frontiers | Research Topics

Ecological consequences of climate change in boreal marginal seas

Edited by
Agneta Andersson, Jacob Carstensen and Anke Kremp

Published in
Frontiers in Marine Science

ISSN 1664-8714
ISBN 978-2-8325-4852-3
DOI 10.3389/978-2-8325-4852-3

About Frontiers

Frontiers is more than just an open access publisher of scholarly articles: it is a pioneering approach to the world of academia, radically improving the way scholarly research is managed. The grand vision of Frontiers is a world where all people have an equal opportunity to seek, share and generate knowledge. Frontiers provides immediate and permanent online open access to all its publications, but this alone is not enough to realize our grand goals.

Frontiers journal series

The Frontiers journal series is a multi-tier and interdisciplinary set of open-access, online journals, promising a paradigm shift from the current review, selection and dissemination processes in academic publishing. All Frontiers journals are driven by researchers for researchers; therefore, they constitute a service to the scholarly community. At the same time, the *Frontiers journal series* operates on a revolutionary invention, the tiered publishing system, initially addressing specific communities of scholars, and gradually climbing up to broader public understanding, thus serving the interests of the lay society, too.

Dedication to quality

Each Frontiers article is a landmark of the highest quality, thanks to genuinely collaborative interactions between authors and review editors, who include some of the world's best academicians. Research must be certified by peers before entering a stream of knowledge that may eventually reach the public - and shape society; therefore, Frontiers only applies the most rigorous and unbiased reviews. Frontiers revolutionizes research publishing by freely delivering the most outstanding research, evaluated with no bias from both the academic and social point of view. By applying the most advanced information technologies, Frontiers is catapulting scholarly publishing into a new generation.

What are Frontiers Research Topics?

Frontiers Research Topics are very popular trademarks of the *Frontiers journals series*: they are collections of at least ten articles, all centered on a particular subject. With their unique mix of varied contributions from Original Research to Review Articles, Frontiers Research Topics unify the most influential researchers, the latest key findings and historical advances in a hot research area.

Find out more on how to host your own Frontiers Research Topic or contribute to one as an author by contacting the Frontiers editorial office: frontiersin.org/about/contact

Ecological consequences of climate change in boreal marginal seas

Topic editors

Agneta Andersson — Umeå University, Sweden

Jacob Carstensen — Aarhus University, Denmark

Anke Kremp — Leibniz Institute for Baltic Sea Research (LG), Germany

Citation

Andersson, A., Carstensen, J., Kremp, A., eds. (2024). *Ecological consequences of climate change in boreal marginal seas*. Lausanne: Frontiers Media SA.

doi: 10.3389/978-2-8325-4852-3

Table of contents

frontiers | Frontiers in Marine Science

TYPE Original Research
PUBLISHED 16 January 2023
DOI 10.3389/fmars.2022.1070377

OPEN ACCESS

EDITED BY
Agneta Andersson,
Umeå University, Sweden

REVIEWED BY
Sabine Dittmann,
Flinders University, Australia
Jan Marcin Weslawski,
Institute of Oceanology, Polish Academy of Sciences, Poland
Regan Nicholaus,
Mbeya University of Science and Technology, Tanzania

*CORRESPONDENCE
Laura Kauppi
laura.kauppi@helsinki.fi

†These authors have contributed equally

SPECIALTY SECTION
This article was submitted to Global Change and the Future Ocean, a section of the journal Frontiers in Marine Science

RECEIVED 14 October 2022
ACCEPTED 28 December 2022
PUBLISHED 16 January 2023

CITATION
Kauppi L, Göbeler N, Norkko J, Norkko A, Romero-Ramirez A and Bernard G (2023) Changes in macrofauna bioturbation during repeated heatwaves mediate changes in biogeochemical cycling of nutrients.
Front. Mar. Sci. 9:1070377.
doi: 10.3389/fmars.2022.1070377

Changes in macrofauna bioturbation during repeated heatwaves mediate changes in biogeochemical cycling of nutrients

Laura Kauppi[1,2]*, Norman Göbeler[1,2], Joanna Norkko[1,2†], Alf Norkko[1,2†], Alicia Romero-Ramirez[3] and Guillaume Bernard[3,4]

[1]Tvärminne Zoological Station, University of Helsinki, Hanko, Finland, [2]Faculty of Biological and Environmental Sciences, University of Helsinki, Helsinki, Finland, [3]Station Marine d'Arcachon, UMR CNRS 5805 EPOC—OASU Université de Bordeaux, Arcachon, France, [4]IFREMER, Department of Oceanography and Ecosystem Dynamics (ODE), Littoral unit, LERAR, Littoral, Arcachon, France

The increasing frequency and intensity of marine heatwaves (MHWs) observed worldwide entails changes in the structure and functioning of ecological communities. While severe and extreme heatwaves often have more destructive effects, the more subtle effects of moderate and strong heatwaves may nevertheless affect ecosystem functioning through complex, context-dependent linkages between different processes. Here we conducted a laboratory experiment to study the effects of repeated short-term, strong MHWs on macrofauna bioturbation and associated solute fluxes as a measure of ecosystem functioning using natural soft-sediment communities from the Baltic Sea. Our results showed changes in both bioturbation and biogeochemical cycling of nutrients following short-term, strong heatwaves, which seemed to contribute to an enhanced degradation of organic matter in the seafloor and an enhanced exchange of solutes across the sediment-water interface as well as increased sediment oxygen consumption. Following changes in these processes, the relative contribution of macrofauna and the environmental context to ecosystem functioning was altered. Our results highlight the potential of even shorter-term, strong MHWs of having system-wide impacts due to changes in the mechanistic process of bioturbation underpinning the biogeochemical cycling of nutrients. This study also highlights the need to measure a wide range of variables for a comprehensive understanding of the changes in functioning under disturbances, such as MHWs.

KEYWORDS

benthic macrofauna, bioturbation, ecosystem functioning, soft sediment, Baltic Sea, climate change

1 Introduction

Soft sediments cover more surface area than any other ecosystem in the world (Snelgrove, 1999). Macrofauna in these soft sediments contribute to the functioning of the whole aquatic ecosystem through their role in benthic-pelagic coupling (Lohrer et al., 2004; Griffiths et al., 2017). Bioturbation by macrofauna links benthic animals to biogeochemical cycling of nutrients through direct consumption of organic matter (Kristensen et al., 1992) and modification of the sediment matrix affecting the redox conditions and activating the microbial degradation processes (Yazdani Foshtomi et al., 2015). The ongoing anthropogenic climate change has caused an increase not only in average temperatures in both aquatic and terrestrial ecosystems (IPCC, 2021), but also in the frequency of periods of abnormally high temperatures, called heatwaves (sensu Hobday et al., 2016). The influence of benthic animals on biogeochemical cycling of nutrients at the seafloor is context-dependent, and is therefore likely to be affected by changes in environmental conditions following climate change (Solan et al., 2004). Only a few studies have looked at the effects of heatwaves on the bioturbation of macrofauna and tried to link that to ecosystem functioning (see Crespo et al., 2017; Dolbeth et al., 2021; Kauppi & Villnäs, 2022) despite the pivotal role this plays in the functioning of marine ecosystems. However, the results of these studies have been somewhat inconclusive with no clear effect on bioturbation due to context-dependent responses and/or the methodology used. Variation in the response could also arise from the duration of the heatwave. There are also interspecific differences in species' response to warming (Harvey et al., 2013; Verdelhos et al., 2015) which could contribute to increasing variation in the observed response and obscure the results. Organisms could also adapt to the increase in any stressor. For example, Fox et al. (2021) observed increases in thermal tolerance in corals following recurrent El Niño heatwaves.

Temperature affects all processes on Earth and thereby also determines ecological patterns and limits the distribution of species (Verdelhos et al., 2015). The frequency and intensity of marine heatwaves (MHW) has already increased following anthropogenic climate change (Hobday et al., 2016; Frölicher et al., 2018; Göbeler et al., 2022). MHWs have the potential to profoundly change the structure of biological communities (e.g. Wernberg et al., 2013; Pansch et al., 2018; Smale et al., 2019), and thereby impair their functioning and provision of goods and services (Smale et al., 2019). Changes in the abundance and/or performance of key species are likely to cause the largest ecological responses to climate change (Reed et al., 2022). Although the effects of heatwaves on the recipient ecosystem are context-dependent (Frölicher & Laufkötter, 2018), severe and extreme heatwaves usually lead to more drastic changes often characterized by mass mortalities of habitat forming species such as corals, kelps or seagrasses (Hobday et al., 2018). Consequences of severe or extreme events might therefore be easier to detect and predict. Even moderate heatwaves, however, may induce changes in species behavior or feeding due to physiological changes following environmental stress associated with increasing temperature (Gillooly et al., 2001; Verdelhos et al., 2015; Amorim et al., 2020; Horwitz et al., 2020; Redfern et al., 2021). While these changes are not lethal, they may still indirectly affect ecosystem processes associated with macrofauna feeding and locomotion activities (Maire et al., 2007; Bernard et al., 2016; Woodin et al., 2016; Pascal et al., 2019). These activities include sediment particle mixing and burrow ventilation (bioirrigation) activities, jointly called bioturbation, which alter the redox conditions of the sediment (Kristensen et al., 2012) and thereby oxygen and nutrient fluxes across the sediment-water interface (Braeckman et al., 2010; Pascal et al., 2019). Any changes in the behavior of macrofauna inducing changes in their bioturbation following changes in temperature could therefore lead to changes in oxygenation of the sediment and cycling of organic matter (Solan et al., 2020).

The Baltic Sea has a long history of eutrophication and coastal areas are suffering from multiple stressors such as hypoxia and pollution. On top of that, mean annual temperature in our study area, an aphotic coastal site at the entrance to the Gulf of Finland, has increased by approximately 2°C since the 1920's and since the late 1980's the increase has been nearly linear (Göbeler et al., 2022). Due to the brackish water and the geologically young age of the Baltic Sea, taxonomic diversity is low, but functional diversity is relatively high (Elmgren & Hill, 1997). Benthic macrofauna communities are dominated by the bivalve *Macoma balthica*, the amphipod *Monoporeia affinis* and the invasive polychaete *Marenzelleria* spp. (e.g. Kauppi et al., 2015). One of the *Marenzelleria* species, *Marenzelleria arctia*, can alone contribute up to 52% of the variation in ammonium fluxes at the sediment-water interface on muddy sites (Kauppi et al., 2018). In shallow coastal sites in the northern Baltic, macrofauna accounted for 25% of the variation in solute fluxes with only a few species having a significant contribution (Gammal et al., 2019) and the same species being responsible for most of the variation in bioturbation rates at these same sites (Bernard et al., 2019a). Bioturbation intensity of the species was defined by the environmental context, with animals having a larger contribution in cohesive than non-cohesive sediments, whereas environmental conditions were more important in non-cohesive sediments (Bernard et al., 2019a). The contribution of macrofauna to variation in solute fluxes can be both direct or indirect through their bioturbation and is also solute-dependent (Kauppi et al., 2018). Given the importance of the macrofauna for the nutrient cycling processes and the relative vulnerability of a system, where the functional contribution is shared by only a few species, any changes in bioturbation following a marine heatwave could have a major effect on ecosystem functioning.

The context-dependent nature of the links between macrofauna, bioturbation and nutrient cycling demonstrated in several earlier studies makes is critical to observe all of these variables together in order to establish a comprehensive understanding of the functioning of the system and how it may change under environmental forcing. To fill in the knowledge gaps regarding the effects of MHWs on benthic macrofauna bioturbation and associated ecosystem functioning in the form of nutrient cycling, we conducted a laboratory experiment using natural sediment communities. More specifically we investigated the effects of repeated, strong MHWs on 1) sediment mixing and bioirrigation processes performed by benthic macrofauna 2) the effects of repeated MHWs on sediment oxygen consumption as a proxy of macrofaunal and microbial activities and 3) changes in solute fluxes as an outcome of remineralisation of organic matter. The results of this study adds to our understanding of the sublethal effects of MHWs that nevertheless might profoundly affect ecosystem processes.

2 Material and methods

2.1 Experiment setup

In total 12 experimental boxes used as experimental units (surface area 34.5 x 29 cm) were retrieved with a box corer onboard "R/V Augusta" on 6th and 7th October, 2020 from a 30 m deep site at Byxholmen (59° 51.734' N, 23° 21.095' E), SW Finland, northern Baltic Sea. The sediment is characterized as clayey mud with elements of sand and gravel. The temperatures chosen for control (CONTROL) and heated (HEAT1/HEAT2) treatments followed climatological temperatures for the reference period 1931-2020 calculated for a monitoring site in close vicinity to the sediment collection site (Göbeler et al., 2022). Of the 12 boxes (a) four boxes functioned as controls and were kept at the climatological mean temperature (about 8.7°C), (b) four boxes received one short-term, strong heatwave and a recovery until the end of the experiment (HEAT1), and (c) the four remaining boxes received two short-term, strong heatwaves with a 7-day recovery period in between (HEAT2; see schematic Figure 1). The first strong MHW had an intensity (relative to the climatological mean) of about 6°C above the climatological mean. As the temperatures naturally decline this time of the year, the 2nd MHW was less intense (about 3.8°C above to the climatological mean) but still of strong category. On 9th October we obtained additional cores with a GEMAX twin corer (diameter of one core 9 cm), that were used to measure porewater and sediment organic content throughout the experiment.

After retrieval, the boxes were carefully transferred to 600 L plastic containers (120 x 80 cm x 80 cm, one box per container) that functioned as water baths. The containers were transferred into two temperature-controlled aquaria rooms (at Tvärminne Zoological Station) set to the climatological mean temperature during the reference period (1931-2020; 8.7°C) and kept in darkness throughout the experiment. Each box received a flow-through of either heated or cooled (down to the control temperature 8.7°C), unfiltered seawater throughout the experiment, except during flux and bromide incubations, but no additional food was given to the macrofauna community. The chl *a* values in the incoming water, however, corresponded to values in the sea at the time of the experiment (1.49 to 1.94 ug/l at 30 m depth; Tvärminne Zoological Station, unpublished data from hydrographic monitoring). Each box was equipped with a circulatory pump to ensure proper mixing of the overlying water. The unfiltered seawater was heated or cooled in header tanks and directed to the experimental units gravitationally. The whole water mass of each box was exchanged ca. 12 times per day. Bottom water temperature in the boxes was followed with an Onset HOBO UA-002-64 Pendant (one pendant in each box logging every 10 minutes). The boxes were left to settle 7 to 8 days prior to experiment start, depending on the retrieval date.

The heatwaves were induced by switching the flow-through from the cooled seawater to the heated seawater. The targeted daily average temperature was reached within twelve hours. Once the heatwave was over, the inflow of heated water was switched back to cooled water to start the recovery period. The first heatwave started 14.10 and ended 21.10, the second heatwave started 28.10 and ended 3.11, first recovery started accordingly on 21.10 and ended 28.10, and second recovery started 3.11 and ended 9.11.

2.2 Luminophore incubations

Sediment mixing was quantified using luminophores as sediment particle tracers incubated during the course of the experiment. In total 36 g DW of pink luminophores (eco-trace®, environmental tracing systems, density = 2.5 g cm^{-3}) were gently spread using a Pasteur pipette on the sediment surface of each box at the beginning of the first heatwave and flow-through was stopped during one hour to allow them to settle. At the start of the second heatwave, a second similar spread of yellow luminophores was performed to study differences in sediment mixing rates under a repeated heatwave (Supplementary Figure 1). The boxes were photographed on each side under UV light (VILBER VL.215.L, wavelength=365nm) using a NIKON D850 digital camera (5408x3600 pixels definition, image resolution of 6 pixels.mm-1) at 12 occasions during the course of the experiment allowing for the assessment of temporal changes in tracer redistribution during each induced phase (Figure 1). Obtained images (JPEG, RGB) were then analyzed using a custom analysis software (Bernard et al., 2016; Bernard et al., 2019b). The sediment-water interface was first manually drawn and then flattened so the vertical location of a given pixel below the interface corresponds to its depth in the sediment. The vertical distribution of tracers in the sediment column (at mm scale) was obtained after a binarization step (based on

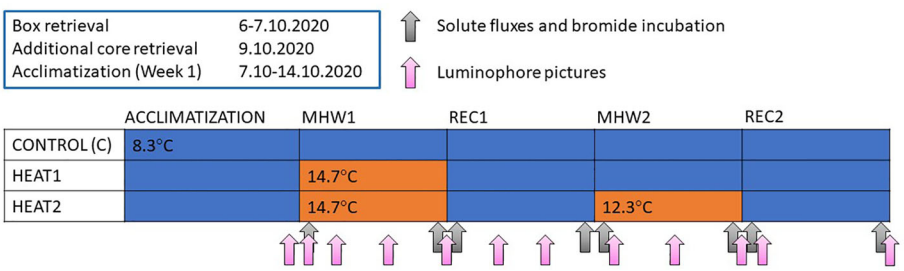

FIGURE 1
Schematic figure representing the experimental design and approximate timepoints when incubations were done and pictures taken. Blue color refers to the control temperature corresponding to the climatological mean and orange color refers to the experimentally induced heatwave, that is CONTROL was kept at control temperature throughout the experiment, HEAT1 received one heatwave and HEAT2 received two heatwaves with a recovery period in between.

the RGB levels). Three metrics were then calculated, characterizing the intensity of the particle mixing performed by the whole community, namely the mean (meanPD), the median (medPD) and the maximum (maxPD) penetration depth of luminophores in the sediment column (Crespo et al., 2017; Dolbeth et al., 2021). For each box, meanPD and medPD measured in the four sides of each box were averaged and the maximum maxPD measured in the four sides was kept. During each of the four tested phases (first MHW, short recovery, second MHW, long recovery from first MHW), increasing rates in the depth of these three variables were assessed using simple linear regressions. The rates were then given in mm day^{-1}.

2.3 Dark incubations of solute fluxes

Dark incubations of solute fluxes were conducted at day 1 and day 5 of each heatwave or recovery period (see Figure 1).The magnitude and direction of solute fluxes at the sediment-water interface link to both macrofauna and the environmental context, such as temperature and organic matter availability (Kauppi et al., 2017; Gammal et al., 2019). Combined they can be used as a measure of nutrient cycling. At the start of the incubations, the inflow of water into the box was stopped and start samples for oxygen (O_2) and nutrients (NH_4^+-N, NO_2-+NO_3^- (hereafter NOX-N), PO_4^{3-}–P, Si^{4+}) were taken from the overlying water column with a syringe. The box was then closed with a lid. The circulatory pump kept the water circulating and prevented the formation of gradients interfering with the diffusion of solutes throughout the incubation. The incubations lasted for 24 hours, thereafter the pump was switched off and the end samples were drawn with a syringe through an opening in the lid. The lid was then removed and the flow-through was started for approximately 30 min-1 hour to exchange the water in the box before starting the bromide incubations. Nutrient samples were filtered through a GF/F filter and stored in the freezer (-20°C) for later analysis in the laboratory at Tvärminne Zoological Station. Oxygen samples were analyzed with Winkler titration either straight after the incubations, or the following day after being stored in the fridge overnight. From the start and end sample, a flux of solutes per square meter per day was calculated considering the volume of water in the box, the incubation time and the area of the box.

2.4 Bioirrigation

Bioirrigation was quantified in each box while assessing the decrease of an inert bromide (Br^-) solute tracer spread in the overlying water. A known volume of stock sodium bromide solution (NaBr, 1 M) was to an initial Br^- concentration of ca. 1 mM in the overlying water after flow-through was stopped. Incubation then lasted 24 h during which overlying water was stirred using gentle air bubbling. After the addition of NaBr solution 5 ml of overlying water samples were taken at 0 (15 min), 6, 12 and 24 hours. Flow-through was restarted after 24 hours. Samples were kept at 4°C until analysis. Concentration of Br- ions in the water samples was analyzed spectrophotometrically (Presley & Claypool, 1971) at Tvärminne Zoological Station (Shimadzu UV-2501 PC) and the relation between bromide concentration in the overlying water and incubation time assessed using simple linear regression (Kauppi et al., 2018). Bioirrigation rates were then given as a pore water exchange rate Q (in ml d^{-1}) calculated after Kauppi et al., 2018.

2.5 Macrofauna community

Box-wise quantification of macrofauna enables the establishment of links between macrofauna, bioturbation and solute fluxes. At the end of the experiment, the sediment was sieved through a 0.5 mm sieve to obtain all macrofauna in the boxes. Macrofauna were stored in 70% ethanol and later identified, measured, counted and weighed.

2.6 Sediment characteristics and porewater nutrients

Vertical profiles of sediment organic content were analyzed at the time of box retrieval (initial values from the field) and for each treatment from GEMAX cores (diameter 9.0 cm) kept in same conditions as the boxes at the end of each experimental phase. The cores were sliced at 0-1, 1-2, 3-4 and 8-9 cm intervals. The slices were transferred to 50 ml Falcon tubes and centrifuged at 2000 rpm for 20 min. The supernatant was then filtered through a GF/F filter and frozen for later analysis of porewater nutrients NH_4^+-N, NOX-N, PO_4^{3-} P and Si^{4+}. At the end of the experiment, three replicate samples of surface sediment (0-2 cm) were taken from each box. One replicate was used for grain size analysis after treatment with 6% H_2O_2 (l) to remove organic material, and two replicates were freeze-dried and pulverized and analyzed for particulate organic nitrogen (PON) and particulate organic carbon (POC) in the laboratory at Tvärminne Zoological Station.

2.7 Statistical analyses

Differences in macrofaunal community structure between the experimental boxes were assessed using non-metric multidimensional scaling (nMDS) based on a Bray-Curtis dissimilary matrix of abundances and biomasses of the taxa. Biomasses (wet weight) were fourth-root transformed to reduce the dominant effect of the clam *Macoma balthica*.

For bioturbation, the increase in mean, median and maximum penetration depth (meanPD, medianPD, maxPD, respectively) of luminophores in the sediment (in mm d^{-1}) and the porewater exchange rate Q (in ml d^{-1}) were calculated for each experimental phase and combined after normalization of the variables into one multivariate distance matrix based on Euclidean distances between the samples. A Principal Coordinated Analysis (PCO) was run to illustrate the patterns in bioturbation throughout the experiment. We used the PERMANOVA –procedure in PRIMER 7 PERMANOVA add-on (Anderson et al., 2008) 1) for differences between treatments during each phase (treatment as a fixed factor) and 2) between phases within each treatment (phase as fixed and box as random factor to account for repeated measures design). If the main test testing for overall differences was significant at the $P < 0.05$ –level, a pairwise test

was run to test for between-treatment or phase differences. The PERMDISP procedure accompanied the PERMANOVAS to test for differences in multivariate dispersions that could affect the PERMANOVA result. To illustrate the changes in the overall bioturbation processes we used PCO. For the second, long recovery period, only differences between CONTROL and HEAT1 were tested. The variables meanPD and medPD showing clearest responses to the induced heatwaves were also studied separately and illustrated with box plots.

Sediment oxygen consumption was studied separately from the other fluxes, since it is so closely related to many of the solutes, such as NOX-N and Si^{4+}, and thus tends to drive the multivariate patterns. Differences in oxygen consumption throughout the experiment were studied using the PERMANOVA procedure between treatments within each experimental phase and between experimental phases within each treatment.

To study differences in the biogeochemical processes between treatments and between different phases of the experiment (heatwave vs. recovery, see Figure 1), we combined the normalized nutrient fluxes (excluding oxygen) into one multivariate distance matrix based on Euclidean distances between the samples. We used the PERMANOVA –procedure in PRIMER 7 PERMANOVA add-on (Anderson et al., 2008) 1) for differences between treatments during each phase (treatment as fixed factor) and 2) between phases within each treatment (phase as fixed and box as random factor to account for repeated measures design). If the main test testing for overall differences was significant at the $P < 0.05$ –level, a pairwise test was run to test for between-treatment or phase differences. The PERMDISP procedure accompanied the PERMANOVAS to test for differences in multivariate dispersions that could affect the PERMANOVA result. To illustrate the changes in the overall biogeochemical processes we used PCO. Draftsman plots with correlations were inspected prior to analysis to inspect the variables for any need of transformations. At the end of the second recovery phase we had lost three boxes from the heated treatments to leakage issues, thus results from the last flux measurements were omitted from the analyses.

3 Results

3.1 Temperature during the experiment

The temperatures aimed for in this experimental setting followed the climatological values of the reference period 1931-2020. The temperature in the controls remained close to the climatological mean at about 8.8°C ± 0.6°C (mean ± SD throughout) over the course of the experiment. Treatment HEAT1 experienced a strong MHW at about 14.9°C ± 0.5 followed by a recovery period at 8.8°C ± 0.8 SD). The HEAT2 treatment experienced the same strong MHW as HEAT1, but followed by a recovery at 8.8°C for 6 days, a repeated strong MHW at 12.0°C ± 0.4 for 5 days and a final recovery at about 8.6°C ± 0.77 SD (Figure 2). Both experimentally induced heatwaves peaked as strong heatwaves but due to the natural cooling this time of the year, the second MHW required less intense temperatures to be categorized as strong MHW.

3.2 Macrofauna

In total 15 different taxa were observed in the boxes of which the clam *Macoma balthica*, the polychaete genus *Marenzelleria* spp. and the amphipod *Monoporeia affinis* were the three most common species in terms of abundance. In terms of biomass, *M. balthica*, *Marenzelleria* spp. and the priapulid worm *Halicryptus spinulosus* were the three dominant species. Based on visual inspection of the nMDS graphs there were no significant differences in the macrofauna structural composition based either on abundances or on wet weight of identified taxa (Figure 3).

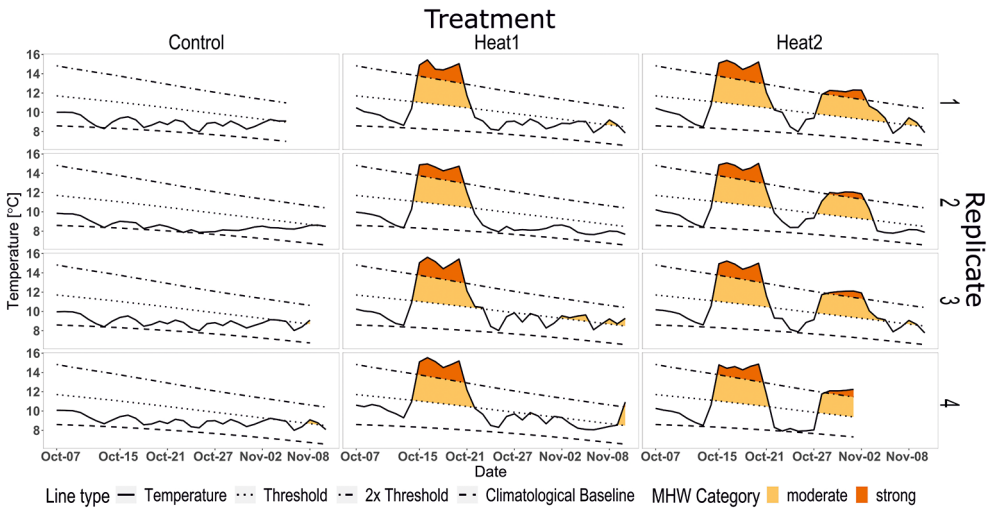

FIGURE 2
Measured temperature (solid line) in the three different treatments during the experiment; CONTROL (first panel), HEAT1 (second panel) and HEAT2 (third panel). Following climatological values (based on reference period 1931-2020) as linetypes (in order from bottom to top for each panel): dashed – climatological baseline; dotted – threshold for moderate MHW; dotdash – 2 x threshold for strong MHW. The HOBO pendant in HEAT2, replicate 4 had stopped working 1st November, which is why no data is presented for this box after that.

3.3 Changes in macrofauna bioturbation

There were no significant changes in the multivariate bioturbation between treatments during the first heatwave and the first and second recovery period (Figure 4A). There was, however, an increasing trend in both the magnitude and the variation of meanPD and medianPD from the CONTROL towards the heated treatments. During the second heatwave, there was a significant difference in multivariate bioturbation between the treatments including the luminophores spread at the beginning of the experiment (Pseudo-F 7.78, P 0.004) but not when including those spread at the beginning of the second heatwave (Figure 4B). This could be due to the significant PERMDISP test for the second layer of luminophores, indicating that the multivariate dispersion was too high to detect a significant difference. Pairwise comparisons showed that HEAT2 differed significantly from both the CONTROL (t 2.46, P 0.02) and HEAT1 (t 4.02, P 0.005) treatments. For meanPD, the CONTROL and HEAT1 differed significantly from HEAT2 (t 10.12, P 0.0002 for C and t 12.96, P 0.0002 for HEAT1). For medianPD, the CONTROL differed significantly from HEAT1 (t 2.62, P 0.05) and from HEAT2 (t 7.79, P 0.0002) and HEAT1 differed significantly from HEAT2 (t 8.64, P 0.0005). The increase in meanPD differed significantly between treatments also for the luminophores spread at the beginning of the second heatwave (Pseudo-F 5.72, P 0.03) with CONTROL differing significantly from HEAT2 (t 2.60, P 0.04) and HEAT1 showing an almost significant difference from HEAT2 (t 2.37, P 0.07).

3.4 Changes in sediment oxygen consumption

There were no significant changes in sediment oxygen consumption between the different experimental phases in any of the treatments (C, HEAT1, HEAT2; Figure 5). However, the oxygen consumption rates are higher during the heatwaves in the heated treatments, and there is a slight decrease in oxygen consumption overall through time in C and HEAT1 after the first heatwave.

3.5 Changes in sediment biogeochemical processes

The clearest changes in sediment biogeochemical processes (multivariate fluxes) happened at the end of the first heatwave in

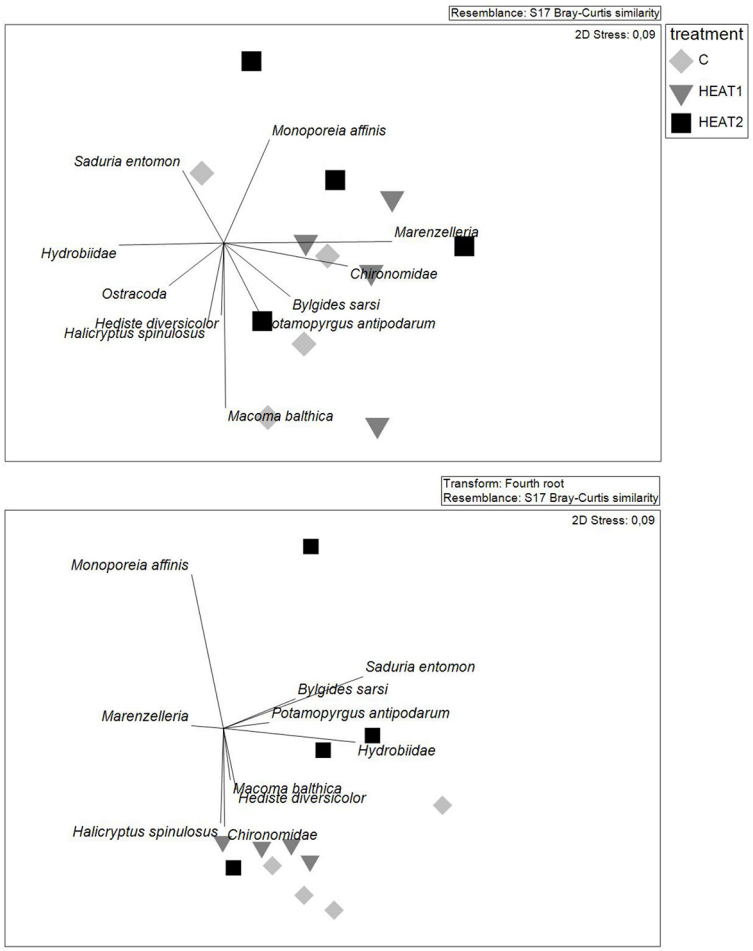

FIGURE 3
Community composition in the experimental boxes illustrated by nMDS plots based on densities (upper panel)) and fourth root transformed wet weights (lower panel) of the different taxa identified from the boxes at the end of the experiment.

10.3389/fmars.2022.1070377

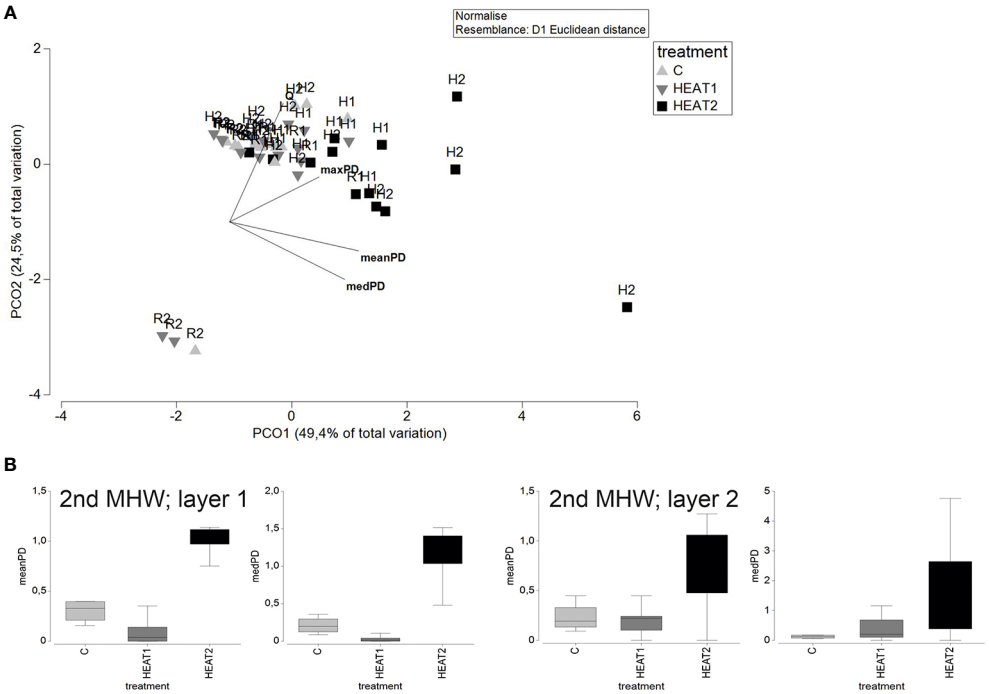

FIGURE 4
A PCO graph on the multivariate distance matrix on bioturbation including the increase in mean penetration depth (meanPD), median penetration depth (medPD) and maximum penetration depth (maxPD) of luminophores and the porewater exchange rate (Q) **(A)**. The vectors overlain on the graph show the correlation of the base variables with the two PCO axes. The labels refer to the different experimental phases: H1= first heatwave, R1= first recovery, H2= second heatwave, R2= second recovery. Vectors show the direction and magnitude of correlation of the variables in the multivariate bioturbation with the PCO axes. In **(B)** the significant differences in meanPD and medPD during the second heatwave are illustrated by box plot graphs with the whiskers representing min and max, the box representing first and third quartiles and the line representing median. CONTROL/C=light grey, HEAT1=dark grey, HEAT2=black. Layer 1 refers to the first set of luminophores spread at the beginning of the first heatwave and layer 2 to the second set of luminophores spread at the beginning of the second heatwave.

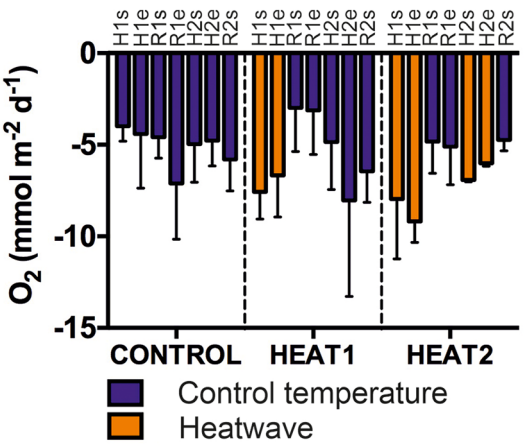

FIGURE 5
Oxygen consumption in mmol/m2/d in the different treatments throughout the course of the experiment. Each bar represents a single flux measurement starting from the start of the first heatwave and ending at the start of the second recovery. Fluxes were measured at the start and end of each experimental phase according to Figure 1. Blue color represents oxygen consumption at control temperature maintained throughout the experiment (8.9°C) and orange color represents oxygen consumption during the experimentally induced heatwaves (at about 14.9°C and 12°C). Bars represent mean consumption and error bars standard deviation.H1s=start of first MHW, H1e=end of first MHW, R1s=start of first recovery, R1e=end of first recovery, H2s=start of second heatwave, H2e=end of second heatwave, R2s=start of second recovery.

HEAT1 and HEAT2 (Figure 6; PERMANOVA main test: Pseudo-F 8.54, P 0.002), where the CONTROL differed significantly from HEAT1 (t 4.19, P 0.002) and from HEAT2 (t 3.52, P 0.005). Also at the end of the second heatwave, HEAT2 differed significantly from CONTROL (PERMANOVA main test: Pseudo-F 4.3011, P 0.05; pairwise comparison between CONTROL and HEAT2: t 3.10, P 0.03). Between the MHWs the recovery of the multivariate fluxes is visible as the disappearance of the separation between the treatments.

There were significant within-treatment differences between the different experimental phases in the biogeochemical processes in HEAT1 and HEAT2 and an almost significant difference in the control (CONTROL: Pseudo-F 1.93, P 0.06; HEAT1: Pseudo-F 4.98, P 0.0001; HEAT2: Pseudo-F 2.53, P 0.01). For the CONTROL treatment, the pair-wise comparisons were not significant at the P=0.05 level. There was a decrease in all the fluxes, except silicate, in the CONTROL treatment throughout the experiment (Supplementary Figure 2). Pairwise comparisons within HEAT1 (Table 1) revealed significant differences between H1_start and H1_end (t 3.04, P 0.003) and H2_start (t 3.78, P 0.002), H1_end and R1_start (t 2.98, P 0.005) and H2_start (t 5.06, P 0.001). In HEAT1, there was also a decrease in all solute fluxes excluding phosphate throughout the course of the experiment (Supplementary Figure 2). Pairwise comparisons in HEAT2 (Table 1) revealed significant differences between H1_end and R1_start (t 3.20 P 0.01), H1_end and R1_end (t3.04, P 0.01), H1_end and H2_start (t 3.95, P 0.004), H1_end and H2_end (t 2.20, P 0.05) and H1_end and R2_start

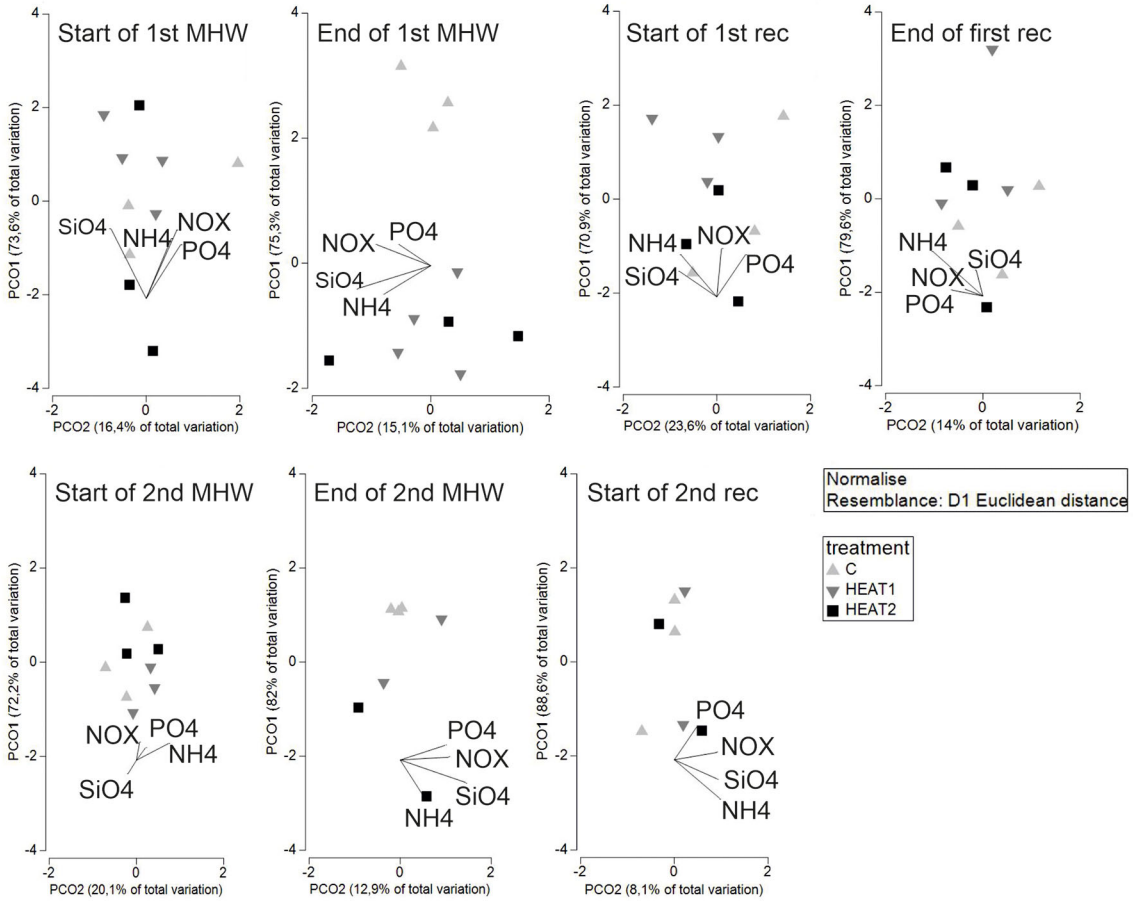

FIGURE 6
PCO graphs showing the multivariate dispersion of fluxes in the different experimental phases. The vectors represent the direction and magnitude of correlation of the different fluxes with the PCO axes.

(t 2.76, P 0.03). In HEAT2, no clear overall increase or decrease in the fluxes were observed, rather the heatwaves could be separated from the recovery phases with higher effluxes at the end of the heatwaves (Figure 6).

3.6 Sediment characteristics and porewater

The two replicate surface sediment samples taken at the end of the experiment were averaged per treatment (n=8 per treatment). The amount of organic carbon was highest in CONTROL (422.1 ± 112.0 µg) and lowest in HEAT2 (390.6 ± 85.6 µg), whereas in HEAT1, the amount of organic carbon was slightly lower than in CONTROL (416.9 ± 96.3 µg). The C/N ratio was highest in HEAT2 (9.4 ± 0.8) and lowest in CONTROL (9.0 ± 0.9), whereas the C/N ratio in HEAT1 was again slightly higher than in CONTROL (9.1 ± 0.8).

In the porewater in CONTROL and HEAT1 treatments, there was a build-up of NH4-N, PO4-P and Si in the porewater below 4 cm depth towards the end of the experiment (Figure 7). NOx-N profiles did not show any difference through time in CONTROL but had a surface peak in HEAT1 at the end of the first and second recovery phases. In HEAT2, on the other hand, the amount of NH4-N, PO4-P and Si in the porewater after 5 cm depth was highest at the end of the second heatwave and lowest at the end of the second recovery period. Similarly to HEAT1, there was a surface peak in NOX-N at the end of the first and second heatwaves, and at the end of the second recovery.

4 Discussion

Given the context-dependent interactions between macrofauna community composition, bioturbation and nutrient cycling, it is essential to measure a wide range of variables together for a more comprehensive understanding of ecosystem functioning when the context (environment) and/or the macrofauna community or bioturbation changes. Since the mean temperature of the oceans and the frequency of heatwaves is increasing, it is imperative to explore the effects of MHWs on the mechanistic effect of macrofauna bioturbation and the associated biogeochemical processes (nutrient cycling). The results of this study indicate an increase in bioturbation activities of macrofauna during short-term, strong heatwaves compared to control temperatures. This increase matches an increase in the biogeochemical cycling of nutrients measured as fluxes of solutes across the sediment-water interface. The increase in sediment oxygen consumption during the heatwaves is likely a consequence of both increased macro- and meiofaunal (bioturbation) as well as microbial (decomposition) activities (Glud, 2008). Oxygen consumption as well as the bioturbation activities and fluxes seem to

TABLE 1 Pair-wise comparisons of the multivariate biogeochemical flux within treatments HEAT1 and HEAT2 (PERMANOVA).

HEAT1			HEAT2		
Groups	*t*	*P(perm)*	*Groups*	*t*	*P(perm)*
H1_S, H1_E	**3.148**	**0.001**	**H1_S, H1_E**	**3.148**	**0.000**
H1_S, R1_S	1.116	0.292	H1_S, R1_S	1.116	0.290
H1_S, R1_E	1.416	0.160	H1_S, R1_E	1.416	0.161
H1_S, H2_S	1.941	0.089	H1_S, H2_S	1.789	0.111
H1_S, H2_E	1.218	0.311	H1_S, H2_E	0.702	0.695
H1_S, R2_S	1.491	0.219	H1_S, R2_S	1.327	0.254
H1_S, R2_E	1.189	0.302	H1_S, R2_E	0.702	0.621
H1_E, R1_S	**3.899**	**0.001**	**H1_E, R1_S**	**3.899**	**0.001**
H1_E, R1_E	**4.029**	**0.001**	**H1_E, R1_E**	**4.029**	**0.001**
H1_E, H2_S	**5.065**	**0.008**	**H1_E, H2_S**	**4.822**	**0.008**
H1_E, H2_E	**3.674**	**0.026**	**H1_E, H2_E**	**2.886**	**0.028**
H1_E, R2_S	**3.661**	**0.029**	**H1_E, R2_S**	**3.653**	**0.028**
H1_E, R2_E	**3.841**	**0.026**	H1_E, R2_E	2.611	0.124
R1_S, R1_E	0.762	0.613	R1_S, R1_E	0.762	0.611
R1_S, H2_S	1.552	0.109	R1_S, H2_S	1.116	0.279
R1_S, H2_E	0.692	0.604	R1_S, H2_E	1.059	0.323
R1_S, R2_S	1.082	0.363	R1_S, R2_S	0.860	0.574
R1_S, R2_E	0.774	0.567	R1_S, R2_E	0.336	0.860
R1_E, H2_S	0.755	0.516	R1_E, H2_S	0.939	0.515
R1_E, H2_E	0.432	0.786	R1_E, H2_E	1.383	0.254
R1_E, R2_S	0.641	0.641	R1_E, R2_S	0.460	0.785
R1_E, R2_E	0.357	0.853	R1_E, R2_E	0.303	1.000
H2_S, H2_E	1.084	0.508	**H2_S, H2_E**	**2.150**	**0.099**
H2_S, R2_S	0.530	0.802	H2_S, R2_S	0.571	0.905
H2_S, R2_E	1.762	0.197	H2_S, R2_E	0.821	0.752
H2_E, R2_S	0.410	0.677	H2_E, R2_S	1.458	0.335
H2_E, R2_E	0.418	1.000	H2_E, R2_E	0.876	0.674
R2_S, R2_E	0.444	1.000	R2_S, R2_E	0.330	1.000

H1_S, start of first heatwave; H1_E, end of first heatwave; R1_S, start of first recovery; R1_E, end of first recovery; H2_S, start of second heatwave; H2_E, end of second heatwave; R2_S, start of second recovery; R2_E, end of second recovery. Significant results in bold.

return to the same level with the control during the recovery phase following the heatwave. A repeated, strong heatwave induced a similar response. During the repeated heatwave, we also observed a difference between treatments in the increase of the penetration depth of tracers that was clearly more marked when considering the first layer of tracers spread in the beginning of the experiment than the second one (spread in the beginning of the second heatwave). This indicates that subsurface sediment is more affected than the surface layer by the enhanced bioturbation activities induced by the heatwave. This corresponds to a known effect of increased temperature on subsurface activity (corresponding to increased foraging for food and burrow maintenance activities) and subsequent bioturbation rates observed in the tellinid bivalves of the genus *Abra* (Maire et al., 2007; Bernard et al., 2016) or burrowing polychaetes (Ouellette et al., 2004; Braeckman et al., 2010). The species mostly responsible for subsurface bioturbation in the soft sediments of the study area are the bivalve *Macoma balthica* and polychaete *Marenzelleria* spp. (Kauppi et al., 2018; Bernard et al., 2019a).

To be considered a heatwave, the period of abnormally high temperature must be at least of 5 days in duration (Hobday et al., 2016; Hobday et al., 2018; Oliver et al., 2021) but is a short-term MHW enough to induce a change? According to the results of this study the answer is yes, a short-term, repeated MHW was enough to generate a significant response in both the bioturbation of the animals

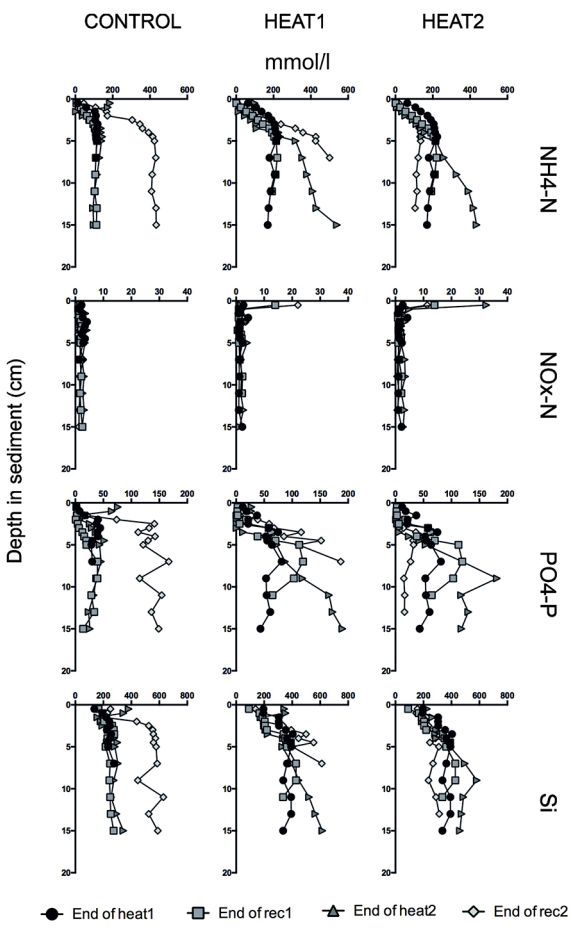

FIGURE 7
Porewater profiles for NH4-N (first row), NOx-N (second row), PO4-P (third row) and Si (last row) from GEMAX cores kept at the same temperature conditions with the experimental units and analyzed at the end of each experimental phase. On the y-axis is the depth of the sediment and on the x-axis the concentration of the solute in mmol/l.

and the biogeochemical processes. Kauppi and Villnäs (2022) detected a similar change in solute fluxes in their short-term moderate heatwave treatment but the effect on bioturbation was less clear. Their strong heatwave treatment peaking at approximately 17°C, however, showed significantly decreased activity based on oxygen consumption, which they considered mostly being due to a shutdown of microbial degradation processes under the strong heatwave conditions since macrofauna still seemed to remain active. In this experiment, the highest amount of organic carbon was lost in the repeated heatwaves treatment. This treatment also had the highest C/N ratio indicating most degraded material. Additionally, the increase in sediment mixing depth was most notable and the porewater profiles indicated lowest concentrations of dissolved solutes in the deeper layers after repeated heatwaves. This implies that the higher activity of macrofauna enhanced the diffusion of solutes from the sediment to the water column and contributed to an increase in the organic matter degradation processes. This contribution was probably both direct through consumption (Kristensen et al., 1992) to meet the higher energetic demand induced by increased activity, and indirect through enhancing microbial activity (Yazdani Foshtomi et al., 2015). Meiofauna, which was not analyzed in this experiment, also has the potential to greatly enhance microbial communities as well as oxygen consumption of the sediment (Bonaglia et al., 2020) and undoubtedly contributed to the increased sediment oxygen consumption observed during the heatwaves.

Microbial processes are central to carbon cycling and their response to warming in marine environments should be included in experiments combining mechanistic effects and bioturbation of macrofauna to biogeochemical processes given the tight links existing between these compartments. Tamelander et al. (2017) suggested that heterotrophic processes in the pelagic compartment would become more important with warmer climate leading to a decrease in organic matter input to the seafloor, resulting in less biomass production (Ehrnsten et al., 2020). Based on the decrease in organic carbon content and increase in C/N ratio in this experiment following repeated, strong heatwaves, organic matter consumption and degradation in the seafloor could also become more efficient with warming thus, at some point, substrate depletion could decrease microbial activity. The low sediment mixing activities of macrofauna in the CONTROL treatment and during the long recovery period of the HEAT1 treatment contributed to a build-up of dissolved nutrients in the sediment as observed from the porewater profiles. This seems to also be the reason for the change in the direction of the solute fluxes from effluxes to influxes towards the end of the experiment in these treatments. Although the differences in carbon and nitrogen content between the treatments are not massive and the porewater profiles are not replicated, the results support each other, highlighting again the importance of studying a range of variables to discern the respective contributions of biological and environmental variables to ecosystem functioning in a changing environment.

Many ecosystems especially along the heavily populated coastlines are already under multiple anthropogenic pressures such as eutrophication, habitat destruction and overfishing (Cloern et al., 2016) on top of which the global climate change further affects ecosystems and their functioning worldwide (Smale et al., 2019). The potential for recovery of an ecosystem after disturbance, such as MHWs, varies depending on the duration and spatial extent of the disturbance event (Thrush and Dayton, 2002). Both the biogeochemical processes as well as the macrofauna activities in this experiment seemed to recover to the control level after the first experimentally induced, strong short-term heatwave. Unfortunately, we could not follow the recovery after the repeated short-term event due to loss of experimental units to leakage, but the immediate response after the repeated heatwave at the start of the (second) recovery period suggested no differences between the treatments. Nevertheless, resources (organic carbon) after the repeated event were more depleted, suggesting that the reason for a decrease in solute fluxes after the repeated heatwaves to a level comparable to the control, could be a combination of lack of material for degradation processes and decreased activity of macrofauna. In the control and after one short-term heatwave, on the other hand, material was still (readily) available. Thus, the system seems to have recovered but despite the similar outcome in terms of ecosystem functioning, the effect of the disturbance on the quantity and quality of resources in the seafloor could in fact have changed the respective contributions of macrofauna and microbial activity and purely diffusional processes to

biogeochemical processes. Studies with longer-term heatwaves of different categories are needed to assess the resilience of the ecosystem to MHWs more thoroughly.

Given the multiple stressors affecting marine ecosystems, heatwaves can and probably will co-occur with other stressors, such as hypoxia (Vaquer-Sunyer & Duarte, 2011; Gruber et al., 2021). Field observations from the Baltic Sea (Tvärminne Zoological Station benthic monitoring program, unpublished data) also indicate increased mortality of *Macoma balthica* following first a prolonged MHW and then the occurrence of a hypoxic event. This highlights the need to include multiple stressors in future studies. Species-specific differences in their response to disturbances, such as MHWs, should also be considered in more detail. Differences in adaptive strategies have been observed for example in fiddler crabs (da Silva Vianna et al., 2020) and limpets (Redfern et al., 2021). Given the low species diversity in the Baltic Sea, changes in the bioturbation, as observed in our experiment, or survival of even one species following an MHW can have substantial effects on the functioning of the system.

In contrast to our results, results from earlier studies indicate a lack of effects of short-term, moderate MHWs (e.g. Crespo et al., 2017; Dolbeth et al., 2021). These studies were, however, conducted on intertidal estuarine populations, naturally subject and adapted to higher and more frequent daily variations of temperature and could therefore tolerate the changes induced by the simulated heatwave (Dolbeth et al., 2021). Nevertheless, our ability to detect significant differences in sediment mixing metrics in response to heatwave also results from the methodological choice of monitoring the distribution of particle tracers through time. Although sensitive to functional trait composition of the animal community and habitat structure (Hale et al., 2014; Crespo et al., 2017), the comparison of the same, but non-time integrated metrics did not end in the detection of significant heatwave effects (Crespo et al., 2017). Following a similar approach to this study, Dolbeth et al. (2021) noted that, although non-significant, "more evident" trends were detected when using time-integrated metrics.

The results of this study clearly demonstrate the potential of even short-term MHWs to alter species burrowing and burrow ventilation activities linked to ecosystem functioning. Significant changes in nutrient cycling in this study were observed earlier than changes in the underlying mechanistic effect of bioturbation. The environmental context (chemical composition of sediment and porewater, organic matter content) also changed following the MHWs, and while the results demonstrate a quick recovery in terms of both bioturbation and the associated solute fluxes even from repeated short-term events, the relative contribution of different factors remains altered after disturbance. The indications of stress responses in this study across a range of variables from environmental and biological to biogeochemical highlights the need to include different types of evidence for a comprehensive understanding of the changes happening in the system as both the environment and the functioning of the organisms are altered. It also implies the concerning fact that already the realised increase in the frequency and intensity of MHWs currently observed (Göbeler et al., 2022) may induce system-wide impacts. There are still important gaps in our knowledge that warrant future studies with regards to for example microbial processes, duration of the heatwaves and multiple stressor effects not only in the Baltic Sea but in marine environments globally.

Data availability statement

The raw data supporting the conclusions of this article will be made available by the authors, without undue reservation.

Author contributions

LK designed and conducted the experiment, performed the data analysis and wrote the manuscript, NG designed and conducted the experiment, JN and AN participated in designing the experiment and provided substantial comments on the manuscript, AR-R participated in the design and substantially contributed to the image analysis and acquisition of data, GB designed the experiment, processed and analyzed the bioturbation data and provided substantial comments on the manuscript. All authors contributed to the article and approved the submitted version.

Funding

Funding for the project was received from Walter and Andrée de Nottbeck Foundation (personal grants to LK, NG and JN), as well as from the ASSEMBLE Plus project (European Union's Horizon 2020 research and innovation programme grant agreement No 730984) to GB and AR-R and the Centre for Coastal Ecosystem and Climate Change Research to AN.

Acknowledgments

We thank Göran Lundberg and Jostein Solbakken for their invaluable help with sampling and handling of the samples and development of the mesocosm space. This study has utilized research infrastructure facilities provided by FINMARI (Finnish Marine Research Infrastructure network).

Conflict of interest

The authors declare that the research was conducted in the absence of any commercial or financial relationships that could be construed as a potential conflict of interest.

Publisher's note

Supplementary material

The Supplementary Material for this article can be found online at: https://www.frontiersin.org/articles/10.3389/fmars.2022.1070377/full#supplementary-material

References

Amorim, V. E., Gonçalves, O., Capela, R., Fernández-Boo, S., Oliveira, M., Dolbeth, M., et al. (2020). Immunological and oxidative stress responses of the bivalve *Scrobicularia plana* to distinct patterns of heatwaves. *Fish Shellf. Immunol.* 106 (June), 1067–1077. doi: 10.1016/j.fsi.2020.09.024

Anderson, M. J., Gorley, R. N., and Clarke, K. R. (2008). *Permanova+ for primer: guide to software and statistical methods* (Plymouth: PERIMER-e).

Bernard, G., Duchêne, J.-C., Romero-Ramirez, A., Lecroart, P., Maire, O., Ciutat, A., et al. (2016). Experimental assessment of the effects of temperature and food availability on particle mixing by the bivalve *Abra alba* using new image analysis techniques. *PloS One* 11, e0154270. doi: 10.1371/journal.pone.0154270

Bernard, G., Gammal, J., Järnström, M., Norkko, J., and Norkko, A. (2019a). Quantifying bioturbation across coastal seascapes: Habitat characteristics modify effects of macrofaunal communities. *J. Sea Res.* 152, 101766. doi: 10.1016/j.seares.2019.101766

Bernard, G., Romero-Ramirez, A., Tauran, A., Pantalos, M., Deflandre, B., Grall, J., et al. (2019b). Declining maerl vitality and habitat complexity across a dredging gradient: Insights from *in situ* sediment profile imagery (SPI). *Sci. Rep.* 9 (1), 1–12. doi: 10.1038/s41598-019-52586-8

Bonaglia, S., Hedberg, J., Marzocchi, U., Iburg, S., Glud, R. N., and Nascimento, F. J. (2020). Meiofauna improve oxygenation and accelerate sulfide removal in the seasonally hypoxic seabed. *Mar. Environ. Res.* 159, 104968. doi: 10.1016/j.marenvres.2020.104968

Braeckman, U., Provoost, P., Gribsholt, B., Van Gansbeke, D., Middelburg, J. J., Soetaert, K., et al. (2010). Role of macrofauna functional traits and density in biogeochemical fluxes and bioturbation. *Mar. Ecol. Prog. Ser.* 399 (January), 173–186. doi: 10.3354/meps08336

Cloern, J. E., Abreu, P. C., Carstensen, J., Chauvaud, L., Elmgren, R., Grall, J., et al. (2016). Human activities and climate variability drive fast-paced change across the world's estuarine–coastal ecosystems. *Global Change Biol.* 22 (2), 513–529. doi: 10.1111/gcb.13059

Crespo, D., Grilo, T. F., Baptista, J., Coelho, J. P., Lillebø, A. I., Cássio, F., et al. (2017). New climatic targets against global warming: will the maximum 2° c temperature rise affect estuarine benthic communities? *Sci. Rep.* 7 (1), 1–14. doi: 10.1038/s41598-017-04309-0

da Silva Vianna, B., Miyai, C. A., Augusto, A., and Costa, T. M. (2020). Effects of temperature increase on the physiology and behavior of fiddler crabs. *Physiol. Behav.* 215, 112765. doi: 10.1016/j.physbeh.2019.112765

Dolbeth, M., Babe, O., Costa, D. A., Mucha, A. P., Cardoso, P. G., and Arenas, F. (2021). Benthic estuarine communities' contribution to bioturbation under the experimental effect of marine heatwaves. *Sci. Rep.* 11 (1), 1–11. doi: 10.1038/s41598-021-90720-7

Ehrnsten, E., Norkko, A., Müller-Karulis, B., Gustafsson, E., and Gustafsson, B. G. (2020). The meagre future of benthic fauna in a coastal sea–benthic responses to recovery from eutrophication in a changing climate. *Global Change Biol.* 26 (4), 2235–2250. doi: 10.1111/gcb.15014

Elmgren, R., and Hill, C. (1997). Ecosystem function at low biodiversity–the Baltic example. *Mar. biodivers.: patterns process.*, 319–336. doi: 10.1017/CBO9780511752360.015

Fox, M. D., Cohen, A. L., Rotjan, R. D., Mangubhai, S., Sandin, S. A., Smith, J. E., et al. (2021). Increasing coral reef resilience through successive marine heatwaves. *Geophys. Res. Lett.* 48 (17), e2021GL094128. doi: 10.1029/2021GL094128

Frölicher, T. L., Fischer, E. M., and Gruber, N. (2018). Marine heatwaves under global warming. *Nature* 560 (7718), 360–364. doi: 10.1038/s41586-018-0383-9

Frölicher, T. L., and Laufkötter, C. (2018). Emerging risks from marine heat waves. *Nat. Commun.* 9 (1), 1–4. doi: 10.1038/s41467-018-03163-6

Gammal, J., Järnström, M., Bernard, G., Norkko, J., and Norkko, A. (2019). Environmental context mediates biodiversity–ecosystem functioning relationships in coastal softsediment habitats. *Ecosystems* 22, 137–151. doi: 10.1007/s10021-018-0258-9

Gillooly, J. F., Brown, J. H., West, G. B., Savage, V. M., and Charnov, E. L. (2001). Effects of size and temperature on metabolic rate. *science* 293 (5538), 2248–2251. doi: 10.1126/science.10619

Glud, R. N. (2008). Oxygen dynamics of marine sediments. *Mar. Biol. Res.* 4 (4), 243–289. doi: 10.1080/17451000801888726

Göbeler, N., Norkko, A., and Norkko, J. (2022). Ninety years of coastal monitoring reveals baseline and extreme ocean temperatures are increasing off the Finnish coast. *Commun. Earth Environ.* 3 (1), 1–11. doi: 10.1038/s43247-022-00545-z

Griffiths, J. R., Kadin, M., Nascimento, F. J. A., Tamelander, T., Törnroos, A., Bonaglia, S., et al. (2017). The importance of benthic–pelagic coupling for marine ecosystem functioning in a changing world. *Global Change Biol.* 23 (6), 2179–2196. doi: 10.1111/gcb.13642

Gruber, N., Boyd, P. W., Frölicher, T. L., and Vogt, M. (2021). Biogeochemical extremes and compound events in the ocean. *Nature* 600 (7889), 395–407. doi: 10.1038/s41586-021-03981-7

Hale, R., Mavrogordate, M. N., Tolhurst, T. J., and Solan, M. (2014). Characterizations of how species mediate ecosystem properties require more comprehensive functional effect descriptors. *Sci. Rep.* 4, 6463. doi: 10.1038/srep06463

Harvey, B. P., Gwynn-Jones, D., and Moore, P. J. (2013). Meta-analysis reveals complex marine biological responses to the interactive effects of ocean acidification and warming. *Ecol. Evol.* 3 (4), 1016–1030. doi: 10.1002/ece3.516

Hobday, A. J., Alexander, L. V., Perkins, S. E., Smale, D. A., Straub, S. C., Oliver, E. C., et al. (2016). A hierarchical approach to defining marine heatwaves. *Prog. Oceanogr.* 141, 227–238. doi: 10.1016/j.pocean.2015.12.014

Hobday, A. J., Oliver, E. C. J., Gupta, A. S., Benthuysen, J. A., Burrows, M. T., Donat, M. G., et al. (2018). Categorizing and naming marine heatwaves. *Oceanography* 31 (2), 162–173. doi: 10.5670/oceanog.2018.205

Horwitz, R., Norin, T., Watson, S. A., Pistevos, J. C., Beldade, R., Hacquart, S., et al. (2020). Near-future ocean warming and acidification alter foraging behaviour, locomotion, and metabolic rate in a keystone marine mollusc. *Sci. Rep.* 10 (1), 1–11. doi: 10.1038/s41598-020-62304-4

IPCC (2021). Summary for Policymakers. In: Climate Change 2021: The Physical Science Basis. In V. Masson-Delmotte, P. Zhai, A. Pirani, S. L. Connors, C. Péan, S. Berger, et al eds. *Contribution of Working Group I to the Sixth Assessment Report of the Intergovernmental Panel on Climate Change.* Cambridge University Press.

Kauppi, L., Bernard, G., Bastrop, R., Norkko, A., and Norkko, J. (2018). Increasing densities of an invasive polychaete enhance bioturbation with variable effects on solute fluxes. *Sci. Rep.* 8 (1), 1–12. doi: 10.1038/s41598-018-25989-2

Kauppi, L., Norkko, J., Ikonen, J., and Norkko, A. (2017). Seasonal variability in ecosystem functions: quantifying the contribution of invasive species to nutrient cycling in coastal ecosystems. *Mar. Ecol. Prog. Ser.* 572, 193–207. doi: 10.3354/meps12171

Kauppi, L., Norkko, A., and Norkko, J. (2015). Large-Scale species invasion into a low-diversity system: spatial and temporal distribution of the invasive polychaetes marenzelleria spp. in the Baltic Sea. *Biol. Invasion.* 17 (7), 2055–2074. doi: 10.1007/s10530-015-0860-0

Kauppi, L., and Villnäs, A. (2022). Marine heatwaves of differing intensities lead to distinct patterns in seafloor functioning. *Proc. R. Soc. B* 289 (1986), 20221159. doi: 10.1098/rspb.2022.1159

Kristensen, E., Andersen, F. Ø., and Blackburn, T. H. (1992). Effects of benthic macrofauna and temperature on degradation of macroalgal detritus: the fate of organic carbon. *Limnol. Oceanogr.* 37 (7), 1404–1419. doi: 10.4319/lo.1992.37.7.1404

Kristensen, E., Penha-Lopes, G., Delefosse, M., Valdemarsen, T., Quintana, C. O., and Banta, G. T. (2012). What is bioturbation? the need for a precise definition for fauna in aquatic sciences. *Mar. Ecol. Prog. Ser.* 446, 285–302. doi: 10.3354/meps09506

Lohrer, A. M., Thrush, S. F., and Gibbs, M. M. (2004). Bioturbators enhance ecosystem function through complex biogeochemical interactions. *Nature* 431 (7012), 1092–1095. doi: 10.1038/nature03042

Maire, O., Duchêne, J. C., Grémare, A., Malyuga, V. S., and Meysman, F. J. R. (2007). A comparison of sediment reworking rates by the surface deposit-feeding bivalve *Abra ovata* during summertime and wintertime, with a comparison between two models of sediment reworking. *J. Exp. Mar. Biol. Ecol.* 343, 21–36. doi: 10.1016/j.jembe.2006.10.052

Oliver, E. C., Benthuysen, J. A., Darmaraki, S., Donat, M. G., Hobday, A. J., Holbrook, N. J., et al. (2021). Marine heatwaves. *Annu. Rev. Mar. Sci.* 13, 313–342. doi: 10.1146/annurev-marine-032720-095144

Ouellette, D., Desrosiers, G., Gagne, J. P., Gilbert, F., Poggiale, J. C., Blier, P. U., et al. (2004). Effects of temperature on *in vitro* sediment reworking processes by a gallery biodiffusor, the polychaete *Neanthes virens*. *Mar. Ecol. Prog. Ser.* 266, 185–193. doi: 10.3354/meps266185

Pansch, C., Scotti, M., Barboza, F. R., Al-Janabi, B., Brakel, J., Briski, E., et al. (2018). Heat waves and their significance for a temperate benthic community: A near-naturalexperimental approach. *Global Change Biol.* 24, 4357–4367. doi: 10.1111/gcb.14282

Pascal, L., Maire, O., Deflandre, B., Romero-Ramirez, A., and Grémare, A. (2019). Linking behaviours, sediment reworking, bioirrigation and oxygen dynamics in a soft-bottom ecosystem engineer: The mud shrimp *Upogebia pusilla* (Petagna 1792). *J. Exp. Mar. Biol. Ecol.* 516, 67–78. doi: 10.1016/j.jembe.2019.05.007

Presley, B., and Claypool, G. (1971). Techniques for analyzing interstitial water samples. *Part 1* 66, 1749–1755.

Redfern, J. C., Foggo, A., and Mieszkowska, N. (2021). Handling the heat: Responses of two congeneric limpet species to environmental temperature differences. *J. Exp. Mar. Biol. Ecol.* 536, 151500. doi: 10.1016/j.jembe.2020.151500

Reed, D. C., Schmitt, R. J., Burd, A. B., Burkepile, D. E., Kominoski, J. S., McGlathery, K. J., et al. (2022). Responses of coastal ecosystems to climate change: Insights from long-term ecological research. *BioScience* 72 (9), 871–888. doi: 10.1093/biosci/biac006

Smale, D. A., Wernberg, T., Oliver, E. C., Thomsen, M., Harvey, B. P., Straub, S. C., et al. (2019). Marine heatwaves threaten global biodiversity and the provision of ecosystem services. *Nat. Climate Change* 9 (4), 306–312. doi: 10.1038/s41558-019-0412-1

Snelgrove, P. V. (1999). Getting to the bottom of marine biodiversity: sedimentary habitats: ocean bottoms are the most widespread habitat on earth and support high biodiversity and key ecosystem services. *BioScience* 49 (2), 129–138. doi: 10.2307/1313538

Solan, M., Bennett, E. M., Mumby, P. J., Leyland, J., and Godbold, J. A. (2020). Benthic-based contributions to climate change mitigation and adaptation. *Philos. Trans. R. Soc. B* 375 (1794), 20190107. doi: 10.1098/rstb.2019.0107

Solan, M., Cardinale, B. J., Downing, A. L., Engelhardt, K. A. M., Ruesink, J. L., and Srivastava, D. S. (2004). Extinction and ecosystem function in the marine benthos. *Science* 306, 1177–1180. doi: 10.1126/science.1103960

Tamelander, T., Spilling, K., and Winder, M. (2017). Organic matter export to the seafloor in the Baltic Sea: Drivers of change and future projections. *Ambio* 46 (8), 842–851. doi: 10.1007/s13280-017-0930-x

Thrush, S. F., and Dayton, P. K. (2002). Disturbance to marine benthic habitats by trawling and dredging: implications for marine biodiversity. *Annu. Rev. Ecol. syst.* 33, 449–473. doi: 10.1146/annurev.ecolsys.33.010802.150515

Vaquer-Sunyer, R., and Duarte, C. M. (2011). Temperature effects on oxygen thresholds for hypoxia in marine benthic organisms. *Global Change Biol.* 17 (5), 1788–1797. doi: 10.1111/j.1365-2486.2010.02343.x

Verdelhos, T., Marques, J. C., and Anastácio, P. (2015). Behavioral and mortality responses of the bivalves *Scrobicularia plana* and *Cerastoderma edule* to temperature, as indicator of climate change's potential impacts. *Ecol. Indic.* 58, 95–103. doi: 10.1016/j.ecolind.2015.05.042

Wernberg, T., Smale, D. A., Tuya, F., Thomsen, M. S., Langlois, T. J., De Bettignies, T., et al. (2013). An extreme climatic event alters marine ecosystem structure in a global biodiversity hotspot. *Nat. Climate Change* 3 (1), 78–82. doi: 10.1038/nclimate1627

Woodin, S., Volkenborn, N., Pilditch, C., Lohrer, A. M., Wethey, D. S., Hewitt, J. E., et al. (2016). Same pattern, different mechanism: Locking onto the role of key species in seafloor ecosystem process. *Sci. Rep.* 6, 26678. doi: 10.1038/srep26678

Yazdani Foshtomi, M., Braeckman, U., Derycke, S., Sapp, M., Van Gansbeke, D., Sabbe, K., et al. (2015). The link between microbial diversity and nitrogen cycling in marine sediments is modulated by macrofaunal bioturbation. *PloS One* 10 (6), e0130116. doi: 10.1371/journal.pone.0130116

frontiers | Frontiers in Marine Science

TYPE Original Research
PUBLISHED 23 January 2023
DOI 10.3389/fmars.2022.1070341

OPEN ACCESS

EDITED BY
Xianghui Guo,
Xiamen University, China

REVIEWED BY
Antonio Busquets Bisbal,
University of the Balearic Islands, Spain
Jingrang Lu,
United States Environmental Protection Agency (EPA), United States

*CORRESPONDENCE
Karolina Ida Anna Eriksson
karolina.eriksson@umu.se

SPECIALTY SECTION
This article was submitted to Global Change and the Future Ocean, a section of the journal Frontiers in Marine Science

RECEIVED 14 October 2022
ACCEPTED 27 December 2022
PUBLISHED 23 January 2023

CITATION
Eriksson KIA, Ahlinder J, Ramasamy KP, Andersson A, Sundell D, Karlsson L, Sjödin A and Thelaus J (2023) Association between *Legionella* species and humic substances during early summer in the northern Baltic Sea.
Front. Mar. Sci. 9:1070341.
doi: 10.3389/fmars.2022.1070341

Association between *Legionella* species and humic substances during early summer in the northern Baltic Sea

Karolina Ida Anna Eriksson[1,2]*, Jon Ahlinder[3], Kesava Priyan Ramasamy[1,2], Agneta Andersson[1,2], David Sundell[3], Linda Karlsson[3], Andreas Sjödin[3] and Johanna Thelaus[3]

[1]Department of Ecology and Environmental Sciences, Faculty of Science and Technology, Umeå University, Umeå, Sweden, [2]Umeå Marine Sciences Centre, Umeå University, Umeå, Sweden, [3]Division of CBRN Defence and Security, Swedish Defence Research Agency (FOI), Umeå, Sweden

Climate change is projected to cause alterations in northern coastal systems, including humification and intensified nutrient loads, which can lead to ecosystem imbalances and establishment of new bacterial species. Several potential pathogens, such as different species of *Legionella*, hide in the environment between infections, some by living inside protozoan host cells. Knowledge about the occurrence of *Legionella* in natural waters is missing, which disable risk assessments of exposure. We performed a study of the species diversity of *Legionella* in the northern Baltic Sea (Gulf of Bothnia) during early summer to map their occurrence and to identify possible environmental drivers. We detected *Legionella* and potential protozoan hosts along gradients of the Gulf of Bothnia. We also for the first time present third generation full-length 16S rRNA amplicon sequencing (Nanopore) to resolve environmental species classification of *Legionella*, with a method suitable to study all bacteria. Our data show that full length 16S rRNA sequences is sufficient to resolve *Legionella* while the standard short Illumina sequences did not capture the entire diversity. For accurate species classification of *Legionella*, harmonization between the Nanopore classification methods is still needed and the bias toward the well-studied *Legionella pneumophila* need to be resolved. Different *Legionella* species occurred both in the Bothnian Sea and in the Bothnian Bay and their abundance were linked to humic substances and low salinity. The relative abundance of *Legionella* was higher in the humic-rich northern waters of the Bothnian Bay. The link between *Legionella* species and humic substances may be indirect *via* promotion of the heterotrophic microbial food web, allowing *Legionella* species and similar bacteria to establish. Humic substances are rich in iron, which has been shown crucial for growth of *Legionella* species and other pathogens. Considering climate change projections in this regional area, with increased humification and freshwater inflow, this bacterial niche containing potential pathogens might become more widespread in the future Baltic Sea. This study demonstrates the significance of

DNA sequencing to monitor public health relevant bacteria like *Legionella* species in the environment. Including sequencing of bacteria and protozoa in the environmental monitoring programs could be used to identify ecosystem imbalances, which enable appropriate responses to emerging diseases.

KEYWORDS

***Legionella*, protozoa, predation resistance, aquatic microbiology, climate change, ecology change, marginal seas, humification**

Introduction

Climate change is projected to cause alterations in the Baltic Sea, such as humification that leads to decreasing salinity and increased water temperatures. This can lead to ecosystem imbalances and the emergence or establishment of new bacterial species. Several bacterial pathogens, such as *Legionella pneumophila*, has its natural lifecycle in the environment and can live inside protozoan host cells. This ecological niche of predation resistant bacteria are relevant for public health, since some species can cause disease in humans (Thomas et al., 2010).

Bacterial defense strategies has evolved due to the co-existence between bacteria and their predators (protozoa). Some of these strategies contribute to the ability of bacteria to cause human disease. *Francisella tularensis*, *Legionella pneumophila, Vibrio cholerae* and *Yersinia pestis* all are examples of pathogenic bacteria that have anti-predator strategies. The mechanisms bacteria use for both of these traits are often similar (Sun et al., 2018; Amaro and Martín-González, 2021). To understand the emergence of diseases from opportunistic or pathogenic bacteria, it is important to complement studies of bacteria in association to the susceptible host (human cells) with studies of bacteria in the environment of their natural lifecycle. It is likely that bacterial traits that result in pathogenicity to humans originally arose as a response to environmental stress such as predation (Park et al., 2020). For example, *Legionella* is a predation resistant bacteria that reside in the environment, and sporadically cause problems in water supplies (Hamilton et al., 2018; Leoni et al., 2018; Holsinger et al., 2022). Still, there is a knowledge gap regarding the occurrence and persistence of pathogenic and predation resistant bacteria like *Legionella* in natural environments including water.

What allows public health relevant species within the genus *Legionella* to survive in environmental water is unknown, even though more than 20 out of 71 reported species within *Legionella* have been recognized as human pathogens and the causative agent of Legionnaires' disease and Pontiac fever (Muder and Yu, 2002; Legionella Species - Special Pathogens Laboratory, 2020; Parte et al., 2020). *L. pneumophila* is the most studied species in human disease as well as in environmental sampling. Other *Legionella* non-*pneumophila* species that cause disease are less studied and undiagnosed (Pascale et al., 2021). Thus, there is a need to investigate non-*pneumophila* species (Duron et al., 2018).

Bacterial species within *Legionella* has been isolated from various types of environments such as soils and drinking water (Chambers et al., 2021). Even though freshwater is considered the major reservoir of *L. pneumophila* (Boamah et al., 2017), the bacterium is mostly studied in man-made water systems such as cooling towers (Brigmon et al., 2020), where the thermophilic bacteria have been shown to dwell (Lesnik et al., 2015). Only a few studies have reported occurrence of DNA sequences specific to the genus *Legionella* in natural aquatic environments such as in lakes, rivers, brackish and marine waters (Carvalho et al., 2007; Parthuisot et al., 2010; Shimada et al., 2021). Thus, there is a need to increase our understanding of the natural diversity of *Legionella* spp. in aquatic systems. One approach to understand driving mechanisms of aquatic bacteria is mapping them across dynamic habitats. Freshwater and marine systems are especially dynamic in coastal zones that function as filters for chemical compounds and organisms entering the ocean through rivers (Lamb et al., 2017). Due to this inflow, the coast is generally more nutrient rich compared to the offshore areas. Thus, bacteria that inhabit these interfaces between freshwater and marine systems are exposed to stresses/disturbances such as nutrient rich river inflow, which may lead to fluctuations in selection dynamics.

The Baltic Sea is at risk for large fluctuations, maybe even to the scale of the structure and function of the ecosystem (Blenckner et al., 2015). Projections indicate that the Baltic Sea will suffer alterations due to climate change, both due to increased temperature and due to increased inflow of organic matter caused by precipitation (Andersson et al., 2015; Harvey et al., 2015; Meier et al., 2022). Bacteria can use humic rich organic substances as food resource, giving them an ecological advantage over other plankton organisms. This, in turn, will cause lowered planktonic food quality as for example high C to N ratios and poorer fatty acid composition (Bandara et al., 2022;

Guo et al., 2022). Previous research show that in the north of the Gulf of Bothnia phosphorus is the most limiting nutrient, while in the south nitrogen limits organismal growth (Andersson et al., 1996; Tamminen and Andersen, 2007). These habitat variations can select for different bacterial species. The brackish Baltic Sea provides a unique opportunity to study drivers along natural environmental gradients, where the northern parts are more similar to freshwater and the southern parts are more saline.

In the middle of the Gulf of Bothnia, along a 10 km coastal area, a previous study reported widespread occurrence of *Legionella* spp. in early summer (Eriksson et al., 2022). To map occurrence of *Legionella* spp. on a larger spatial scale in the Gulf of Bothnia and with the aim to find environmental drivers, we here analyzed samples in the coast-offshore and north-south gradients in early summer. We used two complementary methods for a general bacterial identification to capture the wide ecological niche of predation resistant bacteria. Then, we particularly focused on *Legionella*, with the aim to also resolve the species. The methods used were sequencing the V4 region of the 16S rRNA gene (using Illumina sequencing) and the V1-9 region (using Nanopore sequencing). To support the species classification, we amplified a *L. pneumophila* specific macrophage infectivity potentiator (*mip*) gene that is associated with virulence (Ballard et al., 2000; Nazarian et al., 2008; Collins et al., 2015; Yin et al., 2022). We expected that relatively high concentrations of humic substances in the coast and the open northern basin of the Gulf of Bothnia (Bothnian Bay) would promote bacterial production and their predators (protozoa), which in turn constitute a niche for *Legionella* spp. In the southern open basin, Bothnian Sea, the humic substance concentration is lower and thus we expected lower bacterial production, as well as lower abundance of protozoa and *Legionella* spp.

Materials and methods

Study sites and environmental data

In June 2019, water samples were collected at 9 different stations (5m depth) in the Gulf of Bothnia: Råneå 1 (RA1), Råneå 2 (RA2), A5, A13, Örefjärden (B3), Gavik (GA1), C3, C14 and C24 (Figure 1). Stations RA1, RA2, A5 and A13 are located in the Bothnian Bay basin (northern Gulf of Bothnia). Stations B3, C14, GA1, C3 and C24 are located in Bothnian Sea basin (southern Gulf of Bothnia). Stations RA1, RA2, GA1, B3 and C14 are coastal sampling sites. Coordinates can be found in Supplementary Material 2.

Umeå Marine Science Centre (UMSC) collected the environmental data *via* the Swedish National Environmental monitoring program. Data were analyzed according to the HELCOM Manual for Marine Monitoring in the COMBINE report (Cooperative Monitoring in the Baltic Marine Environment).

The included variables for this study were conductivity, temperature and depth (CTD), bacterial production, humic substances, nutrient salts, dissolved organic carbon (DOC), total nitrogen and total phosphorous, collected at 5m depth. For Chlorophyll-a and primary production, a pooled fraction of the surface water (1-10m) was used. Procedures for the measurements are presented at HELCOM (HELCOM 2017). The data was accessed at SHARKdata (SHARKdata - Datasets, 2022). Differences in environmental concentration levels were estimated using linear models fitted within R, comparing the Bothnian Bay (north) and the Bothnian Sea (south).

Bacterial DNA sampling and extraction

At each sampling site, 75-500 ml water was gently filtered (≤20kPa) onto 0.2 µm filters (Pall Corporation sterilized filters, Supor ® 0.2 µm, 47 mm, S-pack white gridded). For samples from RA1 and RA2, <500ml was filtered due to limitations with the filtering of turbid water (100 ml and 250 ml, respectively). A total of 9 water samples were collected. The filters were folded using cleaned tweezers and placed in 2 ml Eppendorf tubes. The samples were stored in -80°C until the DNA extraction. Filters were thawed and placed into Powerwater bead beating tubes. The DNA was extracted using a DNeasy® PowerWater® kit (Qiagen, Hilden, Germany) according to a modified DNeasy PowerWater protocol, where the samples were treated with an additional heating step (horizontal water bath for 30 min, 65°C) and with a bead-beating step in each direction of 20 Hz, 3x3min with a Tissuelyser II (Qiagen, Hilden, Germany). The concentration of the DNA extracts from the stations ranged from 6-46 ng/µl. Two filter blanks were used as negative control during DNA extraction. The final DNA was frozen before subjected to PCR analysis. Sample preparation, thermal cycling and PCR product preparation were performed in separate rooms.

Illumina amplicon preparation and sequencing

For the 16S rRNA amplicon preparation, DNA was amplified and sequenced as previously described (Hägglund et al., 2018), part from the PCR purification kit used. In short, the DNA was amplified using the No. 5 Hot Mastermix 2.5x kit (5 PRIME, Qiagen, Hilden, Germany) with bacteria/archaeal primers 515F/806R specific for the hypervariable V4 region of the 16S rRNA gene (Caporaso et al., 2012). BSA has been shown to reduce PCR inhibition from humic substances (Opel et al., 2010; Sidstedt et al., 2020). To avoid inhibition, 8 µg of BSA was

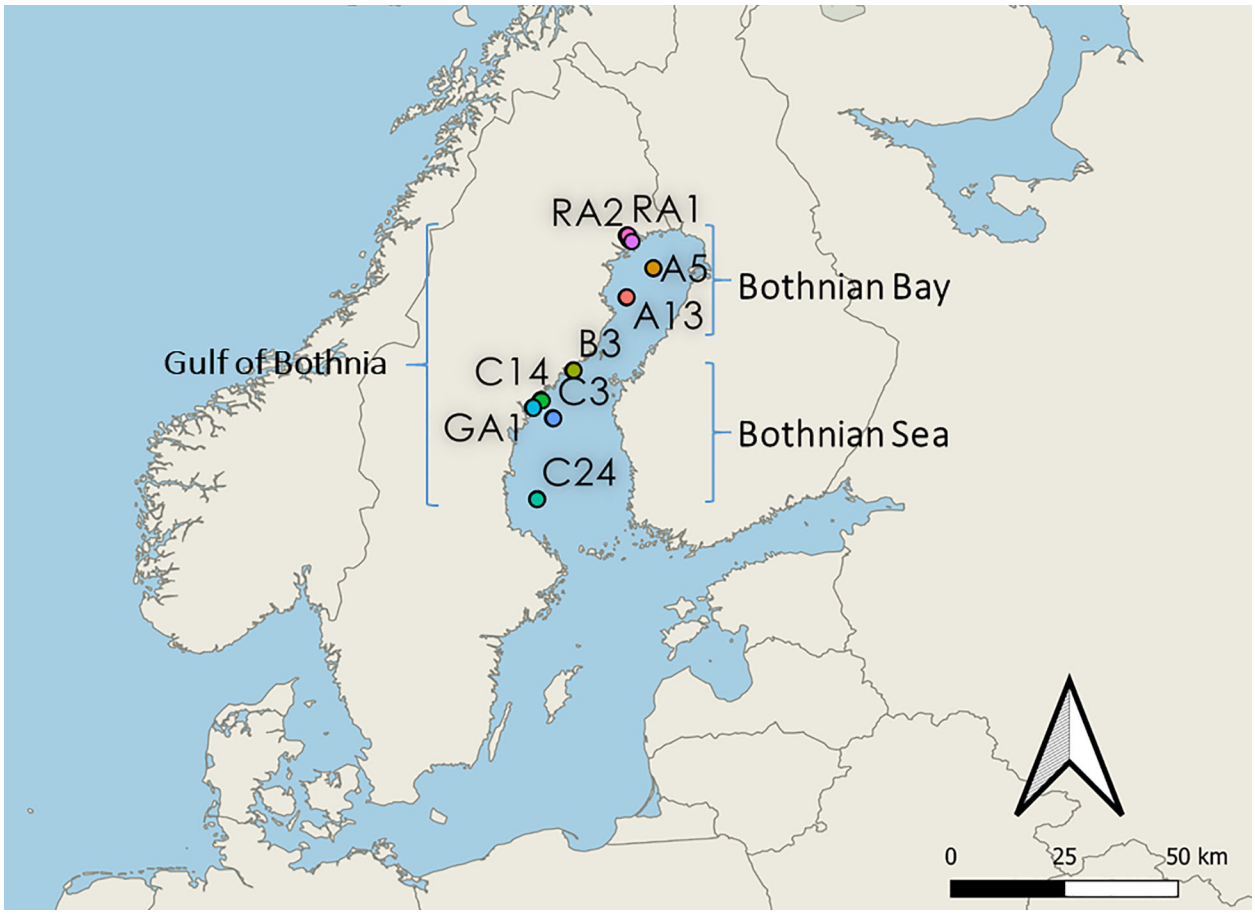

FIGURE 1
Map of the stations in the Gulf of Bothnia. Northern stations RA1, RA2, A5 and A13 are located in the Bothnian Bay basin (northern Gulf of Bothnia). Southern stations B3, C14, GA1, C3 and C24 are located in the Bothnian Sea basin (southern Gulf of Bothnia). Costal stations: RA1, RA2, B3, C14 and GA1. Offshore stations: A5, A13, C3 and C24.

therefore used for each reaction. The forward and reverse primers were modified to incorporate a 12 bp Golay error-correcting barcode that enables sample multiplexing (Caporaso et al., 2012). All samples were amplified in triplets and pooled after PCR amplification (94°C for 3 min; 35 cycles of 94°C for 45 s, 50°C for 1 min, 72°C for 1.5 min; 10 min rest to finish). For PCR, 3 template blank reactions were included by using nuclease free water instead of template.

For the 18S rRNA amplicon preparation, DNA was amplified using the No. 5 Hot Mastermix 2.5x kit (5 PRIME, Qiagen, Hilden, Germany) with eukaryotic primers V6F/V8R (V6F: 5'- AATTYGAHTCAACRCGGG, V8R: 5'-GACRGGCGGTGTGNACAA) specific for the hypervariable V6-V8 region of the 18S rRNA gene. These primers were designed by Eriksson et al. (2022), using higher degeneracies than earlier publications (Edgcomb et al., 2011; Hadziavdic et al., 2014). The benefits of this region is described in detail by Latz et al. (2022). All samples were amplified in triplets and pooled after PCR amplification (94°C for 3 min; 35 cycles of 94°C for 45 s, 57°C for 1 min, 72°C for 1.5 min; 10 min rest to finish).

The PCR product was run on a 1% agarose gel and the DNA concentration was estimated with a Qubit fluorometer (Invitrogen, Carlsbad, CA, United States). The amplicons were pooled at equimolar concentrations and purified with the QIAquick PCR purification kit (Qiagen, Hilden, Germany) following the supplier's instructions. The DNA concentration of the pooled amplicon product was measured with a Qubit fluorometer and adjusted to 2 nM. The library was denatured and diluted as described by Illumina (MiSeq System User Guide, Part # 15027617 Rev. C), before it was loaded onto a MiSeq cartridge (Illumina, San Diego, CA, United States) and sequenced using a 2x300 bp paired-end sequencing protocol (Hägglund et al., 2018).

Illumina quality control and raw data processing

Demultiplexing was done using deML (Renaud et al., 2015). The Quantitative Insights Into Microbial Ecology (QIIME2) pipeline, version 2019.1, was used for processing raw sequence data (Bolyen et al., 2019). Greengenes version 13.8 (McDonald et al., 2012) and PR2 version 4.12.0 (Guillou et al., 2012) databases were used for bacteria and eukaryote taxonomic assignment. Quality filtering was done using dada2 default parameter values. For the 16S rRNA sequence raw data processing, the reads were trimmed to 275 bp for the forward read and to 250 bp for the reverse read. For the 18S rRNA sequence raw data processing, the forward read were trimmed to 290 bp allowing a maximum of 5 expected errors per read. For 18S rRNA, the reverse read were not used due to low quality.

The Illumina 16S rRNA amplicon sequencing yielded 10549128 reads, 5211659 (49.4%) of which remained after the data was processed into amplicon sequence variants (ASVs). The data was filtered, denoised, merged and chimeras were removed, resulting in 4497 ASVs; the number of reads per sample ranged from 242562 to 562960. The Illumina 18S rRNA amplicon sequencing yielded 323690 reads, 63790 of which remained after the data was processed (19.7%, forward read only), resulting in 97 ASVs; the number of reads per sample ranged from 11815 to 2593.

Nanopore amplicon preparation and sequencing

To increase the taxonomic resolution and to compare with Illumina generated data, longer amplicons were also prepared and sequenced using the Oxford Nanopore Technology (ONT). In short for the 16S rRNA amplicons, the DNA was amplified using the Terra PCR Direct Polymerase Mix (Clontech, Mountain View, CA) with bacteria/archaeal primers with ONT overhang (S-D-Bact-0008-c-S-20 (27F): 5'-AG**R**GTT**Y**GAT**YM**TGGCTCAG-3', S-D-Bact-1492-a-A-22 (1492-R): 5'-TACGG**Y**TACCTTGTTACGACTT) (Lane, 1991) amplifying the V1-V9 region of the 16S rRNA gene. To avoid inhibition, 8 µg of BSA was used for each reaction. All samples were amplified in duplicates using 30 and 33 cycles (98°C for 2 min; 30 or 33 cycles of 98°C for 10 s, 57°C for 15 s, 68°C for 1.5 min; 68°C for 5 min rest to finish).

Single stranded DNA were removed from the PCR products using 2 µl ExoSAP-IT (Applied Biosystems, USA) to ~150 fmol/sample and each purified sample were then quantified using the Qubit 1×HS Assay Kit (Thermo Fisher Scientific).

The PCR Barcoding Expansion kit (EXP-PBC096) together with Ligation Sequencing Kit (SQK-LSK109) were used to sequence the 16S rRNA amplicons PCR. After the PCR-barcoding step in the protocol a purification of PCR products were performed using 0.5× of AMPure magnetic beads (Beckmann) following the manufacturer's protocol, thereafter, the purified PCR products were quantified using the Qubit1×HS Assay Kit (Thermo Fisher Scientific), and were pooled in equimolar amounts (200 ng/sample) before proceeding with the protocol. Some modifications were made within the protocol to adjust the volumes for the following sequencing on a MinION Mk1B instrument (ONT) with a Flongle Flow Cell (R9.4.1 chemistry, FLO-FLG001). The MinION instrument was ongoing for approximately 48 hr, or until no further reads could be collected.

Nanopore quality control and raw data processing

Basecalling and demultiplexing were performed using Guppy v6.0.1 (Oxford Nanopore Technologies). The data processing and read classification steps were implemented using the Snakemake workflow management system (Koster and Rahmann, 2012) together with Bioconda (Grüning et al., 2018). For visualization, nanoplot was used (version 1.29.1, https://github.com/wdecoster/NanoPlot/releases). Quality control was done using nanoq (version 0.8.6, https://github.com/esteinig/nanoq). The nanopore data was quality trimmed using Porechop (version 0.2.4, https://github.com/rrwick/porechop). Reads were then filtered by length (0-1 Mb) with Nanofilt (version 2.8.0, https://github.com/wdecoster/nanofilt). We assessed read statistics using NanoStat (version 1.4.0, https://github.com/wdecoster/nanostat) (De Coster et al., 2018). Overall, we obtained 834343 reads, with a mean read quality of 11.7. Otherwise, default settings were used. Taxonomic classification of the consensus sequences was done by kraken2 version 2.1.2 (Wood et al., 2019) and bracken version 2.6.2. (Lu et al., 2017) using a custom database and GTDB v207 (a list of included GCF files and taxonomy can be found in Supplementary Material 2). EMU (version 2.0) was used using the original database (Curry et al., 2022).

Target organisms

To include as many of the possible species of *Legionella*, the ASVs were selected at a higher taxonomic level for the Illumina dataset (at family level Legionellaceae). Phylogenies were estimated based on FastTree 2 (Price et al., 2010). For the Nanopore dataset, the genus *Legionella* was selected.

In order to compare the co-occurrence of *Legionella* and include heterotrophic and mixotrophic protists, other phylogenetic groups were excluded from the eukaryotic data set based on knowledge of feeding style (Olenina et al., 2006).

The supergroup Archaeplastida were excluded. For the supergroup Opisthokonta, Choanoflagellates were kept as they are filter feeders (Richter and Nitsche, 2017), while the Divison of Metazoa and Fungi were excluded. For the supergroup Stramenopiles, heterotrophic and mixotrophic Chrysophyceae was included since they have phagotrophic feeding style. From the Division Ochrophyta, class Chrysophyceae, Dictyochophyceae and unknown assignment (NA) were kept while non-relevant classes were excluded (Bolidophyceae, Bacillariophyta, MOCH-2, Picozoa, Phaeothamniophyceae, MOCH-5 Raphidophyceae, Synurophyceae, Eustigmatophyceae, Phaeophyceae, and Xanthophyceae). The sequence data was visualized using R package phyloseq (McMurdie and Holmes, 2013) and ggplot2 (Wickham, 2016).

Microscopic analysis

To obtain the protist biomass, microscopic counting and analysis of phytoplankton from the environmental monitoring program was included in this study. Phytoplankton were analyzed microscopically using the Utermöhl method according to the Helcom Combine manual (Utermöhl, 1958; Olenina et al., 2006; HELCOM, 2017). Autotrophic and mixotrophic phytoplankton were identified to the highest possible taxonomic level. Most heterotrophic protists were however not counted. The size of the cells was measured and their biovolume calculated (Olenina et al., 2006). Carbon biomass was calculated using biovolume to carbon biomass conversion factors (Menden-Deuer and Lessard, 2000). This microscopic method is constrained to nano- (2-20 µm) and micro scale (20-200 µm), and thus picoeukaryotes (<2 µm) are not included in the analyses.

Phylogenetic analysis of sequences assigned to *Legionella pneumophila*

To investigate the validity of the classification of the ASVs assigned to *Legionella pneumophila* by kraken, a multiple sequence alignment and phylogentic tree was created for the environmental ASVs and *Legionella* spp. The similarity of *Legionella* spp. 16S rRNA sequences was determined using the Basic Local Alignment Search Tool (BLASTN) at the National Centre for Biotechnological Information (NCBI) and EzTaxon-e server (Kim et al., 2012). The 16S rRNA of the closest hit was retrieved from the IMG-JGI database (Chen et al., 2021). The SBDI Sativa curated 16S GTDB database (version 5) (Lundin and Andersson, 2021) was downloaded and sequences annotated as *Legionella* were extracted to construct the phylogeny. The extracted sequences were concatenated with sequences selected in this study and the sequence of *Francisella tularensis* subsp. *tularensis* SCHU S4 was selected as the outgroup. All concatenated sequences were aligned using MAFFT (Katoh and Standley, 2013) and alignment was trimmed using ClipKIT with the smart-gap option (Steenwyk et al., 2020). The evolutionary relationship was inferred by the Maximum Likelihood method using RAxML-NG (Kozlov et al., 2019) with model GTR+G with Transfer Bootstrap Expectation (TBE) calculation (Lemoine et al., 2018) and visualized using Figtree (version 1.4.4, https://github.com/rambaut/figtree/).

Generalized linear latent variable model

A generalized linear latent variable model (GLLVM) was used to estimate the importance of the environmental factors on the occurrence on *Legionella* spp. To include as many of the possible species, the ASVs were selected at a higher taxonomic level (at family level Legionellaceae). For accurate frequency distribution of ASVs, the Illumina dataset was used for the model (a more error prone nanopore dataset lead to many unique ASVs). The GLLVM was fitted to the data using the R-package gllvm (Niku et al., 2019). Gaussian distribution function (i.e. identity link) for the responses was selected: environmental variables was included in the model as continuous predictors: humic substances, TDP and temperature. To avoid including highly correlated variables as predictors in the model, a pre-selection step was performed based on the PCA scoreplot (Figure 2), of the environmental variables (i.e. only one of a group of tightly clustered variables was selected, Figure 2). This resulted in a model with fewer parameters that, according to the theory of Occam's razor, is preferred since they are easier to fit and less prone to convergence issues compared to complex models. For example, temperature and bacterial production were highly correlated (correlation: 0.90), thus bacterial production was excluded from the statistical analyses. In the analysis, it is therefore difficult to disentangle the effect of these variables on the abundance of Legionellaceae. To identify how much of the ASV variation each variable could explain, a separate model was first made for each variable (Table 1). For the selection of the final model, a sensitivity analysis was performed, where the model with the best model of fit and lowest AIC and BIC scores was chosen, i.e. the most optimal trade-off between model fit and complexity (Table 1). Finally, based on the model selection results, humic substances, TDP and temperature were included in the model along with a factor for coastal habitat and a factor for filter volumes (to compensate for when less than 500 ml of water could be filtered).

The continuous variables were normalized so that the mean value and standard deviation were set to zero and one, respectively, for each included predictor. To improve convergence, jitter variance for starting values of latent variables were set to 0.5, and the number of initial runs were set to five. Since additional latent variables did not improve the model, one latent variable was selected to capture the residual

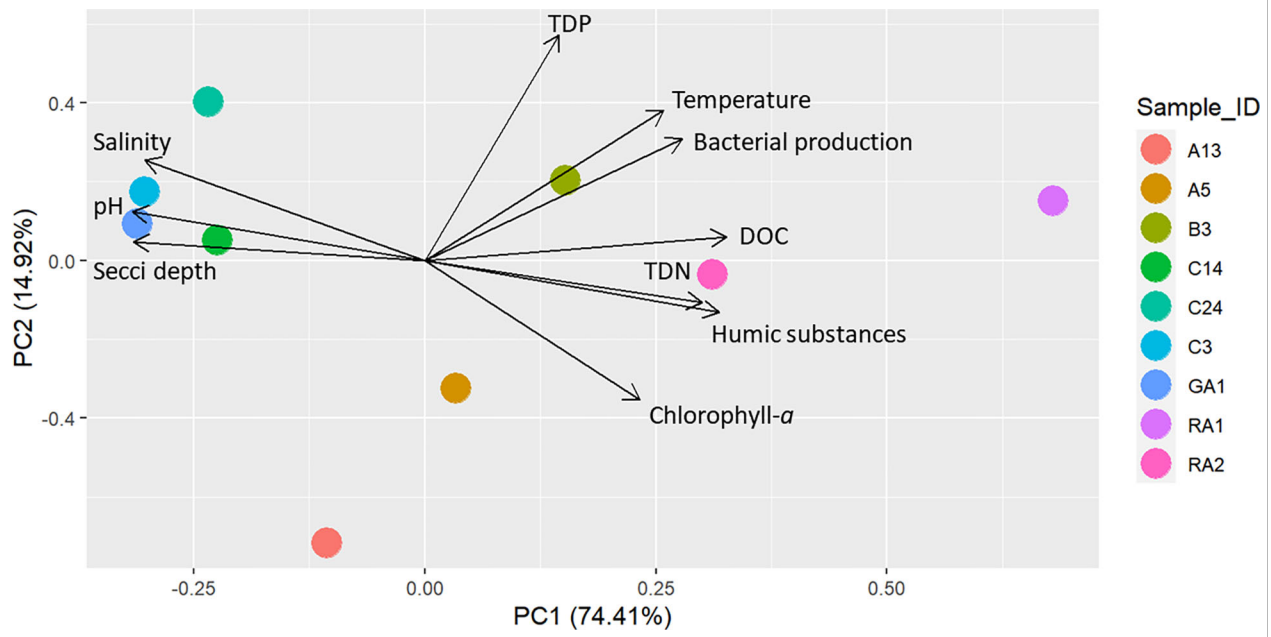

FIGURE 2
PCA of the spatial distribution of environmental variables at the stations. The prcomp function was used in the R package stats with default settings, using normalized and scaled data.

TABLE 1 Variation explained in the Amplicon Sequence Variant (ASV) communities for each environmental variable (according to the ratio of traces).

Predictors	AIC	BIC	Variation explained
Humics, TDP, Coast, Temperature, Filtervol	105	127	0.48
Humics, TDP, Coast, Temperature	210	229	0.48
Humics, TDP, Coast, Bacterial production, Filtervol	214	236	0.59
Humics, TDP, Salinitynorm, Temperature	271	290	0.55
Humics, TDP, Bacterial production, Filtervol	284	304	0.58
Humics, TDP, Salinitynorm, Bacterial production	299	318	0.59
Humics, TDP, Bacterial production	311	327	0.59
Coastal habitat	322	333	0.186
TDP	322	333	0.150
Chl-*a*	319	330	0.105
Bacterial production	302	313	0.104
Temperature	288	299	0.091
Salinity	299	310	0.059
Humics	303	314	0.030
No predictor	310	318	-

The full model includes to the following predictors: Humic substances, TDP, Coast, Temperature, Filter volume.

variation. Otherwise, default values of the GLLVMs function were used. The identified *Legionella* occurred at relatively low abundances in the sequence data, constituting of <1% of the entire bacterial community. To manage rare sequence variants and avoiding bias, and to reduce noise in the models, rare sequence variants that only occurred in one sample were excluded in the model.

Real time PCR - *Legionella* specific amplification

Primer and probe sequences for the *L. pneumophila*-specific *mip* gene target were used (Nazarian et al., 2008). The *L. pneumophila* specific TaqMan® probe had a 6-carboxy-fluorescein (FAM) as the fluorescent reporter on the 5′ end and a 6-carboxytetramethylrhodamine (TAMRA) as the quencher dye on the 3′ end of the probe (Nazarian et al., 2008). SsoAdvanced Universal Probes Supermix was used (Bio-Rad). To avoid inhibition, 8 µg of BSA was used for each reaction. For each reaction, 1 µL of template DNA was used for a total volume of 20 µL. Thermal cycling, fluorescent data collection, and data analysis were carried out on an iCycler (Bio-Rad Laboratories, Hercules, CA). The thermal cycling profile consisted of an initial incubation at 95°C for 3 min, followed by 45 cycles of 95°C for 5 s and 60°C for 30 s.

Primer targeting a 16S rRNA gene region specific for *Legionella* were used. For each reaction 1 µl of template DNA was used in a mix of SsoAdvanced Universal Probes Supermix (Bio-Rad), BSA and primer iQLeg1F 5'-CACTGTATGTCAAGGGTAGGTAAG-3' and iQLeg1R5'-TTAGTGGCGCAGCAAACGCGAT-3' (this study) for a total volume of 20 µL. The thermal cycling profile consisted of an initial incubation at 95°C for 3 min, followed by 40 cycles of 95°C for 5 s and 60°C for 5 s. Water samples spiked with *L. pneumophila* concentrations ranging from 10 to 10^5 colony forming units per mL were analyzed in duplicates to test the limit of detection and generate a standard curve for assessing target DNA concentrations. The standard curve was evaluated with the iQLeg1 primer pair. Positive control mixtures, using DNA from *L. pneumophila* and negative control mixtures without a template, were included in each PCR run.

Results

Environmental conditions

Principal component analysis (PCA) of the environmental variables show that the northern parts of the Gulf of Bothnia was characterized by high DOC and humic substances while the southern parts was clearer, had relatively higher salinity and higher pH (Figure 2). In addition, the spatial distribution of environmental variables was larger in the northern parts of the Gulf of Bothnia compared to the south. There were several significant environmental differences between the north and the south: for humic substances, pH, TDN, chlorophyll-*a*, and salinity (Tables S1, S2 and Supplementary Figure S1).

The concentration of humic substances were highest at station RA1, RA2, and B3 (Figure 3), where the bacterial

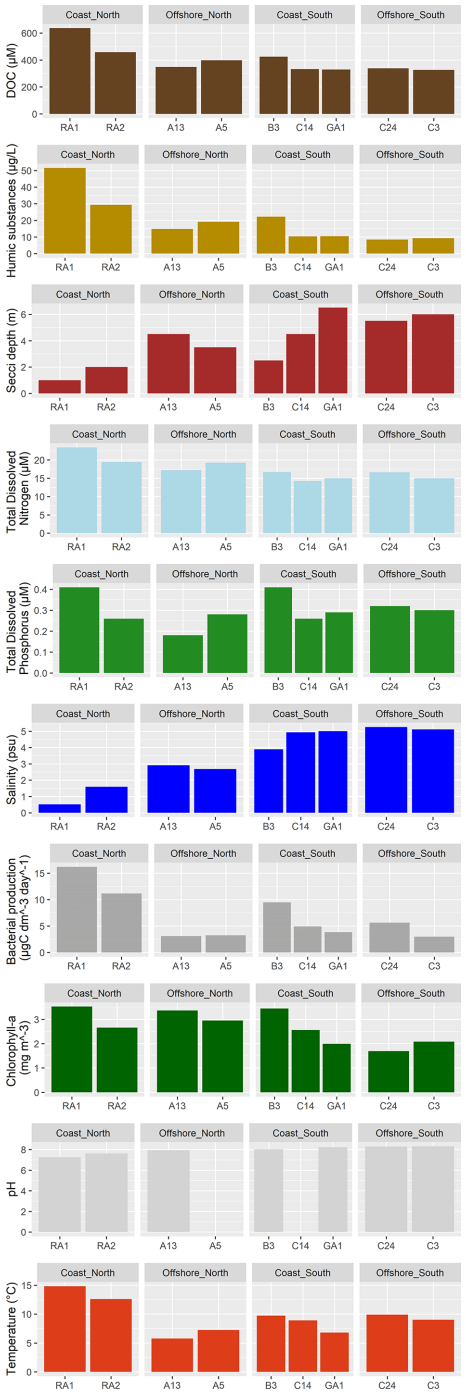

FIGURE 3
Environmental variables at the stations.

production were also high compared to the rest of the stations (>8 compared to <6 µgC/(dm3*day)). Nitrogen concentrations were higher in the north (mean north 19.21 +/- 2.65, mean south 15.22 +/- 1.00, p<0.05, Supplementary Figure S1; Tables S1, S2), especially at the coastal stations (RA1: 23.42 µM and RA2: 19.42 µM), followed by the offshore stations in the north (A13: 17.21 µM and A5: 19.28 µM). Phosphorus concentrations were especially low at station A13 (0.18 µM), while station RA1 and B3 had the highest concentrations of phosphorous (>0.4 µM). The temperature were the highest in the coastal northern RA1 and RA2 stations, followed by the southern C24, B3, C14 and C3 stations.

Occurrence of *Legionella* in the Gulf of Bothnia

Short amplicon (Illumina) sequence variants assigned to genus *Legionella* were only detected in the northern samples (RA1, RA2, A13, A5 and B3), (Supplementary Figure S2, *top*). A total of 2 amplicon sequence variants (ASVs) were identified that were assigned to genus *Legionella* (Supplementary Figure S3, top). Legionellaceae was however detected in all samples from north to south. In total, 24 ASVs were detected (Supplementary Figure S2, *bottom*), 14 occurred in more than one sample (Figure 4). Station A5 had the highest relative abundance of ~0.3%, followed by station A13 and B3 with relative abundances of about 0.25% (Supplementary Figure S2, *top*). The relative abundance in the remaining samples was <0.15%. The relative abundance at A5 was about four times higher compared to the stations with the lowest relative abundance (RA1, C24 and C3).

For the long amplicon sequencing (the nanopore dataset), species were assigned by classification algorithm emu, kraken and bracken. Some differences between the classifiers were observed. For the genus *Legionella*, 5 species were suggested by EMU (Figure 5, *top*), where *L. pneumophila* were the most frequently suggested species (sample A13, A5, B3, GA1 and RA2). According to kraken, 16 species were suggested (Figure 5, *middle*), where *L. waltersii* were the most frequently suggested species (sample A13, A5, B3 and RA2). Bracken assigned 20 species (Figure 5, *bottom*), where *L. pneumophila* were one of the most frequently suggested species (sample A5, B3, C14 and GA1). Correlations between the two 16S rRNA datasets indicated that an assigned species often correlated strongly with several Illumina ASVs (Figure 6). For the turbid samples RA1, Legionellaceae was not detected by the classifier EMU. Also, the classifier did not detect *Legionella* in sample C3 and C24. The relative abundance of ASVs assigned to *Legionella* species was highest at B3 (EMU: ~0.35% of total reads, kraken: ~100 reads out of 48468 and bracken: 0.45% of total reads), about 4-9 times higher relative abundance, according to the different classifiers, compared to the stations with the lowest relative abundance (RA1, C24 and C3). This is supported by qPCR analysis performed targeting a *Legionella* specific region of the 16S rRNA. Occurrence of *Legionella* specific DNA was confirmed for all samples and ranged from 2 to 40 bacteria/

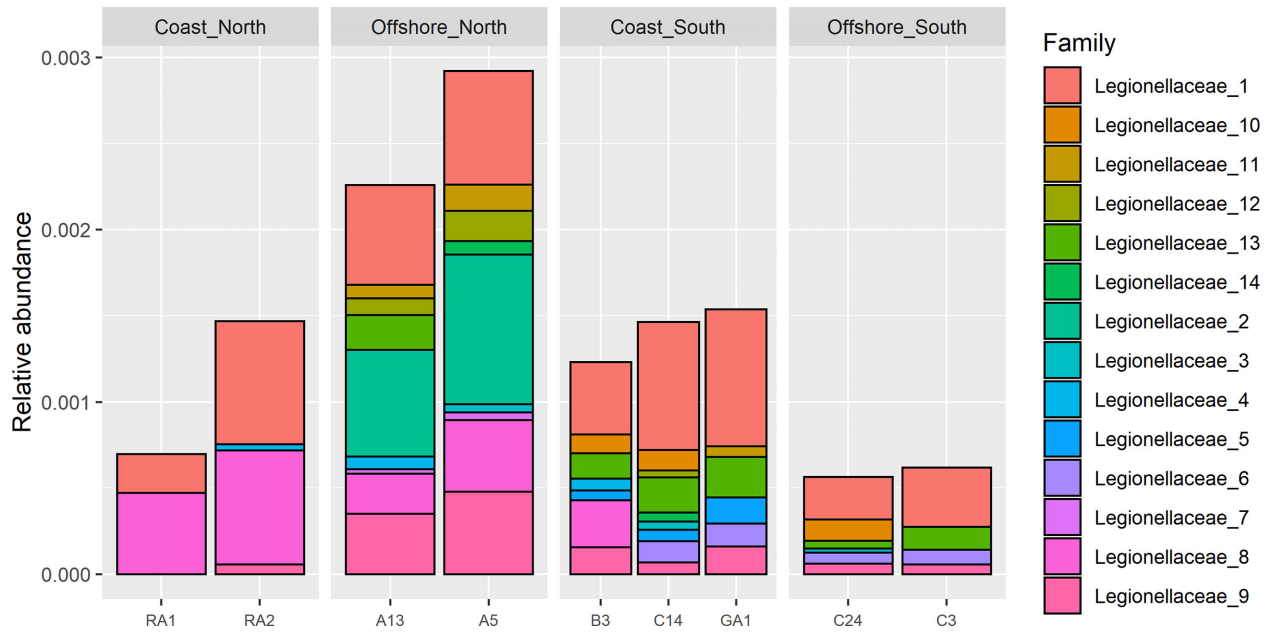

FIGURE 4
Filtered Illumina Legionellaceae ASVs, detected in more than one sample (ASVs used in GLLVM).

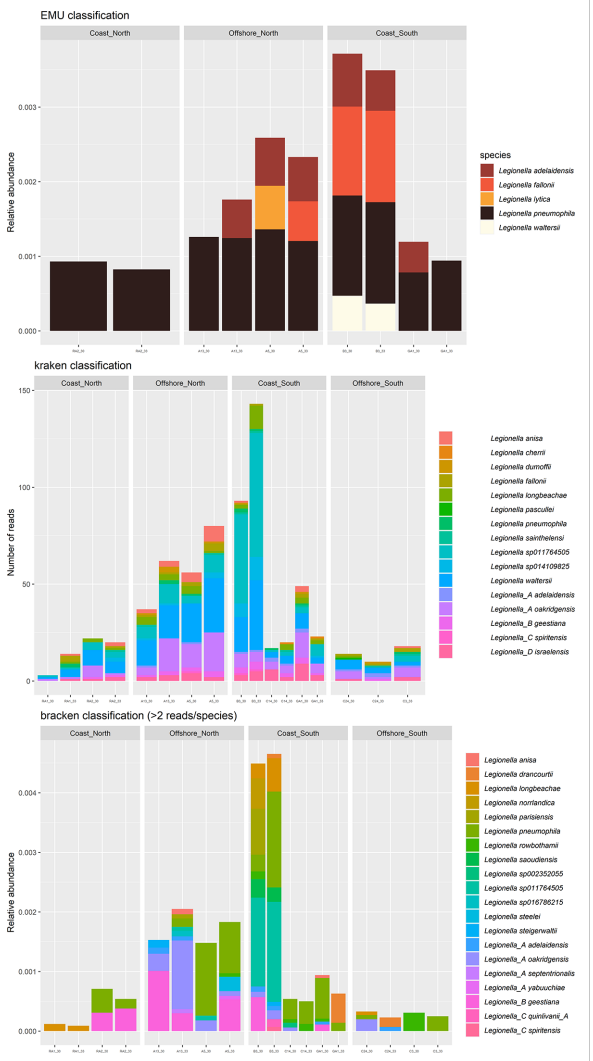

FIGURE 5
Relative abundance of nanopore Amplicon Sequence Variant reads (ASV) of genera *Legionella* at each station, assigned by classification algorithm EMU (top), kraken (middle) and bracken (bottom). Each sample was sequenced twice, after 30 and 33 PCR cycles.

mL sea water (low versus high abundance). The A5, B3, RA1 and RA2 samples all had *Legionella* corresponding to >20 bacteria/mL sea water, while samples from C14, C24, C3 and GA1 all had *Legionella* corresponding to 2 bacteria/mL sea water (Supplementary Figure S4).

The ASVs that were assigned to *L. pneumophila* by kraken was aligned along with other 16S rRNA sequences for other species of *Legionella* (Figure 7). Phylogenetic analysis reveals that most sequences are most similar to *L. sp011764505* (deposited in NCBI as *L. antarctica*). *Legionella* sp. *GA1-1* is closest related to *Legionella A oakridgensis* while *Legionella* sp. A5-1 and *Legionella* sp. A5-2 forms a novel branch in the tree without previous characterized species representative. None of the sequences generated in this study were most similar to *L. pneumophila*. Also, the *Legionella* specific amplification of the *mip* gene were negative for all samples (data not shown), indicating that the *Legionella* species detected in the Gulf of Bothnia samples does not have this exact *mip* variant that is associated with virulence, and suggest that the detected species aren't the virulent *L. pneumophila*.

Potential hosts: Phytoplankton and phagotrophic protozoa

The estimated biomass of phagotrophic protozoa using microscopy are presented in Supplementary Figure S5. Station B3 had the largest phytoplankton biomass, over 70 µgC/L (70000 µgC/m3), while station A13, GA1, C3 and C24 had a biomass around 40 µgC/L. Station RA1 and RA2 had the lowest biomass, around 5 µgC/L (station A5 and C14 were not counted). Diatoms were abundant at the A13, B3 and RA1 stations. For the phagotrophic protists, the biomass were higher in the south, where the ciliate *Mesodinium rubrum* was abundant.

For the genetic method, amplification of the 18S rRNA gene (region V6-V8) indicate that the ciliate *Mesodinium rubrum* was most relatively abundant compared to other phagotrophic protozoans, except in the RA-stations. At the A-stations and at station B3, *Woloszynskia halophila* was detected, an organism that had positive co-occurrence with several *Legionella* ASVs (Supplementary Figures S6, S7). Unlike the 18S V9 region, this longer 18S V6-V8 region were able to assign the majority of the taxa to species level (>70%), which enabled investigation of specific species co-occurrence (Supplementary Figure S7). In general, the co-occurrence varied between *Legionella* ASVs and phagotrophic protozoa. *Legionella* ASVs number 5, 6 and 14 had positive co-occurrence with *Mesodinium, Protaspa lineage, Botuliforma*, and *Telonema*.

GLLVMs analysis identify potential drivers for the occurrence of *Legionella* spp.

To identify drivers for the occurrence of *Legionella* spp. we corrected for sampling location while taking dependencies among taxa into account (Figures 2, 6). Included in the model were ASVs that occurred in more than one sample, 14 in total (Figure 4). Significant parameter estimates for each organismal group show that humic substances had a positive effect on the ASV abundance for 6 of the Legionellaceae ASVs (Figure 8). Humic substances were the predictor with the most significant positive associations for *Legionella* ASVs.

The contribution of each independent variable in the model is found in Table 1, where temperature explain 9% of the total variation of the Legionellaceae ASVs. TDP explains 15%, coastal

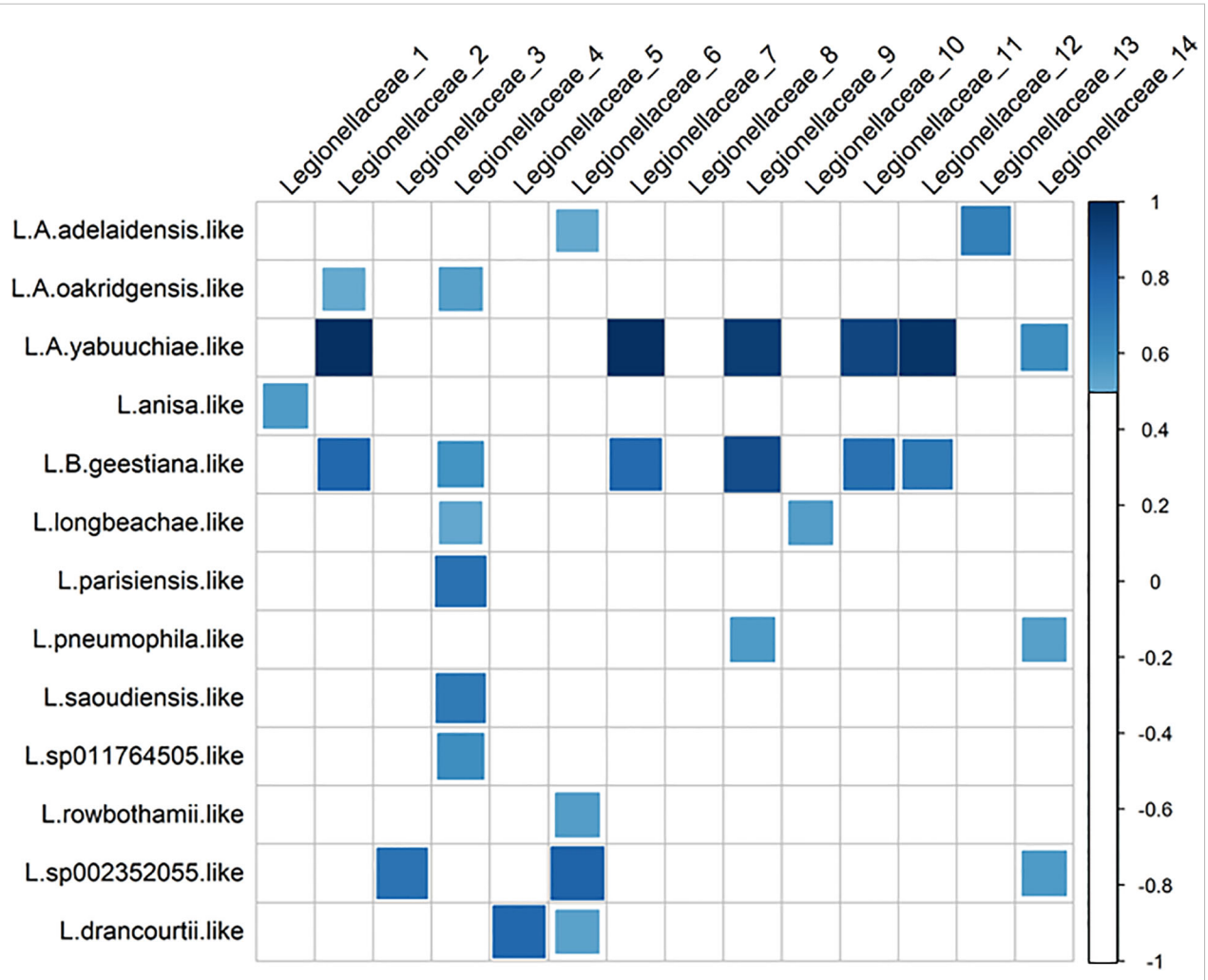

FIGURE 6
Correlations (≥0.5) between ASVs in the family Legionellaceae (Illumina) and species classification in the *Legionella* genus (Nanopore, bracken classification).

habitat explain 19%, bacterial production 10%, chlorophyll-*a* explains 11% of the total variation, salinity explain 6% and humic substances explain 3%. The full model explains 48%, including the predictors Humic substances, TDP, Coast, Temperature and Filtered volume. Salinity were not included in the model since it had a strong negative correlation to humic substances (correlation: -0.94). One ASVs abundance were negatively influenced by TDP and one were positively influenced. Four ASVs abundances were negatively influenced by temperature. Five ASV abundances are significant for a coastal habitat, some ASVs were negatively influenced by reduced filtered volumes (when < 500 ml water were filtered, Supplementary Table S3), only one ASV were significantly negatively impacted. Overall, three potential niches were identified. *Legionella* ASV number 4 and 13 co-occurred. *Legionella* ASV number 5, 6, 8 and 10 were not strongly co-occurring with other taxa. The remaining *Legionella* ASVs were strongly positively correlated (Supplementary Figure S8). This remaining subset of *Legionella* ASVs were positively correlated with humic substances (Figure 8, Supplementary Table S4).

Discussion

Data on occurrence and persistence of potentially pathogenic bacteria like *Legionella* spp. in natural waters are missing, which hinders assessment of the risk of exposure. In this study we identified humic substances to be a potential environmental driver for occurrence of *Legionella* species ASVs (6 out of 14) in the northern Baltic Sea, where the ASVs were more relatively abundant in the humic northern waters. Here, we for the first time present data of the species biodiversity

of *Legionella* from long 16S rRNA sequencing using the Nanopore technologies. This rising technology unravelled opportunities and challenges for describing the occurrence of this public health relevant genus in natural waters.

Geographic variation of *Legionella* species sequences in the Gulf of Bothnia

A previous study identified *Legionella* in a 10 km coastal area in the Bothnian Sea during June 2018 using short 16S rRNA Illumina sequencing (Eriksson et al., 2022). Here, we identify *Legionella* both using standard short 16S rRNA Illumina sequencing and by using longer Nanopore sequencing. With Illumina, *Legionella* was mainly detected in the Bothnian Bay where *Legionella* was confirmed at all stations. In addition to detection in the Bothnian Bay, *Legionella* was detected at station B3, confirming the occurrence in this region. Interestingly, at B3 the relative abundance of *Legionella* ASVs was the highest of all stations, constituting ~0.15% of the reads (Supplementary Figure S2, **top**). Regarding the ASVs of the family Legionellaceae, these were detected in all samples (Supplementary Figure S2, **bottom**). Some specific ASVs were mainly detected in the offshore in the north (e.g. ASV no. 14), while others were mainly detected in the southern samples (e.g. ASV no. 6), indicating a spatial variation of *Legionella* spp. in the Gulf of Bothnia.

Previous studies have suggested temperature as a driver for *Legionellales* in freshwater (Graells et al., 2018). Generally, for the Gulf of Bothnia, the south-north differences in temperature and the salinity gradient makes the Bothnian Bay more similar to freshwater. A study of bacteria (16S rRNA amplicon sequences) along the salinity gradient of the Baltic Sea argued that the Bothnian Bay is an easier habitat to exploit by species adapted to freshwater compared to more saline water (Herlemann et al., 2011), such as *Legionella*. This is consistent with our finding of the highest relative abundance of *Legionella* spp. at the northern stations where the salinity was lower. However, in our model, the relative abundance of only one ASV (no. 5) were significantly correlated to higher temperature. Instead, the occurrence of several ASVs were significantly correlated to lower temperatures (Figure 8). Temperature was thus not found to be a driver for *Legionella* spp. in this study.

The microbial food web link: humic substances, iron and *Legionella*

In contrast to our expectation, predators (protozoa) were more abundant in the south of the Gulf of Bothnia (Supplementary Figure S5), where there were less humic substances. It is, however, notable that the total phytoplankton biomass was highest at station B3, where the relative abundance of *Legionella* spp. were also the highest among the samples (Figure 5, Supplementary Figure S4). Most mixotrophic algae can consume bacteria through phagocytosis (Stoecker et al., 2017). Non-phagotrophic algae such as diatoms have other endocytic mechanisms for ingesting nutrients like iron (Sutak et al., 2020). Interestingly, by taking advantage of the process of endocytosis, it has been shown that bacteria can enter eukaryotic cells (Bonazzi and Cossart, 2006). Since *Legionella* mainly is an intracellular organism, this observation opens for the hypothesis that *Legionella* also can use phytoplankton as host. However, the standard monitoring of the Baltic Sea does not include counting of strictly heterotrophic protists, which is limiting the assessment of potential hosts. DOC and predation pressure from unicellular eukaryotes, such as amoebas, together drive the evolution of bacteria. If the amounts of DOC and predators increase, this bacterial resilience to stress may also rise (Fang

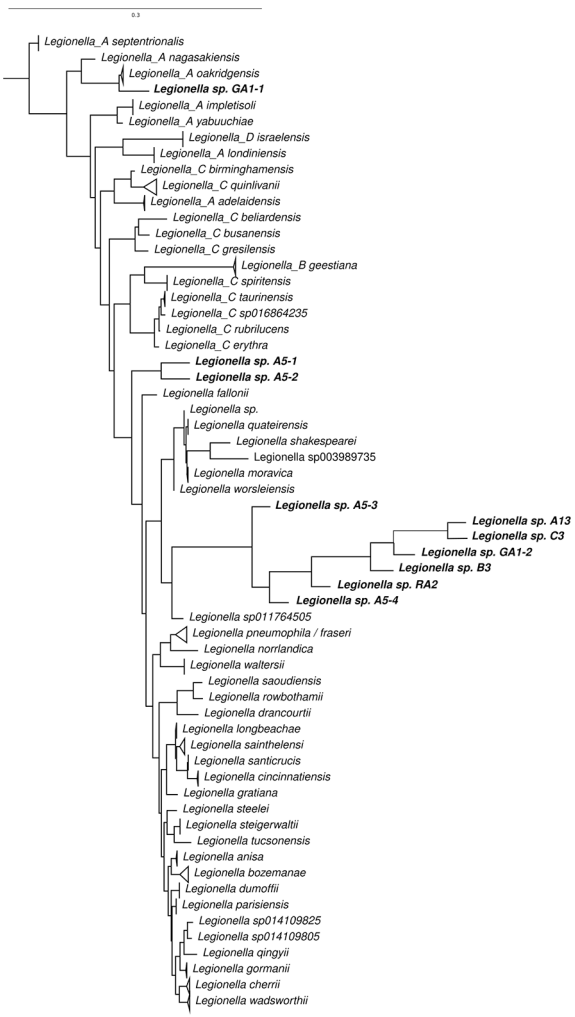

FIGURE 7
Phylogenetic relationship of 16S rRNA gene sequences of species of *Legionella* and ASVs assigned to *L. pneumophila* by kraken.

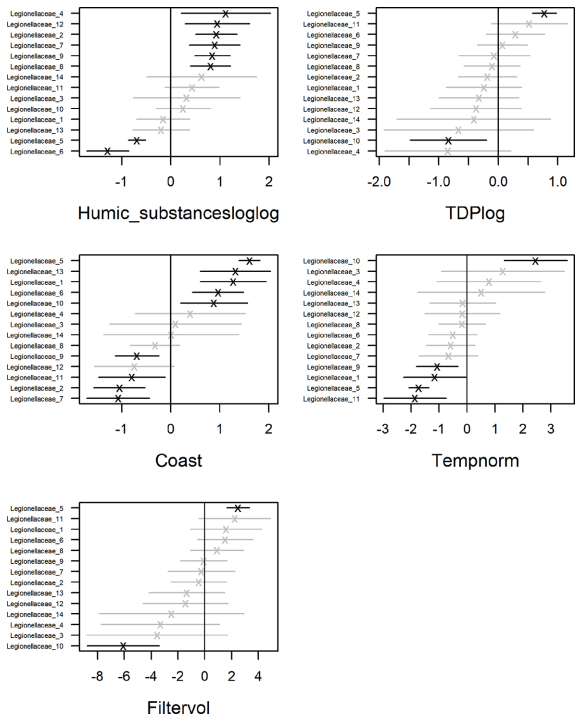

FIGURE 8
Coefficient estimates by GLLVM analysis showing average effect and uncertainty (as 95% CI) for each organismal group.

et al., 2022). Therefore, it can be argued that bacteria that already are resistant to predation might have an ecological advantage.

Another factor that may impact the distribution of *Legionella* is availability of iron, which has shown to play an important role for the growth, survival and virulence of *L. pneumophila*. Several studies showed that the growth of this bacterium depends on the presence of iron (Cianciotto, 2015; Portier et al., 2016). Several intracellular bacteria has mechanisms to carefully take up iron without killing their host (Ratledge and Dover, 2000; Wandersman and Delepelaire, 2004; Leon-Sicairos et al., 2015; Yan et al., 2021). Iron has been described as the most valuable metal from a metabolic perspective, since a multitude of enzymes and co-factor require this vital compound (Klebba et al., 2021). Interestingly, there is a correlation between iron sequestration and pathogenicity, and many gram-negative bacterial pathogens have elaborate pathways to acquire iron (Klebba et al., 2021).

Importantly, iron is bound to humic substances and is transported into the ocean together along with the humic substances, providing iron beyond estuaries, especially during spring when the water flow is higher (Herzog et al., 2020). When the pH is lower, iron can be released. In soils, iron has shown to bind humic acids at pH 7 twice as much compared to at pH 5 (Boguta et al., 2019). Humic substances can thus control the biological availability of iron, also in seawater (Laglera and Van Den Berg, 2009). Several studies have investigated the role of humic substances complexed with iron in seawater (Yang et al., 2017; Whitby et al., 2020), but humic substances potential role in the uptake of iron by *Legionella* in marginal seas is unknown. However, a new iron-regulated gene (IroT/MavN) involved in ferrous iron transport has been identified in *Legionella* (Cianciotto, 2015; Portier et al., 2015). In a climate change perspective, a further understanding of the microbial degradation of humic substances may be of great importance, especially in humic-rich waters like boreal marginal seas.

Along the gradients of the Gulf of Bothnia, the pH ranged from 7.25 (RA1) to 8.31 (C3). Station RA1 is located near a river mouth (Råne river), and is characterized as an estuarine area (Soerensen et al., 2017). Station B3 is also situated 5 km from a river mouth (Öre river). Of the Legionellaceae, several ASV abundances (6 out of 14) were positively linked to humic substances, perhaps as an indirect effect of iron availability. Since climate change most likely will cause increased precipitation in this region of northern Europe (Meier et al., 2022), freshwater inflows of iron-containing terrestrial humic substances can be expected to rise in the northern Baltic Sea. Potentially, this may lead to promotion of iron-demanding *Legionella* spp.

Standard short 16S rRNA Illumina sequencing: Potential misleading conclusions regarding the diverse genus *Legionella*

The study of particular bacterial species in their natural habitat is challenging due to the limitations with the standard methods used to study these organisms. Therefore, bacteria can most often only be resolved to genus level by using the standard short Illumina amplicon sequencing. For *Legionella*, only two ASVs were assigned to the genus, all detected in the northern stations (RA1, RA2, A13, A5 and B3, Supplementary Figure S2). These two ASVs are not representative of the whole family tree of Legionellaceae (Supplementary Figure S3). Thus, potential misleading conclusions could easily be drawn when studying this genus based solely on short amplicon Illumina data, since the majority of the diversity is not considered.

To complement the standard Illumina sequencing, we used Nanopore sequencing. The advancement of the Nanopore sequencing technologies are providing new possibilities to sequence longer amplicons (Benítez-Páez et al., 2016; Heikema et al., 2020; Rodríguez-Pérez et al., 2021), which has the potential to classify the bacteria to species level (Johnson et al., 2019; Urban et al., 2021). We performed full-length nanopore sequencing with the aim to resolve the genus of *Legionella* to species level. To verify the robustness of the technique, we sequenced each sample twice, with 30 and 33 PCR cycles. We used the software EMU that is specifically developed for erogenous ONT sequencing data, since it has been suggested to outcompete other software considering specificity (Curry et al., 2022). In addition, we used classifier

kraken and bracken for comparison. Nanopore sequencing resulted in comparable relative abundances to the Illumina dataset for the family Legionellaceae. It therefore seems that the Nanopore sequencing results suggested species for all of the Legionellaceae reads detected using Illumina sequencing (Figure 5, Supplementary Figure S2).

Error prone Nanopore sequencing remain a challenge for accurate species classification of environmental strains

Nanopore sequencing is a promising technique for bacterial species classification. However, current limitations on base accuracy together with limitations in database completeness, limits classification specificity, especially when working on environmental samples with many uncharacterized environmental species (Latorre-Pérez et al., 2021). Therefore, caution is needed when interpreting read classification data based on ONT sequencing. Comparisons between short and long read 16S rRNA classification has shown that there are different biases in the two methods which complicates direct comparison of the results. A question that arise is how to determine if a particular classified ASV from a Nanopore sequencing run belong to an already sequenced species, or if it comes from a non-sequenced relative? For example, Legionellaceae is a diverse family and the majority of environmental variants remain uncultured (Graells et al., 2018). EMU classified all ASVs to species; the level of uncertainty allowed for classification of taxa in environmental samples could therefore be a target for future optimization.

Classification-bias towards virulent *L. pneumophila*

In addition to the more error prone sequences, the pathogenic strain *L. pneumophila* is well studied and hence overrepresented in databases. Even though *L. pneumophila* is the most virulent among the Legionellaceae, more than 20 other species of *Legionella* have shown to cause disease. The remaining strains are considered to be non-pathogens until the opposite has been proven (Legionella Species - Special Pathogens Laboratory, 2020). Thus, future efforts in the sequencing of isolates from the field and patients could aid in reducing this bias.

The Gulf of Bothnia may harbor understudied species of pathogenic *Legionella* spp.

For non-*L. pneumophila* strains, cases of disease are estimated to be underrepresented due to the standard testing methods to confirm Legionnaires' disease and Pontiac fever (Chambers et al., 2021), and alternative methods for detection is debated, often including specific gene amplification to facilitate time consuming culture based methods (Vittal et al., 2022).

By combining short and long 16S rRNA amplicon sequencing to map the distribution of *Legionella* spp. in the Gulf of Bothnia, this study highlights that there is an environmental niche for several species of *Legionella* in the Gulf of Bothnia. This study also suggest that these public health relevant bacteria that previously has shown the capability to cause disease such as *L. oakridgensis, L. parisiensis, L. longbeachae, L. cherrii* and *L. anisa* (Bibb et al., 1981; Tang et al., 1985; Bornstein et al., 1989; Fang et al., 1989; Lo Presti et al., 1997) can be part of the natural diversity. It is known that pathogenic strains live in natural aquatic environments, and that they are being selected in manmade water systems such as drinking water pipes and cooling towers (Lesnik et al., 2015; Tsao et al., 2019). Therefore, these bacteria could be of importance considering climate change and future water management. Future field studies should thus focus on how species of *Legionella* are influenced by natural gradients such as humic substances, iron, temperature and salinity over time. Genus specific targets such as the non-*Legionella pneumophila* target rpoB gene (Pascale et al., 2021) may also be useful to further resolve the pathogenic and non-pathogenic species of *Legionella* spp. In addition, experimental studies could provide direct evidence of environmental drivers for the occurrence of *Legionella*, preferably separating the effect of humic substances and salinity.

Conclusion and outlook

In conclusion, this study highlights that there is an environmental niche for the occurrence of several species of *Legionella* in the Gulf of Bothnia, and that pathogenic bacteria can be part of the natural diversity. Partial 16S rRNA sequencing did not capture the diversity within *Legionella* while the third generation long Nanopore 16S rRNA sequencing was shown promising for bacterial species classification, even though harmonization between classification methods is still needed. Importantly, the Nanopore classification methods had a bias toward the well-studied *L. pneumophila*, limiting classification of environmental strains. Thus, sequencing environmental isolates could improve the classification using this powerful and rising sequencing method. These bacteria are facultative intracellular, can be pathogenic and have anti-predator strategies. Therefore, knowledge regarding potential hosts for these bacteria such as phagotrophic protozoa could be crucial, since they might provide a niche for emerging pathogens. Currently, taxonomic information of bacteria and heterotrophic protozoa is not included in the environmental monitoring. Here, we

demonstrate the significance of sequencing techniques to map public health relevant bacteria such as *Legionella* spp. in the environment, using a method that can be used to study all bacteria. By applying generalized linear latent variable models (GLLVMs) we show that the occurrence of opportunistic *Legionella* spp. were linked to high concentrations of humic substances and low salinity. Considering climate change projections in this area, with increased humification and freshwater inflow, this bacterial niche might become more widespread in the future Baltic Sea. Environmental monitoring including sequencing of bacteria and protozoa could thus help identify climate change induced ecosystem imbalances and to appropriately respond to emerging diseases.

Data availability statement

The original contributions presented in the study are publicly available. This data can be found here: NCBI, PRJNA901258.

Author contributions

KE and AA conceived the study. AA organized the data collection and KE processed the samples for sequencing. KE, JA and DS processed the data after sequencing. KE and JA conducted the statistical data analyses. KR and AS performed the phylogenetic analysis. AS and LK developed the Nanopore 16S rRNA amplicon workflow. JT organized the qPCR. KE wrote the manuscript together with all co-authors. All authors contributed to the article and approved the submitted version.

Funding

This project was financed by the Industrial doctoral school at Umeå University, the marine research environment EcoChange (FORMAS) and the Swedish Ministry of Defence (grant A4001).

Acknowledgments

We thank Umeå Marine Sciences Centre for chemical analyses, Ingrid Dacklin and Emelie Näslund Salomonsson for help with the sequencing. We thank Stina Bäckman and Mattias Jonsson for the help with the qPCR. Umeå Marine Science Centre is acknowledged for providing data on physicochemical variables and phytoplankton microscopy, *via* the Swedish National Marine Monitoring Program.

Conflict of interest

The authors declare that the research was conducted in the absence of any commercial or financial relationships that could be construed as a potential conflict of interest.

Publisher's note

All claims expressed in this article are solely those of the authors and do not necessarily represent those of their affiliated organizations, or those of the publisher, the editors and the reviewers. Any product that may be evaluated in this article, or claim that may be made by its manufacturer, is not guaranteed or endorsed by the publisher.

Supplementary material

The Supplementary Material for this article can be found online at: https://www.frontiersin.org/articles/10.3389/fmars.2022.1070341/full#supplementary-material

Supplementary data related to this article can be accessed at the Short Read Archive (https://www.ncbi.nlm.nih.gov/sra), project accession: PRJNA, ID: 901258. Supplementary Material 1 contains all associations between ASVs and predictors included in the GLLVM. ASV tables are provided in Supplementary Material 2 and 3.

References

Amaro, F., and Martín-González, A. (2021). Microbial warfare in the wild–the impact of protists on the evolution and virulence of bacterial pathogens. *Int. Microbiol.* 24, 559–571. doi: 10.1007/s10123-021-00192-y

Andersson, A., Hajdu, S., Haecky, P., Kuparinen, J., and Wikner, J. (1996). Succession and growth limitation of phytoplankton in the gulf of bothnia (Baltic Sea). *Mar. Biol.* 126, 791–801. doi: 10.1007/BF00351346

Andersson, A., Meier, H. E. M., Ripszam, M., Rowe, O., Wikner, J., Haglund, P., et al. (2015). Projected future climate change and Baltic Sea ecosystem management. *Ambio* 44, 345–356. doi: 10.1007/s13280-015-0654-8

Ballard, A. L., Fry, N. K., Chan, L., Surman, S. B., Lee, J. V., Harrison, T. G., et al. (2000). Detection of legionella pneumophila using a real-time PCR hybridization assay. *J. Clin. Microbiol.* 38, 4215–4218. doi: 10.1128/JCM.38.11.4215-4218.2000

Bandara, T., Brugel, S., Andersson, A., Chun, D., and Lau, P. (2022). Seawater browning alters community composition and reduces nutritional quality of plankton in a subarctic marine ecosystem. Canadian Journal of Fisheries and Aquatic Sciences 79 1–11. doi: 10.1139/CJFAS-2021-0118

Benítez-Páez, A., Portune, K. J., and Sanz, Y. (2016). Species-level resolution of 16S rRNA gene amplicons sequenced through the MinION^{TM} portable nanopore sequencer. *Gigascience* 5, 4. doi: 10.1186/S13742-016-0111-Z/2720968

Bibb, W. F., Sorg, R. J., Thomason, B. M., Hicklin, M. D., Steigerwalt, A. G., Brenner, D. J., et al. (1981). Recognition of a second serogroup of legionella

longbeachae. *J. Clin. Microbiol.* 14, 674–677. doi: 10.1128/JCM.14.6.674-677.1981

Blenckner, T., Österblom, H., Larsson, P., Andersson, A., and Elmgren, R. (2015). Baltic Sea Ecosystem-based management under climate change: Synthesis and future challenges. *Ambio* 44, 507–515. doi: 10.1007/s13280-015-0661-9

Boamah, D. K., Zhou, G., Ensminger, A. W., and O'Connor, T. J. (2017). From many hosts, one accidental pathogen: The diverse protozoan hosts of legionella. *Front. Cell. Infect. Microbiol.* 7. doi: 10.3389/fcimb.2017.00477

Boguta, P., D'Orazio, V., Senesi, N., Sokołowska, Z., and Szewczuk-Karpisz, K. (2019). Insight into the interaction mechanism of iron ions with soil humic acids. the effect of the pH and chemical properties of humic acids. *J. Environ. Manage.* 245, 367–374. doi: 10.1016/j.jenvman.2019.05.098

Bolyen, E., Rideout, J. R., Dillon, M. R., Bokulich, N. A., Abnet, C. C., Al-Ghalith, G. A., et al. (2019). Reproducible, interactive, scalable and extensible microbiome data science using QIIME 2. *Nat. Biotechnol.* 37, 852–857. doi: 10.1038/s41587-019-0209-9

Bonazzi, M., and Cossart, P. (2006). Bacterial entry into cells: A role for the endocytic machinery. *FEBS Lett.* 580, 2962–2967. doi: 10.1016/j.febslet.2006.04.010

Bornstein, N., Mercatello, A., Marmet, D., Surgot, M., Deveaux, Y., and Fleurette, J. (1989). Pleural infection caused by legionella anisa. *J. Clin. Microbiol.* 27, 2100–2101. doi: 10.1128/JCM.27.9.2100-2101.1989

Brigmon, R. L., Turick, C. E., Knox, A. S., and Burckhalter, C. E. (2020). The impact of storms on legionella pneumophila in cooling tower water, implications for human health. *Front. Microbiol.* 11. doi: 10.3389/fmicb.2020.543589

Caporaso, J. G., Lauber, C. L., Walters, W. A., Berg-Lyons, D., Huntley, J., Fierer, N., et al. (2012). Ultra-high-throughput microbial community analysis on the illumina HiSeq and MiSeq platforms. *ISME. J.* 6, 1621–1624. doi: 10.1038/ismej.2012.8

Carvalho, F. R. S., Vazoller, R. F., Foronda, A. S., and Pellizari, V. H. (2007). Phylogenetic study of legionella species in pristine and polluted aquatic samples from a tropical Atlantic forest ecosystem. *Curr. Microbiol.* 55, 288–293. doi: 10.1007/s00284-006-0589-1

Chambers, S. T., Slow, S., Scott-Thomas, A., and Murdoch, D. R. (2021). Legionellosis caused by non-legionella pneumophila species, with a focus on legionella longbeachae. *Microorganisms* 9, 291. doi: 10.3390/microorganisms9020291

Chen, I.-M. A., Chu, K., Palaniappan, K., Ratner, A., Huang, J., Huntemann, M., et al. (2021). The IMG/M data management and analysis system v.6.0: new tools and advanced capabilities. *Nucleic Acids Res.* 49, D751–D763. doi: 10.1093/nar/gkaa939

Cianciotto, N. P. (2015). An update on iron acquisition by legionella pneumophila: new pathways for siderophore uptake and ferric iron reduction. *Future Microbiol.* 10, 841–851. doi: 10.2217/FMB.15.21

Collins, S., Jorgensen, F., Willis, C., and Walker, J. (2015). Real-time PCR to supplement gold-standard culture-based detection of legionella in environmental samples. *J. Appl. Microbiol.* 119, 1158–1169. doi: 10.1111/JAM.12911

Curry, K. D., Wang, Q., Nute, M. G., Tyshaieva, A., Reeves, E., Soriano, S., et al. (2022). Emu: species-level microbial community profiling of full-length 16S rRNA Oxford nanopore sequencing data. *Nat. Methods* 19, 845–853. doi: 10.1038/s41592-022-01520-4

De Coster, W., D'Hert, S., Schultz, D. T., Cruts, M., and Van Broeckhoven, C. (2018). NanoPack: visualizing and processing long-read sequencing data. *Bioinformatics* 34, 2666–2669. doi: 10.1093/bioinformatics/bty149

Duron, O., Doublet, P., Vavre, F., and Bouchon, D. (2018). The importance of revisiting legionellales diversity. *Trends Parasitol.* 34, 1027–1037. doi: 10.1016/J.PT.2018.09.008

Edgcomb, V., Orsi, W., Bunge, J., Jeon, S., Christen, R., Leslin, C., et al. (2011). Protistan microbial observatory in the cariaco basin, caribbean. i. pyrosequencing vs Sanger insights into species richness. *ISME. J.* 5, 1344–1356. doi: 10.1038/ismej.2011.6

Eriksson, K. I. A., Thelaus, J., Andersson, A., and Ahlinder, J. (2022). Microbial interactions — underexplored links between public health relevant bacteria and Protozoa in coastal environments. *Front. Microbiol.* 13. doi: 10.3389/fmicb.2022.877483

Fang, W., Lin, M., Shi, J., Liang, Z., Tu, X., He, Z., et al. (2022). Organic carbon and eukaryotic predation synergistically change resistance and resilience of aquatic microbial communities. *Sci. Total. Environ.* 830, 154386. doi: 10.1016/j.scitotenv.2022.154386

Fang, G. D., Yu, V. L., and Vickers, R. M. (1989). Disease due to the legionellaceae (other than legionella pneumophila): Historical, microbiological, clinical, and epidemiological review. *Med.* 68, 116–132. doi: 10.1097/00005792-198903000-00005

Graells, T., Ishak, H., Larsson, M., and Guy, L. (2018). The all-intracellular order legionellales is unexpectedly diverse, globally distributed and lowly abundant. *FEMS Microbiol. Ecol.* 94, 185. doi: 10.1093/femsec/fiy185

Grüning, B., Dale, R., Sjödin, A., Chapman, B. A., Rowe, J., Tomkins-Tinch, C. H., et al. (2018). Bioconda: sustainable and comprehensive software distribution for the life sciences. *Nat. Methods* 15, 475–476. doi: 10.1038/s41592-018-0046-7

Guillou, L., Bachar, D., Audic, S., Bass, D., Berney, C., Bittner, L., et al. (2012). The protist ribosomal reference database (PR2): a catalog of unicellular eukaryote small Sub-unit rRNA sequences with curated taxonomy. *Nucleic Acids Res.* 41, D597–D604. doi: 10.1093/nar/gks1160

Guo, J., Brugel, S., Andersson, A., and Lau, D. C. P. (2022). Spatiotemporal carbon, nitrogen and phosphorus stoichiometry in planktonic food web in a northern coastal area. *Estuar. Coast. Shelf. Sci.* 272, 107903. doi: 10.1016/J.ECSS.2022.107903

Hadziavdic, K., Lekang, K., Lanzen, A., Jonassen, I., Thompson, E. M., and Troedsson, C. (2014). Characterization of the 18S rRNA gene for designing universal eukaryote specific primers. *PloS One* 9, e87624. doi: 10.1371/journal.pone.0087624

Hägglund, M., Bäckman, S., Macellaro, A., Lindgren, P., Borgmästars, E., Jacobsson, K., et al. (2018). Accounting for bacterial overlap between raw water communities and contaminating sources improves the accuracy of signature-based microbial source tracking. *Front. Microbiol.* 9. doi: 10.3389/fmicb.2018.02364

Hamilton, K. A., Prussin, A. J., Ahmed, W., and Haas, C. N. (2018). Outbreaks of legionnaires' disease and pontiac fever 2006–2017. *Curr. Environ. Heal. Rep.* 5, 263–271. doi: 10.1007/s40572-018-0201-4

Harvey, E. T., Kratzer, S., and Andersson, A. (2015). Relationships between colored dissolved organic matter and dissolved organic carbon in different coastal gradients of the Baltic Sea. *Ambio* 44, 392–401. doi: 10.1007/s13280-015-0658-4

Heikema, A. P., Horst-Kreft, D., Boers, S. A., Jansen, R., Hiltemann, S. D., de Koning, W., et al. (2020). Comparison of illumina versus nanopore 16S rRNA gene sequencing of the human nasal microbiota. *Genes* 11, 1105. doi: 10.3390/GENES11091105

HELCOM (2017). *Manual for marine monitoring in the COMBINE programme of HELCOM.*

Herlemann, D. P. R., Labrenz, M., Jürgens, K., Bertilsson, S., Waniek, J. J., and Andersson, A. F. (2011). Transitions in bacterial communities along the 2000 km salinity gradient of the Baltic Sea. *ISME. J.* 5, 1571–1579. doi: 10.1038/ismej.2011.41

Herzog, S. D., Persson, P., Kvashnina, K., and Kritzberg, E. S. (2020). Organic iron complexes enhance iron transport capacity along estuarine salinity gradients of Baltic estuaries. *Biogeosciences* 17, 331–344. doi: 10.5194/bg-17-331-2020

Holsinger, H., Tucker, N., Regli, S., Studer, K., Roberts, V. A., Collier, S., et al. (2022). Characterization of reported legionellosis outbreaks associated with buildings served by public drinking water systems: United states 2001–2017. *J. Water Health* 20, 702–711. doi: 10.2166/WH.2022.002

Johnson, J. S., Spakowicz, D. J., Hong, B.-Y., Petersen, L. M., Demkowicz, P., Chen, L., et al. (2019). Evaluation of 16S rRNA gene sequencing for species and strain-level microbiome analysis. *Nat. Commun.* 10, 5029. doi: 10.1038/s41467-019-13036-1

Katoh, K., and Standley, D. M. (2013). MAFFT multiple sequence alignment software version 7: Improvements in performance and usability. *Mol. Biol. Evol.* 30, 772–780. doi: 10.1093/molbev/mst010

Kim, O.-S., Cho, Y.-J., Lee, K., Yoon, S.-H., Kim, M., Na, H., et al. (2012). Introducing EzTaxon-e: a prokaryotic 16S rRNA gene sequence database with phylotypes that represent uncultured species. *Int. J. Syst. Evol. Microbiol.* 62, 716–721. doi: 10.1099/ijs.0.038075-0

Klebba, P. E., Newton, S. M. C., Six, D. A., Kumar, A., Yang, T., Nairn, B. L., et al. (2021). Iron acquisition systems of gram-negative bacterial pathogens define TonB-dependent pathways to novel antibiotics. *Chem. Rev.* 121, 5193–5239. doi: 10.1021/acs.chemrev.0c01005

Koster, J., and Rahmann, S. (2012). Snakemake–a scalable bioinformatics workflow engine. *Bioinformatics* 28, 2520–2522. doi: 10.1093/bioinformatics/bts480

Kozlov, A. M., Darriba, D., Flouri, T., Morel, B., and Stamatakis, A. (2019). RAxML-NG: a fast, scalable and user-friendly tool for maximum likelihood phylogenetic inference. *Bioinformatics* 35, 4453–4455. doi: 10.1093/bioinformatics/btz305

Laglera, L. M., and Van Den Berg, C. M. G. (2009). Evidence for geochemical control of iron by humic substances in seawater. *Limnol. Oceanogr.* 54, 610–619. doi: 10.4319/LO.2009.54.2.0610

Lamb, J. B., van de Water, J. A. J. M., Bourne, D. G., Altier, C., Hein, M. Y., Fiorenza, E. A., et al. (2017). Seagrass ecosystems reduce exposure to bacterial pathogens of humans, fishes, and invertebrates. *Science* 355, 731–733. doi: 10.1126/science.aal1956

Lane, D. J. (1991). *16S/23S rRNA sequencing.* Ed. E. Stackeb (New York: John Wiley and sons).

Latorre-Pérez, A., Gimeno-Valero, H., Tanner, K., Pascual, J., Vilanova, C., and Porcar, M. (2021). A Round Trip to the Desert: In situ Nanopore Sequencing Informs Targeted Bioprospecting. *Front. Microbiol.* 12, 3777. doi: 10.3389/fmicb.2021.768240

Latz, M. A. C., Grujcic, V., Brugel, S., Lycken, J., John, U., Karlson, B., et al. (2022). Short- and long-read metabarcoding of the eukaryotic rRNA operon: evaluation of primers and comparison to shotgun metagenomics sequencing. *Mol. Ecol. Resour* 22 (6):2304-2318. doi: 10.1111/1755-0998.13623

Legionella Species - Special Pathogens Laboratory (2020). Available at: https://specialpathogenslab.com/legionella-species/ (Accessed September 2, 2022).

Lemoine, F., Domelevo Entfellner, J.-B., Wilkinson, E., Correia, D., Dávila Felipe, M., De Oliveira, T., et al. (2018). Renewing felsenstein's phylogenetic bootstrap in the era of big data. *Nature* 556, 452–456. doi: 10.1038/s41586-018-0043-0

Leoni, E., Catalani, F., Marini, S., and Dallolio, L. (2018). Legionellosis associated with recreational waters: A systematic review of cases and outbreaks in swimming pools, spa pools, and similar environments. *Int. J. Environ. Res. Public Heal.* 15, 1612. doi: 10.3390/IJERPH15081612

Leon-Sicairos, N., Reyes-Cortes, R., Guadrón-Llanos, A. M., Madueña-Molina, J., Leon-Sicairos, C., and Canizalez-Román, A. (2015). Strategies of intracellular pathogens for obtaining iron from the environment. *BioMed. Res. Int.* 2015, 1–17. doi: 10.1155/2015/476534

Lesnik, R., Brettar, I., and Höfle, M. G. (2015). Legionella species diversity and dynamics from surface reservoir to tap water: from cold adaptation to thermophily. *ISME. J.* 10, 1064–1080. doi: 10.1038/ismej.2015.199

Lo Presti, F., Riffard, S., Vandenesch, F., Reyrolle, M., Ronco, E., Ichai, P., et al. (1997). The first clinical isolate of legionella parisiensis, from a liver transplant patient with pneumonia. *J. Clin. Microbiol.* 35, 1706–1709. doi: 10.1128/JCM.35.7.1706-1709.1997

Lu, J., Breitwieser, F. P., Thielen, P., and Salzberg, S. L. (2017). Bracken: estimating species abundance in metagenomics data. *PeerJ. Comput. Sci.* 3, e104. doi: 10.7717/peerj-cs.104

Lundin, D., and Andersson, A. (2021). SBDI sativa curated 16S GTDB database. *SciLifeLab Dataset* doi: 10.17044/scilifelab.14869077.v5

McDonald, D., Price, M. N., Goodrich, J., Nawrocki, E. P., DeSantis, T. Z., Probst, A., et al. (2012). An improved greengenes taxonomy with explicit ranks for ecological and evolutionary analyses of bacteria and archaea. *ISME. J.* 6, 610–618. doi: 10.1038/ismej.2011.139

McMurdie, P. J., and Holmes, S. (2013). Phyloseq: An r package for reproducible interactive analysis and graphics of microbiome census data. *PloS One* 8, e61217. doi: 10.1371/journal.pone.0061217

Meier, H. E. M., Kniebusch, M., Dieterich, C., Gröger, M., Zorita, E., Elmgren, R., et al. (2022). Climate change in the Baltic Sea region: a summary. *Earth Syst. Dyn.* 13, 457–593. doi: 10.5194/esd-13-457-2022

Menden-Deuer, S., and Lessard, E. J. (2000). Carbon to volume relationships for dinoflagellates, diatoms, and other protist plankton. *Limnol. Oceanogr.* 45, 569–579. doi: 10.4319/lo.2000.45.3.0569

Muder, R. R., and Yu, V. L. (2002). Infection due to *Legionella* species other than *L. pneumophila*. *Clin. Infect. Dis.* 35, 990–998. doi: 10.1086/342884

Nazarian, E. J., Bopp, D. J., Saylors, A., Limberger, R. J., and Musser, K. A. (2008). Design and implementation of a protocol for the detection of legionella in clinical and environmental samples. *Diagn. Microbiol. Infect. Dis.* 62, 125–132. doi: 10.1016/j.diagmicrobio.2008.05.004

Niku, J., Hui, F. K. C., Taskinen, S., and Warton, D. I. (2019). Gllvm: Fast analysis of multivariate abundance data with generalized linear latent variable models in r. *Methods Ecol. Evol.* 10, 2173–2182. doi: 10.1111/2041-210X.13303

Olenina, I., Hajdu, S., Edler, L., Andersson, A., Wasmund, N., Busch, S., et al. (2006). Biovolumes and size-classes of phytoplankton in the Baltic Sea HELCOM. *Balt. Sea Env. Proc.* 106, 1–44.

Opel, K. L., Chung, D., and McCord, B. R. (2010). A study of PCR inhibition mechanisms using real time PCR. *J. Forensic. Sci.* 55, 25–33. doi: 10.1111/j.1556-4029.2009.01245.x

Park, J. M., Ghosh, S., and O'Connor, T. J. (2020). Combinatorial selection in amoebal hosts drives the evolution of the human pathogen legionella pneumophila. *Nat. Microbiol.* 5, 599–609. doi: 10.1038/s41564-019-0663-7

Parte, A. C., Sardà Carbasse, J., Meier-Kolthoff, J. P., Reimer, L. C., and Göker, M. (2020). List of prokaryotic names with standing in nomenclature (LPSN) moves to the DSMZ. *Int. J. Syst. Evol. Microbiol.* 70, 5607–5612. doi: 10.1099/ijsem.0.004332

Parthuisot, N., West, N. J., Lebaron, P., and Baudart, J. (2010). High diversity and abundance of legionella spp. in a pristine river and impact of seasonal and anthropogenic effects. *Appl. Environ. Microbiol.* 76, 8201–8210. doi: 10.1128/AEM.00188-10

Pascale, M. R., Salaris, S., Mazzotta, M., Girolamini, L., Fregni Serpini, G., Manni, L., et al. (2021). New insight regarding legionella non- pneumophila species identification: Comparison between the traditional mip gene classification scheme and a newly proposed scheme targeting the rpoB gene. *Microbiol. Spectr.* 9, e01161-21. doi: 10.1128/Spectrum.01161-21

Portier, E., Bertaux, J., Labanowski, J., and Hechard, Y. (2016). Iron availability modulates the persistence of *Legionella pneumophila* in complex biofilms. *Microbes Environ.* 31, 387–394. doi: 10.1264/jsme2.ME16010

Portier, E., Zheng, H., Sahr, T., Burnside, D. M., Mallama, C., Buchrieser, C., et al. (2015). IroT/mavN , a new iron-regulated gene involved in l egionella pneumophila virulence against amoebae and macrophages. *Environ. Microbiol.* 17, 1338–1350. doi: 10.1111/1462-2920.12604

Price, M. N., Dehal, P. S., and Arkin, A. P. (2010). FastTree 2 - approximately maximum-likelihood trees for large alignments. *PloS One* 5, e9490. doi: 10.1371/journal.pone.0009490

Ratledge, C., and Dover, L. G. (2000). Iron metabolism in pathogenic bacteria. *Annu. Rev. Microbiol.* 54, 881–941. doi: 10.1146/annurev.micro.54.1.881

Renaud, G., Stenzel, U., Maricic, T., Wiebe, V., and Kelso, J. (2015). deML: robust demultiplexing of illumina sequences using a likelihood-based approach. *Bioinformatics* 31, 770–772. doi: 10.1093/bioinformatics/btu719

Richter, D. J., and Nitsche, F. (2017). "Choanoflagellatea," in *Handbook of the protists: Second edition* (Cham: Springer International Publishing), 1479–1496. doi: 10.1007/978-3-319-28149-0_5

Rodríguez-Pérez, H., Ciuffreda, L., and Flores, C. (2021). NanoCLUST: a species-level analysis of 16S rRNA nanopore sequencing data. *Bioinformatics* 37, 1600–1601. doi: 10.1093/bioinformatics/btaa900

SHARKdata - Datasets (2022). Available at: https://sharkdata.smhi.se/ (Accessed October 11, 2022).

Shimada, S., Nakai, R., Aoki, K., Shimoeda, N., Ohno, G., Kudoh, S., et al. (2021). Chasing waterborne pathogens in Antarctic human-made and natural environments, with special reference to legionella spp. *Appl. Environ. Microbiol.* 87, 1–15. doi: 10.1128/AEM.02247-20

Sidstedt, M., Rådström, P., and Hedman, J. (2020). PCR inhibition in qPCR, dPCR and MPS–mechanisms and solutions. *Anal. Bioanal. Chem.* 412, 2009–2023. doi: 10.1007/s00216-020-02490-2

Soerensen, A. L., Schartup, A. T., Skrobonja, A., and Björn, E. (2017). Organic matter drives high interannual variability in methylmercury concentrations in a subarctic coastal sea. *Environ. pollut.* 229, 531–538. doi: 10.1016/j.envpol.2017.06.008

Steenwyk, J. L., Buida, T. J., Li, Y., Shen, X.-X., and Rokas, A. (2020). ClipKIT: A multiple sequence alignment trimming software for accurate phylogenomic inference. *PloS Biol.* 18, e3001007. doi: 10.1371/journal.pbio.3001007

Stoecker, D. K., Hansen, P. J., Caron, D. A., and Mitra, A. (2017). Mixotrophy in the marine plankton. *Ann. Rev. Mar. Sci.* 9, 311–335. doi: 10.1146/annurev-marine-010816-060617

Sun, S., Noorian, P., and McDougald, D. (2018). Dual role of mechanisms involved in resistance to predation by Protozoa and virulence to humans. *Front. Microbiol.* 9 1017. doi: 10.3389/fmicb.2018.01017

Sutak, R., Camadro, J.-M., and Lesuisse, E. (2020). Iron uptake mechanisms in marine phytoplankton. *Front. Microbiol.* 11. doi: 10.3389/fmicb.2020.566691

Tamminen, T., and Andersen, T. (2007). Seasonal phytoplankton nutrient limitation patterns as revealed by bioassays over Baltic Sea gradients of salinity and eutrophication. *Mar. Ecol. Prog. Ser.* 340, 121–138. doi: 10.3354/MEPS340121

Tang, P. W., Toma, S., and MacMillan, L. G. (1985). Legionella oakridgensis: laboratory diagnosis of a human infection. *J. Clin. Microbiol.* 21, 462–463. doi: 10.1128/JCM.21.3.462-463.1985

Thomas, V., McDonnell, G., Denyer, S. P., and Maillard, J.-Y. (2010). Free-living amoebae and their intracellular pathogenic microorganisms: risks for water quality. *FEMS Microbiol. Rev.* 34, 231–259. doi: 10.1111/j.1574-6976.2009.00190.x

Tsao, H. F., Scheikl, U., Herbold, C., Indra, A., Walochnik, J., and Horn, M. (2019). The cooling tower water microbiota: Seasonal dynamics and co-occurrence of bacterial and protist phylotypes. *Water Res.* 159, 464–479. doi: 10.1016/j.watres.2019.04.028

Urban, L., Holzer, A., Baronas, J. J., Hall, M. B., Braeuninger-Weimer, P., Scherm, M. J., et al. (2021). Freshwater monitoring by nanopore sequencing. *Elife* 10, 1–27. doi: 10.7554/eLife.61504

Utermöhl, H. (1958). Zur vervollkommnung der quantitativen phytoplankton-methodik. *SIL. Commun.* 9, 1–38. doi: 10.1080/05384680.1958.11904091

Vittal, R., Roshini, J., Raj, M., Kumar, B. K., and Karunasagar, I. (2022). Advances in environmental detection and clinical diagnostic tests for legionella species. *J. Heal. Allied Sci. NU.* 12, 168–174. doi: 10.1055/S-0041-1731863

Wandersman, C., and Delepelaire, P. (2004). Bacterial iron sources: From siderophores to hemophores. *Annu. Rev. Microbiol.* 58, 611–647. doi: 10.1146/annurev.micro.58.030603.123811

Whitby, H., Planquette, H., Cassar, N., Bucciarelli, E., Osburn, C. L., Janssen, D. J., et al. (2020). A call for refining the role of humic-like substances in the oceanic iron cycle. *Sci. Rep. 2020. 101.* 10, 1–12. doi: 10.1038/s41598-020-62266-7

Wickham, H. (2016). *ggplot2: Elegant graphics for data analysis* (Cham: Springer International Publishing). doi: 10.1007/978-3-319-24277-4

Wood, D. E., Lu, J., and Langmead, B. (2019). Improved metagenomic analysis with kraken 2. *Genome Biol.* 20, 257. doi: 10.1186/s13059-019-1891-0

Yang, R., Su, H., Qu, S., and Wang, X. (2017). Capacity of humic substances to complex with iron at different salinities in the Yangtze river estuary and East China Sea. *Sci. Rep.* 7, 1–9. doi: 10.1038/s41598-017-01533-6

Yan, Q., Zhang, W., Lin, M., Teymournejad, O., Budachetri, K., Lakritz, J., et al. (2021). Iron robbery by intracellular pathogen *via* bacterial effector–induced ferritinophagy. *Proc. Natl. Acad. Sci.* 118, e2026598118. doi: 10.1073/pnas.2026598118

Yin, X., Chen, Y.-Z., Ye, Q.-Q., Liao, L.-J., Cai, Z.-R., Lin, M., et al. (2022). Detection performance of PCR for legionella pneumophila in environmental samples: a systematic review and meta-analysis. *Ann. Clin. Microbiol. Antimicrob.* 21, 1–12. doi: 10.1186/s12941-022-00503-9

frontiers | Frontiers in Marine Science

TYPE Systematic Review
PUBLISHED 15 March 2023
DOI 10.3389/fmars.2023.1134699

OPEN ACCESS

EDITED BY
Anke Kremp,
Leibniz Institute for Baltic Sea Research (LG), Germany

REVIEWED BY
Liyang Yang,
Fuzhou University, China
Helmut Maske,
Center for Scientific Research and Higher Education in Ensenada (CICESE), Mexico

*CORRESPONDENCE
Johan Wikner
johan.wikner@umu.se

SPECIALTY SECTION
This article was submitted to Global Change and the Future Ocean, a section of the journal Frontiers in Marine Science

RECEIVED 30 December 2022
ACCEPTED 28 February 2023
PUBLISHED 15 March 2023

CITATION
Wikner J, Vikström K and Verma A (2023) Regulation of marine plankton respiration: A test of models.
Front. Mar. Sci. 10:1134699.
doi: 10.3389/fmars.2023.1134699

Regulation of marine plankton respiration: A test of models

Johan Wikner[1,2]*, Kevin Vikström[1,3] and Ashish Verma[1,2]

[1]Department of Ecology and Environmental Science, Umeå University, Umeå, Sweden, [2]Umeå Marine Sciences Centre, Umeå University, Hörnefors, Sweden, [3]Department of Ecology and Genetics, Limnology, Uppsala University, Uppsala, Sweden

Plankton respiration is a major process removing oxygen from pelagic environments and constitutes one of the largest oxygen transformations in the sea. Where the O_2 supplies due to dissolution, advection and oxygenic photosynthesis are not sufficient, hypoxic, or anoxic waters may result. Coastal waters with limited water exchange are especially prone to have low oxygen levels due to eutrophication and climate change. To support marine environmental management in a period of rapid climate change, we investigated the current knowledge of regulating plankton respiration based on field and experimental studies reported in the literature. Models for regulation of plankton respiration was tested on a three-year field data set. Temperature is the most reported predictor positively influencing plankton respiration (mean r^2 = 0.50, n=15). The organic carbon supply driven by primary production has a similar coefficient of determination but fewer reported relationships (mean r^2 = 0.52, n=6). Riverine discharges of dissolved organic carbon can override the influence of primary production in estuaries precluding effects of nutrient reductions. The median predictions of respiration regulation produced by current models vary by a factor of 2 from the median of observed values and extreme values varied even more. Predictions by models are therefore still too uncertain for application at regional and local scales. Models with temperature as predictor showed best performance but deviated from measured values in some seasons. The combined dependence of plankton respiration on temperature, phytoplankton production and discharge of riverine organic carbon will probably lead to increased oxygen consumption and reduced oxygen levels with projected climate change. This will be especially pronounced where increased precipitation is expected to enhance riverine discharges of carbon compounds. The biologically mediated transfer of carbon for long-term storage in deeper layers will slow down. Implementation of plankton respiration measurements in long-term ecological monitoring programs at water body and basin scales is advocated, which would enable future multivariate analyses and improvements in model precision across aquatic environments.

KEYWORDS

climate, effect, plankton, oxygen, respiration, regulation, temperature, carbon

1 Introduction

1.1 Biological and microbial carbon pump concepts

The development of large volumes of sea water with low oxygen concentrations (hypoxic) or where oxygen is absent (anoxic) is of increasing concern for society and for the sustainability of marine ecosystem services (Diaz and Rosenberg, 2008; Rabalais et al., 2010; Zhang et al., 2010; Carstensen et al., 2014; Breitburg et al. 2018). Outgassing due to elevated temperatures and enhanced respiration rates of marine organisms are two major processes that decrease oxygen concentrations in aquatic systems (Oschlies et al., 2018). In addition to removing oxygen, respiration also contributes to elevated atmospheric carbon loads by producing CO_2 (Figure 1) (Rivkin and Legendre, 2001; Sanders et al., 2016). Current estimates show that less than 1% of carbon assimilated in the sea will end up in deep waters over millennia and thus be removed from biosphere cycling. More than 90% of sedimenting carbon is mineralized back to the atmosphere as CO_2 by respiration (Henson et al., 2011; Bach et al., 2019; Fender et al., 2019; Giering et al., 2020). Consequently, the regulation of respiration and associated oxygen consumption will be crucial to accurately model marine and global carbon cycles and to assess the ability of biological and microbial carbon pumps to mitigate CO_2 levels in the biosphere (Dang, 2020). This knowledge is also crucial for stakeholders and environmental managers who are responsible for sustaining ecosystem functions, biodiversity, and chemical compositions in the sea.

Therefore, we investigated the current understanding of the regulation of plankton respiration using reported general models applied on a coastal multi-year data set of plankton respiration from the well-studied Öre Estuary located in the boreal zone (The Baltic Sea, Vikström and Wikner, 2019; Vikström et al., 2020). The boreal zone constitutes the next largest land carbon reservoir on the planet (Pan et al., 2011), and a substantial load of organic carbon is discharged to the coastal zone (Reader et al., 2014). Coastal waters are important due to high marine biodiversity and productivity, load of terrestrial organic carbon by river discharge and that limited water exchange increases risk of hypoxia in some coastal areas (e.g., the Baltic Sea). Pelagic respiration is dominant in the water column and is the focus of this study, while benthic respiration comprises one-fourth of total marine respiration in estuarine waters (Hopkinson and Smith, 2005). In deeper oceanic environments, pelagic respiration is expected to be even more dominant due to degradation of sedimentary matter by bacterioplankton (Cho and Azam, 1988). Plankton respiration will thereby have a major impact on the marine carbon distribution between the organic fraction and CO_2 in both coastal and offshore environments.

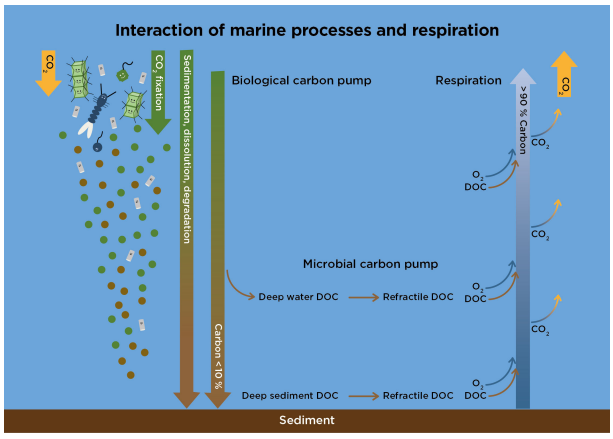

FIGURE 1
Schematic view of the role of respiration in the biological and microbial carbon pumps in the sea. Respiration drives oxygen consumption and mineralization of organic carbon pools to CO_2 and its emission to the atmosphere. Understanding respiration regulation is therefore crucial for the carbon budget of the atmosphere and the capacity of the ocean to assimilate carbon. Phyto-, protozooplankton and prokaryotic plankton are crucial for operating these processes together with mesozooplankton.

1.2 Role of respiration in BCP

The "biological carbon pump" (BCP) is defined as the assimilation of CO_2 and synthesis of biomass by autotrophic plankton, followed by sedimentation of dead and aggregated cells as well as faecal pellets produced by grazing zooplankton to deeper water layers (Figure 1). The major transformation of biomass to CO_2 occurs in surface waters, and less than 10% is transported to deeper waters (Henson et al., 2011). The potential transformation by prokaryotes of the bioavailable carbon substrates reaching the deep water to recalcitrant compounds is named the "microbial carbon pump" (MCP). Direct evidence for the generation of recalcitrant compounds is methodologically challenging, and only limited experimental evidence has been reported thus far (Jiao et al., 2010). The combined action of BCP and MCP has been proposed as a mechanism of the biosphere to remove CO_2 from the atmosphere, a mechanism that is proposed to be bioengineered to speed up CO_2 removal.

BCP and MCP are efficiently counteracted by respiration throughout the entire water column (Robinson, 2019). Prokaryotes not only mineralize dissolved and particulate organic matter in the surface layer but also colonize, dissolve and degrade sedimenting aggregates and faecal pellets (Cho and Azam, 1988; Azam and Malfatti, 2007). Determinations of mainly free-living prokaryotic respiration are relevant, as the contribution from respiration by particle-associated prokaryotes seems limited (Belcher et al., 2016), possibly due to the efficient dissolution of aggregates. Microorganisms perform this degradation of organic matter and thereby dominate oxygen consumption in the sea, where phyto- and bacterioplankton account for approximately 33% each, and protozooplankton accounts for 24% (Figure 2, Robinson et al., 2005). The respiration by microbial plankton in the water column is thereby a major cause of the small fraction of carbon reaching the deep ocean, which originally formed in the marine photic zone. Consequently, oxygen consumption contributing to hypoxia and emission of CO_2 will mainly be caused by microbial activity in the pelagic realm. For coastal

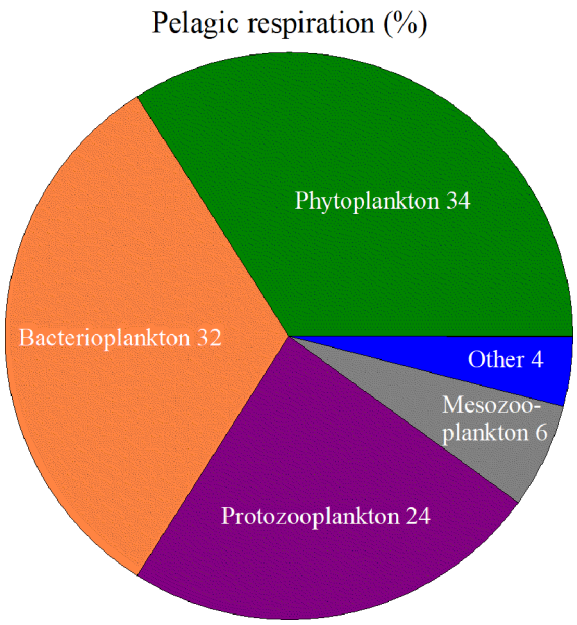

FIGURE 2
Pie diagram showing the distribution of pelagic respiration among phytoplankton, bacterioplankton, protozooplankton, mesozooplankton and other organisms (e.g., fish) based on Robinson and Williams 2005 (their Table 9.2).

and estuarine environments, it is relevant to point out that planktonic respiration is already a major process that converts organic carbon to CO_2 in shallower waters (i.e., > 40 m bottom depth) (Sandberg et al., 2004; Hopkinson and Smith, 2005).

A better understanding of the controlling factors of plankton respiration and how it will be affected by projected climate changes is therefore important. We compile the current understanding of how oxygen consumption is regulated with a particular focus on plankton respiration in the boreal zone. Fish respiration was not investigated, as it constitutes a relatively small part of pelagic respiration (Figure 2, Robinson et al., 2005). Mesozooplankton abundances in Winkler bottle volumes are too low (typically < 150 ml) to contribute to these measurements. Additionally, mesozooplankton respiration constitutes a small share of pelagic respiration (Figure 2, Robinson et al., 2005).

2 Methods

2.1 Study design

Reports providing empirical evidence for how pelagic oxygen consumption is regulated were compiled from the current literature, reviews, and book sections. Models related to pelagic oxygen consumption were also searched in articles using physical-biogeochemical models to project the effects on oxygen status caused by climate change. Pelagic oxygen consumption consists primarily of plankton respiration, including bacterioplankton (i.e., prokaryotic plankton, Figure 2). Benthic respiration and NH_4 oxidation (e.g., nitrification) were not investigated.

The reported mathematical functions with predictors, coefficients of determination (r^2) and coefficients of precision were collected. The r^2-values were used as a measure of the strengths of relationships. When log transformed data were used to define the statistical relationship those relationships were given lesser rank than relationships obtained with untransformed data to predict plankton respiration on regional or local scales.

Selected equations modelling plankton respiration were tested for their predictive powers using a three-year field dataset (Vikström et al., 2020) and a study of bacterioplankton respiration (Vikström and Wikner, 2019), both collected from a boreal estuary in the northern Baltic Sea.

Reported assessments of the expected effects of current climate change projections on oxygen consumption and oxygen concentrations in the references were compiled.

2.2 Collection of references

A comprehensive compilation of the scientific knowledge of aquatic respiration contained in the book by Williams et al. (2005) was used to cover older references. An earlier compilation of bacterioplankton respiration was found in Robinson (2008).

The Web of Science was searched using the following syntaxes: (TS=respiration OR (TS=oxygen AND TS=consumption)) AND (TS=marine OR TS=Sea) AND (TS=climate AND TS=Change) (date of search: 15th September 2022) and (TS=respiration OR (TS=oxygen AND TS=consumption)) AND (TS=marine OR TS=Sea) AND (TS=control AND TS=Regulation) (date of search: 16th September 2022)

References in the authors' EndNote libraries and paper copy libraries from three decades of research were another source for collecting references.

2.3 Search strategy

Articles and chapters were searched for figures that showed relationships between oxygen consumption or respiration versus different predictors. Only marine environments were investigated. The equations for relationships should be reported with at least the coefficient of determination provided. It was also ideal when the statistical significances, number of values and precisions of derived coefficients of the fitted model were reported.

Reports of Q_{10}- or activation energy-values (E_a) for plankton and bacterioplankton respiration were compiled from estuaries and ocean ecosystems.

The texts were screened for titles, subtitles, or conclusions regarding oxygen consumption regulation. In addition, reported assessments of the effect of climate change on oxygen consumption and oxygen status were compiled.

Predictors where significant relationships from several investigations were available were selected for further analysis. Here, the equations reported were compiled and ranked according to their r^2 values as indications of model fit. Ease of prediction was seen as key for application to environmental management.

2.4 Data sources

A three-year multiple season dataset of planktonic respiration that was measured with optode sensors (the OPTOCS method, n=191,Vikström et al., 2020) and bacterioplankton respiration data from two seasons (n=42, Vikström and Wikner, 2019), estimated with the same method. The two datasets are from the boreal Öre Estuary (northern Baltic Sea), with high riverine carbon input and encompasses complementary data such as primary production ($^{14}CO_2$ incorporation), bacterioplankton community growth rates (^{3}H-thymidine incorporation), bacterioplankton carbon contents, temperatures, dissolved organic carbon and nutrients. The datasets were used for testing the different models found in the literature in a coastal boreal environment.

One significant relationship was reported as an r^2 value by Hopkinson and Smith (2005) but lacked derived equations or associated statistical information. To add this model to the analysis, data were extracted from their Figure 8.9 (WebPlotDigitizer, https://apps.automeris.io/wpd/) and were added to Table 1.

2.5 Data analysis

To evaluate the explanatory degrees of models (i.e., Figure 3), the category "plankton respiration" included one "phyto"- and "picoplankton" category each. Additionally, one "planktonic and benthic" category was joined with the plankton category. Discrete values from different depths were used for model testing unless the model was designed for integrated values, where the observed values were integrated in the same manner. Boxplots were used to describe the levels and distributions of values when more than one case occurred. Determinations of model capabilities to predict plankton respiration in the dataset with observations were performed in R Studio (version 2022.07.01 + 554, R_Core_Team, 2021) and packages therein. The conformity between the observed and predicted values of the different models was assessed by boxplots across seasons and residual root mean square error (RMSE) values (Sokal and Rohlf, 1995). Boxplots indicate conformity for both the level and distribution of data, while the RMSEs show residual variances that are not explained by the models. When using temperature as the main driver, the measured temperature at the time of estimation of respiration was used. Complementary data were extracted from the dBotnia database (dBotnia, 1994), which are identical to those reported by Vikström et al. (2020). For the model by Eilola et al. (2009), bioavailable detritus was modelled as 0.75 × [DOC] assuming 50% of marine DOC to be bioavailable and POC constituting 25% of total organic carbon (Forsgren and Jansson, 1992; Sandberg et al., 2004). Bacterioplankton abundances and growth rates were available in the authors' datasets and are presented in Vikström and Wikner (2019). The measurement of oxygen consumption by optodes sensors (OPTOCS method) enables extraction of initial air saturations and oxygen concentrations from individual runs and was used here for Equation 7 (Table 1). Model fits were evaluated by the root mean square error values calculated for each model (Equation 1) and are presented in Supplementary Table S2.

TABLE 1 Functional relationships and their coefficient of determination (r^2) for different quantities of pelagic respiration compiled from the indicated references.

Equation No.	Equation	Explanatory factor	r^2	p	n
3	$PR=0.005e^{0.086T}$	Temperature	0.87	<0.01	14[7]
4	$R=4.94(\pm 2.30)GPP^{0.74\ (\pm 0.087)}$	Gross primary production	0.72[a]	0.041,<0.001	29[5]
5	$PR=0.33(\pm 0.070)T$	Temperature	0.63[a,b]	<0.001	15[6]
6	$\Sigma R= 4.57 + 0.73\Sigma NPP$	Net phytoplankton production	0.54	0.02	65[8]
7	R=-23+0.51NPCP	Net plankton community production	0.48	<0.001	46[9]
8	$R=f(T)C_r(O_2/(O_2+k_1))$	Temperature and oxygen conc.	–	–	-[4]
9	$PR=0.002e^{0.15T}\times[DOC+POC]\times0.0019$	Temperature and organic carbon supply	–	–	-[10]
10	$\log_{10}R=1.0(\log_{10}P)^{0.78(\pm 0.02)}$	Gross primary production	0.66	–	874[1]
11	$\log_{10}BR=3.69(\log_{10}BG)^{0.58}$	Bacterioplankton growth	0.56	<0.001	286[2]
12	$\log_{10}BR=0.05T-0.59$	Temperature	0.32	<0.001	286[2]
13	$\log_{10}BR=1.62(\log_{10}BA)^{0.81}$	Bacterioplankton abundance	0.27	<0.001	260[2]
14	$\log_e\rho=26.49-0.589/kT$	Temperature	0.20	<0.001	205[3]
15	$\log_{10}BR=0.02(\log_{10}DOC)^{0.80}$	Dissolved organic carbon	0.18	<0.001	167[2]

Models are sorted on untransformed and logarithmic values and then descending level of the r^2-value within those categories. The measured quantities are ecosystem respiration (R), plankton respiration (PR), bacterioplankton respiration (BR), and specific prokaryotic respiration (ρ). The standard errors of coefficients are shown in parentheses, probabilities of type I errors (p) and numbers of cases (n) are presented where reported. References are given as exponents next to the n values.
[1]Duarte and Agusti (1998), [2]Robinson (2008), [3] López-Urrutia and Morán (2007) (k is Boltzmann's constant), [4]Bendtsen and Hansen (2013) (k_1 is pelagic O_2 half-saturation constant), [5]Hopkinson and Smith (2005), [6]Panigrahi et al. (2013), [7]Smith and Kemp (1995) (Mid bay, upper layer), [8]Williams (1998) (Σ=depth integrated values), [9]Smith and Kemp (2001), [10]Eilola et al. (2009), -=not reported, [a]Adjusted r^2. [b]Values (26% of total n) recalculated and corrected for observed oversaturation of oxygen.

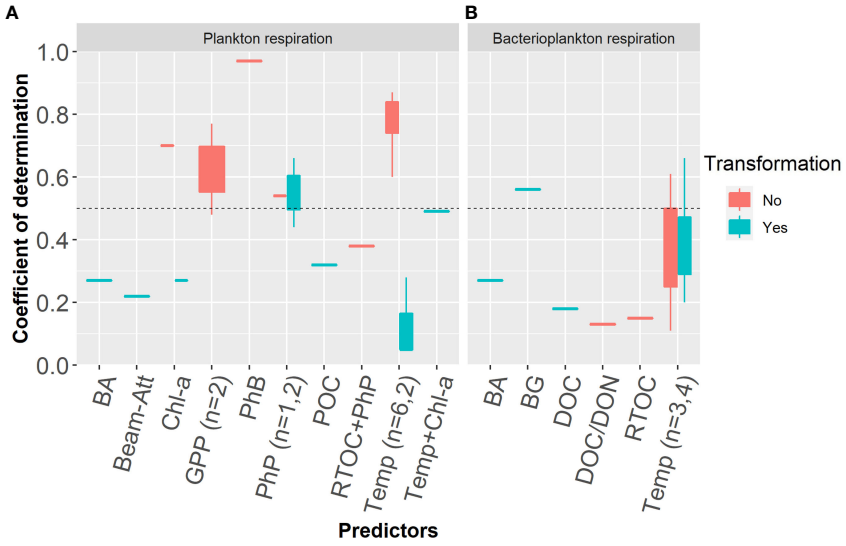

FIGURE 3
Boxplots showing the distributions of the coefficient of determination (r^2) of environmental predictors for plankton respiration **(A)** and bacterioplankton respiration **(B)** reported in the literature. The dashed horizontal black line represents the level for 50% of the explanation. Categories without any boxplot distributions represent values from a single study. The numbers of observations for categories exceeding 1 are shown. The predictors bacterioplankton abundance (BA), beam attenuation (Beam-Att), chlorophyll-a (chl-a), phytoplankton biomass (PhB), phytoplankton production (PhP), particulate organic carbon (POC), riverine total organic carbon (RTOC), temperature (Temp), bacterioplankton growth (BG), dissolved organic carbon (DOC) and dissolved organic nitrogen (DON) are shown.

$$RMSE = \sqrt{\frac{\Sigma(Measured - Predicted)^2}{n}} \quad \text{Eq. 1}$$

3 Results and discussion

A total of 36 references were found that included empirical information regarding plankton respiration regulation (Supplementary Table S1). Three of those lacked coefficients of determination and were removed from the data analysis of r^2. The publication years of the collected articles covered 1991 to 2020. One-third of those came from books that previously reviewed the subject field. In addition, 4 references reporting different coupled physical-biogeochemical models were reviewed.

3.1 Models for regulation of respiration

As a primary strategy to investigate the current knowledge of plankton respiration regulation, we reviewed some of the models that were applied to simulate the marine carbon cycle. However, in several references the equations used for oxygen consumption were not provided, alternatively based on mass balance calculations or on relationships coupled to nitrogen cycling (Neumann et al., 2002; Savchuk, 2002; Eilola et al., 2009; Meier et al., 2011b). Among reported equations, the Swedish Coastal and Ocean Biogeochemical model (SCOBI) calculate pelagic oxygen consumption based on detritus mineralization and temperature (Eilola et al., 2009). Bendtsen and Hansen (2013) provided a model for oxygen consumption that is included in Table 1, referring to White et al. (1991); Pomeroy and Wiebe (2001) and Lomas et al. (2002) regarding temperature control of pelagic respiration. Their relationship uses a temperature sensitivity-dependence (Q_{10}-value) and half-saturation constant for oxygen concentrations that differs from most other relationships presented in Table S1. They also calculated benthic respiration in a similar manner using different parameter values. The inclusion of oxygen concentration is scientifically motivated but rarely used, as many studies of plankton respiration are performed in well oxygenated environments. However, in environments showing hypoxia, this predictor becomes crucial for proper modelling of oxygen consumption. However, no quality measure of the relationship by Bendtsen and Hansen (2013) is provided, such as the explanation degree or other measures of fit to observed data.

3.2 Experimentally derived regulation of respiration

3.2.1 Character of references

Few studies have directly addressed the regulation of plankton respiration. Research with a focus on respiration has been directed toward the trophic balance between pelagic respiration and carbon fixation (Duarte and Agusti, 1998; Williams and Le, 1998; del Giorgio and Duarte, 2002; Williams et al., 2004) and more recently, climate change effects (Lopez-Urrutia et al., 2006; Vazquez-Dominguez et al., 2007; Sarmento et al., 2010; Panigrahi et al., 2013). One study that directly addressed the regulation of bacterioplankton respiration showed a relationship to DOC (Alonso-Saez et al., 2008), and several studies of respiration in Chesapeake Bay also provide valuable results that are relevant to the

regulation of plankton and bacterioplankton respiration (Smith and Kemp, 1995; Smith and Kemp, 2001; Smith and Kemp, 2003). Relationships among respiration and various predictors are also reported in an outstanding review and synthesis of respiration studies in aquatic environments (Williams et al., 2005). For bacterioplankton respiration, a book section by Robinson (2008) provided a comprehensive background. Given the limited community of distinguished researchers in the field who are included in the reference list, earlier reviews of respiration and our own research activity in the field in the past two decades, the risk of having overlooked key reports is assessed to be low.

3.2.2 Explanatory power of predictors

Studies reporting significant relationships with different predictors were compiled to assess the current knowledge of plankton respiration control (Table S1). The reported coefficient of determination (r^2 univariate, R^2 multivariate) were used as measures of the explanatory powers of the relationships. A plot of r^2 versus predictor provides an overview of the current understanding of plankton and bacterioplankton respiration regulation (Figure 3). Due to varying types of respiration that were measured and distributed as untransformed or transformed values, the number of cases for each combination with predictors become low. The ambient temperature in the sampled environment is the most reported governing predictor (grand mean r^2 = 0.50, n=15). Reports using untransformed values for plankton respiration are typically obtained in more homogenous environments and show higher coefficient of determination than those based on logarithm transformed values (i.e., cross-ecosystem studies). Analyses of temperature regulation based on untransformed values alone were performed on aggregated basins or environments that were deemed similar (i.e., estuaries) and resulted in a grand mean r^2 of 0.61 (n=9). Cross-system analyses, which are typically based on logarithm transformed values prior to statistical tests, show a lower mean r^2- value of 0.32 (n=6) for temperature. Coefficient of determination based on untransformed values are higher (r^2 = 0.74, n=6) than when based on logarithm transformed values for plankton respiration, but not so for bacterioplankton respiration. Given the lower coefficient of determination and that back-transformed coefficients are associated with wider confidence intervals, the uncertainties for relationships based on logarithm transformed values are substantial. Increasing imprecision when transforming a predictive function from logarithmic to untransformed measures is of concern when applied to local water bodies or when doing basin scale planning within marine environmental management.

The supply of carbon substrates as a regulator of plankton respiration is also reported, albeit with fewer cases (r^2 = 0.52, n=6). Those encompasses different predictors, such as gross primary production (GPP), net primary production (NPP), net plankton community production (NPCP) and riverine DOC (rDOC). The coefficient of determination are comparably high based on the untransformed values for GPP alone (r^2 = 0.63, n=2), representing estuarine environments. One report of a significant relationship with phytoplankton biomass (i.e., chlorophyll-a) from the Gulf of Riga had the highest r^2 value reported for a predictor but re-analysis resulted in a lower value (r^2 = 0.65, year 1995 data) (Olesen et al., 1999). This value was close to one case of a high explanation for chlorophyll-a based on untransformed values reported from the Chesapeake Bay (r^2 = 0.70) (Smith and Kemp, 2001). The predictive power of phytoplankton abundance may reflect its importance as a source for carbon substrate supplies *via* zooplankton exudation, faeces pellet production and dissolution. A lack of effects of mineral nutrients (e.g., NO_3 and PO_4) on bacterioplankton respiration was reported in a one-year field study (Lemée et al., 2002). The relationship with the supply of organic carbon substrates (including plankton biomass) is directly relevant for assigning eutrophication as a cause of hypoxia development. The high coefficient of determination between plankton respiration and gross primary production from estuaries is the most powerful relationship reported of this type (r^2 = 0.77, n=29, untransformed) (Hopkinson and Smith, 2005).

When comparing results and models from different studies both the environmental conditions and methodology applied may influence the results. Still models for regulation of plankton respiration is typically presented as being generally applicable, and ideally should be so, motivating validation in any environment at this stage. Field studies dominated the data set of 37 studies (Table S1) investigated, with only two microcosm studies and one mesocosm and model study each. Spatial and temporal scale of studies vary and could also influence models. Sampling varies from individual stations, *via* coastal transects to compilation of marine data across sea areas. Temporal scales from days to several years occur. 18 studies were done in estuarine environments, most of them in the boreal zone. Studies representative of oceanic environments amounts to 13. Temperature should have a similar basic effect in most environments, but likely influenced by the level of the ambient water temperature and type of organic matter present. This can be one cause of deviating precision of the models. Estuaries will be directly influenced by input of terrestrial organic matter from rivers with some bioavailable fraction and a large humic component. The influence of riverine discharge is lacking in identified models but shown as a major driver in a Baltic Sea estuary (Vikström et al., 2020). The autochthonous productivity in meso- and eutrophic environments appear to systematically increase plankton respiration, although continued increase (Duarte and Agusti, 1998; Williams and Le, 1998) or levelling off (Hopkinson and Smith, 2005) at higher productivity rates differ between studies.

3.2.3 The dual influence of temperature

Distinguishing between the effects of temperature and substrate supply is challenging. An increase in temperature (T) increases the probability of elements and molecules colliding and thereby the chemical reaction rate (k) at a given activation energy (E_a) for a chemical reaction:

$$k = Ae^{-E_a/RT} \quad \text{Eq. 2}$$

where R is the molar gas constant and A is a collision frequency constant (Dickerson and Geis, 1979). Temperature thereby affects

both enzyme catalysis of reactions by conformational change of the enzyme, and the chemical reactions of the creation and/or breakage of chemical bonds in or between the substrates. Consequently, organisms, especially bacterioplankton, should also experience elevated temperatures as an extended pool of available substrates. Higher temperature makes many chemical reactions more energetically favorable and thereby more substrates should be possible to use for metabolism. To better approach the issue of confounding predictors, we advocate that future research include multivariate collection of data accompanied by multivariate statistical analyses, including predictor influence measures and correlations. Reports where different predictors have been challenged in multiple stepwise regressions are scarce, and it is therefore not possible to assess whether higher coefficient of determination can be achieved using several predictors. Panigrahi et al. (2013) reported results from a multiple regression with temperature and chlorophyll-a, where only temperature remained once the data were adjusted for samples with oxygen oversaturation (>100%).

3.2.4 Riverine DOC as a source of substrates

Riverine discharge of DOC drives a significant share of plankton respiration in the boreal northern Baltic Sea with high freshwater influence (r^2 = 0.38, n=46) (Vikström et al., 2020). Riverine DOC exceeds the carbon supply from estuarine phytoplankton carbon fixation by 4-fold and explains part of the high plankton respiration levels during winter with negligible phytoplankton production (i.e., baseline respiration, del Giorgio and Williams, 2005). Other reports of significant plankton respiration at zero phytoplankton production prevail (Williams and Le, 1998; Du and Shen, 2015), although this was not further discussed by the authors. Thus, riverine DOC can supply coastal respiration with carbon substrates when discharges are sufficient and should be considered together with primary production in coastal areas.

3.2.5 Bacterioplankton growth as a predictor

Bacterioplankton respiration shows a coupling to bacterio plankton growth that is recommended as a preferred predictor (Robinson, 2008). This finding reflects that favorable growth conditions for bacterioplankton in general promote their respiration. When using bacterioplankton biomass growth as an environmental indicator, this can provide valuable information for managers on the trophic status and indicate the level and development of oxygen consumption. In this context, the observation that bacterioplankton respiration lacks a relationship to prokaryotic diversity is relevant (Reinthaler and Herndl, 2005) and is supported by other reports of functional redundancy in prokaryotic communities (Fernandez-Gonzalez et al., 2016). However, a recent report in contrary demonstrate significantly different respiration rates between lineages, but still a positive relationship to growth rate (Munson-McGee et al., 2022). For other questions such as climate change effects, external environmental predictors are of more value for projecting net outcomes for bacterioplankton respiration. As bacterioplankton growth estimates also have marked uncertainty and evaluated factors are $\log_{10}$-transformed, the predictive value of those equations for managing the marine environment is limited (Figure 3 and 4). In addition, uncertainty estimates of the derived coefficients are rarely provided in the covered literature regardless of the predictor involved, which precludes assessments of model precision.

3.2.6 Maintenance activities contribute to respiration

Complicating the relationship between bacterioplankton respiration and growth, the contribution of maintenance respiration of prokaryotes is probably of a sufficient extent to influence plankton respiration regulation in the field (Carlson et al., 2007; Vikström and Wikner, 2019; Verma et al., 2022; Wikner and Vikström, 2023). This should also apply to other planktonic organisms (e.g., Norberg and DeAngelis, 1997) but is not discussed in a review of zooplankton respiration (Hernández-León and Ikeda, 2005). The influence of maintenance respiration should weaken the relationships with growth-related predictors. Temperature plausibly influences maintenance respiration as well, but other factors in the environment that regulate maintenance activities of organisms should also contribute. Activities such as

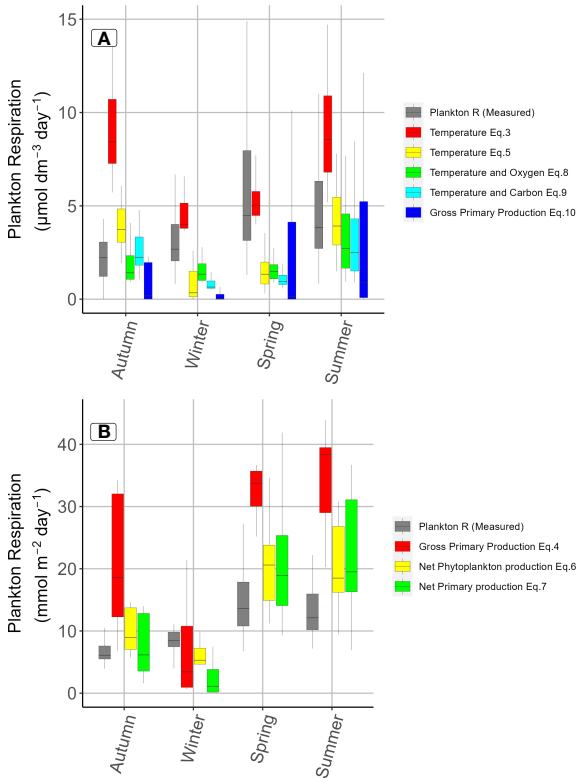

FIGURE 4
Comparison of observed values for plankton respiration in a boreal estuary and modelled values based on indicated functions from the literature (Table 1). Boxplots show the median values, interquartile range (25-75%) and the 0-25% and 75-100% quartiles. Models based in discrete **(A)** or integrated values **(B)**, respectively, are shown in separate panels.

maintaining osmotic potential inside cells requires energy metabolism *via* increased ATP synthesis. Nutrients (e.g., nitrogen and phosphorus) are also required for the synthesis of osmolytes, repair of nucleic acids, enzymes, and other cell constituents. However, as elements for maintenance metabolism can be recycled intracellularly and be independent of biomass increase, a share of pelagic respiration should be uncoupled from external nutrient supply. A better understanding of maintenance activities in plankton is recommended for future research to increase our knowledge of maintenance respiration regulation.

3.3 Fit of relationships to a multiyear dataset

3.3.1 Prediction of plankton respiration

The ability of selected relationships to predict a three-year annual dataset of respiration rates from the boreal northern Baltic Sea at the four major seasons were tested (Table 1, Vikström et al., 2020, Figures S1-S13). The power of models to predict respiration were assessed by median and spread of values in boxplots and by root mean square errors between predicted and observed values (Figures 4, 5). Low values of RMSE indicate good predictive power (Sokal and Rohlf, 1995), while match between observed and modelled data sets regarding median and spread were assessed visually. All functions deviated from the observed values for plankton respiration at some season (Figure 4). Temperature and oxygen (Eq. 8) and temperature and carbon (Eq. 9) showed good match on both level and spread with observed values in autumn and summer, while being clearly lower than observed values in winter and spring. Also, net phytoplankton production (Eq. 6) and net primary production (Eq. 7) showed good match regarding the median, but generally larger spread than observed values (c.f., integrated values). Temperature alone (Eq. 3) matched the median well in winter and spring, while being markedly higher at other seasons. Noticeably, the other temperature equation (Eq. 5) was instead closer to observed values in summer and autumn, but lower in winter and spring, showing a correlation to Eq. 3 but on a markedly lower level. For discrete values, 4 of 5 models showed good match during summer while being more scattered other seasons. Gross primary production (Eq. 4) deviated most for integrated values, despite showing a high r^2-value to data in the original article.

The analysis of root mean square error (RMSE) encompassed all seasons (Table S2). Model Eq. 5, 8, 10, 9, and 3 showed low RMSE values in ascending order (3.3-4.0 μmol dm^{-3} d^{-1}). All these coincided with models performing well in the box-plot analysis above. However, models with low RMSE were also associated with the highest number of cases tested (n>178 per model). For phytoplankton production, related tests could only include 51 cases, and the difference in n may have contributed to the different RMSE observed.

Even if many predicted distributions of plankton respiration remain within a factor of 2 relative to the observed values, substantial deviations occur that contribute to uncertainty in projecting the effects due to climate change and anthropogenic disturbance. Therefore, none of the tested equations could model the observed respiration rates in the northern Baltic Sea with sufficient accuracy and precision in all seasons. A statistically significant relationship between plankton respiration and temperature has previously been reported for the reference estuary (Panigrahi et al., 2013, Table S4). That relationship was based on a multiple regression using samples from 5 m depth (i.e., volumetric data), where chlorophyll-a, phytoplankton production and dissolved organic carbon was removed from the initial model. In a later study, including influence of riverine discharge of total organic carbon and phytoplankton production integrated over the

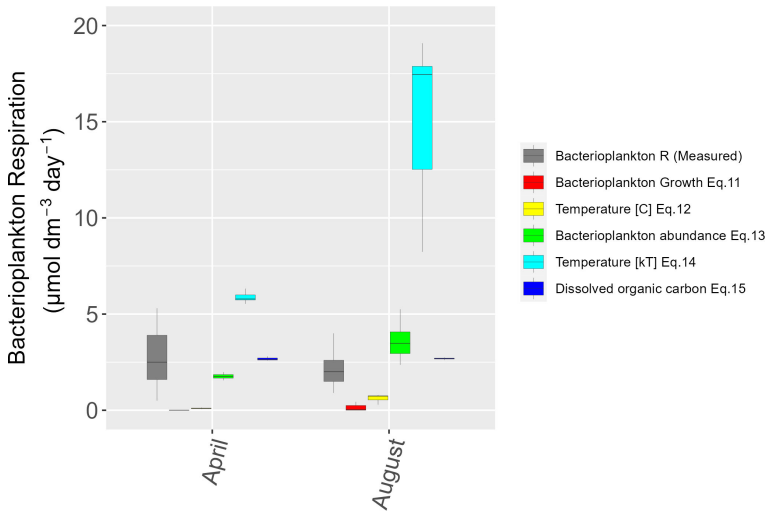

FIGURE 5
Same as Figure 4 but for bacterioplankton respiration.

water column, the sum of those factors (i.e., carbon input) was the only required predictor based on a multiple regression, (Vikström et al., 2020, their Figure 4). Water temperature, chlorophyll-a and dissolved organic carbon were removed from their initial model due to too low influence on plankton respiration. But also those relationships show a moderate predictive ability.

3.3.2 Prediction of bacterioplankton respiration

Modelling bacterioplankton respiration showed the best fit to the observed data for the predictors, DOC and bacterioplankton abundance in April but both had a markedly narrower range of values (Figure 5). The exception was bacterioplankton abundance reproducing the spread well in August, albeit at a higher median value. The observed bacterioplankton respiration rates came from another dataset from the same boreal estuary (Vikström and Wikner, 2019). DOC and bacterioplankton abundance were also the predictors showing the lowest RMSE values (Table S2). Significant maintenance respiration at low values of bacterio plankton growth (0.004-0.1 μmol dm^{-3} d^{-1}) could possibly explain an underestimation by this model in the oligotrophic and comparably cold environment of the boreal estuary with high loads of terrigenous organic matter (Vikström and Wikner, 2019). The analysis of a global data set by (López-Urrutia and Morán, 2007) also find that bacterioplankton respiration is maintained at depleted trophic state while bacterial growth decrease, together reducing the growth efficiency. Taken together, the current models for bacterioplankton respiration also deviates from observed data regarding level, distribution, or both attributes. Consequently, uncertainty in current models precludes precise (< ± 20% CV) prediction of future bacterioplankton respiration in the tested water body.

3.4 Temperature sensitivity of plankton respiration

Given that temperature is a commonly reported and a comparably strong predictor of respiration, current reports of the temperature sensitivity of plankton and bacterioplankton respiration were compiled (Table 2). The Q_{10} values for plankton respiration showed a median value of 3.2 (range 1.8-26). Variations occur between measurements within the same study and these are to some extent related to season (e.g., Panigrahi et al., 2013). Colder ambient temperatures tend to promote higher values but may also be explained by rates closer to the detection limits of current methods, where comparably small difference in untransformed units may mean multiple increases in rates. High inputs of riverine dissolved organic carbon together with low temperatures are also suggested to explain the high Q_{10} values in the northern Baltic Sea (Nydahl et al., 2013; Panigrahi et al., 2013). The DOC concentrations in the northern Baltic Sea are 5-fold higher than those in oceanic waters (Voss et al., 2021). Excess bioavailable carbon substrates should promote larger increases in respiration rates with increasing temperature. Plankton respiration seems to be more temperature sensitive than phytoplankton production and bacterioplankton growth (Lefevre et al., 1994; Vazquez-Dominguez et al., 2007; Panigrahi et al., 2013).

3.5 Effects of climate change on oxygen consumption

Reported assessment of climate change effects on oxygen consumption and concentrations in the current literature were compiled (Table 3). There is a consistent view in these reports that

TABLE 2 Q_{10}-values for oxygen consumption and respiration reported in the literature.

Variable	Q_{10}/E_a-value (-, eV)	Range Q_{10}/E_a	Ambient tempera-ture (°C)	Environment	Citation
Plankton respiration	2.8/-	1.4-24/-	1.0-6.7	Antarctic Ocean	Robinson and Williams (1993)
Plankton respiration	3.2/-	–	3.25	Antarctic Ocean	Vosjan and Olanczukneyman (1991)
Plankton respiration	5.1/-	4.2-10.6/-	9.0-16.0	Atlantic NE coast	Lefevre et al. (1994)
Plankton respiration	2.5/-	0.77-8.4/-	-1.5-1.0	Atlantic NW coast	Pomeroy et al. (1991)
Mesopelagic respiration	3.65/-0.90	–	8.7-14.9	Atlantic South and Indian Ocean	Mazuecos et al. (2015)
Plankton respiration	9/-	0.01-1115/-	-0.2-17.7	Estuary	Panigrahi et al. (2013)[b]
Microbial respiration	26/-	12-2370/-	12.0-15.0	Estuary	Nydahl et al. (2013)
Plankton respiration	2.4/-	1.9-2.8/-	4.4	Mesocosm	Hoppe et al. (2008)
Microbial respiration	-/-0.56	–	-1.0-28.5	Global Ocean	Lopez-Urrutia et al. (2006)
Plankton respiration	-/-0.32	–	-0.1-35	Global Ocean	Lopez-Urrutia et al. (2006)
Plankton respiration	6.8/-	5.9-7.1/-	23.0-24.0	Mediterranean Sea	Robinson (2000)
Microbial respiration	1.9/-	–	12.5-15.5/25.0-27.3	Mediterranean Sea Coast	Vazquez-Dominguez et al. (2007)

-, not available. [a]Mean of reported range. [b]Values (26% of total n) recalculated and corrected for observed oxygen oversaturation.
Cases are sorted by environment for comparison.

TABLE 3 Compilation of the effects of climate change assessed in the literature on oxygen consumption and concentrations.

		Climate change effect on O_2		
Environment	Study type	Consumption	Concentration	Reference
Coastal Mediterranean Sea	Manipulated field samples	↑	–	(Vazquez-Dominguez et al., 2007)
Ocean	Compiled field data	↑	–	(Robinson, 2008)
Ocean	MTE†-analysis of field data	↑	–	(Sarmento et al., 2010)
Baltic Sea	Model assemble	↑	↓	(Meier et al., 2011b)
Coastal Baltic Sea	Microcosm experiment	↑	↓	(Nydahl et al., 2013)
Kattegat	OXYCON model	↑	↓	(Bendtsen and Hansen, 2013)
Coastal Baltic Sea	Manipulated field samples	↑	↓	(Panigrahi et al., 2013)
Ocean	Review	–	↓	(Oschlies et al., 2018)

†Metabolic Theory of Ecology.
Arrows indicate the direction of change. Dashes indicate not reported assessments.

oxygen consumption will increase, and oxygen concentrations will decrease if the current climate projections for temperature are realized. This is in accordance with the evidence that temperature is a major predictor for respiration (Figure 3, Table S1, Figure 6). A literature survey of prokaryotic strains (n=239) and their thermal performance curve support an increase in prokaryotic respiration at higher temperature (Smith et al., 2019), but was mainly related to terrestrial taxa and lacked assessment of changes in substrate supply. Coupled physical-biogeochemical models driven by regionalized meteorological data from global climate simulations also show that oxygen consumption will increase in the Baltic Sea (Meier et al., 2011a). Both direct effect of temperature on plankton respiration and an increased supply of organic matter *via* higher primary production due to nutrient loads contribute to the increase. A mesocosm study from this sea area provides further support for increased plankton respiration and projects a reduction in the biological pump of organic matter to deeper water layers (Wohlers et al., 2009). However, that projection is based on that primary production increase is an outcome of climate change, while the net outcome of climate change for primary production varies with the marine environment. In contrast to the Baltic Sea scenario, a net 12-26% decrease in global primary production is projected when accounting

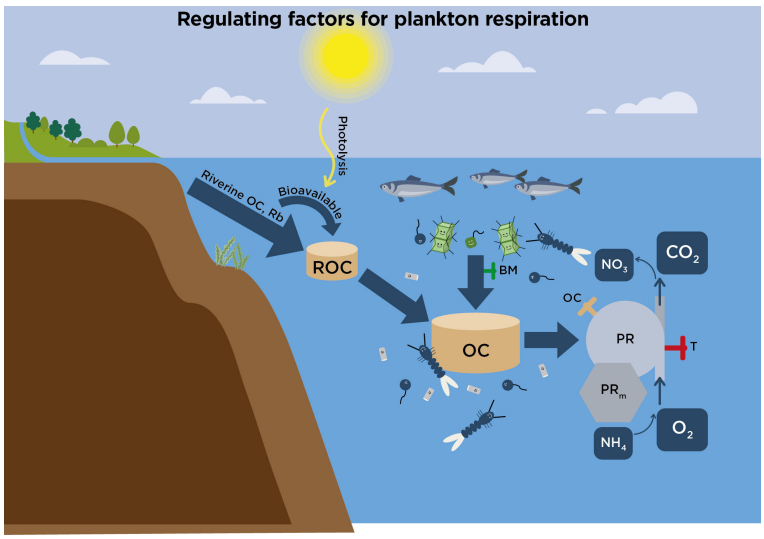

FIGURE 6
Conceptual diagram showing how plankton respiration (PR) is mainly controlled by temperature (T, red valve), and supply of bioavailable organic carbon (OC, yellow valve). OC is provided by excretion from grazing zooplankton and fish, phytoplankton and macroalgal exudation and detritus degradation. Coupling between respiration and biomass (BM, green valve, i.e., Chl-a) may reflect its importance for generating OC *via* zooplankton excretion and viral lysis. Supply of organic matter from riverine DOM discharge (ROC) can be significant in estuaries and contribute to formation of OC. Photolysis increase bioavailability of refractile humic substances. ROC drives basal respiration (PR_b). Oxidation of NH_4 to NO_3 contribute with a smaller share in the marine environment. The significant contribution of maintenance respiration (PR_m) to plankton respiration is also indicated.

for changes in nutrient availability (Couespel et al., 2021). Confidence in effect of climate change on primary production also influence reliability in projection of its effect on oxygen consumption.

In the northern Baltic Sea, primary production is also expected to decline but because of elevated precipitation and discharges of organic carbon (Andersson et al., 2015). In environments where precipitation is projected to increase due to climate change, terrestrial organic carbon, nitrogen and phosphorous discharged will also be elevated. Phytoplankton and macroalgae can use these elevated supplies of nitrogen and phosphorous for growth unless counteracted by reduced light penetration or global insolation (i.e., increased cloudiness). Reduced primary production under elevated freshwater discharges has been demonstrated on basin and multiannual scales in the northern Baltic Sea, explained by reduced light irradiance and intensified competition for limiting mineral nutrients (Wikner and Andersson, 2012). Terrestrial organic carbon from boreal watersheds is colored due to humic substances that hamper light penetration in the water column. Part of the terrestrial organic carbon can also be directly bioavailable to aquatic biota (20%, Pettersson et al., 1997) and should become more bioavailable by photolytic cleavage (Bertilsson et al., 1999), promoting bacterioplankton growth and respiration. Increased competition between bacterioplankton and phytoplankton for limited mineral nutrients will therefore further reduce primary production. The projected climate changes with warmer waters and higher precipitation in the northern Baltic Sea are consequently expected to enhance plankton respiration without an increase in primary production (Meier et al., 2011b; Andersson et al., 2015).

The expected effects of climate change in the Baltic Sea are in accordance with assessments conducted on the global scale. López-Urrutia and Morán (2007) conclude that global warming will lead to an increased flux of CO_2 from the ocean to the atmosphere. Sarmento and Descy (2008) claim that our knowledge and experimental evidence make it probable that bacterioplankton respiration and losses to grazers will increase, making microorganisms even more dominant in a warmer ocean. Robinson (2008) also concluded that bacterioplankton and thus total respiration will increase with the projected temperature increases. Further support for this view is provided by Oschlies et al. (2018), who projected that warming of waters will not change the integrated oxygen loss but will shift the respiration of organic matter closer to the surface, reducing the oxygen concentration there.

Given the significance of temperature as a predictor, a tentative quantitative estimate of the temperature effect on plankton respiration can be calculated based on the reported temperature sensitivity (i.e., Q_{10}-value, Table 2). Rearranging the Q_{10}-function reported by (Sherr and Sherr, 1996) to

$$\frac{R_2}{R_1} = Q_{10}^{(T_2-T_1)/10} \qquad \text{Eq. 16}$$

the effect of increased temperature (T_2-T_1) on increase in plankton respiration (R_2/R_1) can be calculated. Using the median Q_{10}-value from Table 2 of 3.2 and the Representative Concentration Pathway (RCP) scenario 2.6 with projected 1°C increase in water temperature, a 12% increase in plankton respiration is projected (Table S3, IPCC, 2019). For the RCP8.5 scenario, leading to a 4°C increase in water temperature, the result is 59% increase in R. Those projections assume that the supply of organic carbon for fueling plankton respiration is not limiting this increase. Even a 12% increase in plankton respiration can cause hypoxia to develop over longer periods, or enhance current hypoxic waters to anoxia, assuming similar or reduced ventilation of the water column. Reduced oxygen concentration would influence many biogeochemical processes dependent on the redox potential with potential profound impact on the environmental status.

The authors above, however, simultaneously stress the uncertainties in current models regarding oxygen consumption and respiration. In line with the conclusion in this compilation, Robinson (2008) infers that the uncertainty in bacterioplankton respiration regulation is still too large to make meaningful projections. Additionally, Oschlies et al. (2018) state that the current understanding of oxygen consumption is insufficient for confident modelling of climate change effects. The literature thus concordantly stresses the paucity of knowledge regarding plankton respiration. The long-term projections mentioned above should therefore be viewed as educated guesses.

Ideally, a model for regulation of plankton respiration would apply to all water environments if accounting for major regulating factors properly. This justifies our investigation of models reported up to date on a well-studied boreal estuary. We conclude that current models do not predict plankton respiration sufficiently well but emphasizes that characteristics of the tested environment may influence this conclusion. Similar test with data from other water environments is advocated. To advance our knowledge of respiration in the sea, improved model performance across water environments can increase the confidence in future advice for management. The systematic measurements of oxygen consumption, primary production and temperature should be implemented in long-term ecological and monitoring programs covering several years, also advocated by Breitburg et al. (2018). Collaboration with biogeochemical modelers is advocated for experimental design. Selected representative high-frequency sampling sites should cover all seasons with at least monthly sampling. Here, multivariate statistics and time series analysis, possibly combined with artificial intelligence technique should be employed at local basin or water body scales, while avoiding the application of logarithm-transformed relationships. In estuaries, measurements of river discharge of organic carbon and nutrients is needed. Harmonization of methodology and terminology would facilitate cross-ecosystem syntheses. For future applications by environmental management agencies, simple and precise predictors and clear guidelines are needed and can be achieved by concerted efforts between environmental monitoring and research.

Data availability statement

The original contributions presented in the study are included in the article/Supplementary Material. Further inquiries can be directed to the corresponding author.

Author contributions

JW, KV and AV designed the study and contributed to literature search. JW composed introductory and conceptual figures, made Table 1 and S1. AV synthesized degree of explanation and made corresponding figures. KV made modelling of selected equations based on available data sets and completed data into figures and tables. JW was the main author and KV and AV contributed in writing. All authors contributed to the article and approved the submitted version.

Funding

We are grateful for the research environment and funding provided by the strategic research program, EcoChange (224-919-09, JW). Financial support was further provided by the Kempe foundations (SMK-1854) to JW. Open access fee was funded by Umeå University within the Sweden Open Access Publishing Framework Agreement.

Acknowledgments

We acknowledge Marlene Lahti at the Communication Office, Umeå University, for refining figure 1 and 6.

Conflict of interest

The authors declare that the research was conducted in the absence of any commercial or financial relationships that could be construed as a potential conflict of interest.

Publisher's note

Supplementary material

The Supplementary Material for this article can be found online at: https://www.frontiersin.org/articles/10.3389/fmars.2023.1134699/full#supplementary-material

References

Alonso-Saez, L., Vazquez-Dominguez, E., Cardelus, C., Pinhassi, J., Sala, M. M., Lekunberri, I., et al. (2008). Factors controlling the year-round variability in carbon flux through bacteria in a coastal marine system. *Ecosystems* 11 (3), 397–409. doi: 10.1007/s10021-008-9129-0

Andersson, A., Meier, H. E. M., Ripszam, M., Rowe, O., Wikner, J., Haglund, P., et al. (2015). Projected future climate change and Baltic Sea ecosystem management. *Ambio* 44 (3), 345–356. doi: 10.1007/s13280-015-0654-8

Azam, F., and Malfatti, F. (2007). Microbial structure of marine ecosystems. *Nat. Rev.* 5 (10), 782–791. doi: 10.1038/nrmicro1747

Bach, L. T., Stange, P., Taucher, J., Achterberg, E. P., Alguero-Muniz, M., Horn, H., et al. (2019). The influence of plankton community structure on sinking velocity and remineralization rate of marine aggregates. *Global Biogeochemical Cycles* 33 (8), 971–994. doi: 10.1029/2019gb006256

Belcher, A., Iversen, M., Manno, C., Henson, S. A., Tarling, G. A., and Sanders, R. (2016). The role of particle associated microbes in remineralization of fecal pellets in the upper mesopelagic of the Scotia Sea, Antarctica. *Limnology Oceanography* 61 (3), 1049–1064. doi: 10.1002/lno.10269

Bendtsen, J., and Hansen, J. L. S. (2013). Effects of global warming on hypoxia in the Baltic Sea-north Sea transition zone. *Ecol. Model.* 264, 17–26. doi: 10.1016/j.ecolmodel.2012.06.018

Bertilsson, S., Stepanauskas, R., Cuadros-Hansson, R., Graneli, W., Wikner, J., and Tranvik, L. (1999). Photochemically induced changes in bioavailable carbon and nitrogen pools in a boreal watershed. *Aquat. Microbial Ecol.* 19 (1), 47–56. doi: 10.3354/ame019047

Breitburg, D., Levin, L. A., Oschlies, A., Gregoire, M., Chavez, F. P., Conley, D. J., et al. (2018). Declining oxygen in the global ocean and coastal waters. *Science* 359 (6371), 46–4+. doi: 10.1126/science.aam7240

Carlson, C. A., del Giorgio, P. A., and Herndl, G. J. (2007). Microbes and the dissipation of energy and respiration: From cells to ecosystems. *Oceanography* 20 (2), 89–100. doi: 10.5670/oceanog.2007.52

Carstensen, J., Andersen, J. H., Gustafsson, B. G., and Conley, D. J. (2014). Deoxygenation of the Baltic Sea during the last century. *Proc. Natl. Acad. Sci. United States America* 111 (15), 5628–5633. doi: 10.1073/pnas.1323156111

Cho, B. C., and Azam, F. (1988). Major role of bacteria in biogeochemical fluxes in the ocean's interior. *Nature* 332, 441–443. doi: 10.1038/332441a0

Couespel, D. , Levy, M., and Bopp, L. (2021). Oceanic primary production decline halved in eddy-resolving simulations of global warming. *Biogeosciences* 18(14), 4321–4349. doi: 10.5194/bg-18-4321-2021

Dang, H. Y. (2020). Grand challenges in microbe-driven marine carbon cycling research. *Front. Microbiol.* 11. doi: 10.3389/fmicb.2020.01039

dBotnia (1994). *dBotnia* (Umeå, Sweden: Umeå Marine sciences Centre).

del Giorgio, P. A., and Duarte, C. M. (2002). Respiration in the open ocean. *Nature* 420 (6914), 379–384. doi: 10.1038/nature01165

del Giorgio, P. A., and Williams, P. (2005). "The global significance of respiration in aquatic ecosystems: from single cells to the biosphere," in *Respiration in aquatic ecosystems.* Eds. P. A. del Giorgio, P. J. Williams and B. Le (Oxford: Oxford University Press), 267–303.

Diaz, R., and Rosenberg, R. (2008). Spreading dead zones and consequences for marine ecosystems. *Science* 321), 926–929. doi: 10.1126/science.1156401

Dickerson, R. E., and Geis, I. (1979). *Chemistry, matter and the universe* (menlo Park, California: Benjamin/Cummings).

Du, J. B., and Shen, J. (2015). Decoupling the influence of biological and physical processes on the dissolved oxygen in the Chesapeake bay. *J. Geophysical Research-Oceans* 120 (1), 78–93. doi: 10.1002/2014jc010422

Duarte, C. M., and Agusti, S. (1998). The CO2 balance of unproductive aquatic ecosystems. *Science* 281 (5374), 234–236. doi: 10.1126/science.281.5374.234

Eilola, K., Meier, H. E. M., and Almroth, E. (2009). On the dynamics of oxygen, phosphorus and cyanobacteria in the Baltic sea; a model study. *J. Mar. Syst.* 75 (1), 163–184. doi: 10.1016/j.jmarsys.2008.08.009

Fender, C. K., Kelly, T. B., Guidi, L., Ohman, M. D., Smith, M. C., and Stukel, M. R. (2019). Investigating particle size-flux relationships and the biological pump across a range of plankton ecosystem states from coastal to oligotrophic. *Front. Mar. Sci.* 6. doi: 10.3389/fmars.2019.00603

Fernandez-Gonzalez, N., Huber, J. A., and Vallino, J. J. (2016). Microbial communities are well adapted to disturbances in energy input. *Msystems* 1 (5). doi: 10.1128/mSystems.00117-16

Forsgren, G., and Jansson, M. (1992). The turnover of river-transported iron, phosphorus and organic carbon in the Öre estuary, northern Sweden. *Hydrobiologia* 235/236, 585–596. doi: 10.1007/BF00026246

Giering, S. L. C., Cavan, E. L., Basedow, S. L., Briggs, N., Burd, A. B., Darroch, L. J., et al. (2020). Sinking organic particles in the ocean-flux estimates from *in situ* optical devices. *Front. Mar. Sci.* 6. doi: 10.3389/fmars.2019.00834

Henson, S. A., Sanders, R., Madsen, E., Morris, P. J., Le Moigne, F., and Quartly, G. D. (2011). A reduced estimate of the strength of the ocean's biological carbon pump. *Geophysical Res. Lett.* 38:1–5. doi: 10.1029/2011gl046735

Hernández-León, S., and Ikeda, T. (2005). "Zooplankton respiration," in *Respiration in aquatic ecosystems*. Eds. P. A. d. Giorgio, P. J. Williams and B. Le (Oxford: Oxford University Press), 57–82.

Hopkinson, C. S., and Smith, E. M. (2005). "Estuarine respiration: an overview of benthic, pelagic and whole system respiration," in *Respiration in aquatic ecosystems*. Eds. P. A. d. Giorgio, P. J. Williams and B. Le (New York: Oxford University Press Inc), 122–146.

Hoppe, H.-G., Breithaupt, P., Wahlter, K., Koppe, R., Bleck, S., Sommer, U., et al. (2008). Climate warming in winter affects the coupling between phytoplankton and bacteria during the spring bloom: a mesocosm study. *Aquat. Microbial Ecol.* 51, 105–115. doi: 10.3354/ame01198

IPCC (2019). "Summary for policymakers," in *IPCC special report on the ocean and cryosphere in a changing climate*. Eds. H.-O. Pörtner, M.-D. D C Roberts, P. V. Zhai, M. Tignor, E. Poloczanska, K. Mintenbeck, M. Nicolai, A. Okem, J. Petzold, B. Rama and N. Weyer(Cambridge, UK and New York, NY, USA: Cambridge University Press).

Jiao, N., Herndl, G. J., Hansell, D. A., Benner, R., Kattner, G., Wilhelm, S. W., et al. (2010). Microbial production of recalcitrant dissolved organic matter: long-term carbon storage in the global ocean. *Nat. Rev. Microbiol.* 8 (8), 593–599. doi: 10.1038/nrmicro2386

Lefevre, D., Bentley, T. L., Robinson, C., Blight, S. P., and Williams, P. J. L. (1994). The temperature response of gross and net community production and respiration in time-varying assemblages of temperate marine micro-plankton. *J. Exp. Mar. Biol. Ecol.* 184 (2), 201–215. doi: 10.1016/0022-0981(94)90005-1

Lemée, R., Rochelle-Newall, E., Van Wambeke, F., Pizay, M. D., Rinaldi, P., and Gattuso, J. P. (2002). Seasonal variation of bacterial production, respiration and growth efficiency in the open NW Mediterranean Sea. *Aquat. Microbial Ecol.* 29 (3), 227–237. doi: 10.3354/ame029227

Lomas, M. W., Glibert, P. M., Shiah, F. K., and Smith, E. M. (2002). Microbial processes and temperature in Chesapeake bay: current relationships and potential impacts of regional warming. *Global Change Biol.* 8 (1), 51–70. doi: 10.1046/j.1365-2486.2002.00454.x

López-Urrutia, A., and Morán, X. A. G. (2007). Resource limitation of bacterial production distorts the temperature dependence of oceanic carbon cycling. *Ecology* 88 (4), 817–822. doi: 10.1890/06-1641

Lopez-Urrutia, A., San Martin, E., Harris, R. P., and Irigoien, X. (2006). Scaling the metabolic balance of the oceans. *Proc. Natl. Acad. Sci. United States America* 103 (23), 8739–8744. doi: 10.1073/pnas.0601137103

Mazuecos, I. P., Aristegui, J., Vazquez-Dominguez, E., Ortega-Retuerta, E., Gasol, J. M., and Reche, I. (2015). Temperature control of microbial respiration and growth efficiency in the mesopelagic zone of the south Atlantic and Indian oceans. *Deep-Sea Res. Part I-Oceanographic Res. Papers* 95, 131–138. doi: 10.1016/j.dsr.2014.10.014

Meier, H. E. M., Andersson, H. C., Eilola, K., Gustafsson, B. G., Kuznetsov, I., Muller-Karulis, B., et al. (2011a). Hypoxia in future climates: A model ensemble study for the Baltic Sea. *Geophysical Res. Lett.* 38. doi: 10.1029/2011gl049929

Meier, H. E. M., Eilola, K., and Almroth, E. (2011b). Climate-related changes in marine ecosystems simulated with a 3-dimensional coupled physical-biogeochemical model of the Baltic Sea. *Climate Res.* 48 (1), 31–55. doi: 10.3354/cr00968

Munson-McGee, J. H., Lindsay, M. R., Sintes, E., Brown, J. M., D'Angelo, T., Brown, J., et al. (2022). Decoupling of respiration rates and abundance in marine prokaryoplankton. *Nature* 612, 764–770. doi: 10.1038/s41586-022-05505-3

Neumann, T., Fennel, W., and Kremp, C. (2002). Experimental simulations with an ecosystem model of the Baltic Sea: A nutrient load reduction experiment. *Global Biogeochemical Cycles* 16 (3). doi: 10.1029/2001gb001450

Norberg, J., and DeAngelis, D. (1997). Temperature effects on stocks and stability of a phytoplankton-zooplankton model and the dependence on light and nutrients. *Ecol. Model.* 95 (1), 75–86. doi: 10.1016/s0304-3800(96)00033-6

Nydahl, A., Panigrahi, S., and Wikner, J. (2013). Increased microbial activity in a warmer and wetter climate enhances the risk of coastal hypoxia. *FEMS Microbiol. Ecol.* 85 (2), 338–347. doi: 10.1111/1574-6941.12123

Olesen, M., Lundsgaard, C., and Andrushaitis, A. (1999). Influence of nutrients and mixing on the primary production and community respiration in the gulf of Riga. *J. Mar. Syst.* 23 (1-3), 127–143. doi: 10.1016/S0924-7963(99)00054-8

Oschlies, A., Brandt, P., Stramma, L., and Schmidtko, S. (2018). Drivers and mechanisms of ocean deoxygenation. *Nat. Geosci.* 11 (7), 467–473. doi: 10.1038/s41561-018-0152-2

Pan, Y., Birdsey, R. A., Fang, J., Houghton, R., Kauppi, P. E., Kurz, W. A., et al. (2011). A Large and persistent carbon sink in the worlds forests. *Science* 333 (6045), 988–993. doi: 10.1126/science.1201609

Panigrahi, S., Nydahl, A., Anton, P., and Wikner, J. (2013). Strong seasonal effect of moderate experimental warming on plankton respiration in a temperate estuarine plankton community. *Estuar. Coast. Shelf Sci.* 135, 269–279. doi: 10.1016/j.ecss.2013.10.029

Pettersson, C., Allard, B., and Boren, H. (1997). River discharge of humic substances and humic-bound metals to the gulf of bothnia. *Estuar. Coast. Shelf Sci.* 44 (5), 533–541. doi: 10.1006/ecss.1996.0159

Pomeroy, L. R., and Wiebe, W. J. (2001). Temperature and substrates as interactive limiting factors for marine heterotrophic bacteria. *Aquat. Microbial Ecol.* 23 (2), 187–204. doi: 10.3354/ame023187

Pomeroy, L. R., Wiebe, W. J., Deibel, D., Thompson, R. J., Rowe, G. T., and Pakulski, J. D. (1991). Bacterial responses to temperature and substrate concentration during the new foundland spring bloom. *Mar. Ecology-Progress Ser.* 75 (2-3), 143–159. doi: 10.3354/meps075143

R_Core_Team (2021). *R: A language and environment for statistical computing* (Vienna, Austria: R Foundation for Statistical Computing).

Rabalais, N. N., Diaz, R. J., Levin, L. A., Turner, R. E., Gilbert, D., and Zhang, J. (2010). Dynamics and distribution of natural and human-caused hypoxia. *Biogeosciences* 7 (2), 585–619. doi: 10.5194/bg-7-585-2010

Reader, H. E., Stedmon, C. A., and Kritzberg, E. S. (2014). Seasonal contribution of terrestrial organic matter and biological oxygen demand to the Baltic Sea from three contrasting river catchments. *Biogeosciences* 11 (12), 3409–3419. doi: 10.5194/bg-11-3409-2014

Reinthaler, T., and Herndl, G. J. (2005). Seasonal dynamics of bacterial growth efficiencies in relation to phytoplankton in the southern north Sea. *Aquat. Microbial Ecol.* 39 (1), 7–16. doi: 10.3354/ame039007

Rivkin, R. B., and Legendre, L. (2001). Biogenic carbon cycling in the upper ocean: Effects of microbial respiration. *Science* 291 (5512), 2398–2400. doi: 10.1126/science.291.5512.2398

Robinson, C. (2000). Plankton gross production and respiration in the shallow water hydrothermal systems of miles, Aegean Sea. *J. Plankton Res.* 22 (5), 887–906. doi: 10.1093/plankt/22.5.887

Robinson, C. (2008). "Heterotrophic bacterial respiration," in *Microbial ecology of the oceans*, *2nd ed*. Ed. D. L. Kirchman (Hoboken: Johan Wiley & Sons, Inc).

Robinson, C. (2019). Microbial respiration, the engine of ocean deoxygenation. *Front. Mar. Sci.* 5. doi: 10.3389/fmars.2018.00533

Robinson, C., and Williams, P. J. L. (1993). Temperature and antarctic plankton community respiration. *J. Plankt. Res.* 15 (9), 1035–1051. doi: 10.1093/plankt/15.9.1035

Robinson, C., Williams, P. J., and Le, B. (2005). "Respiration and it´s measurement in surface marine waters," in *Respiration in aquatic ecosystems*. Eds. P. A. del Giorgio, P. J. Williams and B. Le (Oxford: Oxford University Press), 147–180.

Sandberg, J., Andersson, A., Johansson, S., and Wikner, J. (2004). Pelagic food web and carbon budget in the northern Baltic Sea: potential importance of terrigenous carbon. *Mar. Ecology-Progress Ser.* 268, 13–29. doi: 10.3354/meps268013

Sanders, R. J., Henson, S. A., Martin, A. P., Anderson, T. R., Bernardello, R., Enderlein, P., et al. (2016). Controls over ocean mesopelagic interior carbon storage (COMICS): Fieldwork, synthesis, and modeling efforts. *Front. Mar. Sci.* 3. doi: 10.3389/fmars.2016.00136

Sarmento, H., and Descy, J. P. (2008). Use of marker pigments and functional groups for assessing the status of phytoplankton assemblages in lakes. *J. Appl. Phycology* 20 (6), 1001–1011. doi: 10.1007/s10811-007-9294-0

Sarmento, H., Montoya, J. M., Vazquez-Dominguez, E., Vaque, D., and Gasol, J. M. (2010). Warming effects on marine microbial food web processes: how far can we go when it comes to predictions? *Philos. Trans. R. Soc. B-Biological Sci.* 365 (1549), 2137–2149. doi: 10.1098/rstb.2010.0045

Savchuk, O. P. (2002). Nutrient biogeochemical cycles in the gulf of Riga: scaling up field studies with a mathematical model. *J. Mar. Syst.* 32 (4), 253–280. doi: 10.1016/s0924-7963(02)00039-8

Sherr, E. B., and Sherr, B. F. (1996). Temporal offset in oceanic production and respiration processes implied by seasonal changes in atmospheric oxygen: the role of heterotrophic microbes. *Aquat. Microb. Ecol.* 11, 91–100. doi: 10.3354/ame011091

Smith, E. M., and Kemp, W. M. (1995). Seasonal and regional variations in plankton community production and respiration for Chesapeake bay. *Mar. Ecol. Prog. Ser.* 116, 217–231f. doi: 10.3354/meps116217

Smith, E. M., and Kemp, W. M. (2001). Size structure and the production/respiration balance in a coastal plankton community. *Limnology Oceanography* 46 (3), 473–485. doi: 10.4319/lo.2001.46.3.0473

Smith, E. M., and Kemp, W. M. (2003). Planktonic and bacterial respiration along an estuarine gradient: responses to carbon and nutrient enrichment. *Aquat. Microbial Ecol.* 30 (3), 251–261. doi: 10.3354/ame030251

Smith, T. P., Thomas, T. J. H., García-Carreras, B., Sal, S., Yvon-Durocher, G., Bell, T., et al. (2019). Community-level respiration of prokaryotic microbes may rise with global warming. *Nat. Commun.* 10 (1) 5124. doi: 10.1038/s41467-019-13109-1

Sokal, R. R., and Rohlf, F. J. (1995). *Biometry* (New York: W.H. Freeman and company).

Vazquez-Dominguez, E., Vaque, D., and Gasol, A. M. (2007). Ocean warming enhances respiration and carbon demand of coastal microbial plankton. *Global Change Biol.* 13 (7), 1327–1334. doi: 10.1111/j.1365-2486.2007.01377.x

Verma, A., Amnebrink, D., Pinhassi, J., and Wikner, J. (2022). Prokaryotic maintenance respiration and growth efficiency field patterns reproduced by temperature and nutrient control at mesocosm scale. *Environ. Microbiol.*, 1–17. doi: 10.1111/1462-2920.16300

Vikström, K., Bartl, I., Karlsson, J., and Wikner, J. (2020). Strong influence of baseline respiration in an oligotrophic coastal ecosystem. *Front. Mar. Sci.* 7 (839). doi: 10.3389/fmars.2020.572070

Vikström, K., and Wikner, J. (2019). Importance of bacterial maintenance respiration in a subarctic estuary: a proof of concept from the field. *Microbial Ecol.* 77 (3), 574–586. doi: 10.1007/s00248-018-1244-7

Vosjan, J. H., and Olanczukneyman, K. M. (1991). Influence of temperature on respratory ETS-activity of microorganisms from admirality bay, king George island, Antarctica. *Netherlands J. Sea Res.* 28 (3), 221–225. doi: 10.1016/0077-7579(91)90019-W

Voss, M., Asmala, E., Bartl, I., Carstensen, J., Conley, D. J., Dippner, J. W., et al. (2021). Origin and fate of dissolved organic matter in four shallow Baltic Sea estuaries. *Biogeochemistry* 154 (2), 385–403. doi: 10.1007/s10533-020-00703-5

White, P. A., Kalff, J., Rasmussen, J. B., and Gasol, J. M. (1991). The effect of temperature and algal biomass on bacterial production and specific growth rate in freshwater and marine habitats. *Microb. Ecol.* 21, 99–118. doi: 10.1007/BF02539147

Wikner, J., and Andersson, A. (2012). Increased freshwater discharge shifts the trophic balance in the coastal zone of the northern Baltic Sea. *Global Change Biol.* 18 (8), 2509–2519. doi: 10.1111/j.1365-2486.2012.02718.x

Wikner, J and K., and Vikström, K. (2023). Extensive prokaryotic maintenance respiration in the sea influenced by osmoregulation. *Frontiers in Marine Science, in press.*

Williams, P. J., and Le, B. (1998). The balance of plankton respiration and photosynthesis in the open oceans. *Nature* 394 (6688), 55–57. doi: 10.1038/27878

Williams, P. J., Le, B., and del Giorgio, P. A. (2005). *Respiration in aquatic ecosystems* (Oxford: Oxford University Press).

Williams, P. J., Le, B., Morris, P. J., and Karl, D. M. (2004). Net community production and metabolic balance at the oligotrophic ocean site: Station ALOHA. *Deep-Sea Res. Part I* 51 (1), 1563–1578. doi: 10.1016/j.dsr.2004.07.001

Wohlers, J., Engel, A., Zollner, E., Breithaupt, P., Jurgens, K., Hoppe, H. G., et al. (2009). Changes in biogenic carbon flow in response to sea surface warming. *Proc. Natl. Acad. Sci. United States America* 106 (17), 7067–7072. doi: 10.1073/pnas.0812743106

Zhang, J., Gilbert, D., Gooday, A. J., Levin, L., Naqvi, S. W. A., Middelburg, J. J., et al. (2010). Natural and human-induced hypoxia and consequences for coastal areas: synthesis and future development. *Biogeosciences* 7 (5), 1443–1467. doi: 10.5194/bg-7-1443-2010

frontiers | Frontiers in Marine Science

TYPE Review
PUBLISHED 15 March 2023
DOI 10.3389/fmars.2023.1101855

OPEN ACCESS

EDITED BY
Agneta Andersson,
Umeå University, Sweden

REVIEWED BY
Juan Andrés López,
University of Alaska Fairbanks,
United States
Anders Frugård Opdal,
University of Bergen, Norway

*CORRESPONDENCE
Leif Andersson
leif.andersson@imbim.uu.se

SPECIALTY SECTION
This article was submitted to
Global Change and the Future Ocean,
a section of the journal
Frontiers in Marine Science

RECEIVED 18 November 2022
ACCEPTED 23 February 2023
PUBLISHED 15 March 2023

CITATION
Andersson L, André C, Johannesson K
and Pettersson M (2023) Ecological
adaptation in cod and herring and
possible consequences of future
climate change in the Baltic Sea.
Front. Mar. Sci. 10:1101855.
doi: 10.3389/fmars.2023.1101855

Ecological adaptation in cod and herring and possible consequences of future climate change in the Baltic Sea

Leif Andersson[1,2*], Carl André[3,4], Kerstin Johannesson[3,4] and Mats Pettersson[1]

[1]Department of Medical Biochemistry and Microbiology, Uppsala University, Uppsala, Sweden, [2]Department of Veterinary Integrative Biosciences, Texas A&M University, College Station, TX, United States, [3]Department of Marine Sciences-Tjärnö, Göteborg University, Strömstad, Sweden, [4]Centre for Marine Evolutionary Biology, University of Gothenburg, Gothenburg, Sweden

The Atlantic herring and Atlantic cod are two marine fish species that have successfully adapted to the brackish Baltic Sea, and the former is able to spawn in near-freshwater conditions in the inner Gulf of Bothnia. Here, we review the state of current knowledge concerning ecological adaptation in the two species and make an attempt to predict how they will be able to cope with future climate change. Previous whole genome sequencing studies in Atlantic herring have revealed hundreds of genetic loci underlying ecological adaptation, including several loci that show very strong associations to variation in salinity and temperature. These results suggest the existence of standing genetic variation available for adaptation to a changing environment. However, although Atlantic herring probably has the genetic potential to adapt, its future status also depends on how climate change will affect plankton production and competing species, such as sprat and three-spined stickleback. In cod, the situation is challenging, as there is only one true Baltic population, spawning east of Bornholm and then dispersing towards the east and north. This Baltic cod population is threatened by overfishing, low oxygen levels in benthic waters and generally bad physiological condition of individual fish, in addition to being completely isolated from gene flow from nearby cod populations at the entrance of the Baltic Sea.

KEYWORDS

Atlantic herring, Atlantic cod, genetic adaptation, climate change, Baltic Sea

1 Introduction

The brackish Baltic Sea is a challenging environment for marine fish, and few marine species have been able to successfully colonize this body of water. Surface salinity drops from 35‰ in the Atlantic Ocean to about 8‰ in the Southern Baltic Sea, and to as low as 2-3‰ in the inner Gulf of Bothnia. Furthermore, the amplitude in temperature variation over the year is higher than in the Atlantic Ocean (Snoeijs-Leijonmalm et al., 2017). Major

anthropogenic impacts on the Baltic Sea ecosystem are eutrophication, leading to algal blooms and hypoxia in certain areas, pollution (dioxin, dioxin-like compounds, and other persistent organic pollutant), and climate change (Snoeijs-Leijonmalm et al., 2017). Climate predictions indicate drastic changes during this century with increasing temperature, lower salinity, and less ice coverage in the winter (Reusch et al., 2018).

The Atlantic herring (*Clupea harengus*) and Atlantic cod (*Gadus morhua*) are two of the most important marine fish that have been able to adapt to the brackish environment in the Baltic Sea (Ojaver et al., 2010). Linnaeus classified the Baltic herring as a subspecies of the Atlantic herring based on its distinct phenotype (small size, reduced fat content compared with Atlantic herring) and named it *Clupea harengus membras* (Linnaeus, 1761). Also, the Atlantic cod present in the Baltic Sea may be considered a distinct subspecies with specific adaptation to the Baltic Sea (Linnaeus, 1761). Both species have been subjected to detailed genetic studies in recent years, which have revealed many of the genes and genomic regions that have contributed to their genetic adaptation. The aim of this review is to summarize the current knowledge of genetic adaptation to the environmental conditions in the Baltic Sea as a basis to speculate how climate change may affect these species.

1.1 Population structure and ecological adaptation in the Atlantic herring

The Atlantic herring has a key ecological role in the North Atlantic Ocean and adjacent waters. It feeds on plankton and thereby constitutes a link between the primary production in the ocean and other fish, including cod, sea birds, and marine mammals that feed on herring (Ojaver et al., 2010). Herring has also been a critical food resource for humans for at least a thousand years (Atmore et al., 2022). It is a benthic spawner that utilizes fully marine environments (35-36‰) as well as brackish environments, including the entire Baltic Sea. Early genetic studies using a handful of biochemical polymorphisms revealed no significant genetic differentiation among populations even between population samples from full marine environments to the inner Gulf of Bothnia (Ryman et al., 1984). This surprising finding was resolved when it became possible to screen large numbers of genetic markers including the sequencing of the entire genome (Lamichhaney et al., 2012; Martinez Barrio et al., 2016; Pettersson et al., 2019; Han et al., 2020). These later studies revealed that there is almost no genetic differentiation at the great majority (>90%) of single nucleotide polymorphisms (SNPs) but highly significant differentiation, often approaching fixation of alternative alleles, between subpopulations for a few percent of the polymorphic sites. The very low genetic differentiation at selectively neutral loci can be explained by the very large population size and some gene flow between subpopulations, resulting in negligible genetic drift. In contrast, natural selection, fueled by the same large population size, is causing striking genetic differentiation at loci underlying ecological adaptation. Thus, whole genome sequencing reveals a considerable degree of local adaptation (Han et al., 2020), in total contrast to the previous results based on a handful of selectively neutral markers. The Atlantic herring data demonstrate that for marine species with large breeding populations, it is essential to study the entire genome to get full insight about population structure and to reveal the genetic markers that confer the most power to distinguish different subpopulations.

Whole genome sequencing has revealed about ten major groups of Atlantic herring that constitute ecotypes genetically adapted to different environmental conditions (Han et al., 2020) (Figure 1). The three major factors distinguishing these ecotypes are (i) spawning time (primarily spring or autumn); (ii) salinity at spawning locations; (iii) water temperature at spawning locations. However, it is clear that there is further genetic differentiation within the major groups. For instance, the spring-spawning herring from the region between the North Sea and the Baltic Sea proper – i.e., the transition zone with a steep salinity gradient – includes genetically differentiated subpopulations. The exact number of subpopulations within the major groups is unknown and it is likewise not known to which extent local populations are isolated from other local populations within the same major group.

1.1.1 Genetic adaptation to low salinity

Difference in salinity is a major environmental factor affecting ecological adaptation in herring. Previous data show that it is the salinity at spawning locations that is more important for local adaptation than salinity at feeding (Han et al., 2020). One example of this is a population spawning under brackish conditions in the Ringköbing fjord (Denmark) but which is feeding under fully marine conditions in the North Sea. This population shows allele frequency patterns shared with other populations spawning in brackish waters (Han et al., 2020). Whole genome sequencing has revealed hundreds of gene regions showing strong genetic differentiation between populations from the Atlantic Ocean and

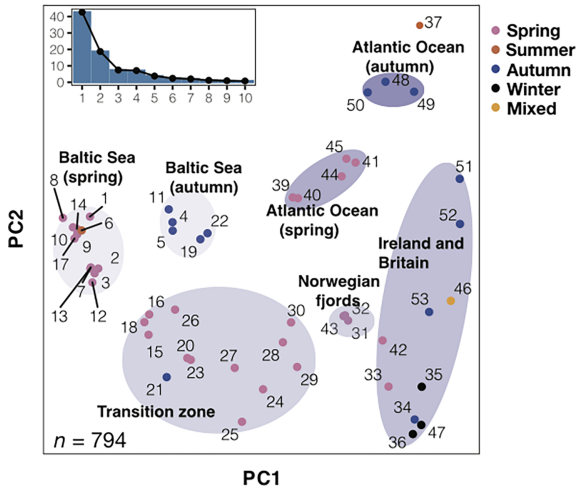

FIGURE 1
Principal component analysis (PCA) of herring populations. PCA based on 794 highly informative markers representing loci likely under natural selection. Color of each population represents spawning season. Inset bar plot indicates the percentage of explained variance by each principal component. *n* = number of SNPs used in the analysis. Adapted from Han et al., 2020, Figure 2.

the brackish Baltic Sea (Han et al., 2020). Some of these are expected to directly affect osmoregulation and two examples of top candidate genes are *LRRC8C* and *PRLR*. *LRRC8C* encodes a volume-regulated ion channel (VRAC) with an important role in osmoregulation in all vertebrates. Members of this family of ion channels are activated when the cell swells and play a key role in cell volume regulation (Osei-Owusu et al., 2018). The most common *LRRC8C* allele present in populations from the Atlantic Ocean differs by four amino acid substitutions from the most common allele in the brackish Baltic Sea (Han et al., 2020) (Figure 2). Interestingly, an intermediate form having two of these substitutions is the most common allele in some populations from the transition zone between the Atlantic Ocean and the Baltic Sea (Figure 2), suggesting that this gene shows a step-wise evolutionary adaptation to low salinity.

Prolactin is best known for its crucial role for lactation in mammals. However, in fish it is well established that prolactin plays a key role in osmoregulation (Manzon, 2002). The *PRLR* gene encodes the receptor of prolactin and the locus shows a very strong signature of selection in relation to adaptation to the brackish Baltic Sea (Han et al., 2020). It is not yet known if this is caused by changes in the protein sequence or in gene regulation.

1.1.2 Genetic adaptation to variation in water temperature

With regard to the ability of the Atlantic herring to adapt to variation in water temperature, insights primarily come from a comparison of allele frequencies in herring spawning in the waters around Great Britain and Ireland with those spawning further north in the Atlantic (Norway, Iceland, Greenland, and Canada) (Han et al., 2020). In this comparison, there are essentially no differences in salinity between regions, but a clear difference in water temperatures; the waters around Ireland and Great Britain are among the warmest where herring reproduction takes place. This

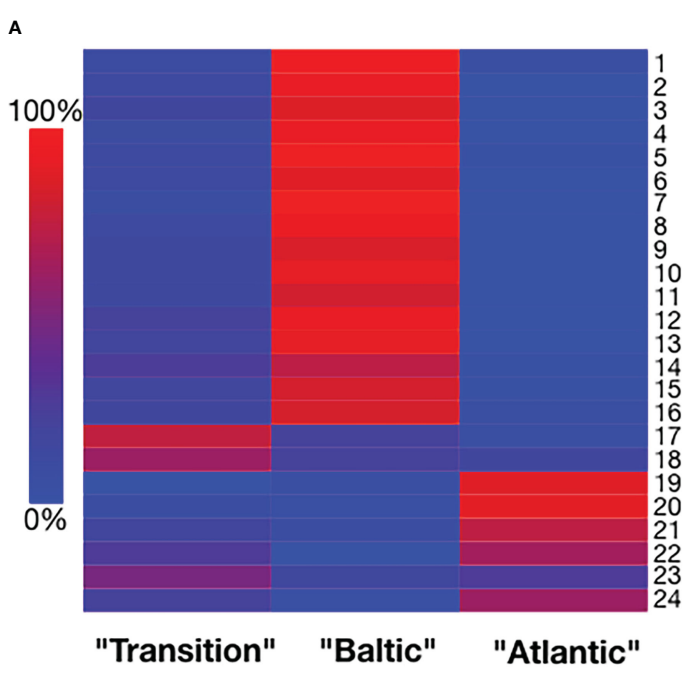

C

	Amino acid position			
	25	242	440	506
Atlantic	D	T	E	E
Transition	D	M	E	K
Baltic	E	M	K	K

FIGURE 2
The frequencies of *LRRC8C* alleles show strong correlation with salinity. **(A)** Heatmap of the frequencies of the three *LRRC8C* alleles. Column labels are colloquial names for the common alleles based on their most prevalent location. Samples were collected and genotyped in the collaborative "Forskarhjälpen" project presented in Pettersson et al. (2019). Each row refers to a population sample (numbered 1-24) collected by one participating school and ordered by geographical location (see panel **B**). Color indicates allele frequency. **(B)** Geographical presentation of the frequency of the Baltic allele (color code for allele frequency the same as in **(A)**. Sample labels correspond to **(A)** Sample (1) lacks a reported location, and is omitted. **(C)** Amino acid residues for the three alleles at the variable positions.

analysis revealed about ten loci with very strong genetic differentiation between the British Isles and northern Atlantic groups (Han et al., 2020) (Figure 3). Interestingly, four of these represent inversions present on chromosome 6, 12, 17, and 23, and ranging in size from 1.2 Mb to 7.8 Mb. Due to the distribution pattern, the two alternate haplotypes at these four inversions are referred to as "Northern" and Southern" and the relative frequencies of the haplotypes at all four show a strong correlation with water temperature at the spawning location. However, it has not yet been proven whether the genetic adaptations at these loci are directly related to water temperatures or to other environmental factors strongly correlated with temperature. Nevertheless, these are obvious candidate loci that may contribute to genetic adaptation to the ongoing climate change.

In the Baltic Sea, the Northern haplotypes are the most common variants at all four inversions, but the Southern haplotypes are also present (Han et al., 2020). This is illustrated for the chromosome 12 inversion in Figure 4. For instance, the Northern haplotype at this locus had a frequency of 94% in a sample from Kalix (BK in Figure 4) while the frequency is about 70% in the Southern Baltic Sea. An interesting finding is that a population sampled from Gamlebyviken (BG in Figure 4) collected on August 20 1979 by one of the authors (LA) had the lowest frequency of the Northern haplotype among all samples from the Baltic Sea. Gamlebyviken is a shallow bay on the east coast of Sweden and it was sampled because it was claimed that it holds a unique local population of Baltic herring. The unusually high frequency of the

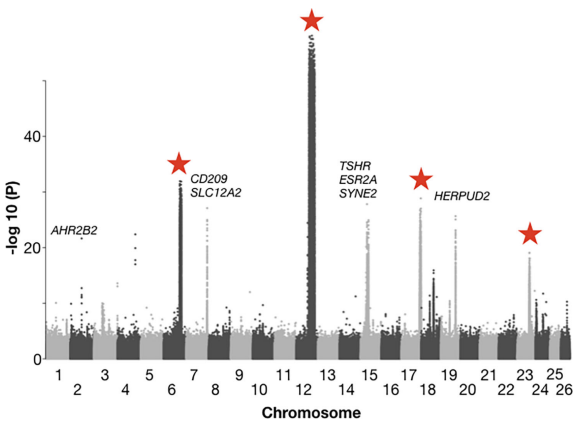

FIGURE 3
Genetic differentiation between herring populations from Ireland and Britain vs. other populations from the Northeast Atlantic. Inversions are located on chromosomes 6, 12, 17, and 23, and are highlighted with red stars. Strong genetic differentiation is observed in the following intervals: chromosome 6: 22.2 – 24.8 Mb, chromosome 12: 17.8 – 25.6 Mb, chromosome 17: 25.8 – 27.5 Mb, and chromosome 23: 16.3 – 17.5 Mb. The Y-axis represents -log10 of the probability (*P*) value in a chi square test per SNP testing the null hypothesis of no allele frequency differences between regions. The following genes associated with genetic differentiation are highlighted: *AHR2B2*, aryl hydrocarbon receptor 2B2; *CD209*, CD209 antigen-like protein; *SLC12A2*, solute carrier family 12 member 2; *TSHR*: thyroid stimulating hormone receptor; *ESR2A*, estrogen receptor 2A; *SYNE2*, spectrin repeat containing nuclear envelope protein 2; *HERPUD2*, HERPUD family member 2. Adapted from Han et al., 2020, Figure 4.

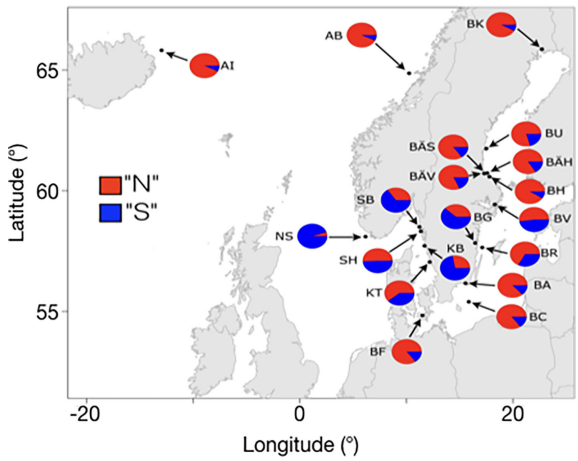

FIGURE 4
Estimated frequencies for the "Northern" and "Southern" haplotypes for the inversion on chromosome 12 in pooled population samples in the Baltic Sea and East Atlantic. Adapted from Pettersson et al., 2019, Figure 6.

Southern haplotype at the chromosome 12 inversion supports this assumption, and highlights the importance of local adaptation of the Atlantic herring in general. It is reasonable to assume that the water in this shallow bay warms up faster in the spring, which is favorable for the fitness of herring carrying the Southern haplotype, a haplotype strongly associated with warm water temperatures at spawning.

1.1.3 Genetic adaptation to altered light conditions in the Baltic Sea

Another gene underlying adaptation to the Baltic Sea is *RHO* encoding rhodopsin, one of the light receptors in the retina of the eye. Hill et al. (2019) demonstrated that a missense mutation (Phe261Tyr) in this gene is absent from Atlantic herring from fully marine environments with a salinity of 35-36‰ but occurs at high frequency throughout the Baltic Sea and is fixed in the inner Baltic Sea. The mutation is expected to cause a red shift in light absorption providing better vision in the brackish Baltic Sea. The light conditions in the Baltic Sea are red-shifted because blue light tends to be absorbed by dissolved organic carbon in the water (Kratzer and Moore, 2018). Interestingly, exactly the same mutation is present in one third of all fish species living in freshwater or brackish waters (Hill et al., 2019), providing a textbook case of convergent evolution.

1.1.4 Why do Atlantic herring show so much genetic differentiation at some loci but essentially no genetic differentiation at neutral loci?

Herring populations spawn under widely different environmental conditions, with regard to salinity, temperature, water depth, light conditions, and biotic factors (prey and predators). This means that the most sensitive phase of life, embryonic and larval development, takes place under drastically different constraints. This has promoted a homing behavior that is a

prerequisite for local genetic adaptation. Indeed, local adaptation in the Baltic Sea is known from a number of other marine fish that also spawn in various coastal or freshwater habitats, such as, cod, plaice, flounder, and stickleback (DeFaveri and Merilä, 2014; Berg et al., 2015; Momigliano et al., 2018; Le Moan et al., 2021). In contrast, the situation is totally different in the European eel, where the entire population spawns in one location, the Sargasso Sea.

Consequently, the eel constitutes a single panmictic population that shows no genetic differentiation between geographic regions (Enbody et al., 2020). This is the situation despite the fact that eels spend most of their adult life under highly variable environmental conditions across Europe and North Africa, but spawning and early development take place under nearly identical conditions in the Sargasso Sea. The homing behavior in the Atlantic herring is not perfect which means that there is some gene flow between subpopulations. Such gene flow combined with the very large size of herring populations is a reasonable explanation for the minute genetic drift in the Atlantic herring and the lack of genetic differentiation at selectively neutral loci. The distribution of F_{ST}-values in the Atlantic herring with a sharp contrast between strong genetic differentiation at a few percent of the loci and no genetic differentiation at the great majority of loci constitutes a major deviation from the one expected for selectively neutral alleles under a drift model (Lamichhaney et al., 2017). The most plausible explanation for this deviation is that the strong genetic differentiation at some loci is due to natural selection.

1.2 The isolated cod population in the Baltic Sea

Atlantic cod is, like herring, an important commercial fish species. It is distributed across the North Atlantic and occurs up to the Bothnian Sea in the Baltic. There are at least two genetically distinct populations of cod in the Baltic Sea: one large population east of Bornholm, and one or several smaller populations that spawn in the western Baltic Sea (Hemmer-Hansen et al., 2019; Weist et al., 2019). Currently, it is believed that the eastern Baltic cod only spawn in the Bornholm deep, and that historical spawning areas in the Gotland and Gdansk deep are now too oxygen-depleted for successful spawning (Köster et al., 2017). The eastern Baltic cod population is adapted to the brackish environment and genetically distinct from the adjacent cod populations in the western Baltic, Belt seas, Öresund, and Kattegat. Adaptations include differences in hemoglobin type, osmoregulatory capacity, egg buoyancy, sperm swimming characteristics, and spawning season. All these adaptations to the brackish environment contribute to an effective reproductive barrier between the eastern and western Baltic cod. SNP genotyping (Berg et al., 2015) and whole genome sequencing (Barth et al., 2019) show that the divergence of eastern Baltic cod is genome wide, indicative of genetic drift in a reproductively isolated population, in addition to specific genetic regions under selection (Figure 5). In contrast, a comparison of cod from Kattegat and the North Sea shows a few regions of strong genetic differentiation most likely underlying genetic adaptation (Figure 5). The reproductive isolation of eastern Baltic cod may be regarded as ongoing ecological speciation.

Successful spawning of Baltic cod is restricted to a layer of water in the Bornholm deep, which has high enough salinity to allow the cod eggs to be neutrally buoyant, while still above critical oxygen levels (Nissling et al., 1994). Experimental studies show that a salinity of ≥ 11‰ and oxygen content above 2 ml O_2 l^{-1} are required for successful fertilization of cod eggs, and that the salinity of neutral buoyancy vary between 10-16‰ (Vallin and Nissling, 2000). Eastern Baltic cod produce larger and lighter eggs compared to cod in the western Baltic (Nissling et al., 1994; Thorsen et al., 1996; Nissling and Westin, 1997), that are neutral buoyant at a lower salinity. Baltic cod also produce sperm that are actively swimming at low salinities (Westin and Nissling, 1991).

Eastern Baltic cod spawn later in the season, in May-August, compared to western Baltic cod that spawn in February-April (Poulsen, 1931; Brander, 2005). This temporal difference likely constitutes an effective barrier to reproduction and gene exchange. However, range expansion and mechanical mixing in the Arkona basin occur regularly (Hemmer-Hansen et al., 2019; Schade et al., 2022), while hybridization seems to be rare.

1.2.1 Genetic adaptation in cod to the Baltic Sea environment

Genome scan studies have detected several regions in the genome of eastern Baltic cod associated with salinity and oxygen conditions at spawning depth (Berg et al., 2015). Most of these

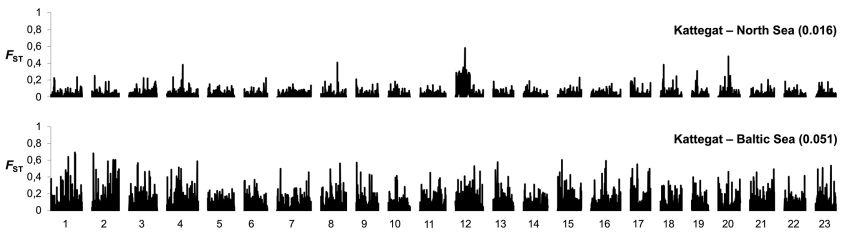

FIGURE 5
Genome-wide differentiation (F_{ST}) in cod based on 8,309 SNPs across all 23 chromosomes in comparisons of cod from Kattegat and North Sea (top) and cod from eastern Baltic Sea and Kattegat (bottom). Median F_{ST} estimates in the two pairwise comparisons are denoted in parentheses. Adapted from Berg et al., 2015, Figure 2.

genomic regions also contain outlier loci, within or close to genes, with high divergence between eastern and western Baltic cod. Several of these candidate genes for selection are known to be involved in fish egg development. One notable example is SNP outlier loci located close to the aquaporin gene, *AQP1A*. The hydration of fish eggs making them larger and lighter, is thought to be governed by water channels or aquaporins (Fabra et al., 2005; Cerdà et al., 2013). Other genes under selection in Baltic cod are members of the solute carrier gene family (SLCs) involved in ion transport, important for egg development. Vitellogenin is involved in hydrolysis of yolk proteins, which produce free amino acids affecting water flux in the egg. Vitellogenin is also important for egg chorion thickness, which is thinner in Baltic cod eggs (Nissling et al., 1994). If a female of western Baltic origin spawns in the Bornholm deep, the eggs will sink down to the anoxic layer and not survive.

Fertilization of eggs is also challenging at low salinity. Baltic cod harbor outlier loci in the vicinity of the zona pellucida glycoprotein-2 gene (*ZP2L1*) on chromosome 8, possibly involved in sperm binding. Other fish species, such as sand goby, show sperm adaptation to low salinity in Baltic populations (Leder et al., 2021).

Osmoregulation and ion exchange in cod larvae, juveniles and adults are controlled by the expression of different enzymes, such as Na^+/K^+-ATPase. Both differential gene expression (Larsen et al., 2011) and signals of selection (Berg et al., 2015) on Na^+/K^+-ATPase genes have been detected in Baltic cod. A SNP located close to the *PRL* gene, coding for prolactin, another protein important for water and salt balance, also show strong environmental correlation in Baltic cod (Berg et al., 2015; Weist et al., 2019). Interestingly and as mentioned above, the gene (*PRLR*) encoding the receptor of prolactin shows a very strong genetic differentiation between Atlantic and Baltic herring (Han et al., 2020).

Already in the early 1960ies, Knud Sick reported a two-allele system with three different hemoglobin genotypes for Atlantic cod, where one allele (HbI-2) was almost fixed in Baltic cod (Sick, 1961). The HbI-2 allele is also dominating in cod populations in colder waters in the North Atlantic. Experimental studies have later shown that oxygen uptake is more efficient at low temperature in fish with the HbI-2 allele (reviewed in Andersen, 2012). Molecular and structural studies have revealed that two non-synonymous mutations in the Hemoglobin beta 1 gene are associated with two amino acid substitutions, Met55Val and Lys62Ala, where the Val-Ala variant corresponds to the HbI-2 allele (Andersen et al., 2009). Several population surveys have identified hemoglobin as a strong genetic outlier between eastern and western Baltic cod (e.g., Weist et al., 2019).

Recent studies show that local adaptation to different environments have been facilitated by chromosomal inversions in the Atlantic cod genome (Matschiner et al., 2022; Sodeland et al., 2022). These inverted chromosomal regions act as supergenes, where multiple neighboring genes are inherited together. Four major supergenes have been identified in Atlantic cod, occurring in different frequencies in different cod populations. Genes involved in adaptation to low salinity in the Baltic are located in inversions on chromosome 2 and 12 (Berg et al., 2015; Barth et al., 2019; Matschiner et al., 2022).

1.3 Can we predict how climate change will affect the herring and cod populations in the Baltic Sea?

As the genetic data for herring and cod clearly show, Baltic populations of these two species are specifically adapted to the Baltic Sea, a marginal marine environment. Increased stress from climate changes will put further pressure on both species. Moreover, the Baltic Sea is an isolated marine basin with narrow openings to the North Sea through the shallow Danish Straits. Consequently, sea warming is more severe and much faster in the Baltic Sea than in the open oceans (Reusch et al., 2018). Currently, the ongoing change in sea surface temperature is about 0.5°C per decade and the average temperature is currently 1.5°C higher than it was 40 years ago (Snoeijs-Leijonmalm et al., 2017). Due to increased precipitation, the salinity is also predicted to decrease in the Baltic Sea (Kniebusch et al., 2019) where most marine species already have adapted to truly marginal levels of salinity (Johannesson and André, 2006; Johannesson et al., 2020). In Atlantic herring, a number of genetic variants show strong correlation with water temperature at spawning (e.g., four inversions) (Han et al., 2020). These will most likely change in frequency in response to increasing temperature. Such a genetic shift might progress smoothly, if the effective sizes of individual subpopulations are large (as is the case in natural populations of herring). However, fishing pressure on the Baltic herring is currently strong and size distributions skewed towards smaller fish (Anonymous, 2021). Furthermore, it is unclear how the current fishing pressure affects local subpopulations, as there is no monitoring at the level of subpopulation. Specific subpopulations, such as the one in Gamlebyviken, may be instrumental to a rapid shift and will be less stressed than other populations by selective mortality as a consequence of increased temperature. From historical samples from the last hundred years, it would be possible to determine the genetic consequences of the current increase of temperature of about 1.5°C.

What appear as additionally problematic for the survival of the Baltic herring is what happens to the ecosystem, not least to the zooplankton communities. For example, in different regions of the Baltic Sea the numbers of three-spined stickleback have increased between 4-fold and 45-fold over the past 35 years, and its predation on fish egg, fish larvae, and zooplankton impacts substantially coastal and open sea food webs (Bergström et al., 2015). Sprat (*Sprattus sprattus*) largely overlaps with herring in distribution in the Baltic Sea and the two species compete for food by targeting the same species of zooplankton, a competition that has increased in intensity with increasing numbers of Baltic sprat (Möllman et al., 2004; Casini et al., 2010). It is unclear how increasing temperature and possibly lower salinity will affect sprat populations in the Baltic. Finally, bladderwrack (*Fucus vesiculosus*) and eelgrass (*Zostera marina*) are important spawning habitats for Baltic herring, and model predictions for the bladderwrack show that it will likely go locally extinct in most of the Baltic Sea over the coming 50-100 years due to increased temperature and reduced salinity (Jonsson et al., 2018; Kotta et al., 2019).

The situation for the isolated eastern cod population is strongly related to the situation of its spawning ground east of the island

Bornholm. The semi-pelagic spawning of the eastern cod is depending on correct buoyancy of the eggs that should neither float, nor sink to the bottom. The Baltic cod has eggs with a buoyancy adapted to the lower salinity of the deep Baltic Sea (Nissling and Westin, 1997). It is furthermore, depending on oxygen in the bottom waters, both for the survival of the eggs and for feeding on benthic invertebrates. Over the past century the area of deep benthic habitat that has become hypoxic inside the Baltic Sea has increased multifold (Reusch et al., 2018). However, data indicate that the hydrographic conditions has remained relatively unchanged in the important cod spawning grounds east of Bornholm the last 60 years (Svedäng et al., 2022). Finally, the cod stock has been heavily depleted by a too intense commercial fishing in the past and today it is in a very poor condition, despite low fishing pressure (ICES, 2021). As cod is also a coldwater species (Asgeirsson et al., 1989), increasing temperatures will put further stress and induce selective mortality, and there is a large risk of local extinction of the Baltic cod east of Bornholm in the near future, partly as a consequence of its complete isolation to other cod stocks (Hemmer-Hansen et al., 2019).

1.4 How can we monitor genetic changes over time?

Genetic studies in Atlantic herring and cod have revealed many genes and genomic regions associated with ecological adaptation. It is now straightforward to set up diagnostic tests to monitor genetic changes at these loci. This can for instance be carried out using so called SNP chips that is a cost-effective way to generate genotypes for many individuals for thousands of SNPs. A fish multi-species SNP chip providing data on thousands of SNPs per species has recently become commercially available (https://www.identigen.com/DnaTraceback/Seafood; accessed November 3, 2022). SNPs for the following species are available on this chip: Atlantic herring, Atlantic horse mackerel, Brown trout, Atlantic cod, Perch, Salmon, and Sprat. This is a valuable resource for many types of population studies, including to monitor stock development as a basis for maintaining genetic diversity and promote sustainable fishery. Careful fishery management is expected to be even more important in the future to avoid population collapse due to the combined effects of climate change and intensive commercial fishing.

The already established genetic markers associated with temperature adaptation, such as the chromosome 12 inversion in the Atlantic herring, that is likely to contribute to the response to future climate changes, should be included in such genetic monitoring. However, it will also be wise to explore genetic changes across the entire genome at regular intervals, on the order once per decade, because new loci may come under selection as the environmental conditions become more extreme. Furthermore, new mutations contributing to genetic adaptation may emerge and need to be included in updated panels of diagnostic genetic markers used for monitoring.

Author contributions

All authors listed have made a substantial, direct, and intellectual contribution to the work and approved it for publication.

Funding

LA's research group is funded by Forskningsrådet (2017-02907) and Knut and Alice Wallenberg Foundation (KAW 2016.0361).

Acknowledgments

CA and KJ acknowledge support from the Linnaeus Centre for Marine Evolutionary Biology, CeMEB.

Conflict of interest

The authors declare that the research was conducted in the absence of any commercial or financial relationships that could be construed as a potential conflict of interest.

Publisher's note

All claims expressed in this article are solely those of the authors and do not necessarily represent those of their affiliated organizations, or those of the publisher, the editors and the reviewers. Any product that may be evaluated in this article, or claim that may be made by its manufacturer, is not guaranteed or endorsed by the publisher.

References

Andersen, Ø. (2012). Hemoglobin polymorphism in atlantic cod – a review of 50 years of study. *Mar. Genomics* 8, 59–65.

Andersen, O., Wetten, O. F., De Rosa, M. C., Andre, C., Carelli Alinovi, C., Colafranceschi, M., et al. (2009). Haemoglobin polymorphisms affect the oxygen-binding properties in atlantic cod populations. *Proc. Biol. Sci.* 276, 833–841.

Anonymous (2021). "Fisk- och skaldjursbestånd i hav och sötvatten 2020. havs och vattenmyndigheten," in *Swedish Agency for marine and water management report*, vol. 2021. (Swedish), 6.

Asgeirsson, B., Fox, J. W., and Bjarnason, J. B. (1989). Purification and characterization of trypsin from the poikilotherm *Gadus morhua*. *Eur. J. Biochem.* 180, 85–94.

Atmore, L. M., Martinez-Garcia, L., Makowiecki, D., André, C., Lougas, L., Barrett, J. H., et al. (2022). Population dynamics of Baltic herring since the Viking age revealed by ancient DNA and genomics. *Proc. Natl. Acad. Sci. U.S.A.* 119, e2208703119.

Barth, J. M., Villegas-Ríos, D., Freitas, C., Moland, E., Star, B., André, C., et al. (2019). Disentangling structural genomic and behavioural barriers in a sea of connectivity. *Mol. Ecol.* 28, 1394–1411.

Berg, P. R., Jentoft, S., Star, B., Ring, K. H., Knutsen, H., Lien, S., et al. (2015). Adaptation to low salinity promotes genomic divergence in Atlantic cod (*Gadus morhua* l.). *Genome Biol. Evol.* 7, 1644–1663.

Bergström, U., Olsson, J., Casini, M., Eriksson, B. K., Fredriksson, R., Wennhage, H., et al. (2015). Stickleback increase in the Baltic Sea – a thorny issue for coastal predatory fish. *Estuarine Coast. shelf Sci.* 163, 134–142.

Brander, K. (2005). Spawning and life history information for north Atlantic cod stocks. *ICES Coop Res. Rep.* doi: 10.17895/ices.pub.5478

Casini, M., Bartolino, V., Molinero, J. C., and Kornilovs, G. (2010). Linking fisheries, trophic interactions and climate: Threshold dynamics drive herring clupea harengus growth in the central Baltic Sea. *Mar. Ecol. Prog. Ser.* 413, 241–252.

Cerdà, J., Zapater, C., Chauvigné, F., and Finn, R. N. (2013). Water homeostasis in the fish oocyte: New insights into the role and molecular regulation of a teleost-specific aquaporin. *Fish Physiol. Biochem.* 39, 19–27.

DeFaveri, J., and Merilä, J. (2014). Local adaptation to salinity in the three-spined stickleback? *J. Evolutionary Biol.* 27, 290–302.

Enbody, E. D., Pettersson, M. E., Sprehn, C. G., Palm, S., Wickström, H., and Andersson, L. (2020). Ecological adaptation in European eels is based on phenotypic plasticity. *Proc. Natl. Acad. Sci. U.S.A.*, 118, e2022620118.

Fabra, M., Raldúa, D., Power, D. M., Deen, P. M. T., and Cerdà, J. (2005). Marine fish egg hydration is aquaporin-mediated. *Science* 307, 545.

Han, F., Jamsandekar, M., Pettersson, M. E., Su, L., Fuentes-Pardo, A. P., Davis, B. W., et al. (2020). Ecological adaptation in Atlantic herring is associated with large shifts in allele frequencies at hundreds of loci. *eLife* 9, e61076.

Hemmer-Hansen, J., Hüssy, K., Baktoft, H., Huwer, B., Bekkevold, D., Haslob, H., et al. (2019). Genetic analyses reveal complex dynamics within a marine fish management area. *Evolutionary Appl.* 12, 830–844.

Hill, J., Enbody, E. D., Pettersson, M. E., Sprehn, C. G., Bekkevold, D., Folkvord, A., et al. (2019). Recurrent convergent evolution at amino acid residue 261 in fish rhodopsin. *Proc. Natl. Acad. Sci. U.S.A.* 116, 18473–18478.

ICES (2021). *Baltic Fisheries assesment working group (WGBFAS)* (Copenhagen: ICES Scientific Reports).

Johannesson, K., and André, C. (2006). Life on the margin: genetic isolation and diversity loss in a peripheral marine ecosystem, the Baltic Sea. *Mol. Ecol.* 15, 2013–2029.

Johannesson, K., Le Moan, A., Perini, S., and André, C. (2020). A Darwinian laboratory of multiple contact zones. *Trends Ecol. Evol.* 35, 1021–1036.

Jonsson, P. R., Kotta, J., Andersson, H. C., Herkul, K., Virtanen, E., Nyström Sandman, A., et al. (2018). High climate velocity and population fragmentation may constrain climate-driven range shift of the key habitat former *Fucus vesiculosus* in the Baltic Sea. *Diversity Distribution* 24, 892–905.

Kniebusch, M., Meier, H. E. M., and Radtke, H. (2019). Changing salinity gradients in the Baltic Sea as a consequence of altered freshwater budgets. *Geophysical Res. Lett.* 46, 9739–9747.

Köster, F. W., Huwer, B., Hinrichsen, Hans-H., Neumann, V., Makarchouk, A., Eero, M., et al. (2017). Eastern baltic cod recruitment revisited—dynamics and impacting factors. *ICES Journal of Marine Science* 74, 3–19. doi: 10.1093/icesjms/fsw172

Kotta, J., Vanhatalo, J., Jänes, H., Orav-Kotta, H., Rugiu, L., Jormalainen, V., et al. (2019). Integrating experimental and distribution data to predict future species patterns. *Sci. Rep.* 9, 1821.

Kratzer, S., and Moore, G. (2018). Inherent optical properties of the Baltic Sea in comparison to other seas and oceans. *Remote Sens.* 10, 418.

Lamichhaney, S., Barrio, A. M., Rafati, N., Sundström, G., Rubin, C.-J., Gilbert, E. R., et al. (2012). Population-scale sequencing reveals genetic differentiation due to local adaptation in Atlantic herring. *Proc. Natl. Acad. Sci. U.S.A.* 109, 19345–19350.

Lamichhaney, S., Fuentes-Pardo, A. P., Rafati, N., Ryman, N., Mccracken, G. R., Bourne, C., et al. (2017). Parallel adaptive evolution of geographically distant herring populations on both sides of the north Atlantic ocean. *Proc. Natl. Acad. Sci. U.S.A.* 114, E3452–E3461.

Larsen, P. F., Nielsen, E. E., Meier, K., Olsvik, P. A., Hansen, M. M., and Loeschcke, V. (2011). Differences in salinity tolerance and gene expression between two populations of Atlantic cod (*Gadus morhua*) in response to salinity stress. *Biochem. Genet.* 50, 454–466.

Leder, E. H., André, C., Le Moan, A., Töpel, M., Blomberg, A., Havenhand, J. N., et al. (2021). Post-glacial establishment of locally adapted fish populations over a steep salinity gradient. *J. Evolutionary Biol.* 34, 138–156.

Le Moan, A., Bekkevold, D., and Hemmer-Hansen, J. (2021). Evolution at two time frames: ancient structural variants involved in post-glacial divergence of the European plaice (*Pleuronectes platessa*). *Heredity* 126, 668–683.

Linnaeus, C. (1761). *Fauna suecica* (Stockholm).

Manzon, L. A. (2002). The role of prolactin in fish osmoregulation: A review. *Gen. Comp. Endocrinol.* 125, 291–310.

Martinez Barrio, A., Lamichhaney, S., Fan, G., Rafati, N., Pettersson, M., Zhang, H., et al. (2016). The genetic basis for ecological adaptation of the Atlantic herring revealed by genome sequencing. *eLife* 5, e12081.

Matschiner, M., Barth, J. M. I., Tørresen, O. K., Star, B., Baalsrud, H. T., Brieuc, M. S. O., et al. (2022). Supergene origin and maintenance in Atlantic cod. *Nat. Ecol. Evol.* 6, 469–481.

Möllman, C., Kornilovs, G., Fetter, M., and Köster, F. W. (2004). Feeding ecology of central Baltic Sea herring and sprat. *J. Fish Biol.* 65, 1563–1581.

Momigliano, P., Jokinen, H., Fraimout, A., Florin, A.-B., Norkko, A., and Merilä, J. (2018). Extraordinarily rapid speciation in a marine fish. *Proc. Natl. Acad. Sci. U.S.A.* 114, 6074–6079.

Nissling, A., Kryvi, H., and Vallin, L. (1994). Variation in egg buoyancy of Baltic cod *Gadus morhua* and its implications for egg survival in prevailing conditions in the Baltic Sea. *Mar. Ecol. Prog. Ser.* 110, 67–74.

Nissling, A., and Westin, L. (1997). Salinity requirements for successful spawning of Baltic and belt Sea cod and the potential for cod stock interactions in the Baltic Sea. *Mar. Ecol. Prog. Ser.* 152, 261–271.

Ojaveer, H., Jaanus, A., MacKenzie, B. R., Martin, G., Olenin, S., et al. (2010). Status of biodiversity in the Baltic Sea. *PLoS ONE* 5 (9), e12467. doi: 10.1371/journal.pone.0012467

Osei-Owusu, J., Yang, J., Vitery, M. D. C., and Qiu, Z. (2018). Molecular biology and physiology of volume-regulated anion channel (VRAC). *Curr. Top. Membr* 81, 177–203.

Pettersson, M. E., Rochus, C. M., Han, F., Chen, J., Hill, J., Wallerman, O., et al. (2019). A chromosome-level assembly of the Atlantic herring genome–detection of a supergene and other signals of selection. *Genome Res.* 29, 1919–1928.

Poulsen, E. M. (1931). "Biological investigations upon the cod in Danish waters," in *Meddelelser fra kommisionen for danmarks fiskeri-og havundersøgelser*, (Copenhagen: C. A. Reitzels publisher) vol. Vol. IX., No 1.

Reusch, T. B. H., Dierking, J., Andersson, H. C., Bonsdorff, E., Carstensen, J., Casini, M., et al. (2018). The Baltic Sea as a time machine for the future coastal ocean. *Sci. Adv.* 4, eaar8195.

Ryman, N., Lagercrantz, U., Andersson, L., Chakraborty, R., and Rosenberg, R. (1984). Lack of correspondence between genetic and morphological variability patterns in Atlantic herring (*Clupea harengus*). *Heredity* 53, 687–704.

Schade, F. M., Weist, P., Dierking, J., and Krumme, U. (2022). Living apart together: Long-term coexistence of Baltic cod stocks associated with depth-specific habitat use. *PloS One* 17, e0274476.

Sick, K. (1961). Haemoglobin polymorphisms in fishes. *Nature* 192, 894–896.

Snoeijs-Leijonmalm, P., Schubert, H., and Radziejewska, T. (2017). *Biological oceanography of the Baltic Sea* (Dordrecht: Springer Science+Business Media).

Sodeland, M., Jentoft, S., Jorde, P. E., Mattingsdal, M., Albretsen, J., Kleiven, A. R., et al. (2022). Stabilizing selection on Atlantic cod supergenes through a millennium of extensive exploitation. *Proc. Natl. Acad. Sci U.S.A.* 119, e2114904119.

Svedäng, H., Savchuk, O., Villnäs, A., Norkko, A., Gustafsson, B. G., Wikström, S. A., et al. (2022). Re-thinking the "ecological envelope" of Eastern Baltic cod (Gadus morhua): conditions for productivity, reproduction, and feeding over time. *ICES J. Mar. Sci.* 79, 689–708.

Thorsen, A., Kjesbu, O. S., Fyhn, H. J., and Solemdal, P. (1996). Physiological mechanisms of buoyancy in eggs from brackish water cod. *J. Fish Biol.* 48, 457–477.

Vallin, L., and Nissling, A. (2000). Maternal effects on egg size and egg buoyancy of Baltic cod, *Gadus morhua*: implications for stock structure effects on recruitment. *Fisheries Res.* 49, 21–37.

Weist, P., Schade, F. M., Damerau, M., Barth, J. M. B., Dierking J,, Andre, C., et al. (2019). Assessing SNP-markers to study population mixing and ecological adaptation in Baltic cod. *PloS One* 14, e0218127.

Westin, L., and Nissling, A. (1991). Effects of salinity on spermatozoa motility, percentage of fertilized eggs and egg development of Baltic cod (Gadus morhua), and implications for cod stock fluctuations in the Baltic. *Mar. Biol.* 108, 5–9.

frontiers | Frontiers in Marine Science

TYPE Original Research
PUBLISHED 19 April 2023
DOI 10.3389/fmars.2023.1130855

OPEN ACCESS

EDITED BY
Songlin Liu,
South China Sea Institute of Oceanology (CAS), China

REVIEWED BY
Raju Sekar,
Xi'an Jiaotong-Liverpool University, China
Benjamin Misson,
Université de Toulon, France

*CORRESPONDENCE
Li Zhao
li.zhao@umu.se

SPECIALTY SECTION
This article was submitted to Global Change and the Future Ocean, a section of the journal Frontiers in Marine Science

RECEIVED 23 December 2022
ACCEPTED 04 April 2023
PUBLISHED 19 April 2023

CITATION
Zhao L, Brugel S, Ramasamy KP and Andersson A (2023) Bacterial community responses to planktonic and terrestrial substrates in coastal northern Baltic Sea. *Front. Mar. Sci.* 10:1130855. doi: 10.3389/fmars.2023.1130855

Bacterial community responses to planktonic and terrestrial substrates in coastal northern Baltic Sea

Li Zhao[1,2]*, Sonia Brugel[1,2], Kesava Priyan Ramasamy[1,2] and Agneta Andersson[1,2]

[1]Department of Ecology and Environmental Science, Umeå University, Umeå, Sweden, [2]Umeå Marine Sciences Centre, Umeå University, Hörnefors, Sweden

Bacteria are major consumers of dissolved organic matter (DOM) in aquatic systems. In coastal zones, bacteria are exposed to a variety of DOM types originating from land and open sea. Climate change is expected to cause increased inflows of freshwater to the northern coastal zones, which may lead either to eutrophication or to increased inputs of refractory terrestrial compounds. The compositional and functional response of bacterial communities to such changes is not well understood. We performed a 2-day microcosm experiment in two bays in the coastal northern Baltic Sea, where we added plankton extract to simulate eutrophication and soil extract to simulate increased inputs of refractory terrestrial compounds. Our results showed that the bacterial communities responded differently to the two types of food substrates but responded in a similar compositional and functional way in both bays. Plankton extract addition induced a change of bacterial community composition, while no significant changes occurred in soil extract treatments. Gammaproteobacteria were promoted by plankton extract, while Alphaproteobacteria dominated in soil extract addition and in the non-amended controls. Carbohydrate metabolism genes, such as aminoglycan and chitin degradation, were enriched by plankton extract, but not soil extract. In conclusion, the coastal bacterial communities rapidly responded to highly bioavailable substrates, while terrestrial matter had minor influence and degraded slowly. Thus, in the northern Baltic Sea, if climate change leads to eutrophication, large changes of the bacterial community composition and function can be expected, while if climate change leads to increased inflow of refractory terrestrial organic matter the bacterial communities will not show fast compositional and functional changes. Degradation of terrestrial organic matter may instead occur over longer periods of time, e.g. years. These findings help to better understand the ability of bacterial communities to utilize different carbon sources and their role in the ecosystem.

KEYWORDS

Microcosm experiment, coastal bacteria, dissolved organic matter, Baltic Sea, metagenome

Introduction

Climate change has different impacts in varying regions on Earth, and in northern Europe both warming and increased precipitation are expected (Meier et al., 2012). In the Baltic Sea, climate change has consequences including eutrophication in certain areas and potential oligotrophication in others (e.g. Andersson et al., 2015). More frequent phytoplankton blooms and increasing production of autochthonous dissolved organic matter (AtDOM) are expected in the southern Baltic Sea, while in the north increased inflow of coloured refractory terrestrial dissolved organic matter (tDOM) may instead nurture heterotrophic bacteria and the "microbial loop" (Andersson et al., 2015; Meier et al., 2022). While tDOM reaching coastal areas is composed of refractory high molecular weight molecules, such as lignin, cellulose, pectin, xylan and humic substances (Pettersson et al., 1997; Akita et al., 2016; Zhao et al., 2021), AtDOM is constituted by plankton derived labile carbon sources, for example chitin, starch and glycogen (e.g. Bertilsson and Jones, 2003).

Dissolved organic matter (DOM) constitute the main energy source for heterotrophic bacteria in surface waters (Jiao et al., 2011). During the bacterial degradation of DOM, complex organic carbon compounds can be broken down into smaller compounds, inorganic nutrients could be released, which can be utilized by other organisms, such as phytoplankton. In turn, phytoplankton excrete organic matter back into the water column, which is degraded by bacteria. Thus, these bacterial communities play an important role in regulating the availability of nutrients and the overall carbon cycle (Azam and Malfatti, 2007; Jiao et al., 2011).

Different DOM types can regulate bacterial community structure due to the occurrence of taxa-specific metabolic capabilities (Logue et al., 2016). In aquatic systems primary producers release large amounts of photosynthetic products, which are food resources for heterotrophic bacteria (Mühlenbruch et al., 2018). The bacterial community composition associated with phytoplankton blooms is often dominated by Gammaproteobacteria, Flavobacteriia and Roseobacter, which is linked to their capability of producing specific exo-enzymes degrading phytoplankton-derived polysaccharides (Teeling et al., 2012). In the Baltic Sea, Gammaprotebacteria have been observed to be common in highly productive areas (Lindh et al., 2015a; Herlemann et al., 2016; Mühlenbruch et al., 2018). Further, this group is known to quickly exploit new environments upon disturbances (Lindh et al., 2015b; Andersson et al., 2018).

Terrestrial DOM, drives communities towards proliferation of Bacteroidetes, Gemmatimonadetes, Planctomycetes, and Alpha- and Betaproteobacteria (Traving et al., 2017; Broman et al., 2019). In coastal areas of the northern Baltic Sea, Burkholderiales dominate the community during the spring river flush period, when tDOM concentrations are elevated (Figueroa et al., 2021). The underlying mechanism may be that Burkholderiales have the capacity for lignin degradation by harbouring a large diversity of catabolic enzymes that can degrade recalcitrant aromatic compounds in a variety of environmental conditions (Morya et al., 2020). Since the transport of tDOM to subarctic coastal zones is huge (Cole et al., 2007; Drake et al., 2018), it can be expected that bacteria with capacity to degrade tDOM are selected in coastal areas receiving freshwater in the northern Baltic Sea.

Previous studies indicate a link between DOM properties and bacterial diversities in aquatic environments, such as glacial systems (Smith et al., 2018), streams (D'Andrilli et al., 2019), river estuaries (Figueroa et al., 2021) and coastal areas (Teira et al., 2009; Traving et al., 2017; Bruhn et al., 2021). The northern Baltic Sea is a particularly interesting region for studying the effects of shifts in DOM properties on bacterial communities, as it is a semi-enclosed brackish basin that receives inputs from both marine and terrestrial sources. Several studies have investigated the effects of various environmental factors on bacterial community composition and diversity in the Baltic Sea (e.g. Andersson et al., 2010; Figueroa et al., 2021). However, the effects of climate change induced DOM shift on bacterial community composition and functional profiles in the northern Baltic Sea are still poorly understood. Therefore, further investigation of the responses of bacterial communities to these changes in the northern Baltic Sea is needed to better understand the potential impacts of climate change on the functioning of this ecosystem. The bacterial community has an important role in biogeochemical cycling and ecological functions in the Baltic Sea. By examining changes in both the taxonomic and functional profiles of bacterial communities, it is possible to gain a more complete understanding of how shifts in DOM properties can affect the ecological and biogeochemical functions of bacterial communities in the Baltic Sea. Metagenomics sequencing techniques can be used to identify genes involved in the degradation of different types of organic matter, such as complex carbon compounds (Lindh and Pinhassi, 2018).

Heterotrophic bacteria play a vital role in the environment by utilizing and breaking down various carbon-rich compounds through the production of exoenzymes, these enzymes facilitate the degradation and utilization of different types of carbon compounds present in the environment (Beier and Bertilsson, 2013; Mühlenbruch et al., 2018). The Carbohydrate-Active enZymes (CAZyme) database describes the genes and functions of relevant enzymes involved in the biosynthesis and breakdown of complex carbohydrates (Drula et al., 2022). By comparing the functional profiles of bacterial communities under different environmental conditions, it is possible to gain insights into the specific enzymatic pathways that are involved in the degradation of different types of organic matter in the Baltic Sea.

To gain insight into how bacterial communities in the northern Baltic Sea may respond to future changes in the dissolved organic matter (DOM) pool resulting from climate change, we conducted a field experiment in a coastal area of the northern Baltic Sea. The study investigated the effects of two types of DOM on bacterioplankton, including labile plankton-derived DOM (plankton extract) and relatively refractory soil-derived DOM (soil extract).

We hypothesized that the varying DOM types would select for bacterial communities with different diversity, community composition and carbohydrate metabolism-related gene profiles. More specifically, that labile plankton-derived DOM amendment would promote Gammaproteobacteria and cause decreased diversity, whereas addition of soil-derived DOM would favour taxa known to be common in terrestrial systems. Bacterial taxa promoted by the addition of plankton-derived DOM were expected to harbour genes for degradation of autochthonous DOM, such as

chitin, alginate, xylan, starch and glycogen. Bacterial taxa favoured by terrestrial DOM were expected to harbour genes for degradation of refractory DOM, such as lignin and cellulose.

To test our hypotheses, we employed 16S rRNA metabarcoding and shotgun metagenomic sequencing to explore the structure of the bacterial communities and their potential metabolic functions. We examined the associations between bacterial taxa and environmental conditions to understand how labile versus refractory DOM impacts the bacterial community assembly. Our overall aim was to investigate the potential shifts of bacterial communities and their functions under climate change scenarios in a coastal region of northern Baltic Sea.

Material and methods

Substrate extraction

To obtain the labile substrate, plankton samples were collected using a WP2 plankton net with a 90 µm mesh at a coastal station (about 20 meters depth) 2 weeks before we performed the experiment, 2018. After combining several vertical net hauls, the collected plankton samples were lysed with a tissue lyser, then the mixture was centrifuged and the supernatant was filtered through a syringe filter with 0.2 µm supor membrane non-polygenic (Pall Corporation). The plankton extract was mainly based on lysates of filamentous cyanobacteria (mainly *Aphanizomenon* sp.) and zooplankton (mainly *Eurytemora* sp., *Acartia* sp. and *Bosmina* sp.), and consisted of high molecular weight (HMW) organic compounds, such as polysaccharides (Zhao et al., 2021), but also inorganic substances. The molar ratio of carbon to nitrogen to phosphorus in the plankton extract was 44:9:1, calculated using the concentrations of dissolved organic carbon (DOC), total dissolved nitrogen (TDN), and total dissolved phosphorus (TDP).

To obtain the refractory terrestrial extract, humic rich river bank soil was collected from a 5-10 cm layer above the sand layer near the Öre River. The soil sample was homogenized and sieved through 4-6 mm sieve nets, then, a 9.8 kg collected soil sample was strongly mixed with 65 l MQ-water for 2 days of vigorous mechanical mixing with a large pump. After that, the mixture was manually pushed through 100 µm nylon net and subsequently through 15 µm nylon net and centrifuged at 10 000 rpm. Then the mixture was stepwise filtered through a filtration system compiled of 25, 5, 3, 1 µm (IFAB product Nr. PPE 025-10, PPE 005-10, SRL 030 250L CZ and SLS 010-250L EF, respectively) by pump suction at high flow rate (~200-400 ml.min^{-1}). Approximately 1.7 l extract was then pushed at low flow rate and high pressure through 0.22 µm filter (250L-CSS-002SFA) before use. The C: N: P molar ratio of the soil extract was 569:36:1, calculated based on the ratio of DOC: TDN: TDP.

Experimental set-up

The experiment aimed to mimic climate change impacts on inputs of terrestrial substances associated with river runoff increasing and on phytoplankton derived substances associated with eutrophication. Two bays situated in the northern Baltic Sea (Figure 1) were selected to conduct the field microcosm experiment (18-20 September 2018), (a) Ängerån (AN) bay (63°32′21″ N, 19.46′29″ E), which receives humic rich river water from the Änger River, (b) Kalvarskatan (KA) bay (63°35′54″N, 19°53′4″ E), which does not have any immediate freshwater inflow (Table 1). The temperature of the water in both bays was 12.7°C. We collected seawater at a depth of 0.5 meters using a Ruttner water sampler (NormecTec, Johanneshov) at each bay, and then filled nine transparent polyethylene cubitainers (10 liters each) with 7.8 liters of seawater filtered through a 200 µm nylon mesh.

In each bay, we incubated seawater samples in triplicate with three different treatments for 2 days. One group received plankton extract addition, resulting in initial concentrations

of ~435 DOC µmol l^{-1}, 2 TDP µmol l^{-1} and 35 TDN µmol l^{-1}, while another group received soil extract addition, resulting in an initial concentration of ~435 DOC µmol l^{-1}, 0.3 TDP µmol l^{-1} and 22 TDN µmol l^{-1}, both of the amendments resulted in approximately a 23-24% increase in carbon concentration. The third group (control) did not receive any addition. We thoroughly mixed the cubitainers and incubated them *in situ* at 0.5 m depth at each bay. We tested the bacterial community response to different treatments by measuring bacterial production and bacterial abundance, inorganic nutrients and dissolved organic carbon (DOC) at the beginning and the end of the experiment. For DNA

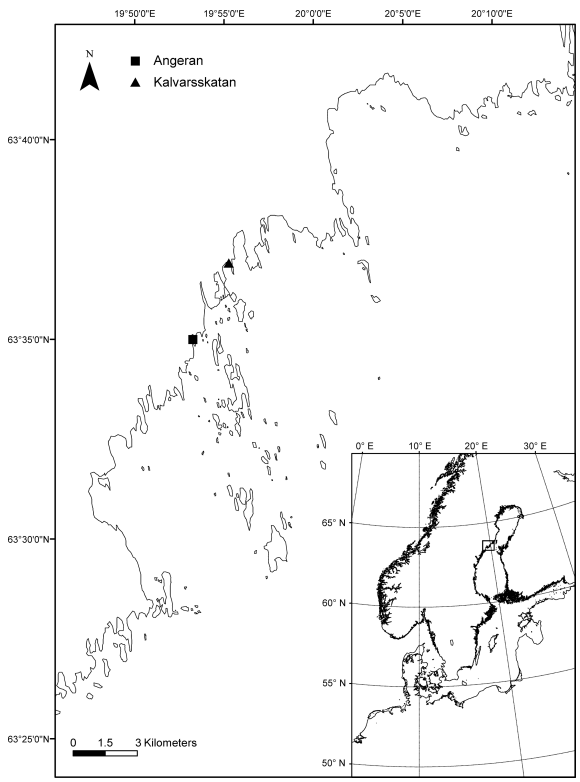

FIGURE 1
Map of experimental sites in coastal northern Baltic Sea. Solid triangle indicates site Kalvarskatan bay receiving no river inflow, and solid square indicates site Angeran bay receiving river inflow.

TABLE 1 Chemical and biological characteristics of the seawater in the two bays.

Bays	Salinity (psu)	DOC (µmol l^{-1})	Humic substances (mg.m^{-3})	TDP (µmol l^{-1})	TDN (µmol l^{-1})	BA (cell.ml^{-1})	BP (mgC.m^{-3}.h^{-1})
Ängerån	3.7	354	14.9	0.2	17.3	4.4×10^6	0.6
Kalvarskatan	3.9	352	13.7	0.2	18.0	4.0×10^6	0.3

BA, bacterial abundance; BP, bacterial production; DOC, dissolved organic carbon; TDP, total dissolved phosphorus; TDN, total dissolved nitrogen.

samples, 1 liter water was filtered on the 47-mm, 0.2 µm PES Supor (Pall Corporation, Ann Arbor) membrane filters, stored at -80°C until DNA extraction.

Bacterial production and bacterial abundance

Bacterial production (BP) was measured using the ^{3}H-thymidine incorporation technique as described in (Berglund et al., 2007). One milliliter of seawater was added to four Eppendorf tubes, one control and triplicate samples. Bacteria in the control were pre-killed by adding 100 µl ice-cold 50% trichloro acetic acid (TCA) and incubating at 2°C for 5 min. After that, 2 µl [^{3}H]-thymidine (83.3 Ci $mmol^{-1}$; PerkinElmer, Massachusetts, USA) were added to each tube to a final concentration of 24 nM. 100 µl of 50% ice-cold TCA were added to the samples after 1 h to terminate the incubations. Samples were analyzed using a Perkin Elmer Tri-Carb 2910TR scintillation counter. The incorporated thymidine was converted to cell production using the conversion factor of 1.4×10^{18} cells mol^{-1} (Fuhrman and Azam, 1982).

Samples for bacterial counts were pre-filtered through a 50 µm mesh, preserved in 0.1% glutaraldehyde (final concentration), frozen at -80°C and analyzed with a BD FACSVerse™ flow cytometer (BD Biosciences). Frozen samples were quickly thawed in a 30°C water bath. Samples were stained with SYBR Green I (Invitrogen) at a final concentration of 1:10 000. As internal standard, 1 µm microspheres (Fluoresbrite plain YG, Polysciences) were added to each sample (Marie et al., 2005).

Chemical analyses

Dissolved organic carbon (DOC) was analyzed in water filtered through a 0.22 µm Supor Membrane Syringe Filter (non-pyrogenic; Acrodisc®) and acidified to 18 mM HCl, final concentration. Samples were analyzed with a high-temperature combustion Shimadzu (Kyoto) TOC-5000 analyzer. Total dissolved phosphorus (TDP) and total dissolved nitrogen (TDN) were measured in 0.22 µm filtered samples, as described for DOC, using a Seal (Norderstedt) QuAAtro39 autoanalyzer after an oxidation step using peroxodisulfate, according to standard analytical methods (Grasshoff et al., 1999).

The concentration of humic substances (HS) was measured from unfiltered water samples using a Perkin Elmer LS 30 fluorometer at 350/450 nm excitation/emission wavelengths, calibrated with a serial dilution of quinine sulfate solution (Hoge et al., 1993).

Picophytoplankton

Samples were pre-filtered through a 50 µm mesh, preserved in 0.1% glutaraldehyde (final concentration) and frozen at −80°C (Marie et al., 2005) for later counts using a BD FACSVerse™ flow cytometer (BD Biosciences) equipped with a 488 nm laser (20 mW output) and a 640 mn laser (output 40 mW). Frozen samples were quickly thawed in a 30°C water bath. Picophytoplankton samples were run with 3 µm microspheres (Fluoresbrite ® plain YG, Polysciences) as internal standard. Picophytoplankton abundance was converted to biomass using carbon conversion factors: 120 fgC cell−1 for picocyanobacteria and 829 fgC $cell^{-1}$ for picoeukaryotic phytoplankton, based on microscopic measurements of cell sizes and use of conversion factors (see above).

Nano- and microphytoplankton, heterotrophic nanoflagellates and ciliates

Samples were preserved with 2% acidic Lugol's solution and stored in darkness at 4°C until analysis. For the analysis of nano- and microplankton, 10-50 ml were settled for 12-48 hours in sedimentation chambers and cells were counted on an inverted microscope (Nikon Eclipse Ti) at 100-400x magnification using phase contrast settings (Utermöhl, 1958). Cells were grouped into three functional groups (AU: autotrophs, HT: heterotrophs, MX: mixotrophs), based on the feeding mode (Olenina et al., 2006). Nutritional characteristics of plankton were identified based on described trophy (Tikkanen and Wille'n, 1992; Hallfors, 2004; Olenina et al., 2006). Further, the coloration of the smallest cells was used to support the trophy classification as Lugol's solution stains Chl a in brown. Plankton biomass was calculated from the geometric shape of cells following Olenina et al. (2006) and cell carbon content was calculated according to Menden-Deuer and Lessard (2000).

DNA extraction

DNA was extracted from filter samples using DNeasy Power Water kit (Qiagen, Sweden) according to a modified DNeasy PowerWater protocol (e.g. extended lysis time, lower elution volume). Further details of the modified protocol can be provided upon request. Two milli-Q water extraction controls and two filter extraction controls were used during DNA extraction, these are samples of Milli-Q water or empty filters that are processed in the same way as the environmental samples, all the extraction controls

were amplified and sequenced in parallel to the samples to monitor possible contamination. The extracted DNA was measured by gel electrophoresis and Qubit fluorometer.

16S rRNA sequencing and data analysis

Prokaryote 16S V4-V5 rRNA gene sequences were generated by PCR amplification using tagged primers 563F (5'-AYTGGGY DTAAAGNG) and 907R (5'-CCGTCAATTCMTTTGAGTTT) (Hugoni et al., 2017). The primers contained sample tags of 8 bp and 4 leading Ns to improve sequence diversity. Q5 High-Fidelity DNA Polymerase was used for the PCR reactions, which included three non-template PCR controls that produced very few reads. Each sample was amplified in triplicate, and the amplicon was purified using magnetic beads. The amplicons were mixed in equimolar proportions and used to construct a 16S library. The amplicons were then mixed in equimolar proportions, and used to construct a 16S library and sequenced on Illumina Hiseq Platform 2500, generated 250 bp paired end reads (Novogene, Beijing, China).

The Obitools package (Boyer et al., 2016) was employed to perform read filtering, primer trimming, merging of paired end reads and demultiplexing. Briefly, the forward and reverse reads were assembled using the illuminapairedend command with a minimum alignment score of 40. Any unpaired reads were eliminated with the obigrep command. Demultiplexing was then carried out using the ngsfilter command (Boyer et al., 2016). The reads were further filtered (maxN = 0, maxEE = 2), and the learnErrors command was applied, and then the reads were denoised using DADA2 version 1.22 (Callahan et al., 2016) to generate amplicon sequence variants (ASVs). Chimers (method = "consensus") and any ASV with a length less than 300 bp were removed. The ASV table was further filtered to exclude potential contaminations identified by the prevalence method of the 'decontam' package (Davis et al., 2018). Taxonomy was assigned using the assignTaxonomy command (minBoot = 80) against the SILVA database v138.1 by Naïve Bayes classifier (Quast et al., 2013). The table was then filtered to exclude the ASVs assigned to mitochondria and chloroplast. Rare taxa with a read number of less than 10 and were prevalent in less than 20% of samples were excluded. Normalization was done by the mirlyn R package with 1000 iterations of rarefaction (without replacement) at a threshold of 49402 reads. Initial analyses of multiple rarefied tables produced similar results, so one representative table from the data set (set.seed =123) was used for the further analyses (Table S1). The ASV table was analyzed and graphically displayed using the R package phyloseq (McMurdie and Holmes, 2013) and ggplot2 (Hadley, 2016). Phyloseq was also used to measure the diversity of bacterial taxa in our samples. Alpha diversity was assessed based on rarefied counts using Shannon-Wiener index, Observed, Chao1, InvSimpson, ACE, Simpson, and Fisher indices were included in Table S2. To compare the microbiota composition between samples, we calculated Bray-Curtis dissimilarity metrics using Phyloseq and visualized the results in a non-metric multidimensional scaling (NMDS) plot. The significant differences between the treatments were determined by Kruskal–Wallis tests from the agricolae R package (de Mendiburu, 2021). We used the DESeq2 package (Love et al., 2014) in R to perform differential abundance testing at the ASV level, comparing addition treatments to control using the contrast function and the Wald test. To account for multiple testing, we applied the Benjamini and Hochberg correction to adjust p-values. ASVs with an adjusted p-value < 0.05 were considered differentially abundant.

In order to estimate the contribution of environmental data to variations in community compositions, we employed a series of redundancy analyses (RDA). We used the Hellinger-transformed ASV matrix created in the R package vegan (Oksanen et al., 2022) as the dependent matrix and the scaled environmental variables as independent matrices. To avoid overfitting the model, only variables with correlation coefficients less than or equal to 0.7 were used in the RDA analysis.

Metagenome sequencing and data analysis

For metagenomics, the DNA extracts from the three replicates of each treatment were pooled, resulting in six samples that were denoted as KAC, KAP, KAS, ANC, ANP and ANS, plus 2 initial samples from day 0, KA0 and AN0. For each sample, 1μg DNA was used for PCR-free library construction with NEBNext® Ultra™ II DNA Library Prep Kit (Cat No. E7645, NEB, USA) according to the instructions of the manufacturer. The library was first quantified using Qubit and real-time PCR, and the size distribution was checked using a bioanalyzer. Quantified libraries were pooled and paired ends (2 × 150 bp) sequenced on a Novaseq 6000 platform.

The basic sequence read quality was checked with FastQC (https://www.bioinformatics.babraham.ac.uk/projects/fastqc/). Adapter sequences and low-quality bases were removed using fastp with default parameters (Chen et al., 2018). The trimmed reads were mapped with PhiX genome to remove potential PhiX reads. Then, the clean reads from the 8 samples were co-assembled using SPAdes v3.13.0 (metaspades model, kmers were 21, 33, and 55). Protein-coding genes were predicted by prodigal (v2.6.3). Predicted genes with a length less than 100 were removed. The remaining gene sequences were clustered by CD-HIT-EST with a minimum of 95% identity and 95% read coverage on amino acid level. Taxonomic assignment up to species level was performed using Kaiju v1.8.2 (Menzel et al., 2016), with an *E*-vale threshold of 0.00001. Salmon v1.8.0 (Patro et al., 2017) was used to quantify the abundance of coding sequences (CDS) abundance, while eggNOG-mapper v2.1.7 (Huerta-Cepas et al., 2019) was used for functional annotation based on precomputed orthology assignments. Differential abundance analysis of CDS under different treatments was performed using EdgeR (Robinson et al., 2010), samples from the same treatment were used as replicates. Genes meeting the criteria of $p < 0.001$ and $|\log2FC| > 5$ were identified as significant differentially abundant genes (DAGs) in both the comparison of plankton extract treatment versus the control and soil extract treatment versus the control (data can be provided upon request). To investigate whether the differences in food substrates might lead to functional differences, Gene ontology (GO) enrichment analysis

of significant DAGs was performed using R package clusterProfiler (Wu et al., 2021). For enrichment analysis, the SQLite-based custom annotation package named as "org. Bpro.org.db" was prepared in R using the AnnotationForge package (Carlson and Pagès, 2023). Using clusterProfiler, significant GO term associated DAGs were identified using enrichGO function. GO terms with both p value and FDR < 0.05 were considered significant and were represented, no significant Gene Ontology (GO) terms were found in the comparison between soil extract treatment and control. To achieve a more precise annotation of carbohydrate-active enzymes (CAZymes), we used the dbCAN2 web server to identify potential CAZymes in CDS (Zhang et al., 2018). To enhance annotation accuracy, we only kept CAZymes that were confirmed by at least two of the following tools: HMMER, DIAMOND and eCAMI (Table S3). We selected genes of interest, such as those encoding for chitinase and glycosidase CAZymes for further discussion. To confirm their function, we conducted a BLAST search against the Uniprot database (https://www.uniprot.org/blast).

Nucleotide sequence accession numbers

All sequencing data is archived in the NCBI SRA database under BioProject accession number PRJNA915349.

Results

Physicochemical and biological characterization of the bay water

Both the Ängerån and Kalvarskatan bays are brackish water systems, but the Ängerån bay is more influenced by freshwater than Kalvarskatan. Consequently, the salinity was slight lower and the concentrations of DOC and humic substances higher in Ängerån (Table 1). The total dissolved nitrogen (TDN) and phosphorus (TDP) were relatively similar in the two bays. The bacterial abundance and bacterial production were also higher in Ängerån than in Kalvarskatan (Table 1).

Carbon biomass of phytoplankton and heterotrophic protozoa

The addition of plankton extract had a stronger effect on primary production because it was rich in inorganic nutrients which promoted both heterotrophic bacterial production and phytoplankton primary production.

The carbon biomass of phytoplankton and heterotrophic protozoa increased 2-3 times in all treatments during the two-day incubation (Figure S1). Approximately 60% of the biomass was constituted by autotrophic pro- and eukaryotic picoplankton. Heterotrophic protozoa, composed of heterotrophic nanoflagellates (HNF) and ciliates, constituted ~10% of the biomass. Their biomass was relatively similar in all samples. At large, the plankton responses were similar in all treatments in the two bays. However, dinoflagellates showed a greater increase in KA than in AN, and therefore the total plankton biomass was higher in KA.

DOC consumption, bacterial abundance and production

The DOC concentration at the start of the experiment was ~350 $\mu molC.l^{-1}$ in the controls and ~435 $\mu molC.l^{-1}$ in the amendment microcosms. Plankton extract was more bioavailable than the soil extract (Table 2). The DOC net consumption in plankton extract treatment was about 18%~20% while below 5% in soil extract treatment (Table 2). The total dissolved phosphorus (TDP) consumption was also high in the plankton extract treatment compared to the control and soil extract treatments.

The bacterial growth in the two bays showed similar trends. The abundance in the KA bay increased from the initial 3.9×10^6 $cell.ml^{-1}$ to 5.3×10^6 $cell.ml^{-1}$ in the control, 5.9×10^6 $cell.ml^{-1}$ in soil extract treatment and 18.0×10^6 $cell.ml^{-1}$ in plankton extract treatment (Figure 2). In AN, the bacterial abundance also showed a similar increase, from initially 4.4×10^6 to 6.4×10^6 in the control, 7.0×10^6 in soil extract treatment and 17.8×10^6 $cell.ml^{-1}$ in plankton extract treatment (Figure 2). Bacterial production (BP) was stimulated by the amendments of both soil extract and plankton extract; it was enhanced 50-123% by soil extract and 1500-3300% by plankton extract relative to the control (Figure 2).

Bacterial diversity and community composition

A total number of 462 ASVs were recovered by 16S rRNA amplicon sequencing of the bacterial communities incubated with the two different substrates in the two bays. Rarefaction curves started to plateau indicating that the diversity of the whole bacterial community was sampled (Figure S2). We used the Shannon-Wiener index as indicator of bacterial diversity. After the 2-day *in situ* incubation, the plankton extract treatment exhibited a significant decrease in bacterial diversity in KA, whereas the soil extract treatment and control group showed only a slight decrease in diversity compared to the initial condition in both bays (Figure 3). The beta-diversity analysis, using nMDS based on Bray–Curtis dissimilarity calculated with ASV relative abundance, indicated that the bacterial structure changed in all treatments compared to the initial condition at Day 0, with no variation between soil treatment and control (Figure 4).

The community composition at the class level was quite similar in both bays, with the Gammaproteobacteria and Alphaproteobacteria being the major class observed, followed by Verricucomicrobiae (Figure 5). However, we observed differences in the relative abundance of these sub-phyla between the treatments. Specifically, the Gammaproteobacteria showed the highest percentages in the plankton extract treatment compared to the soil extract and control treatments. On the other hand, the Alphaproteobacteria did not show much difference between the treatments (Figure 5). These

10.3389/fmars.2023.1130855

TABLE 2 Comparison of the bacterial DOC, TDN and TDP consumption and percentage DOC utilization in different treatments.

	Measure	Control	plankton extract	soil extract
AN	DOC consumption ($\mu molC.l^{-1}$)	–	77.6 (± 3.4)	–
	DOC utilization (%)	–	17.7 (± 0.8)	–
	TDN consumption ($\mu molC.l^{-1}$)	–	14.3 (± 1.5)	–
	TDP ($\mu molC.l^{-1}$)	0.0 (± 0.1)	1.6(± 0.1)	–
KA	DOC consumption ($\mu molC.l^{-1}$)	20.0 (± 2.2)	88.1 (± 8.3)	19.6 (± 8.0)
	DOC utilization (%)	5.7 (± 0.63)	20.2 (± 1.9)	4.5 (± 1.8)
	TDN consumption ($\mu molC.l^{-1}$)	0.5 (± 0.6)	13.2 (± 1.4)	0.0 (± 0.8)
	TDP consumption ($\mu molC.l^{-1}$)	0.0 (± 0.1)	1.3 (± 0.1)	0.1 (± 0.0)

Values are means ± standard deviation of three experimental replicates.
– denotes data not available.

observations suggest that the different treatments may have a selective effect on the abundance of certain bacterial taxa. Gammaproteobacteria were in general promoted by plankton extract (Figure S3), the differential abundance analysis between plankton extract treatment and control showed that ~85% of the increased abundance ASVs were Gammaproteobacteria (58 out of 67 in KA and 39 out of 47 in AN) (Table S4). More specially, the bacterial community in the plankton extract treatment had higher relative abundance of ASVs from genera *Aeromonas*, *Shewanella* and *Motilimonas*. There was a significant increase in the abundance of some taxa in both bays, for example genera *Aeromonas* (ASV3, ASV14), *Shewanella* (ASV8) and *Motilimonas* (ASV17) increased over 100-fold, and from rare taxa in the initial community became dominant taxa after 2 days incubation (Figure 6). The bacterial community in the soil extract treatment had higher relative abundance of ASVs from class Actinobacteria and Verrucomicrobiae, but we identified no ASV as significantly different when comparing the soil extract treatment to the control.

Carbon metabolism-associated genes and relevant taxa

Gene Ontology Annotations of the most differentially abundant genes (DAGs) between plankton extract treatment and control, showed enrichment of genes involved in aminoglycan catabolic processes, peptidoglycan catabolic process and chitin catabolic process (Figure 7). Accordingly, we focused on the analysis of genes related to carbohydrate degradation. Our gene profile analysis revealed the presence of DAGs encoding for the carbohydrate-active enzymes glycoside hydrolases (GHs), polysaccharide lyases (PLs), carbohydrate esterases (CEs), and auxiliary activities (AAs) (Table S5). Based on literature survey, we selected the most enriched CAZyme-coding genes which actively responded to the addition of plankton extract and soil extract (Table 3).

The most abundant CAZy families predicted under the plankton extract treatment belonged to GHs, and among them, Chitinase (GH18), alpha-amylase and maltodextrin glucosidase

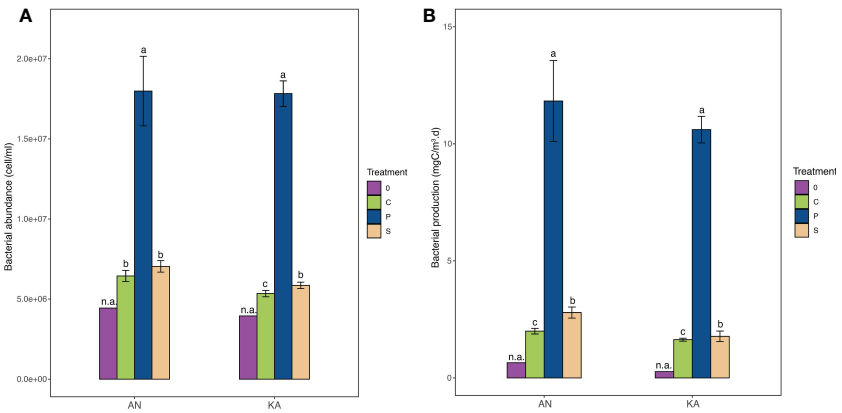

FIGURE 2
Bacterial abundance **(A)** and bacterial production **(B)** in different treatments measured in Kalvarsskatan (KA) and Ängerån (AN) bay at the start (and the end (day 2) of the experiment. The colours in the graph represent different treatments, with purple representing day 0, green representing control, blue representing plankton extract treatment, and brown representing soil extract treatment, day 2. Values are means of 3 replicates ± standard deviation. 0: day 0 (before DOM amendments). Error bars represent the standard deviation. The letter s "a" "b" and "c" placed above each bar indicate significant differences ($\alpha = 0.05$) between the treatments (excluding day 0), as determined by Kruskal–Wallis tests.

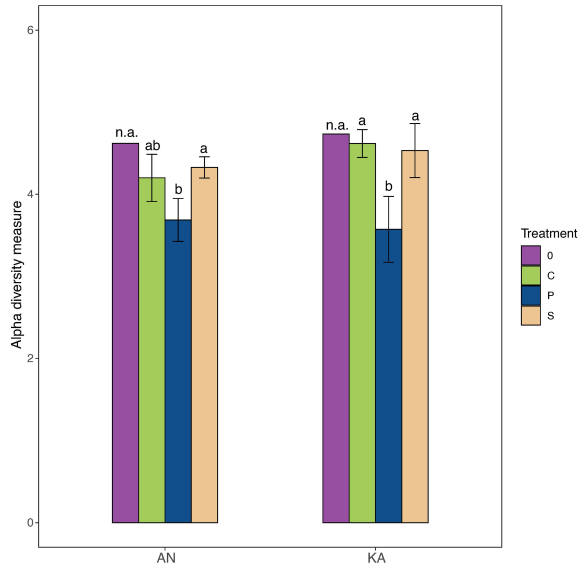

FIGURE 3
Alpha diversity (Shannon–Wiener diversity index) of samples in different treatment for Kalvarsskatan (KA) and Ängerån (AN) at the start (day 0, before DOM amendments) and end of the experiment (day 2). The colours in the graph represent different treatments, with purple representing day 0, green representing control, blue representing plankton extract treatment, and brown representing soil extract treatment, day 2. Error bars represent the standard deviation. The letter s "a" and "b" placed above each bar indicate significant differences (α = 0.05) between the treatments (excluding day 0), as determined by Kruskal–Wallis tests.

(GH13), glucosaminidase (GH73), and amylomaltase/4-α-glucanotransferase (GH77) were responsible for the possible degradation of chitin, starch, and glycogen (Table 3). In contrast, under the soil extract treatment, we observed a higher abundance of genes encoding endo-1,3-β-glucanase/ laminarinase (GH16) by Flavobacteria, and a gene encoding peroxidase (AA2) by the genus *Reyranella*, which may have a function in the degradation of cellulose and lignin, respectively (Table 3). The heatmap of the selected genes encoding for carbohydrate active enzymes (CAZymes) showed their different abundance across different treatments (Figure S4).

Discussion

The results of this study showed that the addition of different DOM types had varying effects on the composition, diversity and carbohydrate metabolism-related gene profiles of the bacterial communities. In general, the addition of autochthonous, plankton derived DOM, induced much larger effects on the bacterial community than the addition of allochthonous, terrestrial DOM. Bacterial production was significantly higher in response to the plankton extract treatment compared to the control in both bays, while the soil extract treatment did not result in such big increase. The high bacterial production in the plankton extract microcosms can be explained by higher bioavailability of the added carbon and higher concentrations of phosphorous compared to the soil extract incubation. The DOC consumption, bacterial abundance, and bacterial production showed that the bacterial community responded rapidly in the plankton extract treatment (Table 2, Figure 2). Our findings suggest that the bacterial community exhibited similar responses to various types of DOM in both bays, indicating a general pattern of community-level response in the northern Baltic Sea.

Alpha-diversity – fast response of the bacterial community to plankton-derived DOM while lack of response to soil-derived DOM

The DOM composition in marine systems has been shown to be highly dynamic and complex (Benner and Amon, 2015), potentially selecting for bacterial communities with high species richness/ diversity and large functional redundancy. However, our study found that the addition of plankton-derived DOM to microcosms resulted in a decrease in species richness, as measured by Shannon-Wiener diversity, while the addition of allochthonous, terrestrial DOM did not significantly affect the diversity compared to the control (Figure 3).

This decrease in species richness in response to plankton-derived DOM could be due to competition for resources. Plankton-derived DOM may contain high-quality organic matter that supports fast-growing, competitive bacterial taxa, leading to the outcompeting of less-competitive taxa and a reduction in diversity (Teeling et al., 2012). Additionally, plankton-derived DOM may select for specific bacterial taxa that are better adapted to utilize this

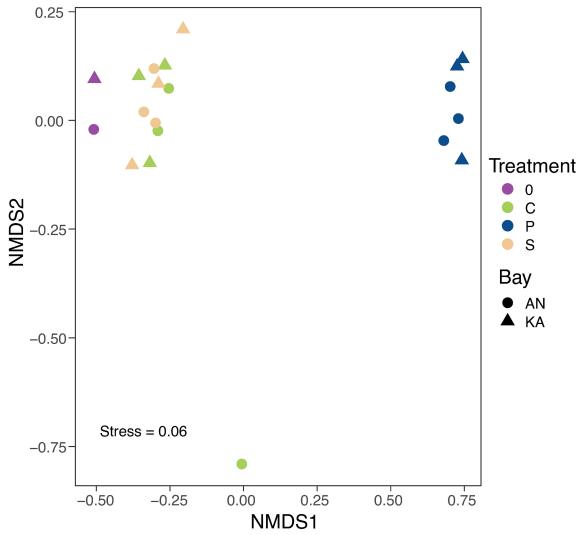

FIGURE 4
NMDS plot based on Bray-Curtis dissimilarities of ASVs relative abundance. The colours in the graph represent different treatments, with purple representing day 0, green representing control, blue representing plankton extract treatment, and brown representing soil extract treatment, day 2. The shapes represent different bays, with triangles representing KA and circles representing AN. The stress value is 0.06 indicates that the NMDS plot provides a highly accurate representation in reduced dimensions.

10.3389/fmars.2023.1130855

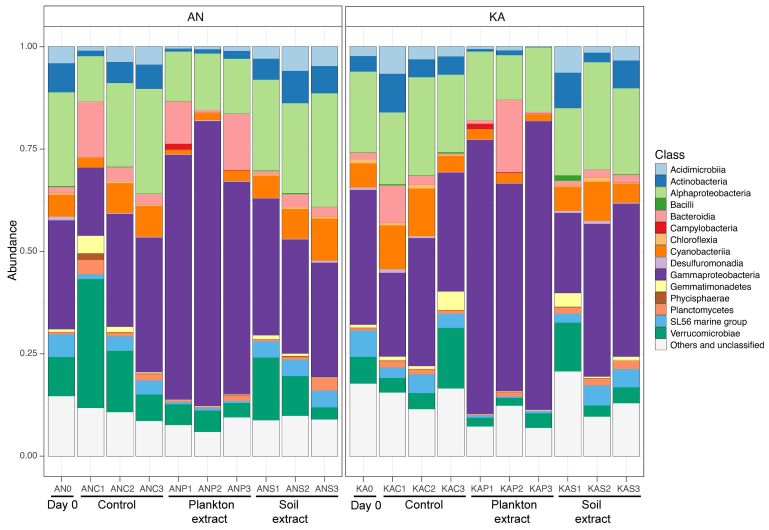

FIGURE 5
Relative abundance of major bacterial taxa at the class level at the start (day 0, before amendments) and end (day 2) of the experiment, in Kalvarsskatan (KA) and Ängerån (AN). AN0 indicates the start sample in Ängerån, and ANC1, ANC2, and ANC3 indicate triplicate samples of the control taken on day 2 in Ängerån. ANP1, ANP2, and ANP3 indicate triplicate samples of the plankton extract treatment taken on day 2 in Ängerån, and ANS1, ANS2, and ANS3 indicate triplicate samples of the soil extract treatment taken on day 2 in Ängerån. KA0 indicates the start sample in Kalvarsskatan, and KAC1, KAC2, and KAC3 indicate triplicate samples of the control taken on day 2 in Kalvarsskatan. KAP1, KAP2, and KAP3 indicate triplicate samples of the plankton extract treatment taken on day 2 in Kalvarsskatan, and KAS1, KAS2, and KAS3 indicate triplicate samples of the soil extract treatment taken on day 2 in Kalvarsskatan. All unidentified and low-abundance ASVs (<0.1%) as "Others and unclassified".

type of organic matter, resulting in a shift in community composition towards more specialized groups, further reducing diversity (Lindh and Pinhassi, 2018).

One possible explanation for the lack of response to soil extract inputs could be related to the lability of the DOM. While previous studies have demonstrated the importance of tDOM for marine bacterial communities and highlighted their positive response to tDOM inputs (Figueroa et al., 2021), it is possible that the soil extract used in our study was not as labile as the tDOM in previous studies. Moreover, the nutrient content could also influence the

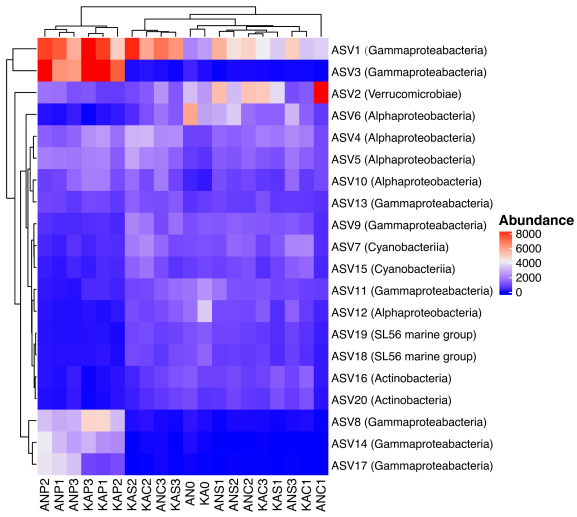

FIGURE 6
Heatmap of the 20 most abundant ASVs in different treatment, each column in the heatmap is an individual sample, each row is an ASV, with the corresponding taxonomic classification indicated at the class level in the parentheses. Clusters based on ASV abundance values. 0: day 0, C: control day 2, P: plankton extract treatment and S: soil extract treatment day 2." to "AN0 indicates the start sample in Ängerån, and ANC1, ANC2, and ANC3 indicate triplicate samples of the control taken on day 2 in Ängerån. ANP1, ANP2, and ANP3 indicate triplicate samples of the plankton extract treatment taken on day 2 in Ängerån, and ANS1, ANS2, and ANS3 indicate triplicate samples of the soil extract treatment taken on day 2 in Ängerån. KA0 indicates the start sample in Kalvarsskatan, and KAC1, KAC2, and KAC3 indicate triplicate samples of the control taken on day 2 in Kalvarsskatan. KAP1, KAP2, and KAP3 indicate triplicate samples of the plankton extract treatment taken on day 2 in Kalvarsskatan, and KAS1, KAS2, and KAS3 indicate triplicate samples of the soil extract treatment taken on day 2 in Kalvarsskatan.

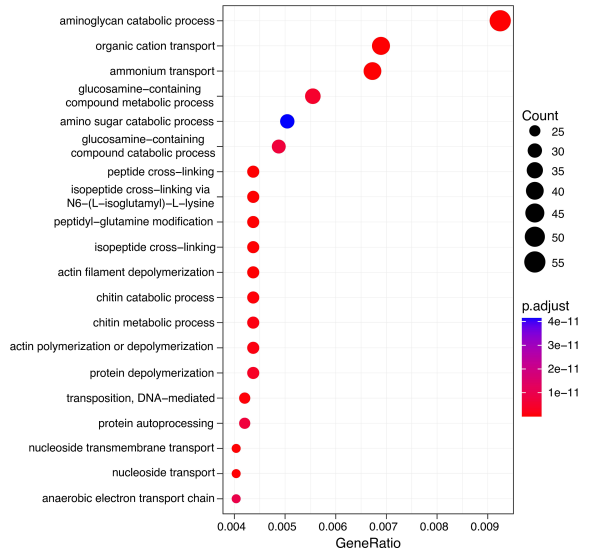

FIGURE 7
Gene ontology (GO) analysis of differentially abundant genes in plankton extract treatment compared to control.

response of bacterial communities to DOM inputs, while the nutrient in the soil extract was quite low in our study. Furthermore, our study was conducted over a short time frame (2 days), which may not be sufficient to capture the functional response of the bacterial community to tDOM inputs. Longer-term experiments and metatranscriptomic or metaproteomic approaches would be needed to better understand the functional response of the bacterial community to soil-derived DOM inputs.

Understanding how different types of organic matter affect bacterial communities can help predict how coastal ecosystems may respond to changes in DOM inputs, such as those resulting from climate change (Andersson et al., 2015). Additionally, understanding the mechanisms behind how specific bacterial taxa utilize different types of organic matter can enhance our comprehension of carbon cycling processes. To achieve this, the potential role of specific bacterial taxa in DOM utilization should be investigated.

Labile plankton-derived DOM induces fast shifts of the bacterial community composition

In both bays, Gammaproteobacteria were promoted when plankton extract was added to the microcosms. Their relative abundance increased from ca. 25 to 75%, thus dominating the bacterial community in this treatment (Figure 5). For example, the data in this study showed that the abundance of the fish pathogen *Aeromonas salmonicida* (Gammaproteobacteria) (McCarthy, 1977) increased in plankton extract treatment. A previous study showed that a representative for coastal Gammaproteobacteria, *Shewanella baltica*, harbors genes for degradation of labile DOM (Zhao et al., 2021). The gene profile analysis in this study however showed that Gammaproteobacteria have diverse metabolic functions potentially enabling them to utilize both refractory and labile substrates. Nevertheless, the differential gene abundance analysis showed that, compared to the control, the addition of plankton extract led to increased abundance of genes coding for carbohydrate-active enzymes degrading labile food substrates. The metabolic specialization of Gammaproteobacteria thus gave them a competitive advantage in the exploitation of labile source, while other bacterial groups were outcompeted in this short time experiment.

In contrast, when soil extract was added as food resource, the bacterial community composition did not change too much compared to the control (Figure 3). This indicates that the initial conditions of the coastal environment were similar refractive to the soil extract, which contains high molecular weight terrestrial DOM (Pettersson et al., 1997; Skoog et al., 2011). We performed a short-time experiment, but the bacterial community will be exposed to increased terrestrial DOM during longer periods of time according to a climate change scenario (Meier et al., 2022). The water turnover time in the Gulf of Bothnia is 5-6 years (Snoeijs-Leijonmalm et al., 2017). Slow growing bacteria did not show any change in the experiment, but in a longer run, we expect the composition of the coastal bacterial community to change towards an increased importance of Actinobacteria and Bacteroidetes, as they have been shown to be dominant in the northern Baltic Sea coast during the spring river flush of terrestrial matter (Figueroa et al., 2021), and in particularly Bacteroidetes which has been reported to responsive to elevated terrestrial DOM (Traving et al., 2017).

Our results conform to previous studies suggesting that the DOM composition in land-sea transitional areas, seasonal cycles and phytoplankton blooms affect the bacterial community composition and function (Lindh et al., 2015b; Mühlenbruch et al., 2018; Broman et al., 2019). However, Langenheder et al. (2005) conducted a study to investigate the relationship between bacterial community composition and functioning in freshwater lakes from mid Sweden. They analyzed the bacterial community composition and the metabolic activity of the bacteria and found that, although there was some correlation between bacterial community composition and function, the relationship was weak. Likely, a certain degree of change of the DOM composition is needed in order to change the bacterial community composition, and the DOM composition in the soil extract and the original coastal water were too similar to induce any major change of the bacterial community composition and function at a short time-scale.

Autochthonous DOM enriches genes encoding for enzymes degrading both labile and refractory carbohydrate substrates

Heterotrophic bacteria utilise DOM based on the molecular weight i.e. low-molecular-weight (LMW) (oligosaccharides, amino acids) and high molecular weight (HMW) polysaccharides. Both the soil and plankton extracts were assumed to at least partly consist of hydrolysable high molecular weight compounds (Pettersson

10.3389/fmars.2023.1130855

TABLE 3 List of selected enriched genes coding for carbohydrate active enzymes (CAZymes) induced by addition of plankton extract and soil extract.

Target CAZy	Gene ID	Enzyme	Target sub-strate	Plankton extract	soil extract	Taxa
GH18	NODE_100286_2*	Chitinase	Chitin		–	*Psychromonas* sp.
GH18	NODE_100737_1*	Chitinase	Chitin		–	*Aeromonas salmonicida*
GH18	NODE_106757_1*	Chitinase	Chitin			*Aeromonas*
GH13	NODE_100965_1*	Glycosidase (Amylase)	Starch		–	*Flavobacterium* sp.
GH13	NODE_1030034_1*	Alpha-amylase	Starch		–	*Aeromonas salmonicida*
GH13	NODE_1039047_1*	Alpha-amylase	Starch			*Shewanella putrefaciens*
GH13	NODE_1030023_1*	Maltodextrin glucosidase	Starch			*Aeromonas*
GH73	NODE_101433_2	Glucosaminidase	Chitin		–	*Rheinheimera* sp.
GH77	NODE_101727_2*	Amylomaltase/4-α-glucanotransferase	Starch		–	Chromatiaceae
GH77	NODE_10469_3*	Amylomaltase/4-α-glucanotransferase	Starch/Glycogen			*Shewanella baltica*
GH43	NODE_102940_2*	Hydrolase	Xylan		–	*Rheinheimera aquimaris*
PL9	NODE_10484_12*	Exopolygalacturonate lyase	Pectin		–	*Aeromonas salmonicida*
PL1	NODE_10484_13*	Pectate lyase	Pectin degradation		–	*Aeromonas*
GH1	NODE_10640_4*	6-phospho-β-galactosidase/β-glucosidase	Starch/Sucrose		–	*Aeromonas salmonicida*
AA2	NODE_241989_1	Peroxidase	Lignin	–		*Reyranella*
GH13	NODE_274175_1	Alpha amylase	Starch	–		Akkermansiaceae
GH16	NODE_150756_1	Endo-1,3-β-glucanase/laminarinase	Cellulose/ Laminarin	–		*Flavobacteria* sp.
GH92	NODE_341680_1	Alpha-mannosidase	Mannose	–		*Flavobacteria* sp.
GH97	NODE_92490_1	Glucoamylase/α-glucosidase	Starch	–		Flavobacteriales
GH4	NODE_119660_2	α-galactosidase	Raffinose	–		*Rhodobacter* sp.

*:denote significant differential abundance.
Encoded enzyme, targeted substrate and functional bacterial taxa are also presented.

et al., 1997; Akita et al., 2016; Mühlenbruch et al., 2018; Zhao et al., 2021). Bacterial exo-enzymes with hydrolytic properties, for example chitinases, would enable degradation of the DOM compounds, and assist in the assimilation of the organic carbon into the bacterial food web (Mühlenbruch et al., 2018).

Our study found that the addition of plankton-derived dissolved organic matter (DOM) resulted in a more than 100-fold increase in the abundance of genes coding for enzymes that are involved in carbohydrate degradation pathways and degrade various polysaccharides, including chitin, starch, glycogen, xylan, and pectin, compared to the control group (Figure 7, Table S5). Chitin is a major component of the exoskeleton of zooplankton, such as copepods (Jeuniaux et al., 1989), while glycogen and starch are the storage compounds of cyanobacteria and other autotrophic plankton (Mühlenbruch et al., 2018). The plankton we collected for our study was dominated by filamentous cyanobacteria and mesozooplankton, suggesting that the plankton extract we used was enriched with chitin, glycogen, and starch, all of which are labile carbon substrates for bacterial utilization. Bacteria, especially Gammaproteobacteria are the major degrader of chitin in aquatic systems, and their chitinases are mostly found in family 18 of glycoside hydrolase families, but are also annotated to other families (Adrangi and Faramarzi, 2013; Beier and Bertilsson, 2013; Wang et al., 2019; Jiang et al., 2022). According to the CAZy database, the α-amylases which hydrolyze starch and glycogen, were categorized in glycoside hydrolase family 13 (GH13) (Drula et al., 2022). Thus, our observed increase in the abundance of genes coding for chitinases and α-amylases in response to the addition of plankton extract might be due to the presence of the GH18 and GH13 families in the identified taxa.

Surprisingly, genes for enzymatic degradation of xylan, pectin and cellulose were also enriched by plankton extract addition, even

though these compounds originate mostly from terrestrial systems (Pettersson et al., 1997; Akita et al., 2016; Zhao et al., 2021). Multiple genes with the same function could occur in a single organism (e.g. Fuchs et al., 1986; Colatriano et al., 2018), which may repeat similar sequences of genes by gene duplication or acquisition of genes from other organisms by lateral gene transfer (Marri et al., 2006; Colatriano et al., 2018). Multiple enzymes of similar function within an individual bacterium could increase the metabolic potential to utilize carbon and enhance the substrate utilization efficiency compared to other organisms. Probably such metabolic capacity could make specific bacteria groups more successful in the bacterial community under certain environmental conditions (Beier and Bertilsson, 2013; Colatriano et al., 2018).

In our study, the enriched genes coding for polysaccharide degradation enzymes were mostly assigned to Gammaproteobacteria (eg. *Aeromonas salmonicida; Shewanella baltica*) and Bacteroidetes (eg. *Flavobacterium* sp.) in the plankton extract addition treatment (Table 3). *Aeromonas salmonicida* harbours various genes simultaneously coding for chitin, starch, pectin and cellulose degradation, *Shewanella baltica* for starch/glycogen degradation. These observations agree with increasing relative abundance of the taxa from Gammaproteobacteria, for example, ASV3 (*Aeromonas*), ASV14 (*Aeromonas*) and ASV8 (*Shewanella*) (Figure 6, Table S1). Xylan is a relatively refractory organic compound, originating from terrestrial systems, which was expected to be enriched in soil extract amended microcosms together with pectin, cellulose and lignin. Interestingly, we observed genes coding for xylan decomposition to be enriched as well in the plankton extract treatment, which was assigned to taxa *Rheinheimera aquimaris*. One of the possible explanations can be a "priming effect", where degradation of labile organic matter stimulates the decomposition of soil extract compounds following the supply of the plankton extract (Bianchi, 2011), but this could also be due to metabolic plasticity of *Rheinheimera*, which support diverse metabolic processes (Lindh et al., 2015b). From our study, we can draw the conclusion that *Flavobacterium* sp. also has metabolic plasticity, as it harbours genes for cellulose, starch and mannose degradation. We observed increased gene abundances under both plankton extract addition and soil extract addition compared to the control. Nevertheless, our study indicated that genes encoding for lignin degradation enzymes from *Reyranella* had higher abundance in soil extract addition than in the control, even though significant difference could not be proven.

Taken together, our study complies with earlier studies showing that autochthonous DOM select for the opportunistic bacteria especially Gammaproteobacteria and *Flavobacteriia* (Beier and Bertilsson, 2013). However, in soil extract addition we only found signs of increased abundances of genes encoding for lignin degradation. Probably long-term studies are needed to get evidence for soil extract being such a driver.

Conclusion and outlook

Our study demonstrates how coastal bacteria can respond compositionally and functionally to climate-induced shifts in dissolved organic matter. The addition of plankton extract induced a change of the bacterial community composition and reduced the species richness, while no significant changes occurred with soil extract. Various genes related to carbohydrate metabolism, such as the degradation of chitin, were enriched by plankton extract amendment, while soil extract only showed slight signs of upregulating genes for lignin degradation. Taken together, coastal bacterial communities showed fast responses to inputs of highly bioavailable autochthonous substrates, while terrestrial matter was not quickly degraded and has minor influence on the bacterial community. We acknowledge the limitations of our short-term study and recognize the need for more comprehensive investigations to better understand the bacterial degradation of terrestrial dissolved organic matter (DOM) in the land-sea transitional zone. Long-term experiments or field studies, in combination with metatranscriptomic or metaproteomic approaches, could provide valuable insights into the functions of slow-growing bacteria and the gradual degradation processes. Such studies would enhance our understanding of how the bacterial community contributes to the overall degradation of terrestrial DOM in the land-sea transitional zone. This information is critical for assessing the impacts of climate change on coastal ecosystems and developing protective strategies.

Data availability statement

The datasets presented in this study can be found in online repositories. The names of the repository/repositories and accession number(s) can be found below: https://www.ncbi.nlm.nih.gov/, PRJNA915349.

Author contributions

LZ, SB and AA conceived the study. LZ and SB carried out the microcosm experiment. SB performed microbial analyses and compiled the environmental data. LZ performed the molecular work and bioinformatics. KR performed the gene analysis related to carbohydrate metabolism. LZ wrote the paper together with all authors. All authors contributed to the article and approved the submitted version.

Funding

This project was financed by the Swedish research council FORMAS (FR-2019/0007), Umeå Marine Sciences Centre, and the Swedish research environment EcoChange.

Acknowledgments

We thank the staff at Umeå Marine Sciences Center and Björn Karlsson for excellent support during performance of the field experiment and for chemical analyses. We thank Eric Cope for the supply of the 16S primers. The bioinformatic data analysis was

enabled by resources provided by the Swedish National Infrastructure for Computing (SNIC) at High Performance Computing Center North (HPC2N) partially funded by the Swedish Research Council through grant agreement no. 2018-05973.

Conflict of interest

The authors declare that the research was conducted in the absence of any commercial or financial relationships that could be construed as a potential conflict of interest.

Publisher's note

All claims expressed in this article are solely those of the authors and do not necessarily represent those of their affiliated organizations, or those of the publisher, the editors and the reviewers. Any product that may be evaluated in this article, or claim that may be made by its manufacturer, is not guaranteed or endorsed by the publisher.

Supplementary material

The Supplementary Material for this article can be found online at: https://www.frontiersin.org/articles/10.3389/fmars.2023.1130855/full#supplementary-material

SUPPLEMENTARY TABLE 1
The table presents an overview of the sequence count and taxonomic annotation per ASV obtained from 16S rRNA sequencing.

SUPPLEMENTARY TABLE 2
Alpha diversity metrics assessed by rarefied count.

SUPPLEMENTARY TABLE 3
The table presents an overview of the potential carbohydrate active enzymes (CAZymes) encoding genes.

SUPPLEMENTARY TABLE 4
The table showing the significant differential abundant ASVs and their taxonomic annotation between plankton extract treatment to control.

SUPPLEMENTARY TABLE 5
The table showing the differential abundant genes and their taxonomic annotation between plankton extract treatment to control or between soil extract treatment to control.

References

Adrangi, S., and Faramarzi, M. A. (2013). From bacteria to human: a journey into the world of chitinases. *Biotechnol. Adv.* 31, 1786–1795. doi: 10.1016/j.biotechadv.2013.09.012

Akita, H., Kimura, Z., Mohd Yusoff, M. Z., Nakashima, N., and Hoshino, T. (2016). Isolation and characterization of burkholderia sp. strain CCA53 exhibiting ligninolytic potential. *Springerplus* 5, 596. doi: 10.1186/s40064-016-2237-y

Andersson, A., Ahlinder, J., Mathisen, P., Hägglund, M., Bäckman, S., Nilsson, E., et al. (2018). Predators and nutrient availability favor protozoa-resisting bacteria in aquatic systems. *Sci. Rep.* 8, 8415. doi: 10.1038/s41598-018-26422-4

Andersson, A., Meier, H. E., Ripszam, M., Rowe, O., Wikner, J., Haglund, P., et al. (2015). Projected future climate change and Baltic Sea ecosystem management. *Ambio* 44 (Suppl 3), 345–356. doi: 10.1007/s13280-015-0654-8

Andersson, A. F., Riemann, L., and Bertilsson, S. (2010). Pyrosequencing reveals contrasting seasonal dynamics of taxa within Baltic Sea bacterioplankton communities. *ISME J.* 4, 171–181. doi: 10.1038/ismej.2009.108

Azam, F., and Malfatti, F. (2007). Microbial structuring of marine ecosystems. *Nat. Rev. Microbiol.* 5, 782–791. doi: 10.1038/nrmicro1747

Beier, S., and Bertilsson, S. (2013). Bacterial chitin degradation-mechanisms and ecophysiological strategies. *Front. Microbiol.* 4, 149. doi: 10.3389/fmicb.2013.00149

Benner, R., and Amon, R. M. (2015). The size-reactivity continuum of major bioelements in the ocean. *Ann. Rev. Mar. Sci.* 7, 185–205. doi: 10.1146/annurev-marine-010213-135126

Berglund, J., Müren, U., Båmstedt, U., and Andersson, A. (2007). Efficiency of a phytoplankton-based and a bacterial-based food web in a pelagic marine system. *Limnol. Oceanogr.* 52, 121–131. doi: 10.4319/lo.2007.52.1.0121

Bertilsson, S., and Jones, J. B. (2003). "Supply of dissolved organic matter to aquatic ecosystems: autochthonous sources," in *Aquatic ecosystems*. Eds. S. E. G. Findlay and R. L. Sinsabaugheds (Burlington: Academic Press), 3–24.

Bianchi, T. S. (2011). The role of terrestrially derived organic carbon in the coastal ocean: a changing paradigm and the priming effect. *Proc. Natl. Acad. Sci. U.S.A.* 108, 19473–19481. doi: 10.1073/pnas.1017982108

Boyer, F., Mercier, C., Bonin, A., Le Bras, Y., Taberlet, P., and Coissac, E. (2016). Obitools: a unix-inspired software package for DNA metabarcoding. *Mol. Ecol. Resour.* 16, 176–182. doi: 10.1111/1755-0998.12428

Broman, E., Asmala, E., Carstensen, J., Pinhassi, J., and Dopson, M. (2019). Distinct coastal microbiome populations associated with autochthonous-and allochthonous-like dissolved organic matter. *Front. Microbiol.* 10, 2579. doi: 10.3389/fmicb.2019.02579

Bruhn, A. D., Stedmon, C. A., Comte, J., Matsuoka, A., Speetjens, N. J., Tanski, G., et al. (2021). Terrestrial dissolved organic matter mobilized from eroding permafrost controls microbial community composition and growth in Arctic coastal zones. *Front. Earth Sci.* 9, 640580. doi: 10.3389/feart.2021.640580

Callahan, B. J., McMurdie, P. J., Rosen, M. J., Han, A. W., Johnson, A. J., and Holmes, S. P. (2016). DADA2: high-resolution sample inference from illumina amplicon data. *Nat. Methods* 13, 581–583. doi: 10.1038/nmeth.3869

Carlson, M., and Pagès, H. (2023) *AnnotationForge: tools for building SQLite-based annotation data packages*. Available at: https://bioconductor.org/packages/AnnotationForge.

Chen, S., Zhou, Y., Chen, Y., and Gu, J. (2018). Fastp: an ultra-fast all-in-one FASTQ preprocessor. *Bioinformatics* 34, i884–i890. doi: 10.1093/bioinformatics/bty560

Colatriano, D., Tran, P. Q., Guéguen, C., Williams, W. J., Lovejoy, C., and Walsh, D. A. (2018). Genomic evidence for the degradation of terrestrial organic matter by pelagic Arctic ocean chloroflexi bacteria. *Commun. Biol.* 1, 90. doi: 10.1038/s42003-018-0086-7

Cole, J. J., Prairie, Y. T., Caraco, N. F., McDowell, W. H., Tranvik, L. J., Striegl, R. G., et al. (2007). Plumbing the global carbon cycle: integrating inland waters into the terrestrial carbon budget. *Ecosystems* 10, 172–185. doi: 10.1007/s10021-006-9013-8

D'Andrilli, J., Junker, J. R., Smith, H. J., Scholl, E. A., and Foreman, C. M. (2019). DOM composition alters ecosystem function during microbial processing of isolated sources. *Biogeochemistry* 142, 281–298. doi: 10.1007/s10533-018-00534-5

Davis, N. M., Proctor, D. M., Holmes, S. P., Relman, D. A., and Callahan, B. J. (2018). Simple statistical identification and removal of contaminant sequences in marker-gene and metagenomics data. *Microbiome* 6, 226. doi: 10.1186/s40168-018-0605-2

de Mendiburu, F. (2021) *Agricolae: statistical procedures for agricultural research*. Available at: https://CRAN.R-project.org/package=agricolae.

Drake, T. W., Raymond, P. A., and Spencer, R. G. M. (2018). Terrestrial carbon inputs to inland waters: a current synthesis of estimates and uncertainty. *Limnol. Oceanogr.* 3, 132–142. doi: 10.1002/lol2.10055

Drula, E., Garron, M. L., Dogan, S., Lombard, V., Henrissat, B., and Terrapon, N. (2022). The carbohydrate-active enzyme database: functions and literature. *Nucleic Acids Res.* 50, D571–D577. doi: 10.1093/nar/gkab1045

Figueroa, D., Capo, E., Lindh, M. V., Rowe, O. F., Paczkowska, J., Pinhassi, J., et al. (2021). Terrestrial dissolved organic matter inflow drives temporal dynamics of the bacterial community of a subarctic estuary (northern Baltic Sea). *Environ. Microbiol.* 23, 4200–4213. doi: 10.1111/1462-2920.15597

Fuchs, R. L., McPherson, S. A., and Drahos, D. J. (1986). Cloning of a *Serratia marcescens* gene encoding chitinase. *Appl. Environ. Microbiol.* 51, 504–509. doi: 10.1128/aem.51.3.504-509.1986

Fuhrman, J. A., and Azam, F. (1982). Thymidine incorporation as a measure of heterotrophic bacterioplankton production in marine surface waters: evaluation and field results. *Mar. Biol.* 66, 109–120. doi: 10.1007/BF00397184

Grasshoff, K., Kremling, K., and Ehrhardt, M. (1999). *Methods of seawater analysis. 3rd Edition* (Weinheim, Germany: Wiley-VCH).

Hadley, W. (2016). *ggplot2: elegant graphics for data analysis-Hadley wickham* (USA: Springer-Verlag New York).

Hallfors, G. (2004). "Checklist of Baltic Sea phytoplankton species (including some heterotrophic protistan groups)," in *HELCOM, balt. Sea environ. proc* (Helsinki, Finland: Helsinki Commission).

Herlemann, D. P., Lundin, D., Andersson, A. F., Labrenz, M., and Jürgens, K. (2016). Phylogenetic signals of salinity and season in bacterial community composition across the salinity gradient of the Baltic Sea. *Front. Microbiol.* 7, 1883. doi: 10.3389/fmicb.2016.01883

Hoge, F. E., Vodacek, A., and Blough, N. V. (1993). Inherent optical properties of the ocean: retrieval of the absorption coefficient of chromophoric dissolved organic matter from fluorescence measurements. *Limnol. Oceanogr.* 38, 1394–1402. doi: 10.4319/lo.1993.38.7.1394

Huerta-Cepas, J., Szklarczyk, D., Heller, D., Hernández-Plaza, A., Forslund, S. K., Cook, H., et al. (2019). eggNOG 5.0: a hierarchical, functionally and phylogenetically annotated orthology resource based on 5090 organisms and 2502 viruses. *Nucleic Acids Res.* 47, D309–D314. doi: 10.1093/nar/gky1085

Hugoni, M., Vellet, A., and Debroas, D. (2017). Unique and highly variable bacterial communities inhabiting the surface microlayer of an oligotrophic lake. *Aquat. Microb. Ecol.* 79, 115–125. doi: 10.3354/ame01825

Jeuniaux, C., Voss-Foucart, M. F., Poulicek, M., and Bussers, J. C. (1989). "Sources of chitin, estimated from new data on chitin biomass and production," in *Chitin and chitosan*. Eds. G. Skjak-Braek, T. Antonsen and P. A. Sandfordeds (London and New York: Elsevier Applied Science), 3–11.

Jiang, W. X., Li, P. Y., Chen, X. L., Zhang, Y. S., Wang, J. P., Wang, Y. J., et al. (2022). A pathway for chitin oxidation in marine bacteria. *Nat. Commun.* 13, 5899. doi: 10.1038/s41467-022-33566-5

Jiao, N., Herndl, G. J., Hansell, D. A., Benner, R., Kattner, G., Wilhelm, S. W., et al. (2011). The microbial carbon pump and the oceanic recalcitrant dissolved organic matter pool. *Nat. Rev. Microbiol.* 9, 555–555. doi: 10.1038/nrmicro2386-c5

Langenheder, S., Lindström, E. S., and Tranvik, L. J. (2005). Weak coupling between community composition and functioning of aquatic bacteria. *Limnol. Oceanogr.* 50, 957–967. doi: 10.4319/lo.2005.50.3.0957

Lindh, M. V., Figueroa, D., Sjöstedt, J., Baltar, F., Lundin, D., Andersson, A., et al. (2015a). Transplant experiments uncover Baltic Sea basin-specific responses in bacterioplankton community composition and metabolic activities. *Front. Microbiol.* 6, 223. doi: 10.3389/fmicb.2015.00223

Lindh, M. V., and Pinhassi, J. (2018). Sensitivity of bacterioplankton to environmental disturbance: a review of Baltic Sea field studies and experiments. *Front. Mar. Sci.* 5, 361. doi: 10.3389/fmars.2018.00361

Lindh, M. V., Sjöstedt, J., Andersson, A. F., Baltar, F., Hugerth, L. W., Lundin, D., et al. (2015b). Disentangling seasonal bacterioplankton population dynamics by high-frequency sampling. *Environ. Microbiol.* 17, 2459–2476. doi: 10.1111/1462-2920.12720

Logue, J. B., Stedmon, C. A., Kellerman, A. M., Nielsen, N. J., Andersson, A. F., Laudon, H., et al. (2016). Experimental insights into the importance of aquatic bacterial community composition to the degradation of dissolved organic matter. *ISME J.* 10, 533–545. doi: 10.1038/ismej.2015.131

Love, M. I., Huber, W., and Anders, S. (2014). Moderated estimation of fold change and dispersion for RNA-seq data with DESeq2. *Genome Biol.* 15, 550. doi: 10.1186/s13059-014-0550-8

Marie, D., Simon, N., and Vaulot, D. (2005). "Phytoplankton cell counting by flow cytometry," in *Algal culturing techniques*. Ed. R. A. Andersen (San Diego: Academic Press), 253–267.

Marri, P. R., Bannantine, J. P., and Golding, G. B. (2006). Comparative genomics of metabolic pathways in *Mycobacterium* species: gene duplication, gene decay and lateral gene transfer. *FEMS Microbiol. Rev.* 30, 906–925. doi: 10.1111/j.1574-6976.2006.00041.x

McCarthy, D. H. (1977). Some ecological aspects of the bacterial fish pathogen - *Aeromonas salmonicida*. *Aquat. Microb.* 6, 299–324.

McMurdie, P. J., and Holmes, S. (2013). Phyloseq: an r package for reproducible interactive analysis and graphics of microbiome census data. *PloS One* 8, e61217. doi: 10.1371/journal.pone.0061217

Meier, H. E. M., Kniebusch, M., Dieterich, C., Gröger, M., Zorita, E., Elmgren, R., et al. (2022). Climate change in the Baltic Sea region: a summary. *Earth Syst. Dynam.* 13, 457–593. doi: 10.5194/esd-13-457-2022

Meier, H. E., Müller-Karulis, B., Andersson, H. C., Dieterich, C., Eilola, K., Gustafsson, B. G., et al. (2012). Impact of climate change on ecological quality indicators and biogeochemical fluxes in the Baltic sea: a multi-model ensemble study. *Ambio* 41, 558–573. doi: 10.1007/s13280-012-0320-3

Menden-Deuer, S., and Lessard, E. J. (2000). Carbon to volume relationships for dinoflagellates, diatoms, and other protist plankton. *Limnol. Oceanogr.* 45, 569–579. doi: 10.4319/lo.2000.45.3.0569

Menzel, P., Ng, K. L., and Krogh, A. (2016). Fast and sensitive taxonomic classification for metagenomics with kaiju. *Nat. Commun.* 7, 11257. doi: 10.1038/ncomms11257

Morya, R., Salvachúa, D., and Thakur, I. S. (2020). Burkholderia: an untapped but promising bacterial genus for the conversion of aromatic compounds. *Trends Biotechnol.* 38, 963–975. doi: 10.1016/j.tibtech.2020.02.008

Mühlenbruch, M., Grossart, H. P., Eigemann, F., and Voss, M. (2018). Mini-review: phytoplankton-derived polysaccharides in the marine environment and their interactions with heterotrophic bacteria. *Environ. Microbiol.* 20, 2671–2685. doi: 10.1111/1462-2920.14302

Oksanen, J., Simpson, G. L., Blanchet, F. G., Kindt, R., Legendre, P., Minchin, P. R., et al. (2022) *Vegan: community ecology package*. Available at: https://CRAN.R-project.org/package=vegan.

Olenina, I., Hajdu, S., Edler, L., Andersson, A., Wasmund, N., Busch, S., et al. (2006). "Biovolumes and size-classes of phytoplankton in the Baltic Sea," in *HELCOM, balt. Sea environ. proc* (Helsinki, Finland: Helsinki Commission), 1–144.

Patro, R., Duggal, G., Love, M. I., Irizarry, R. A., and Kingsford, C. (2017). Salmon provides fast and bias-aware quantification of transcript expression. *Nat. Methods* 14, 417–419. doi: 10.1038/nmeth.4197

Pettersson, C., Allard, B., and Borén, H. (1997). River discharge of humic substances and humic-bound metals to the gulf of bothnia. *Estuar. Coast. Shelf Sci.* 44, 533–541. doi: 10.1006/ecss.1996.0159

Quast, C., Pruesse, E., Yilmaz, P., Gerken, J., Schweer, T., Yarza, P., et al. (2013). The SILVA ribosomal RNA gene database project: improved data processing and web-based tools. *Nucleic Acids Res.* 41, D590–D596. doi: 10.1093/nar/gks1219

Robinson, M. D., McCarthy, D. J., and Smyth, G. K. (2010). edgeR: a bioconductor package for differential expression analysis of digital gene expression data. *Bioinformatics* 26, 139–140. doi: 10.1093/bioinformatics/btp616

Skoog, A., Wedborg, M., and Fogelqvist, E. (2011). Decoupling of total organic carbon concentrations and humic substance fluorescence in a an extended temperate estuary. *Mar. Chem.* 124, 68–77. doi: 10.1016/j.marchem.2010.12.003

Smith, H. J., Dieser, M., McKnight, D. M., SanClements, M. D., and Foreman, C. M. (2018). Relationship between dissolved organic matter quality and microbial community composition across polar glacial environments. *FEMS Microbiol. Ecol.* 94, 1–10. doi: 10.1093/femsec/fiy090

Snoeijs-Leijonmalm, P., Schubert, H., and Radziejewska, T. (2017). *Biological oceanography of the Baltic Sea* (Dordrecht, Netherland: Springer Science & Business Media).

Teeling, H., Fuchs, B. M., Becher, D., Klockow, C., Gardebrecht, A., Bennke, C. M., et al. (2012). Substrate-controlled succession of marine bacterioplankton populations induced by a phytoplankton bloom. *Science* 336, 608–611. doi: 10.1126/science.1218344

Teira, E., Nieto-Cid, M., and Álvarez-Salgado, X. A. (2009). Bacterial community composition and colored dissolved organic matter in a coastal upwelling ecosystem. *Aquat. Microb. Ecol.* 55, 131–142. doi: 10.3354/ame01290

Tikkanen, T., and Wille'n, T. (1992). "Phytoplankton flora," (Solna, Sweden: The Swedish Environmental Protection Agency).

Traving, S. J., Rowe, O., Jakobsen, N. M., Sørensen, H., Dinasquet, J., Stedmon, C. A., et al. (2017). The effect of increased loads of dissolved organic matter on estuarine microbial community composition and function. *Front. Microbiol.* 8, 351. doi: 10.3389/fmicb.2017.00351

Utermöhl, H. (1958). Zur vervolkommung der quantitativen phytoplankton-methodik. *Mitt. Int. Verein. Theor. Angew. Limnol.* 9, 1–38.

Wang, Y. J., Jiang, W. X., Zhang, Y. S., Cao, H. Y., Zhang, Y., Chen, X. L., et al. (2019). Structural insight into chitin degradation and thermostability of a novel endochitinase from the glycoside hydrolase family 18. *Front. Microbiol.* 10, 2457. doi: 10.3389/fmicb.2019.02457

Wu, T., Hu, E., Xu, S., Chen, M., Guo, P., Dai, Z., et al. (2021). clusterProfiler 4.0: a universal enrichment tool for interpreting omics data. *Innovation* 2, 100141. doi: 10.1016/j.xinn.2021.100141

Zhang, H., Yohe, T., Huang, L., Entwistle, S., Wu, P., Yang, Z., et al. (2018). dbCAN2: a meta server for automated carbohydrate-active enzyme annotation. *Nucleic Acids Res.* 46, W95–W101. doi: 10.1093/nar/gky418

Zhao, L., Brugel, S., Ramasamy, K. P., and Andersson, A. (2021). Response of coastal *Shewanella* and *Duganella* bacteria to planktonic and terrestrial food substrates. *Front. Microbiol.* 12, 726844. doi: 10.3389/fmicb.2021.726844

frontiers | Frontiers in Marine Science

TYPE Original Research
PUBLISHED 24 April 2023
DOI 10.3389/fmars.2023.1156487

OPEN ACCESS

EDITED BY
Agneta Andersson,
Umeå University, Sweden

REVIEWED BY
Catherine Legrand,
Halmstad University, Sweden
Sonia Brugel,
Umeå University, Sweden

*CORRESPONDENCE
Lumi Haraguchi
lumi.haraguchi@syke.fi

SPECIALTY SECTION
This article was submitted to Global Change and the Future Ocean, a section of the journal Frontiers in Marine Science

RECEIVED 01 February 2023
ACCEPTED 04 April 2023
PUBLISHED 24 April 2023

CITATION
Haraguchi L, Kraft K, Ylöstalo P, Kielosto S, Hällfors H, Tamminen T and Seppälä J (2023) Trait response of three Baltic Sea spring dinoflagellates to temperature, salinity, and light gradients. *Front. Mar. Sci.* 10:1156487. doi: 10.3389/fmars.2023.1156487

Trait response of three Baltic Sea spring dinoflagellates to temperature, salinity, and light gradients

Lumi Haraguchi*, Kaisa Kraft, Pasi Ylöstalo, Sami Kielosto, Heidi Hällfors, Timo Tamminen and Jukka Seppälä

Marine Ecology Measurements, Research Infrastructure, Finnish Environment Institute, Helsinki, Finland

Climate change is driving Baltic Sea shifts, with predictions for decrease in salinity and increase in temperature and light limitation. Understanding the responses of the spring phytoplankton community to these shifts is essential to assess potential changes in the Baltic Sea biogeochemical cycles and functioning. In this study we use a high-throughput well-plate setup to experimentally define growth and the light acquisition traits over gradients of salinity, temperature and irradiance for three dinoflagellates commonly occurring during spring in the Baltic Sea, *Apocalathium malmogiense*, *Gymnodinium corollarium* and *Heterocapsa arctica* subsp. *frigida*. By analysing the response of cell volume, growth, and light-acquisition traits to temperature and salinity gradients, we showed that each of the three dinoflagellates have their own niches and preferences and are affected differently by small changes in salinity and temperature. *A. malmogiense* has a more generalist strategy, its growth being less affected by temperature, salinity, and light gradients in comparison to the other tested dinoflagellates, with *G. corollarium* growth being more sensitive to higher light intensities. On the other hand, *G. corollarium* light acquisition traits seem to be less sensitive to changes in temperature and salinity than those of *A. malmogiense* and *H. arctica* subsp. *frigida*. We contextualized our experimental findings using data collected on ships-of-opportunity between 1993-2011 over natural temperature and salinity gradients in the Baltic Sea. The *Apocalathium* complex and *H. arctica* subsp. *frigida* were mostly found in temperatures<10°C and salinities 4-10 ‰, matching the temperature and salinity gradients used in our experiments. Our results illustrate that trait information can complement phytoplankton monitoring observations, providing powerful tools to answer questions related to species' capacity to adapt and compete under a changing environment.

KEYWORDS

Baltic Sea, vernal dinoflagellates, light acquisition traits, environmental gradients, high-throughput well-plate

1 Introduction

Primary productivity is a key function in marine ecosystems associated with major energy and matter fluxes, especially during the productive season (Falkowski et al., 1998). In the Baltic Sea, the productive season starts in spring with the growth of cold-water species, which depending on the areas, often occurs under the ice (Ikävalko & Thomsen, 1997; Spilling, 2007). Phytoplankton growth is further stimulated by the stratification of the water column that unlike many marine systems is largely controlled by freshwater advection from coastal waters (which are influenced by snowmelt and rainfall), with temperature having a secondary role (Stipa, 2004). This leads to highly variable physical and biological conditions, with the bloom starting to develop first in the southern parts, then the more northern, and usually occurring in February-May (Kahru and Nömmann, 1990; Spilling et al., 2018). The Baltic Sea spring bloom marks the ecosystem shifts from being net heterotrophic to net autotrophic, acting as a sink of carbon dioxide (Honkanen et al., 2021). During this period about 50% of the annual carbon is fixed and up to 80% of this fixed carbon can sink to the sea bottom (Lignell et al., 1993; Spilling et al., 2018).

Long-term observations have reported trends in the Baltic Sea spring bloom phenology and intensity, with an increase in temperature and light conditions leading to earlier and longer blooms, while reduced nutrient loads are associated with a lower bloom peak intensity (Groetsch et al., 2016). Diatoms and dinoflagellates make up most of the Baltic Sea spring phytoplankton community, with the ratio of these two groups varying over space and time. However, long term trends regarding dominance shifts from diatoms to dinoflagellates have been attributed to changes in local conditions, such as stormier winters and thinner ice, which favour the resuspension of cyst beds and under ice accumulation of dinoflagellates during winter time, allowing them to outcompete diatoms during the spring bloom (Klais et al., 2011; Klais et al., 2013). These shifts are connected to potential changes in the export and cycling patterns of carbon and nitrogen, with the dominance of dinoflagellates being associated with sinking material with a lower C:N:P ratio (Spilling et al., 2014) and slower-sinking particles than diatom dominated communities (Tamelander and Heiskanen, 2004). Ultimately, the spring bloom material will influence patterns in remineralization and food availability, affecting both summer nutrient availability for phytoplankton and food supply for pelagic grazers and benthic communities (Vahtera et al., 2007; Spilling et al., 2018; Hjerne et al., 2019).

Large interannual variations in the bloom composition are still observed (Spilling et al., 2018). The occurrence of dinoflagellate dominated blooms is dependent on the initial environmental conditions and success in the species recruitment, being sensitive to climate change scenarios (Kremp et al., 2008). Albeit all being cold water species, vernal Baltic Sea dinoflagellates have different ecological strategies regarding growth rates, cyst formation and nutrient acquisition, affecting the community composition and the fate of the bloom (Kremp et al., 2009; Spilling et al., 2018). However, challenges in species identification under the light microscope, especially when samples have been preserved, increase the uncertainty of taxonomical assignment and limits the capacity to evaluate relationships with environmental factors (Sundström et al., 2009).

Analysing phytoplankton traits has been proposed as a method to integrate molecular, physiological, morphological and ecological knowledge on phytoplankton and their responses to different drivers, allowing for a more general mechanistic explanation to organisms' occurrence under certain environmental conditions (Litchman and Klausmeier, 2008). Trait-based approaches can be helpful to understand effects of environmental changes in planktonic communities (Litchman et al., 2010). While certain traits can easily be established (e.g. size, motility, pigments), others such as photo-physiology, growth and nutrient uptake require extensive experimental effort to be determined. When considering species that have a similar niche, such as vernal Baltic Sea dinoflagellates, the response of individual species to fine environmental gradients is an important aspect to be explored under climate change scenarios. Thus, in this study we aim to define experimentally the responses of growth parameters over gradients of salinity, temperature, and irradiance for three dinoflagellates commonly found during spring in the Baltic Sea, *Apocalathium malmogiense*, *Gymnodinium corollarium* and *Heterocapsa arctica* subsp. *frigida*. Of these, the two first mentioned are common bloom-formers (Jaanus et al., 2006; Sundström et al., 2010), whereas the latter is regularly occurring, but rarely in bloom-forming amounts (Hällfors, 2013, and references therein). Additionally, we contextualize the findings from our laboratory experiments by comparing the results to a long-term time series of semi-quantitative species data collected using ships-of-opportunity travelling across salinity and temperature gradients in the Baltic Sea.

2 Material and methods

2.1 Experiment setup

Experiments were conducted in the Marine Research Laboratory (Finnish Environment Institute) facilities between February and June 2019. The experimental platform used was a high-throughput well-plate setup and the experiments were conducted in solid, flat bottom, white 96 well-plates (Lumitrac 200, Greiner Bio One). In this setup, each well was individually illuminated by an adjustable light-emitting diode (LED - VLMW41, VISHAY) light from above (Figure 1A) and the LED panel was cooled with a small fan. Each LED plate was set with 12 light levels (10, 15, 20, 30, 40, 75, 100, 125, 150, 200, 350 and 550 µmol photon m^2 s^{-1}) and each light level illuminated eight wells. The measured light spectrum of the LED is depicted in Figure 1C. Prior to the experiments, the PAR levels of each LED were manually checked with a light sensor (Spherical Micro Quantum Sen (US-SQS/L, Walz) connected to a LI-250A (LI-COR) light meter) and the intensity was adjusted according to the specified light treatment of each well. The temperature of each plate was regulated by a cooler plate (liquid cooling block HD-S350 (Bitspower) with a self-built

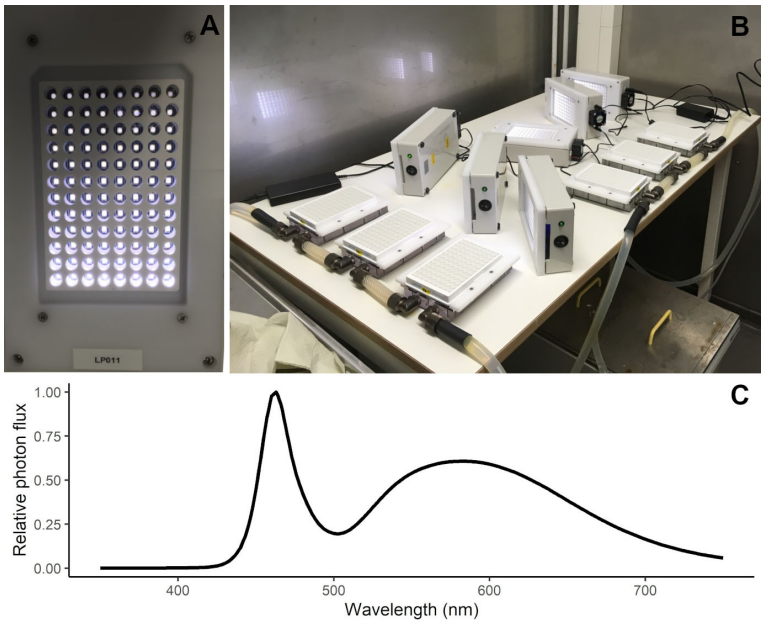

FIGURE 1
High-throughput well-plate setup used in the experiments. Detail on the LED plate for illuminating individual wells **(A)** and experiment setup showing the 96-well plates positioned on the temperature-controlled cooling plates with LED panels to the side, ready to be mounted over the well-plates **(B)**. Measured light spectrum (as relative photon flux) in the LED panels used in the experiment **(C)**.

polyoxymethylene frame, under which the well-plate and an aluminium adapter plate could be pushed and secured) connected to a flow-through temperature-controlled water cooler (DLK 25, Lauda) (Figure 1B). For each taxon, a total of 12 plates were incubated simultaneously in three different temperatures (3, 6, 9° C). Each plate included two out of the six salinity levels (4, 5, 6, 7, 8, 9 ‰, representative of the Baltic proper and Gulf of Finland), resulting in a total of 216 treatments (each one running in quadruplicates). The photoperiod used in the experiments was 14:10 (light:dark).

Three Baltic Sea spring dinoflagellates were selected from the FINMARI Culture Collection/Syke Marine Research Laboratory and Tvärminne Zoological Station (FINMARI CC): *Apocalathium malmogiense* (G. Sjöstedt) Craveiro, Daugbjerg, Moestrup & Calado (strain code SHTV-1, collected in Tvärminne Storfjärden, western Gulf of Finland, in 2002 by A. Kremp), *Gymnodinium corollarium* A.M. Sundström, Kremp & Daugbjerg (strain code GCTV03, collected at station BY15, in the Baltic Proper, in 2007 by A. Kremp) and *Heterocapsa arctica* subsp. *frigida* Rintala & G. Hällfors (strain code HATV-1401, collected in Tvärminne Storfjärden, western Gulf of Finland, in 2014 by P. Hakanen). In the culture collection, these strains are maintained at a 14:10 light: dark cycle, at 4°C, using f/2 medium (Guillard and Ryther, 1962, but excluding the Si), the base of which is filtered and autoclaved Baltic Sea water with the salinity of approximately 6 ‰. Prior to the experiments, the selected strains were pre-acclimated to the used salinities (for 4-12 weeks) and temperatures (for 2-4 weeks). To avoid potential biases associated to dilution of dissolved compounds in the sea water, the f/2 medium with different salinities used in the pre-acclimation and in the experiments was based on artificial sea water and made by diluting sea salt (Tropic Marin, Germany) in Milli-Q water.

Once a culture was pre-acclimated and growing in the different conditions, the cells were inspected using a FlowCam (Fluid Imaging Technologies) equipped with a colour camera, a flow cell FC100 and 10x objective. Images were collected with an auto-image mode and single healthy cells were manually sorted using the Visual Spreadsheet software (Fluid Imaging Technologies). Individual cell volumes were obtained using the area-based diameter algorithm from the Visual Spreadsheet software. To start the experiments, each well was filled with 300 µl of f/2 medium of the appropriate salinity and inoculated with 10-30 µl of the pre-acclimated culture. The amount of inoculum varied according to the density of the stock culture which was determined just before the inoculation by assessing the cell densities and chlorophyll *a in vivo* fluorescence and aiming at a reading of 130-250 fluorescence units. Chlorophyll *a* fluorescence (ex./em.: 440/680 nm) of the medium and the test unit immediately after the inoculation was checked using a fluorescence spectrometer (Cary Eclipse, Agilent), equipped with a plate reader accessory, and using the following parameter settings: excitation 440 nm, excitation slit 5 nm, emissions 680 nm, emission slit 5 nm and high voltage (800 V) setting of the photomultiplier. Thereafter, growth in each well was evaluated from chlorophyll *a in vivo* fluorescence time series, which was measured daily in the same way as described above. A blank plate was filled with f/2 medium and measured daily in the same way as the experimental plates to monitor the background fluorescence of the medium. The daily background medium fluorescence was calculated as the average of the 96 wells each day and this value was subtracted from fluorescence data of that day prior growth rates calculations. To

avoid evaporation and contamination between wells, all the plates were covered with an optical clear film, which was exchanged for a new one every time the plates were taken out for reading. For deciding on which type of film to use, we first ran a pilot using a gas-tight (ultra-clear polyester sealing adhesive film for qPCR (VWR)) and a non-gas-tight cover (the non-adhesive cover back film of the sealing qPCR film) to cover 96 well-plates and monitor growth of our study organisms. No difference in light (spectrum nor intensity) was observed between the cover types, which were then evaluated regarding the chlorophyll *a in vivo* fluorescence growth and evaporation for 20 days at 4 °C. While no difference was observed between cover types for *G. corollarium* growth, growth of *A. malmogiense* and *H. arctica* subsp. *frigida* were slower in plates covered with the gas-tight membranes in comparison to non-gas tight. Thus, although we first intended to use the sealing qPCR film, we opted for using its non-adhesive protective back film instead. Each set of experiments was carried out with one strain at a time, due to the limited amount of available experimental platforms. The experiments lasted between 11 days (for *A. malmogiense* and *G. corollarium*) and 21 days (for *H. arctica* subsp. *frigida*). In some cases, treatments reached readings over 500 fluorescence units earlier than others and were discontinued to ensure that the readings were still within the linear dynamic range of the instrument and that the fluorescence readings were directly proportional to the chlorophyll *a* concentration.

2.2 Statistical analysis

Effects of temperature and salinity on the cell sizes of the three dinoflagellates were tested with cell volume estimates obtained from the FlowCam by the end of the pre-acclimation. For that, a linear model was employed for each taxon, using the cell volumes as response variable and temperature, salinity, and the interaction between them (temperature×salinity) as independent variables. Cell volumes were log-transformed prior to analysis due to their scale-dependent variability. Analysis was done in R version 4.1.0 (R Core Team, 2021). The significance levels for all the analyses were 0.05. All plots were drawn in R using the "ggplot2" package (Wickham, 2016).

Daily fluorescence time series were plotted to follow the growth of each culture under the different experimental conditions and growth rates were determined only from the exponential growth phase. Although the cultures were pre-acclimated to temperature and salinity, this was not done for the light intensities. Thus, in the first days of the incubations (lag growth phase) variations in the chlorophyll *a* fluorescence were under the effect of light acclimation and were not proportional to the biomass, as the cellular pigmentation changed to match an optimum in a given light level. The exponential growth phase was differentiated from lag and stationary growth phases by assessing differences in the slope values of the fluorescence increase over time. For this, a regression model was estimated using piecewise linear relationships for the detection of breakpoints (Muggeo, 2003). The estimated breakpoints were considered to mark the change in the growth phase for each treatment in each experiment. The fitting of regression models with segmented relationships and break-point estimation was carried in R, using the package "segmented" (Muggeo, 2008). The exponential growth phase was considered to start on the first day after the (first) break point and to finish either by the end of the experiment or at the second breakpoint (that was interpreted to mark the start of the stationary phase), when this was detected. When no breakpoints were detected or not significant, the fluorescence time series were individually checked to determine the beginning of the exponential phase. Growth rates for each well were calculated as in Equation 1 (Levasseur et al., 1993):

$$\mu = (\ln F_f - \ln F_0)/t \qquad \text{Equation 1}$$

Where F_f is the chlorophyll *a* fluorescence by the end of the exponential growth phase, F_0 is the chlorophyll *a* fluorescence at the beginning of the exponential growth phase, and t is the number of days between F_0 and F_f .

The resulting growth patterns were used to estimate the photo-physiological traits of each taxon by fitting a growth-irradiance curve at different temperature and salinity levels. At first, we aimed to evaluate the light limitation by fitting the growth-irradiance curve with a simpler two-parameter model (MacIntyre et al., 2002; Equation 2). However, as some of the tested organisms displayed a negative effect of high light intensities on growth, we also fitted a three-parameter model to evaluate light limitation and photoinhibition (Eilers and Peeters, 1988; Equation 3). Note that negative growth rates were excluded prior to model fitting.

$$\mu(E) = \mu_{max} \times e^{\frac{-E}{K_E}} \qquad \text{Equation 2}$$

$$\mu(E) = \frac{\mu_{max} \times E}{\frac{\mu_{max}}{\alpha \times I_{op}^2} \times E^2 + (1 - 2 \times \frac{\mu_{max}}{\alpha \times I_{op}}) \times E + \frac{\mu_{max}}{\alpha}} \qquad \text{Equation 3}$$

In Equation 2, the observed growth (μ) over the different light intensities (E) is parameterized as the maximum growth rate at optimal light intensities (μ_{max}) and the light-saturation parameter (K_E). In Equation 3 the observed growth (μ) over the different light intensities (E) is described by the maximum growth rate at optimal light intensities (μ_{max}), the irradiance in which growth rate is maximum (I_{op}) and the initial slope of the growth-irradiance curve (α) of a given species. The parameters for both models were estimated with nonlinear least squares in R using the package "nlme" (Pinheiro et al., 2021). Only parameters with significant estimates are reported in our results.

2.3 Long-term monitoring data

Alg@line phytoplankton monitoring data (n = 3396) collected across the Baltic Sea (Travemünde-Helsinki) between 1993-2011 using ships-of-opportunity (Finnjet 1993-1997; Finnpartner 1998-2006; Finnmaid 2007-2011) was utilized to put the experiment findings into an environmental context. The sampling focused on spring, summer and autumn, with fewer samplings during the winter months December, January and February. The commercial ferry route across the Baltic Sea reflects multiple environmental gradients, including temperature and salinity. The FerryBox system

pumps water collected at ~ 5 m depth that is representative of the entire productive layer (Rantajärvi et al., 1998). The water is distributed at a flow rate of 2-4 L min^{-1} through different sensors, including a temperature and conductivity sensor from which temperature and salinity were obtained. Along the transect, discrete water samples were collected using an automated sampler (ISCO) and stored in it in refrigerated and unlit conditions until they were brought ashore for analysis. In 1993-1995 sampling was scheduled to take place at specific times, from 1996 onward samples were taken at specific longitudinal positions. Throughout the study period the methods used were essentially the same although the models and makes of some apparatus varied. Phytoplankton samples were preserved with acid Lugol's solution (Willén, 1962) and settled following the Utermöhl method (Utermöhl, 1958). In brief, 50 ml of sample was settled for ≥ 24 hours and the whole chamber bottom was examined under a 10x objective, and two bottom diameters were examined using the 40x objective. The phytoplankton species composition was determined with the accuracy permitted by inverted light microscopy of acid Lugol's preserved samples. The semi-quantitative phytoplankton abundance assessment followed the HELCOM guidelines (HELCOM, 2011) and the occurrence of each taxon in a sample was classified in five ranks: 1 = very sparse (only one or a few cells in the analysed area), 2 = sparse (slightly more cells in the analysed area), 3 = scattered (several cells in many fields of view), 4 = abundant (several cells in most fields of view), and 5 = dominant (many cells in every field of view). For a more detailed description see Hällfors (2013).

Since *Heterocapsa arctica* subsp. *frigida* was formally described only in 2010 (Rintala et al., 2010) this taxon was recorded in the long-term monitoring data mainly at genus level. However, the main person analysing the phytoplankton species composition, Seija Hällfors, who also participated in the species description in 2010, was aware of the distinct morphology of *H. arctica* subsp. *frigida* long before this monitoring began (cf. Hällfors, 2013, and references therein). The overwhelming majority of the records of *Heterocapsa* sp. in the data are *H. arctica* subsp. *frigida*, and based on notes covering the years 1993-2005 (i.e. the data utilized in the study by Rintala et al., 2010), some other *Heterocapsa* sp. observations were excluded for that period. Between 2006-2011, such notes were not evaluated, and while there is a chance that a few other *Heterocapsa* observations are included, we are confident that most of the genus-level records are in fact *H. arctica* subsp. *frigida*. *Apocalathium malmogiense* and *Gymnodinium corollarium* are part of a species complex, the *Apocalathium* complex (also termed *Scrippsiella/Biecheleria/Gymnodinium* complex (Sundström et al., 2010), and *Scrippsiella* complex (Jaanus, 2011)). Because *A. malmogiense* and *G. corollarium* cannot reliably be differentiated in acid Lugol's fixed samples, and furthermore, because in the early years of the monitoring data these species were both identified as *Scrippsiella hangoei*, we chose to sum the occurrences of all species belonging to this species complex and treat it collectively as the *Apocalathium* complex. To recalculate the abundance ranks when taxonomical units were joined within a sample, we used the highest observed rank among the merged taxonomical units, as the maximum number of merged taxonomical units was three (Hällfors, 2013). The occurrences of *H. arctica* subsp. *frigida* and the *Apocalathium* complex in different temperatures and salinities over the years were visualised by kernel density estimates, with peaks denoting where more observations were recorded.

3 Results

3.1 Effects of temperature and salinity on cell volume

Potential effects of temperature (3, 6, and 9°C) and salinity (4-9 ‰) on the cell volume of the three dinoflagellates was evaluated by the end of the pre-acclimation period. At salinity 9 ‰, cell volumes could not be determined for *A. malmogiense* (all temperatures) and for *G. corollarium* (at 3°C) due to technical issues. On average, *A. malmogiense* was larger (mean ± sd = 6451 ± 1947 μm^3, n = 19360) than *G. corollarium* (mean ± sd = 3586 ± 1245 μm^3, n = 26027). As expected, both above mentioned species were markedly larger than *H. arctica* subsp. *frigida* (mean ± sd = 1062 ± 391 μm^3, n = 7289). Cell volumes were significantly affected by temperature for all three dinoflagellates ($p< 0.001$) and by salinity ($p< 0.001$ for *A. malmogiense* and *H. arctica* subsp. *frigida*; $p = 0.004$ for *G. corollarium*). The interaction between temperature and salinity was only significant for *G. corollarium* ($p< 0.01$). Cell volumes were similar across temperature for *A. malmogiense*, but cells were larger at 3°C and smaller at 9°C (Figure 2). *G. corollarium* and *H. arctica* subsp. *frigida* were smaller at 3°C (with slightly larger cells at 6°C) and larger at 9°C, with the increase in cell sizes at 9°C being pronounced for *H. arctica* subsp. *frigida* (Figure 2). The cell volume of *A. malmogiense* did not seem to be affected by variations in salinity, while *H. arctica* subsp. *frigida* cell volume was consistent across salinities at 6°C, but a tendency towards larger cells was observed for the other temperatures at salinity 9 ‰ (Figure 2). At 3 and 6°C, *G. corollarium* cells were smaller at intermediate salinities (5-7 ‰) and increased towards both low and high salinities, however at 9°C average cell decreased with increasing salinity (Figure 2).

3.2 Effects of temperature, salinity and light intensity on growth rates

The three dinoflagellates grew differently in the treatments. *A. malmogiense* was the only species to grow in all temperatures (3, 6, and 9°C), salinities (4-9 ‰) and light intensities (Figure 3). Variability among the replicates of *A. malmogiense* increased at 9°C, more pronouncedly at lower salinities and higher light intensities (Figure 3). *G. corollarium* growth was detected in all salinities at 3 and 6°C, while at 9°C consistent growth among the replicates could only be detected in salinity 5 ‰ (Figure 4). *G. corollarium* did not grow in the highest light intensity (550 µmol photon m^2 s^{-1}) and at 350 µmol photon m^2 s^{-1} growth was only detected in salinities 5-8 ‰ at 3°C and 5-9 ‰ at 6°C (Figure 4). *G. corollarium* replicates exhibited the lowest variability among the three dinoflagellates, being quite consistent in the treatments where growth was detected

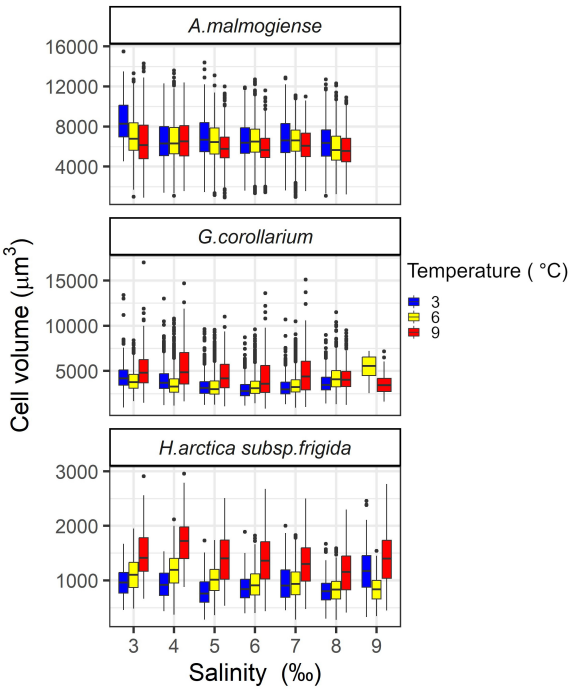

FIGURE 2
Variations in cell volumes of *Apocalathium malmogiense*, *Gymnodinium corollarium*, and *Heterocapsa arctica* subsp. *frigida* after the pre-acclimation to the salinities and temperatures used in the experiment.

(Figure 4). Growth in *H. arctica* subsp. *frigida* was observed for all salinities (4-9 ‰) in temperatures of 3 and 6°C, however at 9°C this species only grew in 6 and 7 ‰ (Figure 5). Although growth was detected at 9°C and 6 ‰, the replicates were not consistent resulting in large variation in these treatments (Figure 5). Similarly to *G. corollarium*, *H. arctica* subsp. *frigida* did not grow at the highest light intensity (Figure 5).

None of the three dinoflagellates grew in all treatments and the highest observed growth rates across all experiments were 0.38, 0.32, and 0.25 d^{-1} for *A. malmogiense*, *G. corollarium* and *H. arctica* subsp. *frigida*, respectively (Figure 6). Growth rates for *A. malmogiense* were higher (>0.25 d^{-1}) at 3°C (all salinities), while at 6 and 9°C such high growth rates were restricted to salinities ≥ 6 ‰ (Figure 6). High growth rates for *G. corollarium* and *H. arctica*

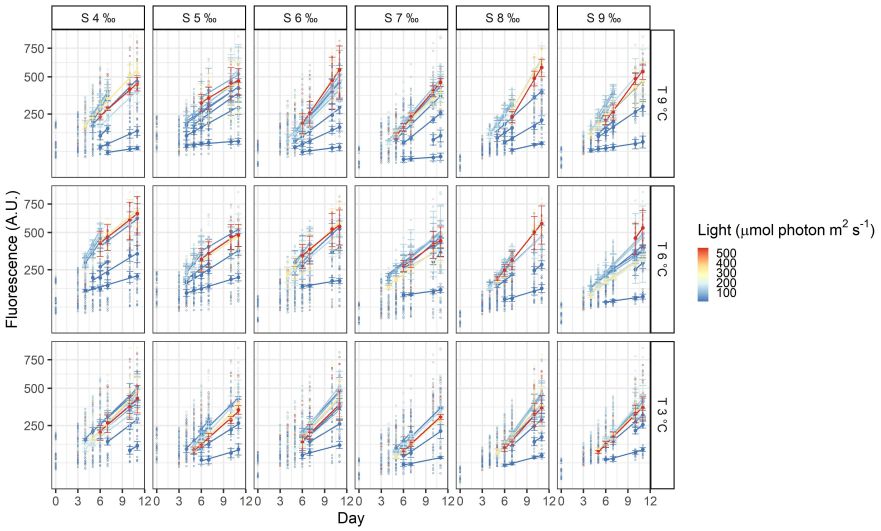

FIGURE 3
Fluorescence time series of *Apocalathium malmogiense*. Each circle is the observed fluorescence of each well in each day. Daily means and standard deviations of the observations used to calculate the growth rates are depicted as full points with the error bars. The lines are linear regressions, included only for visualization purposes.

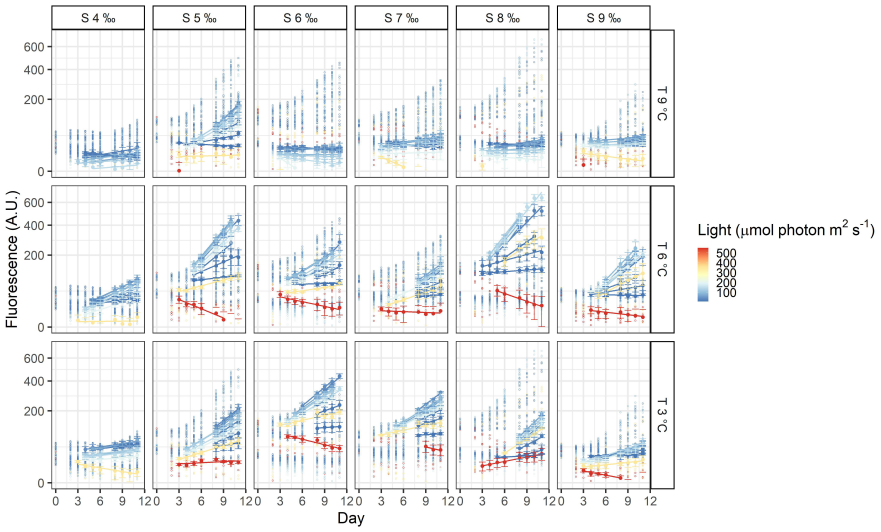

FIGURE 4
Fluorescence time series of *Gymnodinium corollarium*. Each circle is the observed fluorescence of each well in each day. Daily means and standard deviations of the observations used to calculate the growth rates are depicted as full points with the error bars. The lines are linear regressions, included only for visualization purposes.

subsp. *frigida* (≥0.20 d^{-1}) were mostly observed at 6°C, although for the latter growth rates were higher in salinities ≥6 ‰ (Figure 6). Light intensities also affected the dinoflagellates growth, influencing the fitting of the two models. *A. malmogiense* showed a weaker tendency to photoinhibition, which was only featured in few treatments (salinities 6, 8, and 9 ‰ at 3°C and salinity 9 ‰ at 6° C) (Figure 6). In contrast, *G. corollarium* and *H. arctica* subsp. *frigida* were more sensitive to higher light intensities, showing photoinhibition for light intensities > 150 and 175-200 µmol photon m^2 s^{-1}, respectively. Curiously, *H. arctica* subsp. *frigida* was not photoinhibited at 6°C in salinities 8-9 ‰ (Figure 6).

The two growth-irradiance models indicated similar maximum growth rates at optimal light intensities (μ_{max}) and saturation intensities for the three dinoflagellates (Figures 6, 7A, C). Overall, estimated μ_{max} were lower than the observed growth rates (µ) but showed a similar variation pattern over the temperature and salinity gradients (Figures 6, 7A, C). The μ_{max} estimates ranged between 0.09-0.30 d^{-1} for *A. malmogiense* (highest values found at 3°C and 6 ‰), 0.06-0.23 d^{-1} for *G. corollarium* (highest μ_{max} at 6°C and 4 ‰), and 0.04-0.20 d^{-1} for *H. arctica* subsp. *frigida* (highest μ_{max} recorded at 6°C and 6 ‰) (Figures 7A, C). The light saturation of the growth-irradiance curve (K_E) ranged between 7.17-23.89, 12.03-32.39 and

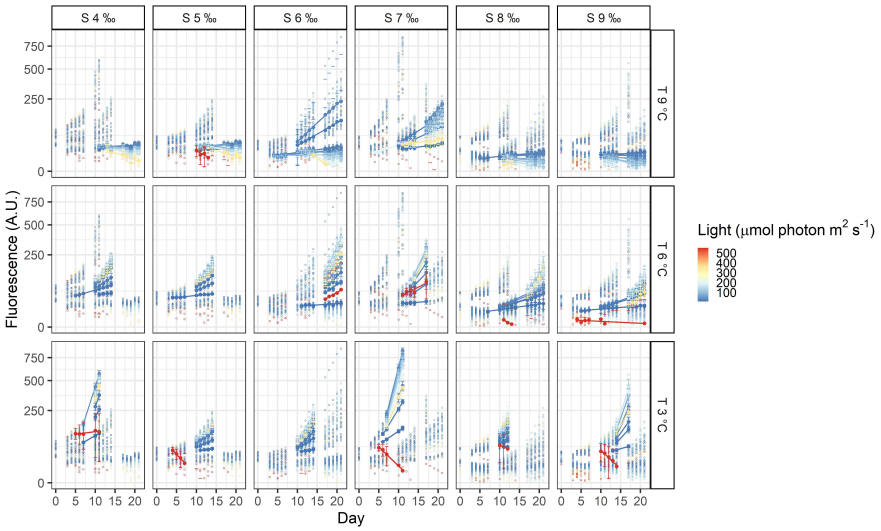

FIGURE 5
Fluorescence time series of *Heterocapsa arctica* subsp. *frigida*. Each circle is the observed fluorescence of each well in each day. Daily means and standard deviations of the observations used to calculate the growth rates are depicted as full points with the error bars. The lines are linear regressions, included only for visualization purposes.

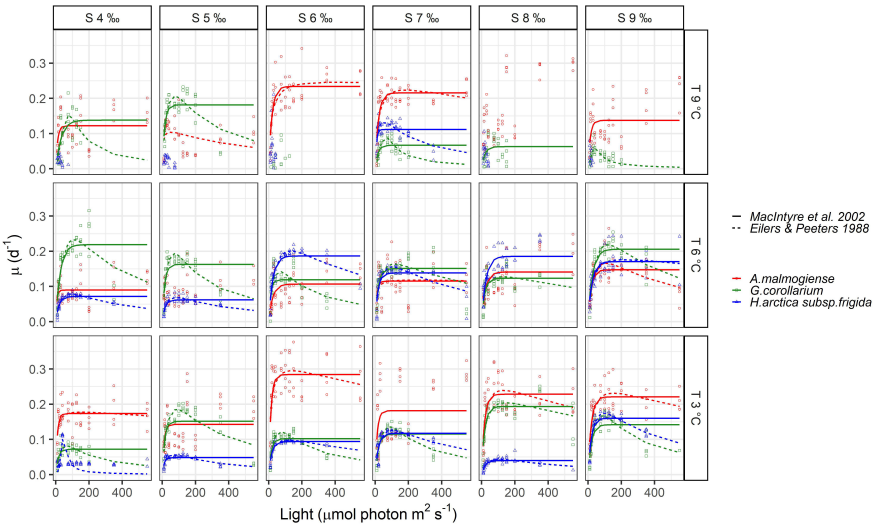

FIGURE 6
Observed growth rates for *Apocalathium malmogiense*, *Gymnodinium corollarium*, and *Heterocapsa arctica* subsp. *frigida*. The curves represent the fitted growth-intensity models (MacIntyre et al., 2002 and Eilers & Peeters, 1988) in different temperatures and salinities.

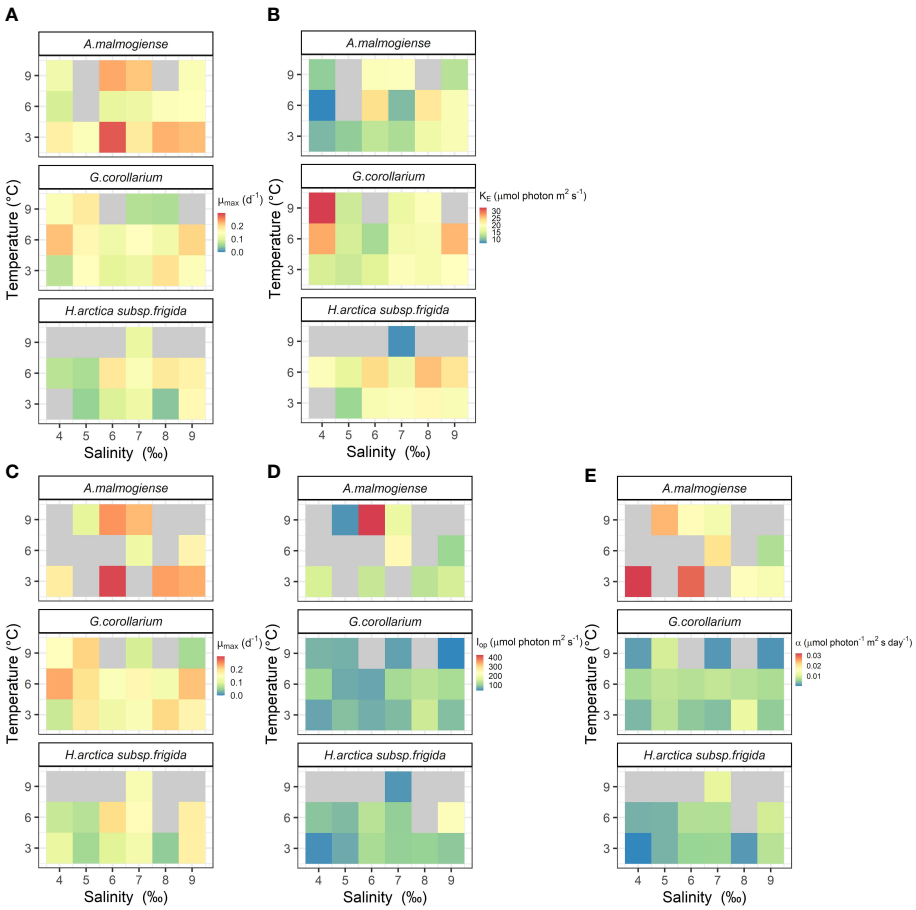

FIGURE 7
Photo-physiological traits estimated for *Apocalathium malmogiense*, *Gymnodinium corollarium*, and *Heterocapsa arctica* subsp. *frigida* at different temperatures and salinities. Parameters estimated using MacIntyre et al. (2002) two-parameter **(A, B)** or Eilers & Peeters (1988) three-parameter models **(C–E)**. Missing and non-significant parameters are depicted in gray.

7.67-25.60 µmol photon m^2 s^{-1} for *A. malmogiense*, *G. corollarium* and *H. arctica* subsp. *frigida*, respectively. Although differences were observed among the dinoflagellates, K_E tended to be higher at 3 and 6°C and salinities ≥6 ‰ for all three tested taxa (Figure 7B). For the three-parameter model, besides μ_{max}, two other parameters were described, I_{op} and α. I_{op} ranged between 51.78-425.41, 40.21-147.11, and 46.61-227.31 µmol photon m^2 s^{-1} for *A. malmogiense*, *G. corollarium*, and *H. arctica* subsp. *frigida* respectively. I_{op} were higher at 3-6°C and salinity >6 ‰ for *G. corollarium*, and for *H. arctica* subsp. *frigida* the values were higher at 6°C and salinity 9 ‰ (Figure 7D). For *A. malmogiense* the highest I_{op} was observed at 9°C and 6 ‰, although the number of estimates for this species was limited using the three-parameter model (Figure 7D). *A. malmogiense* presented the highest α values (0.007-0.032 µmol photon^{-1} m^2 s d^{-1}), with lower α estimates found for *H. arctica* subsp. *frigida* (0.0005-0.012 µmol photon^{-1} m^2 s d^{-1}) and *G. corollarium* (0.001-0.012 m^2 µmol photon^{-1} m^2 s d^{-1}). α was higher at 3°C and salinity ≤ 6 ‰ for *A. malmogiense*, while for *G. corollarium* consistent high values were observed at 6 °C independent on the salinity and for *H. arctica* subsp. *frigida* α values were more sensitive to salinity than temperature, with higher values estimated for salinities ≥ 6 ‰ (Figure 7E). The overall relationships between the estimated parameters of each model distinguish *A. malmogiense* from *G. corollarium* and *H. arctica* subsp. *frigida* for the 3-parameter model (Figures 8A-C), but the difference between dinoflagellates is less clear for the 2-parameter model (Figure 8D).

3.3 Occurrence in the Baltic Sea phytoplankton community

Of the 3396 Alg@line monitoring samples collected in 1993-2011, the *Apocalathium* complex and/or *H. arctica* subsp. *frigida* occurred in a total of 1157 samples and more frequently in the northern than southern part of the transect (Figure 9A). The *Apocalathium* complex was observed in all the months between February to November, although the number of records from July – November is low (less than 15 occurrences for the entire period). *H. arctica* subsp. *frigida* was observed between February – June and August – November, however it was usually observed in March, April and May, with scarce occurrence (<10 observations) in other months. Both the *Apocalathium* complex and *H. arctica* subsp. *frigida* were observed most frequently and with higher abundances in April and May. Overall, the long-term data demonstrated that the *Apocalathium* complex and *H. arctica* subsp. *frigida* are usually found in natural samples in temperatures<10°C and salinities 4-10 ‰ (Figures 9B, C), matching the temperature and salinity gradients used in this study.

Both the *Apocalathium* complex and *H. arctica* subsp. *frigida* seem to prefer similar temperature (2-5°C) and salinity (5-7 ‰) ranges, although the occurrence of *H. arctica* subsp. *frigida* was more constrained than that of the *Apocalathium* complex (Figures 9B, C). Abundant and dominant occurrences (ranks 4 and 5) of the *Apocalathium* complex seem to have a bi-modal distribution for both salinity (peaks at 5 ‰ with highest kernel

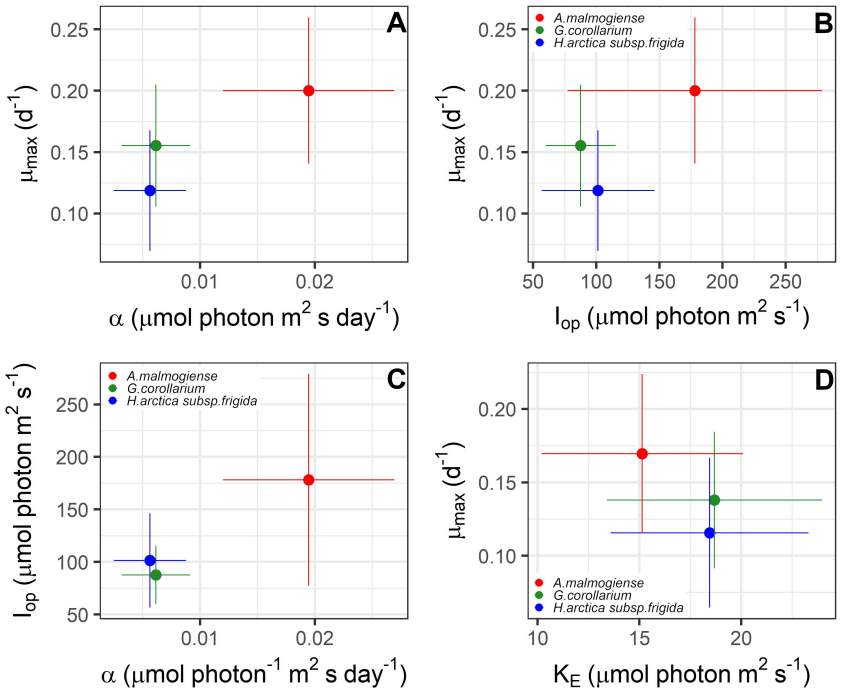

FIGURE 8
Relationships between photo-physiological traits estimated for *Apocalathium malmogiense*, *Gymnodinium corollarium*, and *Heterocapsa arctica* subsp. *frigida*. The points depict the averages and the bars the standard deviations found in all the experiments. **(A–C)** are the parameters estimated using Eilers & Peeters (1988) 3-parameter model; **(D)** depicts relationship between the two-parameter estimated with MacIntyre et al. (2002) model.

10.3389/fmars.2023.1156487

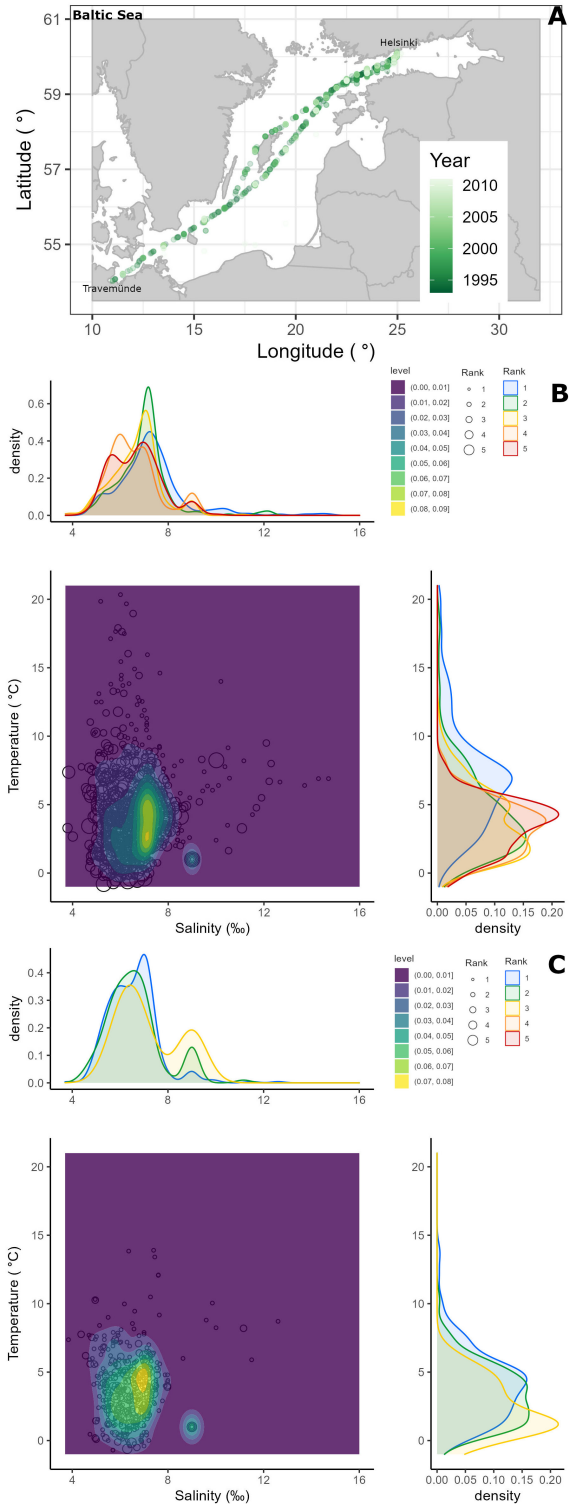

FIGURE 9
Semi-quantitative phytoplankton data (as abundance ranks) from samples collected in 1993-2011 onboard ships-of-opportunity transversing the Baltic Sea **(A)**, depicting the occurrence of the *Apocalathium* complex **(B)** and *Heterocapsa arctica* subsp. *frigida* **(C)** over environmental temperature and salinity gradients.

density estimate ~0.45, and 7 ‰ with highest kernel density estimate 0.4) and temperature (peaks at 4-5°C with highest kernel density estimate ~0.2, and a shoulder at 2.5°C with kernel density estimate 0.12-0.15) (Figure 9B). *H. arctica* subsp. *frigida* most frequently occurred at salinities 6-7 ‰ (kernel density estimate 0.35-0.45) and at 0.5°C (kernel density estimate >0.2), although a shoulder (kernel density estimate 0.1) can be observed at around 5°C (Figure 9C).

4 Discussion

Baltic Sea spring dinoflagellates have similar niches regarding their adaptation to cold water and capacity to sustain growth under low nutrient conditions (Kremp et al., 2008; Spilling and Markager, 2008). It has been shown that the cyst formation strategies and seeding conditions from the sediments are essential for the success of certain dinoflagellates species during spring and are susceptible to climate change (Jaanus et al., 2006; Kremp et al., 2008; Spilling et al., 2018). Yet, those factors operate over longer time scales while physiological responses occur at much shorter time scales, providing a contemporary insight into the population dynamics (Harris, 1980), although those remain largely underexplored. We showed that each one of the three tested vernal dinoflagellates have their own niches and preferences regarding photo-acquisition traits. Additionally, temperature and salinity affect the cell volume and response to light availability differently in the three dinoflagellates. Below we present methodological considerations and discuss the implications of our findings for the understanding of the Baltic Sea spring bloom dynamics in face of climate change.

4.1 The high-throughput well-plate setup for phytoplankton trait studies

The high-throughput well-plate setup used in the experiment allows for controlling the light intensity in each well independently and each well-plate to be under temperature controlled conditions, facilitating the conduction of multiple irradiance (Chen et al., 2012; Thrane et al., 2016) and temperature (Thrane et al., 2017) experiments simultaneously. Such experiments would consume much more time and resources if conducted in larger experimental units. This kind of experimental platform has been successfully used to investigate other ecological applications, such as nutrient stoichiometry, organic carbon transformations and screening of optimal growth conditions (Volpe et al., 2021).

Volpe et al. (2021) listed common problems associated with the use of a high-throughput well-plate setup for assessing growth response on microalgae: the temperature variation across the plate associated with different light intensities, evaporation losses and the potential effects of carbon limitation and pH variations on the algae growth. Unlike the setup used in other experiments, our well-plates were illuminated from above and the bottom of the plate was directly in contact with a cooling plate to reduce temperature fluctuations. Additionally, the illumination plate was equipped with a fan to dissipate the heat generated by the LEDs, an improvement also suggested by Volpe et al. (2021). In our experiments we minimized the potential carbon limitation by not using gas-tight membranes. Pilot results indicated potential carbon limitation for *A. malmogiense* and *H. arctica* subsp. *frigida*, since they showed a tendency to slower growth in plates covered with the gas-tight membranes in comparison to non-gas tight ones, while this was not so strongly manifested in *G. corollarium* (data not shown). It is important to highlight that no difference in the light intensity nor quality was observed between the cover types. During the pilot experiments no significant evaporation loss was observed in the well-plates, regardless of the light intensity, likely because the experiments were carried out at low temperatures.

For the purposes of this study, and taking the precautions explained above, the high-throughput well-plate experimental setup proved to perform well. It should however be noted that some species might not be suitable for testing in the well-plate setup. For example, cultured strains of the chain forming *Peridiniella catenata*, another common spring dinoflagellate in the Baltic Sea, appear to require more space (larger volumes of medium) for growth in culture. We could not include *Biecheleria baltica* (which is also part of the *Apocalathium* complex) in this study, because it failed to grow in the well-plates. As this species does not seem to require larger volumes for its growth, this could result from growing the dinoflagellates in media based on artificial sea water rather than filtered sea water, since some phytoplankton might require certain components, such as organic compounds, not present in artificial mixtures (Berges et al., 2001). We chose to use artificial sea water to account for any potential effects associated with using different salinities, which would require either different dilutions or sea water from different sources, increasing the potential random effects. Future improvements for the design might include testing other growth medium types and/or the addition of soil extract that seems to benefit some organisms. Thus, we recommend testing the growth of a target species in different setups (e.g., culture media, different cover membranes, well-plate suitability) prior to full scale experiments. We also stress that although numerous experiments can be carried out simultaneously in the well-plate setup, the small volume of each well (~300 µl) limits the variables and methods that can be employed to evaluate the experimental responses. Despite the clear suitability of chlorophyll *a* fluorescence for this setup, the method also has limitations due to relatively narrow linear range of fluorescence measurements from white well-plates (as the ones used in this study), and acclimation effects need to be considered, especially when a light gradient is used (as presented in Material and Methods section).

4.2 Growth rates of vernal Baltic Sea dinoflagellates

Growth rates have been previously reported in the literature for *A. malmogiense* and *G. corollarium*, but no such information was found for *H. arctica* subsp. *frigida*. *Scrippsiella hangoei* (syn. *A. malmogiense*) was reported to grow equally well in 0-30 ‰ and to tolerate temperatures > 6°C (Kremp et al., 2005). *A. malmogiense* growth varied from 0.18 to 0.33 d^{-1} in temperatures 0-11°C, but growth was negatively affected for temperatures >11°C, with no growth detected above 14 °C (Hinners et al., 2017). *G. corollarium* was reported to grow well in 1.5-12 ‰ salinities, with optimal growth rates at 9 ‰ (0.51 divisions per day or $\mu = 0.35\ d^{-1}$) and in 2-6°C temperatures, with optimal growth rates at 4°C (0.47 divisions per day or $\mu = 0.33\ d^{-1}$) (Sundström et al., 2009). Thus, the growth rates obtained in our experiments were comparable with previous

studies for both *A. malmogiense* (maximum μ = 0.38 d^{-1}) and *G. corollarium* (maximum μ = 0.32 d^{-1}). Additionally, considering that relatively slow growth rates characterize Baltic Sea spring dinoflagellates, especially in comparison to diatoms, which form the other dominant phytoplankton group during springtime in the Baltic Sea (Kremp et al., 2008; Spilling and Markager, 2008), our growth rates estimates appear to be realistic.

4.3 Considerations on selected growth-irradiance models

Multiple Growth-Irradiance models for phytoplankton have been used (e.g. Eilers & Peeters, 1988; MacIntyre et al., 2002; Edwards et al., 2015; Lacour et al., 2017), but it is not unequivocally clear which of these models best describes the photo-physiology traits. While our primarily choice was the model by MacIntyre et al. (2002) based on its simplicity and robustness, the model is unable to reproduce photoinhibition, as observed in *G. corollarium* and *H. arctica* subsp. *frigida*. To be able to capture the photoinhibition component (I_{op}), which was a relevant aspect for some of the tested organisms, it was clear that another model was needed. In fact, we tested fitting two additional models, a two-parameter model by Steele (1962), which is defined by μ_{max} and I_{op} (data not shown), and the three-parameter model by Eilers & Peeters (1988). Despite the simplicity of the Steele model, it consistently yielded higher estimates for both μ_{max} and I_{op} than the same parameters estimated by the Eilers and Peeters model. Additionally, the μ_{max} estimated with both the MacIntyre et al. and Eilers & Peeters models, were similar (for *H. arctica* subsp. *frigida*) or better (for *A. malmogiense*) related to the observed growth rates than the Steele model, but this was not the case for *G. corollarium*, in which the Eilers & Peeter and Steele models had similar fitting and parameter estimate (data not shown). From those observations we can conclude that although a simpler formulation might be the first target, the model choice should ultimately take into consideration the degree of photoinhibition experienced by the targeted organism. Finally, we chose to present results from fitting both the MacIntyre et al. and Eilers & Peeters models, in order to be as comprehensive as possible, but at the same time provide comparable parameter estimates for the three tested dinoflagellates and more comparability with earlier studies as these models have been used e.g. by Schwaderer et al. (2011); Edwards et al. (2015), and Lacour et al. (2017).

4.4 Vernal Baltic Sea dinoflagellates - from traits to niches

Unicellular, rather nondescript, about 20-30 μm dinoflagellates, known as the *Apocalathium* complex, occur throughout the springtime in the Baltic Sea and occasionally dominate the phytoplankton biomass (Lignell et al., 1993; Larsen et al., 1995; Jaanus et al., 2006). Despite their similar gross morphology (as seen using conventional monitoring methods, i.e. in light microscopical analysis of acid Lugol's preserved samples), morphological, ultrastructural and molecular evidence sustain the classification of these dinoflagellates into three distinct species (*Apocalathium malmogiense*, *Biecheleria baltica* and *Gymnodinium corollarium*), each with slightly different temperature and salinity preferences (Kremp et al., 2005; Sundström et al., 2009; Sundström et al., 2010). It has been shown that this complex is dominated by *Biecheleria baltica* (northern Baltic Sea) and *G. corollarium* (central Baltic Sea), with cyst records indicating a small contribution of *A. malmogiense* (Spilling et al., 2018 and references therein). This species complex was reported to occur at 4.5-8 ‰ salinities and temperatures of -1.2-13.8°C, with high abundances recorded over a narrower temperature range (-1.2-7.9°C) (Jaanus et al., 2006; Hällfors, 2013). Here we show that for the most abundant occurrences (ranks 4 and 5) the *Apocalathium* complex displays a bimodal distribution in both salinity and temperature which may indicate slightly different preferences for different species in the complex. This is corroborated by our experiment results, in which *A. malmogiense* can grow over a broader salinity, temperature and light range than *G. corollarium*, which seems to be better adapted to temperatures around 6°C and salinities between 5-8 ‰ and is more susceptible to photoinhibition. Higher light acquisition trait values characterize *A. malmogiense*, which grew faster than *G. corollarium* at all tested irradiances. However, we evaluated only a limited number of traits and this apparent advantage of *A. malmogiense* might impose costs to other traits, such as nutrient use efficiency and resistance to predators (Edwards et al., 2015), which could change the competitive ability of the species.

The smaller-sized *H. arctica* subsp. *frigida* is a common spring dinoflagellate in the Baltic Sea, usually occurring at< 5°C but being recorded between temperatures -1.2-13.9°C and salinities 4.7-11.5, while occurring more frequently in the lower-salinity northern areas than in the south (Rintala et al., 2010; Hällfors, 2013). *H. arctica* subsp. *frigida* does not often reach high abundances, which is demonstrated by the fact that its highest abundance rank in the environmental data is 3; however it can form under-ice blooms (Niemi and Åström, 1987; Hällfors, 2013). In our study, the highest-abundance observations (scattered, rank 3) were more frequent in temperatures<2°C, whereas the occurrence of those over salinity were bimodal. Very sparse and sparse observations (ranks 1-2) mostly occurred at salinities<8 and between 2-5°C, thus our experiment results agree well with the occurrence observed in natural samples. Likely its slower growth rates, associated with a limited niche for light acquisition, influences the capacity of this dinoflagellate to form blooms. The limited niche for light acquisition can result from an adaptation to also living in sea ice (Rintala et al., 2010), and the fact that α responds to both temperature and salinity may also reflect an adaptation to switching between life in sea ice and open water. *H. arctica* subsp. *arctica* has been shown to form temporary cysts (Iwataki, 2002), although no information on these (beyond a micrograph; Iwataki, 2002: Plate 1, fig. 3) or the cyst formation conditions were provided. In the *H. arctica* subsp. *frigida* original description, no mention of cysts (temporary or resting) is provided (Rintala et al., 2010), however structures resembling temporary cysts were observed in culture but they were not investigated further.

Growth rate and resource acquisition traits partly define the competitive ability of species in a community and these traits will ultimately respond to the expression of multiple physiological characteristics (Litchman and Klausmeier, 2008). When considering steady state growth under nutrient-saturated conditions, variations in the growth-irradiance relationships can be due to: 1) differences in the light-harvesting properties; 2) changes in the photosynthesis quantum requirement; 3) changes in the photosynthesis to respiration ratios; 4) variations in the amount of fixed carbon exudated; and 5) changes in the photosynthetic quotients (Falkowski et al., 1985). We consider that our experimental observations correspond to a steady state growth under nutrient-saturated conditions, as we only analysed the exponential growth phase. Additionally, considering that the phytoplankton growth medium has plenty of macronutrients and the slow exponential growth rates observed for the tested dinoflagellates, we believe that the effects of nutrient limitation in our experiments were negligible.

Light acquisition traits are the manifestation of many underlying cell features (e.g. pigment composition and their cell quotas, metabolism, respiration, photoprotection, ability to capture photon energy and fix carbon) that change in response to changes in the environment, as long as they are within the ranges defined by the cell genotype (Falkowski et al., 1985; Edwards et al., 2015). Thus, temperature variations are likely to affect the light acquisition traits, due to the thermal effects in the cell metabolism that will change the respiration to photosynthesis ratio (Raven and Geider, 1988) and also due to effects of temperature on electron transport rates (Reynolds, 2006). Although temperature variation also affects the enzymes in the photosynthetic apparatus, they are less sensitive to temperature than the cell metabolism (Raven and Geider, 1988; Dewar et al., 1999). However, such effects can be observed over short-term scales (minutes-hours), while over the course of days to weeks (like in this study) a steady state is reached due to the establishment of balanced carbon fluxes (Dewar et al., 1999). Thus, although factors such as the cell volume or cell specific chlorophyll *a* and carbon content were not measured at the end of the experiment, we believe that our results capture the resulting steady state over gradients. Our observations indicate that the light acquisition traits in the three studied dinoflagellates are affected by both temperature and salinity. Although the thermal effect on metabolism is more pronounced, salinity might also affect the respiration to photosynthesis ratio, due to osmoregulation costs. Additionally, salinity variation might also have a direct effect on photosynthesis, as ionic stress was shown to stimulate cyclic electron flow and inhibited non-cyclic flow in the chlorophyte *Dunaliella tertiolecta* (Gilmour et al., 1985). Even though such effects have not been demonstrated for dinoflagellates, one could assume that similarly to temperature, combined effects of salinity on cell metabolism and photosynthetic apparatus can ultimately affect growth rates.

Size is usually a good trait predictor influencing important characteristics such as growth and resource acquisition (Litchman and Klausmeier, 2008). Overall, self-shading is reduced in smaller cells and smaller phytoplankton tend to have a higher light absorption efficiency (α) (Kirk, 2010). Metanalysis studies in freshwater and marine environments found that μ_{max} and α tend to be negatively correlated with cell size, while no significant relationship was found for I_{op} (Tang, 1996; Schwaderer et al., 2011; Edwards et al., 2015). Our cell volumes showed, as was expected, that *H. arctica* subsp. *frigida* is much smaller (mean 1062 μm^3) than *G. corollarium* (mean 3586 μm^3) and *A. malmogiense* (mean 6451 μm^3). Thus, based only on cell size, one could expect *H. arctica* subsp. *frigida* to have the highest μ_{max} and α, with *A. malmogiense* and *G. corollarium* having similar values. However, we observed the highest μ_{max}, I_{op} and α for *A. malmogiense*, while *G. corollarium* and *H. arctica* subsp. *frigida* showed similar values for these parameters. This exemplifies that when assessing species with a similar niche generic assumptions such as the allometric scaling might not always apply, as those relationships are a generalization and more suitable over a broader context. We note that *A. malmogiense* and *H. arctica* subsp. *frigida* are thecate dinoflagellates and the theca is absent in *G. corollarium*, differentiating the tested dinoflagellates regarding their cell wall structure. Although light scatter and absorption might be influenced by cell coverage (Witkowski et al., 1998) and affect the light acquisition traits, the effects of cell sizes, pigment amount and cell contents on those traits are likely to be disproportionally larger than the presence or absence of a theca (Smayda, 1997; MacIntyre & Cullen, 2005).

Our results indicate that the cell sizes of *G. corollarium* and *H. arctica* subsp. *frigida* are more sensitive to temperature variations than that of *A. malmogiense*. Meantime, *G. corollarium* light acquisition traits seem to be relatively constant over the tested salinity and temperature gradients, while growth under low light is negatively affected by salinity for *A. malmogiense*. The efficiency of *H. arctica* subsp. *frigida* to use absorbed light for growth increases with both salinity and temperature. At salinity 9 ‰, α becomes similar among the three dinoflagellates, although irregular growth and/or lower growth rates indicate signs of stress in these dinoflagellates. In light of the predicted milder winters, with increased water temperature and light availability in the Baltic Sea (Groetsch et al., 2016), our results indicate that changes in the environmental conditions during spring will likely affect the size distribution and the photo-acquisition traits within the spring bloom communities. Such changes can affect both matter and energy flow in the system, by altering the photosynthesis/respiration ratio, exudation of organic carbon and particle degradation and sinking (Falkowski et al., 1985; Lacour et al., 2017).

5 Conclusions

In this study, we showed that although Baltic Sea vernal dinoflagellates occur in similar salinity and temperature ranges, they have their own niches. We presented novel data on *H. arctica* subsp. *frigida*, which despite its occurring in low abundances is a ubiquitous component of the Baltic Sea spring bloom. Furthermore, we demonstrate that *G. corollarium* and *A. malmogiense* have distinct niches regarding their light acquisition strategies

reinforcing the occurrence of different traits among the *Apocalathium* complex. Although all three tested dinoflagellates are well adapted to low light conditions, an increase in light availability can impact the vernal Baltic Sea dinoflagellate assembly, selecting for species that can tolerate high light (such as *A. malmogiense*) in contrast to others that are more prone to photoinhibition (such as *G. corollarium* and *H. arctica* subsp. *frigida*). Additionally, the cell volume, growth and light acquisition traits of the three tested dinoflagellates respond differently to small changes in the ranges of temperature and salinity that are found in the Baltic Sea, demonstrating that photo-acquisition traits can also be used to assess climate change effects, especially when considering short-term effects on species competition. Platforms such as the high-throughput well-plate setup used in this study can ease the arduous task of obtaining physiological trait data. Our results illustrate that this kind of information is essential to answer questions related to species capacity to adapt and compete under a changing environment, especially when complemented by long term phytoplankton monitoring data.

Data availability statement

The raw data supporting the conclusions of this article will be made available by the authors, without undue reservation.

Author contributions

LH and JS conceived the experiments. LH and KK performed the experiments with assistance of PY and JS. PY, SK and TT developed the high-throughput well-plate used in the experiments. HH and LH organized the semi-quantitative monitoring data. LH analysed the data and wrote the first manuscript draft. All authors contributed to the article and approved the submitted version.

Funding

This study was funded by the SEASINK project (Academy of Finland, grant # 317297). LH was funded by Academy of Finland (NanOCean, grant # 342223) and KK was supported by Tiina and Antti Herlin Foundation.

Acknowledgments

This study utilized research infrastructure as part of FINMARI (Finnish Marine Research Infrastructure consortium). We thank Lot van Berkel and Johanna Oja for their assistance during the experiments; and the Alg@line team and Seija Hällfors for their contribution to the ship-of-opportunity phytoplankton time series. We are grateful for Tom Andersen and Geir Andersen help for implementing the LED panels. Also, we thank the reviewers for their valuable comments and suggestions, which helped improve the manuscript.

Conflict of interest

The authors declare that the research was conducted in the absence of any commercial or financial relationships that could be construed as a potential conflict of interest.

Publisher's note

References

Berges, J. A., Franklin, D. J., and Harrison, P. J. (2001). Evolution of an artificial seawater medium: improvements in enriched seawater, artificial water over the last two decades. *J. Phycol.* 37 (6), 1138–1145. doi: 10.1046/J.1529-8817.2001.01052.X

Chen, M., Mertiri, T., Holland, T., and Basu, A. S. (2012). Optical microplates for high-throughput screening of photosynthesis in lipid-producing algae. *Lab. Chip* 12 (20), 3870–3874. doi: 10.1039/C2LC40478H

Dewar, R. C., Medlyn, B. E., and Mcmurtrie, R. E. (1999). Acclimation of the respiration/photosynthesis ratio to temperature: insights from a model. *Global Change Biol.* 5 (5), 615–622. doi: 10.1046/j.1365-2486.1999.00253.x

Edwards, K. F., Thomas, M. K., Klausmeier, C. A., and Litchman, E. (2015). Light and growth in marine phytoplankton: allometric, taxonomic, and environmental variation. *Limnol. Oceanogr.* 60 (2), 540–552. doi: 10.1002/LNO.10033/SUPPINFO

Eilers, P. H., and Peeters, J. C. H. (1988). A model for the relationship between light intensity and the rate of photosynthesis in phytoplankton. *Ecol. Model.* 42 (3–4), 199–215. doi: 10.1016/0304-3800(88)90057-9

Falkowski, P. G., Barber, R. T., and Smetacek, V. (1998). Biogeochemical controls and feedbacks on ocean primary production. *Science* 281, 200–206. doi: 10.1126/science.281.5374.200

Falkowski, P. G., Dubinsky, Z., and Wyman, K. (1985). Growth-irradiance relationships in phytoplankton1. *Limnol. Oceanogr.* 30 (2), 311–321. doi: 10.4319/LO.1985.30.2.0311

Gilmour, D. J., Hipkins, M. F., Webber, A. N., Baker, N. R., and Boney, A. D. (1985). The effect of ionic stress on photosynthesis in *Dunaliella tertiolecta*. *Planta* 163 (2), 250–256. doi: 10.1007/BF00393515

Groetsch, P. M. M., Simis, S. G. H., Eleveld, M. A., and Peters, S. W. M. (2016). Spring blooms in the Baltic Sea have weakened but lengthened from 2000 to 2014. *Biogeosciences* 13 (17), 4959–4973. doi: 10.5194/BG-13-4959-2016

Guillard, R. R., and Ryther, J. H. (1962). Studies of marine planktonic diatoms. i. cyclotella nana hustedt, and *Detonula confervacea* (cleve) gran. *Can. J. Microbiol.* 8, 229–239. doi: 10.1139/M62-029

Hällfors, H. (2013). Studies on dinoflagellates in the northern Baltic Sea. PhD thesis (Helsinki: University of Helsinki).

Harris, G. P. (1980). Temporal and spatial scales in phytoplankton ecology. mechanisms, methods, models, and management. *Can. J. Fisheries Aquat. Sci.* 37 (5), 877–900. doi: 10.1139/f80-117

HELCOM (2011) *Manual for marine monitoring in the COMBINE programme of HELCOM. part c. programme for monitoring of eutrophication and its effects. annex 6: guidelines concerning phytoplankton species composition, abundance and biomass*. Available at: http://www.helcom.fi/groups/monas/Combin%0AeManual/AnnexesC/en_GB/annex6/%0A.

Hinners, J., Kremp, A., and Hense, I. (2017). Evolution in temperature-dependent phytoplankton traits revealed from a sediment archive: do reaction norms tell the whole story? *Proc. R. Soc. B: Biol. Sci.* 284, 20171888. doi: 10.1098/RSPB.2017.1888

Hjerne, O., Hajdu, S., Larsson, U., Downing, A., and Winder, M. (2019). Climate driven changes in timing, composition and size of the Baltic Sea phytoplankton spring bloom. *Front. Mar. Sci.* 6. doi: 10.3389/FMARS.2019.00482/BIBTEX

Honkanen, M., Müller, J. D., Seppälä, J., Rehder, G., Kielosto, S., Ylöstalo, P., et al. (2021). The diurnal cycle of pCO_2 in the coastal region of the Baltic Sea. *Ocean Sci.* 17 (6), 1657–1675. doi: 10.5194/OS-17-1657-2021

Ikävalko, J., and Thomsen, H. A. (1997). 'The Baltic Sea ice biota (March 1994): a study of the protistan community'. *Eur. J. Protistol.* 33, 229–243. doi: 10.1016/S0932-4739(97)80001-6

Iwataki, M. (2002). Taxonomic study on the genus heterocapsa (Peridiniales, dinophyceae). PhD thesis (Tokyo: University of Tokyo).

Jaanus, A. (2011). Phytoplankton in Estonian coastal waters – variability, trends and response to environmental pressures. PhD thesis (Tartu: Tartu University).

Jaanus, A., Hajdu, S., Kaitala, S., Andersson, A., Kaljurand, K., Ledaine, I., et al. (2006). Distribution patterns of isomorphic cold-water dinoflagellates *(Scrippsiella/Woloszynskia* complex) causing "red tides" in the Baltic Sea. *Hydrobiologia* 554 (1), 137–146. doi: 10.1007/S10750-005-1014-7

Kahru, M., and Nömmann, S. (1990). The phytoplankton spring bloom in the Baltic Sea in 1985, 1986: multitude of spatio-temporal scales. *Continental Shelf Res.* 10 (4), 329–354. doi: 10.1016/0278-4343(90)90055-Q

Kirk, John T. O. (2010). *Light and photosynthesis in aquatic ecosystems. 3rd edn* (Cambridge: Cambridge University Press). doi: 10.1017/CBO9781139168212

Klais, R., Tamminen, T., Kremp, A., Spilling, K., An, B. W., Hajdu, S., et al. (2013). Spring phytoplankton communities shaped by interannual weather variability and dispersal limitation: mechanisms of climate change effects on key coastal primary producers. *Limnol. Oceanogr.* 58 (2), 753–762. doi: 10.4319/LO.2013.58.2.0753

Klais, R., Tamminen, T., Kremp, A., Spilling, K., and Olli, K. (2011). Decadal-scale changes of dinoflagellates and diatoms in the anomalous Baltic Sea spring bloom. *PloS One* 6 (6), e21567. doi: 10.1371/JOURNAL.PONE.0021567

Kremp, A., Elbrächter, M., Schweikert, M., Wolny, J. L., and Gottschling, M. (2005). *Woloszynskia halophila* (Biecheler) comb. nov.: a bloom-forming cold-water dinoflagellate co-occurring with scrippsiella hangoei (Dinophyceae) in the Baltic Sea. *J. Phycol.* 41 (3), 629–642. doi: 10.1111/J.1529-8817.2005.00070.X

Kremp, A., Rengefors, K., and Montresor, M. (2009). Species specific encystment patterns in three Baltic cold-water dinoflagellates: the role of multiple cues in resting cyst formation. *Limnol. Oceanogr.* 54 (4), 1125–1138. doi: 10.4319/LO.2009.54.4.1125

Kremp, A., Tamminen, T., and Spilling, K. (2008). Dinoflagellate bloom formation in natural assemblages with diatoms: nutrient competition and growth strategies in Baltic spring phytoplankton. *Aquat. Microbial. Ecol.* 50 (2), 181–196. doi: 10.3354/AME01163

Lacour, T., Larivière, J., and Babin, M. (2017). Growth, chl a content, photosynthesis, and elemental composition in polar and temperate microalgae. *Limnol. Oceanogr.* 62, 43–58. doi: 10.1002/lno.10369

Larsen, J., Kuosa, H., Ikävalko, J., Kivi, K., and Hällfors, S. (1995). A redescription of *Scrippsiella hangoei* (Schiller) comb. nov. –a "red tide" dinoflagellate from the northern Baltic. *Phycologia* 34 (2), 135–144. doi: 10.2216/I0031-8884-34-2-135.1

Levasseur, M., Thompson, P. A., and Harrison, P. J. (1993). Physiological acclimation of marine phytoplankton to different nitrogen sources. *J. Phycol.* 29 (5), 587–595. doi: 10.1111/J.0022-3646.1993.00587.X

Lignell, R., Heiskanen, A.-S., Kuosa, H., Gundersen, K., Kuuppo-Leinikki, P., Pajuniemi, R., et al. (1993). Fate of a phytoplankton spring bloom: sedimentation and carbon flow in the planktonic food web in the northern Baltic. *Mar. Ecol. Prog. Ser.* 94, 239–252. doi: 10.3354/meps094239

Litchman, E., de Tezanos Pinto, P., Klausmeier, C. A., Thomas, M. K., and Yoshiyama, K. (2010). Linking traits to species diversity and community structure in phytoplankton. *Hydrobiologia* 653 (1), 15–28. doi: 10.1007/s10750-010-0341-5

Litchman, E., and Klausmeier, C. A. (2008). Trait-based community ecology of phytoplankton. *Annu. Rev.* 39, 615–639. doi: 10.1146/annurev.ecolsys.39.110707.173549

MacIntyre, H. L., and Cullen, J. J. (2005). "Using cultures to investigate the physiological ecology of microalgae," in *Algal culturing techniques*. Ed. R. A. Andersen (Cambridge: Cambridge: Academic Press), 287–326.

MacIntyre, H. L., Kana, T. M., Anning, T., and Geider, R. J. (2002). Photoacclimation of photosynthesis irradiance response curves and photosynthetic pigments in microalgae and cyanobacteria. *J. Phycol.* 38 (1), 17–38. doi: 10.1046/J.1529-8817.2002.00094.X

Muggeo, V. M. R. (2003). Estimating regression models with unknown break-points. *Stat Med.* 22, 3055–3071. doi: 10.1002/sim.1545

Muggeo, V. M. R. (2008) *Segmented: an r package to fit regression models with broken-line relationships*. Available at: https://cran.r-project.org/doc/Rnews/.

Niemi, Å., and Åström, A.-M. (1987). Ecology of phytoplankton in the tvärminne area, SW coast of finland. IV. environmental conditions, chlorophyll a and phytoplankton in winter and spring 1984 at tvärminne storfjärd. *Annales Botanici Fennici* 24 (4), 333–352.

Pinheiro, J., Bates, D., DebRoy, S., Sarkar, D., and Core Team, R. (2021) *Nlme: linear and nonlinear mixed effects models*. Available at: https://cran.r-project.org/package=nlme%3E.

Rantajärvi, E., Olsonen, R., Hällfors, S., Leppänen, J.-M., and Raateoja, M. (1998). Effect of sampling frequency on detection of natural variability in phytoplankton: unattended high-frequency measurements on board ferries in the Baltic Sea. *ICES J. Mar. Sci.* 55 (4), 697–704. doi: 10.1006/JMSC.1998.0384

Raven, J. A., and Geider, R. J. (1988). Temperature and algal growth. *New Phytol.* 110 (4), 441–461. doi: 10.1111/J.1469-8137.1988.TB00282.X

R Core Team (2021). *R: a language and environment for statistical computing* (Vienna, Austria: R Foundation for Statistical Computing). Available at: http://www.r-project.org/.

Reynolds, C. S. (2006). *The ecology of phytoplankton* (Cambridge: Cambridge University Press). doi: 10.1017/CBO9780511542145

Rintala, J.-M., Hällfors, H., Hällfors, S., Hällfors, G., Majaneva, M., and Blomster, J. (2010). *Heterocapsa arctica* Subsp. *frigida* subsp. nov. (Peridiniales, dinophyceae)–description of a new dinoflagellate and its occurrence in the Baltic Sea. *J. Phycol.* 46 (4), 751–762. doi: 10.1111/J.1529-8817.2010.00868.X

Schwaderer, A. S., Yoshiyama, K., de Tezanos Pinto, P., Swenson, N. G., Klausmeier, C. A., and Litchman, E. (2011). Eco-evolutionary differences in light utilization traits and distributions of freshwater phytoplankton. *Limnol. Oceanogr.* 56 (2), 589–598. doi: 10.4319/LO.2011.56.2.0589

Smayda, T. J. (1997). Harmful algal blooms: their ecophysiology and general relevance to phytoplankton blooms in the sea. *Limnol. Oceanogr.* 42, 1137–1153. doi: 10.4319/lo.1997.42.5_part_2.1137

Spilling, K. (2007). Dense sub-ice bloom of dinoflagellates in the Baltic Sea, potentially limited by high pH. *J. Plankton Res.* 29 (10), 895–901. doi: 10.1093/plankt/fbm067

Spilling, K., Kremp, A., Klais, R., Olli, K., and Tamminen, T. (2014). Spring bloom community change modifies carbon pathways and C:N:P: chl a stoichiometry of coastal material fluxes. *Biogeosciences* 11 (24), 7275–7289. doi: 10.5194/BG-11-7275-2014

Spilling, K., and Markager, S. (2008). Ecophysiological growth characteristics and modeling of the onset of the spring bloom in the Baltic Sea. *J. Mar. Syst.* 73 (3–4), 323–337. doi: 10.1016/J.JMARSYS.2006.10.012

Spilling, K., Olli, K., Lehtoranta, J., Kremp, A., Tedesco, L., Tamelander, T., et al. (2018). Shifting diatom-dinoflagellate dominance during spring bloom in the Baltic Sea and its potential effects on biogeochemical cycling. *Front. Mar. Sci.* 5. doi: 10.3389/FMARS.2018.00327/BIBTEX

Steele, J. H. (1962). Environmental control of photosynthesis in the sea. *Limnol. Oceanogr.* 7, 137–150. doi: 10.4319/lo.1962.7.2.0137

Stipa, T. (2004). The vernal bloom in heterogeneous convection: a numerical study of Baltic restratification. *J. Mar. Syst.* 44 (1–2), 19–30. doi: 10.1016/J.JMARSYS.2003.08.006

Sundström, A. M., Kremp, A., Daugbjerg, N., Moestrup, Ø., Ellegaard, M., Hansen, R., et al. (2009). *Gymnodinium corollarium* Sp. nov. (Dinophyceae) – a new cold water dinoflagellate responsible for cyst sedimentation events in the Baltic Sea. *J. Phycol.* 45 (4), 938–952. doi: 10.1111/J.1529-8817.2009.00712.X

Sundström, A. M., Kremp, A., Tammilehto, A., Tuimala, J., and Larsson, U. (2010). Detection of the bloom-forming cold-water dinoflagellate *Biecheleria baltica* in the Baltic Sea using LSU rRNA probes. *Aquat. Microbial. Ecol.* 61 (2), 129–140. doi: 10.3354/AME01442

Tamelander, T., and Heiskanen, A. S. (2004). Effects of spring bloom phytoplankton dynamics and hydrography on the composition of settling material in the coastal northern Baltic Sea. *J. Mar. Syst.* 52 (1–4), 217–234. doi: 10.1016/J.JMARSYS.2004.02.001

Tang, E. P. Y. (1996). Why do dinoflagellates have lower growth rates? *J. Phycol.* 32 (1), 80–84. doi: 10.1111/J.0022-3646.1996.00080.X

Thrane, J. E., Hessen, D. O., and Andersen, T. (2016). The impact of irradiance on optimal and cellular nitrogen to phosphorus ratios in phytoplankton. *Ecol. Lett.* 19 (8), 880–888. doi: 10.1111/ele.12623

Thrane, J. E., Hessen, D. O., and Andersen, T. (2017). Plasticity in algal stoichiometry: experimental evidence of a temperature-induced shift in optimal supply N:P ratio. *Limnol. Oceanogr.* 62 (4), 1346–1354. doi: 10.1002/lno.10500

Utermöhl, H. (1958). Methods of collecting plankton for various purposes are discussed. *SIL Commun.* 9, 1–38. doi: 10.1080/05384680.1958.11904091.

Vahtera, E., Conley, D. J., Gustafsson, B. G., Kuosa, H., Pitkänen, H., Savchuk, O. P., et al. (2007). Internal ecosystem feedbacks enhance nitrogen-fixing cyanobacteria blooms and complicate management in the Baltic Sea. *AMBIO: A J. Hum. Environ.* 36 (2), 186–194. doi: 10.1579/0044-7447(2007)36

Volpe, C., Vadstein, O., Andersen, G., and Andersen, T. (2021). Nanocosm: a well plate photobioreactor for environmental and biotechnological studies. *Lab. Chip* 21 (10), 2027–2039. doi: 10.1039/D0LC01250E

Wickham, H. (2016). *ggplot2: elegant graphics for data analysis* (New York: Springer-Verlag).

Willén, T. (1962). Studies on the phytoplankton of some lakes connected with or recently isolated from the Baltic. *Oikos* 13 (2), 199. doi: 10.2307/3565084

Witkowski, K., Król, T., Zielinski, A., and Kuten, E. (1998). A lightscattering matrix for unicellular marine phytoplankton. *Limnol. Oceanogr.* 43, 859–869. doi: 10.4319/lo.1998.43.5.0859

frontiers | Frontiers in Marine Science

TYPE Original Research
PUBLISHED 01 May 2023
DOI 10.3389/fmars.2023.1161065

OPEN ACCESS

EDITED BY
Jonathan Y.S. Leung,
University of Adelaide, Australia

REVIEWED BY
Henrik Kylin,
Linköping University, Sweden
Xian Sun,
Sun Yat-sen University, China

*CORRESPONDENCE
Terry Bidleman
terry.bidleman@umu.se

SPECIALTY SECTION
This article was submitted to Global Change and the Future Ocean, a section of the journal Frontiers in Marine Science

RECEIVED 07 February 2023
ACCEPTED 10 April 2023
PUBLISHED 01 May 2023

CITATION
Bidleman T, Agosta K, Andersson A, Brugel S, Ericson L, Hansson K, Nygren O and Tysklind M (2023) Sources and pathways of halomethoxybenzenes in northern Baltic estuaries. *Front. Mar. Sci.* 10:1161065. doi: 10.3389/fmars.2023.1161065

Sources and pathways of halomethoxybenzenes in northern Baltic estuaries

Terry Bidleman[1]*, Kathleen Agosta[1], Agneta Andersson[2,3], Sonia Brugel[2,3], Lars Ericson[2], Katarina Hansson[4], Olle Nygren[5] and Mats Tysklind[1]

[1]Department of Chemistry, Umeå University (UmU), Umeå, Sweden, [2]Department of Ecology & Environmental Science, UmU, Umeå, Sweden, [3]Umeå Marine Science Centre, UmU, Hörnefors, Sweden, [4]Swedish Environmental Research Institute (IVL), Gothenburg, Sweden, [5]Dean's Office, Faculty of Medicine, UmU, Umeå, Sweden

Introduction: Thousands of halogenated natural products (HNPs) are generated in the ocean and on land. A subset of these, halomethoxybenzenes (HMBs), are released from both natural and anthropogenic sources. Here we consider: 1. Brominated anisoles (BAs), transformation products of bromophenols. 2. Drosophilin A methyl ether (DAME: 1,2,4,5-tetrachloro-3,6-dimethoxybenzene), a secondary metabolite of terrestrial fungi. 3. Tetrachloroveratrole (TeCV: 1,2,3,4-tetrachloro-5,6-dimethoxybenzene), a lignin byproduct found in bleached kraft mill effluent. 4. Pentachloroanisole (PeCA), a metabolite of the wood preservative pentachlorophenol.

Methods: We examined several ecosystem compartments to determine sources and exchange processes for these HMBs: air, precipitation, rivers, forest fungi and litter, and water from northern Baltic estuaries and offshore. Samples were analyzed for HMBs by capillary gas chromatography – quadrupole mass spectrometry.

Results and discussion: All four types of HMBs were found in air, and BAs, DAME and TeCV were also present in precipitation. BAs and DAME were common in rivers and estuaries, whereas TeCV was low and PeCA was below detection. DAME was identified in several species of fungi and in forest litter; TeCV was occasionally present, but BAs and PeCA were below detection. Concentrations of BAs were higher in estuaries than in rivers or offshore waters, showing that estuaries are hot spots for production. BAs were negatively or not correlated with chlorophyll-a, suggesting contribution by heterotrophic bacteria as well as known production by phytoplankton and macroalgae. DAME was negatively or not correlated with BAs and did not appear to be produced in the estuaries; fungi and forest litter containing fungal mycelia are suggested as sources. HMBs volatilize from sea and land, disperse through the atmosphere, and return *via* precipitation and rivers. Production and biogeochemical cycles are influenced by climate change and we suggest BAs and DAME for following partitioning and exchange processes.

KEYWORDS

halogenated natural products, halomethoxybenzenes, Baltic Sea, estuaries, atmospheric and riverine transport

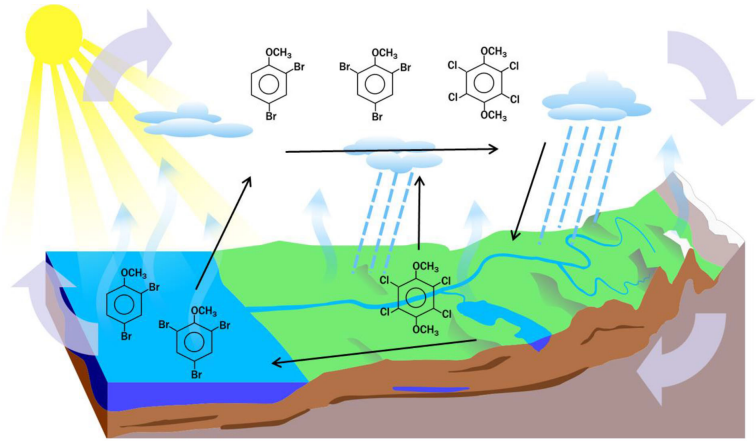

"What goes around, comes around": The sea-land-air cycle of HMBs.

GRAPHICAL ABSTRACT

Highlights:

- Natural HMBs bromoanisoles (BAs) and DAME (drosophin A methyl ether) were measured in ecosystem compartments supplying Baltic estuaries.
- Phytoplankton and macroalgae are known producers of BAs in estuaries and bacteria may contribute.
- DAME is produced by terrestrial fungi, with river transport to estuaries.
- These HMBs are useful for following partitioning and exchange processes.

1 Introduction

Thousands of halogenated natural products (HNPs) are generated in the ocean and on land, and their production and cycling are likely to be impacted by climate change (Bidleman et al., 2020). Halomethoxybenzenes (HMBs) are a subset of HNPs which have both natural and anthropogenic origins (Führer and Ballschmiter, 1998). Dibromo- and tribromoanisoles (DiBA and TriBA) result from bacterial O-methylation of precursor bromophenols (BPs), produced by marine organisms, chlorination of wastewater and industrial activities (Allard et al., 1987; Howe et al., 2005; Koch and Sures, 2018). Drosophilin A methyl ether (DAME: 1,2,4,5-tetrachloro-3,6-dimethoxybenzene), chlorinated anisoles and related compounds are secondary metabolites of terrestrial fungi (DeJong and Field, 1997; Teunissen et al., 1997; Garvie et al., 2015). Tetrachloroveratrole (TeCV: 1,2,3,4-tetrachloro-5,6-dimethoxybenzene) and other chloroveratroles (CVs) are metabolites of the chloroguiaicols formed in bleached kraft mill effluent (Neilson et al., 1983; Neilson et al., 1988; Brownlee et al., 1993). Pentachloroanisole (PeCA) is a metabolite of the wood preservative pentachlorophenol, but may also have unidentified natural sources (Kylin et al., 2017).

BAs and other haloanisoles are undesireable "taste and odor" compounds, arising from the disinfection of drinking water containing halogens (Diaz et al., 2005). They cause "cork taint" in wines (Chatonnet et al., 2004; Alañón et al., 2020), and mustiness in packaged food (Whitfield et al., 1997) and water (Brownlee et al., 1993). On the other hand, BPs are key flavor components in seafood (Chung et al., 2003), and algae are being considered as food additives and in aquaculture to take advantage of BPs and other flavor-enhancing components (Jones et al., 2016; Francezon et al., 2021). The precursor of DAME, drosophilin A (DA = 2,3,5,6-tetrachloro-4-methoxyphenol), has been reported in the meat of wild boar (*Sus scrofa*), apparently due to consuming fungi (Hiebl et al., 2011). Both DAME and DA have antibiotic activity (Kavanaugh et al., 1952; Teunissen et al., 1997). Neilson et al. (1984) reported threshold toxic concentrations and sublethal effects of several HMBs, including TeCV, on zebrafish (*Brachydanio rerio*) embryos and larvae. DAME and TriBA have been found in fish from the Laurentian Great Lakes of North America (Renaguli et al., 2020).

In previous papers, we reported BAs (Bidleman et al., 2017a; Bidleman et al., 2017b; Bidleman et al., 2023), DAME, TeCV and PeCA (Bidleman et al., 2023) in air and precipitation samples collected at Råö on the Swedish west coast and at an inland station Pallas in Subarctic Finland. The relative abundance of these compounds in air was ΣBAs (2,4-DiBA + 2,4,6-TriBA) > DAME > TeCV > PeCA at Råö, and DAME > ΣBAs > TeCV > PeCA at Pallas. These spatial patterns were consistent with marine sources for BAs and terrestrial sources for DAME, while the origins of the TeCV and PeCA were unclear. No temporal trends in air were evident for any HMB compound from 2002-2019. Concentrations in precipitation appeared to be controlled by Henry's law scavenging of the gas-phase compound. A terrestrial source for

DAME was suggested by its presence in several species of fungi, gathered from Swedish forests, and by literature reports of DAME in other fungal species worldwide.

Findings of HMBs in air and precipitation of coastal and inland regimes prompted further examination of their transport and exchange between the marine and terrestrial environment. Here for the first time, we report concentrations and linkages of BAs, DAME and TeCV in air, rivers and northern Baltic estuaries and discuss land-sea-air exchange processes. Climate change is producing profound alterations in the Northern Baltic ecosystem, driven by reduced ice cover and greater runoff of terrestrial dissolved organic carbon (DOC), one consequence being a shift from a phytoplankton-based food web to one based on heterotrophic bacteria (Andersson et al., 2015). In addition to supplying food for bacteria (Figueroa et al., 2021), terrestrial DOC sorbs anthropogenic persistent organic pollutants and other compounds of concern (Ripszam et al., 2015), thus influencing their food web bioaccumulation (Andersson et al., 2015). Along with DOC, HMBs provide tracers of land-sea transfer. Because the HMBs studied here are hydrophobic and accumulate in fish (Renaguli et al., 2020), they may be useful for studying bioaccumulation processes in the nearshore zone. As climate-induced changes bring more terrestrial DOC into the northern Baltic, these processes are likely to be even more relevant in the future.

2 Materials and methods

2.1 Air and precipitation sampling

Collection of air and precipitation samples at Pallas (68°0.0 N, 24°13.8 E) and Råö (57°23.622 N, 11°54.852 E) (Figures 1A, B) (Supplementary Material, S1) was done by the Swedish Environmental Research Institute (IVL). Samples were processed in their laboratory and cleaned extracts were sent to Umeå University (UmU) for analysis of HMBs (Bidleman et al., 2023).

2.2 River, estuary and offshore water sampling

River water was collected periodically in Västerbotten County, Sweden, usually soon after the spring flood, but occasionally in fall (S1, Table S1). Five rivers (Vindel, Ume, Sävar, Öre and Änger) were sampled in 2017, 2018, 2019 and 2022, and are shown in Figure 1, Area C, along with their mean flow rates, modeled from 2017-2021 (Swedish Meteorological and Hydrological Institute (SMHI), 2022). Total samples were 5-6 for the first four rivers and 2 for the Änger.

Estuaries Kalvarskatan (KAL, 63°36.072 N, 19°53.140 E) and Ängerån (ÄNG, 63°34.400 N, 19°50.666 E) were sampled during spring-summer in 2018, 2019, 2021 and 2022 (S1, Table S2). The area is shown as in Figure 1D, with more detail in Figure S1. Water was taken from the upper 0.5 m. KAL has no river, whereas ÄNG has a small river (Änger, Figure 1). Both are called "estuaries" throughout this paper. Water samples were collected at two other estuaries which have fresh water inputs intermediate of KAL and ÄNG (Eriksson et al., 2022; Guo et al., 2022): Stadsviken (SVK, 63° 33.026 N, 19°47.647 E) and Valviken (VVK, 63°32.468 N, 19°46.725 E), offshore of Hörnefors (HÖRN, 63°33.852 N, 19°56.226 E), in Örefjärden sound (ÖREFJ, 63°31.320 N, 19°48.276 E) and at the island group Holmön (63°47.598 N, 20°52.068 E) in 2018-2019 (Figure S1; Table S4). The Holmön samples were taken offshore of Bergudden Light (HOLBER), and in a shallow strait Sörsundet (HOLSÖR), which separates the two main islands.

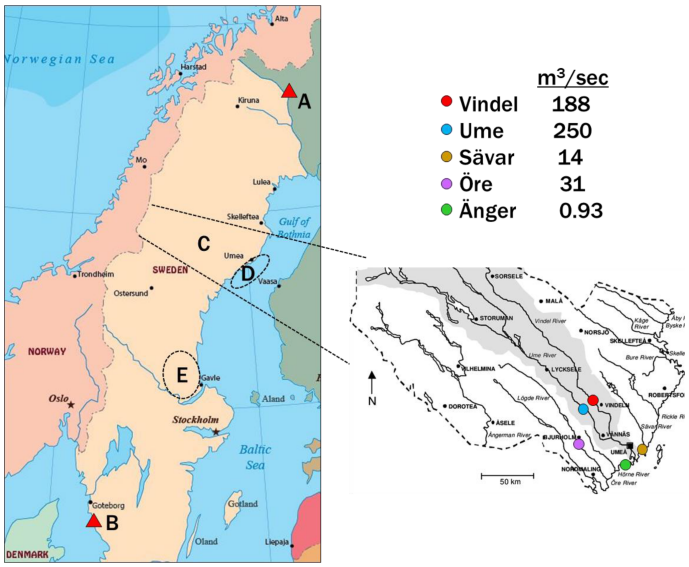

FIGURE 1
Locations for sample collection. Air at Pallas **(A)** and Råö **(B)**, rivers **(C)**, estuaries and offshore water (D, "The Quark") and terrestrial fungi **(C, E)**. The rivers are shown on the side map of Västerbotten County, with their mean flow rates modeled from 2017-2021 (SMHI). Expansion of the estuaries region **(D)** is shown in Figure S1 and Guo et al. (2022).

Water was collected in 20-L stainless steel cans, 3-5 L was filtered through glass fiber filters and the HMBs were sorbed on solid-phase extraction cartridges (Supplementary S1). Samples were processed within five days of collection to minimize changes in TriBA content (Supplementary S5).

2.3 Phytoplankton sampling

Phytoplankton was collected during bloom periods in May and September 2019 and August 2020 (Supplementary S1). The collections were made at the ÖREFJ station (see above). The phytoplankton in May consisted mainly of diatoms (*Skeletonema marinoi*, *Chaetoceros wighamii*), while August and September collections were dominated by the cyanobacterium *Aphanizominon flos-aquae*. Water samples were taken from within and below the *A. flos-aquae* blooms.

2.4 Fungi and forest litter sampling

Fungi and coniferous, deciduous or mixed litter were gathered in fall from forests in Västerbotten and Gävleborg Counties, Sweden (Figure 1, Areas C and E), and were frozen until analysis. They were collected and processed as described in Supplementary S1.

2.5 Chemical analysis

Sources of supplies for sample collection and analysis are reported in Supplementary S2. Samples were analyzed for the HMB compounds 2,4-DiBA, 2,4,6-TriBA, DAME, TeCV and PeCA using capillary gas chromatography- quadrupole mass spectrometry (GC-MSD) (Supplementary S3), monitoring the selected ions in Table S5. Quality control information is reported in Supplementary S4. In addition to HMBs, properties measured in estuarine water were temperature (TMP), salinity (SAL), chlorophyll-a (CHL) and dissolved organic carbon (DOC). Methods for these are outlined in Table S6.

2.6 Data analysis

Statistical analysis (regressions, t-tests, etc.) was done using Excel Version 2302 and XLSTAT 2022, and Prism (GraphPad).

3 Results and discussion

3.1 Air and precipitation

Mean concentrations of HMBs in air and precipitation at Råö and Pallas for 2018-2019 are given in Table 1. Monitoring was also conducted in earlier years and all air and precipitation results are reported in Bidleman et al. (2017a); Bidleman et al. (2023). In these studies, only the polyurethane foam (PUF) trap was analyzed for air samples, and corrections were made for incomplete collection due to breakthrough of gas-phase compounds. As noted in Section 1, the order of abundance of HMBs in air at Råö was ΣBAs > DAME > TeCV > PeCA, whereas at Pallas the order was DAME > ΣBAs > TeCA > PeCA. The same abundance order was also found in precipitation, with the exception that PeCA was generally below detection. Mean concentrations of DAME in air at Råö and Pallas were not significantly different (p >0.05, Welch's t-test of means), whereas precipitation at Pallas showed higher levels of DAME compared to Råö (p = 0.012). Lower abundance of BAs at Pallas can be explained by its remoteness from marine regions (Bidleman et al., 2023).

The apparent enthalpy of surface-to-air exchange ($\Delta_{SA}H$, kJ mol^{-1}) at Råö and Pallas was calculated from Clausius-Clapeyron (CC) plots of log partial pressure in air (P_{air}/Pa) versus reciprocal temperature:

$$\Delta_{SA}H = -slope \star R \star 2.303/1000 \quad (1)$$

where R = 8.314 Pa m^3 mol^{-1} K^{-1} (Bidleman et al., 2023). By comparing observed slopes with those of HMB physicochemical properties (vapor pressure, octanol-air partition coefficient, Henry's law constant), we found that apparent $\Delta_{SA}H$ for TriBA (but not DiBA), DAME and TeCV at Råö were within one standard deviation of property values. At Pallas, $\Delta_{SA}H$ was also within one

TABLE 1 HMBs in air and precipitation.

	Råö				Pallas			
	Air[a,c], pg m^{-3}		Precipitation[a,c], pg L^{-1}		Air[b,c], pg m^{-3}		Precipitation[b,c], pg L^{-1}	
	Mean	SD	Mean	SD	Mean	SD	Mean	SD
DiBA	35	24	20	13	9.0	8.5	16	17
TriBA	44	25	36	26	8.4	6.0	14	8.7
DAME	34	23	37	30	41	43	72	57
TeCV	12	7.2	22	18	2.1	1.5	6.4	3.5
PeCA	1.4	0.6	ND[d]	ND	0.56	0.74	ND	ND

a) Years 2018-2019, N_{air} = 23-24, N_{precip} = 19-22, depending on compound.
b) Years 2018-2019, N_{air} = 24, N_{precip} = 17-24, depending on compound. Monitoring was also done at both stations in earlier years, see Bidleman et al., 2017a, 2023.
c) Mean concentrations of DAME in air at Råö and Pallas were not significantly different (p >0.05, Welch's t-test of means) , whereas precipitation at Pallas showed higher levels of DAME compared to Råö (p = 0.012).
d) ND: below the limit of detection.

standard deviation of property values for DAME, but not for either BA. Values of $\Delta_{SA}H$ that are similar to those of physicochemical properties imply local or regional surface-air exchange (e.g., with soil, vegetation, water) whereas relatively flat slopes of CC plots and low values of $\Delta_{SA}H$ are expected for compounds which arrive *via* long-range transport and show little interaction with local/regional surfaces (Hoff et al., 1998; Wania et al., 1998).

Our interpretation of these observations is that TriBA at Råö is influenced by exchange with coastal seawater, but sources for DiBA may be more dispersed over wider areas of the ocean. Differences between the two BAs might be explained by higher concentrations of TriBA versus DiBA in coastal macroalgae (Bidleman et al., 2023), although we discuss in Section 3.4.1 that BA proportions in water are not necessarily the same as those in macroalgae. BAs have not been reported in Atlantic seawater off the Swedish west coast. DAME may be influenced by exchange with land surfaces around Råö, a conclusion supported by findings of DAME in terrestrial fungi and forest litter (Section 3.3), but a marine contribution is not ruled out, since DAME has been reported in open-ocean seawater (Schreitmüller and Ballschmiter, 1994; Schreitmüller and Ballschmiter, 1995) and offshore water in the northern Baltic (Section 3.5). Being a coastal site, Råö is influenced by alternating land and sea breezes. BAs showed no evidence of local exchange at Pallas, which is expected from its distance from marine sources. However, $\Delta_{SA}H$ for DAME at Pallas was suggestive of contributions from the regional (terrestrial) environment (Bidleman et al., 2023).

Mean atmospheric concentrations of HMBs at our stations are compared in Figure 2 with other measurements made in the northern Baltic (Bidleman et al., 2015), Norway (Bohlin-Nizzetto et al., 2021), and the Canadian Arctic (Su et al., 2008; Wong et al., 2011). TriBA concentrations at Pallas and Norway (Svalbard) were similar to each other and lower than those found in the Canadian Archipelago. TeCV concentrations at Pallas were about twice those reported at circumpolar Arctic stations in 2000-2003 (Su et al., 2008). The mean PeCA concentration at Pallas was similar to that reported at Alert, Canada (Wong et al., 2021). DAME has not been reported at other Arctic-Subarctic stations. DAME concentrations of 2-195 pg m^{-3} have been found at island stations and over the open ocean (Atlas et al., 1986; Wittlinger and Ballschmiter, 1990; Schreitmüller and Ballschmiter, 1994; Schreitmüller and Ballschmiter, 1995).

3.2 Rivers

Mean concentrations of HMBs in rivers are given in Table 2, with details in Table S1. DiBA and TriBA were determined in all samples, DAME and TeCV in only some of them. DAME was the most abundant compound, with a mean concentration over all rivers 5-8 times higher than those of DiBA, TriBA or TeCV. PeCA was generally below detection. No significant correlations were found among the compounds (p >0.05). No differences were evident across the rivers, with the exception that the mean concentration of TriBA in the Öre River (16 ± 5 pg L^{-1}, n=5) was lower than the average of the other four rivers (44 ± 22 pg L^{-1}, n=19) (p<0.001).

Suspected sources of HMBs to the rivers are atmospheric deposition to and drainage from their watersheds. We examined these possibilities by comparing the ratios of mean concentrations of HMBs in rivers (Table S1) to those in precipitation at Råö and Pallas (Table 1). A limitation is that both atmospheric sites are quite distant from the river locations (Figure 1). River/precipitation (R/P) ratios, calculated by assuming mean river concentrations and different scenarios of precipitation contribution, are presented in Table S7. R/P ratios in Scenario 1 assume the Råö precipitation concentrations and are 1.2-3.2 for BAs, 2.0 for TeCV and 9.0 for DAME. Differences in the R/P ratios are obtained if based on precipitation concentrations from Pallas (Scenario 2): 3.1-4.2 for BAs, 6.7 for TeCV and 4.6 for DAME, or averaged precipitation concentrations from both sites (Scenario 3): 1.7-3.5 for BAs, 3.0 for TeCV and 6.1 for DAME. The Västerbotten region (Figure 1C) receives air parcels from all sectors, including from the North Atlantic across Sweden (Newton et al., 2014). Concentrations of BAs at northern Baltic stations, measured in 2011-2012, show the influence of this pathway as well as regional emissions from the Baltic Sea (Bidleman et al., 2015; Bidleman et al., 2017b). Average concentrations of BAs in northern Baltic air, measured in 2011-2012 (23 pg m^{-3} DiBA, 50 pg m^3 TriBA) (Bidleman et al., 2015), are more similar to those at Råö than at Pallas (Figure 2). Based on this consideration, the R/P ratios based on Scenario 1 (precipitation concentrations at Råö) are probably the best of the three estimates of R/P ratios in the Västerbotten region.

An R/P = 1 implies that the precipitation directly drives HMB concentrations in the rivers, whereas R/P >1 suggests additional sources; i.e., runoff from within the watershed. Since R/P >1 for all HMBs and in all scenarios (Table S7), some contribution from within the watershed seems likely. Results from the Scenario 1 calculations suggest greater watershed contribution for DAME than the BAs or TeCV. Atmospheric sources to the watershed are precipitation and atmospheric deposition of gaseous HMBs scavenged by the "forest filter effect" (McLachlan and Horstmann, 1998; Su et al., 2007; Gong et al., 2021). DAME is produced by fungi (Section 3.3) and enters rivers *via* stream and groundwater drainage from the terrestrial environment, as well as being delivered by air

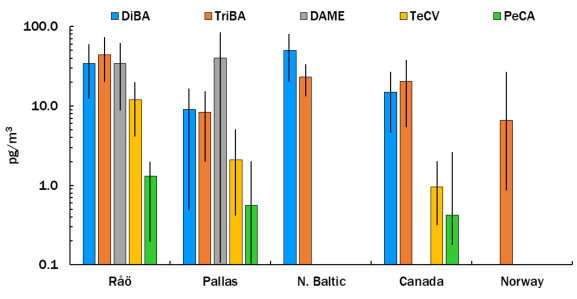

FIGURE 2
Mean ± SD concentrations of HMBs in air at Råö and Pallas (this study) and the Northern Baltic (Bidleman et al., 2015), compared to reported levels at Canadian (Su et al., 2008; Wong et al., 2011; Wong et al., 2021) and Norwegian (Bohlin-Nizzetto et al., 2021) locations. Variations for PeCA in Canada and TriBA in Norway are shown as ranges.

TABLE 2 HMBs in rivers of Västerbotten County, Sweden[a,b], pg L^{-1}.

	Ånger			Öre			Sävar			Vindel			Ume		
	Mean	SD	n	Mean	SD	n	Mean	SD	n	Mean	SD	n	Mean	SD	n
DiBA	42	20	2	74	26	5	81	47	5	80	23	6	57	17	6
TriBA	73	50	2	16	5	5	52	25	5	40	9	6	32	9	6
DAME	481		1	239	64	4	329	98	3	355	277	4	267	87	4
TeCV[c]	64		1	38	4	2	36	7	3	31	18	3	51	3	3

a) See Table S1 for sampling dates.
b) Locations and mean flows in Figure 1.
c) Not quantifiable in some samples due to low concentrations or chromatographic interference.

transport from other regions. Transport to the estuaries takes place by rivers and atmospheric deposition.

3.3 Terrestrial fungi and forest litter

Fruiting bodies of terrestrial fungi (n=19) and litter/underlying humus samples (n=6) were screened for DAME and TeCV. Our method has a limit of detection (LOD) of 0.0016 mg kg^{-1} (S4 Section 4). DAME in four species ranged from 0.3-3.8 mg kg^{-1} fresh weight (fw): *Micromphale perforans* (a saprotroph), *Stereum hirsutum* (a white rot), *Thelephora terrestris* (an ectomycorrhiza) and *Hydnellum mirabile*.(an ectomycorrhiza). Four others (*Stereum subtomentosum* (white rot), *Kuehneromyces mutabilis* (saprotroph), *Cladonia stellaris* (lichen), and *Jackrogersella multiformis* (soft rot, intermediate between white and brown rot) contained 0.015-0.053 mg kg^{-1} fw. The litter/humus samples, which were presumably permeated with fungal mycelia, contained 0.006-1.6 mg kg^{-1} fw.

Only a few samples contained detectable levels of TeCV, 0.0033 and 0.039 mg kg^{-1} fw in *M. perforans* and *T. terrestris*, respectively, and 0.0033-0.016 mg kg^{-1} fw in litter/humus (n=3). The low occurrence of TeCV in fungi and litter is surprising, given its frequency of detection in air and precipitation; however, we note that the number of fungi species screened here is small compared to their diversity. BAs and PeCA were not detected in fungi nor in litter/humus.

The reported range of total chlorine in forest soils of Sweden is 16-458 mg kg^{-1} dry weight, of which two-thirds or more is organically bound (Svensson et al., 2022). The balance between organic and inorganic chlorine is maintained by rates of chlorination and dechlorination (Svensson et al., 2021). Chlorination of organic matter takes place most actively in the rhizosphere and is carried out by diverse organisms, including bacteria, fungi and vascular plants, as well as by abiotic processes (Öberg and Bastviken, 2012; Montelius et al., 2019; Svensson et al., 2022). DeJong and Field (1997) describe several classes of chlorinated fungal metabolites produced by basidiomycetes: amino acids, anisyls, hydroquinones, orsinols, orsellinate sesquiterpenes and others. We found the chlorinated hydroquinone DAME, and it is likely that the forests are also sources of these other fungal metabolite classes. Some of these have been described as "fungal volatiles" (Dickschat, 2017), implying that they are available for atmospheric transport. Degradation pathways also exist for these compounds; e.g., mineralization and biotransformation in forest soils (DeJong and Field, 1997) and reductive dehalogenation in anaerobic sediments (Milliken et al., 2004), but we did not investigate these processes.

3.4 KAL and ÄNG estuaries

DiBA, TriBA and DAME were the main HMBs found in KAL and ÄNG water. TeCV was identified in a few samples at lower levels and PeCA was below detection. Concentrations are summarized in Table 3 and detailed for each sampling event in Tables S2, along with the other supporting chemical and biological factors listed in Table S6.

3.4.1 Bromoanisoles.

Mean concentrations in KAL were 428 ± 380 pg L^{-1} DiBA and 294 ± 153 pg L^{-1} TriBA (n=15), and in ÄNG 281 ± 164 pg L^{-1} DiBA and 242 ± 106 pg L^{-1} TriBA (n=5) (Table 3). Means in the northern and southern Baltic in 2011-2013 were 86 ± 51 pg L^{-1} DiBA and 199 ± 150 pg L^{-1} TriBA, for a set consisting of mostly open-sea samples (Bidleman et al., 2016). The time courses of BAs in the estuaries over the spring-summer are shown in Figures 3A, B, with fits to the curves in Table S3, where all years have been combined. The pattern for BAs in both estuaries was similar, lower concentrations in May-June, a rise in July-August and falling off in September. This seasonal rise-fall trend was noted for BAs, BPs and their transformation products hydroxylated and methoxylated bromodiphenyl ethers (OH-BDEs, MeO-BDEs) in Baltic macroalgae, amphipods and fish (Dahlgren et al., 2015; Dahlgren et al., 2016).

A study in which passive water samples were deployed on the Great Barrier Reef (GBR) from 2007-2013 showed mean concentrations of 450 pg L^{-1} DiBA and 170 pg L^{-1} TriBA (Vetter et al., 2018), within the range of those found in KAL and ÄNG. As in KAL, events of high DiBA on the GBR sometimes corresponded with high TriBA, and sometimes not. The precursor BPs were also found on the GBR. At 3840 pg L^{-1}, the mean concentration of DiBP was over eight times the DiBA concentration, whereas the mean for TriBP (21 pg L^{-1}) was lower than that of TriBA. The TriBP concentration was likely lower because of its near-complete dissociation in seawater, resulting in poor collection by the passive sampler (Vetter et al., 2009).

TABLE 3 HMBs in KAL and ÄNG estuaries[a,b], pg L^{-1}.

	KAL			ÄNG		
	Mean	SD	n	Mean	SD	n
DiBA	428	380	15	281	164	15
TriBA	294	153	15	242	106	15
DAME	189	50	9	271	140	10
TeCV[c]	27	11	4	63	42	3

a) See Table S2 for sampling dates and other physical, chemical and biological properties.
b) KAL: Kalvarskatan, ÄNG: Ängerån.
c) Not quantifiable in some samples due to low concentrations or chromatographic interference.

Correlations among the HMB compounds and other chemical and biological factors are summarized in Table S8, where significant relationships ($p<0.05$) are shown in red, positive correlations are in normal font and negative ones are italicized. DiBA and TriBA were positively and significantly correlated in ÄNG, but not in KAL, where occasional high spikes of DiBA were measured that did not correspond to high TriBA (Figure 3A). SAL and DOC were negatively correlated in both estuaries, more strongly in ÄNG due to delivery of terrestrial dissolved organic matter, which is typical of northern Baltic rivers (Figueroa et al., 2021; Guo et al., 2022). Plots of the BAs and DAME versus SAL, DOC and CHL are shown in Figure 4. TriBA was positively correlated to SAL in both estuaries. A rise in DiBA with SAL was suggested in both estuaries, but the correlations were not significant. DiBA and TriBA were negatively correlated to DOC in ÄNG, but not in KAL, which had a smaller variation in DOC. Both BAs were negatively correlated with CHL in ÄNG (more strongly for DiBA than TriBA) and not correlated with CHL in KAL.

Proportions of the two BAs in KAL and ÄNG water were expressed by the fraction F_{TriBA} = TriBA/(DiBA + TriBA), which varied from about 0.2 to 0.7. F_{TriBA} was slightly lower in midsummer than in spring or fall (Figure 3C). Average F_{TriBA} were 0.46 ± 0.16 in KAL and 0.49 ± 0.11 in ÄNG. There were no significant differences between the two estuaries in mean BAs concentrations nor in mean F_{TriBA} (Welch's t-test, unequal variances, $p > 0.05$). Variations in F_{TriBA} suggest links to production mechanisms. In 16 macroalgae species from the Baltic, and Atlantic coasts of Sweden and Norway, TriBA exceeded DiBA with mean F_{TriBA} = 0.75 ± 0.15 (Bidleman et al., 2019), and TriBA > DiBA in phytoplankton (see below). Thus, these photosynthesizers would be expected to release mainly TriBA to the estuaries, whereas similar abundances of the two BAs in the estuaries suggest additional sources.

Duplicate water samples were collected in September 2019 within and below a bloom of *A. flos-aquae* and showed the following mean concentrations. Within bloom: DiBA 128 ± 7 pg L^{-1}, TriBA 232 ± 16 pg L^{-1}, below bloom: DiBA 76 ± 23 pg L^{-1}, TriBA 173 ± 13 pg L^{-1}. Although suggestive of higher concentrations within the bloom, neither within-below set is significant. In August 2020, only one set of water samples was taken, with DiBA 49 pg L^{-1} and TriBA 228 pg L^{-1} within the bloom, and DiBA 24 pg L^{-1} and TriBA 198 pg L^{-1} below. Analysis of the *A. flos-aquae* for TriBA gave 3.5 ng g^{-1} fw in 2019 and

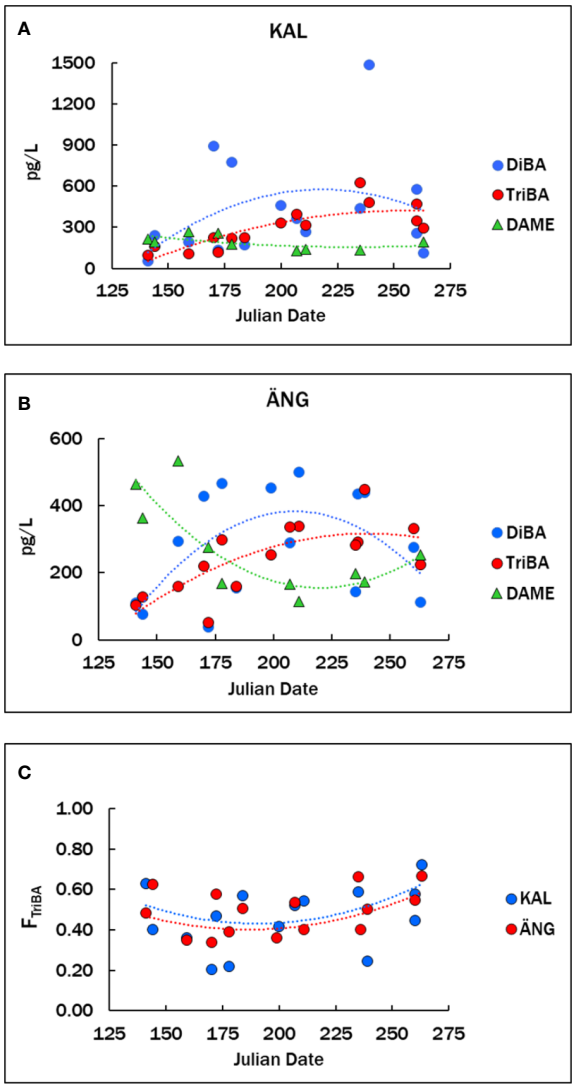

FIGURE 3
(A, B) Concentrations of BAs and DAME in the KAL and ÄNG estuaries from May to September. **(C)** Fraction of TriBA, F_{TriBA} = TriBA/(DiBA + TriBA). Data for all years are plotted versus the Julian date of sampling. Numerical data are given in Table S2. Lines are second-order regressions, $Y = aX^2 + bX + c$, with regression parameters in Table S3.

0.9 ng g^{-1} fw in 2020, DiBA in *A. flos-aquae* was below detection in both years (<0.06 ng g^{-1} fw). Diatoms (*Skeletonema marinoi, Chaetoceros wighamii*) collected in May 2019 showed 0.12 ng g^{-1} fw TriBA and 0.06 ng g^{-1} fw DiBA, well below the concentrations in *A. flos-aquae*. TriBA exceeded DiBA in another phytoplankton species, *Nodularia spumigena* (Löfstrand et al., 2010). Results of this limited study suggest that TriBA is released during *A. flos-aquae* blooms, either from the alga itself or produced by associated bacteria. The F_{TriBA} in water from these experiments ranged from 0.64-0.89, higher than 0.46-0.49 in KAL and ÄNG (see above), but lower than F_{TriBA} in *A. flos-aquae* itself (0.94-0.98).

It is not clear whether CHL is a suitable indicator of BAs production by photosynthesizers in general. In the red alga *Ceramium tenuicorne*, DiBP was positively correlated with CHL but TriBP was not, and DiBP was better correlated to the sum of xanthophylls and carotenoids than to CHL (Lindqvist et al., 2017). We note that TriBA was relative abundant in the fall-collected *A. flos-aquae* but not in the spring-collected diatoms. Thus, TriBA in water might be more related to CHL in the fall than in spring.

BPs are synthesized by marine algae as secondary metabolites by haloperoxidase enzymes (Koch and Sures, 2018) and production is influenced by environmental stress factors (Dahlgren et al., 2015). Genes for BPs production have been identified in marine gamma-proteobacteria, in particular *Pseudoalteromonas* spp. (Agarwal et al., 2014; Busch et al., 2019). Several types of microorganisms are capable of generating haloanisoles by O-methylation of precursor halophenols, including bacteria, cyanobacteria and fungi (Neilson et al., 1988; Zhang et al., 2016; Zhou et al., 2021).

In summary, three lines of evidence support bacteria in addition to macroalgae and phytoplankton as sources of BAs to the estuaries: 1. Nearly equal concentrations of DiBA and TriBA were found in water, whereas TriBA > DiBA in macroalgae and phytoplankton. 2. BAs in water showed negative or no correlation with the photosynthetic variable CHL. 3. Production of BPs and other HNPs has been reported in heterotrophic marine bacteria. As noted above, production of BAs is a two-step process, whereby BPs are first formed and then O-methylated to BAs. Interpretation of BA-BP trends in the estuaries would be aided in the future by also determining concentrations of BPs.

3.4.2 DAME and TeCV

The DAME concentrations averaged 189 ± 50 pg L^{-1} (n=9) in KAL and 271 ± 140 pg L^{-1} (n=10) in ÄNG (Table 3), with no significant difference in these means (p >0.05). Concentrations in ÄNG were higher in spring, declined over the summer, and rose again in early fall (Figure 3B). Mean DAME concentrations early (up to and including Julian day 200) and later (after Julian day 200) were 221 ± 38 pg L^{-1} (n=5) and 149 ± 71 pg L^{-1} (n=4) in KAL (not significant), and 361 ± 145 pg L^{-1} (n=5) and 180 ± 51 pg L^{-1} (n=5) in ÄNG (p = 0.058). The suggested higher spring values in ANG probably result from riverine runoff to ÄNG (see below). TeCV concentrations were lower and undetectable in many samples. Means of positive samples for KAL and ÄNG were 27 ± 11 pg L^{-1} (n=4) and 63 ± 42 pg L^{-1} (n=3).

Few correlations involving DAME were significant, limited by the smaller number of samples analyzed for this HMB. In ÄNG, a terrestrial-riverine source for DAME was supported by a positive association with DOC (p = 0.043) and a negative (but not significant) relationship to SAL (p = 0.079). One DAME point appears to be an outlier (Figures 4C, F), and if that point is rejected, the correlations of DAME with DOC (positive) and SAL (negative) are stronger (p = 0.00044 and 0.0066, respectively). No significant associations between DAME and DOC, or DAME and SAL, were found in KAL, which has smaller ranges of these independent variables. DAME was negatively correlated with TriBA in ÄNG (p = 0.017) and KAL (p = 0.0075). Rejection of the suspect DAME point in ÄNG led to stronger negative correlations with TriBA (p = 0.012) and DiBA (p = 0.026). These trends suggest that, unlike BAs, DAME is not produced within the estuaries but delivered by terrestrial runoff.

3.5 Other estuaries and offshore waters.

Estuaries VVK and SVK, the strait HOLSÖR, and offshore sites HÖRN, ÖREFJ and HOLBER, were each sampled on 2-3 occasions and results are reported in Tables 4, S4. Concentrations of BAs (VVK and SVK) and DAME (VVK only) were within the ranges of those found in KAL and ÄNG (Table S2). HOLSÖR is a shallow area between two Holmön islands with visible aquatic plants when sampled, and levels of BAs in HOLSÖR were even higher than those in the estuaries (Tables 4, S4). Concentrations of BAs in offshore waters at HÖRN, ÖREFJ and HOLBER (Table 4; Figure 5; Table S4) were lower than those in the estuaries and HOLSÖR, and typical of concentrations reported in the open Baltic (Section 3.4.1). Values of F_{TriBA}, calculated from mean concentrations in Table 4, were 0.56 and 0.54 for VVK and SVK, respectively, slightly higher than F_{TriBA} in KAL and ÄNG (0.46 and 0.49, Section 3.4.1), but still showing similar abundance of the two BAs. Higher abundance of DiBA was found in HOLSÖR (F_{TriBA} = 0.39), while TriBA was more dominant in offshore waters ÖREFJ, HÖRN and HOLBER (F_{TriBA} = 0.60-0.67).

Concentrations of DAME were quite similar in the estuaries and offshore; means 189, 271 and 130 pg L^{-1} in KAL, ÄNG and VVK, respectively, versus 180 and 163 pg L^{-1} at HÖRN and ÖREFJ, (Tables 3, 4; Figure 5). This similarity is another indication that DAME is not produced within the estuaries but delivered rather uniformly to coastal waters by riverine runoff and atmospheric deposition. The only other report of DAME in seawater is from a survey in the North and South Atlantic in 1991-1992 (Schreitmüller and Ballschmiter, 1994; Schreitmüller and Ballschmiter, 1995). Concentrations in open-ocean surface water ranged from 1.5-7.7 pg L^{-1}, well below those in our estuaries and offshore waters.

3.6 Atmospheric and riverine loadings versus *in situ* production of BAs in Bothnian Bay.

Our studies were conducted in estuaries and rivers of the "Quark" between the Bothnian Sea and Bothnian Bay (Area D in Figure 1). The Bothnian Bay has a surface area of 36800 km^2 and a catchment area of 260675 km^2 (https://en.wikipedia.org/wiki/

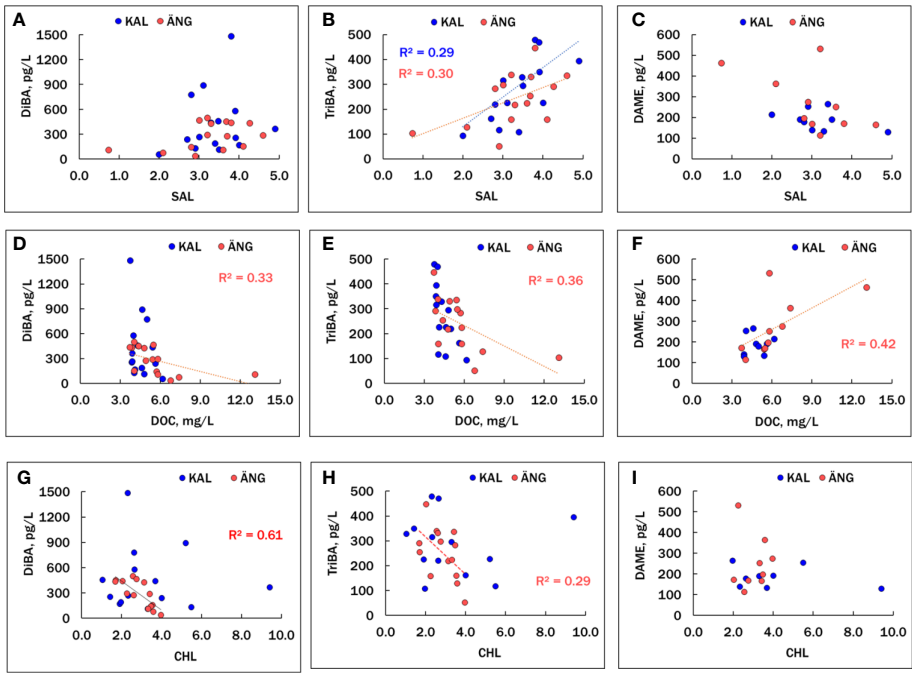

FIGURE 4
Associations of DiBA **(A, D, G)**, TriBA **(B, E, H)** and DAME **(C, F, I)** with variables SAL, DOC and CHL in the KAL and ÄNG estuaries. Only significant ($p<0.05$) regressions are shown. Correlation coefficients (as r^2) are given in Table S8.

Bothnian_Bay) and receives loadings of BAs from atmospheric deposition and riverine runoff, as well as from *in situ* production. In a previous assessment (Bidleman et al., 2015), BAs were judged to be oversaturated in Bothnian Bay surface water with respect to the air (water/air fugacity ratio >1) and the net flux was sea-to-air, removing an estimated ΣBAs = 1360 kg over five-month period from May-September. The reverse process, gaseous deposition of ΣBAs to the Bay, amounted to only 62 kg. Although we sampled only a few of the many rivers flowing into the Bay, we can make a rough estimate of their BAs transport. The annual discharge of eight major rivers into the Bay is 78.5 km^3 (https://en.wikipedia.org/wiki/Bothnian_Bay). Scaling to the concentrations and flows of the rivers in Table 2 gives an estimated ΣBAs = 3.3 kg runoff into the Bay over five months. Thus, rivers deliver some BAs to the Bay, but the oversaturated water concentrations are probably maintained by *in situ* production, which drives the volatilization.

4 Conclusions and implications for climate change influence

The overall picture of HMB transport and exchange can be summed up by "What goes around, comes around". HMBs volatilize from sea and land, disperse through the atmosphere, and return *via* precipitation and rivers. This cycle provides a pathway for marine BAs to reach terrestrial ecosystems. BAs have been found in water and larvae of black flies (*Simuliidae* spp.) from Subarctic streams in Sweden (Kupryianchyk et al., 2018).

TABLE 4 HMBs in other estuaries and offshore water, pg L^{-1}.

Location[a]	DiBA	TriBA	DAME
VVK			
mean	204	261	130
SD	112	43	38
n	3	3	3
SVK			
mean	195	227	NA[b]
SD	36	86	
n	3	3	
ÖREFJ			
mean	85	175	163
SD	31	118	13
n	3	3	2
HÖRN			
mean	68	101	180
SD	23	18	35
n	3	3	2
HOLBER			
mean	85	164	NA

(Continued)

TABLE 4 Continued

Location[a]	DiBA	TriBA	DAME
SD	44	85	
n	2	2	
HOLSÖR			
mean	774	502	NA
SD	614	145	
n	2	2	

[a]See Section D in Figure 1, and Figure S1. VVK: Valviken, SVK: Stadsviken, ÖREFJ: Örefjärden, HÖRN: Hörnefors, HOLBER: Holmön Bergudden, HOLSÖR: Holmön Sörsundet.
[b]NA, not analyzed.

Concentrations of BAs in KAL and ÄNG estuaries and two others (VVK and SVK) are higher than those offshore. Negative or no correlations between BAs and CHL in KAL and ÄNG suggest bacterial production in addition to known production by phytoplankton and macroalgae. Rivers also contribute BAs, but their role in Bothnian Bay appears minor relative to atmospheric processes. DAME is found in terrestrial fungi and forest litter and enters estuaries through watershed drainage.

Production and biogeochemical cycles of HNPs are influenced by climate change (Bidleman et al., 2020). The northern Baltic is transitioning from a phytoplankton-based food web to one based on heterotrophic bacteria, driven by higher precipitation and increased runoff of terrestrial dissolved organic matter (Andersson et al., 2015; Figueroa et al., 2016; Andersson et al., 2018; Figueroa et al., 2021). Phytoplankton blooms and are increasing in the southern Baltic, leading to greater eutrophication (Meier et al., 2019). How and where these shifts will affect the distribution of BAs and other HNPs is uncertain, given that macroalgae, phytoplankton and bacteria are all producers. Changes that can be expected over this century have been modeled for a region of the Baltic that encompasses the upper Bothnian Sea, the Quark, and lower Bothnian Bay; i.e. Regions C and D in Figure 1 (Turkia et al., 2022). Increases are predicted for annual filamentous algae and the perennial macroalgae *Fucus* spp. and *Furcellaria lumbricalis*. Greater production of heterotrophic bacteria and decreased phytoplankton in the northern Baltic (Andersson et al., 2015; Figueroa et al., 2016; Andersson et al., 2018; Figueroa et al., 2021) operate to augment and diminish BAs, respectively, and the net effect of these opposing processes is unknown. Increased precipitation and terrestrial runoff is likely to bring more DAME into the estuaries, but other climate impacts on DAME production have yet to be determined

BAs, BPs and other HNPs bioaccumulate in Baltic amphipods and fish and show seasonal variations in concentration (Dahlgren et al., 2016), and it is likely that DAME would behave similarly (Renaguli et al., 2020). HMBs might be useful indicators of land-sea interactions, as well as to follow migration of fish between estuaries and offshore.

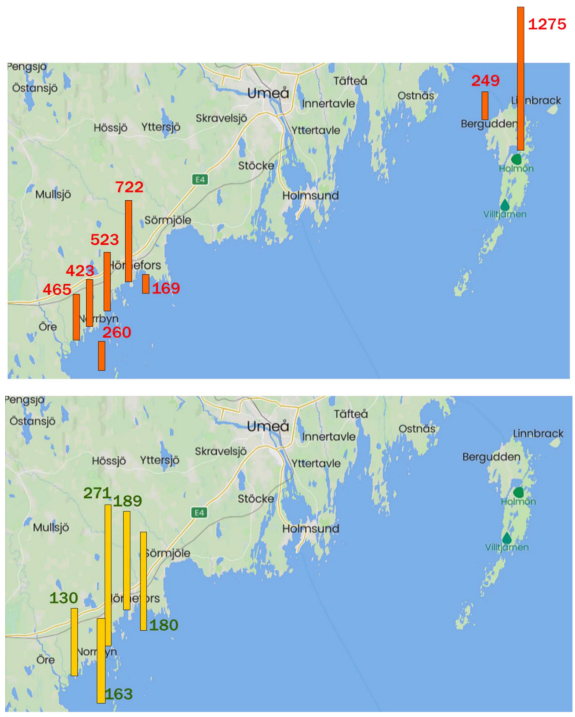

FIGURE 5
Top: ΣBAs (pg L^{-1}) in KAL, ÄNG, VVK and SVK estuaries and in HOLSÖR compared to offshore stations HÖRN, ÖREFJ and HOLBER. Bottom: DAME (pg L^{-1}) in KAL, ÄNG and VVK estuaries compared to offshore stations HÖRN and ÖREFJ. DAME was not measured at Holmön stations. Data from Tables 3 and S4. Station identifications are shown in Figure S1.

Data availability statement

The original contributions presented in the study are included in the article/Supplementary Material. Further inquiries can be directed to the corresponding author.

Author contributions

TB, AA, SB and MT contributed to conception and design of the study. Sample collection was done by TB, KA, SB, LE, KH and ON. Chemical analyses were done by TB, SB and KH. MT provided funding and materials support. TB wrote the first draft of the manuscript. All authors contributed to the article and approved the submitted version.

Acknowledgments

This project was supported by funds from the Swedish marine strategic research environment EcoChange (the Swedish Research Council Formas). We thank the staff at the Umeå Marine Sciences Center for assistance in sampling and chemical analyses, Linda Zetterholm (UmU Chemistry) for assistance with river sampling, and Swedish Meteorological and Hydrological Institute (SMHI) for river flow data (Figure 1).

Conflict of interest

The authors declare that the research was conducted in the absence of any commercial or financial relationships that could be construed as a potential conflict of interest.

Publisher's note

All claims expressed in this article are solely those of the authors and do not necessarily represent those of their affiliated organizations, or those of the publisher, the editors and the reviewers. Any product that may be evaluated in this article, or claim that may be made by its manufacturer, is not guaranteed or endorsed by the publisher.

Supplementary material

The Supplementary Material for this article can be found online at: https://www.frontiersin.org/articles/10.3389/fmars.2023.1161065/full#supplementary-material

References

Agarwal, V., El Gamal, A. A., Yamanaka, K., Poth, D., Kersten, R. D., Schorn, M., et al. (2014). Biosynthesis of polybrominated aromatic organic compounds by marine bacteria. *Nat. Chem. Biol.* 10, 640–647. doi: 10.1038/nchembio.1564

Alañón, M. E., Alarcón, M., Díaz-Maroto, I. J., Pérez-Coello, M. S., and Díaz-Maroto, M. C. (2020). Corky off-flavor compounds in cork planks at different storage times before processing. influence on the quality of the final stopper. *J. Sci. Food. Agric.* 101, 4735–4742. doi: 10.1002/jsfa.11119

Allard, A.-S., Remberger, M., and Nielson, A. (1987). Bacterial O-methylation of halogen-substituted phenols. *Appl. Environ. Microbiol.* 53, 839–845. doi: 10.1128/aem.53.4.839-845.1987

Andersson, A., Brugel, S., Paczkowska, J., Rowe, O. F., Figueroa, D., Kratzer, S., et al. (2018). Influence of allochthonous dissolved organic matter on pelagic basal production in a northerly estuary. *Estuar. Coast. Shelf Sci.* 204, 225–235. doi: 10.1016/j.ecss.2018.02.032

Andersson, A., Meier, H. E. M., Ripszam, M., Rowe, O., Wikner, J., Haglund, P., et al. (2015). Projected future climate change and Baltic Sea ecosystem management. *Ambio* 44 (suppl. 3), 345–356. doi: 10.1007/s13280-015-0654-8

Atlas, E., Sullivan, K., and Giam, C. S. (1986). Widespread occurrence of polyhalogenated aromatic ethers in the marine atmosphere. *Atmos. Environ.* 20, 1217–1220. doi: 10.1016/0004-6981(86)90156-3

Bidleman, T. F., Agosta, K., Andersson, A., Brorström-Lundén, E., Haglund, P., Hansson, K., et al. (2015). Atmospheric pathways of chlorinated pesticides and natural bromoanisoles in the northern Baltic Sea and its catchment. *Ambio* 44 (suppl. 3), 472–483. doi: 10.1007/s13280-015-0666-4

Bidleman, T. F., Agosta, K., Andersson, A., Haglund, P., Hegmans, A., Liljelind, P., et al. (2016). Sea-Air exchange of bromoanisoles and methoxylated bromodiphenyl ethers in the northern Baltic. *Mar. Pollut. Bull.* 112, 58–64. doi: 10.1016/j.marpolbul.2016.08.042

Bidleman, T. F., Andersson, A., Brorström-Lundén, E., Brugel, S., Ericson, L., Hansson, K., et al. (2023). Halomethoxybenzenes in air of the Nordic region. *Environ. Sci. Ecotechnol* 13, 100209. doi: 10.1016/j.ese.2022.100209

Bidleman, T. F., Andersson, A., Brugel, S., Ericson, L., Haglund, P., Kupryianchyk, D., et al. (2019). Bromoanisoles and methoxylated bromodiphenyl ethers in macroalgae from Nordic coastal regions. *Environ. Sci. Proc. Impacts* 21, 881–892. doi: 10.1039/C9EM00042A

Bidleman, T. F., Andersson, A., Haglund, P., and Tysklind, M. (2020). Will climate change influence production and environmental pathways of halogenated natural products? *Environ. Sci. Technol.* 54, 6468–6485. doi: 10.1021/acs.est.9b07709

Bidleman, T. F., Brorström-Lundén, E., Hansson, K., Laudon, H., Nygren, O., and Tysklind, M. (2017a). Atmospheric transport and deposition of bromoanisoles along a temperate to Arctic gradient. *Environ. Sci. Technol.* 51, 10974–10982. doi: 10.1021/acs.est.7b03218

Bidleman, T. F., Laudon, H., Nygren, O., Svanberg, S., and Tysklind, M. (2017b). Chlorinated pesticides and natural brominated anisoles in air at three northern Baltic stations. *Environ. Pollut.* 225, 381–389.

Bohlin-Nizzetto, P., Aas, W., Halvorsen, H. L., Nikiforov, V., and Pfaffhuber, K. A. (2021). "Monitoring of environmental contaminants in air and precipitation," in *Annual report 2020. (NILU report 12/2021; Norwegian environment agency m-2060| 2021)* (Kjeller: Norwegian Institute for Air Research (NILU), 148, ISBN: . ISSN: 2464-3327.

Brownlee, B. G., Macinnis, G. A., and Noton, L. R. (1993). Chlorinated anisoles and veratroles in a Canadian river receiving bleached kraft pulp mill effluent. identification, distribution, and olfactory evaluation. *Environ. Sci. Technol.* 27, 2450–2455. doi: 10.1021/es00048a021

Busch, J., Agarwal, V., Schorn, M., Machado, H., Moore, B. S., Rouse, G. W., et al. (2019). Diversity and distribution of the bmp gene cluster and its polybrominated products in the genus *Pseudoalteromonas*. *Environ. Microbiol.* 21, 1575–1585. doi: 10.1111/1462-2920.14532

Chatonnet, P., Bonnet, S., Boutou, S., and Labadie, M. D. (2004). Identification and responsibility of 2,4,6,-tribromoanisole in musty, corked odors in wine. *J. Agric. Food Chem.* 52, 1255–1262. doi: 10.1021/jf030632f

Chung, H. Y., Ma, W. C. J., and Kim, J.-S. (2003). Seasonal distribution of bromophenols in selected Hong Kong seafood. *J. Agric. Food Chem.* 51, 6752–6760. doi: 10.1021/jf034632r

Dahlgren, E., Enhus, C., Lindqvist, D., Eklund, B., and Asplund, L. (2015). Induced production of brominated aromatic compounds in the alga *Ceramium tenuicorne*. *Environ. Sci. Pollut. Res.* 22, 18107–18114. doi: 10.1007/s11356-015-4907-7

Dahlgren, E., Lindqvist, D., Dahlgren, H., Asplund, L., and Lehtilä, K. (2016). Trophic transfer of naturally produced brominated aromatic compounds in a Baltic Sea food chain. *Chemosphere* 144, 1597–1604. doi: 10.1016/j.chemosphere.2015.10.024

DeJong, E., and Field, J. A. (1997). Sulfur tuft and turkey tail: biosynthesis and biodegradation of organohalogens by basidiomycetes. *Ann. Rev. Microbiol.* 51, 375–414. doi: 10.1146/annurev.micro.51.1.375

Diaz, A., Fabrellas, C., Ventura, F., and Galceran, M. T. (2005). Determination of the odor threshold concentrations of chlorobrominated anisoles in water. *J. Agric. Food Chem.* 53, 383–387. doi: 10.1021/jf049582k

Dickschat, J. S. (2017). Fungal volatiles – a survey from edible mushrooms to moulds. *Nat. Prod. Rep.* 34, 310–328. doi: 10.1039/C7NP00003K

Eriksson, K. I. A., Thelaus, J., Andersson, A., and Ahlinder, J. (2022). Microbial interactions - underexplored links between public health relevant bacteria and protozoa in coastal environments. *Front. Microbiol.* 13, 877483. doi: 10.3389/fmicb.2022.877483

Figueroa, D., Eric Capo, E., Lindh, M. V., Rowe, O. F., Paczkowska, J., Pinhassi, J., et al. (2021). Terrestrial dissolved organic matter inflow drives temporal dynamics of the bacterial community of a subarctic estuary (northern Baltic Sea). *Environ. Microbiol.* 23, 4200–4213. doi: 10.1111/1462-2920.15597

Figueroa, D., Rowe, O. F., Paczkowska, J., Legrand, C., and Andersson, A. (2016). Allochthonous carbon - a major driver of bacterioplankton production in the subarctic northern Baltic Sea. *Microb. Ecol.* 71, 789–801. doi: 10.1007/s00248-015-0714-4

Francezon, N., Tremblay, A., Mouget, J.-L., Pasetto, P., and Beaulieu, L. (2021). Algae as a source of natural flavors in innovative foods. *J. Agric. Food Chem.* 69, 11753–11772. doi: 10.1021/acs.jafc.1c04409

Führer, U., and Ballschmiter, K. (1998). Bromochloromethoxybenzenes in the marine troposphere of the Atlantic ocean: a group of organohalogens with mixed biogenic and anthropogenic origin. *Environ. Sci. Technol.* 32, 2208–2215. doi: 10.1021/es970922a

Garvie, L. A. J., Wilkins, B., Groy, P. L., and Glaeser, J. A. (2015). Substantial production of drosophilin a methyl ether (tetrachloro-1,4-dimethoxybenzene) by the lignicolous basidiomycete *Phellinus badius* in the heartwood of mesquite *(Prosopis juliflora)* trees. *Sci. Nat.* 102, 18. doi: 10.1007/s00114-015-1268-5

Gong, P., Xu, H., Wang, C., Chen, Y., Guo, L., and Wang, X. (2021). Persistent organic pollutant cycling in forests. *Nat. Rev. Earth Environ.* 2, 182–197. doi: 10.1038/s43017-020-00137-5

Guo, J., Brugel, S., Andersson, A., and Lau, D. C. P. (2022). Spatiotemporal carbon, nitrogen and phosphorus stoichiometry in planktonic food web in a northern coastal area. *Estuar. Coast. Shelf Sci.* 272, 107903. doi: 10.1016/j.ecss.2022.107903

Hiebl, J., Lehnert, K., and Vetter, W. (2011). Identification of a fungi-derived terrestrial halogenated natural product in wild boar *(Sus scrofa)*. *J. Agric. Food Chem.* 59, 6188–6192. doi: 10.1021/jf201128r

Hoff, R. M., Brice, K. A., and Halsall, C. J. (1998). Nonlinearity in the slopes of clausius-clapeyron plots for SVOCs. *Environ. Sci. Technol.* 32, 1793–1798. doi: 10.1021/es9709740

Howe, P. D., Dobson, S., and Malcolm, H. M. (2005). "2,4,6-tribromophenol and other simple bromophenols," in *Concise international chemical assessment document 6* (Geneva: World Health Organisation), 47, ISBN: .

Jones, B., Smullen, R., and Carton, A. G. (2016). Flavour enhancement of freshwater farmed barramundi *(Lates calcarifer)*, through dietary enrichment with cultivated sea lettuce, *Ulva ohnoi*. *Aquaculture* 454, 192–198. doi: 10.1016/j.aquaculture.2015.12.017

Kavanaugh, F., Hervey, A., and Robbins, W. J. (1952). Antibiotic substances from basidiomycetes IX. *Drosophila subatrata* (batsch ex fr.) quel. *Proc. Nat. Acad. Sci. (US)* 38, 555–560. doi: 10.1073/pnas.38.7.555

Koch, C., and Sures, B. (2018). Environmental concentrations and toxicology of 2,4,6-tribromophenol (TBP). *Environ. Pollut.* 233, 706–713. doi: 10.1016/j.envpol.2017.10.127

Kupryianchyk, D., Giesler, R., Bidleman, T., Liljelind, P., Lau, D. C. P., Sponseller, R., et al. (2018). Industrial and natural compounds in filter-feeding black fly larvae and water in three tundra streams. *Environ. Toxicol. Chem.* 37, 3011–3017. doi: 10.1002/etc.4267

Kylin, H., Svensson, T., Jensen, S., Strachan, W. M. J., Franich, R., and Bouwman, H. (2017). The trans-continental distributions of pentachlorophenol and pentachloroanisole in pine needles indicate separate origins. *Environ. Pollut.* 229, 688–695. doi: 10.1016/j.envpol.2017.07.010

Lindqvist, D., Dahlgren, E., and Asplund, L. (2017). Biosynthesis of hydroxylated polybrominated diphenyl ethers and the correlation with photosynthetic pigments in the red alga *Ceramium tenuicorne*. *Phytochem.* 133, 51–58. doi: 10.1016/j.phytochem.2016.10.009

Löfstrand, K., Malmvärn, A., Haglund, P., Bignert, A., Bergman, Å., and Asplund, L. (2010). Brominated phenols, anisoles, and dioxins present in blue mussels from the Swedish coastline. *Environ. Sci. Pollut. Res.* 17, 1460–1468. doi: 10.1007/s11356-010-0331-1

McLachlan, M. S., and Horstmann, M. (1998). Forests as filters of airborne organic pollutants, a model. *Environ. Sci. Technol.* 32, 413–420. doi: 10.1021/es970592u

Meier, H. E. M., Dieterich, C., Eilola, K., Gröger, M., Höglund, A., Radtke, H., et al. (2019). Future projections of record-breaking sea surface temperature and cyanobacteria bloom events in the Baltic Sea. *Ambio* 48, 1362–1376. doi: 10.1007/s13280-019-01235-5

Milliken, C. E., Meier, G. P., Watts, J. E. M., Sowers, K. E., and May, H. D. (2004). Microbial anaerobic demethylation and dechlorination of chlorinated hydroquinone metabolites synthesized by basidiomycete fungi. *Appl. Environ. Microbiol.* 70, 385–392. doi: 10.1128/AEM.70.1.385-392.2004

Montelius, M., Svensson, T., Lourino-Cabana, B., Thiry, Y., and Bastviken, D. (2019). Radiotracer evidence that the rhizosphere is a hot-spot for chlorination of soil organic matter. *Plant-Soil* 443, 245–257. doi: 10.1007/s11104-019-04180-0

Neilson, A. H., Allard, A.-S., Hynning, P.Å., Remberger, M., and Landner, L. (1983). Bacterial methylation of chlorinated phenols and guaiacols: formation of veratroles from guaiacols and high molecular weight chlorinated lignin. *Appl. Environ. Microbiol.* 45, 774–783. doi: 10.1128/aem.45.3.774-783.1983

Neilson, A. H., Allard, A. -S., Reiland, S., Remberger, R., Tärnholm, A., Viktor, T., et al. (1984). Tri- and tetrachloroveratrole, metabolites produced by bacterial O-methylation of tri- and tetrachloroguaiacol: an assessment of their bioconcentration potential and their effects on fish reproduction. *Can. J. Fish. Aquat. Sci.* 41, 1502–1512.

Neilson, A. H., Lindgren, C., Hynning, P-Å., and Remberger, M. (1988). Methylation of halogenated phenols and thiophenols by cell extracts of gram-positive and gram-negative bacteria. *Appl. Environ. Microbiol.* 53, 524–530. doi: 10.1128/aem.54.2.524-530.1988

Newton, S., Bidleman, T. F., Bergknut, M., Racine, J., Laudon, H., Giesler, R., et al. (2014). Atmospheric deposition of persistent organic pollutants and chemicals of emerging concern at two sites in northern Sweden. *Environ. Sci. Proc. Impacts* 16, 298–305. doi: 10.1039/c3em00590a

Öberg, G., and Bastviken, D. (2012). Transformation of chloride to organic chlorine interrestrial environments: variability, extent, and implications. *Crit. Rev. Environ. Sci. Technol.* 42, 2526–2545. doi: 10.1080/10643389.2011.592753

Renaguli, A., Fernando, S., Hopke, P. K., Holsen, T. M., and Crimmins, B. S. (2020). Nontargeted screening of halogenated organic compounds in fish fillet tissues from the great lakes. *Environ. Sci. Technol.* 54, 15035–15045. doi: 10.1021/acs.est.0c05078

Ripszam, M., Paczkowska, J., Figueira, J., Veenaas, C., and Haglund, P. (2015). Dissolved organic carbon quality and sorption of organic pollutants in the Baltic Sea in light of future climate change. *Environ. Sci. Technol.* 49, 1445–1452. doi: 10.1021/es504437s

Schreitmüller, J., and Ballschmiter, K. (1994). The equilibrium distribution of semivolatile organochlorine compounds between atmosphere and surface water in the Atlantic ocean. *Angew. Chem. Int. Eng. Ed.* 33, 646–649. doi: 10.1002/anie.199406461

Schreitmüller, J., and Ballschmiter, K. (1995). Air-water equilibrium of hexachlorocyclohexanes and chloromethoxybenzenes in the north and south Atlantic. *Environ. Sci. Technol.* 29, 207–215. doi: 10.1021/es00001a027

Su, Y., Hung, H., Blanchard, P., Patton, G. W., Kallenborn, R., Konoplev, A., et al. (2008). A circumpolar perspective of atmospheric organochlorine pesticides (OCPs): results from six Arctic monitoring stations in 2000–2003. *Atmos. Environ.* 42, 4682–4698. doi: 10.1016/j.atmosenv.2008.01.054

Su, Y., Wania, F., Harner, T., and Lei, Y. D. (2007). Deposition of polybrominated diphenyl ethers, polychlorinated biphenyls, and polycyclic aromatic hydrocarbons to a boreal deciduous forest. *Environ. Sci. Technol.* 41, 534–540. doi: 10.1021/es0622047

Svensson, T., Kylin, H., Montelius, M., Sandén, P., and Bastviken, D. (2021). Chlorine cycling and the fate of cl in terrestrial environments. *Environ. Sci. Pollut. Res.* 28, 7691–7709. doi: 10.1007/s11356-020-12144-6

Svensson, T., Redon, P.-O., Thiry, Y., Montelius, M., and Bastviken, D. (2022). Chlorination of soil organic matter: the role of humus type and land use. *Sci. Total Environ.* 806, 150478. doi: 10.1016/j.scitotenv.2021.150478

Swedish Meteorological and Hydrological Institute (SMHI) (2022) *Vattenwebb*. Available at: https://www.smhi.se/data/hydrologi/vattenwebb.

Teunissen, P. J. M., Swarts, H. J., and Field, J. A. (1997). The *de novo* production of drosophilin a (tetrachloro-4-methoxyphenol) and drosophilin a methyl ether (tetrachloro-1,4-dimethoxybenzene) by ligninolytic basidiomycetes. *Appl. Microbiol. Biotechnol.* 47, 695–700. doi: 10.1007/s002530050997

Turkia, T., Anderssén, E., Lakso, E., Saarinen, A., Berglund, J., Nygård, L., et al. (2022). "What will the sea look like in 2120?," in *Future climate and species distribution models for the central gulf of bothnia* (European Union: ECOnnect Project final report, Interreg Botnia-Atlantica), 65.

Vetter, W., Hasse-Aschoff, P., Rosenfelder, N., Komarova, T., and Mueller, J. F. (2009). Determination of halogenated natural products in passive samplers deployed along the great barrier reef, Queensland/Australia. *Environ. Sci. Technol.* 43, 6131–6137. doi: 10.1021/es900928m

Vetter, W., Kaserzon, S., Gallen, C., Knolla, S., Gallen, M., Hauler, C., et al. (2018). Occurrence and concentrations of halogenated natural products derived from seven years of passive water sampling, (2007–2013) at normanby island, great barrier reef, Australia. *Mar. Pollut. Bull.* 137, 81–90. doi: 10.1016/j.marpolbul.2018.09.032

Wania, F., Haugen, J.-E., Lei, Y. D., and Mackay, D. (1998). Temperature dependence of atmospheric concentrations of semivolatile organic compounds. *Environ. Sci. Technol.* 32, 1013–1021. doi: 10.1021/es970856c

Whitfield, F. B., Hill, J. L., and Shaw, K. J. (1997). 2,4,6-tribromoanisole: a potential cause of mustiness in packaged food. *J. Agric. Food Chem.* 45, 889–893. doi: 10.1021/jf960587u

Wittlinger, R., and Ballschmiter, K. (1990). Studies of the global baseline pollution XIII. C6-C14 organohalogens (α-and γ-HCH, HCB, PCB, 4,4'-DDT, 4,4'-DDE, cis- and trans-chlordane, trans-nonachlor, anisols) in the lower troposphere of the southern Indian ocean. *Fres. J. Anal. Chem.* 336, 193–200. doi: 10.1007/BF00332252

Wong, F., Hung, H., Dryfhout-Clark, H., Aas, W., Bohlin-Nizzetto, P., Breivik, K., et al. (2021). Time trends of persistent organic pollutants (POPs) and chemicals of emerging Arctic concern (CEAC) in Arctic air from 25 years of monitoring. *Sci. Total Environ.* 775, 145109. doi: 10.1016/j.scitotenv.2021.145109

Wong, F., Jantunen, L. M., Pućko, M., Papakyriakou, T., Stern, G. A., and Bidleman, T. F. (2011). Air-water exchange of anthropogenic and natural organohalogens on international polar year (IPY) expeditions in the Canadian Arctic. *Environ. Sci. Technol.* 45, 876–881. doi: 10.1021/es1018509

Zhang, K., Zhang, L., Zhang, T., Mao, M., and Fu, J. (2016). Study on formation of 2,4,6-trichloroanisole by microbial O-methylation of 2,4,6-trichlorophenol in lake water. *Environ. Pollut.* 219, 228–234. doi: 10.1016/j.envpol.2016.10.042

Zhou, X., Zhang, K., Zhang, T., Cen, C., and Pa, R. (2021). Biotransformation of halophenols into earthy-musty haloanisoles: investigation of dominant bacterial contributors in drinking water distribution systems. *J. Haz. Mater.* 403, 123693. doi: 10.1016/j.jhazmat.2020.123693

frontiers | Frontiers in Marine Science

TYPE Original Research
PUBLISHED 03 July 2023
DOI 10.3389/fmars.2023.1175176

OPEN ACCESS

EDITED BY
Anke Kremp,
Leibniz Institute for Baltic Sea Research (LG), Germany

REVIEWED BY
Mikko Olin,
Natural Resources Institute Finland (Luke), Finland
Xian Sun,
Sun Yat-sen University, China

*CORRESPONDENCE
Petter Tibblin
petter.tibblin@lnu.se

RECEIVED 27 February 2023
ACCEPTED 13 June 2023
PUBLISHED 03 July 2023

CITATION
Hall M, Nordahl O, Forsman A and Tibblin P (2023) Maternal size in perch (*Perca fluviatilis*) influences the capacity of offspring to cope with different temperatures.
Front. Mar. Sci. 10:1175176.
doi: 10.3389/fmars.2023.1175176

Maternal size in perch (*Perca fluviatilis*) influences the capacity of offspring to cope with different temperatures

Marcus Hall, Oscar Nordahl, Anders Forsman and Petter Tibblin*

Department of Biology and Environmental Science, Ecology and Evolution in Microbial Model Systems (EEMiS), Linnaeus University, Kalmar, Sweden

Climate change causes earlier and warmer springs in seasonal environments and a higher incidence of extreme weather events. In aquatic environments, this changes the thermal conditions during spawning, and the thermal performance of eggs and embryos may determine the consequences of climate change on recruitment. In iteroparous species with indeterminate growth, the eggs produced by a given female in successive years will increase in size as the female grows larger and likely be exposed to different temperatures during incubation due to annual variation in spring phenology. Still, we know little about whether differences in maternal size impact the temperature-dependent performance and viability of the offspring. Here we utilised a thermal gradient laboratory experiment on Baltic Sea perch (*Perca fluviatilis*) to investigate how maternal size influence the temperature dependent hatching success of the offspring. The results uncovered a positive relationship between maternal size and average hatching success, but the shape of the relationship (reaction norm) linking hatching success to incubation temperature was independent of maternal size. However, we did find an association between maternal size and the variance (S.D. and CV) in hatching success across temperatures, with larger females producing offspring with maintained performance (less sensitive) across temperature treatments, indicative of flatter reaction norms and broader thermal niches. This suggests that maintaining the size distribution of fish populations, for instance through regulations of size-selective fisheries, may be important to aid the long-term productivity and viability of fish populations and ultimately conserve the function and services of ecosystems.

KEYWORDS

Baltic Sea, climate change, hatching, fish, global warming, reproduction, spawning, thermal tolerance

1 Introduction

Global warming is impacting the thermal conditions that organisms experience during key life-history events, such as reproduction and embryo development, which may ultimately influence the dynamics and viability of populations and species (Dahlke et al., 2020). In high latitude biomes, global warming is already causing altered seasonality, increased annual mean temperatures and a higher incidence of extreme weather events that generate more variable and unpredictable thermal conditions among and within years. These effects are also predicted to increase in severity over the next decades (Tamarin-Brodsky et al., 2020). The capacity to tolerate high, variable, and unpredictable thermal conditions during life-history events, such as reproduction, is thus assumed critical for organisms to cope with climate change (Dahlke et al., 2020; Morgan et al., 2020). Previous research has highlighted that this may be mediated both through adaptive evolution of, and phenotypic plasticity in, thermal performance of eggs and embryos (Salinas and Munch, 2012; Seebacher et al., 2015; Chen et al., 2018). This is supported by a firm body of evidence based on comparisons of thermal performance and tolerance among species and populations inhabiting, and exposed to, different thermal regimes (Comte and Olden, 2017; Sunde et al., 2019; Carbonell et al., 2021). Compared with the existing work and understanding of the mechanistic underpinnings of variation among populations and species, much less is known regarding the sources of variation in thermal performance (tolerance) among individuals within populations. For example, a better knowledge of the sources of variation in the thermal performance and tolerance of offspring within and between different families, including the relative contribution of genes, developmental plasticity and maternal effects, is key for understanding evolutionary modifications of thermal tolerance and to generate predictive models on the consequences of global warming for biodiversity and the function and services of ecosystems (Salinas and Munch, 2012; Wennersten and Forsman, 2012; Forsman, 2015; Hall et al., 2021).

Maternal size affects the allocation of resources for reproduction and the distribution of those resources among offspring in most vertebrates (Roff, 1992; Marshall et al., 2018). For example, in fish, larger females tend to produce more and larger eggs with higher nutrient content (Barneche et al., 2018), which can lead to increased offspring size and survival (Heath et al., 1999; Kamler, 2005; Hixon et al., 2014). It is also known that oxygen consumption and metabolic rates often increases with increasing egg size. These are physiological factors that can influence susceptibility to thermal stress, especially in aquatic environments where oxygen solubility decreases with increasing temperature (Martin et al., 2017). From a mechanistic perspective, it has been proposed that because smaller eggs have a higher surface to volume ratio the oxygen demand of the developing embryos can more easily be met (via diffusion) in small than in large eggs, such that smaller eggs should be favorable in low oxygen (i.e. warm) environments (van den Berghe and Gross, 1989; Robertson and Collin, 2015). Still, there are also examples to the opposite effect where larger eggs perform better in low oxygen environments (Einum et al., 2002; Hendry and Day, 2003). Together, this means that there is potential for maternal size to also impact offspring performance in different temperatures, due to size-dependent changes in egg size, although evidence for this effect is limited (Martin et al., 2020; Olin et al., 2022).

Important knowledge on how and why species, populations, and individuals may respond differently to changes in temperature can be achieved by studying their performance under various thermal conditions (i.e., reaction norms or performance curves) (Via et al., 1995; Hall et al., 2021). Flat (shallow) reaction norms would suggest tolerance to environmental fluctuations (*i.e.*, maintained performance), while narrow curvilinear responses are instead indicative of a narrow environmental range for optimal performance, and directional reaction norms suggest that optimal performance peaks at one end of the environmental spectrum. Directional and/or narrow curvilinear recreation norms may increase vulnerability to temperature variation because they reduce the ability to adjust to changing temperatures without incurring fitness costs (Hall et al., 2021). However, not only the shapes of reaction norms are informative concerning the response of genotypes to different environments but also the sensitivity in performance since it may influence population dynamics (e.g. to what degree the number of recruits may be impacted in different environments).

This study aimed to determine whether and how maternal size affects offspring quality and the offspring's ability to perform in different thermal conditions by examining the size-dependent hatching success of anadromous Baltic Sea perch (*Perca fluviatilis*) using a split-brood laboratory temperature gradient experiment. Perch is an iteroparous total spawner with females depositing their eggs in a single egg strand at a specific location and at a single time point (Craig, 2000). The incubation of eggs until hatching is subjected to variable thermal conditions depending on the timing of egg deposition and the prevailing spring phenology (Tibblin et al., 2012; Hall et al., 2021) such that maintained offspring performance in different temperatures may be key for individual reproductive success. For this study, we collected eggs from 69 newly deposited egg strands (the total weight of which served as a proxy for maternal size similar to Lang, 1987) in the field and conducted an experiment in which eggs from the focal females were incubated in the laboratory at four different temperatures (10, 12, 15, and 18 °C). The experiment was designed to answer the following questions: (1) Does maternal size influence the overall hatching success?; (2) Does the shape of reaction norms and/or the sensitivity of egg hatching success to temperature vary among families depending on maternal size?; and (3) Could size-dependent maternal effects on thermal sensitivity of offspring performance be accounted for by differences in egg size?

2 Methods

2.1 Field collection of egg strands

In 2019, we conducted a field survey to identify and sample perch egg strands in the lower stretches of Hossmoån river (56°C 37.530'N, 16°C 14.331'E southeast Sweden) which have previously been identified as an important spawning habitat for Baltic Sea

anadromous perch (Tibblin et al., 2012). Perch typically spawns in shallow water and their eggs can be detected from their characteristic egg strands which are highly visible within reasonable sight depth conditions, as is the case for perch in Hossmoån (Tibblin et al., 2012; Hall et al., 2021). The study took place from April 3 to June 24 during which we identified 511 egg strands (unique females spawning) along transects set in the lower stretch of the river. We monitored the transects three days a week using a combination of polarizing glasses and a bathyscope to detect the egg strands. Each detected egg strand was marked with a red cellulose tape in the nearest reed strand, and its location was marked on a map to avoid double sampling of egg strands. During each sampling occasion (day), we sampled 3-6 of the newly detected egg strands (pending availably of egg strands). The egg strands sampled were chosen haphazardly but with the aim to comprise size variation among strands during each sample occasion. In sampling the egg strands, we first gently loosened them from the spawning substrate (typically reed), and then transferred the egg strand as a whole to a water-filled bucket using a fine-meshed net (see Hall et al., 2021 for details) after which it was weighed (gram wet weight). From each of the weighed egg strands, we took a ~10 cm subsample which was placed in a small water-filled (stream water) container (0.8 L) and brought to the to the laboratory facility at the Linnaeus University. At the laboratory, we divided each egg strand sample into four subsamples after which they were randomly distributed to the different temperature-controlled rooms, set at 10, 12, 15 and 18 C°, to be used for the split-brood temperature hatching experiment.

2.2 Hatching experiment in the laboratory

Once the subsamples had been brought into each of the temperature-controlled rooms and allowed to slowly adjust to room temperatures (~1h), we cut out two replicates (replicate weight 1.23 g ± 0.18 S.D.) from each subsample per temperature treatment. We then transferred each replicate to 0.8 L containers, filled with aerated room temperature adjusted tap-water. The container was made of two stacked 0.8 L containers, with the bottom part cut out of the top container and replaced with a 1.5*1.5 mm mesh-net to allow for throughflow during water exchanges (as water flows out from the bottom container). The containers were placed on racks within the temperature-controlled rooms, with an average light intensity of ~60 $\pi E/m^2/S$. The position of each sample and replicate was assigned randomly prior to the start of the experiment, to minimize potential bias stemming from temperature and light differences within the racks. We conducted complete water exchanges regularly (daily in the 15 and 18 C° temperature-controlled room, and about every second day in the 10 and 12 C° rooms), by overflowing the containers with treatment specific temperature adjusted water. This was done to maintain high oxygen concentrations throughout the incubation period and to remove biological byproducts.

To capture the initial number of eggs and number of viable eggs in each replicate, we took a picture of each replicate at the start of the laboratory experiment (Nikon D5600, F/7.1, 1/60 sec, ISO-400, Focal length 50 mm). In a similar fashion, we also captured images of hatched larvae at the end of the experiment (Nikon D5600, F/11, 1/80 sec, ISO-400, Focal length 50 mm). These images provided us with a starting estimate of the number of viable eggs in each replicate, and the final number of hatched larvae (*i.e.* hatching success).

2.2.1 Counting of eggs and larvae and estimating larvae length

We counted the initial number of eggs and the number of viable eggs in each replicate using ImageJs multipoint tool (Schneider et al., 2012), we excluded dead eggs (opaque) from the estimate of viable eggs. We also counted the number of hatched larvae at the end of the experiment, using the same approach. Hatching success was then estimated as the number of hatched larvae/viable eggs.

2.3 Statistics

All statistical analyses were performed in R v. 3.5.2 and Rstudio v. 1.1.46 (Team, R. S, 2016; Team, R. C, 2018).

2.3.1 Maternal size effects on hatching success

To examine whether and how maternal size influenced hatching success, we used a linear mixed model with hatching success set as the response variable, egg strand size as a continuous fixed effect and family was included as a random effect. Here, we included all egg strand samples (n = 67 in the analysis, while later analyses focused on families with an overall hatching success above 5% to examine the influence of maternal size on thermal performance.

2.3.2 Maternal size and its influence on offspring reaction norms and thermal performance

To examine whether and how maternal size influenced the shape of the reaction norm linking hatching success to incubation temperature we first excluded egg strands (families) with a hatching success lower than 5% in all incubation temperatures. These egg strand samples were excluded to avoid estimating reaction norms and variance estimates from samples with 0 - few hatching individuals, which could severely influence the shape of reaction norms and variance estimates without reflecting true differences in thermal performance (*e.g.*, due to differences in infections/virulence among the replicates). Following that, we used a generalized linear mixed model (GLMM) with a binomial error structure to estimate whether and how the thermal reaction norm changed with maternal size. This was analyzed using the glmer function in the lme4-package (Bates et al., 2014). Here, we set hatching success as the response variable, egg strand size (total weight in gram) and incubation temperature as continuous fixed effects with the effect of incubation temperature estimated using a curvilinear function, and with the interaction between these two factors included to examine whether size influenced temperatures effect on hatching success (*i.e.*, the shape of the reaction norm). Family and its interaction with temperature (family-by-temperature interaction) was included as a random effect to account for among family variation in the temperature dependent reaction norms (slopes),

again using a curvilinear function for the effect of temperature. Significance of fixed effects were evaluated with a type II Wald's chi-square test.

To further investigate how maternal size influenced the thermal sensitivity of performance of the offspring, we used variance estimates to investigate the variance in hatching success among the temperature treatments. Here, we first calculated the mean hatching success within each temperature treatment for each family (from the two replicates). These mean values of hatching success in the temperature treatments (10, 12, 15 and 18 °C) were then used to estimate the standard deviation (S.D.) and the coefficient of variance (CV) in hatching success. Thereafter, we examined the relationship between egg strand size and variance estimates (S.D. and CV, respectively) with a linear regression, using the lm function in R.

2.3.3 Egg size and its influence on temperature-dependent hatching success

As egg size influences metabolism and oxygen diffusion, both of which depend on temperature, and commonly increases with maternal size in fish, we wanted to examine whether egg size per se was associated with changes in the thermal performance of the offspring. We first examined if egg size also increased with increasing maternal size (egg strand size) within this population. Egg size was estimated by dividing the weight of each replicate with its initial number of eggs, and then averaged across replicates and treatments to gather a robust estimate of the average egg size for each egg strand. We then assessed the relationship between egg size and the size of the egg strand with a linear regression, again using the lm function in R. Finally, we examined whether and how egg size influenced the thermal sensitivity of offspring performance across the temperature treatments. Here, the variance estimates (S.D. and CV, respectively) were set as response variables and egg size were set as the explanatory variable, and its relationship was analysed with a linear regression, again using the lm function in R.

2.4 Ethical approval

The laboratory was approved as research facility (Dnr 5.2.18–17988/18), and the study was granted ethical approval (approval Dnr 168677-2018) by the Ethical Committee on Animal Experiments in Linköping, Swedish Board of Agriculture, Sweden.

3 Results

3.1 Maternal size and offspring success

Egg strand sizes varied between 31 and 1502 g, showcasing a substantial variation in the size of the reproducing individuals. These maternal size differences were associated with differences in hatching success, with larger egg strands (females) having an overall higher hatching success (χ^2 = 12.08, *d.f.* = 1, p < 0.001, Figure 1).

3.2 Maternal size and its influence on offspring reaction norms and thermal performance

The shape of the reaction norm linking hatching success to incubation temperature did not change with maternal size (egg strand size × incubation temperature interaction; χ^2 = 0.73, *d.f.* = 2, p = 0.69, Figure 1), while temperature and maternal size, respectively, influenced hatching success (egg strand size, χ^2 = 10.39, *d.f.* = 1, p = 0.001; incubation temperature - curvilinear relationship; χ^2 = 7.82, *d.f.* = 2, p = 0.02). However, variance estimates (S.D. and CV) of the temperature dependent hatching success decreased with increasing maternal size (linear regression; S.D., R^2 = 0.079, $F_{1,59}$ = 5.06, p = 0.028; CV, R^2 = 0.118, $F_{1,59}$ = 7.87, p = 0.007; Figure 1), indicating that the performance of offspring produced by larger females was less sensitive to differences in incubation temperature.

3.3 Egg size and its influence on temperature performance

As egg size increased with increasing female size (linear regression; R^2 = 0.19, $F_{1,65}$ = 15.28, p < 0.001; Figure 2), we wanted to examine whether egg size was a driving mechanism behind the variation in thermal performance of offspring according to maternal size. We did this by examining whether egg size was associated with tolerance in temperature performance (S.D. and CV). Here, we found that larger eggs indeed were associated with maintained offspring performance across temperatures (linear regression; S.D., R^2 = 0.09 $F_{1,\ 59}$ = 5.56, p = 0.022; CV, R^2 = 0.10, $F_{1,59}$ = 6.47, p = 0.0136).

4 Discussion

Thermal regimes are shifting due to climate change which result in higher and more unpredictable temperatures during spawning for fish populations in temperate regions (Lema et al., 2019; IPCC, 2022). Simultaneously, the size distribution of many fish populations is impacted by intense fisheries harvest which typically removes large individuals (Uusi-Heikkilä et al., 2016). This emphasizes the need to understand whether and how the size structure within populations and species impacts their thermal dependence of performance and resilience to climate change. In this study we examined how maternal size of perch was related to offspring size (egg size), offspring quality (hatching success), and whether it influenced the thermal performance of offspring across a laboratory temperature gradient. We found that egg size and the overall hatching success increased with increasing maternal size. We also found that the shape (i.e. slope or curvature) of the reaction norm linking hatching success to incubation temperature did not seem to differ significantly depending on maternal size (as indirectly estimated by the weight of the egg strand). However, the variance estimates of the thermal performance (CV/S.D.) decreased

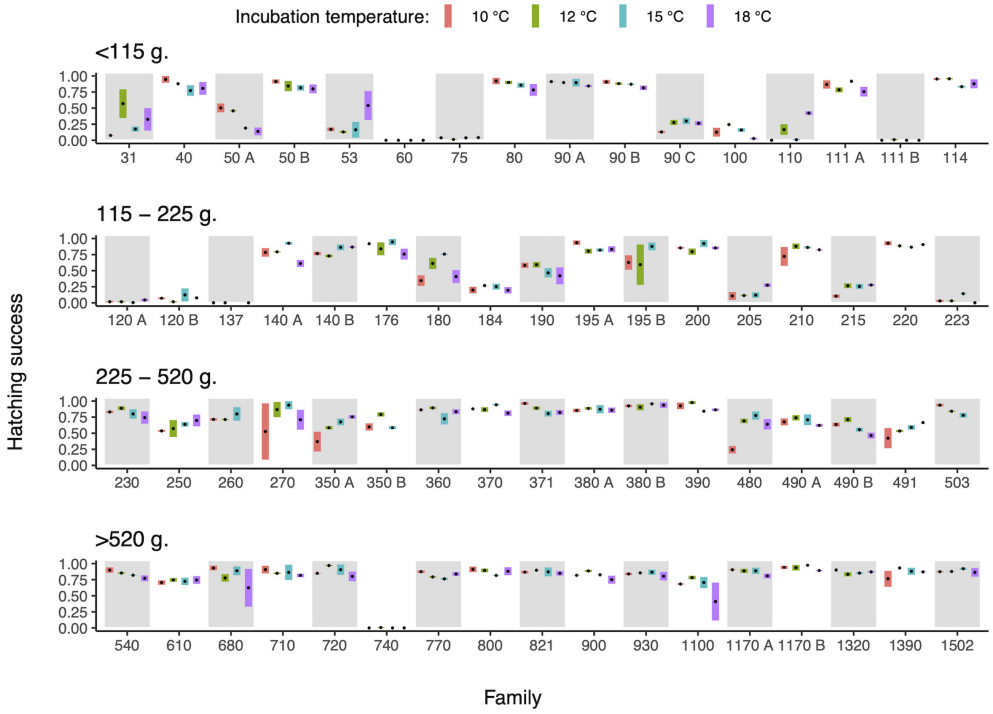

FIGURE 1
Relationship between maternal size (estimated through egg strand weight) and hatching success of the eggs when exposed to different incubation temperatures. The bar within each temperature treatment shows the range between the two replicates, and the black mark is the mean temperature specific hatching success of that family. Families have been ordered based on egg strand weight and split into four panels with different size classes. Families are labelled with their egg strand weight (g) with the addition of letters (A, B) to separate families that shared the same size. Data from temperature treatments are ordered from lowest to highest temperature within each family.

with increasing maternal size, indicating higher tolerance in performance across temperatures in offspring produced by large females. Further analysis indicated that this association between variance in offspring thermal performance and maternal size was mediated by egg size rather than maternal size itself, such that larger eggs had higher tolerance in performance. Although our study does not implicitly investigate whether and how this was related to oxygen conditions, the results support a growing body of evidence that challenge the conventional "bigger is worse during incubation" hypothesis stating that smaller eggs should be favoured in high temperatures due to improved diffusion of oxygen relating to the higher surface to volume ratio (van den Berghe and Gross, 1989; Hendry et al., 2001; Einum et al., 2002; Hendry and Day, 2003; Martin et al., 2017). Together, our findings suggest that maintaining the size structure of fish populations, for instance through fisheries regulations, may be fundamental for the ability to cope with the future climate change (Hidalgo et al., 2011).

Our finding of an increase in egg size with increasing maternal size aligns with numerous previous studies in fish (Berggren et al., 2016; Rollinson and Rowe, 2016), and in perch specifically (Olin et al., 2012), where egg size commonly increases with maternal size. This pattern is also consistent across many other taxa including birds, amphibians and reptiles (see Lim et al., 2014 for a meta-analysis). This points towards a general size dependent shift in the optimal trade-off between fecundity and individual offspring investment, increasing the likelihood that offspring quality also increases with maternal size (Rollinson and Rowe, 2016). Indeed, our results also support this notion as offspring quality, estimated through hatching success, increased with maternal size. This in turn indicates that the size structure within populations could affect the overall recruitment success and ultimately impact population dynamics (Shelton et al., 2006).

Our split-brood hatching experiment across a temperature gradient did not reveal any statistically significant differences in the shape of the reaction norms depending on maternal size. This could perhaps partly be attributed to that smaller females had rather variable reactions norms (positive, negative, and curvilinear) whereas the reaction norms of larger females were predominantly flat (Figure 1) resulting in similar mean reaction norms across size classes. In agreement with this interpretation, the intraindividual variation (CV and S.D.) in hatching success across the temperature gradient decreased with increasing maternal size, indicating that the thermal tolerance of performance of offspring produced by larger individuals was broader. This suggests that the recruitment potential of larger females was less sensitive to thermal variation than that of smaller females (Sinclair et al., 2016). In the light of that climate change is expected to skew the size distributions of many temperate fish species and populations towards smaller individuals (Walters and Hassall, 2006; Estlander et al., 2015; Campana et al., 2020), our result of a positive size-dependent resilience to temperature variation suggests that there may be additive negative effects of climate change on the viability and productivity of

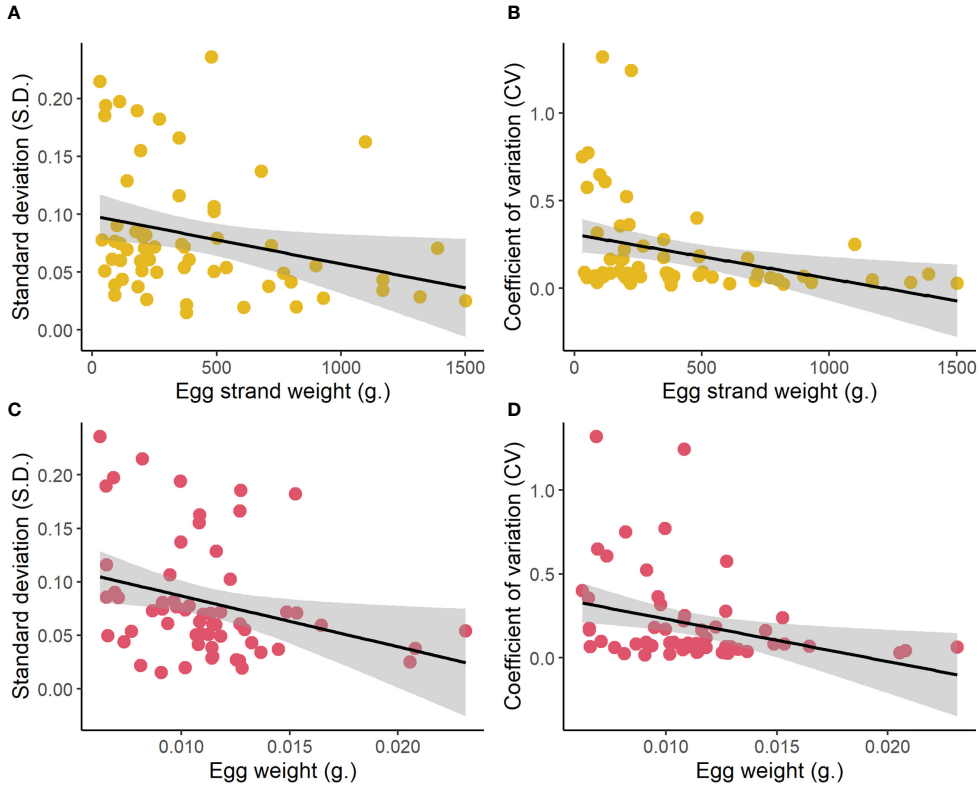

FIGURE 2
The relationship between: maternal size (egg strand weight) **(A, B)** and egg size **(C, D)** with the temperature sensitivity of the offspring estimated as the variance (standard deviation S.D, and coefficient of variance CV) in hatching success across the temperature treatments.

populations. This finding also constitutes an important argument to why it is essential for fisheries management to maintain the size distribution of exploited fish stocks in the context of maintaining their capacity to cope with climate change (Hidalgo et al., 2011; Dahlke et al., 2020).

Based on a rather large body of evidence, we predicted that differences in egg size would offer a mechanistic explanation to putative patterns of size-dependent maternal effects on offspring thermal performance (Parker and Begon, 1986; Hendry et al., 2001; Martin et al., 2017) which was indeed supported by our data. However, our results did not cohere to the notion of smaller eggs performing better in high temperatures (and assumedly lower oxygen concentrations) due to improved oxygen diffusion through a higher surface to volume ratio (van den Berghe and Gross, 1989; Fleming and Gross, 1990), instead larger eggs had both higher and less variable performance across temperatures. A similar pattern of a positive association between egg size and thermal performance have been shown in salmonids (Einum et al., 2002) which was attributed to that the rate of oxygen consumption *does not*, as previously assumed, increase more rapidly with increasing egg size than the rate at which the egg surface area available for oxygen diffusion increases. Unfortunately, our study design does not allow to make any casual inference about the effects of egg size on thermal performance and it is possible that it may be related to other factors correlating with increasing size of the females and the eggs. For instance, the number of spawning events (which is strongly correlated with age and body size) may influence the temperature performance in eggs through epigenetic mechanisms relating to the variation in temperature conditions during spawning experienced by the female (Salinas and Munch, 2012; Tibblin et al., 2016). Another explanation may be that the higher temperature tolerance of offspring produced by larger mothers indicated by our results is accompanied by a higher buffering capacity and temperature tolerance also of other aspects of individual performance, and that broader thermal niches improve survival (Franzen et al., 2022).

Taken together, our results show that larger females, in general, produce larger eggs and eggs with an overall higher quality (increased hatching success). Furthermore, we also found indications of an increased tolerance to different temperature conditions in eggs from larger females, and that these differences may be due to maternally driven differences in egg sizes. At times when many fish populations are challenged by intense size-selective harvest this knowledge emphasize the great value in conserving the natural size distribution to avoid further negative impacts of climate change on the productivity and viability of fish populations.

Data availability statement

The raw data supporting the conclusions of this article will be made available by the authors, without undue reservation.

Ethics statement

The animal study was reviewed and approved by the Ethical Committee on Animal Experiments in Linköping, Swedish Board of Agriculture, Sweden. Dnr 168677-2018.

Author contributions

MH and PT conceived the study. MH, ON, AF and PT designed the study. MH, ON and PT conducted the field and laboratory work. MH analyzed the data with support from PT and AF. All authors contributed to interpretation of results. MH and PT wrote the manuscript, with input from ON and AF. All authors contributed to the revision process and approved the submitted version.

Funding

This work was supported by funds kindly provided by the Swedish Research Council FORMAS (grant 2018-00605 to PT; grant 2017-00346 to AF and PT; and *via* EcoChange grant to PT).

Acknowledgments

We are grateful to Ole Tiesch, Emma Svahn and Christofer Osbeck for excellent field assistance, and Per Koch-Schmidt, Per Larsson and Johanna Sunde for important input on the research questions and advise on the set-up of the laboratory experiment. We thank Mikko Olin and Xian Sun for constructive feedback during the review process. We are grateful to Hossmo FVOF, Ola Sennefjord and Kjell Linyr for granting us access to the study system.

Conflict of interest

The authors declare that the research was conducted in the absence of any commercial or financial relationships that could be construed as a potential conflict of interest.

Publisher's note

References

Barneche, D. R., Robertson, D. R., White, C. R., and Marshall, D. J. (2018). Fish reproductive-energy output increases disproportionately with body size. *Science* 360, 642–645. doi: 10.1126/science.aao6868

Bates, D., Mächler, M., Bolker, B., and Walker, S. (2014). Fitting linear mixed-effects models using lme4. *arXiv* 1–51. doi: 10.18637/jss,v067.i01

Berggren, H., Nordahl, O., Tibblin, P., Larsson, P., and Forsman, A. (2016). Testing for local adaptation to spawning habitat in sympatric subpopulations of pike by reciprocal translocation of embryos. *PloS One* 11, e0154488. doi: 10.1371/journal.pone.0154488

Campana, S. E., Stefánsdóttir, R. B., Jakobsdóttir, K., and Sólmundsson, J. (2020). Shifting fish distributions in warming sub-Arctic oceans. *Sci. Rep.* 10, 16448. doi: 10.1038/s41598-020-73444-y

Carbonell, J. A., Wang, Y.-J., and Stoks, R. (2021). Evolution of cold tolerance and thermal plasticity in life history, behaviour and physiology during a poleward range expansion. *J. Anim. Ecol.* 90, 1666–1677. doi: 10.1111/1365-2656.13482

Chen, Z., Farrell, A. P., Matala, A., and Narum, S. R. (2018). Mechanisms of thermal adaptation and evolutionary potential of conspecific populations to changing environments. *Mol. Ecol.* 27, 659–674. doi: 10.1111/mec.14475

Comte, L., and Olden, J. D. (2017). Evolutionary and environmental determinants of freshwater fish thermal tolerance and plasticity. *Global Change Biol.* 23, 728–736. doi: 10.1111/gcb.13427

Craig, J. F. (2000). *Percid fishes: systematics, ecology and exploitation* (Oxford: Blackwell Science).

Dahlke, F. T., Wohlrab, S., Butzin, M., and Pörtner, H.-O. (2020). Thermal bottlenecks in the life cycle define climate vulnerability of fish. *Science* 369, 65. doi: 10.1126/science.aaz3658

Einum, S., Hendry, A., and Fleming, I. (2002). Egg-size evolution in aquatic environments: does oxygen availability constrain size? *Proc. R. Soc. B: Biol. Sci.* 269, 2325–2330. doi: 10.1098/rspb.2002.2150

Estlander, S., Nurminen, L., Mrkvička, T., Olin, M., Rask, M., and Lehtonen, H. (2015). Sex-dependent responses of perch to changes in water clarity and temperature. *Ecol. Freshw. Fish* 24, 544–552. doi: 10.1111/eff.12167

Fleming, I. A., and Gross, M. R. (1990). Latitudinal clines: a trade-off between egg number and size in pacific salmon. *Ecology* 71, 2–11. doi: 10.2307/1940241

Forsman, A. (2015). Rethinking phenotypic plasticity and its consequences for individuals, populations and species. *Heredity* 115, 276–284. doi: 10.1038/hdy.2014.92

Franzen, M., Francioli, Y., Askling, J., Kindvall, O., Johansson, V., and Forsman, A. (2022). Differences in phenology, daily timing of activity, and associations of temperature utilization with survival in three threatened butterflies. *Sci. Rep.* 12, 7534. doi: 10.1038/s41598-022-10676-0

Hall, M., Nordahl, O., Larsson, P., Forsman, A., and Tibblin, P. (2021). Intra-population variation in reproductive timing co-varies with thermal plasticity of offspring performance in perch (*Perca fluviatilis*). *J. Anim. Ecol.* 90, 2236–2247. doi: 10.1111/1365-2656.13542

Heath, D. D., Fox, C. W., and Heath, J. W. (1999). Maternal effects on offspring size: variation through early development of chinook salmon. *Evolution* 53, 1605–1611. doi: 10.2307/2640906

Hendry, A., and Day, T. (2003). Revisiting the positive correlation between female size and egg size. *Evolutionary Ecol. Res.* 5, 421–429.

Hendry, A. P., Day, T., and Cooper, A. B. (2001). Optimal size and number of propagules: allowance for discrete stages and effects of maternal size on reproductive output and offspring fitness. *Am. Nat.* 157, 387–407. doi: 10.1086/319316

Hidalgo, M., Rouyer, T., Molinero, J. C., Massutí, E., Moranta, J., Guijarro, B., et al. (2011). Synergistic effects of fishing-induced demographic changes and climate variation on fish population dynamics. *Mar. Ecol. Prog. Ser.* 426, 1–12. doi: 10.3354/meps09077

Hixon, M. A., Johnson, D. W., and Sogard, S. M. (2014). BOFFFFs: on the importance of conserving old-growth age structure in fishery populations. *ICES J. Mar. Sci.* 71, 2171–2185. doi: 10.1093/icesjms/fst200

IPCC (2022). *Climate change 2022: impacts, adaptation, and vulnerability* (Cambridge, UK and New York, NY, USA: Cambridge University Press).

Kamler, E. (2005). Parent-egg-progeny relationships in teleost fishes: an energetics perspective. *Rev. Fish Biol. Fisheries* 15, 399. doi: 10.1007/s11160-006-0002-y

Lang, C. (1987). Mortality of perch, *Perca fluviatilis l.*, estimated from the size and abundance of egg strands. *J. Fish Biol.* 31, 715–720. doi: 10.1111/j.1095-8649.1987.tb05274.x

Lema, S. C., Bock, S. L., Malley, M. M., and Elkins, E. A. (2019). Warming waters beget smaller fish: evidence for reduced size and altered morphology in a desert fish following anthropogenic temperature change. *Biol. Lett.* 15, 20190518. doi: 10.1098/rsbl.2019.0518

Lim, J. N., Senior, A. M., and Nakagawa, S. (2014). Heterogeneity in individual quality and reproductive trade-offs within species. *Evolution* 68, 2306–2318. doi: 10.1111/evo.12446

Marshall, D. J., Pettersen, A. K., and Cameron, H. (2018). A global synthesis of offspring size variation, its eco-evolutionary causes and consequences. *Funct. Ecol.* 32, 1436–1446. doi: 10.1111/1365-2435.13099

Martin, B. T., Dudley, P. N., Kashef, N. S., Stafford, D. M., Reeder, W. J., Tonina, D., et al. (2020). The biophysical basis of thermal tolerance in fish eggs. *Proc. R. Soc. B: Biol. Sci.* 287, 20201550. doi: 10.1098/rspb.2020.1550

Martin, B. T., Pike, A., John, S. N., Hamda, N., Roberts, J., Lindley, S. T., et al. (2017). Phenomenological vs. biophysical models of thermal stress in aquatic eggs. *Ecol. Lett.* 20, 50–59. doi: 10.1111/ele.12705

Morgan, R., Finnøen, M. H., Jensen, H., Pélabon, C., and Jutfelt, F. (2020). Low potential for evolutionary rescue from climate change in a tropical fish. *Proc. Natl. Acad. Sci.* 117, 33365–33372. doi: 10.1073/pnas.2011419117

Olin, M., Jutila, J., Lehtonen, H., Vinni, M., Ruuhijärvi, J., Estlander, S., et al. (2012). Importance of maternal size on the reproductive success of perch, *Perca fluviatilis*, in small forest lakes: implications for fisheries management. *Fisheries Manage. Ecol.* 19, 363–374. doi: 10.1111/j.1365-2400.2012.00845.x

Olin, M., Kotakorpi, M., Nurminen, L., and Ruuhijärvi, J. (2022). The maternal effects on pikeperch (*Sander lucioperca*) larvae depend on temperature. *Ecol. Freshw. Fish* 31, 280–290. doi: 10.1111/eff.12629

Parker, G. A., and Begon, M. (1986). Optimal egg size and clutch size: effects of environment and maternal phenotype. *Am. Nat.* 128, 573–592. doi: 10.1086/284589

Robertson, D. R., and Collin, R. (2015). Inter- and intra-specific variation in egg size among reef fishes across the isthmus of Panama. *Front. Ecol. Evol.* 2. doi: 10.3389/fevo.2014.00084

Roff, D. A. (1992). *The evolution of life histories* (New York: Chapman & Hall).

Rollinson, N., and Rowe, L. (2016). The positive correlation between maternal size and offspring size: fitting pieces of a life-history puzzle. *Biol. Rev.* 91, 1134–1148. doi: 10.1111/brv.12214

Salinas, S., and Munch, S. B. (2012). Thermal legacies: transgenerational effects of temperature on growth in a vertebrate. *Ecol. Lett.* 15, 159–163. doi: 10.1111/j.1461-0248.2011.01721.x

Schneider, C. A., Rasband, W. S., and Eliceiri, K. W. (2012). NIH Image to ImageJ: 25 years of image analysis. *Nat. Methods* 9, 671. doi: 10.1038/nmeth.2089

Seebacher, F., White, C. R., and Franklin, C. E. (2015). Physiological plasticity increases resilience of ectothermic animals to climate change. *Nat. Climate Change* 5, 61–66. doi: 10.1038/nclimate2457

Shelton, P. A., Sinclair, A. F., Chouinard, G. A., Mohn, R., and Duplisea, D. E. (2006). Fishing under low productivity conditions is further delaying recovery of Northwest Atlantic cod (*Gadus morhua*). *Can. J. Fisheries Aquat. Sci.* 63, 235–238. doi: 10.1139/f05-253

Sinclair, B. J., Marshall, K. E., Sewell, M. A., Levesque, D. L., Willett, C. S., Slotsbo, S., et al. (2016). Can we predict ectotherm responses to climate change using thermal performance curves and body temperatures? *Ecol. Lett.* 19, 1372–1385. doi: 10.1111/ele.12686

Sunde, J., Larsson, P., and Forsman, A. (2019). Adaptations of early development to local spawning temperature in anadromous populations of pike (*Esox lucius*). *BMC Evolutionary Biol.* 19, 148. doi: 10.1186/s12862-019-1475-3

Tamarin-Brodsky, T., Hodges, K., Hoskins, B. J., and Shepherd, T. G. (2020). Changes in northern hemisphere temperature variability shaped by regional warming patterns. *Nat. Geosci.* 13, 414–421. doi: 10.1038/s41561-020-0576-3

Team, R.C (2018). *A language and environment for statistical computing* (Vienna, Austria: R Foundation for Statistical Computing).

Team, R.S (2016). *RStudio: integrated development environment for r* (Boston, MA: RStudio, Inc).

Tibblin, P., Forsman, A., Borger, T., and Larsson, P. (2016). Causes and consequences of repeatability, flexibility and individual fine-tuning of migratory timing in pike. *J. Anim. Ecol.* 85, 136–145. doi: 10.1111/1365-2656.12439

Tibblin, P., Koch-Schmidt, P., Larsson, P., and Stenroth, P. (2012). Effects of salinity on growth and mortality of migratory and resident forms of Eurasian perch in the Baltic Sea. *Ecol. Freshw. Fish* 21, 200–206. doi: 10.1111/j.1600-0633.2011.00537.x

Uusi-Heikkilä, S., Lindström, K., Parre, N., Arlinghaus, R., Alós, J., and Kuparinen, A. (2016). Altered trait variability in response to size-selective mortality. *Biol. Lett.* 12, 20160584. doi: 10.1098/rsbl.2016.0584

van den Berghe, E. P., and Gross, M. R. (1989). Natural selection resulting from female breeding competition in a pacific salmon (coho: *Oncorhynchus kisutch*). *Evolution* 43, 125–140. doi: 10.2307/2409169

Via, S., Gomulkiewicz, R., Dejong, G., Scheiner, S. M., Schlichting, C. D., and Vantienderen, P. H. (1995). Adaptive phenotypic plasticity - consensus and controversy. *Trends Ecol. Evol.* 10, 212–217. doi: 10.1016/S0169-5347(00)89061-8

Walters, R. j., and Hassall, M. (2006). The temperature-size rule in ectotherms: may a general explanation exist after all? *Am. Nat.* 167, 510–523. doi: 10.1086/501029

Wennersten, L., and Forsman, A. (2012). Population-level consequences of polymorphism, plasticity and randomized phenotype switching: a review of predictions. *Biol. Rev.* 87, 756–767. doi: 10.1111/j.1469-185X.2012.00231.x

frontiers | Frontiers in Marine Science

TYPE Original Research
PUBLISHED 25 July 2023
DOI 10.3389/fmars.2023.1170054

OPEN ACCESS

EDITED BY
Donald F. Boesch,
University of Maryland, College Park, United States

REVIEWED BY
Jennifer L. Bowen,
Northeastern University, United States
Sarah K. Hu,
Woods Hole Oceanographic Institution, United States
Diane Stoecker,
University of Maryland, College Park, United States

*CORRESPONDENCE
Agneta Andersson
agneta.andersson@umu.se

†PRESENT ADDRESS
Matyas Ripszam,
Department of Chemistry and Industrial Chemistry, University of Pisa, Pisa, Italy

RECEIVED 20 February 2023
ACCEPTED 04 July 2023
PUBLISHED 25 July 2023

CITATION
Andersson A, Grinienė E, Berglund ÅMM, Brugel S, Gorokhova E, Figueroa D, Gallampois C, Ripszam M and Tysklind M (2023) Microbial food web changes induced by terrestrial organic matter and elevated temperature in the coastal northern Baltic Sea.
Front. Mar. Sci. 10:1170054.
doi: 10.3389/fmars.2023.1170054

Microbial food web changes induced by terrestrial organic matter and elevated temperature in the coastal northern Baltic Sea

Agneta Andersson[1,2]*, Evelina Grinienė[1,3], Åsa M. M. Berglund[1], Sonia Brugel[1,2], Elena Gorokhova[4], Daniela Figueroa[1,2], Christine Gallampois[5], Matyas Ripszam[5†] and Mats Tysklind[5]

[1]Department of Ecology and Environmental Science, Umeå University, Umeå, Sweden, [2]Umeå Marine Sciences Centre, Umeå University, Hörnefors, Sweden, [3]Marine Research Institute, Klaipėda University, Klaipėda, Lithuania, [4]Department of Environmental Science, Stockholm University, Stockholm, Sweden, [5]Department of Chemistry, Umeå University, Umeå, Sweden

Climate change has been projected to cause increased temperature and amplified inflows of terrestrial organic matter to coastal areas in northern Europe. Consequently, changes at the base of the food web favoring heterotrophic bacteria over phytoplankton are expected, affecting the food web structure. We tested this hypothesis using an outdoor shallow mesocosm system in the northern Baltic Sea in early summer, where the effects of increased temperature (+ 3°C) and terrestrial matter inputs were studied following the system dynamics and conducting grazing experiments. Juvenile perch constituted the highest trophic level in the system, which exerted strong predation on the zooplankton community. Perch subsequently released the microbial food web from heavy grazing by mesozooplankton. Addition of terrestrial matter had a stronger effect on the microbial food web than the temperature increase, because terrestrial organic matter and accompanying nutrients promoted both heterotrophic bacterial production and phytoplankton primary production. Moreover, due to the shallow water column in the experiment, terrestrial matter addition did not reduce the light below the photosynthesis saturation level, and in these conditions, the net-autotrophy was strengthened by terrestrial matter enrichment. In combination with elevated temperature, the terrestrial matter addition effects were intensified, further shifting the size distribution of the microbial food web base from picoplankton to microphytoplankton. These changes up the food web led to increase in the biomass and proportion of large-sized ciliates (>60 µm) and rotifers. Despite the shifts in the microbial food web size structure, grazing experiments suggested that the pathway from picoplankton to nano- and microzooplankton constituted the major energy flow in all treatments. The study implies that the microbial food web compartments in shallow coastal waters will adjust to climate induced increased inputs of terrestrial matter and elevated temperature, and that the major energy path will flow from picoplankton to large-sized ciliates during the summer period.

KEYWORDS

mesocosm experiment, climate change, microbial food web, Baltic Sea, terrestrial matter effects, temperature effect

Introduction

Autotrophic and heterotrophic microorganisms are important components at the base of aquatic food webs. The microbes are involved in a continuum of trophic pathways depending on the physicochemical environment. The trophic structure stretches from herbivorous food webs, dominated by autotrophic microplankton grazed by mesozooplankton to microbial loops dominated by heterotrophic bacteria grazed by small protozoa, nanoflagellates (Azam et al., 1983, Legendre and Rassoulzadegan, 1995). Climate change affects the physicochemical environment in aquatic systems, thus likely altering the microbial community structure and function.

Severe temperature alterations, precipitation and extreme weather events have been attributed to climate change, affecting all Earth environments (Pörtner et al., 2022). In northern Europe, and especially the northern Baltic Sea areas, both elevated temperature and increased precipitation are projected, which will lead to higher river inflows of terrestrial matter and nutrients to the coast (Meier et al., 2012; Andersson et al., 2015; Meier et al., 2022). However, how those combined changes will affect the trophic pathways and food web functions is unclear.

Warming will induce several food web changes, including a decrease in size of organisms like bacteria, phytoplankton, protozoa and mesozooplankton (Andersson et al., 1986; Andersson et al., 1994; Suikkanen et al., 2013). This decrease would be due to the combined effects of nutrient limitation and temperature (Mousing et al., 2014). Increased temperature will lead to faster assimilation of nutrients by osmotrophic organisms (heterotrophic bacteria and phytoplankton), and nutrient depletion will promote small-sized organisms due to their large surface-to-volume ratio (Samuelsson et al., 2002). In turn, small-sized phytoplankton and bacteria may, facilitate feeding of smaller micro- and mesozooplankton grazers, as the food chain is size-structured (Fenchel, 1987). As a result, new niches in the food web can appear, including intermediate trophic levels. Furthermore, higher temperatures may disfavor autotrophy and promote heterotrophic processes (Hoppe et al., 2002; Müren et al., 2005), i.e., heterotrophic bacterial production and grazing by heterotrophic protists (Hoppe et al., 2002; Rose et al., 2009).

In coastal areas receiving terrestrial matter the microbial food web often dominates, where heterotrophic bacterial production is enhanced, and phytoplankton primary production is hampered due to darkening (browning) of the water (e.g. Figueroa et al., 2016; Andersson et al., 2018). However, if terrestrial matter inflows are accompanied by large amounts of nutrients, phytoplankton growth can be promoted, supporting microphytoplankton rather than picoplankton in microbial loops (Legendre and Rassoulzadegan, 1995; Paczkowska et al., 2019).

Inflows of terrestrial matter to coastal waters have been shown to promote protozoa, such as heterotrophic and mixotrophic nanoflagellates (2-20 µm) and ciliates (30-100 µm) (Vähätalo et al., 2002; Paczkowska et al., 2019). The large size range of ciliate communities reflects co-existence of different functional groups with varying food preferences. The present paradigm states that, in terrestrial matter rich waters, ciliates constitute an important link from the microbial food web to mesozooplankton, which in turn are food for planktivorous fish (Vähätalo et al., 2002; Andersson et al., 2015; Paczkowska et al., 2019). However, in-depth knowledge of how terrestrial matter inputs drive the ciliate functional ecology and community structure is lacking.

To approach these questions, we performed a mesocosm study to elucidate how warming and increased terrestrial matter inputs affect the energy flows in the microbial food web in a shallow coastal system, consistent with a climate change scenario. The experimental system consisted of a natural plankton community and larval planktivorous fish from the coastal northern Baltic Sea. Effects on the energy flow in the microbial food web and ecosystem functions were assessed by compiling changes in production and biomass of different functional groups. We expected that increased temperature would favor small-sized plankton organisms, such as picoplankton and heterotrophic microbes, driving the system towards net-heterotrophy. Also, we expected that terrestrial matter addition would promote the heterotrophic microbial food web, thus further enhancing net-heterotrophy. Therefore, when temperature elevation was combined with terrestrial matter addition, the strongest net-heterotrophy stimulation was expected.

Materials and methods

Mesocosm experiment

A 35-day mesocosm experiment was performed at Umeå Marine Sciences Center (Sweden), May-July 2013, using seawater from the northern coastal Baltic Sea (63°56'N, 19°54'E). The experiment had 4 treatments (3 replicates each) representing systems with and without inputs of terrestrial matter (tM) (5.2 and 7 mg C l^{-1}, respectively) at two temperatures (15°C as "present day" and 18°C as "climate altered" conditions). +3°C was chosen as the surface water temperature is projected to increase by 2-4°C in the Baltic Sea (HELCOM, 2013a; HELCOM, 2013b). Treatments were named 15, 18, tM15 and tM18, to indicate temperature and tM enrichment.

In total, 12 polypropylene tanks (Allembalage AB, Jordbo, Sweden), with a height of 1 m and volume of 1000 l were immersed in four large pools. All tanks were simultaneously filled with seawater collected 1 km offshore in the northern Bothnian Sea (63° 34'N, 19°54'E) using a Flygt 3152.181 pump (Xylem Sundbyberg Sweden). The salinity was 3‰, which is normal for the sea area Andersson et al. (2018). The water was filtered (1 mm slit filter, Bernoulli System Lund, Sweden) to remove fish and allow natural communities of bacteria, phytoplankton, protozoa and mesozooplankton to populate the mesocosms. A computer-controlled cooling/heating system kept the temperature constant in the pools. Each pool contained three mesocosms and treatment allocation was randomized, with at least one treatment represented in each appropriate block. Ambient air was gently bubbled at the bottom of each mesocosm to create a well-mixed water column, and a semi-transparent polyethylene-phthalate roof covered the mesocosms.

Terrestrial matter was extracted from natural humic soils in a nearby mesic mixed forest, dominated by *Picea abies* and *Betula pubescens* (co-dominant). The field layer was of *Vaccinium myrtillus* type. The soil was extracted as described in Ripszam et al. (2015), and filtered through a 90 µm mesh. The carbon concentration of the soil extract was ~2.1 g C l^{-1}, and the C: N: P molar ratio was approximately 2985:33:1, calculated based on the ratio of DOC: TDN: TDP. Terrestrial matter addition started directly after filling the mesocosms with seawater, by gradual addition to each of the 6 mesocosms (tM treatment) reaching a total addition of 2 mg l^{-1} of DOC at the end of the experiment. This corresponds to a 40% increase, which is approximately what is forecasted over the next 100 years due to climate change (Hägg et al., 2010). 25% of this amount (0.5 mg.l^{-1}) were added on the first day of the experiment, to boost the system, and after that 6.8% were added three times a week (0.14 mg C l^{-1} per 3 days).

In addition to carbon, the soil extract also contained dissolved nitrogen and phosphorus. Previous studies have shown that the bioavailable portion of dissolved nitrogen and phosphorus in riverine and coastal waters is ~20-30% and 75%, respectively (Stepanauskas et al., 2002; Lignell et al., 2008). Therefore, to target the effects of increased carbon, we added equal amounts of dissolved inorganic nitrogen (DIN) and dissolved inorganic phosphorus (DIP) to the non-enriched mesocosms to match the nutrient concentrations in the tM treatments and balance their bioavailability. Nutrient addition started directly after filling the mesocosms with seawater.

As the top consumer, we used larval perch (*Perca fluviatilis*), hatched from egg strands collected from a coastal spawning bay. 10 individuals (6.26 ± 0.25 mm, mean ± 1 SD) were added to each tank on the 5th of June and collected on the 26th of June. Results of fish responses to the experimental treatments are presented elsewhere (Åsa Berglund submitted).

Sampling and analyses of physicochemical and biological variables

Samples were taken 3-6 times during the experiment to measure physicochemical and biological variables. In general, the samples were collected in the middle of the mesocosms.

Light, nutrients and chlorophyll *a*

Photosynthetically active radiation (PAR) was measured around noon (11 am-1 pm) three times during the experiment (start, mid and end), using a PAR Licor sensor (LICOR -193SA). The measurements were performed at midday at five positions: in the four corners and the middle at three different depths: 0, 0.45 and 0.90 m; the average PAR value per mesocosm was calculated from the 15 data points.

Concentrations of dissolved organic carbon (DOC) were analyzed using a high-temperature carbon analyzer (Shimadzu TOC-L) and total N, total P, dissolved inorganic nitrogen (DIN) and dissolved inorganic phosphorus (DIP) were analysed using a Seal Analytical QUAATRO auto analyzer.

To measure chlorophyll *a* (Chl *a*), 100 ml samples were filtered onto 25 mm GF/F filters under low vacuum and stored at -80°C. The pigments were extracted in 95% ethanol in the dark at 4°C overnight, and measured with a Perkin Elmer LS 30 fluorometer (433/674 nm excitation/emission wavelengths) (HELCOM, 2013b).

Heterotrophic bacterial production and phytoplankton primary production

Heterotrophic bacterial production and primary production samples were collected in the middle of each mesocosm. Heterotrophic bacterial production (BP) was measured using the [^{3}H-methyl]-thymidine technique (Fuhrman and Azam, 1982). 1 ml of mesocosm water was added to three Eppendorf tubes, one control and technical duplicates for the test samples. Bacteria in the control were pre-killed by adding 100 µl ice-cold 50% TCA and incubation at -20°C for 5 minutes. 2 µl [^{3}H]-thymidine (84 Ci mmol l^{-1}; Perkin Elmer, Massachusetts, USA) were added to each tube to a final concentration of 24 nM. The incorporated thymidine was converted to cell production using the conversion factor of 1.4 x10^{18} cells mol^{-1} (Wikner and Hagström, 1999). To calculate carbon biomass production, a bacterial carbon content of 20 fg C $cell^{-1}$ was assumed (Lee and Fuhrman, 1987), which has been shown to be representative for the coastal area (data not shown). Daily production rates were calculated assuming stable uptake rates over the day.

Primary production (PP) was measured using the ^{14}C technique. 5 ml seawater were added to three 20 ml transparent glass vials with one dark tube as a control. 7.2 µl ^{14}C were added to each vial (^{14}C Centralen Denmark, activity 100 µCi/ml) and incubated at 80-cm depth for ~3 hours. The samples were analysed in a Beckman 6500 scintillation counter. Daily primary production was calculated as described in Andersson et al. (1996).

Picoplankton: heterotrophic bacteria and picophytoplankton

Samples for analysis of picophytoplankton and heterotrophic bacteria were collected in the middle of the mesocosms, preserved in 0.1% glutaraldehyde (final concentration) and frozen at −80°C (Marie et al., 2005) for later counts using a BD FACSVerse^{TM} flow cytometer (BD Biosciences) equipped with a 488 nm laser (20 mW output) and a 640 mn laser (output 40 mW). The frozen samples were quickly thawed in a 30°C water bath and pre-filtered through a 50 µm mesh. Picophytoplankton samples were run with 3 µm microspheres (Fluoresbrite R plain YG, Polysciences) as internal standard. Picophytoplankton abundance was converted to biomass using carbon conversion factors 120 fgC $cell^{-1}$ for picocyanobacteria and 829 fgC $cell^{-1}$ for picoeukaryotic phytoplankton, based on microscopic measurements of cell sizes (see below).

Heterotrophic bacteria samples were diluted with 0.2-µm filtered seawater, stained with SYBR Green I (Invitrogen)

(1:10000, final concentration) and kept in the dark at room temperature for 10 min. 1 µm microspheres (Fluoresbrite R plain YG, Polysciences) were added to each sample as internal standard and analyses were run at a low flow rate of 30 µl min^{-1} with an acquisition time of 2 min. Heterotrophic bacteria abundance was converted to biomass using carbon conversion factor 20 fgC $cell^{-1}$ (Lee and Fuhrman, 1987).

Nano- and microphytoplankton

Samples were collected in the middle of the mesocosms, fixed with 2% acidic Lugol's solution and stored in darkness at 4°C until analysis. To analyse nano- and microphytoplankton and heterotrophic nanoflagellates, 10-50 ml were settled for 12-48 hours in sedimentation chambers and cells were counted with an inverted microscope (Nikon Eclipse Ti) at 100-400x magnification using phase contrast settings (Utermöhl, 1958). Cells were grouped into three functional groups (AU: autotrophs, HT: heterotrophs, MX: mixotrophs), based on the feeding mode (Olenina et al., 2006), and two size classes (nanophytoplankton: 2–20 µm, microphytoplankton: >20 µm), based on the measurements of the longest cell axis. Filamentous cyanobacteria were assigned to the microphytoplankton category based on the size of the tightly clustered amalgamations of cells. Nutritional characteristics of plankton were identified based on their trophy (Tikkanen and Willen, 1992; Hällfors, 2004; Olenina et al., 2006). As Lugol's solution stains Chl *a* brown, the color of the smallest cells was used to support the trophy classification.

Biomass of pico, nano and microphytoplankton

Phytoplankton and heterotrophic nanoflagellates biomass was calculated from the geometric shape of cells following Olenina et al. (2006), and cell carbon content was calculated according to Menden-Deuer and Lessard (2000). Total phytoplankton biomass (TB) was the sum of autotrophs carbon biomass, including pico-, nano- and microplankton and mixotrophs (for example *Mesodinium rubrum*). The relative contribution of different size classes and functional groups to the total biomass was calculated.

Ciliates

For the analysis of ciliates, 25–50 ml were settled for at least 24-48 h in Utermöhl's chambers and counted with an inverted microscope at 200× magnification. The entire content of each Utermöhl's chamber was surveyed, and an additional subsample was counted if the total number of organisms was <150. Ciliate biovolume was calculated by their geometric shape using measurements of the cell length and width of at least 20 cells of each species/taxa per sample. Cell carbon biomass of aloricated ciliates was calculated according to Menden-Deuer and Lessard (2000), and carbon biomass of tintinnids was estimated using the experimentally derived factor of 0.053 pg C pm^{-3} lorica volume (Verity and Lagdon, 1984). Different functional groups of ciliates were classified according to Mironova et al. (2013): pico-filterers (bacterivorous), nano-filterers (algivorous), pico/nano- filterers (bacterio/algivorous), omnivores (heterotrophic flagellates, algae and ciliates) and predators (ciliates). Further, the ciliates were grouped into the following size classes: <20 µm, 20-30 µm, 30-60 µm and >60 µm.

Zooplankton

Once per week, zooplankton was sampled using a 25 µm nylon net (mouth diameter 0.14 m). Three vertical tows per sampling were performed, comprising a total volume of 40 liters. The samples were preserved with RNAlater and stored at 4°C until analysis. The entire sample content was counted using a counting chamber and an inverted microscope (Leitz fluovert FS, Leica) at 80× magnification. Copepods were classified according to species, developmental stage (nauplii, copepodites CI–III, CIV–V and adults), and sex, whereas cladocerans were classified according to species, maturity (adults and juveniles) and sex. Biomass was calculated using abundance data and species- and stage-specific weights (Hernroth, 1985).

Photosynthetic efficiency, heterotrophic bacterial growth rate and ecosystem trophy

Phytoplankton photosynthetic efficiency was calculated by dividing primary production rate by the Chl *a* concentration according to Andersson et al. (2018). Heterotrophic bacterial specific growth rate was calculated by dividing the bacterial production by the bacterial biomass according to Andersson et al. (2018). Ecosystem trophy, defined as net-heterotrophy or net-autotrophy, was calculated as a difference between primary production and heterotrophic bacterial production, with positive and negative values indicating ecosystem net-autotrophy and net-heterotrophy, respectively.

Statistical analyses

In mesocosm experiments, it usually takes a few weeks to stabilize physicochemical and biological parameters in the system (e.g. Paczkowska et al., 2020). We were mainly interested in treatment effects of the stabilized systems. For example, in our experiment the primary production was relatively high in the beginning of the experiment, but after three weeks of incubation it stabilized at a lower level (Supplementary Figure 1). Heterotrophic bacterial production also showed decreasing values during the first weeks of the experiment, but during the three last weeks the values stabilized (Supplementary Figure 1). Therefore, data from the last two-three weeks of the experiment (week 3 – 5) were used, translating into 2-3 data points per mesocosm. The differences between the treatments were evaluated using Kruskal-Wallis test for each abiotic and biotic variable. The non-parametric approach was chosen because the

homogeneity assumption was violated for most variables, as shown by the Levene test. Arcsine transformation was used for percentage data. Multiple comparisons of mean ranks for all variables were used, with $p<0.05$ indicating significant differences between the groups. Statistical tests were performed using STASTISTICA 7.0 (StatSoft Ltd.).

Grazing experiment

Towards the end of the experiment (weeks 4-5), dilution experiments were conducted to estimate nano- and microzooplankton (2-200 µm) grazing on heterotrophic bacteria and phytoplankton (size fractions <3 and 3-50 µm) in randomly chosen mesocosms from different treatments (15, 18, tM15 and tM18). For these experiments, 20 l water from each mesocosm were taken; half of the volume was used to prepare the particle-free water (FW) and the rest was used as whole water (WW). FW was prepared by pre-filtering through 50-µm plankton mesh to remove larger particles and then through 0.2-µm Millipore filter under a slight vacuum. The filtration process took about one hour. WW was gently poured through a 200 µm mesh to remove mesozooplankton. For the 15 and tM15 mesocosms, the WW was diluted by FW to four target dilutions in ratios of 1:0, 3:1, 1:1, 1:3 (dilution factor or decimal fraction of WW: 1; 0.75; 0.5; 0.25 respectively). For the 18 and tM18 mesocosms, a fifth treatment was added, where WW was diluted by FW in ratio of 1:9 (dilution factor 0.1). The exposure was carried out in duplicates, in 1 l transparent glass sterile bottles that were incubated at the same temperature and light conditions as in the mesocosm tanks for 24-48 h. To ensure that nutrients are available to phytoplankton at all dilution levels, nitrate (10 µg N l^{-1}) and phosphate (1 µg P l^{-1}) were added in excess to each bottle (Landry and Hassett, 1982). For bacteria, a carbon source (mixed glucose, galactose, mannitol and sodium acetate) was added to a final concentration of 140 µmol l^{-1} (Stepanauskas et al., 2002).

At the start and the end of experiment, 300 ml of each dilution mixture were sampled for heterotrophic bacteria, <3 and 3-50 µm phytoplankton fractions. For nutrient analysis (nitrate, nitrite, ammonium, phosphate and silicate) and microzooplankton counts, samples were taken only from 1:0 treatment (WW only) at the beginning and the end of the experiment.

The data analysis was performed according to Landry and Hassett (1982). The prey apparent growth rate (AGR, d^{-1}) was estimated as:

$$AGR = Ln\,(P_t/P_o)/t;$$

Where P_t and P_o are final and initial concentrations of prey (heterotrophic bacteria, phytoplankton <3 and 3-50 µm size fractions), and t is incubation time (d). Heterotrophic bacteria and phytoplankton were analyzed using flow cytometry, as described above.

The rates of prey growth and grazing mortality were calculated using the linear regression of AGR versus dilution factor. The regression slope is the microzooplankton grazing rate (g, d^{-1}), and the intercept is the growth rate of prey in the absence of grazing (μ, d^{-1}). A significant negative slope (one-tailed t-test, $p<0.05$) was used as evidence for measurable grazing. When statistically non-significant regression or positive slope were observed, the grazing rates were not determined.

Grazing of the potential production of heterotrophic bacteria and different size fractions of phytoplankton (< 3 µm, 3-50 µm) were calculated ($P_{p,}$% d^{-1}):

$$P_p = (e^{\mu} - e^{\mu-g})/(e^{\mu} - 1);$$

Where µ is growth rate of prey and g is grazing rate of microzooplankton (James and Hall, 1998) calculated as described above.

Results

Temporal variation

Temporal dynamics of bottom up and top-down factors

Temperature, nutrients (DOC, TN, DIN TP and DIP) and light (PAR) constituted bottom-up factors for microbial food web responses. The temperature was successfully maintained at 15°C and 18°C with a variation of <0.5%. The DOC concentrations were stable over time in the non-enriched mesocosms, averaging 5.2 mg C l^{-1}, while in the tM enriched systems, the concentrations increased steadily during the experiment to reach 7 mgC l^{-1} at the end of the experiment (Figure 1).

Total organic nitrogen and phosphorus showed similar temporal patterns as DOC (Supplementary Figure 2). In the non-enriched mesocosms, the dissolved inorganic nitrogen and phosphorus decreased, except for the high temperature 18°C that showed more varying values (Supplementary Figure 2). In the tM enriched mesocosms the DIP showed high values at the start, decreased in the middle and increased again towards the end of the experiment (Supplementary Figure 2). Light (PAR) showed low temporal variation within treatment (coefficient of variation <10%), but the values were ca. 40% lower in the tM-enriched mesocosms (Figure 1).

The mesozooplankton community consisted of cladocerans, rotifers and copepods (Supplementary Figure 3). The mesozooplankton biomass decreased over time in all treatments (Figure 2), and the mean size declined significantly, mostly in the tM18 treatment, where the fraction of small-bodied zooplankton (mostly rotifers) increased from ~30 to 45% during the latter part of the experiment (Supplementary Figure 4).

Temporal variation of microbial food web components

Ciliates represented the highest trophic level of the microbial food web. The ciliate community showed high versatility, with five feeding types: pico-filterers, pico-nano-filterers, nano-filterers, omnivores and predators (Table 1). Pico-filterers were mostly dominated by oligotrichids (*Lohmanniella* spp. and *Strombidium* spp.), whereas pico-nano-filterers were represented by peritrichids (*Vorticella* spp. and *Epystilis* spp.), and scuticociliates (*Uronema* spp. and *Cyclidium* spp.). The dominant omnivorous ciliate was the hypotrichid *Stylonychia* sp. (Supplementary Figure 5). Within the predator

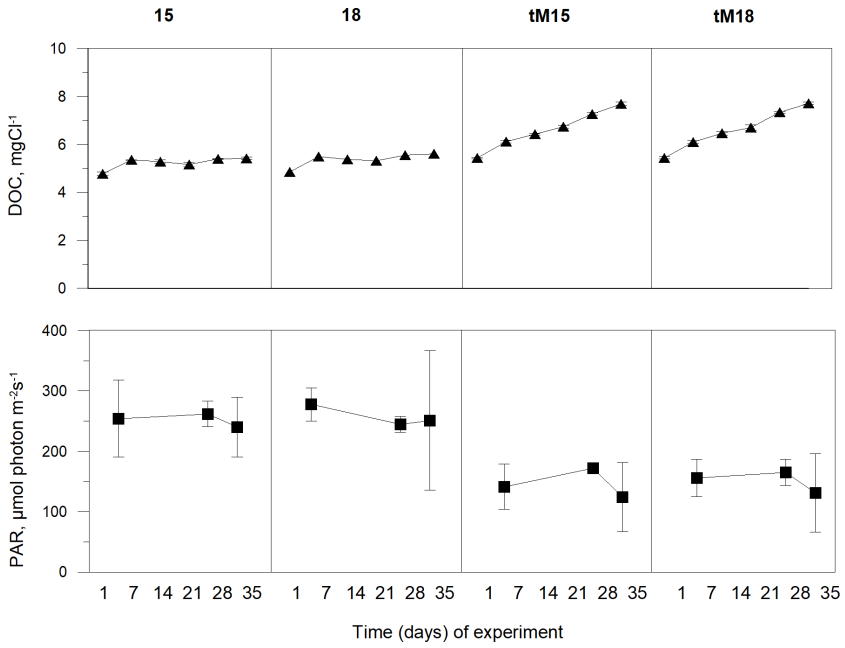

FIGURE 1
Dissolved organic carbon (DOC) and photosynthetically active radiation (PAR) during the experiment in different treatments: 15, 18, tM15 and tM18. Error bars denote standard deviation.

group, haptorids *Monodinium* sp., *Didinium* sp. and *Lacrymaria* sp. were common (Table 1). The total ciliate biomass increased in all treatments during the first week, and after that further increases were observed in the tM-enriched mesocosms (Figure 2). The ciliate biomass plateaued/stabilized during the last two weeks of the experiment in all treatments (Figure 2). Omnivorous and predatory ciliates increased over time in the tM-enriched mesocosms (Supplementary Figure 6), while other groups showed a more fluctuating pattern. No clear temporal trend was observed in the non-enriched mesocosms (Supplementary Figure 6).

Micro-, nano- and picoplankton constituted the base of the microbial food web. Microphytoplankton was dominated by autotrophic diatoms in all mesocosms, while heterotrophic, mixotrophic and autotrophic taxa constituted nanoplankton; many of those were flagellates. In the tM-enriched mesocosms, the micro and nanoplankton remained relatively constant (except for one outlier, microphytoplankton tM15, day 35), while their biomass decreased over time in the non-enriched treatments. Picophytoplankton consisted of pigmented eukaryotic cells and picocyanobacteria. In the tM-enriched mesocosms, picophytoplankton increased during the first weeks of the experiment and decreased after that (Figure 2). However, in the non-enriched mesocosms, their biomass was relatively constant throughout the experiment. Heterotrophic bacteria showed a similar temporal pattern as picophytoplankton (Figure 2).

Stabilized treatment effects

Bottom-up factors

Regardless of the incubation temperature (15 and 18°C), the DOC concentrations were significantly higher (ca 40%) in the tM-enriched than in the non-enriched mesocosms (Figure 3, Supplementary Table 1). The added terrestrial matter was colored, causing a decrease in the average photosynthetically active radiation (PAR) from ~250 to 150 µmol photon m^{-2} s^{-1} (Figure 3, Supplementary Table 1). The terrestrial matter also contained nitrogen and phosphorus, causing an approximate doubling of the total (TN and TP) and inorganic nitrogen and phosphorus (DIN and DIP) concentrations compared to the non-enriched mesocosms (Figure 3, Supplementary Table 1).

Standing stocks of major plankton groups

During the last weeks of the experiment, the copepod + cladoceran biomass was low in all treatments, and no significant difference was observed between the treatments (Figure 4, Supplementary Table 1). The rotifer biomass was similar in most treatments, but the lowest in the 18°C incubation (Figure 4, Supplementary Table 1). Terrestrial matter addition caused increased biomass of ciliates, total phytoplankton and heterotrophic bacteria, while temperature increase alone did not cause any general increase or decrease of these groups (Figure 4, Supplementary Table 1). Heterotrophic nanoflagellates (HNF) showed a similar pattern, albeit not significant (Figure 4, Supplementary Table 1). In the tM-enriched systems, phytoplankton and heterotrophic bacteria tended to decrease at the highest temperature (Figure 4, Supplementary Table 1).

Size-structure of the microbial food web base

Autotrophic and heterotrophic picoplankton constituted the largest pool, 60-90%, of the microbial biomass in all treatments, whereas nanoplankton contributed ~5-10% (Figure 5). Neither tM addition nor elevated temperature affected the picoplankton

10.3389/fmars.2023.1170054

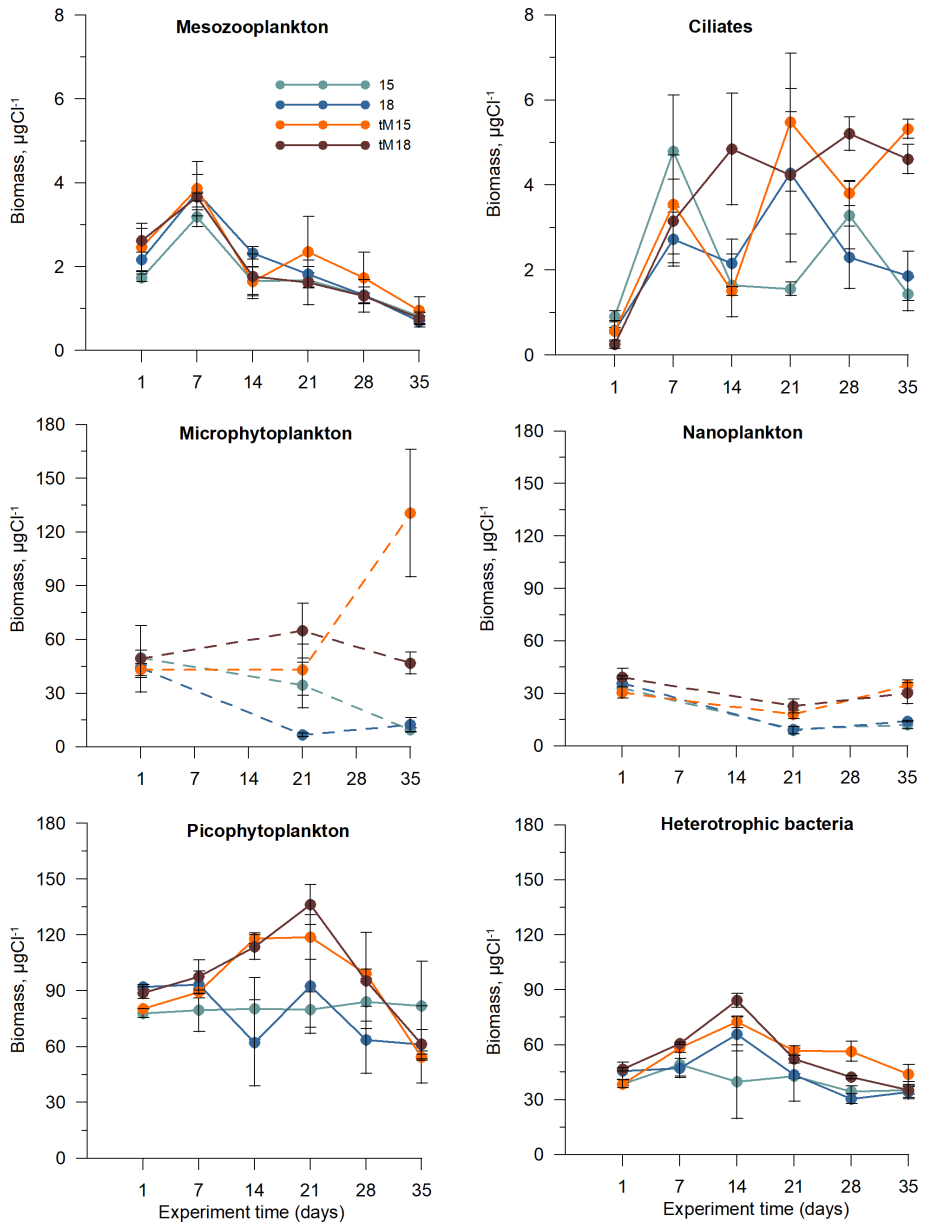

FIGURE 2
Temporal variation of mesozooplankton, ciliates, microphytoplankton (autotrophic (AU) and mixotrophic (MX)), nanoplankton (heterotrophic (H), MX and AU), picophytoplankton (picocyanobacteria + picophytoeukarytotes, AU) and heterotrophic bacteria (HT) in different treatments. Error bars denote standard error. Dashed lines indicate few sampling points.

TABLE 1 Cell size range (min-max and mean in brackets) and feeding type of ciliate taxa in the mesocosm experiment: O, omnivorous; P, predator.

Ciliate taxonomic order	Taxa	Cell size range (mean), µm	Feeding type	Literature source
Haptorida	*Actinobolina* sp.	65–85 (75)	nano/micro-interceptor (P)	a
Haptorida	*Askenasia* sp.	25–35 (29)	nano-interceptor (O)	a, c
Haptorida	*Mesodinium pulex* (Claparède and Lachmann, 1859)	10–25 (15)	pico/nano-interceptor (O)	a
Haptorida	*Monodinium* sp.	30–40 (33)	nano/micro-interceptor (P)	a, c
Haptorida	*Didinium* sp.	45–70 (58)	nano/micro-interceptor (P)	a, c

(Continued)

10.3389/fmars.2023.1170054

TABLE 1 Continued

Ciliate taxonomic order	Taxa	Cell size range (mean), µm	Feeding type	Literature source
Haptorida	*Lacrymaria* sp.	60–110 (79)	nano/micro-interceptor (P)	b
Haptorida	*Mesodinium rubrum* Jankowski, 1976	10–30 (19)	Autotrophic	
Haptorida	*Trachelius ovum* Ehrenberg, 1831	125–150 (146)	nano/micro-interceptor (P)	a
Prostomatida	*Holophrya* sp.	50–65 (54)	nano-interceptor	a
Prostomatida	*Coleps hirtus* (O. F. Müller, 1786)	35–50 (40)	nano/micro-interceptor (O)	a
Prostomatida	*Urotricha* sp.	25–35 (29)	pico-nano-interceptor	a
Prostomatida	*Prorodon* sp.	90	nano/micro-interceptor (P)	a
Oligotrichida	*Lohmanniella* sp.	30–35 (31)	pico/nano-filterer	h
Oligotrichida	*Lohmanniella oviformis* Leegaard, 1915	15-25 (20)	pico/nano-filterer	e, m
Oligotrichida	*Strobilidium* spp.	10–40 (30)	pico/nano-filterer	c
Oligotrichida	*Strombidium conicum* Lohmann, 1908	40–75 (63)	pico/nano-filterer	b, i
Oligotrichida	*Strombidium* cf. *vestitum*	20–35 (25)	pico/nano-filterer	i
Oligotrichida	*Strombidium* sp.	50–60 (58)	pico/nano-filterer	h
Oligotrichida	*Strombidium* cf. *acutum*	30–55 (39)	nano-filterer	k
Oligotrichida	*Limnostrombidium viride* (Stein, 1867)	15–25 (20)	pico/nano-filterer	a
Oligotrichida	*Tintinnopsis* sp.1	40–100 (71)	nano-filterer	d, c
Oligotrichida	*Tintinnopsis* sp.2	100–150 (125)	nano-filterer	d, c
Oligotrichida	*Tintinnopsis* sp.3	90	nano-filterer	d, c
Oligotrichida	*Tintinnopsis baltica* Brandt, 1896	85	nano-filterer	d, c
Oligotrichida	*Tintinnopsis beroidea* Stein, 1867	60–65 (63)	pico-nano-filterer	e
Oligotrichida	*Codonella cratera* Leidy, 1877	55	nano-filterer	a
Oligotrichida	*Tintinnopis pistillum* Kofoid and Campbell, 1929	100–200 (147)	nano-filterer	d, c
Oligotrichida	*Tintinnopsis tubulosa* Levander, 1900	50–100 (72)	nano-filterer	a
Hypotrichida	*Euplotes affinis* Dujardin, 1842	30–50 (41)	pico-micro filterer (O)	l, a
Hypotrichida	*Stylonychia* sp.	75– 150 (105)	pico-micro filterer (O)	f
Pleurostomatida	*Litonotus cygnus* (O. F. Müller,1776)	80–155(129)	nano/micro-interceptor (P)	a
Peritrichida	*Charchesium pectinatum* (Zacharias, 1897)	30–50 (45)	pico-filterer	a
Peritrichida	*Vorticella* sp.1	30–40 (34)	pico-filterer	c
Peritrichida	*Vorticella* sp.2	20–25 (24)	pico-filterer	c
Peritrichida	*Vorticella* sp.3	44–48 (45)	pico-filterer	c
Peritrichida	*Vorticella* sp.4	65–90 (78)	pico-filterer	c
Peritrichida	*Epystilis* sp.	75	pico-filterer	a
Scuticociliatida	*Uronema* sp.	35–40 (36)	pico-filterer	g
Scuticociliatida	*Cyclidium* spp.	20–30 (22)	pico-filterer	g

a – Foissner and Berger (1996); b – Fenchel (1987); c – Gaedke and Wickham (2004); d – Rassoulzadegan et al. (1988); e – Kivi and Setälä (1995); f – Pfister and Arndt (1998); g – Ayo et al. (2001); i – Agatha and Riedel-Lorjé (1997); h – Maeda and Carey (1985); Maeda (1986), k – Stürder-Kypke et al. (2000); l – Hausman (1988); m – Jonsson (1986).

biomass (Supplementary Table 1), and nanoplankton biomass increased with tM addition (Figure 5, Supplementary Table 1), with no significant temperature effect. Microphytoplankton constituted the second largest biomass pool, contributing 10-30%, increasing with the tM addition and showing some indication of decrease at elevated temperature (Figure 5, Supplementary Table 1). These variations in relative contributions of the micro-, nano- and picoplankton biomass resulted in a changed size structure of the

10.3389/fmars.2023.1170054

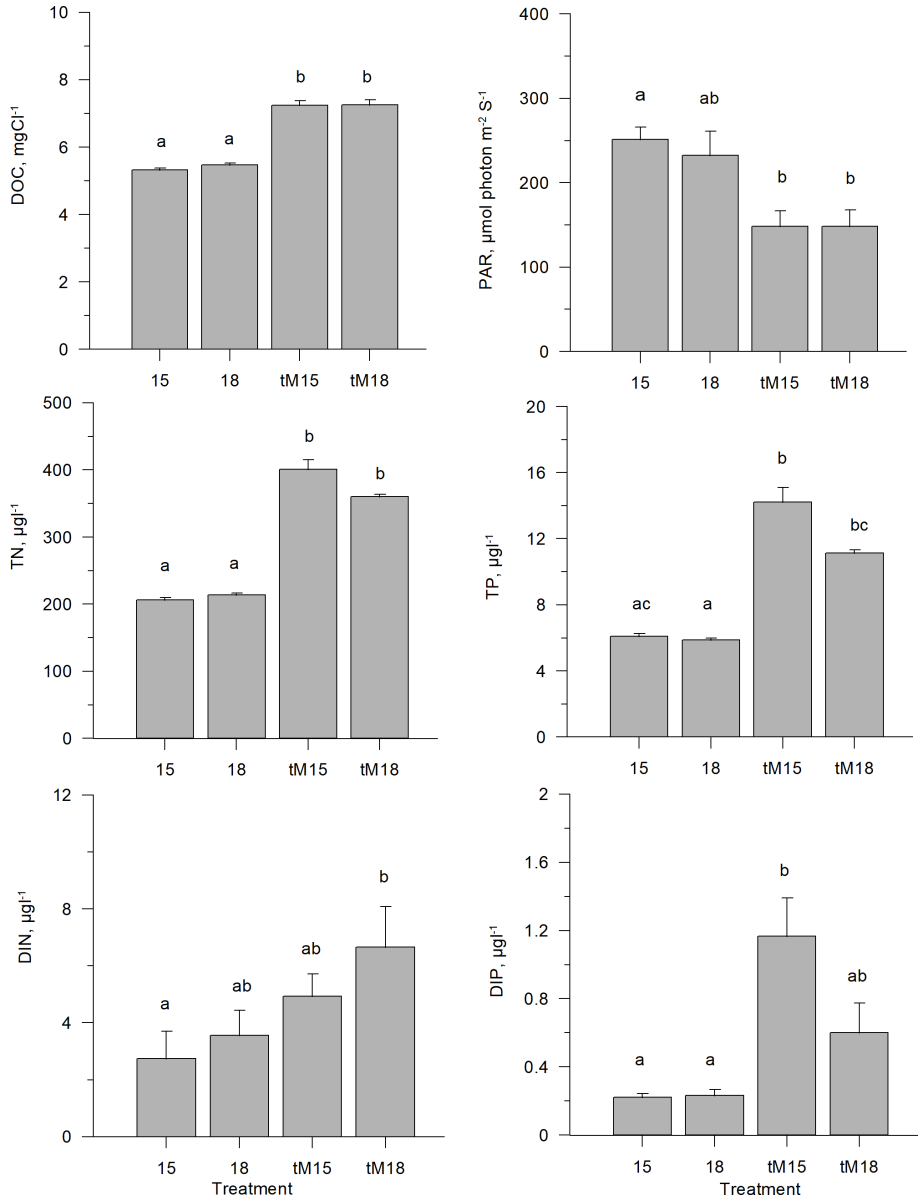

FIGURE 3
Abiotic variable averages during the last three weeks of experiment; dissolved organic carbon (DOC), photosynthetically active radation (PAR), total nitrogen (TotN), total phosphorus (TotP), dissolved inorganic nitrogen and dissolved inorganic phosphorus in different treatments. Error bars denote standard error. Letters indicate the results of the Kruskal-Wallis test and *post-hoc* means of ranks for all groups test. Treatments with the same letters are not significantly different based on mean ranks comparison test (p>0.05).

microbial food web base. The tM addition facilitated large-sized organisms (microphytoplankton), while small-sized organisms benefitted from the higher temperature (Figure 5, Supplementary Table 1). Moreover, the tM addition had a larger impact on the size structure than the temperature increase.

Size-structure of the ciliate community

Omnivorous ciliates were the only group that responded positively to tM addition, with significant differences found between 15 and tM18 (Figure 6, Supplementary Table 1). Pico-nano filtering ciliates constituted the largest biomass in the ciliate community, but their biomass did not respond significantly to any treatment (Figure 6, Supplementary Table 1). Pico-filterers, nano-filterers and predators constituted somewhat smaller shares of the ciliate community, and with tM addition no significant difference could be identified (Figure 6, Supplementary Table 1).

The tM addition favored large ciliates (Figure 6, Supplementary Table 1), as indicated by the increased proportion of >60 µm ciliates in the tM18 treatment. No significant temperature effect on the ciliate size structure was found.

10.3389/fmars.2023.1170054

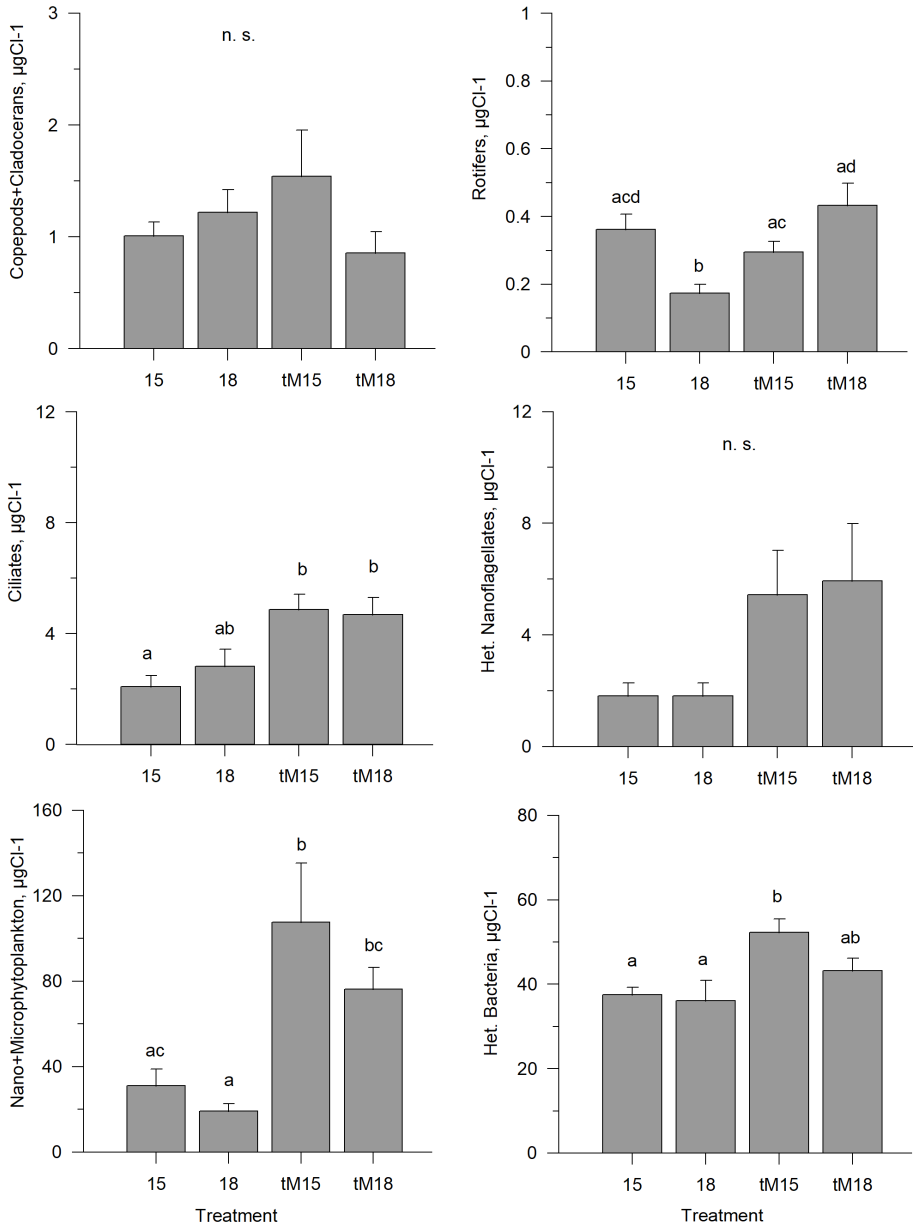

FIGURE 4
Average biomass of key functional groups of organisms during the last three weeks of the experiment in different treatments. Error bars denote standard error. Letters indicate the results of the Kruskal-Wallis test and *post-hoc* means of ranks for all groups test. Treatments with the same letters are not significantly different based on mean ranks comparison test (p>0.05), n.s., not significant.

Basal production and energy flow in the microbial food web

Phytoplankton primary production and heterotrophic bacterial production constituted the base of the microbial food web. The phytoplankton primary production was relatively similar in the 15°C and 18°C mesocosms during the last weeks of the experiment, but in the tM-enriched mesocosms the primary production rates were approximately twice as high (Figure 7, Supplementary Table 1). A similar pattern was observed for heterotrophic bacterial production (Figure 7, Supplementary Table 1), which was significantly higher in all treatments with tM enrichment. The photosynthetic efficiency in the tM-enriched mesocosms was approximately half that in the non-enriched tanks; however, this difference was not significant (Figure 7, Supplementary Table 1). The lowest heterotrophic bacterial specific growth rates were observed in the non-enriched low-temperature incubations (15°C) and the highest in the tM-enriched mesocosms at 18°C (Figure 7, Supplementary Table 1).

In the grazing experiment, grazers consisted of phagotropic nanoflagellates (heterotrophs and mixotrophs) and phagotrophic ciliates (heterotrophs and mixotrophs). In the non-enriched mesocosms, the experimental start biomass of phagotrophic nanoflagellates was twice as high as that of phagotrophic ciliates (Supplementary Table 2). In the tM enriched mesocosms, the initial biomass of phagotrophic nanoflagellates and phagotrophic ciliates

10.3389/fmars.2023.1170054

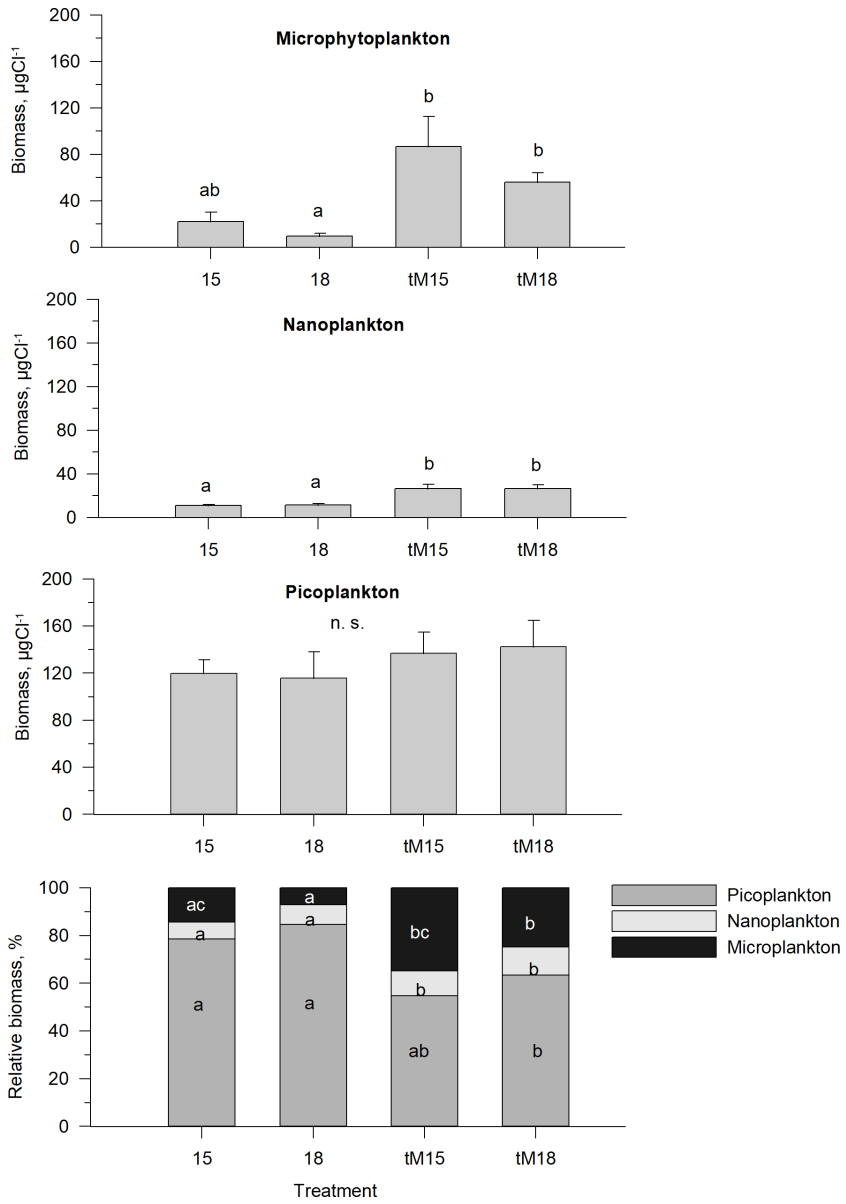

FIGURE 5
Average biomass and relative biomass of the microbial food web base during the last three weeks of the experiment: microphytoplankton, nanoplankton and picoplankton, including autotrophs, mixotrophs and heterotrophs in different treatments. Error bars denote standard error. Letters indicate the results of the Kruskal-Wallis test and *post-hoc* means of ranks for all groups test. Treatments with the same letters are not significantly different based on mean ranks comparison test ($p>0.05$), n.s., not significant.

was similar (Supplementary Table 2). The total grazer biomass was 2.5 times higher in the tM enriched samples (Supplementary Table 2). The grazing experiments indicated that both heterotrophic and autotrophic picoplankton were strongly grazed by microzooplankton in most of the mesocosms independent of temperature and tM addition (Table 2), with as much as 60-100% of their potential production consumed daily. By contrast, microzooplankton grazing on nano- and microphytoplankton was not detectable (Table 2).

Ecosystem trophy

Average values indicated that all mesocosms were net-autotrophic, i.e., the difference between primary production (PP) and heterotrophic bacterial production (BP) estimates was positive (Figure 7). However, no statistically significant differences between the treatments were found due to the large within-treatment variations (Figure 7, Supplementary Table 1). In the tM-enriched systems, the average PP-BP value was 3-fold higher than in the non-enriched mesocosms, indicating that tM drove the system towards

10.3389/fmars.2023.1170054

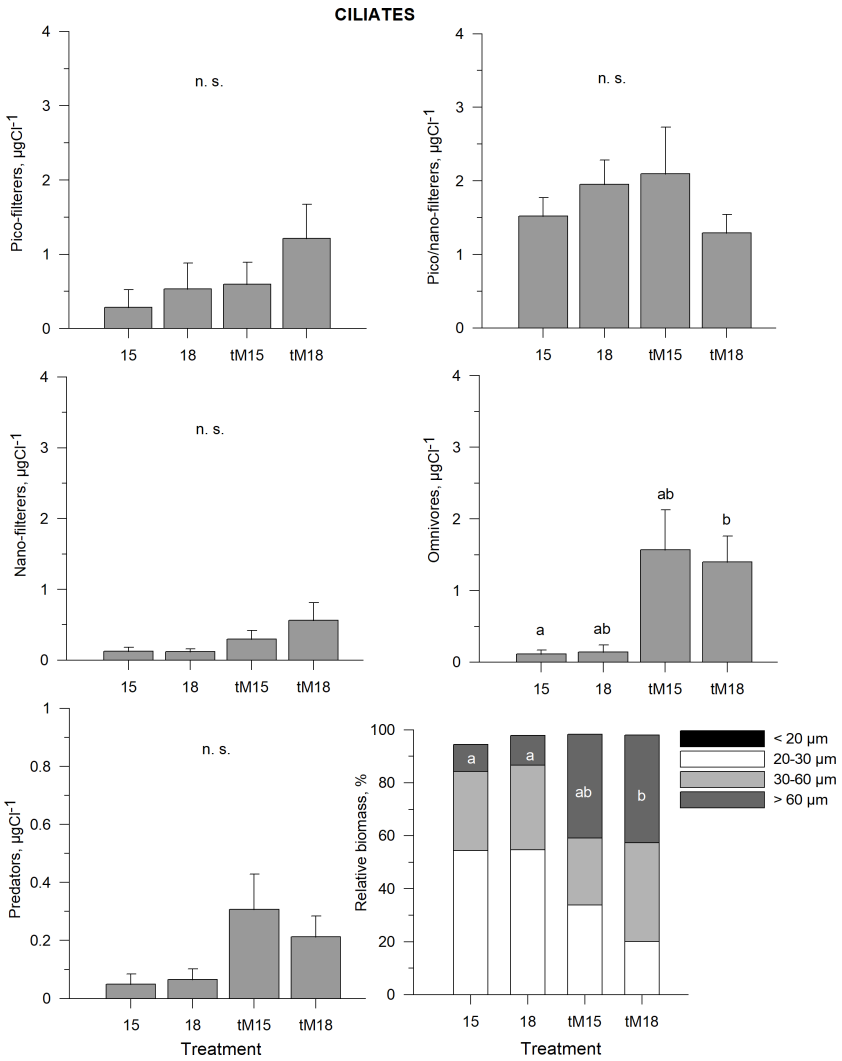

FIGURE 6
Average biomass of different feeding types of ciliates during the last three weeks of the experiment: picoplankton feeders, pico/nanoplankton feeders, nanoplankton feeders, omnivorous and predators in different treatments. Error bars denote standard error. Letters indicate the results of the Kruskal-Wallis test and *post hoc* means of ranks for all groups test. Treatments with the same letters are not significantly different based on mean ranks comparison test (p>0.05), n.s., not significant.

increased net-autotrophy. No indication of temperature effects on the ecosystem trophy was found (Figure 7).

Discussion

The experiment started during the spring bloom, but after a few weeks of incubation the plankton communities and production rates were similar to that of a natural summer community in the study area (e.g. Andersson et al., 2018). The plankton composition and production varied in different treatment, implying that the results would mimic environmental changes during the summer period. We found that the addition of terrestrial organic matter induced significant changes in the production and structure of the microbial food web, including its base (phytoplankton and heterotrophic bacteria) and consumers (ciliates), while elevated temperature only had a slight restructuring effect on the different food web components.

Although the treatments induced changes in mesozooplankton structure, the mesozooplankton community was unlikely to exert substantial predation on the microbial food web because it was heavily predated upon by the fish present in the system. During the experiment, the mesozooplankton biomass decreased from 4 to 2 µg C l^{-1}, corresponding to the lower range of the biomass observed in the Baltic Sea (e.g. Dahlgren et al., 2010). The mesozooplankton to ciliate ratio was low (0.25). We, therefore, assume that

10.3389/fmars.2023.1170054

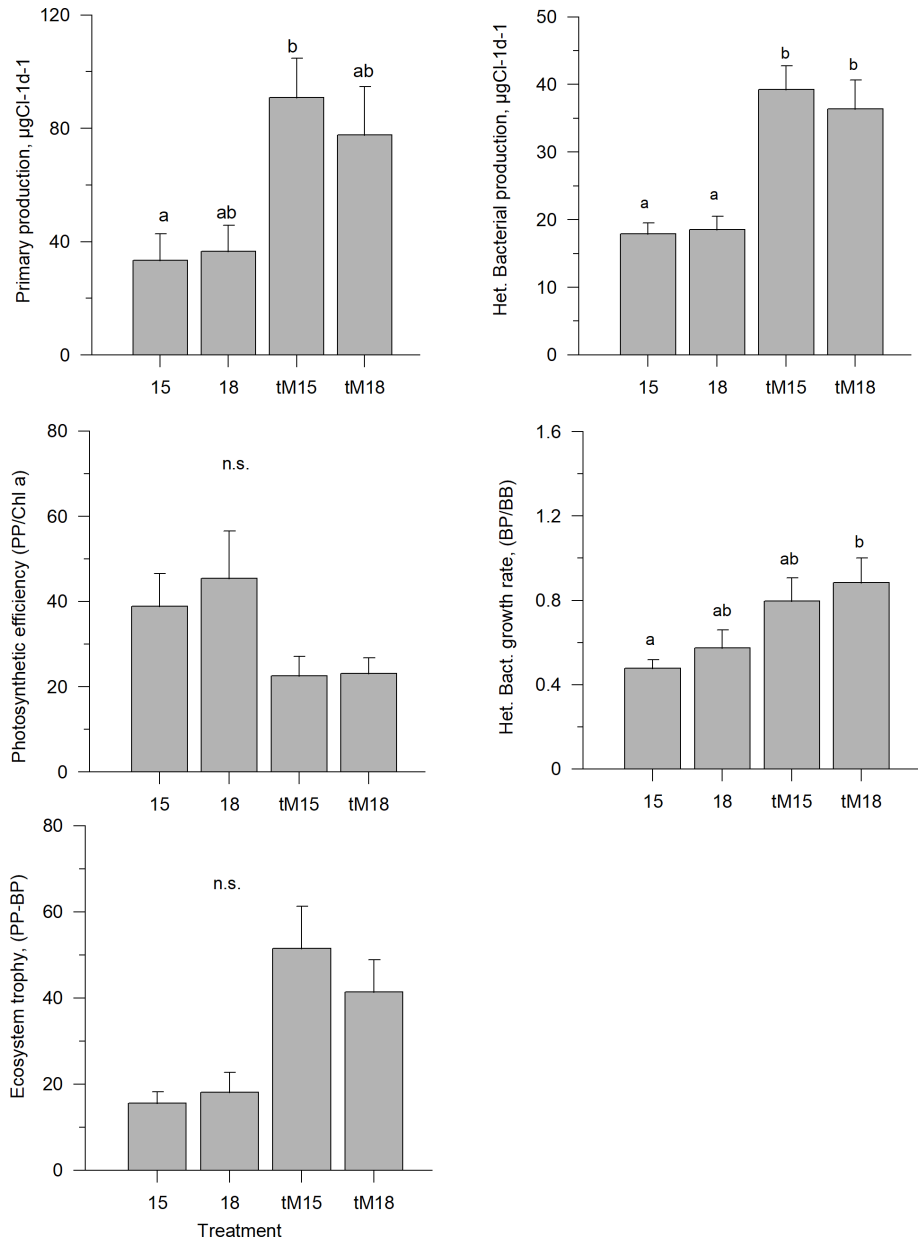

FIGURE 7
Average phytoplankton and heterotrophic bacterial production rates during the last three weeks of experiment; primary production (PP), bacterial production (BP), photosynthetic efficiency (PP/Chla), bacterial specific growth rate (BP/BB) and ecosystem trophy in different treatments. Error bars denote standard error. Letters indicate the results of the Kruskal-Wallis test and *post hoc* means of ranks for all groups test. Treatments with the same letters are not significantly different based on mean ranks comparison test ($p>0.05$), n.s., not significant.

mesozooplankton grazing on the microbial food was relatively low and that we can interpret the treatment effects on the microbial food web structure and function as bottom-up effects.

Terrestrial matter promoted both autotrophs and heterotrophs at the food web base

Both primary production and heterotrophic bacterial production were elevated in the tM treatments. The high inorganic nutrient concentrations due to the tM addition have likely promoted phytoplankton growth. In fact, the DIN and DIP concentrations were 1-4 fold higher in the tM-enriched systems. Even though the brown color of the tM caused decreased photosynthetically active radiation (PAR) by 35%, from ~250 to 150 µmol photon m^{-2} s^{-1} (midday), these values indicate that light would be sufficient for light-saturated photosynthesis (Andersson et al., 1994). The mesocosm light conditions were similar to that in surface water in the study area during summer (Andersson et al., 2018). Nevertheless, the lower light levels require higher cell pigment content leading to decreased photosynthetic efficiency in the tM-enriched mesocosms.

10.3389/fmars.2023.1170054

TABLE 2 Initial abundances of bacteria and phytoplankton size fraction <3 µm and 3-50 µm, growth rates of bacteria and phytoplankton (µ, day^{-1}), grazing rates (g, day^{-1}) and potential production grazed per day (%) in different treatments.

Prey type	Treatment	Initial abund.ml^{-1}	µ	g	R^2	Potential production grazed, %
Bacteria	15	1832051	0.52	0.46	0.82	91
	18	1206263	0.60	0.55	0.93	94
	tM15	1538119	0.39	0.21	0.61	59
	tM18	1652092	0.36	0.41	0.72	111
Phytoplankton fractions	<3 µm					
	15	31611	n.s.	n.s.	n.s.	n.s.
	18	62795	0.35	0.37	0.92	105
	tM15	68286	0.23	0.21	0.67	92
	tM18	62327	n.s.	n.s.	n.s.	n.s.
	3-50 µm					
	15	3238	n.s.	n.s.	n.s.	n.s.
	18	3404	n.s.	n.s.	n.s.	n.s.
	tM15	10249	n.s.	n.s.	n.s.	n.s.
	tM18	8593	n.s.	n.s.	n.s.	n.s.

n.s., not significant.

Promotion of heterotrophic bacterial growth and production by terrestrial matter agrees with the earlier field and experimental studies. Two field studies in the northern Baltic Sea coast showed peaks of bacterial production during the spring river flush and positive correlations between heterotrophic bacterial production and DOC, humic substances and colored dissolved organic matter (CDOM) (Figueroa et al., 2016; Andersson et al., 2018). Other mesocosm experiments have also shown that terrestrial matter enrichment induces elevated heterotrophic bacterial production in coastal waters of the northern Baltic Sea (e.g. Lefébure et al., 2013). Thus, the heterotrophic bacterial growth response can be explained by terrestrial matter being available as a substrate for bacteria, even though a large proportion is refractory (Zhao et al., 2022).

Terrestrial matter shifted the microbial food web towards larger cell size

The addition of terrestrial matter shifted the organism size distribution of the food web base (autotrophic and heterotrophic picoplankton, nanoflagellates and microphytoplankton) towards a larger size. The promotion of large-sized plankton at the food web base was likely caused by the 2-4 fold increase in the nutrient concentrations following the tM addition, implying that the tM-enriched mesocosms had a higher carrying capacity for the standing stocks. Although small osmotrophic cells, with their large surface-to-volume ratios, are more competitive in nutrient uptake at low nutrient concentrations, large cells have an advantage when nutrients are abundant (Samuelsson et al., 2002).

Since the aquatic food web is size-structured (Fenchel, 1987), we could expect that the highest trophic level of the microbial food web, e.g. ciliates, would also show increased cell size. This was indeed observed (Figure 6), and the total biomass and contribution of ciliates >60 µm were higher in the tM-enriched mesocosms. The dominant >60 µm taxa, *Stylonichia* sp, is an omnivorous ciliate, which is known to feed on a large size range of organisms (Pfister and Arndt, 1998). The results agree with earlier modeling and experimental studies showing that an increase in carrying capacity facilitates the propagation of omnivorous ciliates in microbial systems (Diehl and Feissel, 2000).

Rotifers that responded positively to the terrestrial matter addition, albeit only at the higher temperature (Figure 4), could likely exert a strong predation pressure on the small-sized ciliates, thus exacerbating the shift towards larger ciliates in the community. The rotifer species in the mesocosms, *Keratella quadrata* and *Synchaeta* spp., prey preferably on small ciliates and can affect their abundances (Gilbert and Jack, 1993). Therefore, both bottom-up and top-down control mechanisms were most probably contributing to the observed size pattern of the consumers in the microbial food web.

Taken together, terrestrial matter addition promoted larger cell size at the base of the food web. The higher overall production by heterotrophic bacteria and phytoplankton in tM mesocosms caused increased biomass of nano- and microphytoplankton, resulting in an increased fraction of autotrophic microphytoplankton (>20 µm) driven by the high nutrient concentrations. All these changes at the base cascaded to the highest trophic level of the microbial food web composed of larger size ciliates. Moreover, at the higher temperature, the food base and ciliate community changes passed on mesozooplankton and promoted rotifers, which could exacerbate the shift to the large ciliates by selective feeding on small ciliates.

Elevated temperature increased heterotrophic bacterial growth rate and induced smaller size at the food web base

As expected, the elevated temperature increased heterotrophic bacterial growth in both the tM and the non-enriched mesocosms. These results comply with earlier studies showing that increased temperature causes increased bacterial growth rate when nutrients and other resources are available (e.g. Degerman et al., 2013). Apparently, sufficient resources were available in our experiment to support bacterial growth even though inorganic nutrients, especially dissolved inorganic phosphorus (DIP), decreased to very low values (close to the detection limit) in the non-enriched incubations. A fast turn-over with re-mineralized nutrients immediately taken up by bacteria after their release by protozoa, mesozooplankton and fish would result in very low inorganic nutrient values. Since a complete food web was present in all mesocosms, from microbes to fish, re-mineralization of nitrogen and phosphorus and release of DOC by heterotrophic organisms would have continuously renewed and recycled these nutrients (Andersson et al., 1985; Legendre and Rassoulzadegan, 1995). Nevertheless, a nutrient limitation was likely in the non-enriched high-temperature incubations (18°C) compared to the control (15°C). However, no net effect of temperature on total heterotrophic bacterial production was observed, which may have been due to predation control from microzooplankton (phagotrophic nanoflagellates and ciliates).

Increased temperature led the food web base to shift towards smaller cell size, primarily due to the decreased microphytoplankton, while the nano- and picoplankton remained stable. This pattern was observed in both the tM-enriched and non-enriched mesocosms. These results comply with earlier studies reporting that increased temperature promoted smaller-size plankton (e.g., Suikkanen et al., 2013; Mousing et al., 2014). Changed size structure can be caused by faster consumption of nutrients, increased metabolism at the higher temperature, or a combination of both factors. Nutrient measurements showed that DIN and DIP concentrations were reduced during the first week of incubation in all mesocosms. However, later in the experiment, the DIN and DIP concentrations in the tM-enriched mesocosms were twice as high as in the non-enriched irrespective of temperature. As a reduction of the microphytoplankton fraction in both the non-enriched and the tM-enriched mesocosms was found at elevated temperatures, one can speculate that the smaller-celled organisms benefitted due to a faster metabolism combined with the fast nutrient uptake by nano- and picoplankton than by microphytoplankton.

Elevated temperature alone did not cause any major change in either the food base (heterotrophic bacteria, HNF, and total phytoplankton) or the ciliate community during the latter part of the experiment. Pico/nano filtering ciliates dominated the non-enriched mesocosms, with frequently occurring *Strombidium*, *Strobilidium* and *Lohmaniella*, which are common in the study area, the northern Baltic Sea (Samuelsson et al., 2002; Samuelsson and Andersson, 2003). Our results agree with those of Aberle et al. (2007), who observed that the ciliate abundance temporarily increased under elevated temperature due to increased phytoplankton growth in a spring bloom mesocosm experiment (Kiel Bight southern Baltic Sea). However, the growth pulse was shortened by increased temperature. In both studies, the ciliate community was dominated by *Strobilidium* and *Lohmaniella*, and a short, one-week growth pulse was observed due to elevated temperature. Taken together, the plankton succession likely speeds up at elevated temperature, which would be a significant ecological consequence of climate change in coastal waters.

Major energy flow from picoplankton to nanoflagellates and ciliates

The major energy flow from heterotrophic and autotrophic picoplankton to nano- and microzooplankton was apparent in all treatments (Table 2, Figure 8).

In the non-enriched mesocosms, the grazers of the microbial food-web were dominated by heterotrophic and mixotrophic nanoflagellates (71% of the grazers carbon biomass), feeding on bacteria (Andersson et al., 1985; Andersson et al., 1986; Andersson et al., 1989), and <30 µm ciliates (29% of the grazers carbon biomass), which are known to feed on pico-nanoplankton (Foissner and Berger, 1996, Agatha and Riedel-Lorjé, 1997, Gaedke and Wickham, 2004). These findings are in agreement with Rassoulzadegan et al. (1988), who reported that ciliates <30 µm mainly feed on picoplankton (70%) and to a lesser extent on nanoplankton (30%). As we did not detect any significant grazing on 3-50 µm phytoplankton, we assume that ciliate feeding on nanoplankton was minor. We presume that there was a larger energy flow from picoplankton to nanoflagellates than from picoplankton to ciliates in the non-enriched mesocosms, as the microbial food-web grazers were dominated by nanoflagellates (Figure 8).

In the tM-enriched mesocosms, the microbial food-web grazers were dominated by heterotrophic and mixotrophic nanoflagellates (51% of the grazers carbon biomass) feeding on bacteria, and ciliates >30 µm (49% of the grazers carbon biomass), known to feed on various organisms, from pico- to microplankton (Rassoulzadegan et al., 1988; Foissner and Berger, 1996; Gaedke and Wickham, 2004). Common genera within this size group were *Tintinnopsis* and *Holophrya*, and *Stylonychia*, a relatively large (100 µm) ciliate feeding on pico-, nano- and microplankton (Pfister and Arndt, 1998). Although the grazing experiment did not detect any significant ciliate feeding on nano- and microphytoplankton by these ciliates, we assume that such pathways exist (Figure 8). The grazing experiment might have a greater capacity to detect grazing on more abundant small organisms (picoplankton) than on relatively rare larger organisms (nano- and microplankton). Another concern regarding the grazing experiment design is the excess of nutrients added to the microcosms to exclude the possibility of nutrient limitation. As these nutrients can introduce nonlinearity in the phytoplankton growth, the results should be interpreted with caution. We presume that the energy flow from picoplankton was similarly supplied to nanoflagellates and ciliates in the tM-treated mesocosms, as the microbial food-web grazer biomass was equally distributed between nanoflagellates and ciliates (Figure 8).

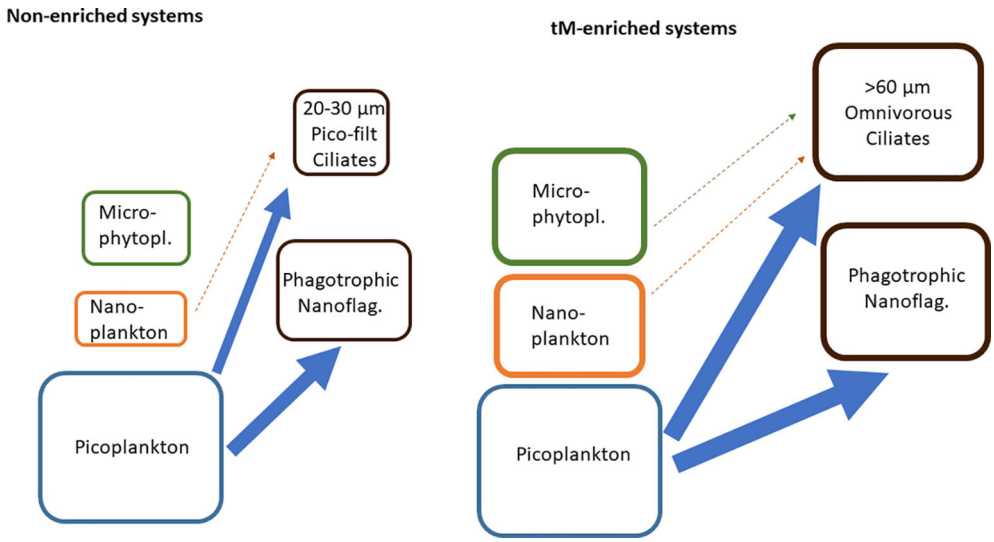

FIGURE 8
Simplified view of the energy flows in the non-enriched and tM enriched mesocosms. *Potential food sources:* picoplankton (heterotrophic bacteria, cyanobacteria and autotrophic eukaryotes), nanoplankton (heterotrophic, autotrophic and mixotrophic organisms), microphytoplankton (autotrophic organisms). *Grazers* phagotrophic nanoflagellates (heterotrophic and mixotrophic flagellates), ciliates (20-30 µm filtering ciliates and >60 µm omnivorous ciliates). Arrows indicate energy flows.

In tM-enriched mesocosms, the nano- and microphytoplankton biomass increased, while the picoplankton did not. Concurrently, the heterotrophic bacterial production and growth rate increased in the tM-enriched mesocosms, which, together with the grazing experiment results, suggests a fast turnover of the heterotrophic bacterial biomass (24 hours, Table 2). We did not measure the picophytoplankton production; however, the picophytoplankton peaked in the middle of the experiment in the tM-enriched mesocosms, indicating that autotrophic picoplankton also had a fast turnover due to its rapid growth and grazing.

Taken together, we found picoplankton to be a key group in the energy flows of the microbial food webs, irrespective of treatment, thus supporting the findings of Paczkowska et al. (2020). However, this pathway has been overlooked in many previous studies that did not analyze autotrophic eukaryotic picoplankton (e.g., Andersson et al., 1996). One reason for that could be technical challenges, because the Utermöhl technique does not allow detection of picoplankton, and epifluorescence microscopy has practical limitations for detecting this group of organisms. Using flow cytometry gives cost-efficient, accurate measures of picophytoplankton (Sosik et al., 2010), and should be considered when designing field- and experimental studies of microbial food webs.

Terrestrial organic matter affected ecosystem trophy

Average values indicate that all mesocosms were net-autotrophic, further strengthened by terrestrial matter enrichment. Although the addition of terrestrial matter promoted both heterotrophic bacterial production and primary production, primary production increased more than bacterial production. However, these results are only indicative due to the high variability between the mesocosms. This finding contrasts previous studies on coastal waters showing that terrestrial matter hampers primary production while increasing heterotrophic bacterial production (Andersson et al., 2013; Figueroa et al., 2016; Andersson et al., 2018; Paczkowska et al., 2020), leading to ecosystem net-heterotrophy. Nevertheless, in ecosystems undergoing critical transitions, a high variability often proceeds the functional change (Dakos et al., 2012). Ecosystem trophy is an important functional trait, and our study indicates that shallow coastal areas can shift between net-heterotrophy and net-autotrophy. In shallow lakes, terrestrial matter inflows can positively affect primary production because these inflows also bring nutrients. Moreover, light has been pointed out as a critical factor of the adverse effects of terrestrial matter on primary production (Seekell et al., 2015). Yet, in shallow lakes where light can reach pelagic and benthic primary producers, terrestrial matter inflows can support their growth. Therefore, it is plausible that terrestrial matter can promote primary production in shallow coastal environments where light is not limiting.

Conclusions

If climate change follows current projections (Meier et al., 2022), heterotrophic bacterial production and phytoplankton production will likely increase in shallow coastal areas in the northern Baltic Sea. The combined effects of elevated temperature and increased inflows of terrestrial matter in coastal microbial food webs would mainly be driven by the increased terrestrial matter inflow, while increased temperature may only induce a slight increase of the bacterial

growth rates and a minor size-spectrum change of the food web base. Even though phytoplankton photosynthetic efficiency may decrease due to water darkening, the overall increase in nutrient availability will promote phytoplankton production, and higher temperature will likely speed up the succession. The size structure of the microbial food web base would change towards large-sized microphytoplankton, although picoplankton will still constitute the major biomass pool during the summer season. The restructuring of the food web base may favor relatively large omnivorous ciliates, which feed on different size groups of plankton, pico-, nano-, and microphytoplankton, and microphagous mesozooplankton, such as rotifers. Our study also indicates that terrestrial matter inputs in the nearshore shallow coastal zone might lead to a flipping between net-autotrophy and net-heterotrophy. In conclusion, this study demonstrates that the microbial food web compartments adjust due to increased inputs of terrestrial matter and elevated temperature. In climate altered northern coastal systems the major energy path will likely flow from picoplankton to large-sized ciliates during the summer period.

Data availability statement

The original contributions presented in the study are included in the article/Supplementary Materials. Further inquiries can be directed to the corresponding author.

Ethics statement

The experimental procedures comply with the current laws of Sweden and were approved by the Regional Ethics Committee of the Swedish National Board for Laboratory Animals in Umeå (CFN, license no. A24-11).

Author contributions

AA and MT conceived the study; ÅB, CG, MR, DF, AA and MT further developed the initial design and prepared for practical implementation; ÅB, CG, MR, DF and EGr carried out the mesocosm study; SB analyzed picoplankton and EGo analyzed mesozooplankton; EGr carried out the grazing experiment and performed the statistical analyzes; AA and EGr drafted the initial version of the manuscript; all authors reviewed and improved the manuscript to its final version.

Funding

The project was funded by the Swedish Institute (SI reference number 00140/2014), the Swedish research council FORMAS (FR-2019/0007) and the Swedish strategic marine research program EcoChange.

Acknowledgments

We thank the staff at Umeå Marine Sciences Center for excellent support during the mesocosm study and Jonas Forsberg for analysis of nano- and microplankton. Special thanks Dr. Ekaterina I. Mironova (Institute of Cytology, Russian Academy of Sciences, St. Petersburg) for consultancy on identification of ciliates.

Conflict of interest

The authors declare that the research was conducted in the absence of any commercial or financial relationships that could be construed as a potential conflict of interest.

Publisher's note

Supplementary material

The Supplementary Material for this article can be found online at: https://www.frontiersin.org/articles/10.3389/fmars.2023.1170054/full#supplementary-material

References

Aberle, N., Lengfellner, K., and Sommer, U. (2007). Spring bloom succession, grazing impact and herbivore selectivity of ciliate communities in response to winter warming. *Oecologica* 150, 668–681. doi: 10.1007/s00442-006-0540-y

Agatha, S., and Riedel-Lorjé, J. (1997). Morphology, infraciliature, and ecology of halteriids and strombidiids (Ciliophora, oligotrichea) from coastal brackish water basins. *Archiv für Protistenkunde* 148, 445–459. doi: 10.1016/S0003-9365(97)80021-8

Andersson, A., Falk, S., Samuelsson, G., and Hagström, Å. (1989). Nutritional characteristics of a mixotrophic nanoflagellate, ochromonas sp. *Microb. Ecol.* 17, 251–262 . doi: 10.1007/BF02012838

Andersson, A., Haecky, P., and Hagström, Å. (1994). Effect of temperature and light on the growth of micro- nano- and pico-plankton: impact on algal succession. *Mar. Biol.* 120, 511–520. doi: 10.1007/BF00350071

Andersson, A., Hajdu, S., Haecky, P., Kuparinen, J., and Wikner, J. (1996). Succession and growth limitation of phytoplankton in the gulf of bothnia. *Mar. Biol.* 126, 791–801. doi: 10.1007/BF00351346

Andersson, A., Jurgensone, I., Rowe, O. F., Simonelli, P., Bignert, A., Lundberg, E., et al. (2013). Can humic water discharge counteract eutrophication in coastal waters? *PloS One* 8, 4. doi: 10.1371/journal.pone.00061293

Andersson, A., Larsson, U., and Hagström, Å. (1986). Size-selective grazing by a microflagellate on pelagic bacteria. *Mar. Ecol. Prog. Ser.* 33, 51–57. doi: 10.3354/meps033051

Andersson, A., Lee, C., Azam, F., and Hagström, Å. (1985). Release of amino acids and inorganic nutrients by heterotrophic marine microflagellates. *Mar. Ecol. Prog. Ser.* 23, 99–106. doi: 10.3354/meps023099

Andersson, A., Meier, H. E. M., Ripszam, M., Rowe, O., Wikner, J., Haglund, P., et al. (2015). Projected future climate change and Baltic Sea ecosystem management. *Ambio* 44 (Supplementary 3), 345–356. doi: 10.1007/s13280-015-0654-8

Andersson, A., Paczkowska, J., Brugel, S., Figueroa, D., Rowe, O., Kratzer, S., et al. (2018). Influence of allochthonous dissolved organic matter on pelagic basal production in a northerly estuary. *Estuar. Coast. Shelf Sci.* 204, 225–235. doi: 10.1016/j.ecss.2018.02.032

Ayo, B., Santamaria, E., Latatu, A., Artolozaga, I., Azua, I., and Iriberri, J. (2001). Grazing rates of diverse morphotypes of bacterivorous ciliates feeding on four allochthonous bacteria. *Lett. Appl. Microbiol.* 33, 455–460. doi: 10.1046/j.1472-765X.2001.01034.x

Azam, F., Fenchel, T., Field, J. G., Gray, J. S., Meyer-Reil, L. A., and Thingstad, F. (1983). The ecological role of water-column microbes in the sea. *Mar. Ecol. Prog. Ser.* 10, 257–263. doi: 10.3354/meps010257

Dahlgren, K., Andersson, A., Larsson, U., Hajdu, S., and Båmstedt, U. (2010). Planktonic production and carbon transfer efficiency along a north-south gradient in the Baltic Sea. *Mar. Ecol. Prog. Ser.* 409, 77–94. doi: 10.3354/meps08615

Dakos, V., Carpenter, S. C., Brock, W. A., Ellison, A. M., Guttal, V., Ives, A. R., et al. (2012). Methods for detecting early warnings of critical transitions in time series illustrated using simulated ecological data. *Plosone* 7, e41010. doi: 10.1371/journal.pone.0041010

Degerman, R., Dinasquet, J., De Luna Sjöstedt, S., Riemann, L., and Andersson, A. (2013). Effect of resource availability on bacterial community responses to increased temperature. *Aquat. Microbial Ecol.* 68, 131–142. doi: 10.3354/ame01609

Diehl, S., and Feissel, M. (2000). Effects of enrichment on three-level food chains with omnivory. *Am. Nat.* 155, 200–218. doi: 10.1086/303319

Fenchel, T. (1987). *Ecology of protozoa: the biology of free-living phagotrophic protists* (US: Science Tech Publishers), 197.

Figueroa, D., Rowe, O. F., Paczkowska, J., Legrand, C., and Andersson, A. (2016). Allochthonous carbon–a major driver of bacterioplankton production in the subarctic northern Baltic Sea. *Microbial Ecol.* 71, 789–801. doi: 10.1007/s00248-015-0714-4

Foissner, W., and Berger, H. (1996). A user-friendly guide to the ciliates (Protozoa, ciliophora) commonly used by hydrobiologists as bioindicators in rivers, lakes, and waste waters, with notes on their ecology. *Freshw. Biol.* 35, 375–482. doi: 10.1111/j.1365-2427.1996.tb01775.x

Fuhrman, J., and Azam, F. (1982). Thymidine incorporation as a measure of heterotrophic bacterioplankton production in marine surface waters: evaluation and field results. *Mar. Biol.* 66, 109–120. doi: 10.1007/BF00397184

Gaedke, U., and Wickham, S. (2004). Ciliate dynamics in response to changing biotic and abiotic conditions in a large, deep lake (Lake constance). *Aquat. Microbial Ecol.* 34, 247–261. doi: 10.3354/ame034247

Gilbert, J. J., and Jack, J. D. (1993). Rotifers as predators on small ciliates. *Hydrobiologia* 255, 247–253. doi: 10.1007/BF00025845

Hägg, H. E., Humborg, C., Morth, C. M., Medina, M. R., and Wulff, F. (2010). Scenario analysis on protein consumption and climate change effects on riverine n export to the Baltic Sea. *Environ. Sci. Technol.* 44, 2379–2385. doi: 10.1021/es902632p

Hällfors, G. (2004). *Checklist of Baltic Sea phytoplankton species* (Nairobi: United Nations Environment Programme).

Hausman, K. (1988). *Protozoologiya (Protozoology)* (Moscow, Russia: Mir).

HELCOM. (2013a). Climate change in the Baltic Sea Area: HELCOM thematic assessment in 2013. . *Balt. Sea Environ.* No. 137

HELCOM. (2013b). Manual for marine monitoring in the COMBINE programme of HELCOM. Available at: https://helcom.fi/action-areas/monitoring-and-assessment/monitoring-guidelines/combine-manual/

Hernroth, L. (1985). *Recommendations on methods for marine biological studies in the Baltic Sea: mesozooplankton biomass assessment, Baltic marine biologists* (Lysekil: Institute of Marine Research).

Hoppe, H.-G., Gocke, K., Koppe, R., and Begler, C. (2002). Bacterial growth and primary production along a north-south transect of the Atlantic ocean. *Nature* 416, 168–171. doi: 10.1038/416168a

James, M. R., and Hall, J. A. (1998). Microzooplankton grazing in different water masses associated with the subtropical convergence round the south island, new Zealand. *Deep Sea Res. I* 45, 1689–1707. doi: 10.1016/S0967-0637(98)00038-7

Jonsson, P. R. (1986). Particle size selection, feeding rates and growth dynamics of marine plankton oligotrichous ciliates (Ciliophora: oligotrichina). *Mar. Ecol. Prog. Ser.* 33, 265–277. doi: 10.3354/meps033265

Kivi, K., and Setälä, O. (1995). Simultaneous measurement of food particle selection and clearance rates of planktonic oligotrich ciliates (Ciliophora: oligotrichina). *Mar. Ecol. Prog. Ser.* 119, 125–137. doi: 10.3354/meps119125

Landry, M. R., and Hassett, R. P. (1982). Estimating the grazing impact of marine micro-zooplankton. *Mar. Biol.* 67, 283–288. doi: 10.1007/BF00397668

Lee, S., and Fuhrman, J. (1987). Relationship between biovolume and biomass of naturally derived bacterioplankton. *Appl. Environ. Microbiol.* 53, 1298–1303. doi: 10.1128/aem.53.6.1298-1303.1987

Lefébure, R., Degerman, R., Andersson, A., Larsson, S., Eriksson, L. O., Båmstedt, U., et al. (2013). Impacts of elevated terrestrial nutrient loads and temperature on pelagic food-web efficiency and fish production. *Global Change Biol.* 19, 1358–1372. doi: 10.1111/gcb.12134

Legendre, L., and Rassoulzadegan, F. (1995). Plankton and nutrient dynamics in marine waters. Ophelia. *Ophelia* 41, 153–172. doi: 10.1080/00785236.1995.10422042

Lignell, R., Hoikkala, H., and Lahtinen, T. (2008). Effects of inorganic nutrients, glucose and solar radiation on bacterial growth and exploitation of dissolved organic carbon and nitrogen in the northern Baltic Sea. *Aquat. Microbial Ecol.* 51, 209–221. doi: 10.3354/ame01202

Maeda, M. (1986). An illustrated guide to the species of the families halteriidae and strobilidiidae (Oligotrichida, ciliophora), free swimming protozoa common in the aquatic environment. *Bull. Ocean Res. Inst. Univ. Tokyo* 2, 1–67.

Maeda, M., and Carey, P. (1985). An illustrated guide to the species of the family strombidiidae (Oligotrichida, ciliophora), free swimming protozoa common in the aquatic environment. *Bull. Ocean Res. Inst. Univ. Tokyo* 19, 1–68.

Marie, D., Simon, N., and Vaulot, D. (2005). "Phytoplankton cell counting by flow cytometry," in *Algal culturing techniques*. Ed. R. A. Andersen (San Diego: Academic Press), 253–267. doi: 10.1016/B978-012088426-1/50018-4

Meier, H. E. M., Kniebusch, M., Dieterich, C., Gröger, M., Zorita, E., Elmgren, R., et al. (2022). Climate change in the Baltic Sea region: a summary. *Earth System Dynamics* 13, 457–593. doi: 10.5194/esd-13-457-2022

Meier, H. E. M., Muller-Karulis, B., Andersson, H. C., Dieterich, C., Eilola, K., Gustafsson, B. G., et al. (2012). Impact of climate change on ecological quality indicators and biogeochemical fluxes in the Baltic Sea: a multi-model ensemble study. *Ambio* 41, 558–573. doi: 10.1007/s13280-012-0320-3

Menden-Deuer, S., and Lessard, E. J. (2000). Carbon to volume relationships for dinoflagellates, diatoms, and other protist plankton. *Limnology Oceanography* 45, 569–579. doi: 10.4319/lo.2000.45.3.0569

Mironova, E., Telesh, I., and Skarlato, S. (2013). Planktonic ciliates of the Neva estuary (Baltic sea): community structure and spatial distribution. *Acta Protozoologica* 52, 13–23. doi: 10.4467/16890027AP.13.002.0830

Mousing, E. A., Ellegaard, M., and Richardson, K. (2014). Global patterns in phytoplankton community size structure [[/amp]]mdash; evidence for a direct temperature effect. *Mar. Ecol. Prog. Ser.* 497, 25–38. doi: 10.3354/meps10583

Müren, U., Samuelsson, K., Berglund, J., and Andersson, A. (2005). Potential effects of elevated seawater temperature on pelagic food webs. *Hydrobiologia* 545, 153–166. doi: 10.1007/s10750-005-2742-4

Olenina, I., Hajdu, S., Edler, L., Andersson, A., Wasmund, N., Busch, S., et al. (2006). Biovolumes and size-classes of phytoplankton in the Baltic Sea. *HELCOM Baltic Sea Environ. Proc.* 106, 1–144.

Paczkowska, J., Brugel, S., Rowe, O. F., Lefébure, R., Brutemark, A., and Andersson, A. (2020). Response of coastal phytoplankton to high inflows of terrestrial matter. *Front. Mar. Sci.* 7-2020 doi: 10.3389/fmars.2020.00080

Paczkowska, J., Rowe, O., Figueroa, D., and Andersson, A. (2019). Drivers of phytoplankton production and community structure in nutrient-poor estuaries receiving terrestrial organic inflow. *Mar. Environ. Res.* 151, 1-10. doi: 10.1016/j.marenvres.2019.104778

Pfister, G., and Arndt, H. (1998). Food selectivity and feeding behaviour in omnivorous filter-feeding ciliates: a case study for Stylonychia. *European Journal for Protistology* 34, 446–457. doi: 10.1016/S0932-4739(98)80013-8

Pörtner, H.-O., Roberts, D. C., Poloczanska, E. C., Mintenbeck, K., Tignor, M., Alegría, A., et al. (2022). "Technical summary," in *Climate change 2022: impacts, adaptation and vulnerability. contribution of working group II to the sixth assessment report of the intergovernmental panel on climate change* (Cambridge, UK and New York, NY, USA: Cambridge University Press), 37–118. doi: 10.1017/9781009325844.002

Rassoulzadegan, F. E., Laval-Peuto, M., and Sheldon, R. W. (1988). Partitioning of the food ration of marine ciliates between pico- and nanoplankton. *Hydrobiologia* 159, 75–88. doi: 10.1007/BF00007369

Ripszam, M., Gallampois, C., Berglund, Å., Larsson, H., Andersson, A., and Tysklind, M. (2015). Effects of predicted climatic changes on fates of organic contaminants in brackish water mesocosms. *Sci. Total Environ.* 517, 10–21. doi: 10.1016/j.scitotenv.2015.02.051

Rose, J. M., Feng, Y., Gobler, C. J., Gutierrez, R., Hare, C. E., Leblanc, K., et al. (2009). Effects of increased pCO2 and temperature on the north Atlantic spring bloom. II. microzooplankton abundance and grazing. *Mar. Ecol. Prog. Ser.* 388, 27–40. doi: 10.3354/meps08134

Samuelsson, K., and Andersson, A. (2003). Predation limitation in the pelagic microbial food web in an oligotrophic aquatic system. *Aquat. Microbial Ecol.* 30, 239–250. doi: 10.3354/ame030239

Samuelsson, K., Haecky, P., Berglund, J., and Andersson, A. (2002). Structural changes in an aquatic microbial food web caused by inorganic nutrient addition. *Aquat. Microbial Ecol.* 29, 29–38. doi: 10.3354/ame029029

Seekell, D. A., Lapierre, J. F., Ask, J., Bergstrom, A. K., Deininger, A., Rodriguez, P., et al. (2015). The influence of dissolved organic carbon on primary production in northern lakes. *Limnology Oceanography* 60, 1276–1285. doi: 10.1002/lno.10096

Sosik, H. M., Olson, R. J., and Armbrust, E. V. (2010). Flow cytometry in phytoplankton research. In: DJ Suggett O Prášil, M.A. Borowitzka (eds.) Chlorophyll a Fluorescence in Aquatic Sciences: Methods and Applications, Developments in Applied Phycology 4, Springer Dordrecht. doi: 10.1007/978-90-481-9268-7_8

Stepanauskas, R., Jorgensen, N. O. G., Eigaard, O. R., Zvikas, A., Tranvik, L. J., and Leonardson, L. (2002). Summer inputs of riverine nutrients to the Baltic Sea: bioavailability and eutrophication relevance. *Ecol. Monogr.* 72, 579–597. doi: 10.1890/0012-9615(2002)072[0579:SIORNT]2.0.CO;2

Stürder-Kypke, M. C., Kypke, E. R., Agatha, S., Warwick, J., and Motagnes, D. J. S. (2000). The "user friendly" guide to coastal planktonic ciliates. The Planktonic Ciliate Project by University of Liverpool on the internet. Available at: http://www.liv.ac.uk/ciliate/intro.htm

Suikkanen, S., Pulina, S., Engström-Öst, J., Lehtiniemi, L., Lehtinen, S., and Brutemark, A. (2013). Climate change and eutrophication induced shifts in northern summer plankton communities. *PloS One* 6, e66475. doi: 10.1371/journal.pone.0066475

Tikkanen, T., and Willen, T. (1992). *Phytoplankton flora* (Solna: The Swedish Environmental Protection Agency).

Utermöhl, H. (1958). Zur vervollkommnung der quantitativen phytoplankton-methodik. *Internationale Vereinigung für theoretische und angewandte Limnologie: Mitt.* 9, 1–38.

Vähätalo, A. V., Aarnos, H., Hoikkala, L., and Lignell, R. (2002). Photochemical transformation of terrestrial dissolved organic matter supports hetero- and autotrophic production in coastal waters. *Mar. Ecol. Prog. Ser.* 423, 1–14. doi: 10.3354/meps09010

Verity, P. G., and Lagdon, C. (1984). Relationships between lorica volume, carbon, nitrogen, and ATP content of tintinnids in Narragansett bay. *J. Plankton Res.* 6, 859–868. doi: 10.1093/plankt/6.5.859

Wikner, J., and Hagström, Å. (1999). Bacterioplankton intra-anual variability: importance of hydrography and competition. *Aquat. Microbial Ecol.* 20, 245–260. doi: 10.3354/ame020245

Zhao, L., Brugel, S., Ramasamy, K. P., and Andersson, A. (2022). Response of coastal *Shewanella* and *Duganella* bacteria to planktonic and terrestrial food substrates. *Front. Microbiol.* 12-2021 doi: 10.3389/fmicb.2021.726844

frontiers | Frontiers in Marine Science

TYPE Review
PUBLISHED 02 August 2023
DOI 10.3389/fmars.2023.1198263

OPEN ACCESS

EDITED BY
Jacob Carstensen,
Aarhus University, Denmark

REVIEWED BY
Yanbin Li,
Ocean University of China, China
Dandan Duan,
Hainan Normal University, China

*CORRESPONDENCE
Juanjo Rodríguez
jj.rserrano@gmail.com

RECEIVED 31 March 2023
ACCEPTED 10 July 2023
PUBLISHED 02 August 2023

CITATION
Rodríguez J (2023) Mercury methylation in boreal aquatic ecosystems under oxic conditions and climate change: a review. *Front. Mar. Sci.* 10:1198263. doi: 10.3389/fmars.2023.1198263

Mercury methylation in boreal aquatic ecosystems under oxic conditions and climate change: a review

Juanjo Rodríguez*

Department of Ecology and Environmental Sciences, Umeå University, Umeå, Sweden

Methylmercury (MeHg) formation is a concerning environmental issue described in waters and sediments from multiple aquatic ecosystems. The genetic and metabolic bases of mercury (Hg) methylation have been well described in anoxic environments, but a number of factors seem to point towards alternative pathways potentially occurring in pelagic waters under oxic conditions. Boreal aquatic ecosystems are predicted to undergo increasing concentrations of dissolved organic matter (DOM) as a result of higher terrestrial runoff induced by climate change, which may have important implications in the formation of MeHg in the water column. In this review, different Hg methylation mechanisms postulated in the literature are discussed, with particular focus on potential pathways independent of the *hgcAB* gene pair and occurring under oxic conditions. Potential effects of DOM on Hg methylation and MeHg bioaccumulation are examined in the context of climate in boreal aquatic ecosystems. Furthermore, the implementation of meta-omic technologies and standardized methods into field measurements and incubation experiments is discussed as a valuable tool to determine taxonomic and functional aspects of Hg methylation in oxic waters and under climate change-induced conditions.

KEYWORDS

mercury methylation, oxic waters, climate change, omic technologies, microbial communities

Introduction

Mercury (Hg) is a heavy metal with no physiological role for any known life form. It can be naturally found in geological deposits and coal, but human activities have greatly enhanced the mobilisation and transport of Hg into natural environments (Streets et al., 2011; Mason et al., 2012). Anthropogenic activities, such as coal combustion, mining, and technology industries, release large quantities of mercury into the atmosphere every year (~ 2000 metric tons), which is mainly transported as elemental mercury (Hg^0) by atmospheric currents (Pirrone et al., 2010; Zhang et al., 2016; Kuss et al., 2018; Ghimire et al., 2019). In the global biogeochemical cycle of mercury (Figure 1), Hg^0 is oxidized by different molecules present in

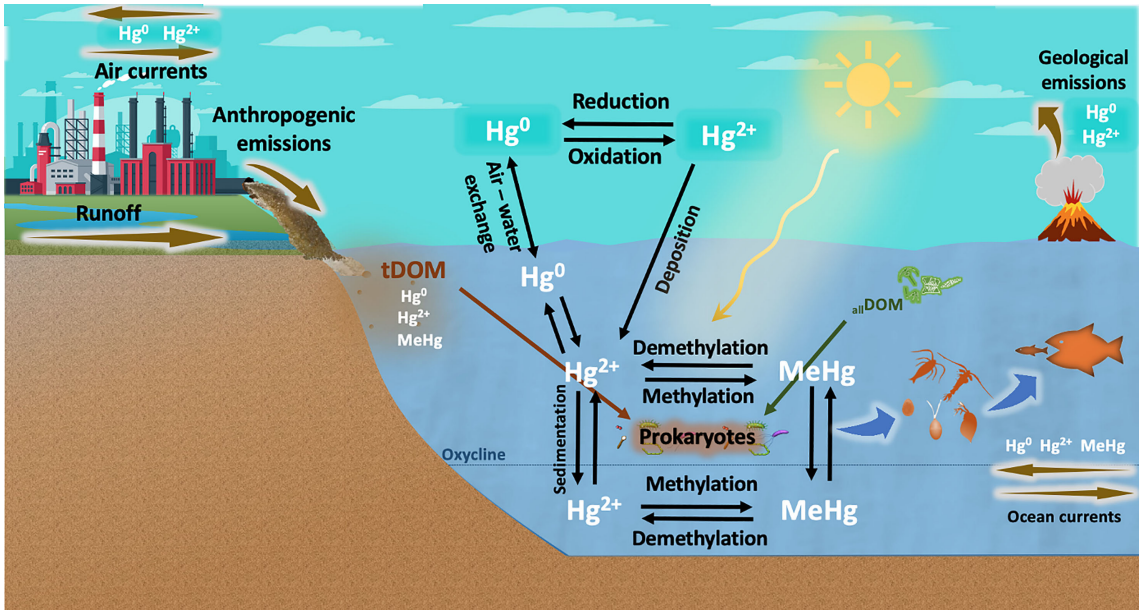

FIGURE 1
Geobiochemical cycle of mercury (Hg) in aquatic environments. Hg is released by anthropogenic activities and geological processes. Elemental mercury (Hg^0) is transported by atmospheric currents and oxidized to divalent inorganic mercury (Hg^{2+}), which is eventually deposited in aquatic ecosystems. Part of this Hg^{2+} is reduced to Hg^0 and recirculated back into the atmosphere, but a substantial portion of Hg^{2+} is bound to DOM molecules and transformed into methylmercury (MeHg) by abiotic processes (e.g., UV radiation) and, to a greater extent, by prokaryotic communities. MeHg formation can be enhanced by DOM from terrestrial origin (tDOM) and DOM freshly produced by phytoplankton communities (allochthonous DOM, $_{all}$DOM), and is then bioaccumulated up to the food web. Hg methylation has been well described to occur in anoxic layers of the water column through metabolic pathways involving *hgcAB* genes. However, the biotic methylation of Hg under oxic conditions is not well understood and is currently under debate.

the atmosphere (e.g., halogen compounds, nitrate radicals or ozone) and eventually converted into divalent inorganic mercury (Hg^{2+}), which is then deposited into aquatic and terrestrial environments (Ariya and Peterson, 2005; Kuss et al., 2018; Bowman et al., 2020). Thereafter, part of the Hg^{2+} is reduced and recirculated back to the atmosphere as Hg^0, but, due to its high reactivity, Hg^{2+} tends to rapidly bind to more stable molecules present in waters and sediments, remaining in these ecosystems for long periods (Krabbenhoft and Sunderland, 2013). Once in aquatic environments, mercury is transformed and uptaken by the resident biota as methylmercury (MeHg), which is bioaccumulated and biomagnified as it is transferred up to the food chain (Boening, 2000; Ullrich et al., 2001; Jonsson et al., 2014). This organic form of mercury is known to be a potent neurotoxin with severe effects for ecosystem health. On humans, MeHg can cause multiple adverse effects, such as neurological and endocrine disorders, cardiovascular problems, or fetal death (Tsubaki and Irukayama, 1977; Grandjean et al., 2004; Tan et al., 2009).

MeHg problematic and early studies

The problematic of MeHg as environmental pollutant dates back to 1960s, where Minamata Disease was postulated to be caused by MeHg poisoning (Minamata Disease Research Group, 1966). Similarly, Westoo (1967) reported abnormally high concentrations of mercury in fish and other foodstuff in Sweden, where 80% to 100% of the mercury was present as MeHg. Considering these and other similar major public health outbreaks worldwide, the microbial participation in MeHg formation in natural aquatic ecosystems was postulated for the first time in a series of studies by Jernelov (1969), where mercury chloride was added into bottom lake sediments and MeHg was observed to be formed after 5-10 days. MeHg was not detected when the sediments were previously sterilized, which led to the conclusion that this process must involve microbial activity, although no microbial species or genes were postulated at the time (Jensen and Jernelöv, 1969; Jernelov, 1969). In addition, one year earlier, Wood et al. (1968) had shown that MeHg could be formed from methylcobalamin when an extract of a methanogenic bacterium (isolated from a canal mud) was incubated with ATP and Hg^{+2} under a hydrogen atmosphere (anoxic conditions).

In light of the emerging knowledge of biotic methylation as the primary source of MeHg, important progress was made by further studies identifying microbial species capable of Hg methylation, particularly in anoxic conditions. Initially, several studies reported microbial methylators under culture-based conditions, isolates and cell extracts (Wood et al. 1968; Taira, 1975; Ridley et al., 1977; Robinson and Tuovinen, 1984), which left yet unresolved the methylation of Hg by complex communities under natural conditions. Compeau and Bartha (1985) was the first comprehensive study identifying and isolating a particular bacterial species capable of Hg methylation in natural aquatic environments. They demonstrated *Desulfovibrio desulfuricans*

capability to methylate Hg^{2+} in low-salinity anoxic estuarine sediments, postulating, for the first time, sulfate-reducing bacteria as major methylators in anoxic aquatic environments. Multiple later studies continued reporting new bacterial species and entire functional groups responsible for MeHg formation in natural environments, from sulfate- and iron-reducing bacteria (e.g., *Geobacter sulfurreducens*, *Desulfuromonas palmitatis*, *Desulfosporosinus acidiphilus*) to methanogenic *Archaea* (e.g., *Methanolobus tindarius*, *Methanobrevibacter smithii*, *Methanoculleus bourgensis*) (Kerin et al., 2006; Ranchou-Peyruse et al., 2009; Gilmour et al., 2013; Podar et al., 2015; Bravo et al., 2018; Jones et al., 2019; Capo et al., 2020b; Gionfriddo et al., 2020). However, the molecular bases (genes and enzymes) behind Hg methylation remained unclear, which implied a substantial gap towards a full understanding of this process. This gap would be in turn fulfilled with the discovery of the hgcAB gene cluster.

HgcAB pathway and the emerging paradigm shift

Since its discovery in 2013 (Parks et al., 2013), the hgcAB gene cluster has captured most of the attention in studies on Hg methylation, as *hgc*A and *hgc*B genes have been proven to be involved in the formation of the bulk of MeHg found in aquatic environments. In a series of experiments, Parks et al. (2013) demonstrated that the biotic formation of MeHg requires the presence of both *hgc*A and *hgc*B genes in the methylator's genome. The deletion of either of these genes supresses the ability to methylate Hg through the reductive acetyl–coenzyme A pathway, but it does not hamper cell growth, which suggests that *hgc*A and *hgc*B are not essential for survival (Parks et al., 2013). *Hgc*A has been described to encode the putative protein HgcA, which is responsible for the transfer of methyl groups to Hg^{2+}. On the other hand, *hgc*B encodes a 2[4Fe-4S] ferredoxin (HgcB protein) capable of reducing a corrinoid cofactor present in HgcA, which enables the acceptance of a methyl group by HgcA. Therefore, the redox potential is an important physicochemical factor that can control Hg uptake and MeHg production by regulating the enzymatic activity of the methylators (Beckers et al., 2019; Regnell and Watras, 2019; Wang et al., 2021).

After a decade of numerous studies on the mechanism of Hg methylation, hgcAB gene cluster has been found in every known anaerobic Hg methylator and in metagenomes from multiple anoxic sediments and waters containing substantial MeHg concentrations (Paranjape and Hall, 2017; Gionfriddo et al., 2019; Ma et al., 2019; Regnell and Watras, 2019; Capo et al., 2020a). This fact has led to the use of *hgcAB* genes as indicators of potential Hg methylation occurring in anoxic aquatic environments. However, recent studies have reported environmentally high concentrations of MeHg in surface waters (Lehnherr et al., 2011; Kirk et al., 2012; Paranjape and Hall, 2017; Villar et al., 2020), where the concentration of oxygen would not allow Hg methylators to perform through the acetyl-CoA/hgcAB pathway. These observations were hypothesised by early studies to be caused by MeHg production in anoxic coastal sediments, which would be then transported to the overlying water column and open waters (Kraepiel et al., 2003; Hammerschmidt and Fitzgerald, 2006). However, this hypothesis conflicts with results from more recent studies showing high demethylation rates and short MeHg lifetime (Monperrus et al., 2007; Whalin et al., 2007; Lehnherr et al., 2011; Ortiz et al., 2015; Wang et al., 2020), which would prevent MeHg to remain in substantial quantities throughout such journey (Cossa et al., 2017). Furthermore, this hypothesis also contrasts with MeHg profiles reported by numerous studies, where the highest concentrations are found in subsurface layers, while deeper waters show lower concentrations (Mason and Fitzgerald, 1993; Cossa et al., 2009; Sunderland et al., 2009; Heimbürger et al., 2015; Munson et al., 2015). External sources, such as atmospheric MeHg deposition and riverine transport, could also be regarded as significant factors, but they are currently considered to be minor sources for the MeHg concentrations found in most marine pelagic environments (Mason et al., 2012; Liu et al., 2021; Wang et al., 2022).

Alternatively, *in situ* methylation of inorganic Hg has been suggested by numerous studies to be the main source of MeHg in the water column. In an incubation experiment, Lehnherr et al. (2011) reported water-column Hg methylation as a significant source of monomethylmercury in Arctic pelagic marine food webs, estimating this process to account for up to 47% of the total monomethylmercury found in these seawaters. Similar studies have also reported MeHg formation in oxygenated marine waters where no known anaerobic methylators or *hgc*AB genes were detected (Malcolm et al., 2010; Podar et al., 2015; Bowman et al., 2019; Rodríguez et al., 2022). These observations pose an apparent paradox where MeHg is produced in non-anoxic waters through a process where anaerobic methylators are considered the main players. As a result, four main explanations can be postulated (Figure 2): 1) Hg methylation by abiotic processes; 2) Biotic MeHg production within anoxic micro-environments; 3) Biotic MeHg production under oxic conditions through metabolic pathways involving *hgcAB* (or *hgcAB*-like) genes or 4) independent of *hgc*AB genes.

The abiotic methylation of Hg has been repeatedly addressed in numerous studies (Celo et al., 2006; Li and Cai, 2013; Regnell and Watras, 2019; Chetelat et al., 2022). While photochemical and non-photochemical methylation are partially responsible for the production of MeHg in oxic waters, these abiotic mechanisms do not generally account for a substantial fraction of the MeHg found in pelagic environment (Monperrus et al., 2007; Lehnherr et al., 2011; Munson et al., 2018; Wang et al., 2022). Therefore, this review will mainly focus on the biotic mechanisms potentially occurring in oxic waters.

Anoxic micro-environments as Hg methylation hotspots in oxic waters

The existence of settling particles in the pelagic zone, enriched in organic matter and showing marked oxygen and pH gradients has been documented since the 1980s (Alldredge and Cohen, 1987; Decho, 1990; Shanks and Reeder, 1993). These particles can range in size from colloids (< 0.2 μm) to aggregates (> 300 μm). In

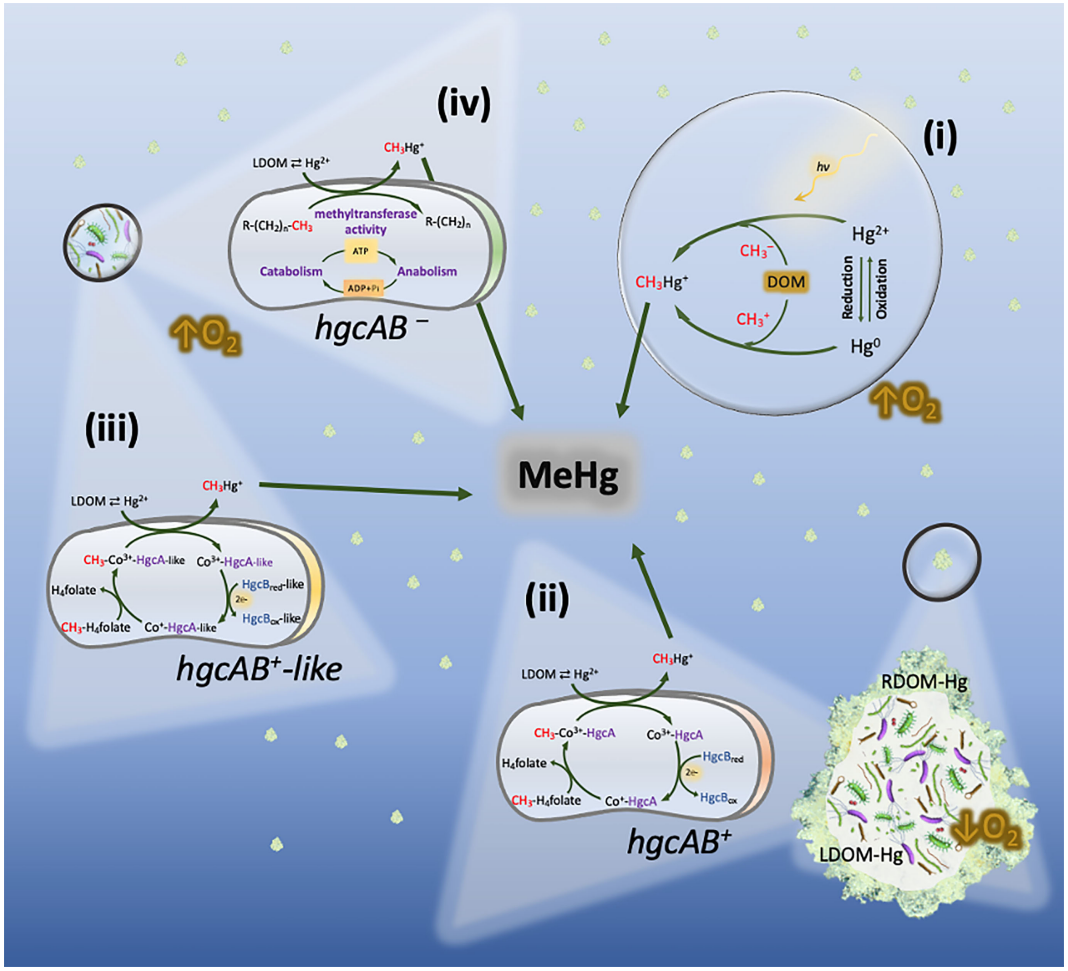

FIGURE 2
Hg methylation pathways potentially co-occurring in oxic layers of the water column. (i) Abiotic Hg methylation, with photochemical and non-photochemical (involving DOM molecules) processes taking place simultaneously. (ii) Biotic Hg methylation by hgcAB^{+} anaerobes (e.g., *Shewenella, Desulfobacula*, or *Desulforhopalus*) inhabiting settling marine snow. The formation of methylmercury (CH_3Hg^+) is carried out under anoxic micro-environments through the acetyl- CoA/hgcAB pathway. (iii) Hg methylation potentially carried out through metabolic pathways similar to the acetyl-CoA/hgcAB pathway by aerobic prokaryotes carrying *hgcAB*-like genes, such as bacteria belonging to the genus Nitrospina. (iv) Hg methylation postulated to take place under truly oxic conditions by unknown aerobic methylators. The formation of MeHg may respond to housekeeping genes which increase their overall activity when carbon, nutrients and Hg^{2+} are present.

particular, marine snow has been widely described as aggregated mixtures of large particles (> 300 µm) mostly composed by organic matter from plankton fecal pellets, living cells, detritus, and exudates (Alldredge and Silver, 1988; Turner, 2015). Alldredge and Cohen 1987 was one of the first studies reporting oxygen-depleted microenvironments within and around such particles, where microbial processes requiring low oxygen conditions, such as denitrification, may occur. Respiratory and photosynthetic activities were measured in light and dark conditions. Their results showed significant oxygen depletion (up to 45%) particularly during dark conditions, when respiration by the bacterial communities inhabiting these particles overtakes the photosynthetic production of oxygen carried out by phytoplankton communities. This respiratory activity is enhanced by the presence of organic matter and essential nutrients present in these particles, which further stimulates bacterial activity (Azam and Long, 2001). These observations were supported by later studies (Ploug et al., 1997; Tang et al., 2011; Decho and Gutierrez, 2017; Bianchi et al., 2018). In a combination of laboratory experiments and field observations, Shanks and Reeder 1993 also found oxygen-depleted conditions within marine snow particles, where sulfide was detected in concentrations far exceeding the values in the surrounding oxic waters. The production of sulfide was also attributed to microbial activity supported by the organic matter within the particles, and shed light to a similar paradox on the production of sulfide in oxygenated layers of the water column.

Marine snow particles are not the only structures where anoxic microenvironments can be formed within oxic waters. The interior of planktonic biota, particularly zooplankton, has also been described to enclose anoxic conditions where anaerobic bacteria can thrive. Glud et al. (2015) reported anoxic microenvironments within carcasses of the copepod *Calanus finmarchicus* in fully oxygenated seawater from Godthåbsfjord (Greenland). They detected denitrification activity by the bacterial communities

naturally inhabiting the interior of these copepods, suggesting sinking *C. finmarchicus* carcasses as hotspots of pelagic denitrification. The gut of living zooplankton has also been reported to show anoxic conditions where different bacterial processes take place (PROCTOR, 1997; Braun et al., 1999). Tang et al. (2011) measured oxygen levels inside the guts of the copepods *Calanus hyperboreusand* and *C. glacialis* from arctic and subarctic waters. The recorded oxygen profiles indicated microbial respiration, which can deplete oxygen levels inside the guts and maintain anoxic conditions.

Considering previous studies reporting the existence of these anoxic microenvironments, the hypothesis of such microenvironments being responsible for MeHg production in oxic pelagic waters started to gain importance as an explanation for the MeHg paradox (Monperrus et al., 2007; Cossa et al., 2009; Sunderland et al., 2009; Lehnherr et al., 2011; Sonke et al., 2013; Schartup et al., 2015). Ortiz et al. (2015) was one of the first studies directly measuring the production of MeHg within settling marine particles. In a microcosm experiment, marine aggregates ranging in size (0.2 µm to > 300 µm; including marine snow) were produced from sieved estuarine seawater and spiked with MeHg ($CH_3{}^{199}Hg$) and inorganic Hg ($^{200}Hg^{+2}$). Methylation and demethylation rates were measured based on changes in isotopic composition of ^{199}Hg and ^{200}Hg. The results pointed to a net Hg methylation particularly in larger particles such as marine snow, which was comparable to rates found in benthic sediments. Gascón Díez et al. (2016) carried out a similar study in the largest freshwater lake in Western Europe (Lake Geneva). Over a period of two years, sediments and settling particles from this lake were collected monthly. Total Hg/MeHg concentrations and methylation rates were measured in the upper first cm of the sediments and in settling particles. Interestingly, MeHg concentrations were 10-fold higher in settling particles compared to sediments, whereas total Hg concentrations were similar in both compartments. Furthermore, while demethylation rates were similar in sediments and particles, methylation rate constants (k_m) were 2-fold greater in settling particles, which suggests a net MeHg formation in settling particles 10 orders of magnitudes higher than sediments. In order to determine the biological origin of this MeHg production, they amended the sediments and particles with molybdate, a known inhibitor of sulfate reducing metabolism, which resulted in a reduction of MeHg production by 80%. In a more recent study, Capo et al. (2020a) addressed this question by a genetic and phylogenetic approach. They analysed 81 metagenomes collected from Baltic Sea waters ranging in oxygen levels from normoxic (2 mL O_2 L^{-1}) to hypoxic (< 2 mL O_2 L^{-1}) and anoxic (no detectable O_2). The *hgcAB* genes were mainly detected in settling particles (marine snow) from anoxic waters, with lower presence under hypoxic and normoxic conditions. However, higher *hgcAB* abundance was found in marine snow compared to filtered water with no aggregates, confirming that settling particles can be hotspots of MeHg production. In addition, a phylogenetic study revealed a Hg methylator community predominantly composed by sulfate reducing bacteria affiliated with *Deltaproteobacteria*.

Hg methylation under oxic conditions: is there an alternative methylation pathway?

The production of MeHg in oxic waters by anaerobic methylators (microenvironments) and, to a lesser extent, by abiotic processes may represent a substantial fraction of the total MeHg pool in certain pelagic environments, but it does not satisfactorily resolve the MeHg paradox in oxic waters where no *hgcAB* genes or anaerobic Hg methylator are detected. Are there Hg methylation mechanisms other than the hgcAB pathway? Or do we need higher-resolution molecular tools to detect *hgcAB* abundances below the current detection thresholds?

Podar et al. (2015) carried out the first comprehensive study on the distribution and prevalence of *hgcAB* genes and unknown Hg methylators across different environments on Earth (>3500 microbial metagenomes), including oxic pelagic waters. The *hgcAB* gene pair was found in every anoxic environment, whereas these genes were only detected in 7 of the 138 metagenomes from pelagic marine water columns. These observations are supported by a more recent study (Bowman et al., 2019) where *hgcAB* genes were screened but not detected in the upper water column (< 800 m) from Arctic Ocean seawater. These findings support the hypothesis of alternative Hg methylation pathways carried out under true oxic conditions. On the contrary, other studies have reported the presence of hgcAB-like genes in surface waters. Gionfriddo et al. (2016) identified for the first time hgcAB-like genes in two *Nitrospina* genomes from waters of the East Antarctic Sea. These microaerophilic bacteria were therefore proposed to play an important role as Hg methylators in pelagic waters, although the authors still referred to microenvironments, such as brine pockets and periphytic biofilms associated with settling organic matter, as the most probable niches where Hg methylation may occur. A more recent study on the distribution of the *hgcAB* genes and Hg methylators in the global ocean (Villar et al., 2020) detected the presence and expression of *hgcAB* homologues in seawaters from most of ocean basins worldwide (except in the Arctic Ocean). These genes were linked to taxonomic relatives of known Hg methylators belonging to *Deltaproteobacteria*, *Firmicutes*, *Chloroflexi*, and particularly *Nitrospina*, which was suggested to be the predominant and widespread bacteria carrying and expressing *hgcAB*-like genes. However, as in Gionfriddo et al. (2016), the methylating activity of *Nitrospina* was not tested under true oxic conditions, and the authors attributed its methylating capacity to be likely perform in oxygen-deficient microenvironments within sinking marine particles. Moreover, although *hgcAB*-like genes are predicted to encode corrinoid iron-sulphur and transmembrane domains distinctive of HgcA and a 4Fe-4S ferredoxin motif characteristic of HgcB, to date organisms carrying these genes have not been proven to produce MeHg (Podar et al., 2015; Gilmour et al., 2018).

To address this controversy, Rodríguez et al. (2022) carry out a microcosm experiment (37 L aquaria) where surface water from the

Baltic Sea was filtered through 0.7 µm to remove sinking particles potentially creating anoxic microenvironments, while preserving the natural prokaryotic communities. The water was exposed to increased concentration of inorganic Hg (250 pM Hg^{+2}) and an air-bubbling system ensured continuous oxygen saturation. Interestingly, MeHg production was detected above ambient levels after addition of inorganic Hg. Using 16S amplification and shotgun metagenomics, neither *hgcAB* genes nor known Hg methylators were detected in this study (including *Nitrospina*). Concentration of MeHg was highly correlated with bacterial activity, which strongly suggest the existence of an alternative Hg methylation pathway under truly oxic conditions where *hgcAB* gene pair is not involved.

MeHg formation and climate change

The potential magnification in MeHg formation and bioaccumulation as a consequence of climate change is currently of great concern for national and international environmental authorities (Stern et al., 2012; Krabbenhoft and Sunderland, 2013; Marnane, 2018; Chetelat et al., 2022). But what is the link between climate change and MeHg formation in boreal aquatic systems? The key factor is organic matter. Prediction models point to an increase of precipitation regimes in the Northern hemisphere as a result of climate change, which in turn will lead to higher terrestrial runoff and river inflows into boreal aquatic ecosystems (Meier et al., 2011; Andersson et al., 2015). These terrestrial inflows contain high concentrations of dissolved organic matter (DOM) swept from the catchment area, thus increasing the overall concentration of DOM in the water column. The reactive nature of organic matter to interact with different environmental pollutants has been object of study for decades, and Hg has been particularly targeted by numerous studies (Hsu-Kim et al., 2013; Ripszam et al., 2015b; Schartup et al., 2015; Alava et al., 2017; Jiang et al., 2018; Rodríguez et al., 2018). Thus, evidence of the role of DOM on Hg methylation and bioaccumulation has exponentially increased over the last years, pointing to several levels at which DOM can interact with Hg (Figure 3): 1) As a complexing agent on Hg^{+2} speciation (Hsu-Kim et al., 2013; Chiasson-Gould et al., 2014; Jiang et al., 2018) and providing methyl groups required for methylation (Nagase et al., 1982, 1984; Weber et al., 1985; from Wang et al., 2022); 2) by enhancing microbial metabolism (Hall et al., 2004; Paranjape and Hall, 2017); and 3) by promoting changes in the physiology and permeability of the bacterial cell membrane (Campbell et al., 1997; Vigneault et al., 2000).

DOM-Hg chemical interactions

The chemical interactions between DOM and Hg largely depend on both DOM concentration and composition. Different ligands within the DOM molecular pool strongly bind to Hg, which can have a dual effect on Hg bioavailability and MeHg production. On the one hand, Hg^{+2} can rapidly bind to biologically labile DOM (LDOM), forming LDOM-Hg aggregates that are highly bioavailable for prokaryotic uptake (Hsu-Kim et al., 2013; Chiasson-Gould et al., 2014; Jiang et al., 2018). This higher bioavailability increases the internalization of Hg into the cytoplasm, where it is transformed into MeHg. A typical example

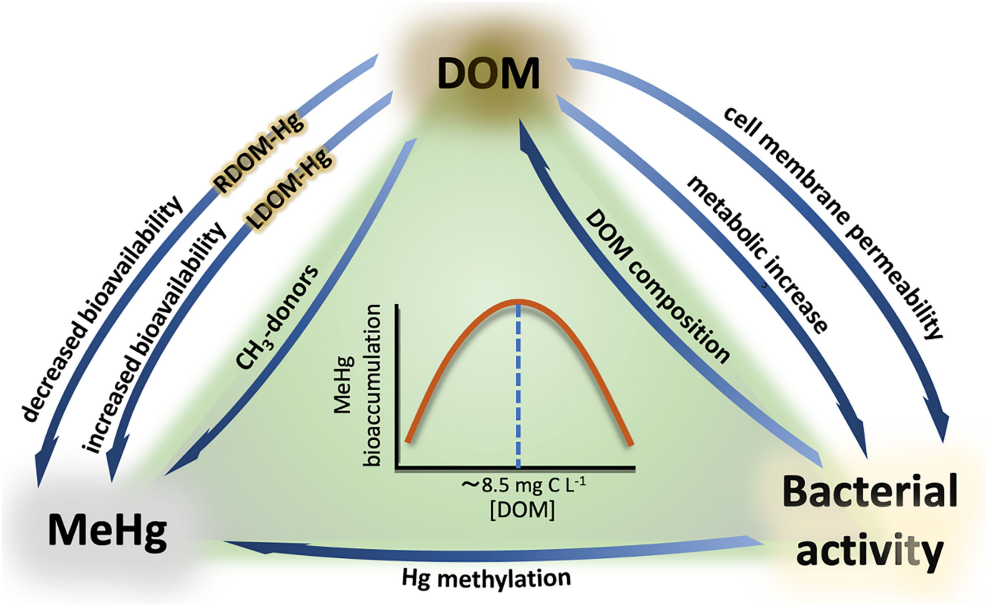

FIGURE 3
Interactions between DOM, MeHg, and bacterial activity. RDOM-Hg and LDOM-Hg refer to the aggregates formed by Hg and refractory compounds (RDOM) and labile compounds (LDOM). The relationship between MeHg bioaccumulation and DOM concentration is represented by a bell-shaped pattern, where MeHg bioaccumulation increases with increasing DOM concentration until a threshold (~8.5 C L^{-1}), from which Hg bioavailability starts to progressively decrease with increasing DOM concentration.

of LDOM is the autochthonous DOM produced by phytoplankton, also known as exudates (Seymour et al., 2017; Mühlenbruch et al., 2018; Eigemann et al., 2022). These molecules can be easily degraded or directly uptaken by prokaryotes, and consequently they have been linked to high MeHg production rates (Kim et al., 2011; Lázaro et al., 2013; Bravo et al., 2017). On the other hand, the bioavailability of Hg can be reduced when refractory compounds (RDOM) act as the main ligands for Hg binding, forming RDOM-Hg aggregates. These molecules are more recalcitrant for biodegradation and, therefore, Hg uptake and MeHg formation are reduced in these situations (Chiasson-Gould et al., 2014; French et al., 2014; Bravo et al., 2017). Furthermore, more complex interactions have been suggested to occur between LDOM-Hg and RDOM-Hg aggregates, where Hg^{+2} can be dissociated from RDOM under photochemical oxidation or microbial degradation and bind to LDOM, thus becoming more bioavailable (Chiasson-Gould et al., 2014). The opposite situation has also been described, where Hg^{+2} bioavailability is reduced due to the progressive degradation of the most labile fraction of DOM by heterotrophic activity, which leads to higher RDOM : LDOM ratios and thus more abundant RDOM-Hg aggregates. These complex interactions between different fractions of DOM and Hg were hypothesized in two companion studies by Chiasson-Gould et al. (2014) and French et al. (2014). In both studies, a bell-shaped relationship between DOM concentration and Hg bioavailability was observed, where Hg bioavailability increased with increasing DOM concentration until a threshold (8.5 – 10 mg C L^{-1}), from which Hg bioavailability started to progressively decrease with increasing DOM concentration. Each of these studies focused on different aspects of the Hg pathway. Whereas French et al. (2014) examined MeHg bioaccumulation in littoral amphipods collected from 26 Arctic lakes (Canada), Chiasson-Gould et al. (2014) used a modified strain of *Escherichia coli* as bioreporter under oxic conditions. This bacterium contains a *merlux* construct that emits bioluminescence when Hg^{+2} is actively transported through the cell membrane, which is used to quantify intracellular Hg^{+2} levels. Interestingly, both studies observed similar patterns in DOM-Hg interactions.

In addition, Chiasson-Gould et al. (2014) also studied Hg^{+2} bioavailability under two conditions: pseudoequilibrium and nonequilibrium at different DOM concentrations. They observed a decrease in bioavailability when Hg^{+2} was pre-incubated with DOM over 24 h (i.e., DOM-Hg pseudoequilibrium), which was explained by Hg^{+2} being mostly bound to strong binding sites in humic and fluvic acids. However, bioavailability increased when Hg^{+2} was freshly added (i.e., DOM-Hg nonequilibrium) to solutions already containing cells and humic/fluvic acids at increasing concentrations (0 to 10 mg C L^{-1}), after which bioavailability started to decrease (bell-shaped pattern).

These observations suggest that the formation of DOM-Hg aggregates is a slow process involving competitive ligand exchange dynamics with multiple functional groups within the DOM pool, which may have important implications in a changing climate where DOM is expected to increase in the water column of boreal aquatic systems. DOM chemical structure and content should be considered of capital importance when studying effects on Hg bioavailability, MeHg production and bioaccumulation, particularly considering that organic matter in aquatic ecosystems is a heterogeneous mixture of molecules derived from terrestrial (allochthonous) and internal (autochthonous) sources, as well as the fact that DOM present in aquatic systems is usually more diverse in molecular structure and primary sources than in terrestrial environments (Jaffe et al., 2008; Schartup et al., 2015).

MeHg production enhanced by increasing microbial metabolism

As discussed above, Hg bioavailability and MeHg formation can be increased through chemical interactions with different DOM molecules, which ultimately interact with the Hg methylators. However, since Hg bio-methylation is an enzymatic process, it can also be enhanced by direct stimulation of the microbial metabolic activity, which has been observed to take place in pelagic waters (French et al., 2014; Paranjape and Hall, 2017; Rodríguez et al., 2022). Numerous studies have provided large evidence of the effects of DOM on the overall increase of microbial metabolism and the importance of organic matter remineralization in the methylation of Hg (Hall et al., 2004; Heimbürger et al., 2010; Bowman et al., 2016; Bravo et al., 2017; Kim et al., 2017; Herrero Ortega et al., 2018; Regnell and Watras, 2018). In fact, the role of settling particles on Hg methylation can be understood to operate at two different levels: 1) By providing low-oxygen micro-environments; 2) By providing organic matter as fuel to increase microbial metabolism. In line with this, Lehnherr et al. (2011) found significant correlations between POC remineralization and MeHg concentrations in the Arctic Sea, but referred to poor POC availability as probable cause for the low methylation rates detected in their experiments, which may have been higher if the water samples had been collected during the seasonal phytoplankton blooms. This relationship between phytoplankton production and Hg methylation is also supported by other studies where peak MeHg concentrations were detected in oxic subsurface euphotic zones during chlorophyll maximum (Bowman et al., 2015; Wang et al., 2018).

Oxygen deficient zones (ODZ) have been suggested as major sources of MeHg linked to organic matter remineralization (Wang et al., 2012; Bowman et al., 2015; Cossa et al., 2017; Kim et al., 2017; Gallorini and Loizeau, 2021). A common ground hypothesis is that POC (such as phytoplankton exudates) and DOM originated in surface and subsurface waters gradually sink to deeper layers, scavenging Hg in its path and forming aggregates that are later metabolized by prokaryotic communities under anoxic or hypoxic conditions. However, while ODZ may be the main source of MeHg in the water column, MeHg production has also be linked to DOM degradation under fully oxygenated waters. Rodríguez et al. (2022) found strong positive correlations between bacterial production and MeHg formation in oxygenated coastal waters from the Baltic Sea under increasing DOM concentrations, where micro-particles larger than 0.7 µm were discarded. Considering projected climate change scenarios for the Northern hemisphere (Meier et al., 2011; Andersson et al., 2015), the addition of terrestrial DOM led to an increase of the overall bacterial activity and diversity, as well as the

relative abundance of genes related to enzymatic activity and energy generation. Furthermore, MeHg formation was detected shortly after the addition of Hg^{+2} (13 h), pointing to a rapid response of bacterial communities to methylate Hg. This quick metabolic response was also suggested by the rapid increase in relative abundance of genes related to cellular activity, with no significant changes in taxonomic composition. These observations may indicate that Hg methylation under oxic conditions just responds to housekeeping genes which increase their overall activity when carbon, nutrients or temperature are provided, but further studies are required to determine the exact mechanisms.

The rapid response of microbial communities to methylate Hg^{+2} may have important implications under a changing climate where DOM concentration in the water column is expected to increase. Although terrestrial DOM flushed from the catchment area in boreal systems is usually rich in refractory organic carbon (Asmala et al., 2013; Bravo et al., 2017), MeHg formation could potentially be increased through a rapid methylation of newly deposited Hg by the local prokaryotic communities boosted by high DOM concentrations, before Hg^{+2} becomes complexed with recalcitrant compounds in the DOM pool (Chiasson-Gould et al., 2014; Rodríguez et al., 2022). In addition, the overall MeHg concentration may be further increased by inputs of allochthonous MeHg derived from runoff (Jonsson et al., 2012; Krabbenhoft and Sunderland, 2013; Jonsson et al., 2014), as well as by reducing MeHg photo-demethylation due to water brownification and subsequent light attenuation typically induced by terrestrial dissolved organic matter (tDOM) (Poste et al., 2015; Wu et al., 2021).

Impacts of DOM on cell membrane permeability

Hg bioavailability can also increase by changes in the physiology of the bacterial cell membrane resulting in higher permeability. Humic and fluvic acids from natural DOM have been shown to act as surfactants, affecting the chemical properties of biological membranes and particularly the level of permeability to neutrally charged chemical species (Vigneault et al., 2000; Slaveykova et al., 2003; Ojwang' and Cook, 2013; Graham et al., 2017), which could constitute a potential pathway for Hg^{+2} internalization (Benoit et al., 1999; Benoit et al., 2001). Chiasson-Gould et al. (2014) studied changes in the bacterial membrane permeability under different DOM concentrations and oxic conditions using bile salts, which reduce cell growth due to increased membrane permeability. They observed no significant increase in membrane permeability, and attributed the higher internalization of Hg^{+2} to interactions between DOM and the bacterial cell wall that resulted in the destabilization of the lipopolysaccharide layer, which could make Hg transport sites more accessible. Nonetheless, these conclusions should be taken with caution as other studies have reported decreased uptake and toxicity of charged metals by humic substances (Koukal et al., 2003; Kostić et al., 2013; Perelomov et al., 2018).

Temperature is also a substantially important factor

The central aspect from which all climate change effects derive is global warming. The increasing temperatures have multiple impacts on a variety of biogeochemical systems, from ice melting in polar and alpine regions to changes in hydrological patterns, increased sea levels, and frequency of extreme atmospheric events (i.e., droughts and deluges), among others (Stern et al., 2012; Andersson et al., 2015; Stott, 2016). Therefore, raising temperatures can have indirect and direct effects on Hg methylation. Permafrost thaw in polar and sub-polar regions has been observed to mobilize significant amounts of Hg accumulated over decades, which can be ultimately transported into aquatic systems (Schuster et al., 2018; Schaefer et al., 2020; Dastoor et al., 2022). Particularly in boreal regions, increased precipitation regimes are predicted to import higher organic matter from catchment areas, with effects on Hg methylation already discussed in the above sections. This increased terrestrial runoff will also import higher amounts of both Hg^{+2} and MeHg into aquatic ecosystems (Stern et al., 2012; Jonsson et al., 2014). Together with nutrients and organic carbon from tDOM, prokaryotic communities have all the necessary elements to potentially carry out Hg methylation (Rodríguez et al., 2022). In addition, a more direct impact of increasing temperatures is the positive effects on microbial activity, further stimulating the overall microbial metabolism, including the methylation activity (Monperrus et al., 2007; Johnson et al., 2016). On the other hand, negative effects on Hg methylation should be also considered by Hg cycling prediction models. For instance, higher rates of demethylation may be caused by the overall increase of microbial activity (Lu et al., 2016; Lu et al., 2017; Paranjape and Hall, 2017), as well as by higher exposure to solar radiation due to loss of sea ice (Stern et al., 2012).

Other indirect effects may account for a potential increase of Hg methylation as a result of increasing temperatures. Thermal stratification of the water column is associated with warmer air temperatures, and it has been shown to promote hypoxic conditions as oxygenated surface waters are prevented from mixing with the bottom layers (Cloern, 2001; Altieri and Keryn, 2015). This may lead to higher Hg methylation rates under anoxic conditions. Furthermore, oxygen levels can also be depleted by heterotrophic activity boosted by both higher temperatures and higher DOM concentration, where the eutrophication levels may increase Hg methylation (Soerensen et al., 2016; Ji et al., 2020; Yao et al., 2020).

Experimental approaches to study MeHg formation in oxic waters

With so many confounding factors affecting the Hg methylation process, how do we conduct suitable experimental strategies and measurements? Studying biological systems is a particularly complex task due to the outstanding complexity derived from numerous interdependent metabolic pathways, number of

biological and chemical species involved, and bidirectional interactions with multiple physicochemical factors.

Field measurements and laboratory incubation experiments are the most employed approaches in the study of Hg methylation (Paranjape and Hall, 2017; Ma et al., 2019; Regnell and Watras, 2019; Gallorini and Loizeau, 2021). Since MeHg is a potent neurotoxin naturally bioaccumulated in natural environments, field experiments within aquatic systems are very constrained due to the exposure of Hg or MeHg to the natural biota. Furthermore, both field measurements and incubation experiments are restricted to a limited framework of variables, as it is virtually impossible to account for all the variables that operate in natural ecological systems. However, a combination of field measurements and controlled experiments is a valuable approach that has been used in a number of studies on Hg methylation in pelagic environments (Lehnherr et al., 2011; French et al., 2014; Paranjape and Hall, 2017; Wang et al., 2022). In some instances, either field measurements or controlled experiments may be sufficient to advance our knowledge towards a particular research question, but both approaches are subjected to their own limitations (Wang et al., 2020).

Field measurements

Field measurements typically consist of the collection of water and sediments to determine physical variables (e.g., temperature and light intensity), chemical variables (e.g., Hg/MeHg concentrations, organic matter content, oxygen, pH, salinity, etc.) and/or biological variables (e.g., metabolic activity, taxonomic composition, gene expression, etc.). Since Hg methylation is primarily a biochemical process, comprehensive studies should include a combination of such bio-physico-chemical variables. However, until recently, field measurements generally considered only chemical factors such as organic matter, oxygen, or relevant chemical species such as thiols (in addition to Hg/MeHg) (Monperrus et al., 2007; Merritt and Amirbahman, 2009; Li and Cai, 2013). Following the breakthrough of meta-omic technologies, more recent studies have introduced taxonomic and metabolic parameters principally through the sequencing of environmental DNA (eDNA). Bowman et al. (2019) and Villar et al. (2020) are among the most recent studies that have greatly contributed to survey the occurrence of Hg/MeHg concentrations and relevant microbial genes in oxic waters from the global oceans. In Bowman et al. (2019), water samples (<800 m depth) were collected from multiple areas ranging from Arctic to equatorial Pacific oceans, where detailed Hg speciation measurements were conducted, as well as targeted and shotgun metagenomics to evaluate the presence of Hg-cycling genes (*hgcAB* and *mer*) and other relevant genes potentially involved in Hg transportation and methylation. On the other hand, Villar et al. (2020) carried out a compilation of metagenomic and metatranscriptomic data obtained from locations covering most of the global ocean basins, with the purpose of addressing the paradox between MeHg production in the upper water column and absence of known anaerobic Hg methylating prokaryotes. Similarly, Podar et al. (2015) also conducted a compilation study using data generated by several metagenome sequencing projects. The compiled sequences were assembled and annotated to study the occurrence of *hgcAB* genes and Hg methylators across different environments, including boreal aquatic systems. Interestingly, these studies reached similar conclusions, where no *hgcAB* genes were generally detected in the oxic water column. Although hgcAB-like genes were found in Bowman et al. (2019) and Villar et al. (2020), to date these genes have not been proven to be involved in the methylation of Hg.

Incubation experiments

Incubation experiments have traditionally relied on experimental models consisting of one or few microbial species (Benoit et al., 2001; Kerin et al., 2006; Gilmour et al., 2013; Parks et al., 2013). Microbial isolates have been used to target specific aspects of the Hg methylation mechanism by simplifying the bio-physico-chemical system. Although this approach has been extensively used under anoxic conditions, only a few experiments have been conducted to investigate Hg methylation under oxic conditions. Chiasson-Gould et al. (2014) is one of the few examples, where the experimental system was reduced to a single bacterial strain (*E. coli* HMS174) genetically modified to study Hg^{+2} bioavailability. A natural DOM extract was used for incubation at different DOM concentrations, which allowed the identification of biochemical interactions between DOM, Hg^{+2} and the bacterial membrane that determined Hg^{+2} bioavailability and methylation. In a similar study, Golding et al. (2002) carried out an incubation experiment where the same *E. coli* strain (HMS174), as well as *Vibrio anguillarum* (a natural aquatic species), were exposed to both anaerobic and aerobic conditions under increased Hg^{+2} concentrations. By using this simplified experimental system, they observed higher uptake of Hg^{+2} under aerobic conditions, mediated by facilitated uptake mechanisms. In Cao et al. (2021), the aerobic methylation of Hg by two γ-proteobacteria strains (*P. fluorescens* TGR-B2 and *P. putida* TGR-B4) was evaluated under different oxygen concentrations, where they detected MeHg formation under both conditions, although Hg methylation under anaerobic conditions appeared to be more efficient.

As new molecular tools have been progressively developed in the field of Microbial Ecology, more integrated experimental designs have shown to be more valuable to study the complex interactions among the vast consortium of microbial species. Fundamental ecological functions are typically carried out by entire microbial communities, where syntrophic interactions between different members provide the necessary physicochemical conditions (Kato and Watanabe, 2010; Morris et al., 2013; Kouzuma et al., 2015). Therefore, whereas highly simplified experimental systems have the potential to unravel specific aspects of the genetic and metabolic bases of Hg methylation, the absence of certain microbial members can significantly alter the natural functioning of this process (Kerin et al., 2006; Ranchou-Peyruse et al., 2009; Bravo and Cosio 2019). Mesocosm model ecosystems have been used in an attempt to reproduce natural conditions while isolating the system to apply controlled conditions. Combined with recently developed Hg isotope tracer methodologies (Jonsson et al., 2012; Jonsson et al.,

2014) and high-throughput sequencing techniques, these experimental designs constitute powerful tools for comprehensive studies of how Hg methylation works in natural environments, and particularly under climate change-induced conditions. In a series of recent studies, Jonsson et al. (2017; 2022) used a 2000 L mesocosm setup to determine MeHg production and bioaccumulation in brackish waters and sediments collected from the Bothnian Sea, where multiple variables were included: increasing concentrations of DOM, nutrients, different Hg isotope tracers, a pelagic food web model (native heterotrophic bacteria, phytoplankton, protozoa, and mesozooplankton), light conditions, and controlled temperature. In a similar incubation experiment, Rodríguez et al. (2022) combined shotgun metagenomics with Hg/MeHg measurements to study Hg methylation by natural bacterial communities in oxygen-saturated pelagic waters, where variables such as DOM, Hg^{+2} concentration, oxygen level, and light intensity were considered.

In order to further improve our experimental models, it is important to point out potential biases and limitations from incubation studies based on the addition of isotopically enriched Hg species. In a recent critique article, Wang et al. (2020) evaluated the validity of this type of experimental approach as a method to study Hg methylation and demethylation rates in seawater. Based on field measurements and incubation experiments conducted along the Canadian Arctic Archipelago, they drew attention to potential reliability issues derived from methylation and demethylation at time zero, as well as the widely accepted assumption of first-order kinetics to calculate methylation and demethylation constants. Although these observations may respond to particular experimental procedures (Tsui et al., 2020; Zhang et al., 2021), and therefore generalizations should be taken with caution, future holistic studies should rely on an integration of field measurements and incubation experiments that allows the identification of potential experimental biases. Thus, field surveys can be highly valuable to guide subsequent incubation experiments where environmental parameters can be tuned to investigate hidden and emergent properties within the complex biological systems, as well as to generate prediction models for future scenarios under a changing climate.

Meta-omic technologies as tools to address the MeHg formation problematic

Until recently, simplified experimental systems were the main source of knowledge to study complex environmental microbial processes such as Hg methylation. After the discovery of the microbial bases of Hg methylation (Parks et al., 2013), early studies essentially relied on culture-dependent approaches to further advance our knowledge on the metabolic pathways, genes and species involved (Benoit et al., 2001; Kerin et al., 2006; Gilmour et al., 2013). The irruption of sequencing-based meta-omic technologies gave rise to a new kind of approach based on the generation of large quantities of sequencing data from entire microbial assemblages. Being culture-independent, this approach has allowed the implementation of more sophisticated experimental designs to disentangle the complex interactions between Hg methylators, their syntrophs, and relevant environmental variables (such as DOM) under natural or modelled conditions (Quince et al., 2017; Pérez-Cobas et al., 2020; Cho, 2021). In particular, metagenetics, metagenomics and metatranscriptomics (sequencing-based meta-omics) have been the meta-omic approaches most frequently used in the field of Microbial Ecology (Table 1), mainly due to: 1) cost-time effectiveness (simultaneous analyses of multiple samples); 2) analytical depth to cover even rare members of microbial communities; and 3) direct applicability in both field surveys and controlled experiments.

Metagenetics (also known as amplicon sequencing, marker-gene metagenomics, or targeted metagenomics) is a targeted approach where specific genes (called marker genes) present in the community gene pool are amplified by PCR, sequenced and aligned against an existing reference database for taxonomic and/or functional characterization of the community. The most frequently used gene marker for taxonomic characterization of bacterial communities is the 16S rRNA gene, which is universally found in bacteria with enough variability (nine hypervariable regions) as to allow taxonomic classification and biodiversity profiling (Větrovský and Baldrian, 2013). As discussed in previous sections, the marker

TABLE 1 Description of the main sequencing-based meta-omic approaches.

	Main applications	Advantages	Disadvantages
Metagenetics (targeted DNA sequencing)	• 16S/18S rRNA taxonomy. • Detection of hgcAB genes.	• Detailed taxonomic characterization. • High detection power for hgcAB genes. • Cost/time effective sample processing.	• Limitation to detect unknown genes potentially involved in Hg methylation in oxic waters. • Very limited information of functional potential.
Metagenomics (non-targeted DNA sequencing)	• 16S/18S rRNA taxonomy. • Detection of hgcAB and other functional genes.	• Overall screening of entire microbial metagenome. • Full characterization of the community functional potential, including hgcAB and other genes potentially involved. • Cost/time effective sample processing.	• Lower taxonomic resolution. • Lower power to detect hgcAB genes. • Limited information of the actual metabolic activity.
Metatranscriptomics (non-targeted mRNA sequencing)	• Characterization of gene expression levels, including hgcAB and other functional genes.	• Higher functional resolution. • Measure of the active microbial fraction. • Potential to detect unknown genes actively involved in Hg methylation in oxic waters.	• Potential non-correlation between hgcAB expression and concentration of MeHg or Hg methylation rates. • Cost/time demanding sample GO to Settings windows processing.

genes in Hg methylation studies have consistently been the *hgcAB* gene pair. In a recent study, Capo et al. (2022) presented a *hgc* gene database (Hg-MATE) covering Hg-cycling microorganisms from terrestrial and aquatic ecosystems. This catalogue compiles isolated, single-cell and metagenome-reconstructed genomes, which can be used as a reference database to identify *hgcAB* genes from complex meta-omic datasets. Due to the lack of knowledge about alternative Hg methylation pathways potentially operating under truly oxic conditions, studies only relying on *hgcAB* genes may be limiting our ability to detect important Hg methylators in pelagic waters (Podar et al., 2015; Jones et al., 2019; Lin et al., 2021).

Shotgun metagenomics (or simply metagenomics) is a non-targeted approach where fragments of the metagenome (i.e., collection of all genomes present in a community) are randomly sequenced and, therefore, taxonomically relevant genes (such as 16S rRNA) as well as functional genes (i.e., involved in physiological processes) can be represented in the dataset, including bacteria, archaea, eukaryotes, and viruses (Quince et al., 2017). One advantage of shotgun metagenomics is the possibility to create biodiversity and functional profiles simultaneously from the very same environmental sample, which can be a valuable tool to detect intercorrelations between the presence of Hg-cycling genes and abundance of potential methylators, as well as other functional genes potentially involved in the Hg methylation process (Rodríguez et al., 2022). Another advantage is the recovery of metagenome-assembled genomes (MAGs), which can provide taxonomic and functional information on specific taxa (down to strain-level diversity) potentially involved in Hg methylation (Bowers et al., 2017; Gionfriddo et al., 2019; McDaniel et al., 2020; Peterson et al., 2020; Lin et al., 2021; Capo et al., 2022). On the other hand, some drawback must be also pointed out, such as the lower sequencing depth compared to specific targeted approaches, where the latter can direct the totality of the sequencing effort towards detecting marker genes such as 16S rRNA or *hgcAB*. In addition, although this technique can offer valuable insights about the functional potential of microbial communities (i.e., presence of genes involved in different metabolic pathways), it does not reflect the actual metabolic activity, as genes need to be transcribed to carry out their biological functions. Other meta-omic techniques are employed to address these aspects, such as metatranscriptomics or metaproteomics (Yap et al., 2022). Overall, shotgun metagenomics represents a cost-time-effective approach to obtain an integral picture of complex microbial communities where detailed resolution is not required.

Metatranscriptomics refers to the non-targeted sequencing of the mRNA pool from biological samples, which offers a higher level of functional resolution as compared to shotgun metagenomics. Multiple studies on Hg methylation have used this approach, particularly to determine levels of *hgcAB* gene expression and thus estimate Hg methylation activity (Vishnivetskaya, 2018; Christensen et al., 2019; Lin et al., 2021). However, the association between these two variables must be taken with caution, as increases in *hgcAB* transcripts may be caused by higher abundance of Hg methylators, and not necessarily by higher cell-specific *hgcAB* expression (Lin et al., 2021). In addition, the expression of *hgcAB* does not confer the capacity for Hg methylation on its own, as the cellular uptake of Hg (i.e., Hg bioavailability) is a necessary requirement. In fact, a number of studies have shown lack of correlation between *hgcAB* expression and concentration of MeHg or Hg methylation rates (Goñi-Urriza et al., 2015; Bravo et al., 2016; Vishnivetskaya, 2018; Christensen et al., 2019), although demethylation activity must be considered as a potential confounding factor for the lack of correlation. Despite these drawbacks, metatranscriptomics is one of the most promising tools in our repertory to potentially elucidate novel Hg methylation pathways occurring in oxic waters. In addition, the analysis of RNA is a measure of the active microbial fraction, allowing the distinction between viable and nonviable cells (Villar et al., 2020; Lin et al., 2021). DNA-based meta-omics (i.e., metagenetics and metagenomics) are still significantly more employed in Hg methylation studies, mainly due to more simplified and cost/time-effective sample preparation procedures. As new methods are developed to improve technical aspects of mRNA isolation, library preparation and sequencing, metatranscriptomics is becoming an extremely useful approach to disentangle complex microbial processes in natural environments.

Considering the advantages and disadvantages of the above-discussed sequencing-based meta-omic techniques, an increasingly popular approach is the combination of metagenomics and metatranscriptomics (multi-omics) to obtain a more comprehensive overview of natural microbial communities (Lin et al., 2021). This approach can facilitate the study of how relevant climate change-related variables (e.g., DOM and temperature) may affect the interconnections between community structure (i.e., occurrence of Hg methylators and syntrophs) and functioning (i.e., Hg methylation activity and overall metabolism). Functional redundancy is a typical property of natural prokaryotic communities that confers high levels of resistance and resilience under environmental disturbance, which can lead to the decoupling of community composition, functional potential, and the actual metabolic activity (Allison and Martiny, 2008; Bissett et al., 2013; Rodríguez et al., 2022). In this context, multi-omics offers an excellent tool for incubation experiments aiming the study of how the metabolic potential to perform Hg methylation and, more importantly, the actual ability to methylate Hg, may be affected under climate change scenarios.

Need for standardized methods and current challenges

A common issue frequently reported is the lack of standardization among different Hg methylation studies employing meta-omic approaches, which may lead to rather disparate results even from samples from the same sampling areas (Capo et al., 2022; Yap et al., 2022). Previous studies have addressed the standardization of analytical methods related to Hg and MeHg concentration and characterization (Creswell et al., 2013; Wen et al., 2017). This review will briefly address potential ways to standardize the analysis of microbial communities, from sample collection to bioinformatic data processing.

Meta-omic studies on aquatic environments usually begin with the collection of water, which is commonly carried out by filtration methods where the cellular fraction is captured onto a fine-pored matrix such as membrane filters (e.g., Lin et al., 2021; Rodríguez et al., 2022). The preservation of the matrix is a crucial step to maintain the integrity of the DNA and, especially, the RNA molecules. Inadequate preservation methods can easily result in loss of genetic material and hence can reduce the accuracy and resolution of the sequencing techniques. In addition, the degradation rate of DNA/RNA molecules can be related to their molecular size and nucleotide composition, which can vary among different taxonomic groups (Mitchell and Takacs-Vesbach, 2008; Kumar et al., 2020; Pavlovska et al., 2021). Therefore, deficient preservation can lead to dissimilar degradation of different DNA/RNA species, resulting in an artificial selection towards certain taxonomic groups over others, and potential loss of low-abundant members of the communities. Similar to *hgcAB*$^{+}$ Hg methylators, other potential methylators using different pathways in oxic waters may be rare members of the communities and, therefore, a proper sample preservation is required to ensure detection and sufficient representation for subsequent analyses. Although preservation buffers have been frequently used (e.g., DNA/RNA Shield™ and RNAlater®), the most prevalent method in meta-omic studies is the use of deep freezing, which is usually achieved by liquid nitrogen (Anchordoquy and Molina, 2007; Pavlovska et al., 2021). The use of pre-fixative solutions can also improve the preservation of the original DNA/RNA pool, particularly when the filtration process takes prolonged periods of times (i.e., up to hours). In these cases, microbial communities may experience changes in community composition and gene expression while enclosed in collection bottles, which can be partially prevented by the addition of fixative alcoholic solutions (such as phenol-ethanol solution) to stop all biological activity while maintaining the original taxonomic and functional composition (Charvet et al., 2019; Rodríguez et al., 2022). Furthermore, the processing of samples immediately after collection is an emerging approach promoted by the development of the portable sequencers MinION (Oxford Nanopore Technologies), which eliminates the need for preservation and thus ensures a greater integrity of DNA and RNA molecules (Tyler et al., 2018; Runtuwene et al., 2019).

The detection of Hg methylators using *hgcAB* primers is also a controversial aspect widely discussed in Hg methylation studies (Capo et al., 2020a; Gionfriddo et al., 2020; McDaniel et al., 2020). The characterization of *hgcAB* genes can be biased by primer design, sequence length, or by the use of different classification methods. Since the first characterization of the *hgcAB* gene pair by Parks et al., 2013, a number of *hgcAB* variants have been described for different Hg methylators (Jones et al., 2019; Villar et al., 2020; Capo et al., 2022). While the design of hgcAB primers in early studies was based on the limited knowledge of a reduced number of Hg methylators (Liu et al., 2014; Bae et al., 2014; Schaefer et al., 2014), newly developed primers increasingly capture a wider diversity (Christensen et al., 2019; Bravo and Cosio, 2019; Jones et al., 2019 Gionfriddo et al., 2020). More efficient primers may help to detect Hg methylators in oxic pelagic environments, where *hgcAB* genes are scarce and sequencing depths can be insufficient for the detection of low-abundant genes. On the other hand, due to the lack of knowledge of the genetic bases and species involved, the study of alternative Hg methylation pathways potentially occurring under oxic conditions will require the design of more universal 16S rRNA primers to cover a wider range of prokaryotic diversity, as well as the use of non-targeted metagenomic approaches (such as MAGs by shotgun metagenomics) for a comprehensive functional characterization of specific taxa potentially involved.

Bioinformatic analysis of sequencing data is another aspect with little consensus among the literature. The existence of multiple bioinformatic pipelines to analyse metagenomic and metranscriptomic data has been shown to cause contrasting results (Cho, 2021; Yap et al., 2022). Bioinformatic analyses typically include a series of steps such as cleaning, assembly, read mapping, gene prediction, gene identification, and gene counting. However, within every step, multiple bioinformatic programs have been developed over the years (Pérez-Cobas et al., 2020). In particular, the use of common, standardized reference databases (either for taxonomic identification or for *hgcAB* genes) has been reiterated in the literature as an important step to facilitate comparisons across different studies (Gallorini and Loizeau, 2021; Capo et al., 2022; Wang et al., 2022). Normalization of gene counts is another key aspect to determine the prevalence of different members of the microbial communities, as well as to allow comparative analyses with similar studies. For instance, in meta-omic studies considering *hgcAB* genes, number of mapped reads and expression levels of housekeeping genes (such as *rpoB*, *gyrB*, and *recA*) are frequently used to normalize *hgcAB* read counts (Tada et al., 2020; Vigneron et al., 2021; Lin et al., 2021; Capo et al., 2022). Rarefaction to a common library size and normalization to gene length and metatranscriptomic sequencing depth are also normalization approaches frequently used in microbial community studies (Rodríguez et al., 2018; Pérez-Cobas et al., 2020). Considering that different normalization approaches can cope with different analytical biases, it is recommended to employ several normalization methods when reporting meta-omic data, which may facilitate data interpretation and inter-study comparisons.

Summary and concluding remarks

The study of Hg methylation in the water column under oxic conditions is still in its infancy. The formation of MeHg in pelagic areas where no anaerobic methylators are detected poses an apparent paradox that may be explained by different processes: 1) Abiotic Hg methylation; 2) Biotic MeHg production within anoxic micro-environments; 3) Biotic MeHg production under oxic conditions through metabolic pathways involving *hgc*AB genes or 4) independent of *hgc*AB genes. Anoxic microenvironments within settling particles have been frequently postulated as the main source of MeHg in the oxic water column, but recent studies suggest that Hg methylation can take place in fully oxygenated waters where anoxic microenvironments are not present. Given the current controversy, more studies on Hg methylation under truly oxic conditions are required to clarify whether Hg methylation is also

performed through metabolic pathways different to the reductive acetyl–CoA pathway involving *hgcAB* genes.

Boreal aquatic ecosystems are predicted to be impacted by global warming through increases in temperatures and DOM concentration in the water column. In particular, DOM is known to affect Hg methylation at different levels: 1) Through chemical interactions affecting Hg^{+2} speciation and providing methyl groups; 2) Enhancing microbial metabolism; 3) Promoting changes in the bacterial cell membrane which affect Hg uptake. These aspects have been poorly studied in boreal aquatic systems under oxic conditions, and, therefore, comprehensive studies including the main biochemical factors involved are required to predict potential ecosystem effects under climate change scenarios.

Meta-omic approaches represent promising tools to accomplish this task. A combination of metagenetics, metagenomics, and metatranscriptomics is advised to simultaneously study taxonomic and functional aspects of Hg methylation, which is particularly valuable in the study of unknown pathways not involving *hgcAB* genes. Due to the wide variety of techniques for sample processing, DNA/RNA sequencing, and data analysis, standardization of meta-omic approaches may improve data interpretation and inter-study comparisons. In addition, an integration of field measurements and incubation experiments is recommended to improve our experimental models when studying how Hg methylation works in natural aquatic environments under oxic conditions, and particularly under climate change-induced conditions.

Author contributions

The author confirms being the sole contributor of this work and has approved it for publication.

Funding

This study was supported by Swedish Environmental Protection Agency (Naturvårdsverket): Project: 2020-00032.

Conflict of interest

The author declares that the research was conducted in the absence of any commercial or financial relationships that could be construed as a potential conflict of interest.

Publisher's note

References

Alava, J. J., Cheung, W. W., Ross, P. S., and Sumaila, U. R. (2017). Climate change–contaminant interactions in marine food webs: Toward a conceptual framework. *Global Change Biol.* 23 (10), 3984–4001. doi: 10.1111/gcb.13667

Alldredge, A. L., and Silver, M. W. (1988). Characteristics, dynamics and significance of marine snow. *Prog. Oceanography* 20.1, 41–82. doi: 10.1016/0079-6611(88)90053-5

Alldredge, A. L., and Cohen, Y. (1987). Can microscale chemical patches persist in the sea? Microelectrode study of marine snow, fecal pellets. *Science* 235 (4789), 689–691. doi: 10.1126/science.235.4789.689

Allison, S. D., and Martiny, J. B. (2008). Resistance, resilience, and redundancy in microbial communities. *Proc. Natl. Acad. Sci.* 105, 11512–11519. doi: 10.1073/pnas.0801925105

Altieri, A. H., and Keryn, B. G. (2015). Climate change and dead zones. *Global Change Biol.* 21.4, 1395–1406. doi: 10.1111/gcb.12754

Anchordoquy, T. J., and Molina, M. C. (2007). Preservation of DNA. *Cell Preserv. Technol.* 5 (4), 180–188. doi: 10.1089/cpt.2007.0511

Andersson, A., Meier, H. M., Ripszam, M., Rowe, O., Wikner, J., Haglund, P., et al. (2015). Projected future climate change and Baltic Sea ecosystem management. *Ambio* 44, 345–356. doi: 10.1007/s13280-015-0654-8

Ariya, P. A., and Peterson, K. A. (2005). "Chemical transformation of gaseous elemental Hg in the atmosphere," in *Dynamics of Mercury Pollution on Regional and Global Scales* (Boston, MA: Springer US), 261–294. doi: 10.1007/0-387-24494-8_12

Asmala, E., Autio, R., Kaartokallio, H., Pitkänen, L., Stedmon, C. A., and Thomas, D. N. (2013). Bioavailability of riverine dissolved organic matter in three baltic sea estuaries and the effect of catchment land use. *Biogeosciences* 10 (11), 6969–6986. doi: 10.5194/bg-10-6969-2013

Azam, F., and Long, R. A. (2001). Sea snow microcosms. *Nature* 414 (6863), 495–498. doi: 10.1038/35107174

Bae, H. S., Dierberg, F. E., and Ogram, A. (2014). Syntrophs dominate sequences associated with the mercury methylation-related gene hgcA in the water conservation areas of the florida everglades. *Appl. Environ. Microbiol.* 80 (20), 6517–6526. doi: 10.1128/AEM.01666-14

Beckers, F., Mothes, S., Abrigata, J., Zhao, J., Gao, Y., and Rinklebe, J. (2019). Mobilization of mercury species under dynamic laboratory redox conditions in a contaminated floodplain soil as affected by biochar and sugar beet factory lime. *Sci. Total Environ.* 672, 604–617. doi: 10.1016/j.scitotenv.2019.03.401

Benoit, J. M., Gilmour, C. C., and Mason, R.P. (2001). The influence of sulfide on solid phase mercury bioavailability for methylation by pure cultures of Desulfobulbus propionicus (1pr3). *Environ. Sci. Technol.* 35 (1), 127–132. doi: 10.1021/es001415n

Benoit, J. M., Gilmour, C. C., Mason, R. P., and Heyes, A. (1999). Sulfide controls on mercury speciation and bioavailability to methylating bacteria in sediment pore waters. *Environ. Sci. Technol.* 33 (6), 951–957. doi: 10.1021/es9808200

Bianchi, D., Weber, T. S., Kiko, R., and Deutsch, C. (2018). Global niche of marine anaerobic metabolisms expanded by particle microenvironments. *Nat. Geosci.* 11 (4), 263–268. doi: 10.1038/s41561-018-0081-0

Bissett, A., Brown, M. V., Siciliano, S. D., and Thrall, P. H. (2013). Microbial community responses to anthropogenically induced environmental change: towards a systems approach. *Ecol. Lett.* 16, 128–139. doi: 10.1111/ele.12109

Boening, D. W. (2000). Ecological effects, transport, and fate of mercury: a general review. *Chemosphere* 40, 1335–1351. doi: 10.1016/S0045-6535(99)00283-0

Bowers, R. M., Kyrpides, N. C., Stepanauskas, R., Harmon-Smith, M., Doud, D., Reddy, T. B. K., et al. (2017). Minimum information about a single amplified genome (MISAG) and a metagenome-assembled genome (MIMAG) of bacteria and archaea. *Nat. Biotechnol.* 35 (8), 725–731. doi: 10.1038/nbt.3893

Bowman, K. L., Collins, R. E., Agather, A. M., Lamborg, C. H., Hammerschmidt, C. R., Kaul, D., et al. (2019). Distribution of mercury-cycling genes in the arctic and equatorial pacific oceans and their relationship to mercury speciation. *Limnology Oceanography* 65, S310–S320. doi: 10.1002/lno.11310

Bowman, K. L., Lamborg, C. H., and Agather, A. M. (2020). A global perspective on mercury cycling in the ocean. *Sci. Total Environ.* 710, 136166. doi: 10.1016/j.scitotenv.2019.136166

Bowman, K. L., Hammerschmidt, C. R., Lamborg, C. H., and Swarr, G. (2015). Mercury in the north atlantic ocean: The US GEOTRACES zonal and meridional sections. *Deep Sea Res. Part II: Topical Stud. Oceanography* 116, 251–261. doi: 10.1016/j.dsr2.2014.07.004

Bowman, K. L., Hammerschmidt, C. R., Lamborg, C. H., Swarr, G. J., and Agather, A. M. (2016). Distribution of mercury species across a zonal section of the eastern tropical

South Pacific Ocean (US GEOTRACES GP16). *Marine Chemistry* 186, 156–166. doi: 10.1016/j.marchem.2016.09.005

Braun, S. T., Proctor, L. M., Zani, S., Mellon, T. M., and Zehr, P. J. (1999). Molecular evidence for zooplankton-associatednitrogen-fixing anaerobes based on amplification of the nifHgene. *FEMS Microbiol. Ecol.* 28, 273–279. doi: 10.1111/j.1574-6941.1999.tb00582.x

Bravo, A. G., Loizeau, J. L., Dranguet, P., Makri, S., Bjoürn, E., Ungureanu, V. G., et al. (2016). Per- sistent Hg contamination and occurrence of Hg- methylating transcript (hgcA) downstream of a chlor-alkali plant in the Olt River (Romania). *Environ. Sci. pollut. Res.* 23, 10529–10541. doi: 10.1007/s11356-015-5906-4

Bravo, A. G., Zopfi, J., Buck, M., Xu, J., Bertilsson, S., Schaefer, J. K., et al. (2018). Geobacteraceae are important members of mercury-methylating microbial communities of sediments impacted by waste water releases. *ISME J.* 12 (3), pp.802–pp.812. doi: 10.1038/s41396-017-0007-7

Bravo, A. G., Bouchet, S., Tolu, J., Björn, E., Mateos-Rivera, A., and Bertilsson, S. (2017). Molecular composition of organic matter controls methylmercury formation in boreal lakes. *Nat. Commun.* 8, 1–9. doi: 10.1038/ncomms14255

Bravo, A. G., and Cosio, C. (2019). Biotic formation of methylmercury: A bio–physico–chemical conundrum. *Limnology Oceanography* 65 (5), 1010–1027. doi: 10.1002/lno.11366

Campbell, P. G., Twiss, M. R., and Wilkinson, K. J. (1997). Accumulation of natural organic matter on the surfaces of living cells: implications for the interaction of toxic solutes with aquatic biota. *Can. J. Fish. Aquat. Sci.* 54, 2543–2554. doi: 10.1139/f97-161

Cao, D., Chen, W., Xiang, Y., Mi, Q., Liu, H., Feng, P., et al. (2021). The efficiencies of inorganic mercury bio-methylation by aerobic bacteria under different oxygen concentrations. *Ecotoxicol. Environ. Saf.* 207, 111538. doi: 10.1016/j.ecoenv.2020.111538

Capo, E., Bravo, A. G., Soerensen, A. L., Bertilsson, S., Pinhassi, J., Feng, C., et al. (2020a). Marine snow as a habitat for microbial mercury methylators in the Baltic Sea. *bioRxiv*, 2020–2003. doi: 10.1101/2020.03.04.975987

Capo, E., Bravo, A. G., Soerensen, A. L., Bertilsson, S., Pinhassi, J., Feng, C., et al. (2020b). Deltaproteobacteria and spirochaetes-like bacteria are abundant putative mercury methylators in oxygen-deficient water and marine particles in the Baltic Sea. *Front. Microbiol.* 11, 574080. doi: 10.3389/fmicb.2020.574080

Capo, E., Peterson, B. D., Kim, M., Jones, D. S., Acinas, S. G., Amyot, M., et al. (2022). A consensus protocol for the recovery of mercury methylation genes from metagenomes. *Mol. Ecol. Resour.* 23 (1), 190–204. doi: 10.1101/2022.03.14.484253

Celo, V., Lean, D. R., and Scott, S. L. (2006). Abiotic methylation of mercury in the aquatic environment. *Sci. Total Environ.* 368 (1), 126–137. doi: 10.1016/j.scitotenv.2005.09.043

Charvet, S., Riemann, L., Alneberg, J., Andersson, A. F., von Borries, J., Fischer, U., et al. (2019). AFISsys-An autonomous instrument for the preservation of brackish water samples for microbial metatranscriptome analysis. *Water Res.* 149, 351–361. doi: 10.1016/j.watres.2018.11.017

Chetelat, J., McKinney, M. A., Amyot, M., Dastoor, A., Douglas, T. A., Heimbürger-Boavida, L. E., et al. (2022). Climate change and mercury in the Arctic: Abiotic interactions. *Sci. Total Environ.* 824, 153715. doi: 10.1016/j.scitotenv.2022.153715

Chiasson-Gould, S. A., Blais, J. M., and Poulain, A. J. (2014). Dissolved organic matter kinetically controls mercury bioavailability to bacteria. *Environ. Sci. Technol.* 48, 3153–3161. doi: 10.1021/es4038484

Cho, J. C. (2021). Omics-based microbiome analysis in microbial ecology: from sequences to information. *J. Microbiol.* 59, 229–232. doi: 10.1007/s12275-021-0698-3

Christensen, G. A., Gionfriddo, C. M., King, A. J., Moberly, J. G., Miller, C. L., Somenahally, A. C., et al, et al. (2019). Determining the reliabil- ity of measuring mercury cycling gene abundance with cor- relations with mercury and methylmercury concentrations. *Environ. Sci. Technol.* 53, 8649–8663. doi: 10.1021/acs.est.8b06389

Cloern, J. E. (2001). Our evolving conceptual model of the coastal eutrophication problem. *Mar. Ecol. Prog. Ser.* 210, 223–253. doi: 10.3354/meps210223

Compeau, G. C., and Bartha, R. (1985). Sulfate-reducing bacteria: principal methylators of mercury in anoxic estuarine sediment. *Appl. Environ. Microbiol.* 50 (2), 498–502. doi: 10.1128/aem.50.2.498-502.1985

Cossa, D., Averty, B., and Pirrone, N. (2009). The origin of methylmercury in open Mediterranean waters. *Limnol. Oceanography* 54 (3), 837–844. doi: 10.4319/lo.2009.54.3.0837

Cossa, D., de Madron, X. D., Sch€afer, J., Lanceleur, L., Guedron, S., Buscail, R., et al. (2017). The open sea as the main source of methylmercury in the water column of the Gulf of Lions (Northwestern Mediterranean margin). *Geochim. Cosmochim. Acta* 199, 222–237. doi: 10.1016/j.gca.2016.11.037

Creswell, J. E., Engel, V., Carter, A., and Davies, C. (2013). "Results from three years of the world's largest interlaboratory comparison for total mercury and methylmercury: Method performance and best practices," in *AGU Fall Meeting Abstracts* 2013, B41C–0405. doi: 2013AGUFM.B41C0405C

Dastoor, A., Angot, H., Bieser, J., Christensen, J. H., Douglas, T. A., Heimbürger-Boavida, L. E., et al. (2022). Arctic mercury cycling. *Nat. Rev. Earth Environ.* 3 (4), 270–286. doi: 10.1038/s43017-022-00269-w

Decho, A. W. (1990). Microbial exopolymer secretions in ocean environments: their role (s) in food webs and marine processes. *Oceanogr. Mar. Biol. Annu. Rev.* 28 (7), 73–153, doi: 10.4319/lo.1990.35.5.1039

Decho, A. W., and Gutierrez, T. (2017). Microbial extracellular polymeric substances (EPSs) in ocean systems. *Front. Microbiol.* 8, 922. doi: 10.3389/fmicb.2017.00922

Eigemann, F., Rahav, E., Grossart, H. P., Aharonovich, D., Sher, D., Vogts, A., et al. (2022). Phytoplankton exudates provide full nutrition to a subset of accompanying heterotrophic bacteria *via* carbon, nitrogen and phosphorus allocation. *Environ. Microbiol.* 24 (5), pp.2467–2483. doi: 10.1111/1462-2920.15933

French, T. D., Houben, A. J., Desforges, J. P. W., Kimpe, L. E., Kokelj, S. V., Poulain, A. J., et al. (2014). Dissolved organic carbon thresholds affect mercury bioaccumulation in Arctic lakes. *Environ. Sci. Technol.* 48, 3162–3168. doi: 10.1021/es403849d

Gallorini, A., and Loizeau, J. L. (2021). Mercury methylation in oxic aquatic macro-environments: a review. *J. Limnol.* 80 (2). doi: 10.4081/jlimnol.2021.2007

Gascón Díez, E, Loizeau, J. L., Cosio, C., Bouchet, S., Adatte, T., Amouroux, D., et al. (2016). Role of settling particles on mercury methylation in the oxic water column of freshwater systems. *Environ. Sci. Technol.* 50 (21), 11672–11679. doi: 10.1021/acs.est.6b03260

Ghimire, P. S., Tripathee, L., Zhang, Q., Guo, J., Ram, K., Huang, J., et al. (2019). Microbial mercury methylation in the cryosphere: Progress and prospects. *Sci. Total Environ.* 697, 134150. doi: 10.1016/j.scitotenv.2019.134150

Gilmour, C. C., Podar, M., Bullock, A. L., Graham, A. M., Brown, S. D., Somenahally, A. C., et al. (2013). Mercury methylation by novel microorganisms from new environments. *Environ. Sci. Technol.* 47 (20), pp.11810–11820. doi: 10.1021/es403075t

Gilmour, C. C., Bullock, A. L., McBurney, A., Podar, M., and Elias, D. A. (2018). Robust mercury methylation across diverse methanogenic archaea. *MBio* 9 (2), 10–1128. doi: 10.1128/mbio.02403-17

Gionfriddo, C., Podar, M., Gilmour, C., Pierce, E., and Elias, D. (2019). *ORNL compiled mercury methylator database (No. MCI533). ORNLCIFSFA (Critical Interfaces Science Focus Area)* (TN (United States: Oak Ridge National Lab. (ORNL), Oak Ridge).

Gionfriddo, C. M., Wymore, A. M., Jones, D. S., Wilpiszeski, R. L., Lynes, M. M., Christensen, G. A., et al. (2020). An improved hgcAB primer set and direct high-throughput sequencing expand Hg-methylator diversity in nature. *Front. Microbiol.* 11, 541554. doi: 10.3389/fmicb.2020.541554

Gionfriddo, C. M., Tate, M. T., Wick, R. R., Schultz, M. B., Zemla, A., and Thelen, M. P. (2016). MicrobialmercurymethylationinAntarctic sea ice. *Nat. Microbiol.* 1, 16127–16112. doi: 10.1038/nmicrobiol.2016.127

Glud, R. N., Grossart, H. P., Larsen, M., Tang, K. W., Arendt, K. E., Rysgaard, S., et al. (2015). Copepod carcasses as microbial hot spots for pelagic denitrification. *Limnol. Oceanography* 60 (6), 2026–2036. doi: 10.1002/lno.10149

Golding, G. R., Kelly, C. A., Sparling, R., Loewen, P. C., Rudd, J. W., and Barkay, T. (2002). Evidence for facilitated uptake of Hg (II) by Vibrio anguillarum and Escherichia coli under anaerobic and aerobic conditions. *Limnol. Oceanography* 47 (4), pp.967–pp.975. doi: 10.4319/lo.2002.47.4.0967

Goñi-Urriza, M. Y., Corsellis, L., Lanceleur, E., Tessier, J., Gury, M., Monperrus,, et al. (2015). Relationships between bacterial energetic metabolism, mercury methylation potential, and hgcA/hgcB gene expression in Des- ulfovibrio dechloroacetivorans BerOc1. *Environ. Sci. pollut. Res.* 22, 13764–13771. doi: 10.1007/s11356-015-4273-5

Graham, A. M., Cameron-Burr, K. T., Hajic, H. A., Lee, C., Msekela, D., and Gilmour, C. C. (2017). Sulfurization of dissolved organic matter increases Hg–sulfide–dissolved organic matter bioavailability to a Hg-methylating bacterium. *Environ. Sci. Technol.* 51 (16), 9080–9088. doi: 10.1021/acs.est.7b02781

Grandjean, P., Murata, K., Budtz-Jørgensen, E., and Weihe, P. (2004). Cardiac autonomic activity in methylmercury neurotoxicity: 14-year follow-up of a Faroese birth cohort. *J. Pediatr.* 144 (2), 169–176. doi: 10.1016/j.jpeds.2003.10.058

Hall, B. D., Louis, V. L. S., and Bodaly, R. D. (2004). The stimulation of methylmercury production by decomposition of flooded birch leaves and jack pine needles. *Biogeochemistry* 68, 107–129. doi: 10.1023/B:BIOG.0000025745.28447.8b

Hammerschmidt, C. R., and Fitzgerald, W. F. (2006). Methylmercury cycling in sediments on the continental shelf of southern New England. *Geochim. Cosmochim. Acta* 70 (4), 918–930. doi: 10.1016/j.gca.2005.10.020

Heimbürger, L.-E., Cossa, D., Marty, J.-C., Migon, C., Averty, B., Dufour, A., et al. (2010). Methyl mercury dis- tributions in relation to the presence of nano-and picophytoplankton in an oceanic water column (Ligurian Sea, north-western Mediterranean). *Geochim. Cosmochim. Acta* 74 (19), 5549–5559. doi: 10.1016/j.gca.2010.06.036

Heimbürger, L.-E., Sonke, J. E., Cossa, D., Point, D., Lagane, C., Laffont, L., et al. (2015). Shallow methylmercury production in the marginal sea ice zone of the central Arctic Ocean. *Sci. Rep.* 5 (1), 1–6. doi: 10.1038/srep10318

Herrero Ortega, S., Catalaín, N., Bjoürn, E., Groüntoft, H., Hilmarsson, T. G., Bertilsson, S., et al. (2018). High methylmercury formation in ponds fueled by fresh humic and algal derived organic matter. *Limnol. Oceanogr.* 63, S44–S53. doi: 10.1002/lno.10722

Hsu-Kim, H., Kucharzyk, K. H., Zhang, T., and Deshusses, M. A. (2013). Mechanisms regulating mercury bioavailability for methylating microorganisms in the aquatic environment: a critical review. *Environ. Sci. Technol.* 47, 2441–2456. doi: 10.1021/es304370g

Jaffe, R., McKnight, D., Maie, N., Cory, R., McDowell, W. H. ;., Campbell,, et al. (2008). Spatial and temporal variations in DOM composition in ecosystems: The importance of long-term monitoring of optical properties. *J. Geophys. Res.* 113, 1–15. doi: 10.1029/2008JG000683

Jensen, Sören, and Jernelöv, A. (1969). Biological methylation of mercury in aquatic organisms. *Nature* 223, 753–754, 5207. doi: 10.1038/223753a0

Jernelov, A. (1969). Are there any differences between" biologically" and "chemically" synthesized methyl mercury. *Vatten* 3, 304.

Ji, X., Liu, C., Zhang, M., Yin, Y., and Pan, G. (2020). Mitigation of methylmercury production in eutrophic waters by interfacial oxygen nanobubbles. *Water Res.* 173, 115563. doi: 10.1016/j.watres.2020.115563

Jiang, T., Bravo, A. G., Skyllberg, U., Björn, E., Wang, D., Yan, H., et al. (2018). Influence of dissolved organic matter (DOM) characteristics on dissolved mercury (Hg) species composition in sediment porewater of lakes from Southwest China. *Water Res.* 146, 146–158. doi: 10.1016/j.watres.2018.08.054

Johnson, N. W., Mitchell, C. P. J., Engstrom, D. R., Bailey, L. T., Coleman Wasik, J. K., and Berndt, M. E. (2016). Methylmercury production in a chronically sulfate-impacted sub-boreal wetland. *Environ. Sci.: Processes Impacts* 18 (6), 725–734. doi: 10.1039/c6em00138f

Jones, D. S., Walker, G. M., Johnson, N. W., Mitchell, C. P., Coleman Wasik, J. K., and Bailey, J. V. (2019). Molecular evidence for novel mercury methylating microorganisms in sulfate-impacted lakes. *ISME J.* 13 (7), 1659–1675. doi: 10.1038/s41396-019-0376-1

Jonsson, S., Skyllberg, U., Nilsson, M. B., Lundberg, E., Andersson, A., and Björn, E. (2014). Differentiated availability of geochemical mercury pools controls methylmercury levels in estuarine sediment and biota. *Nat. Commun.* 5, 4624. doi: 10.1038/ncomms5624

Jonsson, S., Skyllberg, U., Nilsson, M. B., Westlund, P.-O., Shchukarev, A., Lundberg, E., et al. (2012). Mercury methylation rates for geochemically relevant HgII species in sediments. *Environ. Sci. Technol.* 46, 11653–11659. doi: 10.1021/es3015327

Jonsson, S., Andersson, A., Nilsson, M. B., Skyllberg, U., Lundberg, E., Schaefer, J. K., et al. (2017). Terrestrial discharges mediate trophic shifts and enhance methylmercury accumulation in estuarine biota. *Sci. Adv.* 3 (1), e1601239. doi: 10.1126/sciadv.1601239

Jonsson, S., Liem-Nguyen, V., Andersson, A., Skyllberg, U., Nilsson, M. B., Lundberg, E., et al. (2022). Geochemical and dietary drivers of mercury bioaccumulation in estuarine benthic invertebrates. *Environ. Sci. Technol.* 56 (14), 10141–10148. doi: 10.1021/acs.est.2c03265

Kato, S., and Watanabe, K. (2010). Ecological and evolutionary interactions in syntrophic methanogenic consortia. *Microbes Environments* 25 (3), 145–151. doi: 10.1264/jsme2.ME10122

Kerin, E. J., Gilmour, C. C., Roden, E., Suzuki, M. T., Coates, J. D., and Mason, R. P. (2006). Mercury methylation by dissimilatory Iron-reducing bacteria. *Appl. Environ. Microbiol.* 72, 7919–7921. doi: 10.1128/AEM.01602-06

Kim, M., Han, S., Gieskes, J., and Deheyn, D. D. (2011). Importance of organic matter lability for monomethylmercury production in sulfate-rich marine sediments. *Sci. Total Environ.* 409 (4), 778–784. doi: 10.1016/j.scitotenv.2010.10.050

Kim, H., Soerensen, A. L., Hur, J., Heimburger, L. E., Hahm, D., Rhee, T. S., et al. (2017). Methylmercury mass budgets and distribution characteristics in the Western Pacific Ocean. *Environ. Sci. Technol.* 51 (3), 1186–1194. doi: 10.1021/acs.est.6b04238

Kirk, J. L., Lehnherr, I., Andersson, M., Braune, B. M., Chan, L., Dastoor, A. P., et al. (2012). Mercury in Arctic marine ecosystems: sources, pathways and exposure. *Environ. Res.* 119, 64–87. doi: 10.1016/j.envres.2012.08.012

Kostić, I. S., Anđelković, T. D., Nikolić, R. S., Cvetković, T. P., Pavlović, D. D., and Bojić, A. L. (2013). Comparative study of binding strengths of heavy metals with humic acid. *Hemijska Industrija* 67 (5), 773–779. doi: 10.2298/HEMIND121107002K

Koukal, B., Gueguen, C., Pardos, M., and Dominik, J. (2003). Influence of humic substances on the toxic effects of cadmium and zinc to the green alga Pseudokirchneriella subcapitata. *Chemosphere* 53 (8), 953–961. doi: 10.1016/S0045-6535(03)00720-3

Kouzuma, A., Kato, S., and Watanabe, K. (2015). Microbial interspecies interactions: recent findings in syntrophic consortia. *Front. Microbiol.* 6, 477. doi: 10.3389/fmicb.2015.00477

Krabbenhoft, D. P., and Sunderland, E. M. (2013). Global change and mercury. *Science* 341 (6153), 1457–1458. doi: 10.1126/science.1242838

Kraepiel, A. M., Keller, K., Chin, H. B., Malcolm, E. G., and Morel, F. M. (2003). Sources and variations of mercury in tuna. *Environ. Sci. Technol.* 37 (24), 5551–5558. doi: 10.1021/es0340679

Kumar, G., Eble, J. E., and Gaither, M. R. (2020). A practical guide to sample preservation and pre-PCR processing of aquatic environmental DNA. *Mol. Ecol. Resour.* 20 (1), 29–39. doi: 10.1111/1755-0998.13107

Kuss, J., Krüger, S., Ruickoldt, J., and Wlost, K. P. (2018). High-resolution measurements of elemental mercury in surface water for an improved quantitative understanding of the Baltic Sea as a source of atmospheric mercury. *Atmospheric Chem. Phys.* 18 (6), 4361–4376. doi: 10.5194/acp-18-4361-2018

Lázaro, W. L., Guimarães, J. R. D., Ignácio, A. R., Da Silva, C. J., and Díez, S. (2013). Cyanobacteria enhance methylmercury production: a hypothesis tested in the periphyton of two lakes in the Pantanal floodplain, Brazil. *Sci. Total Environ.* 456, 231–238. doi: 10.1016/j.scitotenv.2013.03.022

Lehnherr, I., Louis, V. L. S., Hintelmann, H., and Kirk, J. L. (2011). Methylation of inorganic mercury in polar marine waters. *Nat. Geosci.* 4, 298–302. doi: 10.1038/ngeo1134

Li, Y., and Cai, Y. (2013). Progress in the study of mercury methylation and demethylation in aquatic environments. *Chin. Sci. Bull.* 58, 177–185. doi: 10.1007/s11434-012-5416-4

Lin, H., Ascher, D. B., Myung, Y., Lamborg, C. H., Hallam, S. J., Gionfriddo, C. M., et al. (2021). Mercury methylation by metabolically versatile and cosmopolitan marine bacteria. *ISME J.* 15 (6), 1810–1825. doi: 10.1038/s41396-020-00889-4

Liu, M., Zhang, Q., Maavara, T., Liu, S., Wang, X., and Raymond, P. A. (2021). Rivers as the largest source of mercury to coastal oceans worldwide. *Nat. Geosci.* 14 (9), 672–677. doi: 10.1038/s41561-021-00793-2

Liu, Y. R., Yu, R. Q., Zheng, Y. M., and He, J. Z. (2014). Analysis of the microbial community structure by monitoring an hg methylation gene (hgcA) in paddy soils along an hg gradient. *Appl. Environ. Microbiol.* 80, 2874–2879. doi: 10.1128/AEM.04225-13

Lu, X., Gu, W., Zhao, L., Farhan Ul Haque, M., DiSpirito, A. A., Semrau, J. D., et al. (2017). Methylmercury uptake and degradation by methanotrophs. *Sci. Adv.* 3 (5), e1700041. doi: 10.1126/sciadv.1700041

Lu, X., Liu, Y., Johs, A., Zhao, L., Wang, T., Yang, Z., et al. (2016). Anaerobic mercury methylation and demethylation by Geobacter bemidjiensis Bem. *Environ. Sci. Technol.* 50 (8), 4366–4373. doi: 10.1021/acs.est.6b00401

Ma, M., Du, H., and Wang, D. (2019). Mercury methylation by anaerobic microorganisms: A review. *Crit. Rev. Environ. Sci. Technol.* 49 (20), 1893–1936. doi: 10.1080/10643389.2019.1594517

Malcolm, E. G., Schaefer, J. K., Ekstrom, E. B., Tuit, C. B., Jayakumar, A., Park, H., et al. (2010). Mercury methylation in oxygen deficient zones of the oceans: no evidence for the predominance of anaerobes. *Mar. Chem.* 122, 11–19. doi: 10.1016/j.marchem.2010.08.004

Marnane, I. (2018). *Mercury in Europe's environment a priority for European and global action*. European Environmental Agency; EEA Report 2018 No.11/2018 pp.72 pp. Record Number doi: 20219947452

Mason, R. P., Choi, A. L., Fitzgerald, W. F., Hammerschmidt, C. R., Lamborg, C. H., Soerensen, A. L., et al. (2012). Mercury biogeochemical cycling in the ocean and policy implications. *Environ. Res.* 119, 101–117. doi: 10.1016/j.envres.2012.03.013

Mason, R. P., and Fitzgerald, W. F. (1993). The distribution and biogeochemical cycling of mercury in the equatorial Pacific Ocean. *Deep Sea Res. Part I.: Oceanographic Res. Papers* 40 (9), 1897–1924. doi: 10.1016/0967-0637(93)90037-4

McDaniel, E. A., Peterson, B. D., Stevens, S. L., Tran, P. Q., Anantharaman, K., and McMahon, K. D. (2020). Expanded phylogenetic diversity and metabolic flexibility of mercury-methylating microorganisms. *Msystems* 5 (4), e00299–e00220. doi: 10.1128/mSystems.00299-20

Meier, M., Andersson, H., Dieterich, C., Eilola, K., Gustafsson, B., Hoüglund, A., et al. (2011). Transient scenario simulations for the Baltic Sea Region during the 21st century. In *SMHI, 2011*, p. 81. DiVA id: diva2:947527

Merritt, K. A., and Amirbahman, A. (2009). Mercury methylation dynamics in estuarine and coastal marine environments—a critical review. *Earth-Sci. Rev.* 96 (1-2), 54–66. doi: 10.1016/j.earscirev.2009.06.002

Minamata Disease Research Group (1966). *[Minamata Disease: Studies About Methyl-Mercury Poisoning] (in Japanese)* (Kumamoto, Japan: Kumamoto University School of Medicine).

Mitchell, K. R., and Takacs-Vesbach, C. D. (2008). A comparison of methods for total community DNA preservation and extraction from various thermal environments. *J. Ind. Microbiol. Biotechnol.* 35 (10), 1139–1147. doi: 10.1007/s10295-008-0393-y

Monperrus, M., Tessier, E., Amouroux, D., Leynaert, A., Huonnie, P., and Donald, O. F. X. (2007). Mercury methylation, demethylation and reduction rates in coastal and marine surface waters of the Mediterranean Sea. *Mar. Chem.* 107, 49–63. doi: 10.1016/j.marchem.2007.01.018

Morris, B. E., Henneberger, R., Huber, H., and Moissl-Eichinger, C. (2013). Microbial syntrophy: interaction for the common good. *FEMS Microbiol. Rev.* 37 (3), 384–406. doi: 10.1111/1574-6976.12019

Mühlenbruch, M., Grossart, H. P., Eigemann, F., and Voss, M. (2018). Mini-review: Phytoplankton-derived polysaccharides in the marine environment and their interactions with heterotrophic bacteria. *Environ. Microbiol.* 20 (8), pp.2671–2685. doi: 10.1111/1462-2920.14302

Munson, K. M., Lamborg, C. H., Boiteau, R. M., and Saito, M. A. (2018). Dynamic mercury methylation and deme- thylation in oligotrophic marine water. *Biogeosciences* 15 (21), 6451–6460. doi: 10.5194/bg-15-6451-2018

Munson, K. M., Lamborg, C. H., Swarr, G. J., and Saito, M. A. (2015). Mercury species concentrations and fluxes in the central tropical Pacific Ocean. *Global Biogeochem. Cycles* 29 (5), 656–676. doi: 10.1002/2015GB005120

Nagase, H., Ose, Y., Sato, T., and Ishikawa, T. (1982). Methylation of mercury by humic substances in an aquatic environment. *Sci. Total Environ.* 25 (2), 133–142. doi: 10.1016/0048-9697(82)90082-1

Nagase, H., Ose, Y., Sato, T., and Ishikawa, T. (1984). Mercury methylation by compounds in humic material. *Sci. total Environ.* 32 (2), 147–156. doi: 10.1016/0048-9697(84)90127-X

Ojwang', L. M., and Cook, R. L. (2013). Environmental conditions that influence the ability of humic acids to induce permeability in model biomembranes. *Environ. Sci. Technol.* 47 (15), pp.8280–8287. doi: 10.1021/es4004922

Ortiz, V. L., Mason, R. P., and Ward, J. E. (2015). An examination of the factors influencing mercury and methylmercury particulate distributions, methylation and

demethylation rates in laboratory-generated marine snow. *Mar. Chem.* 177, 753–762. doi: 10.1016/j.marchem.2015.07.006

Paranjape, A. R., and Hall, B. D. (2017). Recent advances in the study of mercury methylation in aquatic systems. *Facets* 2, 85–119. doi: 10.1139/facets-2016-0027

Parks, J. M., Johs, A., Podar, M., Bridou, R., Hurt, R. A., Smith, S. D., et al. (2013). The genetic basis for bacterial mercury methylation. *Sci. (New York N.Y.)* 339 (6125), 1332–1335. doi: 10.1126/science.1230667

Pavlovska, M., Prekrasna, I., Parnikoza, I., and Dykyi, E. (2021). Soil sample preservation strategy affects the microbial community structure. *Microbes Environments* 36 (1), ME20134. doi: 10.1264/jsme2.ME20134

Perelomov, L. V., Sarkar, B., Sizova, O. I., Chilachava, K. B., Shvikin, A. Y., Perelomova, I. V., et al. (2018). Zinc and lead detoxifying abilities of humic substances relevant to environmental bacterial species. *Ecotoxicol. Environ. Saf.* 151, 178–183. doi: 10.1016/j.ecoenv.2018.01.018

Pérez-Cobas, A. E., Gomez-Valero, L., and Buchrieser, C. (2020). Metagenomic approaches in microbial ecology: an update on whole-genome and marker gene sequencing analyses. *Microbial. Genomics* 6 (8). doi: 10.1099/mgen.0.000409

Peterson, B. D., McDaniel, E. A., Schmidt, A. G., Lepak, R. F., Janssen, S. E., Tran, P. Q., et al. (2020). Mercury methylation genes identified across diverse anaerobic microbial guilds in a eutrophic sulfate-enriched lake. *Environ. Sci. Technol.* 54 (24), 15840–15851. doi: 10.1021/acs.est.0c05435

Pirrone, N., Cinnirella, S., Feng, X., Finkelman, R. B., Friedli, H. R., Leaner, J., et al. (2010). Global mercury emissions to the atmosphere from anthropogenic and natural sources. *Atmospheric Chem. Phys.* 10 (13), 5951–5964. doi: 10.5194/acp-10-5951-2010

Ploug, H., Buchholz, B., and Jørgensen, B. (1997). Anoxic aggregates an ephemeral phenomenon in the ocean. *Aquat. Microbial. Ecol.* 13, 285–294. doi: 10.3354/ame013285

Podar, M., Gilmour, C. C., Brandt, C. C., Soren, A., Brown, S. D., Crable, B. R., et al. (2015). Global prevalence and distribution of genes and microorganisms involved in mercury methylation. *Sci. Adv.* 1, e1500675. doi: 10.1126/ sciadv.1500675

Poste, A. E., Braaten, H. F. V., de Wit, H. A., Sørensen, K., and Larssen, T. (2015). Effects of photodemethylation on the methylmercury budget of boreal Norwegian lakes. *Environ. Toxicol. Chem.* 34 (6), 1213–1223. doi: 10.1002/etc.2923

PROCTOR, L. M. (1997). Nitrogen-fixing, photosynthetic, anaerobicbacteria associated with pelagic copepods. *Aquat. Microb. Ecol.* 12, 105–113. doi: 10.3354/ame012105

Quince, C., Walker, A. W., Simpson, J. T., Loman, N. J., and Segata, N. (2017). Shotgun metagenomics, from sampling to analysis. *Nat. Biotechnol.* 35 (9), 833–844. doi: 10.1038/nbt.3935

Ranchou-Peyruse, M., Monperrus, M., Bridou, R., Duran, R., Amouroux, D., Salvado, J. C., et al. (2009). Over- view of mercury methylation capacities among anaerobic bacteria including representatives of the sulphate-reducers: implications for environmental studies. *Geomicrobiol. J.* 26, 1–8. doi: 10.1080/01490450802599227

Regnell, O., and Watras, C. J. (2018). Microbial mercury methylation in aquatic environments: a critical review of published field and laboratory studies. *Environ. Sci. Technol.* 53, 4–19. doi: 10.1021/acs.est.8b02709

Regnell, O., and Watras, C. J. (2019). Microbial mercury methylation in aquatic environments: A critical review of published field and laboratory studies. *Environ. Sci. Technol.* 53 (1), 4–19. doi: 10.1021/acs.est.8b02709

Ridley, W. P., Dizikes, L. J., and Wood, J. M. (1977). Biomethylation of toxic elements in the environment. Science. *Science* 197, 4301, 329–332. doi: 10.1126/science.877556

Ripszam, M., Paczkowska, J., Figueira, J., Veenaas, C., and Haglund, P. (2015b). Dissolved organic carbon quality and sorption of organic pollutants in the Baltic Sea in light of future climate change. *Environ. Sci. Technol.* 49, 1445–1452. doi: 10.1021/es504437s

Robinson, J. B., and Tuovinen, O. (1984). Mechanisms of microbial resistance and detoxification of mercury and organomercury compounds: physiological, biochemical, and genetic analyses. *Microbiol. Rev.* 48 (2), 95–124. doi: 10.1128/mr.48.2.95-124.1984

Rodríguez, J., Andersson, A., Björn, E., Timonen, S., Brugel, S., Skrobonja, A., et al. (2022). Inputs of terrestrial dissolved organic matter enhance bacterial production and methylmercury formation in oxic coastal water. *Front. Microbiol.* 13. doi: 10.3389/fmicb.2022.809166

Rodríguez, J., Gallampois, C. M., Timonen, S., Andersson, A., Sinkko, H., Haglund, P., et al. (2018). Effects of organic pollutants on bacterial communities under future climate change scenarios. *Front. Microbiol.* 9, 2926. doi: 10.3389/fmicb.2018.02926

Runtuwene, L. R., Tuda, J. S., Mongan, A. E., and Suzuki, Y. (2019). On-site minION sequencing. In: *ingle Molecule and Single Cell Sequencing; Advances in Experimental Medicine and Biology*. Singapore: Springer, 1129, 143–150. doi: 10.1007/978-981-13-6037-4_10

Schaefer, K., Elshorbany, Y., Jafarov, E., Schuster, P. F., Striegl, R. G., Wickland, K. P., et al. (2020). Potential impacts of mercury released from thawing permafrost. *Nat. Commun.* 11 (1), 4650. doi: 10.1038/s41467-020-18398-5

Schaefer, J. K., Kronberg, R. M., Morel, F. M., and Skyllberg, U. (2014). Detection of a key hg methylation gene, hgcA, in wetland soils. *Environ. Microbiol. Rep.* 6 (5), 441–447. doi: 10.1111/1758-2229.12136

Schartup, A. T., Ndu, U., Balcom, P. H., Mason, R. P., and Sunderland, E. M. (2015). Contrasting effects of marine and terrestrially derived dissolved organic matter on mercury speciation and bioavailability in seawater. *Environ. Sci. Technol.* 49 (10), 5965–5972. doi: 10.1021/es506274x

Schuster, P. F., Schaefer, K. M., Aiken, G. R., Antweiler, R. C., Dewild, J. F., Gryziec, J. D., et al. (2018). Permafrost stores a globally significant amount of mercury. *Geophysical Res. Lett.* 45 (3), 1463–1471. doi: 10.1002/2017GL075571

Seymour, J. R., Amin, S. A., Raina, J. B., and Stocker, R. (2017). Zooming in on the phycosphere: the ecological interface for phytoplankton–bacteria relationships. *Nat. Microbiol.* 2 (7), 1–12. doi: 10.1038/nmicrobiol.2017.65

Shanks, A. L., and Reeder, M. L. (1993). Reducing microzones and sulfide production in marine snow. *Mar. Ecol. Prog. Ser.* 96 (1), 43–47. doi: 10.3354/meps096043

Slaveykova, V. I., Wilkinson, K. J., Ceresa, A., and Pretsch, E. (2003). Role of fulvic acid on lead bioaccumulation by Chlorella kesslerii. *Environ. Sci. Technol.* 37 (6), 1114–1121. doi: 10.1021/es025993a

Soerensen, A. L., Schartup, A. T., Gustafsson, E., Gustafsson, B. G., Undeman, E., and Bjoürn, E. (2016). Eutrophication increases phytoplankton methylmercury concentrations in a coastal sea: a baltic sea case study. *Environ. Sci. Technol.* 50 (21), 11787–11796. doi: 10.1021/acs.est.6b02717

Sonke, J. E., Heimbürger, L.-E., and Dommergue, A. (2013). Mercury biogeochemistry: paradigm shifts, outstanding issues and research needs. *Comptes Rendus Geosci.* 345, 213–224. doi: 10.1016/j.crte.2013.05.002

Stern, G. A., Macdonald, R. W., Outridge, P. M., Wilson, S., Chetelat, J., Cole, A., et al. (2012). How does climate change influence arctic mercury? *Sci. Total Environ.* 414, 22–42. doi: 10.1016/j.scitotenv.2011.10.039

Stott, P. (2016). How climate change affects extreme weather events. *Science* 352 (6293), 1517–1518. doi: 10.1126/science.aaf7271

Streets, D. G., Devane, M. K., Lu, Z., Bond, T. C., Sunderland, E. M., and Jacob, D. J. (2011). All-time releases of mercury to the atmosphere from human activities. *Environ. Sci. Technol.* 45 (24), 10485–10491. doi: 10.1021/es202765m

Sunderland, E. M., Krabbenhoft, D. P., Moreau, J. W., Strode, S. A., and Landing, W. M. (2009). Mercury sources, distribution, and bioavailability in the north Pacific Ocean: Insights from data and models. *Global Biogeochem. Cycles* 23 (2), n/a–n14. doi: 10.1029/2008GB003425

Tada, Y., Marumoto, K., and Takeuchi, A. (2020). Nitrospina-like bacteria are potential mercury methylators in the mesopelagic zone in the east china sea. *Front. Microbiol.* 11. doi: 10.3389/fmicb.2020.01369

Taira, M. (1975). Studies on microbial synthesis and decomposition of organomercury compounds. *Nippon Eiseigaku Zasshi (Japanese J. Hygiene)* 30 (4), 461–489. doi: 10.1265/jjh.30.461

Tan, S. W., Meiller, J. C., and Mahaffey, K. R. (2009). The endocrine effects of mercury in humans and wildlife. *Crit. Rev. Toxicol.* 39 (3), 228–269. doi: 10.1080/10408440802233259

Tang, K. W., Glud, R. N., Glud, A., Rysgaard, S., and Nielsen, T. G. (2011). Copepod guts as biogeochemical hot- spots in the sea: Evidence from microelectrode profiling of Calanus spp. *Limnol. Oceanography* 56 (2), 666–672. doi: 10.4319/lo.2011.56.2.0666

Tsubaki, T., and Irukayama, K. (1977). *Minamata disease. Methylmercury poisoning in Minamata and Niigata, Japan* (Amsterdam, The Netherlands: North-Holland Publishing Company, PO Box 211).

Tsui, M. T. K., Blum, J. D., and Kwon, S. Y. (2020). Review of stable mercury isotopes in ecology and biogeochemistry. *Sci. Total Environ.* 716, 135386. doi: 10.1016/j.scitotenv.2019.135386

Turner,, and Jefferson, T. (2015). Zooplankton fecal pellets, marine snow, phytodetritus and the ocean's biological pump. *Prog. Oceanography* 130, 205–2485. doi: 10.1016/j.pocean.2014.08.005

Tyler, A. D., Mataseje, L., Urfano, C. J., Schmidt, L., Antonation, K. S., Mulvey, M. R., et al. (2018). Evaluation of Oxford Nanopore's MinION sequencing device for microbial whole genome sequencing applications. *Sci. Rep.* 8 (1), 1–12. doi: 10.1038/s41598-018-29334-5

Ullrich, S. M., Tanton, T. W., and Abdrashitova, S. A. (2001). Mercury in the aquatic environment: a review of factors affecting methylation. *Crit. Rev. Environ. Sci. Technol.* 31, 241–293. doi: 10.1080/20016491089226

Větrovský, T., and Baldrian, P. (2013). The variability of the 16S rRNA gene in bacterial genomes and its consequences for bacterial community analyses. *PloS One* 8 (2), e57923. doi: 10.1371/journal.pone.0057923

Vigneault, B., Percot, A., Lafleur, M., and Campbell, P. G. (2000). Permeability changes in model and phytoplankton membranes in the presence of aquatic humic substances. *Environ. Sci. Technol.* 34 (18), pp.3907–3913. doi: 10.1021/es001087r

Vigneron, A., Cruaud, P., Aubé, J., Guyoneaud, R., and Goñi-Urriza, M. (2021). Transcriptomic evidence for versatile metabolic activities of mercury cycling microorganisms in brackish microbial mats. *NPJ Biofilms Microbiomes* 7 (1), 83. doi: s41522-021-00255-y

Villar, E., Cabrol, L., and Heimbürger-Boavida., L.-E. (2020). Widespread microbial mercury methylation genes in the global ocean. *Environ Microbiol Rep* 12 (3), 277–287. doi: 10.1111/1758-2229.12829

Vishnivetskaya, T. A. (2018). Microbial community structure with trends in methylation gene diversity and abundance in mercury-contaminated rice paddy soils in Guizhou, China. *Environ. Sci. Process. Impacts* 20, 673–685. doi: 10.1039/C7EM00558J

Wang, K., Liu, G., and Cai, Y. (2022). Possible pathways for mercury methylation in oxic marine waters. *Crit. Rev. Environ. Sci. Technol.* 52 (22), 3997–4015. doi: 10.1080/10643389.2021.2008753

Wang, F., Macdonald, R. W., Armstrong, D. A., and Stern, G. A. (2012). Total and methylated mercury in the Beaufort Sea: The role of local and recent organic remineralization. *Environ. Sci. Technol.* 46 (21), 11821–11828. doi: 10.1021/es302882d

Wang, K., Munson, K. M., Armstrong, D. A., Macdonald, R. W., and Wang, F. (2020). Determining seawater mercury methylation and demethylation rates by the seawater incubation approach: A critique. *Mar. Chem.* 219, 103753. doi: 10.1016/j.marchem.2020.103753

Wang, K., Munson, K. M., Beaupre-Laperriere, A., Mucci, A., Macdonald, R. W., and Wang, F. (2018). Subsurface seawater methylmercury maximum explains biotic mercury concentrations in the canadian arctic. *Sci. Rep.* 8 (1), 1–5. doi: 10.1038/s41598-018-32760-0

Wang, J., Shaheen, S. M., Jing, M., Anderson, C. W., Swertz, A.-C., Wang, S.-L., et al. (2021). Mobilization, methylation, and demethylation of mercury in a paddy soil under systematic redox changes. *Environ. Sci. Technol.* 55 (14), 10133–10141. doi: 10.1021/acs.est.0c07321

Weber, J. H., Reisinger, K., and Stoeppler, M. (1985). Methylation of mercury (II) by fulvic acid. *Environ. Technol.* 6 (1-11), 203–208. doi: 10.1080/09593338509384337

Wen, Q., Su, Z., Cai, W., Huang, W., Fan, J., Huang, H., et al. (2017). Recent progress on detection methods of methyl mercury. *J. Food Saf. Qual.* 8 (3), 845–853. doi: 20173134599

Westoo, G. (1967). Determination of methylmercury compounds in foodstuffs. *Acta Chem. Scand.* 21, 1790–1800. doi: 10.3891/acta.chem.scand.21-1790

Whalin, L., Kim, E.-H., and Mason, R. (2007). Factors influencing the oxidation, reduction, methylation and deme- thylation of mercury species in coastal waters. *Mar. Chem.* 107 (3), 278–294. doi: 10.1016/j.mar-chem.2007.04.002

Wood, J. M., Kennedy, F. S., and Wolfe, R. S. (1968). Reaction of multihalogenated hydrocarbons with free and bound reduced vitamin B12. *Biochemistry* 7 (5), 1707–1713. doi: 10.1021/bi00845a013

Wu, P., Kainz, M. J., Valdés, F., Zheng, S., Winter, K., Wang, R., et al. (2021). Elevated temperature and browning increase dietary methylmercury, but decrease essential fatty acids at the base of lake food webs. *Sci. Rep.* 11 (1), 16859. doi: 10.1038/s41598-021-95742-9

Yao, C., He, T., Xu, Y., Ran, S., Qian, X., and Long, S. (2020). Mercury bioaccumulation in zooplankton and its relationship with eutrophication in the waters in the karst region of Guizhou Province, Southwest China. *Environ. Sci. pollut. Res.* 27, 8596–8610. doi: 10.1007/s11356-019-07479-8

Yap, M., Ercolini, D., Álvarez-Ordóñez, A., O'Toole, P. W., O'Sullivan, O., and Cotter, P. D. (2022). Next-generation food research: use of meta-omic approaches for characterizing microbial communities along the food chain. *Annu. Rev. Food Sci. Technol.* 13, .361–.384. doi: 10.1146/annurev-food-052720-010751

Zhang, Y., Jacob, D. J., Horowitz, H. M., Chen, L., Amos, H. M., Krabbenhoft, D. P., et al. (2016). Observed decrease in atmospheric mercury explained by global decline in anthropogenic emissions. *Proc. Natl. Acad. Sci.* 113, 526–531. doi: 10.1073/pnas.1516312113

Zhang, L., Liang, X., Wang, Q., Zhang, Y., Yin, X., Lu, X., et al. (2021). Isotope exchange between mercuric [Hg (II)] chloride and Hg (II) bound to minerals and thiolate ligands: Implications for enriched isotope tracer studies. *Geochim. Cosmochim. Acta* 292, 468–481. doi: 10.1016/j.gca.2020.10.013

frontiers | Frontiers in Marine Science

TYPE Original Research
PUBLISHED 19 October 2023
DOI 10.3389/fmars.2023.1244434

OPEN ACCESS

EDITED BY
Xin Lin,
Xiamen University, China

REVIEWED BY
Xiangqi Yi,
Xiamen University, China
Yong Zhang,
Fujian Normal University, China

*CORRESPONDENCE
Åsa M. M. Berglund
asa.berglund@umu.se

RECEIVED 22 June 2023
ACCEPTED 27 September 2023
PUBLISHED 19 October 2023

CITATION
Berglund ÅMM, Gallampois C, Ripszam M, Larsson H, Figueroa DA, Grinienė E, Byström P, Gorokhova E, Haglund P, Andersson A and Tysklind M (2023) Effects on the food-web structure and bioaccumulation patterns of organic contaminants in a climate-altered Bothnian Sea mesocosms.
Front. Mar. Sci. 10:1244434.
doi: 10.3389/fmars.2023.1244434

Effects on the food-web structure and bioaccumulation patterns of organic contaminants in a climate-altered Bothnian Sea mesocosms

Åsa M. M. Berglund[1]*, Christine Gallampois[2], Matyas Ripszam[2,3], Henrik Larsson[4], Daniela A. Figueroa[1], Evelina Grinienė[5], Pär Byström[1], Elena Gorokhova[6], Peter Haglund[2], Agneta Andersson[1,4] and Mats Tysklind[2]

[1]Department of Ecology and Environmental Science, Umeå University, Umeå, Sweden, [2]Department of Chemistry, Umeå University, Umeå, Sweden, [3]Department of Chemistry and Industrial Chemistry, University of Pisa, Pisa, Italy, [4]Umeå Marine Sciences Centre, Umeå University, Hörnefors, Sweden, [5]Marine Research Institute, Klaipėda University, Klaipėda, Lithuania, [6]Department of Environmental Science, Stockholm University, Stockholm, Sweden

Climate change is expected to alter global temperature and precipitation patterns resulting in complex environmental impacts. The proposed higher precipitation in northern Scandinavia would increase runoff from land, hence increase the inflow of terrestrial dissolved organic matter (tDOM) in coastal regions. This could promote heterotrophic bacterial production and shift the food web structure, by favoring the microbial food web. The altered climate is also expected to affect transport and availability of organic micropollutants (MPs), with downstream effects on exposure and accumulation in biota. This study aimed to assess climate-induced changes in a Bothnian Sea food web structure as well as bioaccumulation patterns of MPs. We performed a mesocosms-study, focusing on aquatic food webs with fish as top predator. Alongside increased temperature, mesocosm treatments included tDOM and MP addition. The tDOM addition affected nutrient availability and boosted both phytoplankton and heterotrophic bacteria in our fairly shallow mesocosms. The increased tDOM further benefitted flagellates, ciliates and mesozooplankton, while the temperature increase and MP addition had minor effect on those organism groups. Temperature, on the other hand, had a negative impact on fish growth and survival, whereas tDOM and MP addition only had minor impact on fish. Moreover, there were indications that bioaccumulation of MPs in fish either increased with tDOM addition or decreased at higher temperatures. If there was an impact on bioaccumulation, moderately lipophilic MPs (log K_{ow} 3.6 – 4.6) were generally affected by tDOM addition and more lipophilic MPs (log K_{ow} 3.8 to 6.4) were generally affected by increased temperature. This study suggest that both increased temperatures and addition of tDOM likely will affect bioaccumulation patterns of MPs in shallow coastal regions, albeit with counteracting effects.

KEYWORDS

organic contaminants, climate impact, food web, bioaccumulation, ecology, Bothnian Sea

1 Introduction

The expected consequences of climate change are not uniform around the globe. While some areas are predicted to have dryer and warmer climates, others will receive more precipitation (IPCC, 2022). Climate change is further expected to affect the global distribution patterns and effects of organic micropollutants (MPs), including persistent organic pollutants (POPs), with a risk of increased redistribution of and exposure to pollutants in different ecosystems (Kallenborn et al., 2012; Borgå et al., 2022). In Scandinavia, increased temperature and precipitation are expected due to a changing climate (Meier et al., 2022), with increased land runoff to rivers and streams (Bergström et al., 2001). This would enhance the load of terrestrial dissolved organic matter (tDOM) into freshwater systems and coastal areas with both changes in the food web structure (Andersson et al., 2015; Creed et al., 2018) as well as changes in the distribution and partitioning of pollutants (Noyes et al., 2009; Kallenborn et al., 2012; Gilbreath and McKee, 2015; Ripszam et al., 2015; Borgå et al., 2022). During recent years the Swedish monitoring of rivers and streams also confirms increasing trends of the water color (browning) and total organic carbon in the majority of investigated areas connected to the Baltic Sea (Swedish Institute for the Marine Environment, 2023).

The Baltic Sea is a semi-enclosed sea with limited water exchange from the high-saline Atlantic Ocean in the south. As a result, the Sea is highly influenced by river runoff, especially in the northern basins (Bothnian Sea and Bothnian Bay). Due to the restricted exchange of water in the Bothnian Sea, the relatively large catchment area, and the occurrence of industries such as pulp and paper mills, the environment has been severely contaminated over the last decades (Sundqvist et al., 2009; Miller et al., 2013; Assefa et al., 2014; Lester and van Riper, 2014). Although concentrations of several POPs have declined, they remain high in sediment and biota (Miller et al., 2013; Assefa et al., 2014; Assefa et al., 2019). With the ongoing climate changes, we expect an increased discharge of both tDOM and MPs into the Baltic Sea with complex direct and indirect effects on the transport, availability and toxicity of POPs (reviewed in Noyes et al., 2009; Kallenborn et al., 2012; Borgå et al., 2022). Climate change also increase water temperatures, influencing MP partitioning, leading to increased bioavailability, but also higher evaporation rates of volatile compounds (Noyes et al., 2009). High temperatures generally speed up the metabolism in biota; thus, the uptake but also elimination of compounds are expected to increase (Noyes and Lema, 2015). In addition, the sensitivity to MPs with increased temperatures, may be species specific (Borgå et al., 2022). As increased temperature may have multiple impacts on MPs, their bioavailability has been proposed to increase, decrease or have no net effect in the warmer climate (Borgå et al., 2010; Carrie et al., 2010; Borgå et al., 2022).

Availability of tDOM may have multiple effects on MP availability and accumulation. Hydrophobic contaminants will adsorb to particles and tDOM (Ripszam et al., 2015), thus decreasing their bioavailability via direct uptake from the water (Haitzer et al., 1998). However, organic material can also serve as a source of nutrients for heterotrophic bacteria (Stepanauskas et al., 2002) favoring heterotrophic bacteria over phytoplankton at the base of the food chain (Andersson et al., 2015; Figueroa et al., 2016). Furthermore, increased tDOM often result in browning of waters, and phytoplankton will have a disadvantage over heterotrophic bacteria due to shading (Creed et al., 2018). The decrease in phytoplankton production may lead to a shift in the food web, favoring the microbial food web (heterotrophic bacteria, flagellates, ciliates and mesozooplankton) over the phototrophic food web constituted of phytoplankton and mesozooplankton (Berglund et al., 2007; Lefebure et al., 2013; Andersson et al., 2015). Many of the legacy POPs (e.g., DDT and PCBs) are known to biomagnify in the food web (Gobas et al., 1999; Borgå et al., 2004). Thus, the shift towards a heterotrophic bacteria-based system would increase the number of trophic levels and potentially increase the accumulation of POPs at the top of the food web. Although the interest in climate-driven pollutant impacts has increased, especially in the Arctic (Noyes et al., 2009; Kallenborn et al., 2012; Su et al., 2018), only a few studies have focused on the climate-driven ecological processes that may impact the availability and transfer of MPs (Alava et al., 2017; Borgå et al., 2022).

In this mesocosm study, we exposed a pelagic food web from the Bothnian Sea to a cocktail of MPs under different climate scenarios, including the future climate conditions represented by increased temperature and tDOM levels as well as present-day conditions. The aim was to evaluate how bioaccumulation patterns of legacy and currently used MPs respond to the future climate scenario considering direct and indirect effects, including ecological shifts in the food web. The hypothesis was that top consumers accumulate more MPs under future climate conditions due to increased heterotrophy of the food web. In addition, we expect that the effects on the bioaccumulation of compounds with high persistence and lipophilicity will be more pronounced, due to their tendency to biomagnify in the food web.

2 Methods

2.1 Experimental setup and treatments

The outdoor mesocosm experiment took place during 34 days between May and July 2013, at the Umeå Marine Science Centre (UMF), Sweden (63' 33'N, 19' 49'E). Three experimental treatments were applied, alone or in combination (three replicates each), with tDOM addition, temperature increase and MP addition as treatment factors (Figure 1A). We used the maximum predicted increase in temperature and tDOM (an increase of 3°C and 30% tDOM, respectively), as suggested earlier (Meier, 2006; Neumann, 2010), and the present day conditions in the region during summer, resulting in experimental settings of 15 and 18°C and 4mg/L and 6mg/L DOC (dissolved organic carbon) for the present-day and climate-altered conditions, respectively. In total 24, mesocosms were established in clean 1 m^3 cubic shaped (1×1×1m) polypropylene tanks (Allembalage AB, Jordbo, Sweden), sheltered by a semi-transparent roof. All tanks were simultaneously filled with 947 L sea water (3‰ salinity) collected 1 km offshore in the northern Bothnian sea (63° 34'N, 19°54'E) using the large pumps of the UMF field station Flygt 3152.181 (Xylem Sundbyberg Sweden).

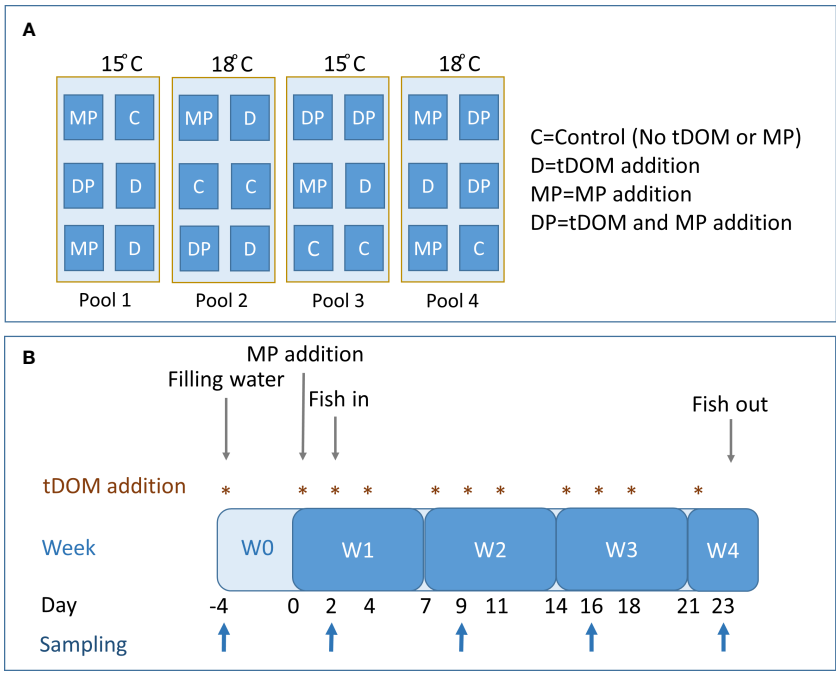

FIGURE 1
Design and layout of the mesocosm experiment **(A)**, and the treatment and sampling scheme over the experiment duration **(B)**.

The water was filtered (1 mm slit filter, Bernoulli System Lund, Sweden) to remove fish and allow natural communities of bacteria, phytoplankton, protozoa and mesozooplankton to populate the mesocosms. The mesocosms were completely immersed in four swimming pools (Ultra Frame Pool 7", Intex, Long Beach; Ca, USA) filled with seawater and connected to a temperature-control system, that maintain the target water temperatures. A block design included six mesocosms per swimming pool, and the position of each mesocosm was randomized to avoid systematic errors (Figure 1A). The temperatures in the pools were recorded daily, yielding an average of 18.0 ± 0.01, 15.2 ± 0.02, 18.0 ± 0.01, and 14.9 ± 0.01°C, for pool 1 – 4 respectively. Individual temperature measurements in each mesocosm was not conducted as each mesocosm was fully immersed in the pools, and hence unlikely would deviate from the temperature in the pools. The mesocosm were aeriated via a compressed air-valve system and to prevent insect colonization mosquito nets were mounted on the top of the mesocosms.

To mimic the increased runoff of organic material, tDOM was prepared using natural humic soil from a typical forest of the area (mix of deciduous and coniferous trees) as described by Ripszam et al. (2015). The humic soil extract was analyzed for DOC, DIN (dissolved inorganic nitrogen, i.e. nitrate, nitrite and ammonium), DIP (dissolved inorganic phosphorous), total N and total P, to calculate the appropriate soil extract volume and nutrient amount for addition. The tDOM-treated mesocosms were pre-treated with 0.5mg/L DOC; after that, tDOM was added weekly (0.14 mg C/L 3 times a week) in concert with water replacement (see below and Figure 1B). To account for the nutrient addition in the tDOM-treated mesocosms, a corresponding amount of dissolved nitrogen and phosphorous (initial boost: 0.95 µg PO4-P/L, 4.43 µg NO_3/L and 0.72 µg NH_4/L, followed by 0.20 µg PO4-P/L, 0.94 µg NO_3/L and 0.15 NH_4/L 3 times a week) was added in control mesocosms (Stepanauskas et al., 2002; Lignell et al., 2008).

The mesocosms were left to equilibrate, and 4 days after the initial tDOM treatment (hereafter referred to time = 0), 2.5 mL of a methanol spiking solution containing a mixture of 33 MPs was added to half of the mesocosms. For a complete list of compounds and the initial concentrations as well as final concentrations, see Ripszam et al. (2015, Table 1 and Figure 3). The MPs were selected based on the hazardous substance list provided by the European Commission (Directive 2008/105/EC, 2008) and spanned four orders of magnitude of lipophilicity, viz. log octanol-water partition coefficients (log K_{ow}) between 2.1 and 6.4 (Table S1). The mixture included legacy POPs, recently and currently used pesticides, high-volume production compounds and some benchmark compounds for modelling (Ripszam et al., 2015).

Two days after the MP addition, fish was introduced to the mesocosms and kept in the system for 21 days. In total, 10 perch (*Perca fluviatilis*) larvae (6.3 ± 0.1mm, 0.8 ± 0.05mg) were added as top predators in each mesocosm. Perch was hatched from egg strands, collected from a coastal spawning bay (63°45'14" N, 20° 32'18" E) and kept at 16°C until the start of the experiment. During the initial stage (pre-exposure), they were fed a mixture of live zooplankton. One week before the planned experiment termination (day 30), the fish were removed due to low zooplankton abundance and risk of starvation. Thus, on day 23, all surviving perch were collected with a large 3-mm net and killed by overdosing of M222 (Ethyl 3-aminobenzoate methanesulfonate, Fluka; Ethical approval No. A28-13, Umeå University). Samples were kept frozen at –20°C until chemical analysis was performed.

2.2 Weekly sampling

Twenty liters of water were replaced three times a week with an equal volume of filtered (20 µm) seawater (see Figure 1B for the sampling scheme). At the same time, nutrients or tDOM (depending on treatment) were added to mesocosms to gradually reach the target of 6 mg/L DOC in the tDOM-treated mesocosms. Once a week, an aliquot of water was sampled, filtered (90 µm), and used to analyze pH, DOC, total nitrogen (Ntot), DIN, total phosphorous (Ptot), DIP, particulate organic phosphorous (PO4-P), primary production (PP), Chlorophyll α (Chl α), bacterial production (BP), and bacterial abundance (BA), phytoplankton, flagellate and ciliates. Mesozooplankton was collected weekly from each mesocosm by three bottom-to-surface hauls with a 65 µm net (14 cm diameter); 40.16 L/sample were filtered. Phytoplankton, flagellates and PO4-P were only counted/analyzed at the start (day -4), mid-point (day 16) and after fish was sampled (day 30, not included in this paper). Light (photosynthetically active radiation, PAR) was measured weekly during mid-day using a PAR Licor sensor (LICOR -193SA) at three depths (top, middle and bottom) and five positions and calculated as an average value for each mesocosm.

2.3 Water chemistry

All parameters for water chemistry (DOC, pH, DIN, DIP, Ntot, Ptot, PO4-P) were determined on the day of sampling. DOC was measured in a high-temperature carbon analyzer (Shimadzu TOC-5000, Shimadzu Corporation) with platinum-coated Al_2O_3 granulate as a catalyst, according to Berglund et al. (2007). A benchtop pH meter (pHenomenal, VWR International AB, Spånga Sweden) with a combined glass electrode (PHENOMENAL 221, avantor, VWR Spånga Sweden), calibrated with three (4.00, 7.00 and 10.01) buffers, AVS Titronorm traceable to SRM from NIST (BDH Chemicals) was used for pH measurements. Concentrations of inorganic nutrients (DIN and DIP) and total nutrient content (Ntot and P tot) were analyzed using a 4-channel auto-analyzer (Quaatro Marine, Braan and Luebbe) according to the Swedish Standards Institute (Grasshoff et al., 1999). The detection limit for DIN and DIP were 1.5 µg DIN/L N and 0.7 µg DIP/L P, respectively. Particulate organic phosphorous (PO4-P) was quantified using the ash-hydrolysis method, with a lower range of measurement from 0.08 µM (Solórzano and Sharp, 1980).

2.4 Biological variables

Primary production, BP and Chl α were analyzed at the day of sampling; all other analyses/counts (BA, phytoplankton, flagellates, ciliates and mesozooplankton) were performed later. Samples for analysis of biomasses and abundances of phytoplankton, heterotrophic flagellates, ciliates and mesozooplankton were fixed with 2% acidic Lugol's solution according to Utermöhl (1958) and stored at 4°C until analysis. Ten µL of glutaraldehyde was added to samples used for BA analyses, and samples were kept for 15 min in the dark followed by storage at -80°C until analysis.

2.5 Bacterial production and abundance

Bacterial production was measured using the [^{3}H-methyl]-thymidine technique (Fuhrman and Azam, 1982). In short, 1 mL of mesocosms water was added to Eppendorf tubes (one control and triplicate samples). In the controls, bacteria were pre-killed by adding 100 µl ice-cold 50% trichloroacetic acid (TCA) and incubated at -20°C for 5 minutes. Then, 2 µL of [^{3}H]-thymidine (84 Ci mmol^{-1}; Perkin Elmer, Massachusetts, USA) were added to each tube to a final concentration 24 nM. Samples were incubated for 1h in the dark, during the early afternoon, at the respective temperature treatment (15 or 18°C). The incubation was terminated by adding 100 µL ice-cold 50% TCA and centrifuging at 13,000 rpm for 10 min. After washing the pellet with 5% TCA, 1 mL scintillation cocktail was added before analyses in a scintillator counter (Beckman Coulter LS 6500/Packard Tri-Carb 1600 TR). The incorporated thymidine was converted to cell production using the conversion factor of $1.4x10^{18}$ cells mol^{-1} (Wikner and Hagström, 1999). Carbon biomass production was estimated from cell production and average cell carbon biomass according to Fuhrman and Azam (1982), using a bacterial carbon content of $1.7x10^{-9}$ µmol C cell^{-1}.

Bacterial abundance was analyzed using a BD FACSVerseTM flow cytometer (BD Biosciences) fitted with a 488-nm laser (20 mW output). Samples were stained with SYBR Green I (Invitrogen) to a final concentration of 1: 10 000 (Marie et al., 2005) and diluted with filtered (0.2 µm) seawater. Samples were run for 1 min at a flow rate of 30 mL min^{-1} and 1 µm microspheres (Fluoresbrite plain YG, Polysciences) served as an internal standard in each sample. Forward light scatter (FSC), side light scatter (SSC), and green fluorescence from SYBR Green I (527 ± 15) were measured to estimate bacteria abundance. Bacterial biomass was then calculated using a conversion factor of 20 fg C cell^{-1} (Lee and Fuhrman, 1987).

2.6 Primary production and chlorophyll α

Primary production (PP) was measured *in situ* using the ^{14}C method according to Gargas (1975). Five mL of sample were added to 20 mL transparent polycarbonate tubes in triplicate and one dark tube as control. ^{14}C was added to each tube (7.2 µL, ^{14}C Centralen Denmark, activity 100 µCi mL^{-1}), and incubation of samples was carried out at 80 cm depth inside the pools, during early afternoon, for about 3 hours. Controls were incubated in the dark, at the respective temperature treatment (15 or 18°C). The activity was stopped by the addition of 150 µL 6M HCl. The samples were analyzed in a scintillation counter (Beckman Coulter LS 6500/Packard Tri-Carb 1600 TR) following addition of 15 mL scintillation cocktail (Optiphase HiSafe 3). Daily PP was calculated as described in Andersson et al. (1996) using factor F according to Gargas (1975).

Samples for Chl α (100 mL) were filtered onto 25 mm GF/F filters, extracted in 10 mL 96% ethanol overnight and measured with a Perkin Elmer LS 30 fluorometer (433/674 nm excitation/emission wavelengths; Waltham®, Middlesex, MA, USA). The protocol was based on US EPA (1997), protocol 446, with the following modifications: a) Ethanol 96% was used in place of 90% acetone and b) glass fiber filters were crushed using ball milling with 5 mm steel beads instead of a mechanical tissue grinder.

2.7 Phytoplankton, flagellates, ciliates and mesozooplankton

Phytoplankton and nanoflagellates were only counted at the start (day -4), mid-point (day 16) and after fish was removed (day 30). Hence, only data for the first two sampling occasions, with relevance for fish, are presented in this paper. Using sedimentation chambers, 10-50 mL of a Lugol-fixed sample were settled for 12-48 hours. The cells were counted using an inverted microscope (Nikon Eclipse Ti) at 100-400x magnification with phase contrast settings (Utermöhl, 1958). Cell biovolume was calculated according to Olenina et al. (2006). Chl α was used as a proxy for phytoplankton stock, as phytoplankton counts (data not shown) were performed on a limited number of samples, and Chl α and phytoplankton biomass correlated well (R^2 = 0.66, p<0.0001).

For ciliate analysis, 25–50 mL of the fixed sample were settled for at least 24-48 h in Utermöhl's chambers and counted with an inverted microscope at 200× magnification, as described in Andersson et al. (2023). The entire bottom of each chamber was surveyed, and an additional subsample was counted if the total number of organisms was below 150. Ciliate biomass was based on their biovolume, which was calculated by their geometric shape using measurements of the cell length and width of at least 20 cells of each species/taxa per sample. Cell carbon content for flagellates and ciliates was calculated according to Menden-Deuer and Lessard (2000).

For mesozooplankton analysis, each sample (entire volume) was counted using a counting chamber and an inverted microscope (Leitz fluovert FS, Leica) at 80× magnification. Copepods were classified according to species and developmental stage (nauplii, copepodites CI–III, CIV–V and adults), whereas cladocerans (*Bosmina coregoni*) were classified according to species, maturity (adults and juveniles) and sex. Biomass (wet weight) was calculated using abundance data, species- and stage-specific individual weights (Hernroth, 1985). Three mesozooplankton groups were considered for the abundance and biomass aggregation: copepods, cladocerans and rotifers. To account for potential differences in ciliate and mesozooplankton abundances, due to the variations in the communities of the root sample (day -4), the relative change in ciliate and mesozooplankton biomass and abundance were calculated:

$$Relative\ \ change\ (\Delta) = \frac{(t_x - t_{-4})}{t_{-4}}$$

where t_x is the biomass/abundance at the time of interest and t_{-4} is the biomasss/abundance at the start of the experiment (day -4).

2.8 Chemical analyses, MPs

Organic contaminants were extracted from whole fish using 1.5 mL cyclohexane: etylacetate (3:1v/v). Internal standard, 20 µL (Ripszam et al., 2015), was added, and the fish samples were homogenized with zirconium beads in a Mini Beadbeater (Biospec. Bartlesville, USA) for 4 min at 3500 oscillations/min. The homogenate was centrifuged at 14 000 rpm for 10 min and the supernatant was collected. The procedure was repeated thrice, and the combined supernatants were evaporated to 500 µL. Lipid removal was accomplished by gel permeation chromatography (GPC) cleanup (Sundkvist et al., 2010). Organic micropollutant concentrations were analyzed by gas chromatography – high-resolution mass spectrometry (GC-HRMS) using an Agilent 6890 GC (Agilent, Santa Clara, CA USA) equipped with an ultra-inert J&W DB-5MS GC column (30m*0.25mm*0.25µm, Agilent, Santa Clara, CA, USA) and a Waters Micromass AutoSpec Ultima HRMS (Waters Corp., Milford, MA, USA) (Sundkvist et al., 2010). The HRMS was operated in electron ionization (EI) mode at >8,000 resolution, utilizing selected ion monitoring (SIM) of two abundant ions of each target compound and internal standard.

Dissolved MPs in water were determined in the sub-0.7µm fraction by liquid-liquid extraction of 300mL water, passed through GF/F filters. Internal standard (20 µL) was added, and extraction occurred in 100 mL dichloromethane (50 mL once and 25 mL twice). Chemical analysis was performed by GC-MS using an Agilent 7890N GC coupled to an HRT-TOF-MS instrument (Leco, St. Joseph, MI), equipped with an ultra-inert J&W DB-5MS GC column (30m*0.25mm*0.25µm, Agilent, Santa Clara, Ca, USA), as described in Ripszam et al. (2015). One sample (MP15 treatment) was lost during the analysis. If concentrations of any contaminants (in fish or water) exceeded 10% of the highest concentration measured in blanks, compounds were omitted from further analysis.

2.9 Statistical analyses

One control mesocosm (18°C) showed low phytoplankton abundance (measured as Chl α), throughout the experiment and only one fish survived. This mesocosm was regarded as an outlier and thus not included in the statistical analyses, nor figures. Data are shown as mean ± SD and all statistical analyses were performed with R 3.6.1 (R Core Team, 2019). Data points below detection limit (i.e. DIP) were not substituted with a constant value.

Multifactorial analysis (MFA; package: FactoMineR) was used on the combined data on water chemistry and biological variables to explore variability within and between treatments. The MFA uses weighed principal axis methods applied on a mixture of quantitative, categorical and frequency variables, and the basis of MFA can be viewed as a weighted PCA applied to a multiple table in which different sets of quantitative variables are juxtaposed (Bécue-Bertaut and Pagès, 2008). The data (DOC, Ptot, Ntot, pH, PP, BP, BA, Chl α, ciliate and mesozooplankton abundances and biomasses) was scaled and grouped by five sampling occasions, and the treatment factors were used as supplementary qualitative

variables. Dissolved inorganic nutrients (DIN and DIP) were not included in the MFA due to the low frequency of detection (up to 65% of samples were below the detection limit), and flagellates and PO4-P were excluded due to low sampling resolution (two of the five sampling occasions). One data point for Ptot was missing due to analytical errors and thus replaced using data imputation (package: missMDA-package).

Changes in water chemistry (pH, DOC and nutrients) and food web structure (primary, heterotrophic bacteria and total basal production, flagellates, ciliates and mesozooplankton) were assessed using linear mixed models (package: nlme), with normal distribution. To provide linear fit of models, all dependent variables except Ntot, Δ flagellate biomass, proportions of copepods and rotifer abundance, fish biomass and FWE were log-transformed, adding a constant (+1) when necessary to prevent infinite values. Visual interpretation of residuals of the fitted model (QQ-plots) were used to assess the need to transform the data. The following treatments were included as independent fixed categorical factors: temperature, MPs, tDOM, and time and three-way interactions were considered in the most complex model. Mesocosm was included as a random factor to account for repeated measures over time. Due to many samples below the detection limit (65%), statistical analyses of DIP did not include time as a factor. Relationships between DOC concentration and nutrient availability (DIN, DIP, PO4-P, Ntot and Ptot) was assessed using the Spearman correlation test.

Food web efficiency (FWE), defined as the cumulative annual production rate of fish over the pelagic primary and heterotrophic bacterial production was determined as the ratio between fish production ($Fish_p$) and total basal production (PP + BP) (Rand and Stewart, 1998):

$$FWE = \frac{\text{Fish}_p}{\text{PP} + \text{BP}}$$

where fish production, PP and BP estimates were expressed as mg C L^{-1} d^{-1}. Fish production was estimated as the total mass change of all surviving individuals assuming carbon content to be 20% of the wet weight (Jobling, 1995), and basal production was estimated as the average BP + PP production during the time when fish was present in the mesocosms.

Differences in total fish biomass and FWE were also assessed with the linear mixed models, and fish survival was analyzed using a generalized linear model with binomial distribution and logit-function (package: stats). All fish models included MPs, temperature and tDOM, and their three-way interactions as independent fixed categorical effects. The correlation between total mesozooplankton biomass and fish survival or total biomass was estimated using the Spearman correlation test.

Bioaccumulation factors (BAF) were calculated using lipid normalized (BAF_l) and wet weight (BAF_{ww}) concentrations in fish and soluble MPs in the sub-0.7 µm fraction:

$$BAF = \frac{MP\ concentration\ in\ fish\ (based\ on\ wet\ weight\ or\ lipid\ weight)}{MP\ concentration\ in\ water}$$

Due to small individual mass (10-19 mg fish, ww), the lipid content was determined for a bulk sample of control fish, yielding 1.4% lipid in the wet mass, and used for all fish samples. This does not allow exact calculation of BAF_l as lipid content may be affected by the treatments, but it provides a crude estimate of BAF_l. The soluble MP fraction was calculated as an average based on weekly water analyses; these results have been reported elsewhere (Ripszam et al., 2015). Treatment effects on the fish MPs concentrations and BAF values (log-transformed) were also analyzed using linear mixed models with normal distribution using temperature, MPs, and tDOM as independent fixed factors (including interactions) and mesocosm as a random factor.

The variable selection in the mixed models was applied using a likelihood ratio test, with stepwise selection (package: MuMIn). The best-fit model was selected based on the corrected Akaike information criterion (AICc), and the simplest model with the lowest AICc was chosen, provided that the ΔAICc > 2 (Burnham et al., 2011). If ΔAICc ≤ 2, the models in question were compared and simplified, if possible, using backward elimination, starting with omitting the interaction effects, and comparing models using ANOVA.

3 Results

3.1 Overall system changes

The multifactorial analysis (MFA) revealed that the water chemistry (pH, DOC, Ntot and Ptot) and biological variables (Chl α, PP, BP, BA, ciliate and mesozooplankton abundance, and ciliate and mesozooplankton biomass) shared similarities within treatments. The 1st dimension, explaining 33.7% of the variance, was strongly driven by tDOM, and mesocosms with tDOM addition had positive scores whereas mesocosms without tDOM addition had negative scores on dimension 1 (Supplementary Figure S1A). The 2nd dimension (13.9%) was driven by MP addition, with generally positive scores for treatments without MP addition and negative scores for mesocosms with MP addition. The third dimension (Supplementary Figure S1B) explained 12.7% of the variance and was mainly driven by temperature, with generally positive scores for 18°C treatments and negative loadings for 15° C treatments.

The general trends in water chemistry data are summarized in the text and available in Table 1, whereas detailed statistical outcome for all the variables included in the final global models can be found in Supplementary Table S2. pH was on average 7.8 ± 0.061, fluctuated over time (7.8 – 7.9, $p < 0.0001$), and was higher in 18 than 15°C mesocosms (7.9 ± 0.069 *vs.* 7.8 ± 0.046, $p < 0.001$). DOC concentrations were on average 5.6 ± 0.53 mg/L in mesocosms without soil addition, whereas in mesocosms with tDOM addition, DOC reached 7.4 ± 0.73 mg/L by the end of the experiment (2-way interaction time × tDOM: $p < 0.0001$), and addition of MP also increased the DOC concentrations ($p < 0.0001$). Moreover, tDOM increased the shading, with reduced light availability by approximately 30% ($p < 0.0001$) in tDOM-

10.3389/fmars.2023.1244434

TABLE 1 Summary (average ± SD) of water chemistry (pH, dissolved organic carbon (DOC), photosynthetically active radiation (PAR), total nitrogen (Ntot) and phosphorous (Ptot), dissolved inorganic nitrogen (DIN) and phosphorous (DIP), particulate organic phosphorous (PO-4P)) for the following treatments: Control (C), tDOM addition (D), organic micropollutant addition (MP) and tDOM + micropollutant addition (DP) at different temperatures (15 or 18°), during the duration of the experiment (MP addition at time=0).

Variable	Time (day)	C15	C18	D15	D18	MP15	MP18	DP15	DP18
pH	-4	7.9 ± 0.023	8.0 ± 0.084	7.8 ± 0.027	7.9 ± 0.072	7.9 ± 0.054	8.0 ± 0.060	7.9 ± 0.018	8.0 ± 0.085
	2	7.8 ± 0.027	7.8 ± 0.042	7.8 ± 0.044	7.8 ± 0.011	7.8 ± 0.016	7.8 ± 0.021	7.8 ± 0.0061	7.8 ± 0.0093
	9	7.8 ± 0.013	7.9 ± 0.0014	7.8 ± 0.018	7.8 ± 0.035	7.8 ± 0.014	7.8 ± 0.049	7.8 ± 0.038	7.9 ± 0.021
	16	7.8 ± 0.050	7.8 ± 0.034	7.8 ± 0.013	7.9 ± 0.020	7.8 ± 0.015	7.8 ± 0.025	7.8 ± 0.033	7.8 ± 0.052
	23	7.8 ± 0.018	7.9 ± 0.013	7.8 ± 0.015	7.8 ± 0.054	7.8 ± 0.030	7.8 ± 0.030	7.8 ± 0.012	7.8 ± 0.038
DOC[a]	-4	4.8 ± 0.062	4.9 ± 0.057	5.4 ± 0.029	5.4 ± 0.050	4.8 ± 0.13	4.9 ± 0.058	5.4 ± 0.038	5.4 ± 0.010
	2	5.4 ± 0.010	5.5 ± 0.057	6.1 ± 0.050	6.1 ± 0.059	6.4 ± 0.038	6.5 ± 0.075	7.2 ± 0.025	7.2 ± 0.44
	9	5.3 ± 0.071	5.4 ± 0.18	6.4 ± 0.027	6.5 ± 0.076	6.1 ± 0.087	6.2 ± 0.12	7.3 ± 0.023	7.3 ± 0.12
	16	5.2 ± 0.11	5.3 ± 0.085	6.7 ± 0.066	6.7 ± 0.12	5.8 ± 0.017	5.8 ± 0.12	7.2 ± 0.072	7.1 ± 0.12
	23	5.4 ± 0.015	5.6 ± 0.19	7.3 ± 0.059	7.3 ± 0.045	5.8 ± 0.035	5.7 ± 0.23	7.4 ± 0.15	7.5 ± 0.15
PAR[b]	0	250 ± 63	280 ± 27	140 ± 37	160 ± 31	200 ± 53	240 ± 46	170 ± 27	200 ± 32
	7	170 ± 33	94 ± 1.5	110 ± 46	100 ± 45	120 ± 60	170 ± 16	100 ± 40	73 ± 22
	22	260 ± 21	240 ± 13	170 ± 6.7	170 ± 22	260 ± 21	230 ± 11	150 ± 19	150 ± 31
Ntot[c]	-4	218 ± 1.19	220 ± 3.11	283 ± 8.21	286 ± 5.23	229 ± 11.9	232 ± 5.15	286 ± 12.6	273 ± 4.38
	2	241 ± 6.14	255 ± 2.62	320 ± 10.8	320 ± 12.3	252 ± 11.9	253 ± 14.8	318 ± 6.92	311 ± 0.115
	9	215 ± 8.88	215 ± 10.5	311 ± 13.1	303 ± 11.5	213 ± 2.89	219 ± 8.19	316 ± 5.55	305 ± 8.65
	16	219 ± 3.12	221 ± 15.7	356 ± 20.1	360 ± 7.22	218 ± 3.37	228 ± 8.68	337 ± 6.27	339 ± 18.5
	23	196 ± 0.577	207 ± 5.44	402 ± 34.0	354 ± 10.6	200 ± 3.57	217 ± 13.4	340 ± 13.5	329 ± 6.05
DIN[c]	-4	8.6 ± 0.59	7.4 ± 0.28	13 ± 4.1	7.9 ± 2.1	8.9 ± 0.81	8.4 ± 4.8	11.4 ± 2.1	6.3 ± 1.4
	2	5.7 ± 4.4	3.9 ± 1.7	9.4 ± 5.8	14 ± 18	7.5 ± 4.4	18 ± 18	11.4 ± 12	14 ± 11
	9	5.2 ± 0.55	10 ± 8.5	13 ± 3.3	18 ± 2.0	5.3 ± 1.5	10 ± 8.3	19.1 ± 7.0	15 ± 11
	16	2.2 ± 2.1	28 ± 36	6.4 ± 3.0	5.5 ± 1.2	5.8 ± 4.6	6.1 ± 5.7	10.3 ± 6.9	13 ± 7.0
	23	3.4 ± 4.6	1.8 ± 1.6	2.5 ± 0.61	2.2 ± 0.76	0.67 ± 0.058	3.8 ± 4.9	1.6 ± 1.3	1.2 ± 0.92
Ptot[c]	-4	8.7 ± 0.058	8.8 ± 0.071	12 ± 0.50	12 ± 0.91	10 ± 0.42	9.9 ± 0.59	11 ± 0.90	11 ± 0.31
	2	7.6 ± 0.21	8.4[d]	10 ± 0.67	11 ± 1.8	8.8 ± 0.23	8.4 ± 0.57	10 ± 0.49	10 ± 0.40
	9	6.5 ± 0.47	6.6 ± 1.3	9.2 ± 0.21	9.0 ± 0.15	6.3 ± 0.42	7.1 ± 0.81	9.8 ± 0.87	9.8 ± 0.38
	16	6.7 ± 0.42	6.2 ± 0.21	12 ± 0.62	11 ± 0.15	7.1 ± 1.1	6.4 ± 0.46	10 ± 0.57	9.6 ± 0.81
	23	5.8 ± 0.058	5.9 ± 0.42	15 ± 3.2	11 ± 0.71	6.3 ± 0.35	7.1 ± 0.72	10 ± 0.96	9.9 ± 0.36
DIP[c]	-4	0.83 ± 0.31	0.85 ± 0.35	2.2 ± 0.61	2.0 ± 0.30	1.5 ± 0.75	0.90 ± 0.44	1.8 ± 0.50	1.6 ± 0.15
	2	BDL	BDL	0.85 ± 0.21	0.75 ± 0.071	BDL	BDL	0.55 ± 0.071	1.1 ± 0.71
	9	BDL	BDL	BDL	BDL	BDL	BDL	0.40[d]	BDL
	16	BDL	BDL	0.90 ± 0.28	0.70 ± 0.42	BDL	BDL	BDL	0.80[d]
	23	BDL	BDL	1.7 ± 0.00	BDL	BDL	BDL	0.70[d]	BDL
PO4-P[c]	-4	5.6 ± 0.68	6.1 ± 0.21	9.3 ± 1.6	9.7 ± 2.2	7.2 ± 1.0	7.8 ± 0.85	7.9 ± 1.2	7.5 ± 0.60
	16	2.6 ± 0.40	2.0 ± 0.071	6.2 ± 2.0	7.3 ± 1.4	2.6 ± 0.21	1.7 ± 0.00	3.9 ± 0.38	4.1 ± 1.6

[a]mg L^{-1}.
[b]µmol Quanta m^{-2} s^{-1}.
[c]µg L^{-1}.
[d]Only represented by one sample per treatment.
[BDL] All samples below detection limit.

treated mesocosms, although the average PAR generally exceeded 100 µmol Quanta m^{-2} s^{-1} (Table 1).

tDOM had a positive effect on total N, total P, DIN and PO4-P, although this was insignificant for DIN ($p = 0.051$; Supplementary Table S2). Nutrients were generally consumed over time in the mesocosms ($p< 0.0001$ for Ntot, Ptot, DIN and PO-4P) and DIP was below detection limit in 65% of the analyzed samples, however, tDOM also had an interactive effect on the temporal patterns. tDOM addition increased Ntot as the experiment progressed, and Ptot and PO-4P were more stable in tDOM-treatments, whereas they decreased in mesocosms without tDOM (2-way interactions time × tDOM; $p< 0.0001$). Temperature had minor effects on nutrient availability, but the highest Ntot concentrations were found in 15°C treatments with tDOM addition and the lowest Ntot concentrations were found in 15°C treatments without tDOM (2-way interactions tDOM × temp, $p< 0.05$). If any, MP addition showed interactive effects with tDOM and time, revealing the highest Ntot and Ptot availability in tDOM treatments followed by tDOM × MP, MP and control treatments (2-way interactions tDOM × MP; $p< 0.0001$). Ntot increased over time in mesocosms without MP addition, but remained stable when MPs were added and PO-4P decreased more between the two sampling occasions if MPs were added (2-way interactions time × MP; $p< 0.01$).Total N, Ptot and DIN, but not DIP and PO4-P, correlated positively with DOC concentration (Ntot: $R_s = 0.86$, $p< 0.0001$; Ptot: $R_s = 0.80$, $p< 0.0001$; DIN: $R_s = 0.21$, $p< 0.05$).

3.2 Food web changes

The general trends of the food web components are presented in the text, whereas detailed statistical outcome for all the variables included in the final global models can be found in Supplementary Table S2. The experiment started during the spring bloom, reflected by high Chl α and PP concentration at the start of the experiment (Figure 2). Both Chl α and PP were slightly boosted in tDOM treatments, although most mesocosms showed a temporal decline after the initial bloom conditions ($p< 0.01$ for both). The temporal decrease in Chl α and PP was greater in mesocosms without tDOM (2-way interaction: time × tDOM; $p< 0.01$ for both). In addition, there was an increase in Chl α by the end of the experiments in mesocosms without MP, but with tDOM, suggesting inhibition of algal growth in MP treated mesocosms (2-way interactions: time × MP; time × tDOM and tDOM × MP). The trends of BP converged with that of Chl α and PP, except for the initial peak in production during the spring bloom (Figure 2). BP was more stable over time with tDOM addition, especially in MP treated mesocosms (3-way interaction: time × tDOM × MP; $p< 0.05$). Total basal production (PP + BP), were strongly influenced by the PP and followed the same patterns as PP (Figure 2).

Abundances of bacteria, flagellates and mesozooplankton (but not ciliates) were stimulated by tDOM addition ($p< 0.05$ for all but ciliates; Figure 3). The temperature effect on the abundance was minor and the temporal trends differed between these four plankton groups (Supplementary Table S2). Bacterial abundance peaked in the middle of the experiment, with no significant unidirectional time effect, although it appeared to decline most in 18°C mesocosms (Figure 3). Flagellate communities were only sampled twice over the experiment (start and mid-time), and abundances were lower in mesocosms without tDOM at the last sampling occasion but also lower in 18°C treatments at the last sampling occasion (Figure 3; 2-way interactions time × tDOM and time × temp: $p< 0.01$ for both). Although the general pattern indicated that there was a peak in ciliate abundance at the later stage of the experiment, the timing of the peak differed between treatments (Figure 3; 2-way interactions time × tDOM and time × temp: $p< 0.05$ for both). These temporal patterns in ciliate abundance was, however, not significant ($p > 0.06$) when the relative change from the start of the experiment (Δ abundance) was assessed (Supplementary Figure S2, and Table S2).

After an early peak in mesozooplankton abundance (Figure 3), mesozooplankton were strongly reduced throughout the experiment ($p< 0.0001$). The only MP effect on abundance was found for mesozooplankton, with lower abundances when MP was added ($p< 0.05$). However, the abundance of mesomesozooplankton was higher in control mesocosms, even prior to MP addition (day -4), and this MP–effect disappeared when the relative (Δ) mesozooplankton abundance was taken into account (Supplementary Figure S2). Early in the experiment, copepods were generally the most common zooplankton group based on abundances (52 ± 12%), followed by rotifers (41 ± 12%) and cladocerans (6.5 ± 4.0%). However, copepod contribution decreased with time to 34 ± 12% (Supplementary Figure S3), and by the end of the experiment, rotifers (59 ± 13%) were the most abundant mesozooplankton. The temporal decline in the percentage of copepods was more pronounced in mesocosms without tDOM (2-way interaction, time × tDOM: $p< 0.05$), especially at the lower temperature (15°C) (3-way interaction, time × tDOM × temp: $p< 0.05$). There were no significant treatment effect on the contribution of the older copepodite stages (stage 5 and adults; $p > 0.05$ for all treatments, data not shown) and they remained stable, albeit low (0.91 ± 0.61 ind L^{-1}). Cladocera abundance fluctuated over the duration of the experiment, with a slight decrease toward the end (Supplementary Figure S3).

The absolute and Δ biomasses of flagellates, ciliates and mesozooplankton generally followed similar patterns as the absolute and Δ abundances. The biomass of flagellate and mesozooplankton decreased with time (Figure 4; $p< 0.0001$ for both), however Δ biomass of ciliates increased with time (Supplementary Figure S2; $p< 0.05$). There was a positive tDOM effect on flagellate and ciliate biomass, especially as the experiment progressed ($p< 0.001$ for all), but no such effect was observed for mesozooplankton. As observed for the abundance of mesozooplankton, MP addition decreased the biomass of mesozooplankton, although again, no such affect was observed for the Δ biomass of mesozooplankton. Due to their larger body sizes, and occurrence of older copepodite stages, the biomass of copepods (0.63 ± 0.48 µg L^{-1}) was still higher than that of rotifers (0.29 ± 0.17 µg L^{-1}) by the end of the experiment, despite the numerical dominance of the rotifers (Supplementary Figure S4). Still, the biomass of copepod, rotifer and cladocera were strongly reduced (from 1.85 ± 0.46 at day 2 to 0.63 ± 0.48 µg L^{-1}, from 0.69 ± 0.20 at day 2 to 0.29 ± 0.174 µg L^{-1}, and from 0.78 ± 0.23 µg L^{-1} at day 2 to 0.17 ± 0.11 µg L^{-1} by the end of the experiment, respectively; $p< 0.001$ for all). Although there was no effect of tDOM on absolute biomass of mesozooplankton (Figure 4),

10.3389/fmars.2023.1244434

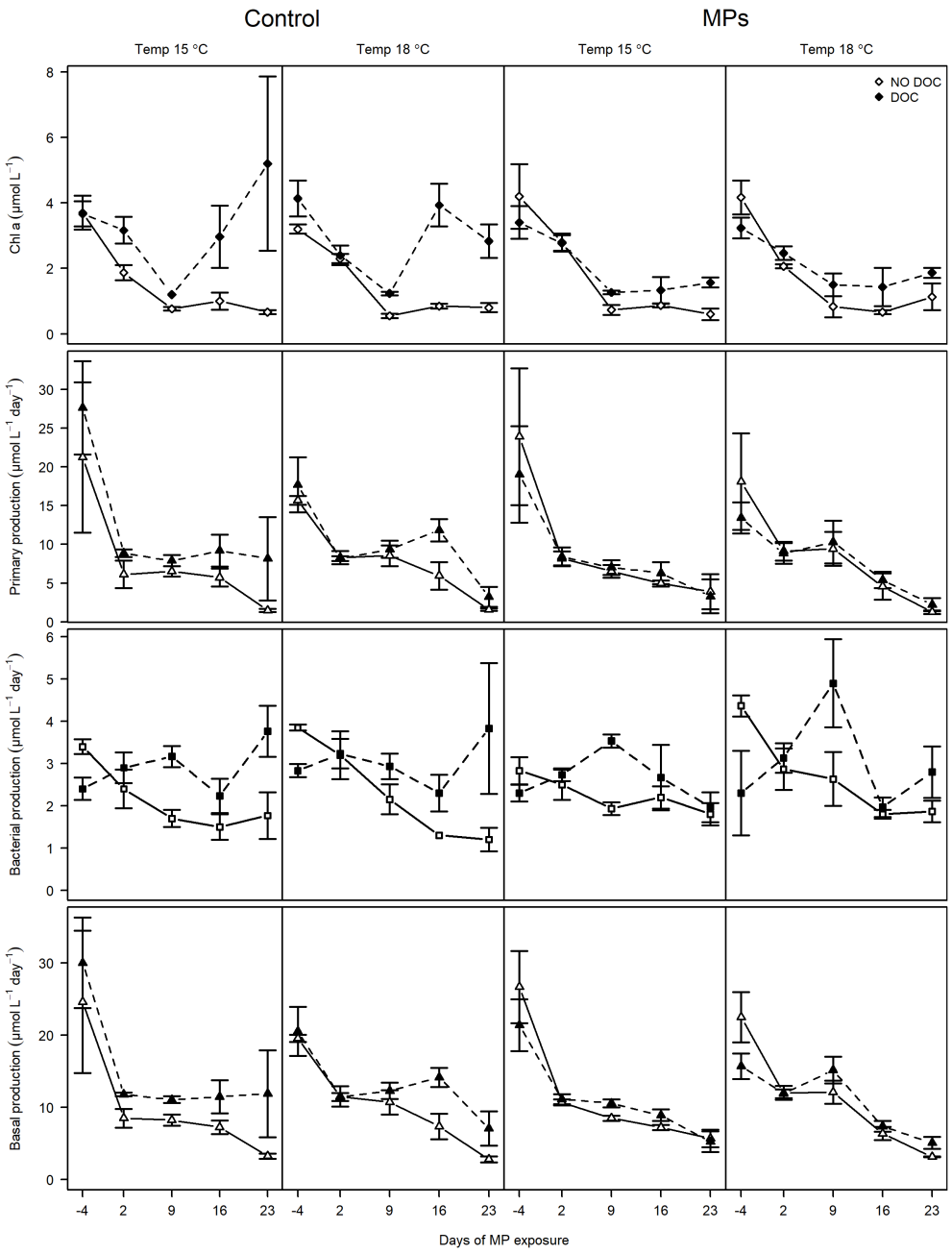

FIGURE 2
Temporal changes in Chlorophyll α, primary production, bacterial production and total basal production in different MP, tDOM and temperature factor combinations. The two columns to the left represent control mesocosms at 15 and 18°C and the two columns to the right represent MP exposed mesocosms at 15 and 18°C. Filled symbols and dashed lines are treatments with tDOM addition and open symbols with solid lines represent treatments without tDOM.

both rotifer and cladocera biomasses were higher in tDOM treated mesocosms (Supplementary Figure S4, $p < 0.05$ for both). Concurring with absolute biomass of mesozooplankton, all three mesozooplankton groups had higher biomasses in mesocosms without MP addition ($p < 0.05$ for all).

Fish biomass and survival were generally higher in 15°C mesocosms (Figures 5A, B). However, there was a three-way interaction between tDOM, MP and temperature, revealing a more complex temperature effect on fish survival, with the highest survival found in both 15 and 18°C mesocosms without MP and tDOM addition, and the lowest survival in 18°C mesocosms with tDOM addition or MP addition (Figure 5B). There was no correlation between mesozooplankton biomass and fish survival ($p > 0.39$ for all), but there was a positive correlation between mesozooplankton biomass and fish biomass ($R = 0.45$, $p = 0.03$). The FWE was lower in tDOM-treated mesocosms and at 18°, at least in mesocosms without MP addition (Figure 5C; 2-way interaction tDOM × MP; $p < 0.05$). In MP treated mesocosms, only temperature affected the FWE.

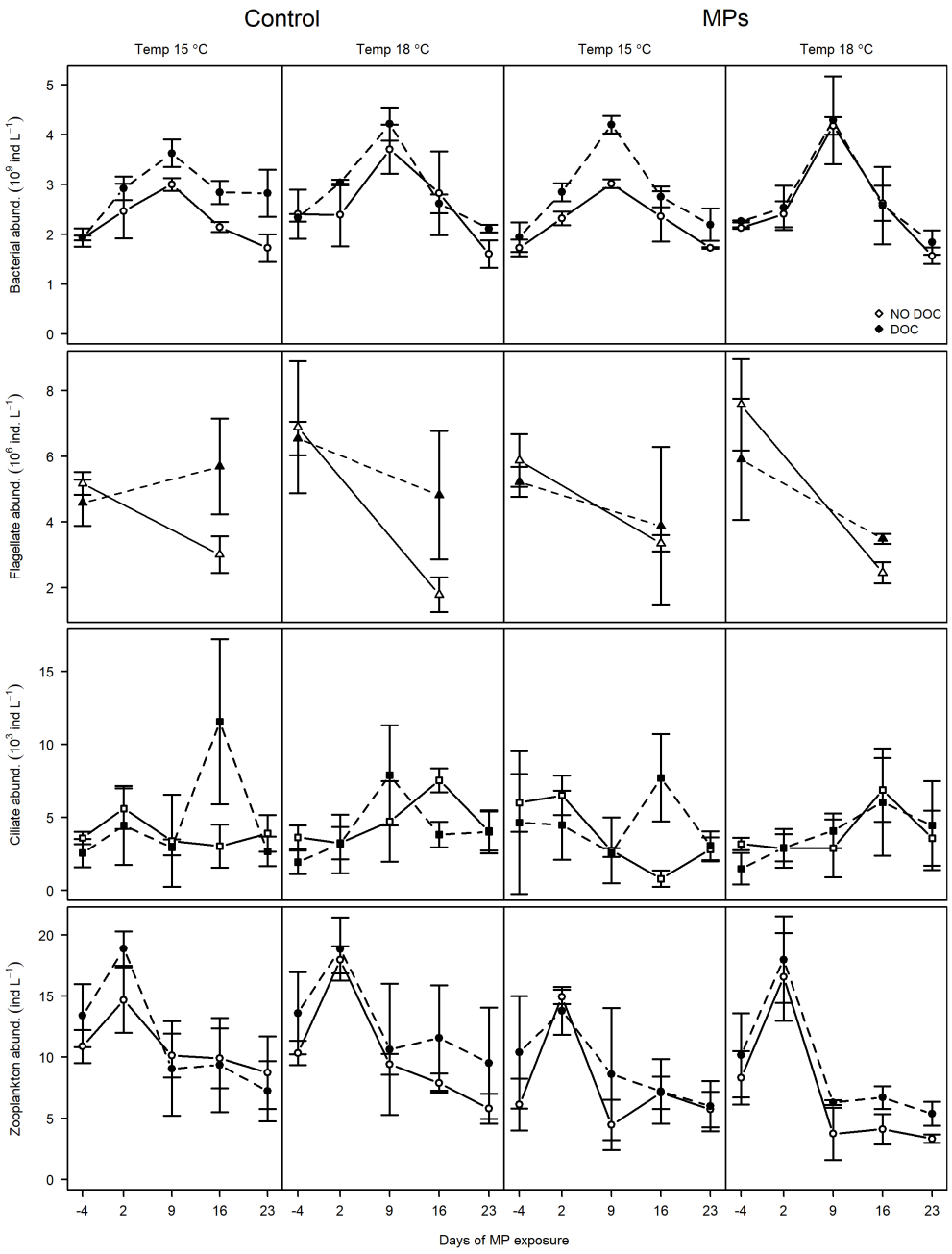

FIGURE 3
Temporal change in the abundance of bacteria (top panels), flagellates (upper middle panels), ciliates (lower middle panels) and mesozooplankton (bottom panels) in different MP, tDOM and temperature factor combinations. The two columns to the left represent control mesocosms at 15 and 18°C and the two columns to the right represent MP exposed mesocosms at 15 and 18°C. Filled symbols and dashed lines are treatments with tDOM addition and open symbols with solid lines represent treatments without tDOM.

3.3 Organic micropollutant bioaccumulation in fish

Twenty-four organic MPs were detected in fish (excluding 9 of the 33 spiked compounds with blank concentrations >10%), and 19 of these compounds were detected in the water after taking blanks into account (Ripszam et al., 2015). In fish, there was a general trend of higher MP concentrations at 15°C compared to 18°C treatments for most compounds (Supplementary Table S1). However, this was only significant for 10 compounds, viz. trifluralin, γ-HCH, 2,4,6-tribromoaniline, PCB28, chlorthal dimethyl, endosulfan I and II, mitotane, TPP and diflufenican and marginally non-significant for two additional compounds, viz. hexachlorobutadiene and α-HCH ($p = 0.07 - 0.09$, Supplementary Table S3). 2,4,6-tribromoaniline concentrations were also higher in fish from tDOM treated mesocosms (39 ± 10 *vs.* 94 ± 28 pg g^{-1}), however no other compound showed an effect of tDOM.

The median BAF_{ww} ranged between 0.87 (ethoprophos) and 1.1×10^4 (phenanthrene) (for lipid normalized BAF, see Supplementary Table S1). Overall, BAFs were generally slightly

10.3389/fmars.2023.1244434

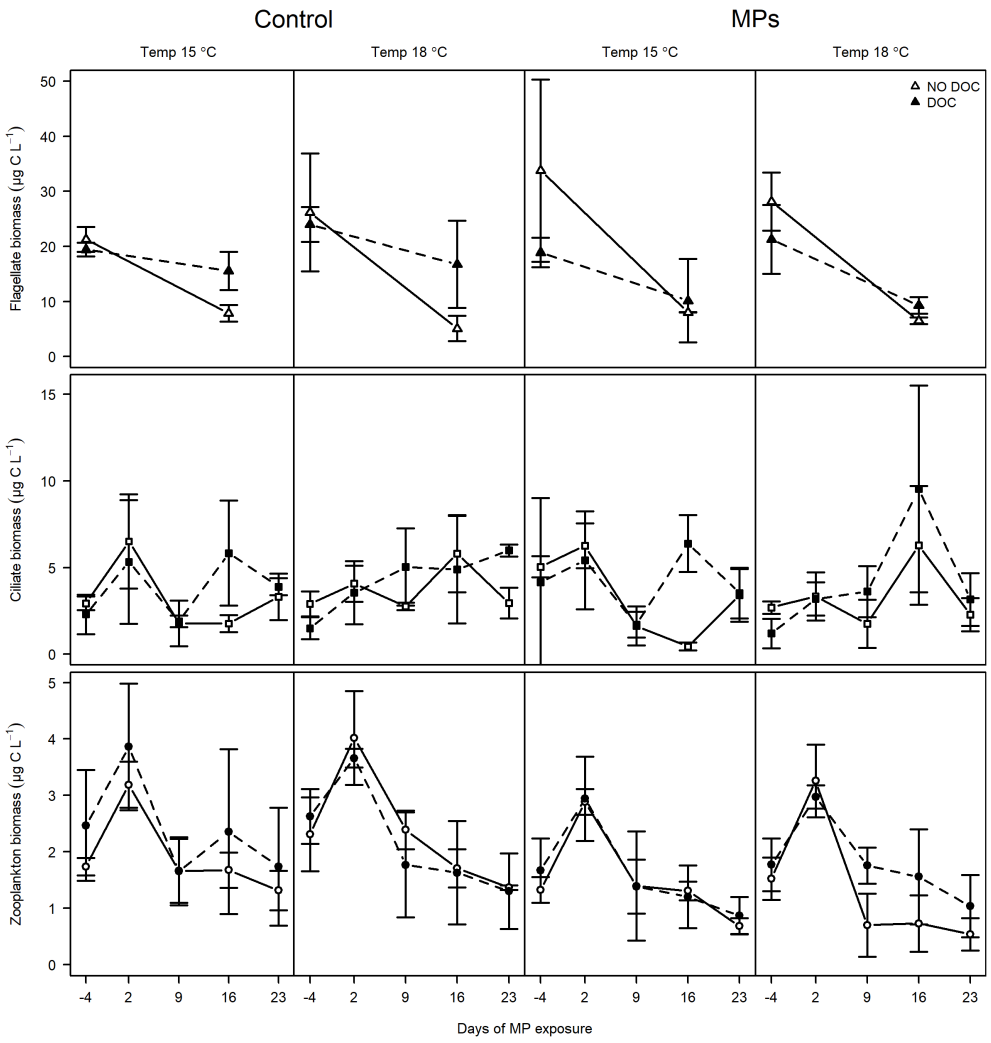

FIGURE 4
Temporal change in biomass of flagellates (top panels), ciliates (middle panels) and mesozooplankton (bottom panels) in different MP, tDOM and temperature factor combinations. The two columns to the left represent control mesocosms at 15 and 18°C and the two columns to the right represent MP exposed mesocosms at 15 and 18°C. Filled symbols and dashed lines are treatments with tDOM addition and open symbols with solid lines represent treatments without tDOM.

higher either at lower temperatures or in tDOM-treated mesocosms (Figure 6, Table S1). However, large within-treatment variability occurred due to the small sample size (n= 2-3 per treatment). In general, the variation in BAF_{ww} was especially pronounced in tDOM-treated mesocosms at lower temperature (15°C). Within the 15°C tDOM treatment, there was one mesocosm where fish accumulated considerably less MPs than the other mesocosms of the same treatment, but that mesocosm did not diverge from the other 15°C and tDOM-treated mesocosms with regard to the biological responses (e.g. survival, growth or biomass of fish). Despite of a large within-treatment variation, there were significantly higher BAF_{ww} for fish from 15°C than 18°C treatments with respect to chlorthal dimethyl and mitotane (Supplementary Table S4), and marginally higher BAF_{ww} for PCB28 and γHCH ($p< 0.08$). BAF_{ww} in fish was significantly higher in tDOM-treated mesocosms than mesocosms without tDOM for ethoprophos (Supplementary Table S4), and marginally higher for 2,4,6-tribromoaniline, TPP and TDCIPP ($p< 0.09$). The log K_{ow} and Henry's law constant for the compounds that showed a temperature-effect ranged between 3.8 and 6.4, and 0.22 and 27 Pa*m^3/mol, respectively, and the log K_{ow} and Henry's law constant for compounds that showed a tDOM-effect ranged between 3.6 and 4.6, and 0.00026 and 0.21 Pa*m^3/mol, respectively (Supplementary Table S1). However, the majority of the compounds within the same range of K_{ow} and Henry's law constant was not significantly affected by either temperature or tDOM.

4 Discussion

As expected, our results indicate that ecosystems in Baltic coastal regions, receiving high river discharge with future climate changes, can be influenced by foremost the nutrient enrichment due to the tDOM addition and, to a minor extent, by the elevated temperature at the bottom of the food web (Berglund et al., 2007;

10.3389/fmars.2023.1244434

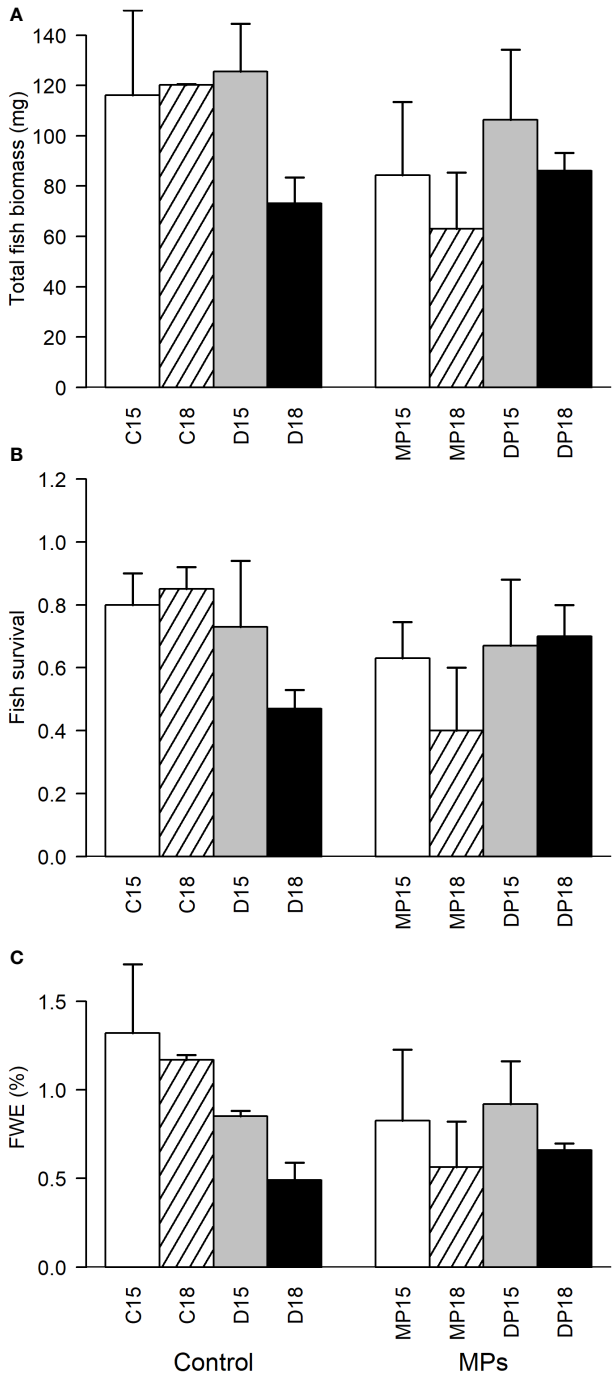

FIGURE 5
Total fish biomass **(A)**, fish survival **(B)**, and food web efficiency (FWE; **C**) at the final sampling of fish (day 23), in different MP, tDOM and temperature factor combinations. Left panel (Control) correspond to treatments without organic micropollutant addition, and right panel treatments with organic micropollutants. 15 and 18 correspond to the two temperature treatments (15 and 18°C), C is controls without tDOM or MP addition, D with tDOM addition, MP with micropollutants, and DP with both tDOM and micropollutants.

Lefebure et al., 2013; Andersson et al., 2015; Liess et al., 2015). If any, MP addition had a minor effect at the base of the food web. MP addition resulted in slightly higher nutrient and DOC concentrations than control mesocosms, and at the applied levels, phytoplankton was negatively affected by the MP addition, while heterotrophic bacteria was slightly benefitted. Although care was taken not to exceed toxic thresholds in the spiking mixture, the negative effect on PP and Chl α might indicate a toxic effect of the herbicides in the MP mixture. As such, the higher nutrient concentrations in MP treated mesocosms might be a consequence of the lower phytoplankton growth. The higher DOC concentration with MP-addition could be caused by the solvent for MPs, i.e. methanol (Rodriguez et al., 2018) and higher DOC concentrations may partly explain the positive MP-effect on bacteria, although bacteria probably also benefitted from a relaxed competition with phytoplankton. Terrestrial DOM-addition stimulated both heterotrophic bacteria and phytoplankton at the base of the food web. That tDOM stimulated phytoplankton was unexpected as shading of phytoplankton and thus reduced photosynthetic activity is expected when tDOM inflow increases in lakes and estuaries (Ask et al., 2012; McGovern et al., 2019). Although tDOM resulted in reduced PAR, the light was still intense enough to saturate photosynthesis (Andersson et al., 1994), which may be attributed to our relatively shallow (0.8 m) mesocosms. Our study thus suggest that an increase in tDOM inflow is unlikely to limit photosynthesis in the shallowest coastal areas. Although tDOM addition stimulated the food web from heterotrophic bacteria and phytoplankton to mesozooplankton, the temperature was generally more influential for fish survival and biomass. Increased temperature generally results in increased fish metabolism (Brown et al., 2004), and with limited food availability, as seen in our experiment, less resources can be allocated to growth. A higher metabolism with increasing temperature (18°C) could explain the lower FWE and total fish biomass in 18°C mesocosms, in line with previous studies (Berglund et al., 2007). Lower FWE in climate-altered food webs may indicate a food chain elongation, with more energy allocated via the heterotrophic microbial food web (Andersson et al., 2015). However, as both primary and heterotrophic bacterial production was benefitted in climate altered mesocosms, especially when MPs were absent, this needs to be interpreted with caution. In addition, MP treated mesocosms had slightly lower PP and Chl α, and MP treated mesocosms only showed marginal effects on FWE. Further, a more detailed study pinpointing the microbial food web in mesocosms without MP addition indicated that the systems tended to be net-autotrophic (Andersson et al., 2023). As such, it is less likely that the reduced FWE in climate-altered food web is an indication of an increase in trophic levels.

In addition to efficiently decreasing total mesozooplankton biomass, perch predation also shifted mesozooplankton community structure from more preferred copepods and cladocerans to the smaller and less preferred rotifers (Byström and García-Berthou, 1999). Higher growth rates in the latter and the temperature effect have most likely also contributed to the observed community shift. As such, fish suffered from strong resource limitation, and by the end of the experiment, mesozooplankton densities were approximately ten times lower than in coastal areas in the Bothnian Bay (Lefebure et al., 2014). The number of reproducing copepoids remained relatively low throughout the experiment, which may have contributed to limited mesozooplankton

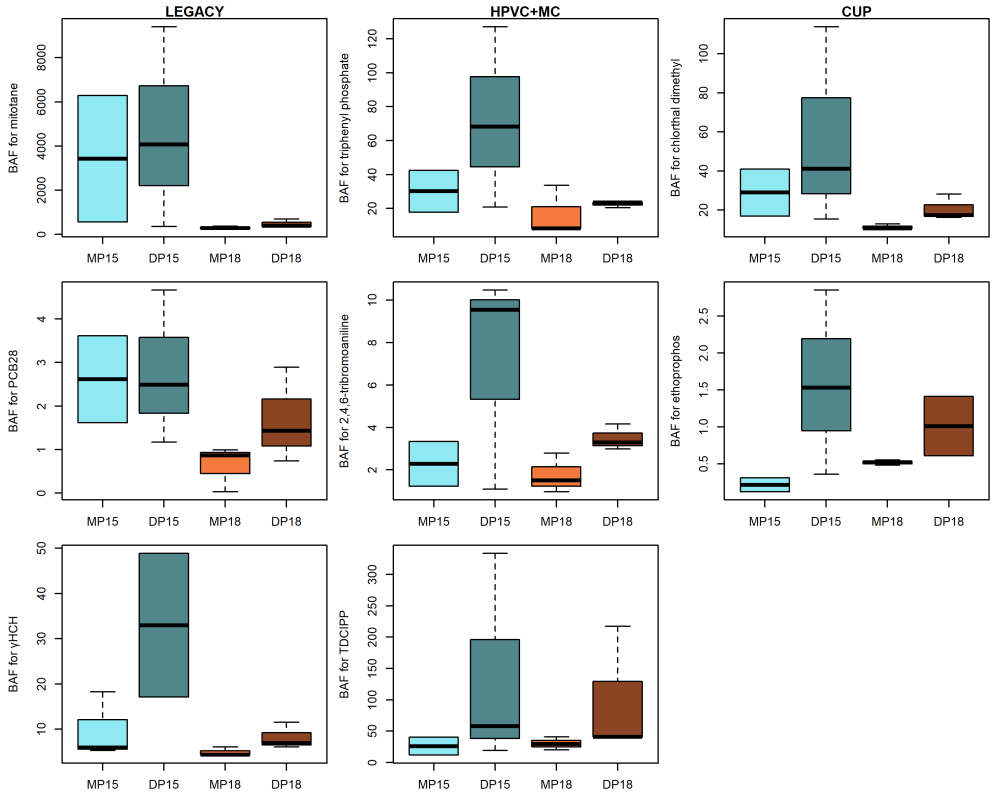

FIGURE 6
Bioaccumulation factors (based on wet weight) for organic micropollutants grouped into legacy pests/POPs (left panels), high production volume compounds as well as model compounds (HPVC + MC, middle panels) and currently and recently used pesticides (CUP, right panels). Pollutants are ordered based on their lipophilicity, with highest logK_{ow} at the top and lowest at the bottom. Blue boxes represent 15°C mesocosms and brown 18° C mesocosms. MP denotes mesocosms amended with organic micropollutants only, and DP represent mesocosms with organic MPs and tDOM. The boxes illustrate the interquartile range and the median, while whiskers represent the upper and lower quartile.

densities. Hence, it is likely that the observed low lipid content of fish (1.4%) and high mortality rates were caused by the food limitation. The predation pressure on mesozooplankton also released ciliates from mesozooplankton grazing, with cascading effects in the microbial food web. The more detailed study pinpointing the microbial food web in mesocosms without MP addition showed that tDOM addition increased the abundance of larger ciliates (> 60µm, dominated by *Stylonychia* sp.) (Andersson et al., 2023). A shift toward cilates of larger size could explain the higher Δ ciliate biomass in tDOM treated mesocosms in the present study (also including MP treatments).

There are many studies on the potential effects of climate change on contaminant distribution and fate, focusing on Arctic ecosystems, but they have mostly been based on modeling approaches (Borgå et al., 2010; Wang et al., 2016; Alava et al., 2018). According to the present study, bioaccumulation of MPs could either decrease or increase with a changing climate, depending on the compound and main driving factor (temperature or tDOM). The risk of bioaccumulation in fish would decrease for compounds that seem to be more temperature sensitive (e.g., mitotane, chlorthal dimethyl, PCB28 and γHCH), whereas for others (e.g., ethoprophos, TDCIPP, TPP, and 2,4,6-tribromoaniline) it would increase if tDOM increases. There were no obvious common denominators such as logK_{ow}, Henry's law constant, group, or type of compounds, which could help foresee how MPs would be affected by temperature or tDOM. Although there was an overlap in log K_{ow} between compounds that was affected by temperature and tDOM, compounds that bioaccumulated less when temperatures increased tended to have a higher log K_{ow} (> 3.8) and compounds that bioaccumulated to a higher extent in tDOM treated mesocosms tended to have a slightly lower log K_{ow} (< 4.6). However, this was not unanimous for all compounds. For example, trifluralin, with log K_{ow} 5.07 showed no tendency of temperature-dependent bioaccumulation, even though chlorthal dimethyl and PCB28 with K_{ow} 4.4 and 5.8, respectively, accumulated significantly less in fish from 18° C than 15°C treatments. In agreement, bioconcentration factors (BCF) in fish for a diverse set of pharmaceutical compounds showed deviating mechanisms for fish uptake, not following a lipophilicity-driven manner (Fick et al., 2010). These factors alone or in combination might explain the lack of consistent pattern between logK_{ow} and BAF, which are usually expected to be affected by the lipophilicity of a compound (Fisk et al., 1998). Also, assessing biomagnification factor (BMF) or trophic magnification factors (TMF) would have been useful in determining the biomagnification patterns and impact of food web changes (Borgå et al., 2012). However, limited amount of prey material prevented such studies.

Terrestrial DOM is expected to decrease the bioavailability of MPs due to increased partitioning to organic matter (Noyes et al., 2009). Micropollutants tended to partition to tDOM in the present

study (Ripszam et al., 2015), which may have reduced the bioavailability for direct (diffusive) uptake in fish (Larsson et al., 1992). This would contrast our results, where tDOM increased the bioaccumulation, if a tDOM affect occurred. Increased biomagnification in fish, due to an increase in trophic levels with a more dominant microbial food web, could have explained the observed tDOM effect. However, we found limited support for a food chain elongation in MP treated mesocosms and the compounds that was affected by tDOM was intermediate, in terms of lipophilicity, i.e. not the compounds where biomagnification was primarily expected. Compound with log K_{ow} > 5 are expected to be associated with tDOM and be largely absorbed via the diet (Gobas, 2001). As such, contrary to what was observed, we expected more lipophilic compounds to bioaccumulated with tDOM addition. An optional explanation for increased bioaccumulation in fish from tDOM treated mesocosms for intermediately lipophilic compounds may be that MPs could be transferred by bacteria up the food chain, when bacteria consume tDOM (Wallberg et al., 2001). As such, reduced bioavailability and diminished passive uptake in fish, due to MP-tDOM complexation (Ripszam et al., 2015), would be counteracted by the increased availability via contaminated diet, due to heterotrophic bacteria consuming contaminant-rich tDOM. However, the pathways for an increased bioaccumulation with increased tDOM, needs to be explored further. In addition, variation in BAF was considerable for tDOM treatments at 15°C due to one mesocosm with consistently lower MP concentrations in fish and a high variability may have prevented us from identifying additional compounds that were influenced by tDOM. There was no apparent biological explanation for the low MP concentrations in fish from this particular mesocosms, such as fish growth, survival and various food web responses. Data on individual lipid content may have helped understand this variation and generate more accurate BAF_l estimates; unfortunately, mesocosm-specific lipid measurements were impossible due to the low amount of the sample material. However, the usefulness of BAF_{ww} and BAF_l varies, depending on a compound's lipophilicity and absorption route (Mackay et al., 2018). In addition, as the food availability was low and fish were close to starvation, the calculated BAF values may rather represent BCF.

The reduced bioaccumulation of MPs in warmer climates has been suggested previously (Noyes et al., 2009; Borgå et al., 2010; Kong et al., 2014), although both increased and decreased bioconcentration have been observed in mussels, depending on compound (Serra-Compte et al., 2018). However, the variability in temperature adaptation among species, and, more specifically, their growth response to the temperature increase, may affect MP accumulation. In particular, cold-water species are expected to have lower bioaccumulation than warm- or temperate species in a warmer climate (Gewurtz et al., 2006; Borgå et al., 2022). The limited growth response in our boreal perch probably explains the lack of corresponding bioaccumulation responses. Also, we found higher losses and lower partitioning of MPs to tDOM at higher temperatures (Ripszam et al., 2015). Thus, increased temperatures may promote MP evaporation and thus reduce the risk of accumulation in biota. However, at the regional scale, higher temperatures may also increase the runoff of MPs from secondary sources (Noyes et al., 2009; Wang et al., 2016; Borgå et al., 2022), which could counteract the effect of increased evaporation in coastal regions.

Higher temperatures not only directly affect MPs but also increase the physiological rates of fish, such as their metabolism (Brown et al., 2004). Thus, MP elimination and depuration are expected to increase in warmer conditions (Paterson et al., 2007; Alava et al., 2017). As such, reduced MP bioaccumulation at the higher temperature (Figure 6) was most likely a combination of the increased contaminant losses through evaporation (Ripszam et al., 2015) and increased fish metabolism. The generally lower biomass of fish in warmer mesocosms could also reflect an increased metabolism and energy expenditure, a response that agrees with previous studies (Gardner et al., 2011; Alava et al., 2017). It has also been suggested that adaptation to climate warming may reduce fish metabolic costs (Moffett et al., 2018). If this holds, and MPs are subsequently eliminated in fish at a slower pace, with a changing climate, the observed positive effects of increasing temperatures (i.e., reduced bioaccumulation of contaminants) may be diminished.

5 Conclusions

This study indicates that the projected climate change in northern Baltic Sea will promote the base of the food chain in shallow coastal areas. An efficient basal production, due to increased tDOM input, also affected the rest of the food web (from flagellates to mesozooplankton) and resulted in increased FWE in mesocosms without MPs. The temperature increase had little impact on lower trophic levels, but resulted in generally reduced growth and survival of the top consumer (fish). The climate-related conditions had differential effects on MP bioaccumulation: temperature increase led to lower bioaccumulation, potentially due to increased evaporation and fish metabolism, whereas tDOM addition increased bioaccumulation, potentially due to a food chain elongation or efficient contaminant transfer from heterotrophic bacteria. The mechanisms behind the temperature and tDOM-dependent bioaccumulation and their interactions need further exploration.

Data availability statement

The datasets presented in this study can be found in online repositories. The names of the repository/repositories and accession number(s) can be found below: Swedish national data service, https://doi.org/10.5878/p8sx-n445.

Ethics statement

The animal study was approved by the Swedish Ethical Review Authority (No. A28-13). The study was conducted in accordance with the local legislation and institutional requirements.

Author contributions

ÅB, CG, MR, HL, PB, PH, AA and MT designed the mesocosm experiment. ÅB, CG, MR, and HL conducted the experiment, and ÅB, CG, MR, HL, DF, EvG, PB, ElG, PH and AA performed analyzes. ÅB performed statistical analyzes and wrote the first draft of the manuscript with support from MT. All authors contributed to manuscript revision, read and approved the submitted version.

Funding

This work was financed by the EcoChange project (Dnr 2009-149) and the Kempe Foundation.

Acknowledgments

We would also like to acknowledge Jonas Forsberg for counting phytoplankton and the staff at Umeå Marine Sciences Centre (UMSC) for assistance and facilitation of the experiment.

Conflict of interest

The authors declare that the research was conducted in the absence of any commercial or financial relationships that could be construed as a potential conflict of interest.

Publisher's note

Supplementary material

The Supplementary Material for this article can be found online at: https://www.frontiersin.org/articles/10.3389/fmars.2023.1244434/full#supplementary-material

References

Alava, J. J., Cheung, W. W. L., Ross, P. S., and Sumaila, U. R. (2017). Climate change-contaminant interactions in marine food webs: Toward a conceptual framework. *Global Change Biol.* 23, 3984–4001. doi: 10.1111/gcb.13667

Alava, J. J., Cisneros-Montemayor, A. M., Sumaila, U. R., and Cheung, W. W. L. (2018). Projected amplification of food web bioaccumulation of MeHg and PCBs under climate change in the Northeastern Pacific. *Sci. Rep.* 8:13460. doi: 10.1038/s41598-018-31824-5

Andersson, A., Grinienė, E., Berglund, Å. M. M., Brugel, S., Gorokhova, E., Figueroa, D., et al. (2023). Microbial food web changes induced by terrestrial organic matter and elevated temperature in the coastal northern Baltic Sea. *Front. Mar. Sci.* 10. doi: 10.3389/fmars.2023.1170054

Andersson, A., Haecky, P., and Hagström, Å. (1994). Effect of temperature and light on the growth of micro-plankton, nano-plankton and pico-plankton - impact on algal succession. *Mar. Biol.* 120, 511–520. doi: 10.1007/BF00350071

Andersson, A., Hajdu, S., Haecky, P., Kuparinen, J., and Wikner, J. (1996). Succession and growth limitation of phytoplankton in the Gulf of Bothnia (Baltic Sea). *Mar. Biol.* 126, 791–801. doi: 10.1007/BF00351346

Andersson, A., Meier, H. E. M., Ripszam, M., Rowe, O., Wikner, J., Haglund, P., et al. (2015). Projected future climate change and Baltic Sea ecosystem management. *Ambio* 44, S345–S356. doi: 10.1007/s13280-015-0654-8

Ask, J., Karlsson, J., and Jansson, M. (2012). Net ecosystem production in clear-water and brown-water lakes. *Global Biogeochemical Cycles* 26:GB1017. doi: 10.1029/2010gb003951

Assefa, A. T., Sobek, A., Sundqvist, K. L., Cato, I., Jonsson, P., Tysklind, M., et al. (2014). Temporal trends of PCDD/fs in baltic sea sediment cores covering the 20th century. *Environ. Sci. Technol.* 48, 947–953. doi: 10.1021/es404599z

Assefa, A., Tysklind, M., Bignert, A., Josefsson, S., and Wiberg, K. (2019). Sources of polychlorinated dibenzo-p-dioxins and dibenzofurans to Baltic Sea herring. *Chemosphere* 218, 493–500. doi: 10.1016/j.chemosphere.2018.11.051

Bécue-Bertaut, M., and Pagès, J. (2008). Multiple factor analysis and clustering of a mixture of quantitative, categorical and frequency data. *Comput. Stat Data Anal.* 52, 3255–3268. doi: 10.1016/j.csda.2007.09.023

Berglund, J., Müren, U., Båmstedt, U., and Andersson, A. (2007). Efficiency of a phytoplankton-based and a bacteria-based food web in a pelagic marine system. *Limnology Oceanography* 52, 121–131. doi: 10.4319/lo.2007.52.1.0121

Bergström, S., Carlsson, B., Gardelin, M., Lindström, G., Pettersson, A., and Rummukainen, M. (2001). Climate change impacts on runoff in Sweden' assessments by global climate models, dynamical downscaling and hydrological modelling. *Climate Res.* 16, 101–112. doi: 10.3354/cr016101

Borgå, K., Fisk, A. T., Hoekstra, P. F., and Muir, D. C. G. (2004). Biological and chemical factors of importance in the bioaccumulation and trophic transfer of persistent organochlorine contaminants in arctic marine food webs. *Environ. Toxicol. Chem.* 23, 2367–2385. doi: 10.1897/03-518

Borgå, K., Kidd, K. A., Muir, D. C. G., Berglund, O., Conder, J. M., Gobas, F. A. P. C., et al. (2012). Trophic magnification factors: Considerations of ecology, ecosystems, and study design. *Integrated Environ. Assess. Manage.* 8, 64–84. doi: 10.1002/ieam.244

Borgå, K., McKinney, M. A., Routti, H., Fernie, K. J., Giebichenstein, J., Hallanger, I., et al. (2022). The influence of global climate change on accumulation and toxicity of persistent organic pollutants and chemicals of emerging concern in Arctic food webs. *Environ. Science-Processes Impacts* 24, 1544–1576. doi: 10.1039/d1em00469g

Borgå, K., Saloranta, T. M., and Ruus, A. (2010). Simulating climate change-induced alterations in bioaccumulation of organic contaminants in an Arctic marine food web. *Environ. Toxicol. Chem.* 29, 1349–1357. doi: 10.1002/etc.159

Brown, J. H., Gillooly, J. F., Allen, A. P., Savage, V. M., and West, G. B. (2004). Toward a metabolic theory of ecology. *Ecology* 85, 1771–1789. doi: 10.1890/03-9000

Burnham, K. P., Anderson, D. R., and Huyvaert, K. P. (2011). AIC model selection and multimodel inference in behavioral ecology: some background, observations, and comparisons. *Behav. Ecol. Sociobiology* 65, 23–35. doi: 10.1007/s00265-010-1029-6

Byström, P., and García-Berthou, E. (1999). Density dependent growth and size specific competitive interactions in young fish. *Oikos* 86, 217–232. doi: 10.2307/3546440

Carrie, J., Wang, F., Sanei, H., Macdonald, R. W., Outridge, P. M., and Stern, G. A. (2010). Increasing contaminant burdens in an arctic fish, burbot (*Lota lota*), in a warming climate. *Environ. Sci. Technol.* 44, 316–322. doi: 10.1021/es902582y

Creed, I. F., Bergström, A.-K., Trick, C. G., Grimm, N. B., Hessen, D. O., Karlsson, J., et al. (2018). Global change-driven effects on dissolved organic matter composition: Implications for food webs of northern lakes. *Global Change Biol.* 24, 3692–3714. doi: 10.1111/gcb.14129

Directive 2008/105/EC (2008). *Directive 2008/105/EC.* (Brussels: THE EUROPEAN PARLIAMENT AND THE COUNCIL OF THE EUROPEAN UNION).

Fick, J., Lindberg, R. H., Parkkonen, J., Arvidsson, B., Tysklind, M., and Larsson, D. G. J. (2010). Therapeutic levels of levonorgestrel detected in blood plasma of fish: results from screening rainbow trout exposed to treated sewage effluents. *Environ. Sci. Technol.* 44, 2661–2666. doi: 10.1021/es903440m

Figueroa, D., Rowe, O. F., Paczkowska, J., Legrand, C., and Andersson, A. (2016). Allochthonous carbon—a major driver of bacterioplankton production in the subarctic northern baltic sea. *Microbial Ecol.* 71, 789–801. doi: 10.1007/s00248-015-0714-4

Fisk, A. T., Norstrom, R. J., Cymbalisty, C. D., and Muir, D. C. G. (1998). Dietary accumulation and depuration of hydrophobic organochlorines: Bioaccumulation parameters and their relationship with the octanol/water partition coefficient. *Environ. Toxicol. Chem.* 17, 951–961. doi: 10.1002/etc.5620170526

Fuhrman, J. A., and Azam, F. (1982). Thymidine incorporation as a measure of heterotrophic bacterioplankton production in marine surface waters - evaluation and field results. *Mar. Biol.* 66, 109–120. doi: 10.1007/bf00397184

Gardner, J. L., Peters, A., Kearney, M. R., Joseph, L., and Heinsohn, R. (2011). Declining body size: a third universal response to warming? *Trends Ecol. Evol.* 26, 285–291. doi: 10.1016/j.tree.2011.03.005

Gargas, E. (1975). *A manual for Phytoplankton Production Studies in the Baltic* (Horsholm, Denmark: Water Quality Institute).

Gewurtz, S. B., Laposa, R., Gandhi, N., Christensen, G. N., Evenset, A., Gregor, D., et al. (2006). A comparison of contaminant dynamics in arctic and temperate fish: A modeling approach. *Chemosphere* 63, 1328–1341. doi: 10.1016/j.chemosphere.2005.09.031

Gilbreath, A. N., and McKee, L. J. (2015). Concentrations and loads of PCBs, dioxins, PAHs, PBDEs, OC pesticides and pyrethroids during storm and low flow conditions in a small urban semi-arid watershed. *Sci. Total Environ.* 526, 251–261. doi: 10.1016/j.scitotenv.2015.04.052

Gobas, F. A. P. C. (2001). "Assessing bioaccumulation factors of persistent Organic Pollutants in Aquatic Food-Chains," in *Persistent Organic Pollutants: Environmental Behaviour and Pathways of Human Exposure*. Ed. S. Harrad (US, Boston, MA: Springer), 145–165.

Gobas, F. A. P. C., Wilcockson, J. B., Russell, R. W., and Haffner, G. D. (1999). Mechanism of biomagnification in fish under laboratory and field conditions. *Environ. Sci. Technol.* 33, 133–141. doi: 10.1021/es980681m

Grasshoff, K., Kremling, K., and Ehrhardt, M. (1999). *Methods of Seawater Analysis* (Weinheim: Wiley-VCH).

Haitzer, M., Hoss, S., Traunspurger, W., and Steinberg, C. (1998). Effects of dissolved organic matter (DOM) on the bioconcentration of organic chemicals in aquatic organisms - A review. *Chemosphere* 37, 1335–1362. doi: 10.1016/s0045-6535(98)00117-9

Hernroth, L. (1985). *Recommendations on Methods for Marine Biological Studies in the Baltic Sea: Mesozooplankton Biomass Assessment; Individual Volume Technique* (Lysekil: Institute of Marine Research).

IPCC (2022). *Climate Change 2022: Impacts* (Cambridge:Adaptation and Vulnerability).

Jobling, M. (1995). Fish bioenergetics. *Oceanographic Literature Rev.* 9, 785.

Kallenborn, R., Halsall, C., Dellong, M., and Carlsson, P. (2012). The influence of climate change on the global distribution and fate processes of anthropogenic persistent organic pollutants. *J. Environ. Monit.* 14, 2854–2869. doi: 10.1039/C2EM30519D

Kong, D. G., MacLeod, M., and Cousins, I. T. (2014). Modelling the influence of climate change on the chemical concentrations in the Baltic Sea region with the POPCYCLING-Baltic model. *Chemosphere* 110, 31–40. doi: 10.1016/j.chemosphere.2014.02.044

Larsson, P., Collvin, L., Okla, L., and Meyer, G. (1992). Lake productivity and water chemistry as govenors of the uptake of persistent pollutants in fish. *Environ. Sci. Technol.* 26, 346–352. doi: 10.1021/es00026a016

Lee, S., and Fuhrman, J. A. (1987). Relationships between biovolume and biomass of naturally dervied marine bacterioplankton. *Appl. Environ. Microbiol.* 53, 1298–1303. doi: 10.1128/aem.53.6.1298-1303.1987

Lefebure, R., Degerman, R., Andersson, A., Larsson, S., Eriksson, L. O., Bamstedt, U., et al. (2013). Impacts of elevated terrestrial nutrient loads and temperature on pelagic food-web efficiency and fish production. *Glob Chang Biol.* 19, 1358–1372. doi: 10.1111/gcb.12134

Lefebure, R., Larsson, S., and Bystrom, P. (2014). Temperature and size-dependent attack rates of the three-spined stickleback (Gasterosteus aculeatus); are sticklebacks in the Baltic Sea resource-limited? *J. Exp. Mar. Biol. Ecol.* 451, 82–90. doi: 10.1016/j.jembe.2013.11.008

Lester, M. B., and van Riper, C. (2014). The distribution and extent of heavy metal accumulation in song sparrows along Arizona's upper Santa Cruz River. *Environ. Monit. Assess.* 186, 4779–4791. doi: 10.1007/s10661-014-3737-2

Liess, A., Rowe, O., Francoeur, S. N., Guo, J., Lange, K., Schröder, A., et al. (2015). Terrestrial runoff boosts phytoplankton in a Mediterranean coastal lagoon, but these effects do not propagate to higher trophic levels. *Hydrobiologia* 766, 275–291. doi: 10.1007/s10750-015-2461-4

Lignell, R., Hoikkala, L., and Lahtinen, T. (2008). Effects of inorganic nutrients, glucose and solar radiation on bacterial growth and exploitation of dissolved organic carbon and nitrogen in the northern Baltic Sea. *Aquat. Microbial Ecol.* 51, 209–221. doi: 10.3354/ame01202

Mackay, D., Celsie, A. K. D., Powell, D. E., and Parnis, J. M. (2018). Bioconcentration, bioaccumulation, biomagnification and trophic magnification: a modelling perspective. *Environ. Science-Processes Impacts* 20, 72–85. doi: 10.1039/c7em00485k

Marie, D., Simon, N., and Vaulot, D. (2005). "Phytoplankton cell counting by flow cytometry," in *Algal Culturing Techniques*. Ed. R. A. Andersen (San Diego, CA: Academic Press), 253–267.

McGovern, M., Evenset, A., Borgå, K., de Wit, H. A., Braaten, H. F. V., Hessen, D. O., et al. (2019). Implications of coastal darkening for contaminant transport, bioavailability, and trophic transfer in northern coastal waters. *Environ. Sci. Technol.* 53, 7180–7182. doi: 10.1021/acs.est.9b03093

Meier, H. E. M. (2006). Baltic Sea climate in the late twenty-first century: a dynamical downscaling approach using two global models and two emission scenarios. *Climate Dynamics* 27, 39–68. doi: 10.1007/s00382-006-0124-x

Meier, H. E. M., Kniebusch, M., Dieterich, C., Gröger, M., Zorita, E., Elmgren, R., et al. (2022). Climate change in the Baltic Sea region: a summary. *Earth Syst. Dynam* 13, 457–593. doi: 10.5194/esd-13-457-2022

Menden-Deuer, S., and Lessard, E. J. (2000). Carbon to volume relationships for dinoflagellates, diatoms, and other protist plankton. *Limnology Oceanography* 45, 569–579. doi: 10.4319/lo.2000.45.3.0569

Miller, A., Hedman, J. E., Nyberg, E., Haglund, P., Cousins, I. T., Wiberg, K., et al. (2013). Temporal trends in dioxins (polychlorinated dibenzo-p-dioxin and dibenzofurans) and dioxin-like polychlorinated biphenyls in Baltic herring (Clupea harengus). *Mar. pollut. Bull.* 73, 220–230. doi: 10.1016/j.marpolbul.2013.05.015

Moffett, E. R., Fryxell, D. C., Palkovacs, E. P., Kinnison, M. T., and Simon, K. S. (2018). Local adaptation reduces the metabolic cost of environmental warming. *Ecology* 99, 2318–2326. doi: 10.1002/ecy.2463

Neumann, T. (2010). Climate-change effects on the Baltic Sea ecosystem: A model study. *J. Mar. Syst.* 81, 213–224. doi: 10.1016/j.jmarsys.2009.12.001

Noyes, P. D., and Lema, S. C. (2015). Forecasting the impacts of chemical pollution and climate change interactions on the health of wildlife. *Curr. Zoology* 61, 669–689. doi: 10.1093/czoolo/61.4.669

Noyes, P. D., McElwee, M. K., Miller, H. D., Clark, B. W., Van Tiem, L. A., Walcott, K. C., et al. (2009). The toxicology of climate change: Environmental contaminants in a warming world. *Environ. Int.* 35, 971–986. doi: 10.1016/j.envint.2009.02.006

Olenina, I., Hajdu, S., Edler, L., Andersson, A., Wasmund, N., Busch, S., et al. (2006). Biovolumes and size-classes of phytoplankton in the Baltic Sea. HELCOM Balt. *Sea Environ. Proc.* 106, 1–144.

Paterson, G., Drouillard, K. G., and Haffner, G. D. (2007). PCB elimination by yellow perch (*Perca flavescens*) during an annual temperature cycle. *Environ. Sci. Technol.* 41, 824–829. doi: 10.1021/es060266r

Rand, P. S., and Stewart, D. J. (1998). Prey fish exploitation, salmonine production, and pelagic food web efficiency in Lake Ontario. *Can. J. Fisheries Aquat. Sci.* 55, 318–327. doi: 10.1139/f97-254

Ripszam, M., Gallampois, C. M. J., Berglund, Å, Larsson, H., Andersson, A., Tysklind, M., et al. (2015). Effects of predicted climatic changes on distribution of organic contaminants in brackish water mesocosms. *Sci. Total Environ.* 517, 10–21. doi: 10.1016/j.scitotenv.2015.02.051

Rodriguez, J., Gallampois, C. M. J., Timonen, S., Andersson, A., Sinkko, H., Haglund, P., et al. (2018). Effects of organic pollutants on bacterial communities under future climate change scenarios. *Front. Microbiol.* 9. doi: 10.3389/fmicb.2018.02926

R Core Team (2019). *R: A language and Environment for Statistical Computing R Foundation for Statistical Computing* (Austria: Vienna).

Serra-Compte, A., Maulvault, A. L., Camacho, C., Alvarez-Munoz, D., Barcelo, D., Rodriguez-Mozaz, S., et al. (2018). Effects of water warming and acidification on bioconcentration, metabolization and depuration of pharmaceuticals and endocrine disrupting compounds in marine mussels (&ITMytilus galloprovincialis&IT). *Environ. pollut.* 236, 824–834. doi: 10.1016/j.envpol.2018.02.018

Solórzano, L., and Sharp, J. H. (1980). Determination of total dissolved phosphorus and particulate phosphorus in natural waters1. *Limnology Oceanography* 25, 754–758. doi: 10.4319/lo.1980.25.4.0754

Stepanauskas, R., Jorgensen, N. O. G., Eigaard, O. R., Zvikas, A., Tranvik, L. J., and Leonardson, L. (2002). Summer inputs of riverine nutrients to the Baltic Sea: Bioavailability and eutrophication relevance. *Ecol. Monogr.* 72, 579–597. doi: 10.2307/3100058

Su, C., Song, S., Lu, Y. L., Liu, S. J., Giesy, J. P., Chen, D. L., et al. (2018). Potential effects of changes in climate and emissions on distribution and fate of perfluorooctane sulfonate in the Bohai Rim, China. *Sci. Total Environ.* 613, 352–360. doi: 10.1016/j.scitotenv.2017.09.021

Sundkvist, A. M., Olofsson, U., and Haglund, P. (2010). Organophosphorus flame retardants and plasticizers in marine and fresh water biota and in human milk. *J. Environ. Monit.* 12, 943–951. doi: 10.1039/B921910B

Sundqvist, K. L., Tysklind, M., Cato, I., Bignert, A., and Wiberg, K. (2009). Levels and homologue profiles of PCDD/Fs in sediments along the Swedish coast of the Baltic Sea. *Environ. Sci. pollut. Res.* 16, 396–409. doi: 10.1007/s11356-009-0110-z

Swedish Institute for the Marine Environment (2023) *Swedish Water Environment*. Available at: https://www.sverigesvattenmiljo.se/.

Utermöhl, H. (1958). Zur vervollkommnung der quantitativen phytoplankton-methodik. Internationale Vereinigung für theoretische und angewandte Limnologie. *Mitteilungen* 9, 1–38. doi: 10.1080/05384680.1958.11904091

US EPA (1997). "Method 446.0: *In Vitro* Determination of Chlorophylls a, b, c + c and Pheopigments in Marine And Freshwater Algae by Visible Spectrophotometry," in *National Exposure Research Laboratory Office of Research and Development. U.S. Environmental protection Agency C, Ohio 45268* (Cincinnati, Ohio: U.S. Environmental Protection Agency).

Wallberg, P., Jonsson, P. R., and Andersson, A. (2001). Trophic transfer and passive uptake of a polychlorinated biphenyl in experimental marine microbial communities. *Environ. Toxicol. Chem.* 20, 2158–2164. doi: 10.1897/1551-5028(2001)020<2158:ttapuo>2.0.co;2

Wang, X. P., Sun, D. C., and Yao, T. D. (2016). Climate change and global cycling of persistent organic pollutants: A critical review. *Sci. China-Earth Sci.* 59, 1899–1911. doi: 10.1007/s11430-016-5073-0

Wikner, J., and Hagström, Å. (1999). Bacterioplankton intra-anual variability: importance of hydrography and competition. *Aquat. Microbial Ecol.* 20, 245–260. doi: 10.3354/ame020245

Frontiers in Marine Science

Explores ocean-based solutions for emerging global challenges

The third most-cited marine and freshwater biology journal, advancing our understanding of marine systems and addressing global challenges including overfishing, pollution, and climate change.

Discover the latest Research Topics

See more →

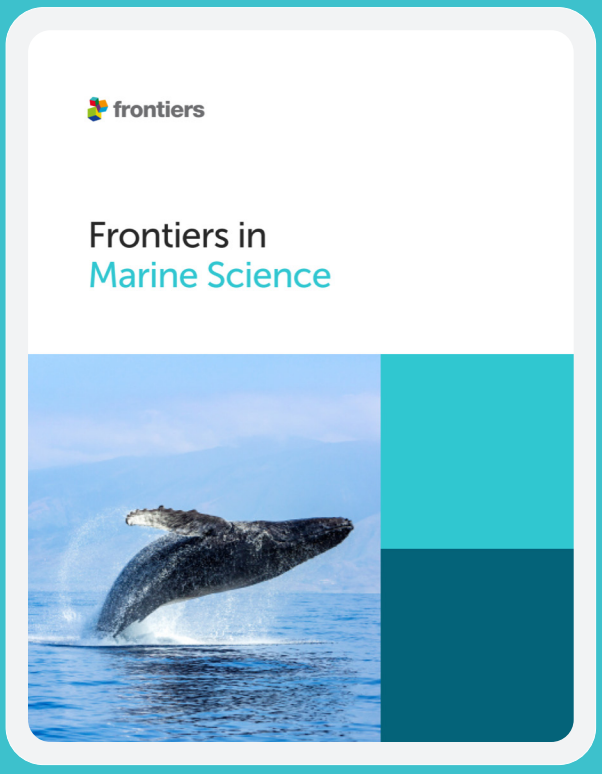

Frontiers

Avenue du Tribunal-Fédéral 34
1005 Lausanne, Switzerland
frontiersin.org

Contact us

+41 (0)21 510 17 00
frontiersin.org/about/contact